University of Alberta

Isolation of Reactive Bonding Environments in the Main Group *via* New Donor-Acceptor and Kinetic Stabilization Pathways

by

S. M. Ibrahim Al-Rafia

A Thesis submitted to the Faculty of Graduate Studies and Research in partial fulfillment of the requirements for the degree of

Doctor of Philosophy

Department of Chemistry

Spring 2013
Edmonton, Alberta

Abstract

The research presented in this Thesis is focused on the synthesis of highly reactive molecules featuring Group 14 elements with the aim of discovering new bonding environments which can be translated into new forms of reactivity.

Kinetic stabilization with the use of sterically demanding ligands containing umbrella-shaped triarylsilyl groups was one of the approaches that was engaged in the pursuit of abovementioned goal. The area of research involving this strategy was the isolation of reactive bonds such as Ge=O and Ge=S double bonds. Due to the presence of a high degree of structural flexibility within the developed amidosilyl ligands, kinetic stabilization of the targeted reactive bonds was not successful. Nevertheless, the steric bulk offered by the amidosilyl ligands presented in this Thesis could be a useful component for future advancement of the transition metal chemistry.

Electronic stabilization with the aid of Lewis basic donors and Lewis acidic acceptors was the other method explored to isolate reactive inorganic species in this Thesis. This donor-acceptor stabilization protocol was employed to isolate parent heavy Group 14 methylenes (EH_2), ethylenes (H_2E-EH_2), hydridoamides (EH-NHDipp; E = Si, Ge and Sn) and oligo dichlorogermanes [$(GeCl_2)_x$, x >2]. The isolation of these reactive molecules in the form of stable adducts represents a promising avenue to study the chemistry of these species under milder condition (with possible applications as precursors to nanomaterials envisioned).

Table of Contents

List of Tables

List of Figures

Lists of Schemes

Lists of Charts

List of Symbols, Abbreviations and Nomenclature

Symbols	Meaning
{X}	Decoupled-nucleus X
2D	Two-dimensional
Å	Angström
bp	Boiling point
ca.	cira; approximately
Equiv	Equivalent
diox.	Dioxane
FT	Fourier transform
g	Gram
gCOSY	Gradient-enhanced correlation spectroscopy
gHMQC	Gradient heteronuclear multiple quantum coherence
gHSQC	Gradient heteronuclear single quantum coherence
Hz	Hertz
IR	Infrared
kJ	kilojoule
Mes	Mesityl
mg	Milligram
MHz	Megahertz
min	Minute
mL	Milliliter
mmol	Millimole
mol	mole
$^{n}J_{AB}$	n-bond AB coupling constant
NMR	Nuclear magnetic resonance
$^{\circ}$C	Degree Celcius
ORTEP	Oak Ridge Thermal Ellipsoid Plot
OTf	Triflate

Ph	Phenyl
ppm	Parts per million
RT	Room temperature
THF	Tetrahydrofuran
TMS	Tetramethylsilane
vs.	versus
δ	Partial charge or chemical shift in ppm
μ	Micro
υ_{AB}	A–B bond stretching frequency
HOMO	Highest occupied molecular orbital
LUMO	Lowest unoccupied molecular orbital
eV	Electron-volt
mp	Melting point
LA	Lewis acid
LB	Lewis base
IPr	1,3-diisopropylphenylimidizole-2-ylidene
NHC	N-heterocyclic carbene
CAAC	Cyclic alkyl amino acrbene
DCM	Dichloromethane
ε	Molar absorption coefficient
MO	Molecular orbital

Chapter 1

Introduction

Chapter 1

Introduction

1.1 Preface

Spectacular discoveries in the chemistry of main Group elements in the beginning of the 21st century has lead to the foundation of an era where new bonding modes have been uncovered, and main group elements have started to adopt reactivity once reserved for transition metals complexes.[1,2] As a synthetic chemist, the primary motivation of this Thesis was to make new molecules featuring new bonding environments that stretch the limit of what current theories predict is possible; moreover, in the pursuit of this goal, new forms of reactivity will hopefully be discovered. The research presented in this Thesis can be divided into two different themes: (1) ligand design and kinetic stabilization of heavy ketone analogues, and (2) the electronic stabilization of low oxidation state Group 14 hydrides.

In brief, the first research chapter of this Thesis (Chapter 2) describes the synthesis of a new ligand class featuring triarylsilyl "Umbrella" motifs and application of these ligands for the isolation of heavier element analogues of ketones. The second research chapter (Chapter 3) involves the synthesis of Lewis acid-base stabilized heavy Group 14 element methylene analogues (EH_2; E = Si, Ge and Sn), and exploration of the reactivity of these species. The third research chapter (Chapter 4) builds upon the synthetic strategy outlined in Chapter 3 and

reports the isolation of heavy ethylene analogues ($H_2EE'H_2$) *via* donor-acceptor stabilization chemistry. The next research chapter (Chapter 5) involves the synthesis of low oxidation state heavy Group 14 element amidohydrides and exploration of their thermal decomposition including a rare carbene ring-expansion/activation reaction. Chapter 6 describes the attempted synthesis of $(PN)_3$, a heavier oligomeric analogue of N_2, while the final research Chapter illustrates recent progress involving the carbene-assisted growth of dichlorogermanium oligomers, $(GeCl_2)_x$.

1.2 Kinetic and electronic stabilization

Kinetic stabilization, or more specifically steric stabilization, describes the isolation of reactive species with the use of steric protection offered by bulky ligands. Sterically demanding ligands act as "kinetic shields" that prevent incoming molecules from reacting with the protected reactive functionality in a molecule. The role of the bulky ligand is to raise the activation energy (E_a) of detrimental oligomerization or decomposition processes, as in many instances these reactions would be thermodynamically favorable on the grounds of the bond enthalpies involved. A classic example of kinetic stabilization would be the isolation of the first stable diphosphene Mes*P=PMes* (**1**) (Mes* = 2,4,6-^{t}Bu$_3$C$_6$H$_2$), (Figure 1.1) in 1981 by Yoshifuji and coworkers. The kinetically stabilized P-P double bond in **1** helped to overturn the widely accepted "double bond rule"[3] and ligand-assisted kinetic stabilization has played a remarkable ongoing role in accessing many new reactive bonding motifs across the Periodic

Table.[4,5] For example, the isolation of kinetically stable digermynes, distannynes and diplumbynes Ar'EEAr' [Ar' = C_6H_3-2,6-(C_6H_3-2,6-$^iPr_2$)$_2$, E = Ge, Sn and Pb; **2**, **3** and **4** respectively], was achieved by the Power group with the aid of sterically demanding terphenyl ligands (Figure 1.1).[6] The bonding features of these heavy acetylene analogues are particularly interesting due to the fact that they all form *trans*-bent structures and the degree of *trans*-bending increases as the Group 14 element becomes heavier. In fact, in diplumbyne (**4**) the terphenyl ligands bonded with Pb form a Pb-Pb-C angle almost 90° (please refer to section 1.7 for more details). In addition, the element-element bond order decrease by roughly 0.5 units with each increase in the period number of the valence orbitals on the Group 14 elements, with the Pb-Pb bond order in **4** approaching unity.

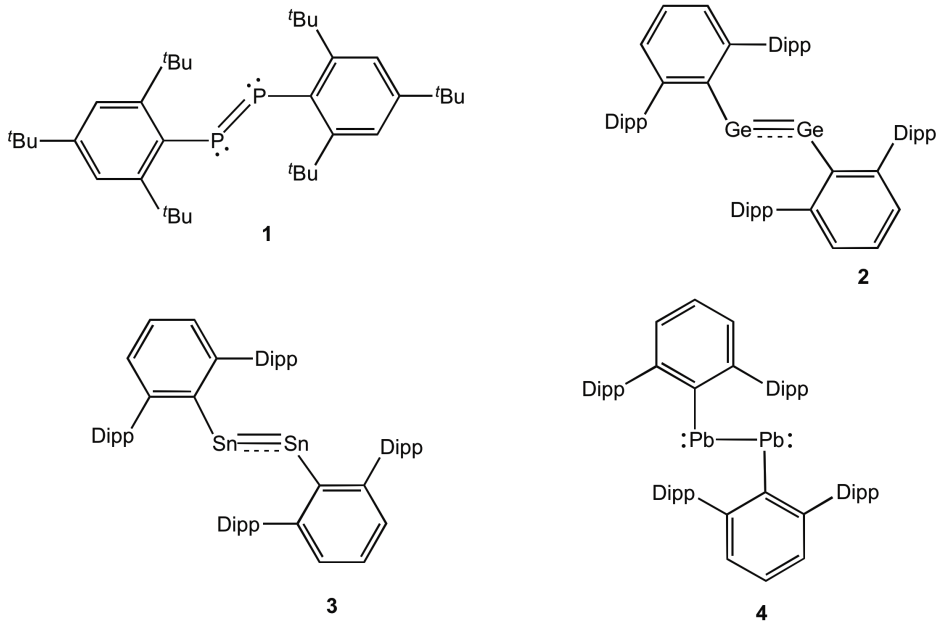

Figure 1.1. Kinetically stabilized reactive bonds, diphosphene (**1**) and the heavy alkyne analogues, Ar'EEAr' (E = Ge, Sn and Pb; **2**, **3** and **4**, respectively).

Electronic stabilization refers to the protection of reactive sites such as filled (lone pair) or vacant orbitals on a molecule with the use of an appropriate donor or acceptor, so that interaction of the ancillary ligand with the reactive site effectively suspends undesired decomposition pathways. Electron deficient boron-containing molecules, such as $B(C_6F_5)_3$, are generally prone to nucleophilic attack due to the presence of a vacant p orbital perpendicular to the sp^2 bonds involving boron. This reactivity pathway can often be prevented by occupying the empty orbital with a neutral donor ligand to form a donor-acceptor adduct, $R_3B{\bullet}LB$ (LB = Lewis basic donor). An excellent recent example of this principle is the isolation of of a stable compound featuring a boron-boron triple bond, IPr•B≡B•IPr (**5**), by Braunschweig and coworkers (Figure 1.2); notably B_2 is highly reactive in the absence of N-heterocyclic carbene IPr ligands (IPr = $[(HCNDipp)_2C:]$; Dipp = 2,6-$^{i}Pr_2C_6H_3$), and only be isolated by matrix isolation at very low temperatures (*ca*. 8 K).[7a,7e] Other excellent examples of this form of stabilization include the formation of dialane (H_2AlAlH_2, **6**),[7b] diphosphinidene (P_2, **7**)[7c] and borylene (:HB, **8**) complexes.[7d]

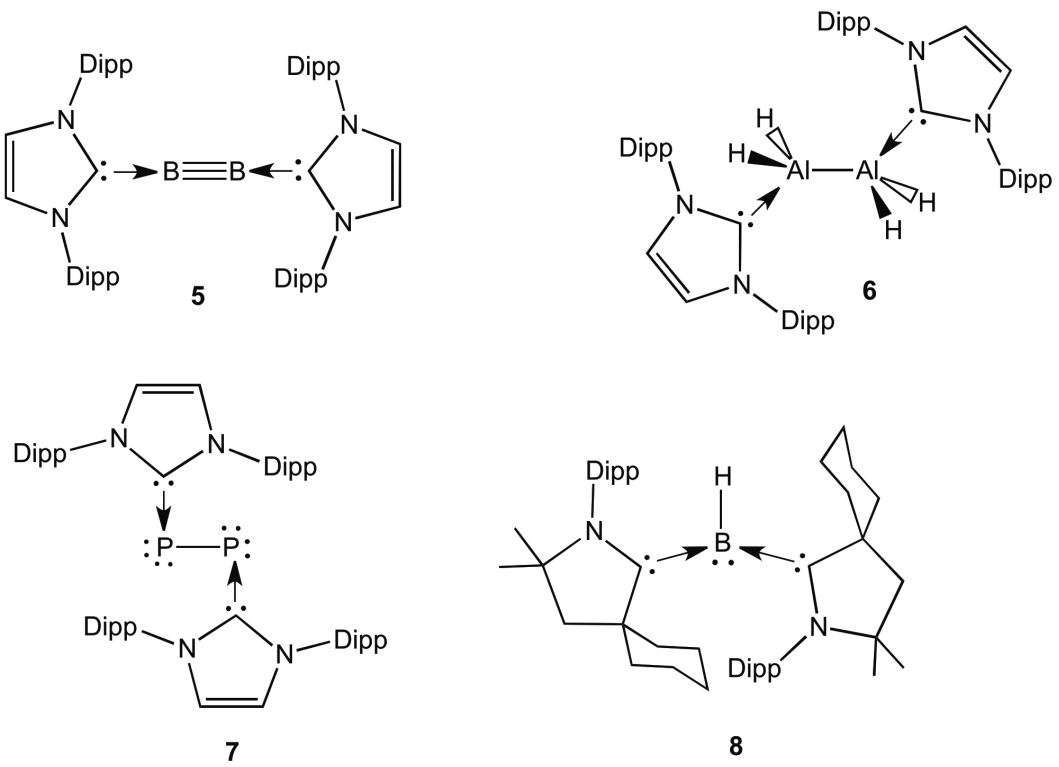

Figure 1.2. Donor-stabilized reactive main-group species: a boron-boron triple bond (**5**), a dialane (**6**), a diphosphinidene (**7**) and parent borylene (**8**).

In addition, some molecules are ambiphilic or bifunctional, in other words they contain an energetically low lying vacant orbital (Lewis acidic site) and a lone pair (Lewis basic site), and thus exhibit electrophilic and nucleophilic character. One possible strategy to stabilize such reactive molecules involves a combined approach termed donor-acceptor stabilization. Relevant examples of this principle were initially reported by the Scheer group to isolate the parent Group 13/15 hydrides H_2PBH_2, H_2PAlH_2 and H_2PGaH_2 in the form of stable adducts (Chart 1.1).[8] This stabilization protocol was later used by the Rivard group to isolate the parent heavy methylenes $:EH_2$ and ethylene adducts

H_2SiGeH_2, H_2SiSnH_2 and H_2GeGeH_2 and this research is the focus of Chapters 3 and 4 in this Thesis (Chart 1.1).[9,10]

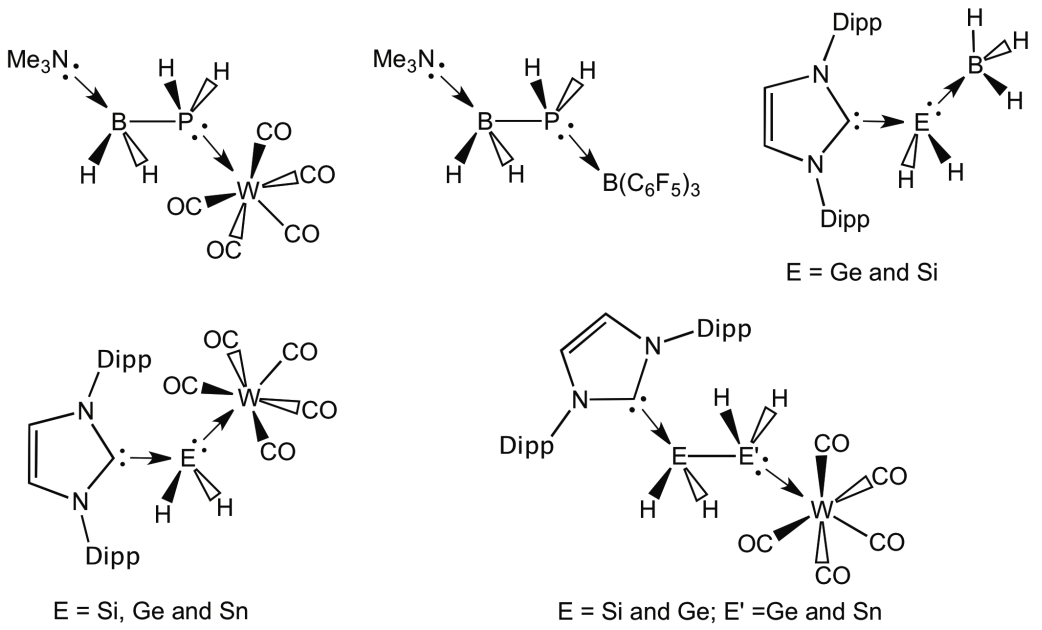

Chart 1.1. Donor-acceptor stabilization of main group hydrides.

1.3 Multiple bonding in heavier main group elements stabilized by sterically encumbered ligands

The synthesis of molecular species featuring unusual bonding environments is a major area of modern inorganic chemistry. In general, a drive to better understand the fundamental bonding principles of inorganic elements serves to inspire researchers in this area. In addition, these types of studies often lead to the discovery of unexpected reactivity.[11] The application of ligand-based stabilization to intercept new bonding modes was elegantly shown by Lappert and coworkers in the early 1970s, when they prepared the novel Sn(II) dialkyl dimer

$L'_2Sn=SnL'_2$ [L' = $CH(SiMe_3)_2$] (**9**).[12] This compound contains a weak Sn-Sn double bond in the solid state (which dissociates into monomeric stannylene units $Sn[CH(SiMe_3)_2]_2$ in solution). This breakthrough instigated a completely new area of research focused on the isolation of compounds featuring formal multiple bonding between heavy main group elements. Afterwards, West and coworkers prepared the first stable disilene $Mes_2Si=SiMes_2$ (Mes = 2,4,6-$Me_3C_6H_2$) (**10**) in 1981.[13] This disilene represented the first inorganic alkene analogue isolated in condensed phase that did not dissociate into monomeric ER_2 units in solution (E = Si, Ge, Sn or Pb). As mentioned, Yoshifuji et al. used a slightly different ligand to stabilize the diphosphine Mes*P=PMes*.[3] The Power group has investigated a series of hindered terphenyl ligands, with the general formula -C_6H_3-2,6-$Aryl_2$ (Figure 1.3) for the synthesis of many low coordinate main group and transition metal species. The presence of flanking aryl groups about the central ligating ring generates a concave steric pocket that is large enough to accommodate various types of reactive bonds while inhibiting the approach of incoming molecules that can contribute to degradation processes.[14] For example, Power and coworkers reported the isolation of a Cr-Cr quintuple bond in the dimeric chromium(I) complex Ar'CrCrAr' [Ar' = C_6H_3-2,6-(C_6H_3-2,6-$^iPr_2$)$_2$] in 2005 with the aid of sterically demanding supporting terphenyl ligands.[15] It also should be mentioned that the Robinson group played an important role in advancing the chemistry of terphenyl ligands.[14b]

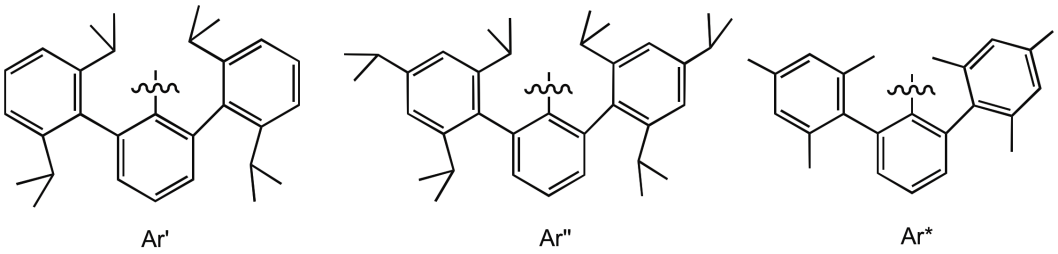

Figure 1.3. Commonly used sterically demanding terphenyl ligands in main group chemistry.

Inspired by the abovementioned successes in the kinetic stabilization of heavy main group element multiple bonds, the Rivard research group became interested in isolating heavier element congeners of ketones and thioketones, R_2E=Ch, (E = Si and Ge; Ch = O and S). The motivation behind this research is partially derived from the rarity of these species in the general literature.[16] In addition, Si=O and Ge=O π-bonds have been postulated to be present in partially oxidized nanocrystalline materials and are often implicated to be responsible for the interesting optical properties of these nanomaterials.[17] The major obstacle to the isolation of heavy element ketones R_2Si=O and R_2Ge=O is their high reactivity due to the weakened π-interactions and concomitantly polarized nature of the E=O bonds, especially towards oligomerization to form $(-R_2E\text{-}O\text{-})_n$ oligomers/polymers, where the value of n is a function of the steric bulk of the substituents (R).[18] In the absence of bulky groups at the Group 14 element, the oligomerization reaction is exothermic and proceeds with no barrier. Nagase and coworkers theoretically determined that the dimerization energy of H_2Si=O was 106 kcal/mol and that this value decreases as the steric bulk of the substituents on silicon increases; this study also suggested that with very hindered substituents on

the silicon center, the dimerization reaction becomes endothermic, thus isolation of a monomeric silanone $R_2Si=O$ might be possible.[19]

In 1901, Kipping and Lloyd reported the synthesis of the first silanone, Ph_2SiO, and proposed a monomeric structure and coined the term "silicone".[20] Although Ph_2SiO was later found to be polymeric, the name "silicone" became a general term for polysiloxanes in the silicon industry. In 2009, Driess reported the synthesis of carbene supported silanone complex $L(ImMe_4)Si=O$ (**11**) [L = $[HC(CMeNDipp)_2]$, Dipp = 2,6-$^i Pr_2C_6H_3$, $ImMe_4$ = $(MeCNMe)_2C$:) (Figure 1.4), wherein the carbene donates electron density into a Si-O π*-orbital of the silanone, effectively suppressing silanone oligomerization.[21a] It should also be mentioned that Si-O π-bonding is significantly decreased as a result of this carbene-silicon interaction. Isolation of a base-coordinated silathione, **12**, was in fact achieved in 1989 by Corriu and coworkers.[22] Approximately a decade later, Goto reported the successful isolation of a monomeric silanethione Tbt(Tip)Si=S (Tbt = 2,4,6-$[(Me_3Si)_2CH]_3C_6H_2$; Tip = 2,4,6-$^i Pr_3C_6H_2$) (**13**) from the desulfurization reaction of Tbt- and Tip-substituted tetrathiasilolane (**14**) using Ph_3P as a desulfurizing agent.[23]

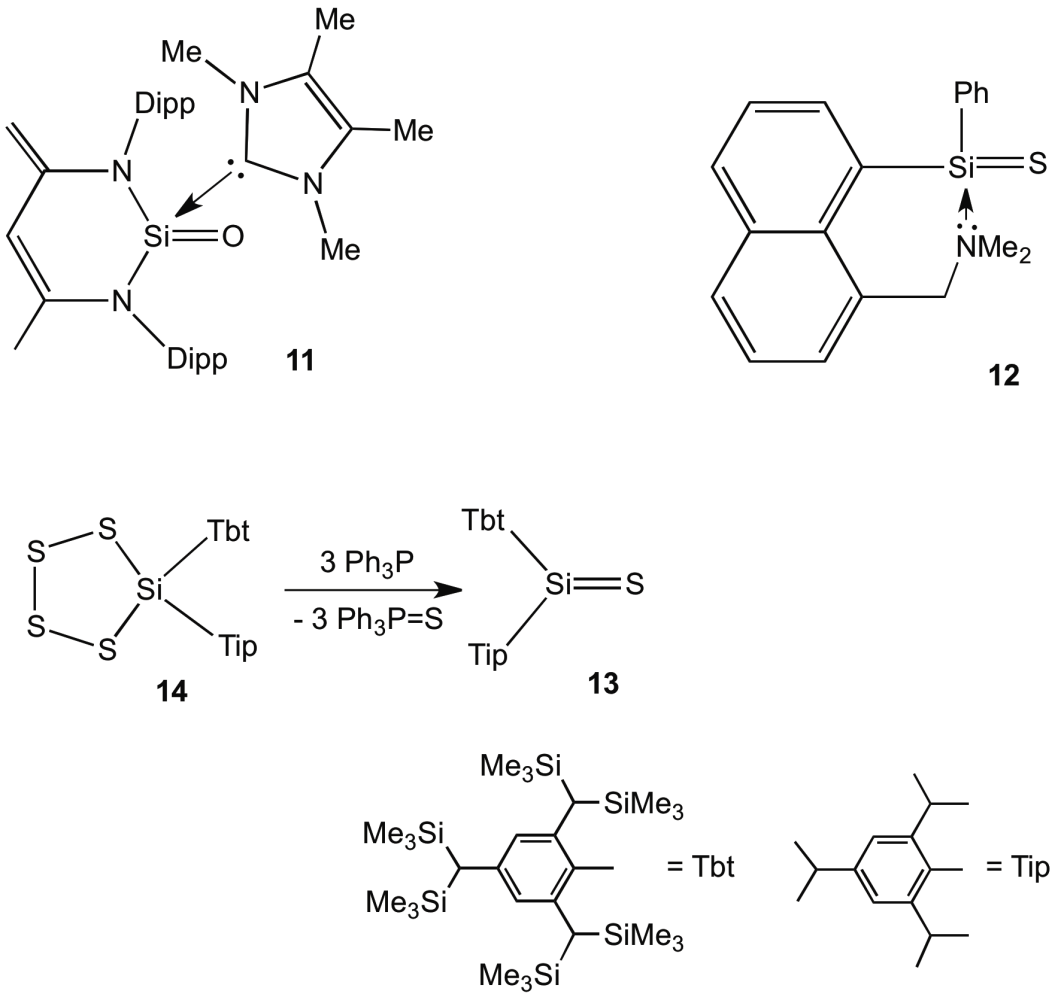

Figure 1.4. Donor-stabilized silanone (**11**) and silathione (**12**); synthesis of the monomeric silanethione Tbt(Tip)Si=S (**13**).

The first example of a stable germanethione, Tbt(Tip)Ge=S (**15**) was disclosed in 1993 (Scheme 1.1).[24] Since this time, a large number of attempts were devoted towards isolating $R_2Ge=O$ as a stable monomeric species and in the vast majority of instances the formation of dimers or oligomers transpired.[25] A stable germanone with an NHC supporting ligand was reported by Driess, which has similar bonding features as its lighter congener, $L(ImMe_4)Si=O$ (**11**),[26] a stable

germanone with a intact Ge-O π-bond was only reported in 2012, when Tamao prepared $(Eind)_2Ge{=}O$ (**16**) (Eind = 1,1,3,3,5,5,7,7-octaethyl-shydridecane-4-yl) *via* oxidation of the two-coordinate germylene (**17**) with Me_3NO (Scheme 1.1).[27]

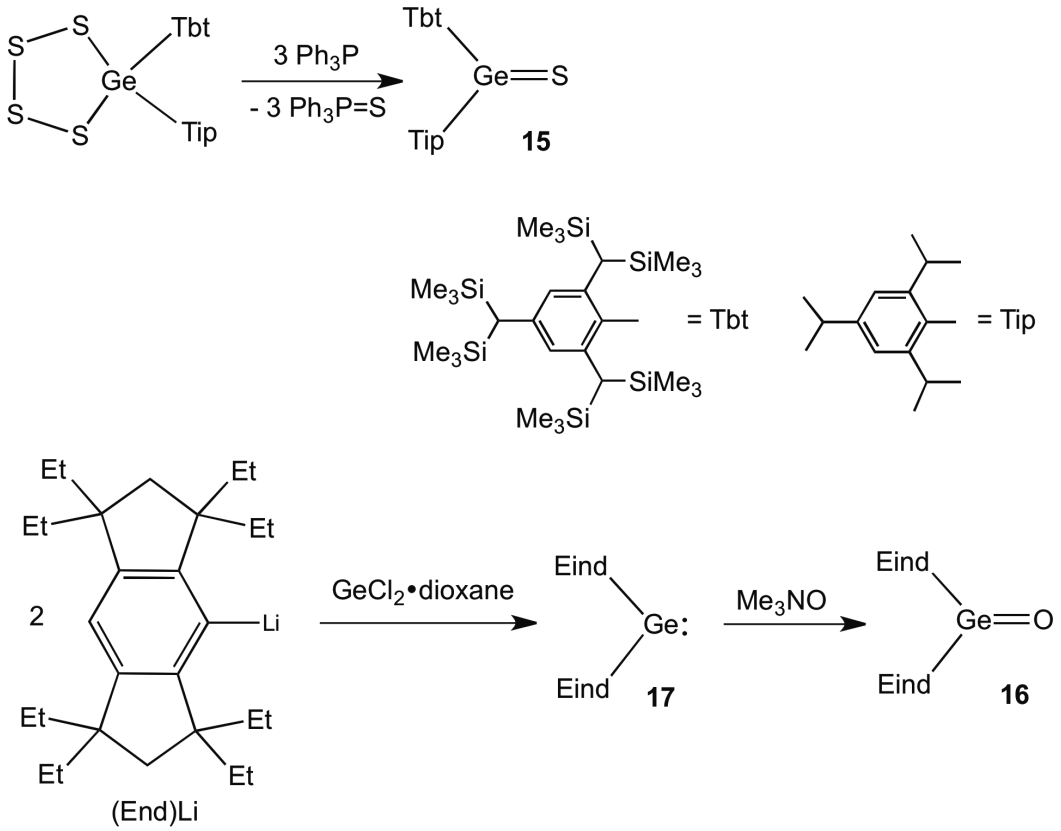

Scheme 1.1. Synthesis of the monomeric germanethione (**15**) and germanone (**16**).

1.4 Carbenes and their heavier analogues

Carbenes represent a class of organic compounds which contain a neutral dicoordinate carbon atom in a divalent state with two non-bonding valence electrons in singly occupied degenerate orbitals (triplet state) or both in the same orbital with anti-parallel spins (singlet state). The first attempts to prepare the parent carbene, CH_2, were reported in the 1830s.[28] At that time, the bonding properties were not well understood, thus the synthesis of a stable divalent carbene was thought to be quite straightforward. Duma (1835) and Regnault (1839) attempted to synthesize methylene (CH_2) by dehydrating MeOH with either phosphorous pentaoxide or concentrated sulfuric acid.[29,30] Later, Butlerov formed ethylene from the reaction of methyl iodide in the presence of copper and suggested that the formation of $H_2C{=}CH_2$ arose from the dimerization of two methylene molecules.[28] In 1862 Geuther proposed that the basic hydrolysis of chloroform proceeded through the transient formation of dichloromethylene ($:CCl_2$), which has now been verified experimentally.[28]

A second vigorous period of carbene research was initiated by the discovery of isonitrile (RNC) and fulminic acid derivatives (RCNO) in the late nineteenth century.[31] Subsequent pioneering work was carried out by Staudinger, who studied the decomposition of diazo compounds, R_2CN_2 to give carbon-carbon double-bonded species; this reaction was believed to proceed *via* the transient formation of carbenes.[32] In 1957, Breslow proposed that an N-heterocyclic carbene, thiozole-2-ylidene, was involved in the catalytic cycle of vitamin B1

which yields furoin from furfural. Through a deuterium labeling experiment, Breslow et al. demonstrated that under the standard reaction conditions (in D_2O), the C2-proton was rapidly exchanged for a deuterium in a statistical equilibrium (**18**), and postulated that the exchange reaction proceeds *via* the formation of a stable carbene intermediate (**19**) (Scheme 1.2).[33] In 1960 the Wanzlick group prepared the first imidazol-2-ylidene carbene (**20**), by the deprotonation of an imidazole salt (**21**) using KO^{t}Bu as a base. Wanzlick and Hoffmann attributed the stability of these imidazole-based carbenes to the presence of 4n+2 π-electrons in the heterocycle. Although (**20**) was not isolated, a stable coordination complex between this N-heterocyclic carbene and mercury was obtained (**22**, Scheme 1.2).[34]

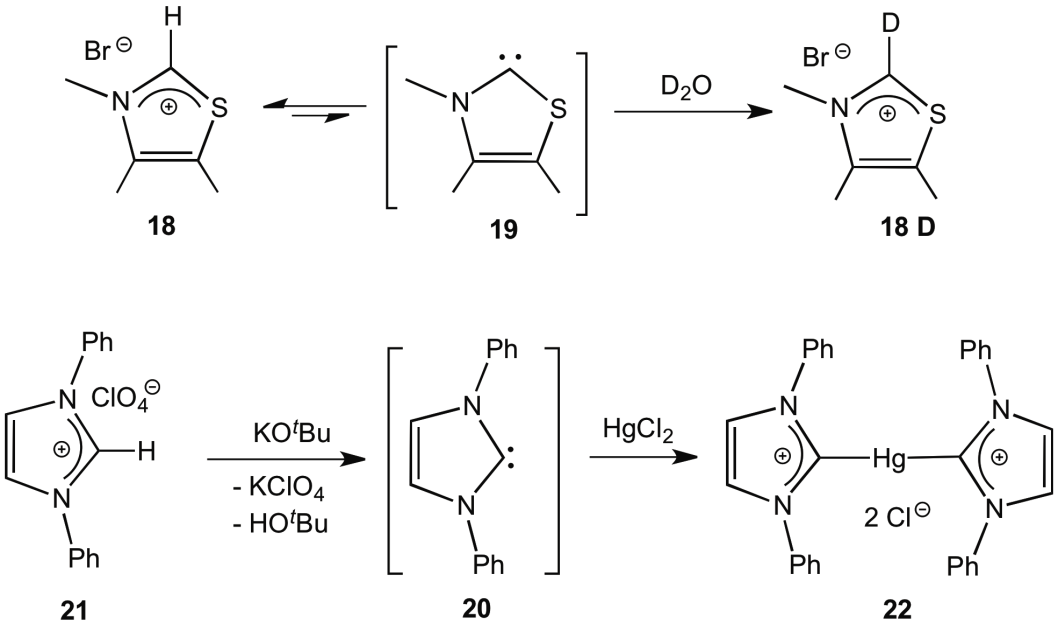

Scheme 1.2. Breslow's isotope labeling experiment and mercury complex of carbene prepared by Wanzlick.

Fischer and Maasbol initiated the application of carbenes in the field of organometallic chemistry in 1964 with the synthesis of the stable chromium-carbene complex $[Cr\{COCH_3(Ph)\}(CO)_5]$.[35] In 1988, the group of Bertrand reported the synthesis of the first carbene that is stable in the condensed phase at ambient temperature; the phosphinocarbene $(^iPr_2N)_2PCSiMe_3$ (**23**) was prepared as a distillable red oil from the reaction of the lithiated diazomethane, $Li[Me_3SiC(N_2)]$ with $ClP(N^iPr_2)_2$.[36] Unfortunately, this phosphinocarbene proved to be a poor σ-donor ligand due to the presence of $P\text{-}C_{carbene}$ multiple bond character. Another major breakthrough in the field of carbene chemistry occurred in 1991 when Arduengo described the synthesis and solid state structure of 1,3-diadamantylimidazol-2-ylidene (**24**), the first unambiguously stable diamino carbene (Figure 1.5).[37]

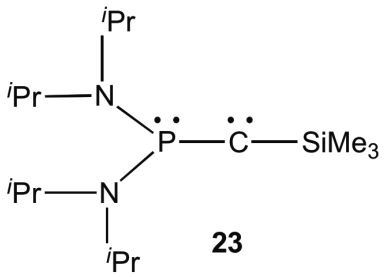

23

Boiling point: 75-80 °C/10^{-2} Torr

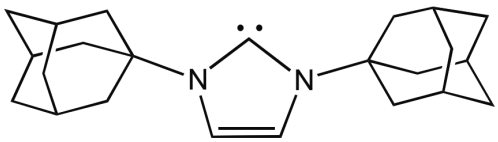

24

Melting point: 240 °C

Figure 1.5. Bertrand's phosphinocarbene $(^iPr_2N)_2PCSiMe_3$ (**21**) and Arduengo's N-heterocyclic carbene (**22**) prepared by Arduengo.

The nature of the groups attached to the carbene carbon dictates whether a singlet or triplet electronic ground state is adopted. The substituents bound to the carbene carbon atom can either be arranged in linear or bent geometries with varying degrees of s and p character in the required C-R bonding orbitals. In the linear geometry, the carbene carbon forms two bonds using degenerate sp hybridized orbitals (according to the Valence Bond Model) while Hund's rule dictates that the remaining p orbitals would be singly occupied to form a triplet ground state (Figure 1.6). While in the bent geometry, the degeneracy of the p orbitals would be removed and the carbene carbon atom adopts an sp^2-type hybridization; as a result, the p_y orbital remains almost unchanged while the initially pure p_x orbital acquires some s character and formally becomes an sp^2 hybrid orbital. The orbital perpendicular to the plane defined by the three atoms (p_y) is assigned as "p" while the non-bonding orbital parallel to the plane is termed as "σ". Thus the dicoordinated divalent carbene carbon can have four possible non-bonding electronic configurations: σ^1p^1 (T_1), σ^1p^1 (S_1), σ^2 (S_0), p^2 (S_2) (Figure 1.6). In the σ^1p^1 configurations the electron spins can either be anti-parallel to give a singlet state (S_1) or parallel to form a triplet state (T_1), while the σ^2 and p^2 configurations are each electron-paired singlet states. In general, the σ^2-configuration is calculated to be lowest energy configuration amongst the possible singlet arrangements, while in the parent carbene, methylene (CH_2), in the linear geometry the energy of the triplet state was calculated to be 14 kcal/mol lower than the singlet ground state (S_1).[38] The singlet-triplet energy separation, ΔE_{ST} [E(triplet)-E(singlet)], is roughly equal to the electron-electron Coulombic

repulsion energy associated with pairing electrons in a σ-type orbital minus the energy required to promote an electron from a non-bonding σ to a p orbital. Therefore, as the energy separation between σ and p_π increases, the promotion energy becomes larger compared to the repulsion energy, thus $S_0(\sigma^2)$ electronic configuration becomes energetically favorable and the carbene center is termed a singlet carbene. On the other hand, if the value of ΔE_{ST} is negative, the triplet (T_1) state becomes the lowest energy configuration and carbene moiety is defined as triplet a carbene (Figure 1.6).

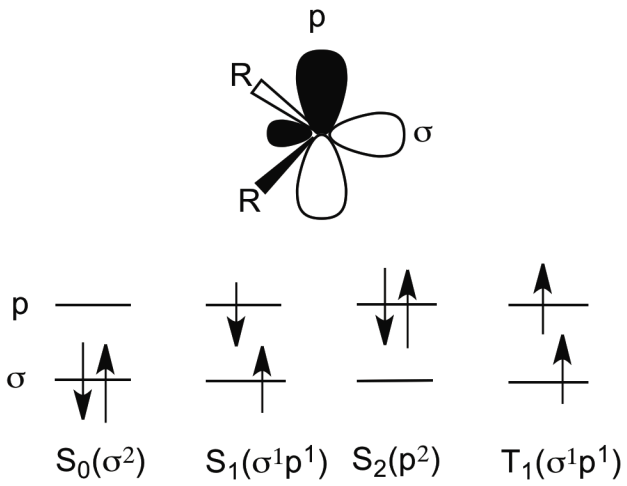

Figure 1.6. Electronic configurations of carbenes.

The electronic and steric properties of the substituents bonded to the carbene carbon directly impacts the electronic configuration adopted by the carbene center. For example, the p orbital of the carbene carbon can participate in a π-type interaction with the substituent. These interactions can be broadly classified into three groups: X-type π-electron donors such as -OR, $-NR_2$, -SR, F, Cl, Br and I; Z-type π-electron acceptors such as –COR, -SOR, $-SO_2R$, -NO and

NO_2; and C-type conjugating groups such as alkenes, alkynes, or aryl substituents. As illustrated in Figure 1.7, an X-type substituent can form a dative π-interaction with the p_π orbital of the carbene carbon, a consequence of this secondary dative interaction, the energy separation between the p and σ orbitals increases, thus leading towards an energetic preference for singlet carbenes. Z-type substituents have empty p or π* orbitals of correct symmetry to interact with the p orbital on the carbene center while C-type substituents have empty π and π* orbitals proximal to the carbene carbon. In both instances conjugation of these substituent-based orbitals with the p orbital on the carbene carbon lowers the energy of the LUMO (in other words lowers the energy of σ-p transition), therefore the formation of a triplet carbene is often favored.

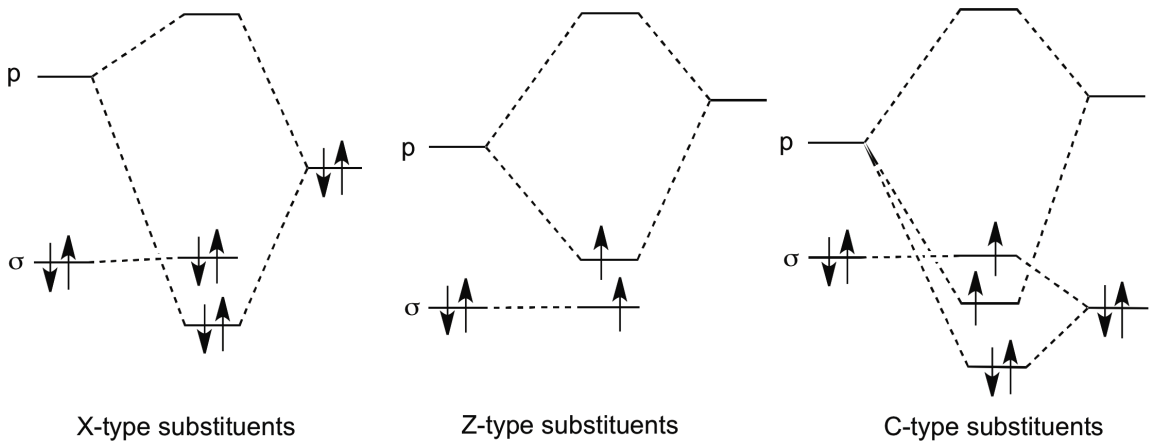

Figure 1.7. Molecular orbital energy diagram describing the effects of different types of substituents on the singlet-triplet energy separation of carbenes.

As mentioned already, the electronic nature of the substituent also plays an important role on the electronic configuration of carbene. In general, electron-withdrawing substituents favor singlet ground states over the triplet states as

electron-withdrawing substituents inductively stabilize the nonbonding σ-orbital by withdrawing electron density while the energy of the p orbital remains relatively unchanged. As a consequence, the energy separation between σ and p orbitals increases leading to the preference of singlet states. On the other hand, σ-electron donating groups induce a smaller σ-p energy separation, thereby favoring triplet states. In support of this trend, Harrison and coworkers theoretically showed that the ground state of carbenes change from triplet to singlet when the substituents on the carbene carbon are changed from electropositive lithium to electronegative fluorine.[39]

The abovementioned mesomeric effect can also be used to explain the strong σ-donor ability of N-heterocyclic carbenes (NHCs) such as Arduengo's N-heterocyclic carbene (**22**). The σ-electron withdrawing nitrogen atoms inductively stabilizes the σ-nonbonding orbital of the carbene carbon center, while the energy of the p orbital increases due to the π interaction with the lone pairs on the adjacent nitrogen centers; the combination of these two effects make NHCs strong σ-donors and weak π-acceptors (Figure 1.8).

Figure 1.8. Electronic stabilization of N-heterocyclic carbenes (NHCs).

Stable singlet carbenes, with a lone pair of electrons and an energetically accessible vacant orbital, have frontier orbitals that might allow for transition metal-like reactivity (*e.g.* splitting of H_2). Unfortunately, since heteroatoms with lone pairs, such as nitrogen, are generally present adjacent to the carbene carbon atoms, strong intramolecular π-interactions are formed. Consequently the carbene based p-orbital is not available for cooperative interaction with incoming substrates, instead carbenes generally use their nonbonding σ-electrons to form dative bonds with various substrates. Recently, Bertrand and coworkers reported the synthesis of stable cyclic (alkyl)(amino)carbenes (CAACs) that can heterolytically cleave hydrogen and activate an N-H bond in ammonia.[1b] Unlike transition metal complexes, these new carbenes do not form "Werner-like" adducts (*i.e* M←:NH_3), instead they exhibit facile N-H bond activation chemistry. The transition metal-like reactivity of CAACs stems from the higher energy of the HOMO and smaller singlet-triplet energy difference in CAACs in comparison to NHCs due to the presence of fewer π-donating substituents adjacent to the carbene carbon center. Due to the higher energy of the HOMO, CAACs are stronger nucleophiles and at the same time, they are also potent electrophiles; thus CAACs can interact synergistically with H_2 (Scheme 1.3).

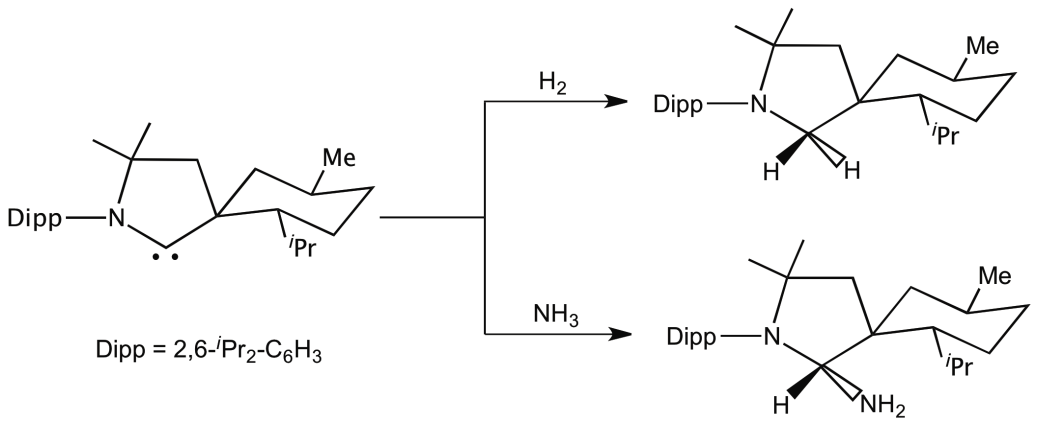

Scheme 1.3. Hydrogen and N-H bond activation by cyclic alkyl(amino)carbenes (CAACs).

The proposed mechanism for H_2 activation involves the donation of carbene σ-electron density into the H-H σ*-orbital, while the bonding σ-electron density in H_2 is donated into the vacant p orbital on the carbene carbon center (Figure 1.9). Theoretical calculations suggest that the mechanism of this reaction is similar to the heterolytic H-H bond cleavage involving a transition metal center; the proposed mechanism for the activation of NH_3 by CAACs is analogus to that of H_2 activation.

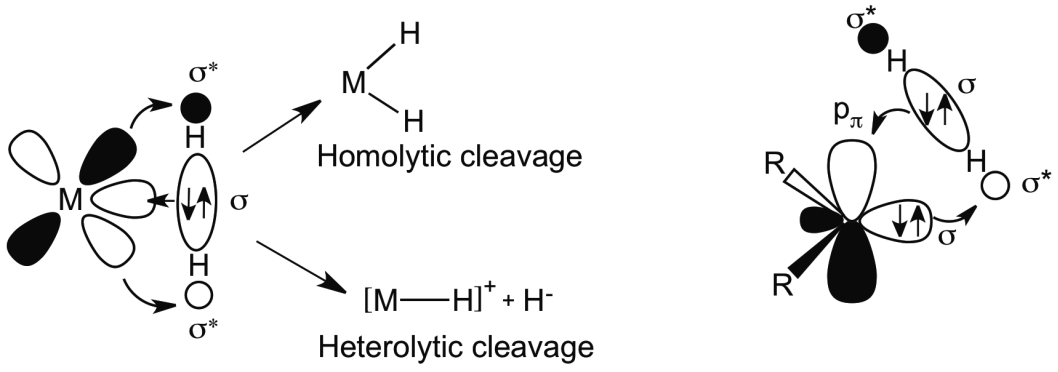

Figure 1.9. Schematic representation of H_2 activation on a transition metal center (left) and proposed mechanism of H_2 activation at a carbene carbon (right).

Due to their strong σ-donating properties, the use of N-heterocyclic carbenes (NHCs) as stabilizing ligands represents a fertile area of research in organometallic and main group chemistry. Recently a number of novel inorganic species have been isolated/stabilized using NHCs as supporting ligands. In this regard, the synthesis of NHC adducts featuring reactive entities such as HB=BH, B≡B, :SiX_2 (X = Cl and Br), :Si=Si:, P_2, and PH represent particularly noteworthy achievements.[40,41] Chart 1.2 contains a list of the most commonly used NHCs, with the bulky derivative IPr used most frequently by the main group chemistry community (including in this Thesis).

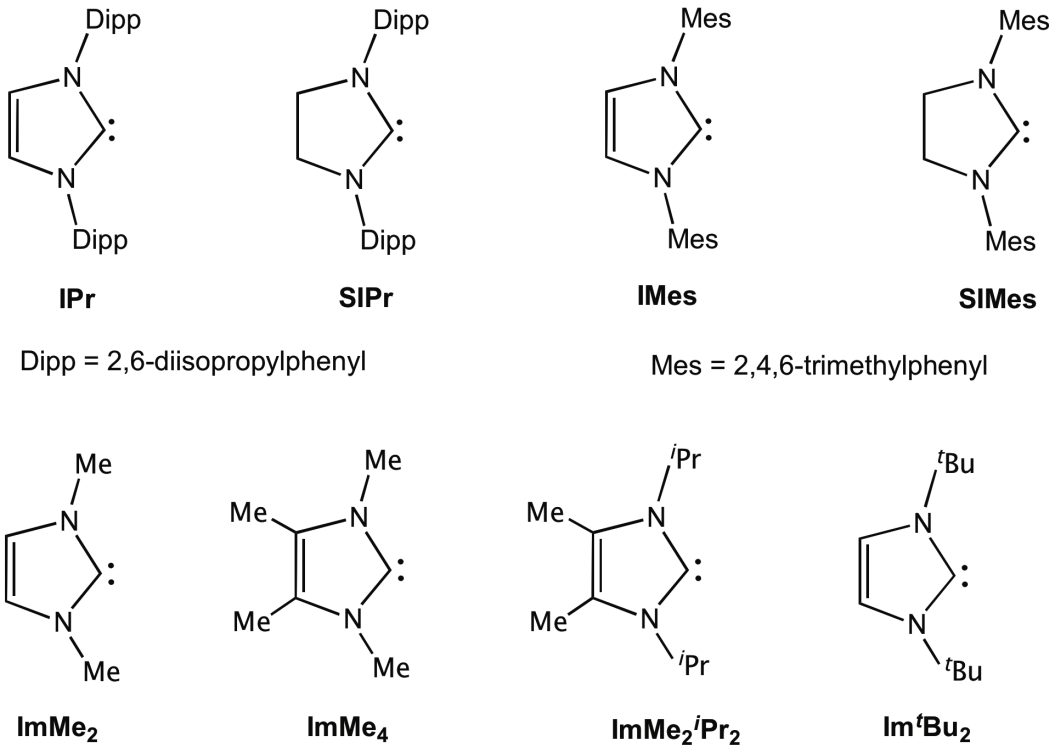

Chart 1.2. Commonly used N-heterocyclic carbenes (NHCs) in main group chemistry.

N-heterocyclic carbenes (NHCs) are similar to phosphines as they are both neutral, two electron σ-donor ligands.[42] NHCs are better σ-donor ligands than phosphines due to the mesomeric and inductive effects exerted by the nitrogen atoms adjacent to carbene carbons and the strong electron donating power of carbenes has led to the discovery of many carbene-bound metal complexes with important catalytic activity. For example, Grubbs et al. recognized the electron donating potential of NHCs and replaced a phosphine ligand in his first generation metathesis catalyst, $[Ru(CHPh)Cl_2(PCy_3)_2]$ (**25**), with an N-heterocyclic carbene to give a modified Ru catalyst with higher catalytic activity (Figure 1.10).[43]

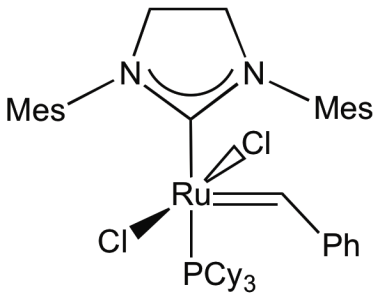

25

Figure 1.10. Second-generation Grubbs catalyst $[Ru(CHPh)Cl_2(PCy_3)(SIMes)]$ (**25**).

Silylenes, R_2Si:, are divalent and dicoordinate neutral silicon species that are heavier congeners of carbenes. Unlike the parent carbene, CH_2, which exists in a thermodynamically favorable triplet state, silylene ($:SiH_2$) adopts a singlet ground state due to the large energy separation and spatial difference between the valence 3s and 3p orbitals on silicon.[44] On the basis of the theoretical calculations, the singlet-triplet energy separation ΔE_{ST} [$\Delta E_{ST} = E_{triplet} - E_{singlet}$] for CH_2 was found to be -14.0 kcal/mol, while the value of ΔE_{ST} for SiH_2 was determined to be 16.7

kcal/mol.[38] However SiH_2 is extremely reactive due to the presence of a low lying empty p orbital and an electron lone pair which leads to ambiphilic character.[45] During the 1980s a number of organosilylenes were prepared and studied in low temperature argon or hydrocarbon matrices, and reported to react rapidly with solvent or themselves above cryogenic temperature.[46]

After the discovery of stable N-heterocyclic carbenes (NHCs) by Arduengo, examples of stable (isolable) rigorously two-coordinate silylenes were unknown, despite the earlier successful synthesis of stable germylenes (R_2Ge:) and stannylenes (R_2Sn:).[47] Notably, Jutzi reported the synthesis of decamethylsilicocene, :Si(η^5-$C_5Me_5)_2$, which possessed a divalent silicon center with two Cp* ligands in a nearly linear arrangement.[47] However, in 1994 West and coworkers prepared the first stable N-heterocyclic silylene (**26**) (Figure 1.10).[48] Interestingly, compound **26** is stable at room temperature for an infinite period of time and it is stable in the solid state (under N_2) to 220 °C. This stabilization originates from a combination of inductive and mesomeric effects due to the presence of nitrogen atoms adjacent to the silicon center, which is similar to the electronic stabilization in N-heterocyclic carbenes. After the isolation of the first stable N-heterocyclic silylene, a number of other groups reported stable silylenes with different structural frameworks. For example, Lappert et al. prepared the benzo-fused silylene in 1995, while Heinicke and coworkers reported the synthesis of pyrido-fused analogue (compounds **27** and **28**, respectively) (Figure 1.11).[49]

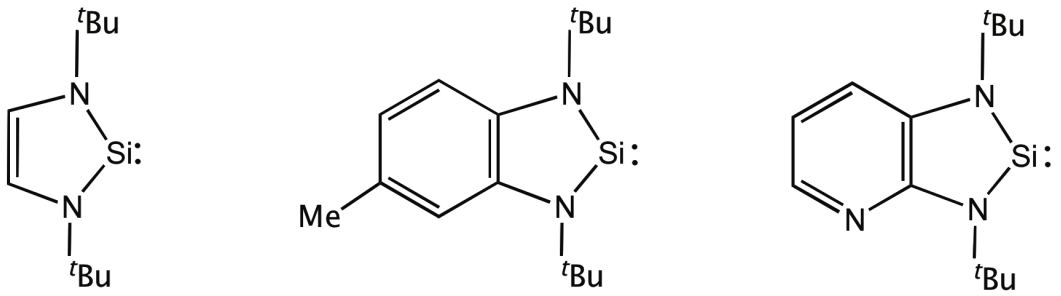

26 **27** **28**

Figure 1.11. N-heterocyclic silylene (**26**), benzo-fused silylene (**27**) and pyrido-fused silylene (**28**).

Silylenes without heteroatom donor stabilization are predicted to be highly unstable and highly reactive due to the lack of electronic stabilization gained from the secondary interaction of empty p orbitals of silylene with heteroatom based lone pairs. However, Kira et al. showed that when bulky $SiMe_3$ groups are positioned close to the silylene center, the synthesis of the unsupported dialkylsilylene (**29**) was possible from KC_8 reduction of the corresponding dibromo compound **30** at -50 °C.[50] Notably, compound **29** is sterically protected by the neighboring bulky $SiMe_3$ groups and is believed to be electronically stabilized by σ-π conjugation (interaction of vacant p orbital of silicon with C-Si σ-bonding orbitals); however **29** isomerizes slowly at 0 °C to give the cyclic silene (**31**) (Scheme 1.4).

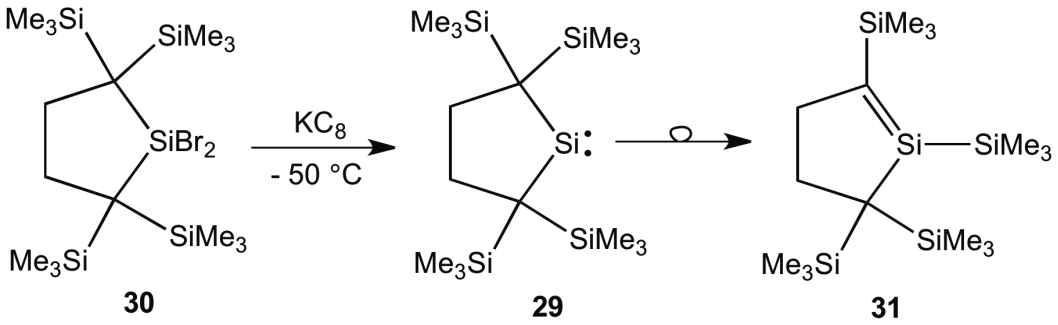

30 **29** **31**

Scheme 1.4. Synthesis of dialkylsilylene (**29**) and its isomerization reaction to give the cyclic silene (**31**).

In 2006, the Driess group discovered a new class of N-heterocyclic silylene featuring a modified β-diketiminate ligand.[14g] The β-diketiminate ligand containing silylene (**32**) displays a wide range of reactivity towards small molecules.[51,52] For example, compound **32** reacts with H_2O to give a mixed-valent siloxy silylene species **33**, which is highly nucleophilic and capable of reacting with small molecules such as CO_2 and N_2O to form the silanoic silyl ester complex **34** *via* oxygen transfer to the Si(II) center (Scheme 1.5). Besides the abovementioned examples, the groups of Roesky and Baceiredo contributed greatly to advance the chemistry of cyclic silylenes through their own syntheses of Si(II) heterocycles.[53,54]

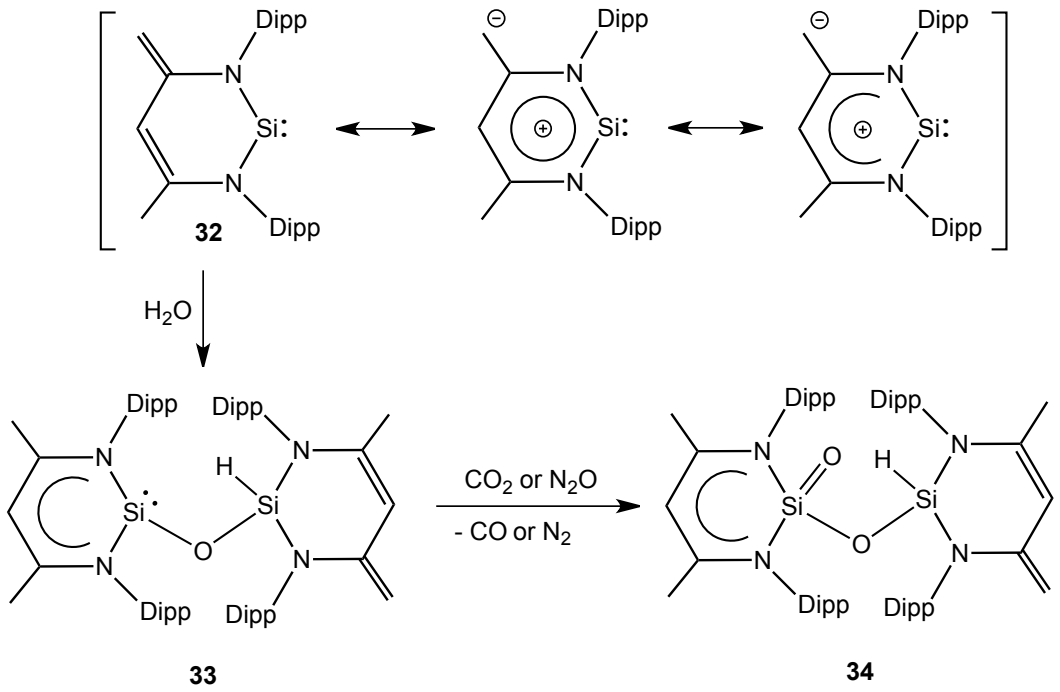

Scheme 1.5. Resonance structures of the β-diketiminate-supported N-heterocyclic silylene (**32**) and its reaction with water (**33**), CO_2 and/or N_2O (**34**).

Despite significant advances made in the chemistry of cyclic silylenes, their acyclic analogues are comparatively rare and difficult to synthesize. West and coworkers reported the synthesis of the acyclic diaminosilylene $[(Me_3Si)_2N]_2Si$:, which is stable at -20 °C for 12 hrs but decomposes to give a complex product mixture at higher temperature.[55] The higher reactivity of acyclic silylenes can be explained by the singlet-triplet energy difference (ΔE_{ST}), which decreases as the bond angle around the silicon center increases and therefore, tuning the bond angles about the silicon atom can alter the reactivity of silylenes. Bond angle adjustment can be achieved by two different ways: (1) use of bulky substituents so that a large bond angle results from steric repulsion;[56,57] (2) placing electropositive substituents at Si in order to reduce the s-character of σ-type

orbital, thus increasing the energy of the HOMO, and as a result, the value of ΔE_{ST} decreases.[58] Also according to Bent's rule, the presence of electron withdrawing substituents will increase the p-character of silicon-substituent bonds and consequently the bond angle around Si center will become narrower.[59] Taking these two important factors into consideration, the groups of Power, Jones and Aldridge reported the syntheses of two-coordinate acyclic silylenes (Scheme 1.6).[60,61] The Power group used sterically encumbered thiolate ligands to kinetically stabilize a silylene $:Si(SAr^*)_2$ ($Ar^* = C_6H_3$-2,6-(C_6H_2-2,4,6-$Me_3)_2$) (**35**). The bond angle around the silicon center (S-Si-S) in **35** was determined to be 90.519(19)° and the HOMO-LUMO energy separation was calculated to be 4.3 eV (414.9 kJ/mol). The acyclic silylene **35** did not show any reactivity towards hydrogen gas and the inertness of **35** was attributed to the high singlet-triplet energy separation, which inhibits the synergic interaction of H_2 with the silicon-based lone pair and 3p orbital in **35**.

Jones, Aldridge et al. discovered a highly reactive divalent silylene, $:Si\{B(NDippCH)_2\}\{N(SiMe_3)Dipp\}$ (**36**) with a singlet-triplet energy separation of 103.9 kJ/mol, which is significantly lower than the related energy gap in Power's silylene. In order to achieve a lower HOMO-LUMO energy separation, Jones and Aldridge used a strongly σ-donating ligand, $B(NDippCH)_2$ to raise the energy of the HOMO (σ-orbital) by inductive effects. Interestingly, compound **36** shows transition metal-like reactivity, and undergoes facile oxidative addition chemistry with H_2 and with C-H bonds at mild temperatures. It is important to

note that the singlet-triplet energy gap (ΔE_{ST}) in the silylene is the key factor that controls the distinctive reactivity of the acyclic silylenes **35** and **36**.

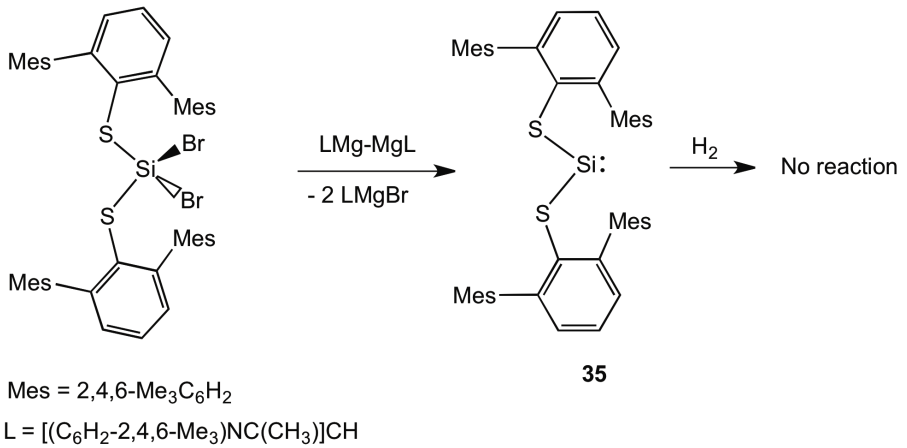

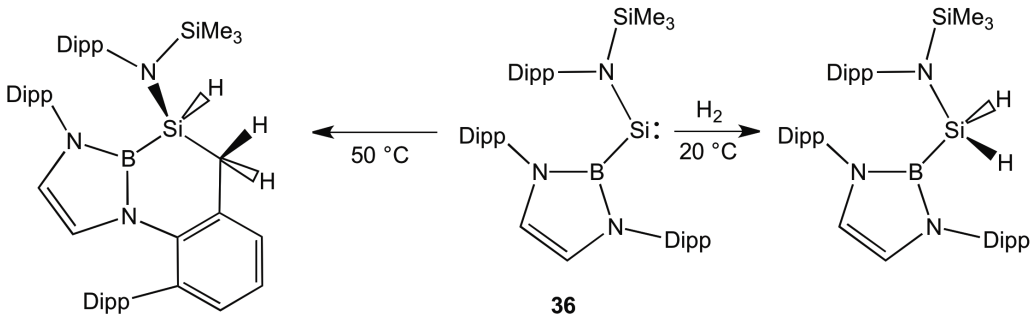

Scheme 1.6. Synthesis of two-coordinate acyclic silylenes (**35** and **36**) and their reactivity.

1.5. Recent progress in the isolation of low valent main group complexes using N-heterocyclic carbenes

The use of N-heterocyclic carbenes as stabilizing σ-donor ligands for main group element complexes has increased dramatically after the pioneering work by Robinson and coworkers in 2007, where they prepared stable neutral diborene, IPr•HB=BH•IPr (**37**) (IPr = 1,3-Bis-(2,6-diisopropylphenyl)-imidazol-2-ylidene)

and diborane IPr•H_2B-BH_2•IPr (**38**) complexes from the reduction of IPr•BBr_3 with excess KC_8 (Scheme 1.7).[62] The boron-boron bond distance in **37** [1.561(18) Å] was determined to be shorter than previously known doubly bonded diboron species, suggesting the presence of a strong B-B π bond.[63,64] The formation of compounds **37** and **38** are proposed to proceed *via* hydrogen abstraction from the diethyl ether solvent during the course of the reaction.[62] Taking advantage of the strong σ-donor ability and large steric bulk of IPr, Robinson prepared an adduct containing a Si_2 unit IPr•Si=Si•IPr (**39**).[40a] The neutral silylene complex **39** was obtained *via* reduction of IPr•$SiCl_4$ in THF with KC_8. Interestingly, when the KC_8 reduction of IPr•$SiCl_4$ was performed in hexanes the major product isolated was chlorosilylene adduct IPr•(Cl)Si-Si(Cl)•IPr (**40**). The analogous digermene adduct,IPr•Ge=Ge•IPr (**41**) was later reported by Jones and coworkers in 2009.[41a] The digermene complex **41** was synthesized by the reduction of IPr•$GeCl_2$ (**42**) using the milder soluble β-diketiminate-stabilized Mg(I) reagent [{Mg[N(Mes)CMe]$_2$CH}$_2$] (Mes = 2,4,6-$Me_3C_6H_2$);[65] interestingly, the reaction of **42** with the common reducing agents such as Na, K or KC_8 gave only free IPr as a soluble product with no sign of the target digermene adduct **41**. Compound **41** was isolated as an air- and moisture-sensitive red crystalline solid and displayed high thermal stability under nitrogen ($T_{dec.}$ = 162-165 °C). The Ge-Ge bond distance [2.3490(8) Å] in **41** was consistent with the presence of a germanium-germanium double bond.[41a] Recently, the Jones group also reported the synthesis of a related distannene adduct IPr•Sn=Sn•IPr (**43**) *via* the reduction of corresponding tin dichloride adduct IPr•$SnCl_2$ (**44**) with the Mg(I) reagent

[{Mg[N(Mes)CMe]$_2$CH}$_2$] (Mes = 2,4,6-Me$_3$C$_6$H$_2$).[66] The molecular structure of **43** was found to be similar with its lighter congeners **39** and **41**, with a characteristic *trans*-bent geometry (please refer to Section 1.7 for details). The IPr ligands in **43** were found to be almost orthogonal to the Sn=Sn plane with a C-Sn-Sn bond angle of 91.82(8)°. As expected from the presence of a weak Sn-Sn bond in **43**, it decomposes at room temperature in the solid state, while in solution decomposition occurs at 20 °C to give free IPr and tin metal. Although, the heaviest analogue of the series IPr•Pb=Pb•IPr is theoretically calculated to be stable in the gas phase, it has thus far remained elusive to synthetic chemists.[67]

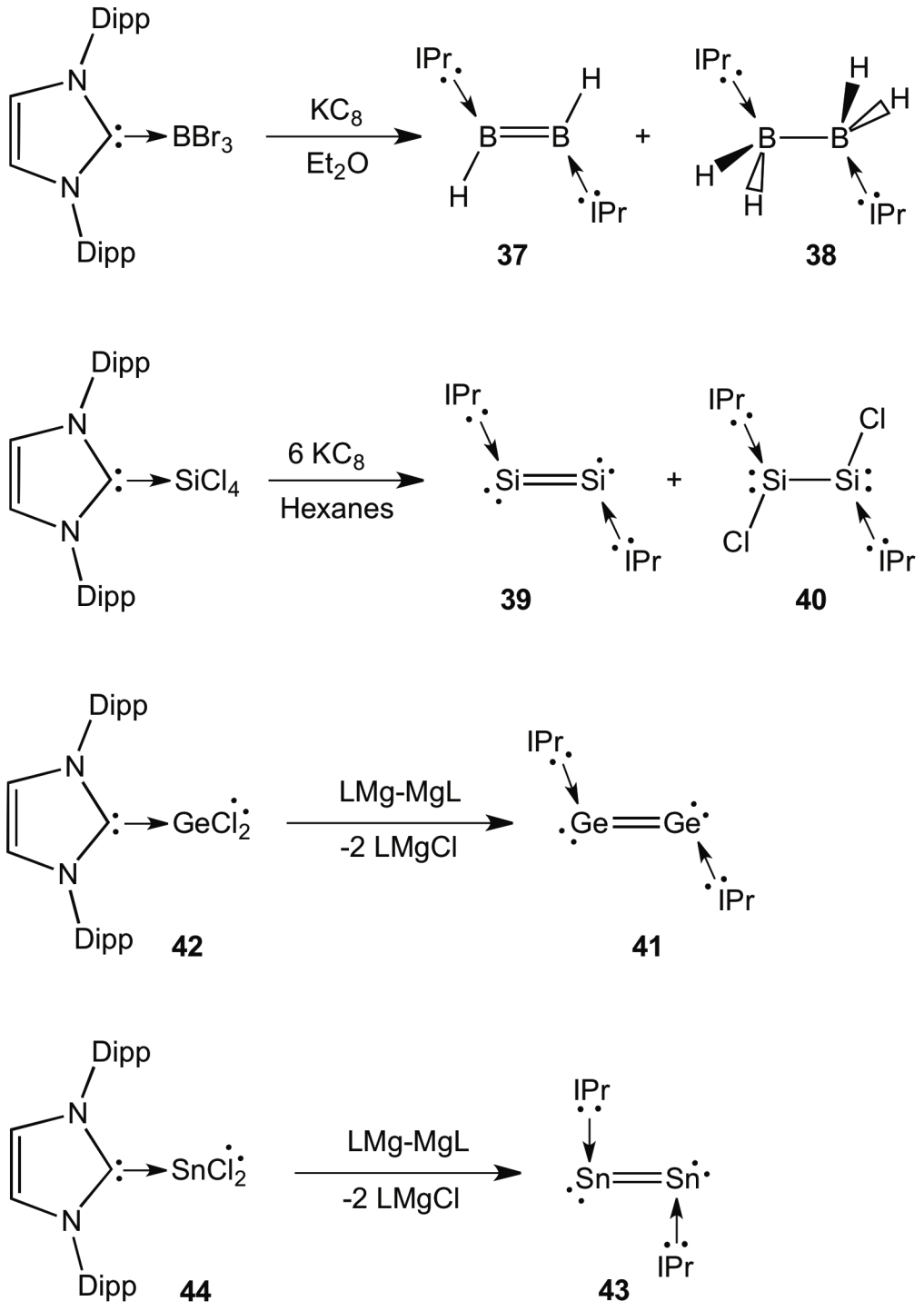

Scheme 1.7. Synthesis and stabilization of diborene (**37**), diborane (**38**), disilene (**39**), chlorosilylene (**41**), digermene (**42**), distannene (**43**) using IPr as supporting ligands.

Another major advance in the synthesis of low-coordinate Si(II) complexes was concurrently made by the groups of Roesky and Filippou.[40b,40c] In 2009 they independently developed the synthesis of the stable dihalosilane adducts IPr•SiX_2 (X = Cl and Br). The dichloro adduct IPr•$SiCl_2$ (**45**) was synthesized by Roesky from the reaction of two equivalents of IPr with $HSiCl_3$ in toluene (**45**) (Scheme 1.7). The synthetic route used by Filippou to form IPr•$SiBr_2$ (**46**) involved the reduction of the Si(IV) salt [IPr•$SiBr_3$]Br with KC_8 (Scheme 1.8). Compounds **45** and **46** each show a high degree of stability both in solution and the solid state, and the stability of these compounds originates from the electronic stabilization imparted by IPr donor. The IPr donor occupies the empty p orbital of the SiX_2 moiety, thereby preventing the SiX_2 units from reacting with each other.[68] The bonding in these IPr•SiX_2 adducts was also studied by DFT calculations, and the $C_{IPr\text{-}Si}$ interactions were found to be highly dative in nature with minimum π-interactions consistent with the poor π-accepting ability of NHCs. These Si(II) adducts possess a stereochemically active lone pair, and as expected, they react with Lewis acids to form dative LA•LB bonds (LA = Lewis acid, LB = Lewis base). Accordingly, IPr•$SiCl_2$ (**45**) reacts with $B(C_6F_5)_3$ to form the donor-acceptor adduct IPr•$SiCl_2$•$B(C_6F_5)_3$ and the bis-adduct $(IPr•SiCl_2)_2Ni(CO)_2$ is formed by the reaction of **45** with $Ni(CO)_4$.[69-71] Due to the nucleophilicity of IPr•$SiCl_2$ (**45**), this species undergoes a clean cycloaddition reaction with benzophenone to give the novel silaoxirane adduct, while the reaction of **45** with bulky azides Ar'N_3 and Ar*N_3 affords the oxidized silazene adducts IPr•Cl_2SiNAr' and IPr•Cl_2SiNAr'.[52c,72] The coordination chemistry of IPr

with the heavier Group 14 element dichlorides EX_2 (E = Ge, Sn and Pb; X = Cl ot Br) is also known. The Rivard group first reported the synthesis of IPr•$GeCl_2$ and IPr•$SnCl_2$ from the reaction of IPr with $GeCl_2$•dioxane and $SnCl_2$, respectively.[9a] Very recently, Jones et al. discovered the synthesis of IPr•$PbBr_2$ by reacting $PbBr_2$ with carbene in THF.[67] Strong carbene-E (E = Si-Pb) sigma interactions were present in each of these adducts with very minimal π contribution.

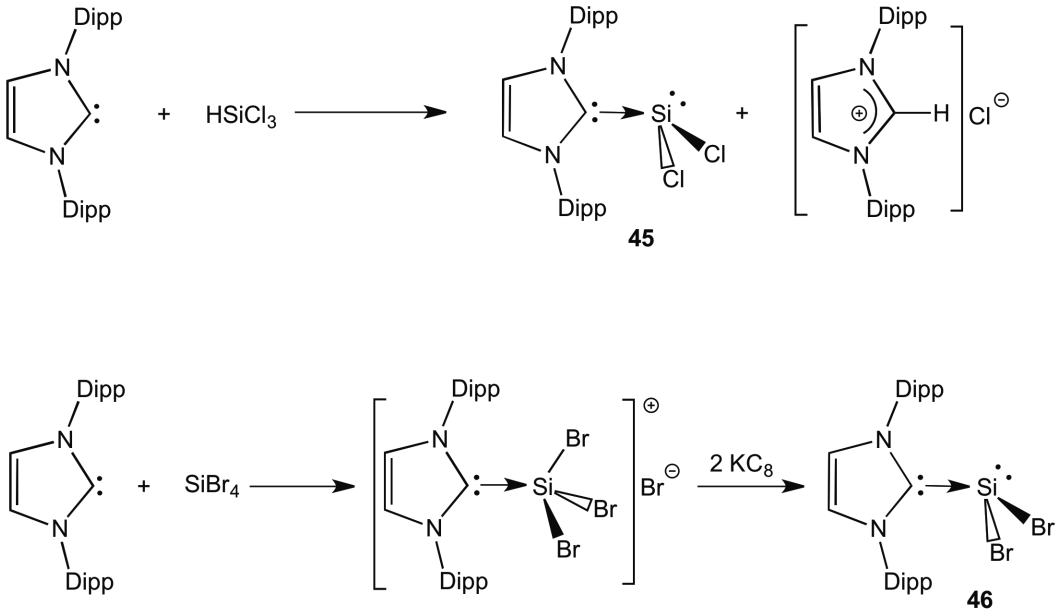

Scheme 1.8. Synthesis of dihalosilylene adducts IPr•$SiCl_2$ (**45**) and IPr•$SiBr_2$ (**46**).

1.6. Hydrides of Group 14 elements

The hydrides of Group 14 elements are of practical interest due to their widespread applications in synthetic organic chemistry (e.g. in hydrosilylation, hydrogermylation and hydrostannylation chemistry) and in material chemistry as precursors for the synthesis of high purity elements and alloys for the electronic industry.[73-78] Although most of these applications involve use of tetravalent species E(IV) (E = Si-Sn), many of these transformations are believed to proceed *via* the formation of $:EH_2$ intermediates.[76] For example, silylene ($:SiH_2$) and germylene ($:GeH_2$) have been postulated as intermediates in the synthesis of semi-conducting Si and Ge films *via* the thermal decomposition of silane (SiH_4) and germane (GeH_4), respectively.[76] In addition, $:EH_2$ units in the coordination sphere of a transition metal $M{=}EH_2$ are postulated to occur during metal catalyzed E-E (E = Si and Ge) bond forming reactions.[76,77] Despite their interesting chemical and bonding properties, heavier Group 14 element methylene analogues $:EH_2$ (E = Si-Pb) have remained elusive due to a lack of suitable synthetic methods and the expected instability of these entities in the condensed phase.[78,79] However, free heavy methylene analogues $:EH_2$ have been identified and studied under cryogenic conditions (*i.e.* matrix isolation at <10 K).[78,79] For example, Andrews and coworkers have studied the reaction of Sn with H_2 *via* laser-assisted codeposition at 3.5 K and detected a mixture of products that contained SnH_x (x = 1-4) species.[77b] Although these hydride species should be stable in the gas phase, they are still unstable (x = 1-3) due to the presence of weak E-H bonds and the

presence of reactive sites (vacant p orbital and lone pairs) that allow low energy decomposition pathways to be accessed.

Earlier approaches for the isolation of low valent Group 14 hydrides involved application of a sterically demanding ligand that is capable of kinetically stabilizing the E-H moiety. The first example illustrating this approach was made by the group of Power in 2000 when they showed that the divalent Sn(II) hydride, $(Ar^*SnH)_2$ (**47**) can be prepared by using the sterically encumbered Ar* ligand ($Ar^* = C_6H_3$-2,6-(2,4,6-$^i Pr_3C_6H_2)_2$).[15f] Later on, the same group also prepared the low coordinate germanium hydrides Ar′(H)GeGe(H)Ar′ (**48**) and $Ar'(H)_2GeGe(H_2)Ar'$ (**47**), along with the aryl germane H_3GeAr' (**50**) from the reaction of digermyne Ar′GeGeAr′ (**51**) (Ar′ = C_6H_3-2,6-(2,6-$^i Pr_2C_6H_2)_2$) with H_2 under ambient conditions (Scheme 1.9).[2c] Using a different approach, Roesky and coworkers synthesized the β-diketiminate supported Ge(II) and Sn(II) monohydrides $[CH(CMeNAr)_2]EH$ (Ar = 2,6-$^i Pr_2C_6H_2$ or 2,6-$Me_2C_6H_2$; E = Ge and Sn; **52** and **53,** respectively) using a hydride/chloride metathesis reaction.[80] Compounds **52** and **53** both are capable of activating small molecules. For example, compound **52** reacts with carbon dioxide at room temperature to give the germanium formate, $[CH(CMeNAr)_2]$Ge-OCOH, and interestingly, the formate group can be liberated with the regeneration of a Ge-H group in the presence of $Li[H_2NBH_3]$.[81,82] The group of Roesky also used a slightly modified ligand to synthesize the Lewis base-capped Si(II) hydride $[PhC(N^tBu)_2]SiH•BH_3$ (**54**).[83]

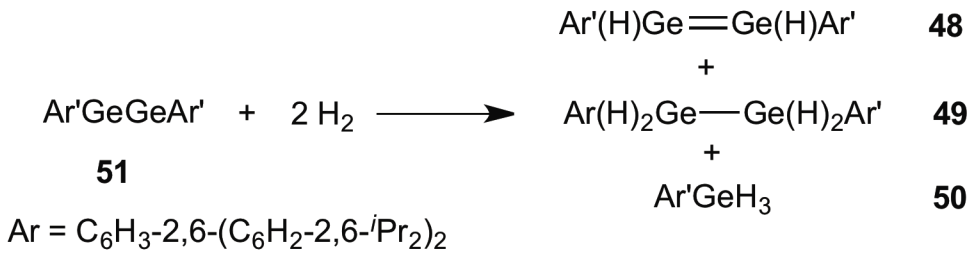

Scheme 1.9. Dihydrogen activation by digermyne (**51**) to give a mixture of digermene (**48**), digermane (**49**) and germane (**50**).

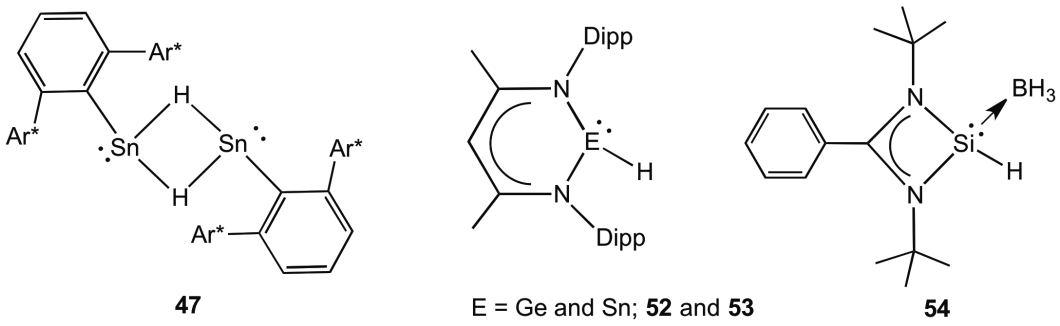

Figure 1.12. Sterically stabilized Group 14 hydrides: $(Ar^*SnH)_2$ (**47**), $[CH(CMeNAr)_2]EH$ (E = Ge and Sn; **52** and **53** respectively) and $[PhC(N^tBu)_2]SiH{\bullet}BH_3$ (**54**).

Despite the fact that E-H (E = Si-Sn) bonds can be stabilized and isolated in the condensed phase with the use of bulky anionic ligands, the parent $:EH_2$ species remained elusive in the solid state. Since the heavy methylene analogues, $:EH_2$ (E = Si-Sn) have been predicted to exhibit dual Lewis acid and basic character due to the presence of a vacant p orbital and a low energy lone pair, the Rivard group intercepted these species using an electronic stabilization procedure termed as "donor-acceptor" stabilization (Figure 1.13). The donor-acceptor stabilization protocol involves capping of the reactive sites of these bifunctional molecules $:EH_2$ (E = Si-Sn) with the use of a carbene donor (to occupy the Lewis

acidic empty p orbital on the Group 14 element) and a Lewis acid acceptor (to bind the lone pair) (Figure 1.13). Rivard et al. successfully implemented this strategy to isolated the parent Ge(II) dihydride as a donor-acceptor adduct IPr•GeH_2•BH_3 from the reaction of IPr•$GeCl_2$ with excess Li[BH_4] in 2009 (please refer to Chapter 3).[9a] IPr•GeH_2•BH_3 showed excellent thermal stability under nitrogen both in the solid state ($T_{dec.}$ = 130 °C) and solution. The parent stannylene :SnH_2 was also intercepted by the Rivard group in 2010 within the coordination sphere of a transition metal complex IPr•SnH_2•$W(CO)_5$.[9b]

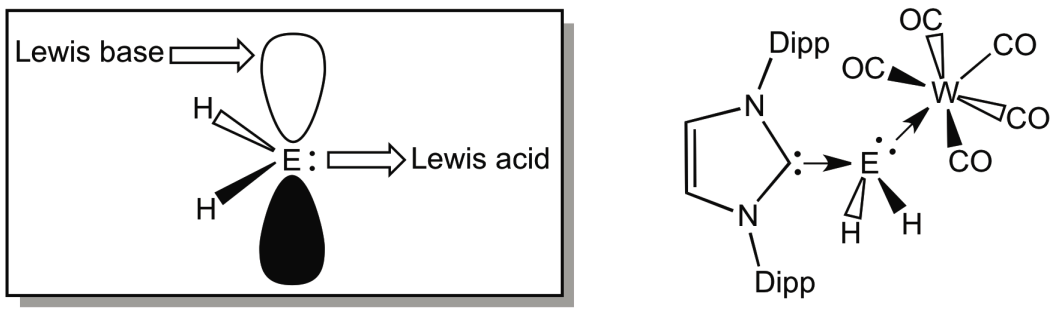

Figure 1.13. The donor-acceptor stabilization protocol.

The "*push-pull*" stabilization technique was also used by Robinson and workers to stabilize the parent silylene complex IPr•SiH_2•BH_2-$SiH(B_3H_7)$•IPr *via* a borane-induced Si–Si cleavage reaction involving the disilene bis-adduct IPr•Si=Si•IPr.[9g] The Rivard group later discovered a more expedient synthesis of SiH_2 complexes IPr•SiH_2•BH_3 and IPr•SiH_2•$W(CO)_5$ from either a chloride/hydride metathesis reaction or by using a BH_3/$W(CO)_5$ exchange reaction starting from IPr•$SiCl_2$•BH_3 and IPr•SiH_2•BH_3, respectively (please refer to

Chapter 3 for details).[9e] In addition to the isolation of stable heavy methylene analogues :EH_2 (E = Si, Ge and Sn), the donor-acceptor strategy was extended further by the Rivard group to isolate inorganic ethylenes as donor-acceptor complexes IPr•EH_2•E'H_2•$W(CO)_5$ (E = Si and Ge; E' = Ge and Sn).[9d] These heavy ethylene complexes are potential precursors for the synthesis of heterostructured nanomaterials (please refer to Chapter 4).[85] More importantly, these results show that the strategy of donor-acceptor stabilization can be a general strategy to access a wide range of reactive molecules containing Lewis acidic and Lewis basic reactive sites.

1.7 The nature of π-bonding in heavy main group elements and the origin of *trans*-bent geometry

Chapter 4 describes the isolation of donor-acceptor adducts of heavy Group 14 ethylene analogues (H_2EEH_2). Accordingly some introduction to multiple bonding involving heavy main group elements is described. The study of stable compounds featuring multiple bonding between two heavier main group elements is one of the core aspects of organometallic and main group chemistry.[86] In general, molecules containing multiple bonding between two heavier main group elements often have *trans*-bent geometries instead of idealized planar or linear arrangements found in the lighter congeners (e.g. ethylenes and acetylenes).[87] The *trans*-bent geometries in the heavier Group 14 element complexes and pyramidal coordination at the element centers can be explained by the Carter-Goddard-Malrieu-Trinquier (CGMT) model which is based on the

correlation between the singlet-triplet excitation energy of the molecular fragments (ER_2) with the electronic and structural characteristics of the complete molecule, and can be summarized by equation 1.[88,89]

$$E_{\pi+\sigma} = E_{INT} - 2\,\Delta E_{ST} \qquad (1)$$

In equation 1, $E_{\pi+\sigma}$ is the E-E double bond energy, E_{INT} is the intrinsic bond energy of the molecule, and ΔE_{ST} represents the value of singlet-triplet energy separation. On the basis of this equation, Trinquier and Malrieu provided a set of general rules considering the relative values of singlet-triplet energy separation (ΔE_{ST}) versus the energy of the E-E bonds. According to these generalized rules, molecules with E-E double bond energy > 2 ΔE_{ST} form classical planar structures, while molecules with $E_{\pi+\sigma}$ < 2 ΔE_{ST} adopt *trans*-bent molecular structures; if the value of $E_{\pi+\sigma}$ less than ΔE_{ST} the individual molecular fragments (ER_2) will not interact to form a double bond. Since the intrinsic bond energy of the E-E double bond decreases and singlet-triplet energy gap increases with increasing atomic number, according to the CGMT model non-classical, *trans*-bent structures become the thermodynamically favorable geometries for the heavy Group 14 (tetrel) elements.

Another generalized way to describe the pyramidal or bent geometries in the heavier tetrel compounds $R_2E{=}ER_2$ (E = Si-Pb) starts from the realization that the singlet ground state of the monomeric moieties with a non-bonding lone pair R_2E: become energetically more stable compared to their triplet states with increasing atomic number. Instead of promoting an electron from the singlet ground state to form a triplet state (requires high energy), these singlet fragments

with a lone pair and empty p orbital combine together in a donor-acceptor fashion to form a formal double bond where each molecular fragment becomes electron donor and electron acceptor; the bond formed in this approach is known as polarized σ or paw-paw bond. The dimerization or the formation of double bond in this manner results in considerable repulsion between the lone pairs and the molecule transform into a bent or pyramidal geometry to minimize the repulsion. However, this model has significant limitations when it comes to describing the geometries of molecules where bond angles are decreased to 90°. In these circumstances, the donor-acceptor interactions should leave the two R_2E: moieties connected by a π-interaction rather than a single σ bond, which is contrary to experimental and computational findings. Thus this simplified donor-acceptor model can only explain structures with moderate degrees of pyramidalization.[89b] For example, in diplumbyne Ar*PbPbAr* (Ar* = C_6H_3-2,6-(2,4,6-^{i}Pr$_3C_6H_2)_2$) (**53**), the Pb-Pb-C bond angle is *ca*. 94° and the long Pb-Pb bond of approximately 3.2 Å strongly suggests the presence of a single bond in this compound.[91]

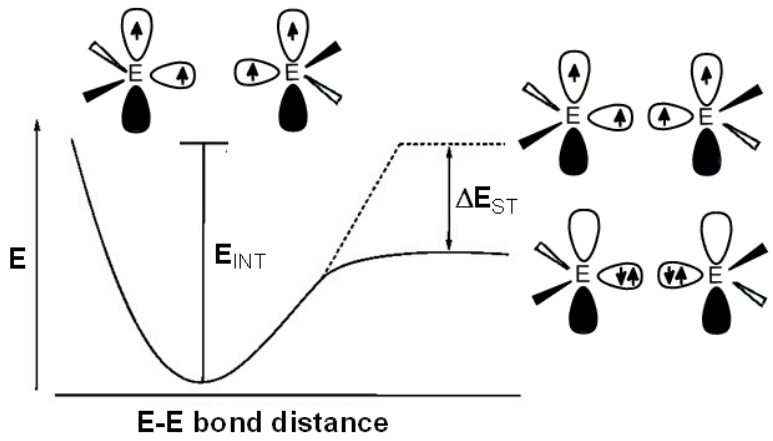

Figure 1.14. Energy profile for the dissociation of a double bond into two triplet fragments. E_{INT} stands for the double bond energy (E_2H_4, in this diagram), ΔE_{ST} is the singlet-triplet energy separation.

According to molecular orbital theory, the *trans*-bent geometry or the geometrical distortion in heavy ethylene analogues $R_2E{=}ER_2$ can be explained by different degrees of mixing of molecular energy levels as the group is descended which is known as second order Jahn-Teller mixing or *pseudo*-Jahn-Teller distortion.[91] This mixing of molecular orbitals occurs in heavy element (E = Si-Pb in the case of Group 14 elements) compounds because the frontier orbitals which having different symmetries in a planar structure transform into orbitals with the same symmetry upon formation of pyramidalized or bent geometries. In addition, the weak E-E bonding interaction in the heavier elements makes the energy difference between the frontier molecular orbitals of same symmetry relatively low, which facilitates secondary mixing and consequently lower energy bent geometries are formed. For example, the E-E π orbital (b_u symmetry) mixes with the σ* orbital (b_u symmetry) to transform into an occupied non-bonding (n_-)

orbital and an unoccupied (n_+) orbital (Figure 1.14).[92,93] As a result of this mixing, electron density is effectively transferred away from the weak π-orbital of E-E bond into a non-bonding type orbital also known as "slipped π-bond" and therefore the E-E bond order decreases. In addition in the pyramidalized or bent geometries the E-E σ-bonding orbital has same symmetry as the π* molecular orbital and thus these orbitals mix further to from a new σ-bonding orbital with lower energy. As the atomic number increases, the E-E σ* and π orbitals become closer in energy and the orbital mixing is more prominent and consequently higher degrees of *trans*-bending are observed and the overall bond order of the molecules decreased. The overall effect of Jahn-Teller mixing or *pseudo*-Jahn-Teller distortion is a lowering of the overall energy of bonding molecular orbitals, thus increasing the stability of the $R_2E{=}ER_2$ molecules.

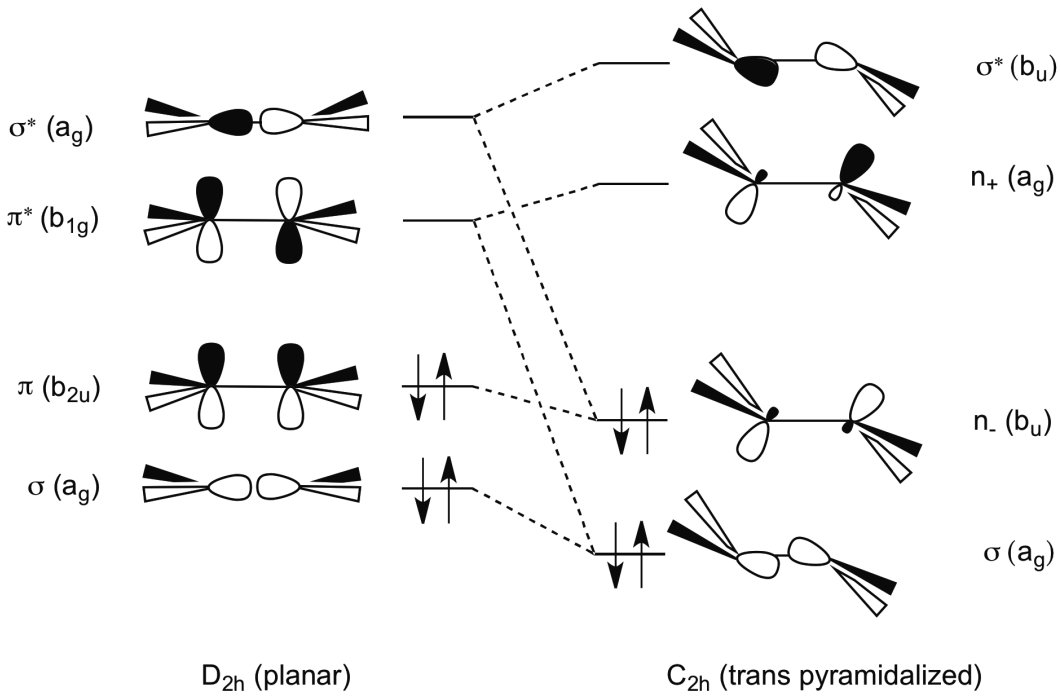

Figure 1.15. Second order Jahn-Teller mixing of σ* and π as well as σ and π* orbitals that leads to lone pair character in the heavy Group 14 ethylene analogues.

1.8 Acknowledgement of Collaborators

Portions of the work discussed in this Thesis were completed in collaboration with other researchers within the Rivard group in the Department of Chemistry at the University of Alberta.

All the X-ray crystallographic studies described in this Thesis were performed by Dr. R. McDonald and Dr. M. Ferguson, including mounting of crystals, setup and operation of the diffractometer, refinement of structures and preparation of all crystallographic data tables.

In Chapter 2, the ligand modification and the chalcogen transfer chemistry were studied in collaboration with S. K. Liew, J. T. Goettle, P. A. Lummis, S. M. McDonald, L. J. Miedema.

In Chapter 3, S. K. Liew explored the initial reactivity of the tin hydride complex, IPr•SnH_2•$W(CO)_5$. In addition, the synthesis of IPr=CH_2 was developed in conjunction with S. K. Liew. K. C. Thimer initially made the carbene adducts, IPr•ECl_2 (E = Ge and Sn).

Mr. M. Miskolzie, Ms. N. Dabral, Dr. M. Richards, and Dr. T. McDougall helped to run ^{29}Si and low-temperature NMR experiments.

Elemental analyses and mass spectrometry were performed by the Analytical and Instrumentation Laboratory at the University of Alberta.

Computational analyses were made by A. C. Malcolm, are not included in this Thesis.

According to the policy in our research group, each chapter of this Thesis is essentially self-contained, and prepared in the form of a paper that is intended

for publication in peer-reviewed journals. The author wrote the first drafts of each Chapter.

A portion of this Thesis has been published previously and the publications are listed below:

Chapter 2 (1) Liew, S. K.; Al-Rafia, S. M. I.; Goettle, J. T.; Lummis, P. A.; McDonald, S. M.; Miedema, L. J.; Ferguson, M. J.; McDonald, R.; Rivard, E. *Inorg. Chem.* **2012**, *51*, 5471.

(2) Al-Rafia, S. M. I.; Lummis, P.A.; Ferguson, M. J.; McDonald, R.; Rivard, E.; *Inorg. Chem.* **2010**, *49*, 9709.

Chapter 3 (1) Thimer, K. C.; Al-Rafia, S. M. I.; Ferguson, M. J.; McDonald, R.; Rivard, E. *Chem. Commun.* **2009**, 7119.

(2) Al-Rafia, S. M. I.; Malcolm, A. C.; Liew, S. K.; Ferguson, M. J.; Rivard, E. *J. Am. Chem. Soc.* **2011**, *133*, 777.

(3) Al-Rafia, S. M. I.; Malcolm, A. C.; Liew, S. K.; Ferguson, M. J.; McDonald, R.; Rivard, E. *Chem. Commun.* **2011**, *47*, 6987.

(4) Al-Rafia, S. M. I.; Malcolm, A. C.; McDonald, R.; Ferguson, M. J.; Rivard, E. *Chem. Commun.* **2012**, *48*, 1308.

Chapter 4 Al-Rafia, S. M. I.; Malcolm, A. C.; McDonald, R.; Ferguson, M. J.; Rivard, E. *Angew. Chem., Int. Ed.* **2011**, *50*, 8354.

Chapter 5 Al-Rafia, S. M. I.; McDonald, R.; Ferguson, M. J.; Rivard, E. *Chem. Eur. J.* **2012**, *18*, 13810.

Chapter 6 Al-Rafia, S. M. I.; Ferguson, M. J.; Rivard, E. *Inorg. Chem.* **2011**, *50*, 10543.

1.9 References

(1) (a) Power, P. P. *Nature* **2010**, *463*, 171. (b) Frey, G. D.; Lavallo, B.; Donnadieu, B.; Schoeller, W. W.; Bertrand, G. *Science* **2007**, *316*, 439. (c) Welch, G. C.; San Juan, R. R.; Masuda, J. D.; Stephan, D. W. *Science* **2006**, *314*, 1124. (d) Peng, Y.; Ellis, B. D.; Wang, X.; Fettinger, J. C.; Power, P. P. *Science* **2009**, *325*, 1668. (e) Li, J.; Schenk, C.; Goedecke, C.; Frenking, G.; Jones, C. *J. Am. Chem. Soc.* **2011**, *133*, 18622.

(2) (a) Power, P. P. *Chem. Rev.* **1999**, *99*, 3463. (b) Peng, Y.; Ellis, B. D.; Wang, X.; Power, P. P. *J. Am. Chem. Soc.* **2008**, *130*, 12268. (c) Spikes, G. H.; Fettinger, J. C.; Power, P. P. *J. Am. Chem. Soc.* **2005**, *127*, 12232. (d) Breher, F. *Coord. Chem. Rev.* **2007**, *215*, 1007. (e) Stephan, D. W. *Dalton Trans.* **2009**, 3129. (e) Power, P. P. *Chem. Rev.* **2003**, *103*, 739.

(3) Yoshifuji, M.; Shima, I.; Inamoto, N.; Hirotsu, K.; Higuchi, T. *J. Am. Chem. Soc.* **1981**, *103*, 4587.

(4) (a) King, R. B.; Bisnette, M. B. *J. Organomet. Chem.* **1967**, *8*, 287. (b) Bradley, D. C.; Chisholm, M. H. *Acc. Chem. Res.* **1976**, *9, 273*. (c) Eaborn, C. *J. Organomet. Chem.* **1982**, *239*, 93. (d) Trofimenko, S. *Chem. Rev.* **1993**, *93*, 943. (e) Schrock, R. R. *Acc. Chem. Res.* **1997**, *30*, 9. (f) Cummins, C. C. *Chem. Commun.* **1998**, 1777. (g) Power, P. P. *J. Organomet. Chem.* **2004**, *689*, 3904. (h) MacLachlan, E. A.; Fryzuk, M. D. *Organometallics* **2006**, *25*, 1530. (i) Holland, P. L. *Acc. Chem. Res.* **2008**, *41*, 905. (j) Wolczanski, P. T. *Chem. Commun.* **2009**, 740.

(5) (a) Cummins, C. C.; Baxter, S. M.; Wolczanski, P. T. *J. Am. Chem. Soc.* **1988**, *110*, 8732. (b) Laplaza, C. E.; Cummins, C. C. *Science* **1995**, *268*, 861. (c) Albrecht, M.; van Koten, G. *Angew. Chem., Int. Ed.* **2001**, *40*, 3750. (d) Pool, J. A.; Lobkovsky, E.; Chirik, P. J. *Nature* **2004**, *427*, 527. (e) Betley, T. A.; Peters, J. C. *J. Am. Chem. Soc.* **2004**, *126*, 6252. (f) Gunanathan, C.; Ben-David, Y.; Milstein, D. *Science* **2007**, *317*, 790. (g) Ni, C.; Ellis, B. D.; Long, G. J.; Power, P. P. *Chem. Commun.* **2009**, 2332. (h) Takaoka, A.; Mankad, N. P.; Peters, J. C. *J. Am. Chem. Soc.* **2011**, *133*, 8440. (i) Rodriguez, M. M.; Bill, E.; Brennessel, W. W.; Holland, P. L. *Science* **2011**, *334*, 780.

(6) Phillips, A. D.; Wright, R. J.; Olmstead, M. M.; Power, P. P. *J. Am. Chem. Soc.* **2002**, *124*, 5930.

(7) (a) Braunschweig, H.; Dewhurst, R. D.; Hammond, K.; Mies, J.; Radacki, K.; Vargas, A. *Science* **2012**, *336*, 11420. (b) Bonyhady, S. J.; Collis, D.; Frenking, G.; Holzmann. N.; Jones, C.; Stasch, A. *Nature Chemistry*, **2010**, *2*, 865. (c) Wang, Y.; Xie, Y.; Wei, P.; King, R. B.; Schaefer, H. F., III; Schleyer, P. v. R.; Robinson, G. H. *J. Am. Chem. Soc.* **2008**, *130*, 14970. (d) Kinjo, R.; Donnadieu, B.; Celik, M. A.; Frenking, G.; Bertrand, G. *Science* **2011**, *333*, 610. (e) Zhou, M.; Tsumori, N.; Fan, K.; Andrews, K.; Xu, Q. *J. Am. Chem. Soc.* **2002**, *124*, 12936.

(8) (a) Adolf, A.; Vogel, U.; Zabel, M.; Timoshkin, A. Y.; Scheer, M. *Eur. J. Inorg. Chem.* **2008**, 3482. (b) Schwan, K.–C.; Timoshkin, A. Y.; Zabel,

M.; Scheer, M. *Chem. Eur. J.* **2006**, *12*, 4900. (c) Vogel, U.; Timoshkin, A. Y.; Scheer, M. *Angew. Chem., Int. Ed.* **2001**, *40*, 4409.

(9) (a) Thimer, K. C.; Al-Rafia, S. M. I.; Ferguson, M. J.; McDonald, R.; Rivard, E. *Chem. Commun.*, **2009**, 7119. (b) Al-Rafia, S. M. I.; Malcolm, A. C.; Liew, S. K.; Ferguson, M. J.; Rivard, E. *J. Am. Chem. Soc.* **2011**, *133*, 777. (c) Al-Rafia, S. M. I.; Malcolm, A. C.; Liew, S. K.; Ferguson, M. J.; McDonald, R.; Rivard, E. *Chem. Commun.* **2011**, *47*, 6987. (d) Al-Rafia, S. M. I.; Malcolm, A. C.; McDonald, R.; Ferguson, M. J.; Rivard, E. *Angew. Chem., Int. Ed.* **2011**, *50*, 8354. (e) Al-Rafia, S. M. I.; Malcolm, A. C.; McDonald, R.; Ferguson, M. J.; Rivard, E. *Chem. Commun.* **2012**, *48*, 1308. (f) Inoue, S.; Driess, M. *Angew. Chem., Int. Ed.* **2011**, *50*, 5614. (g) Abrahim, M. Y.; Wang, Y.; Xie, Y.; Wei, P.; Schaefer III, H. F.; Schleyer, P. v. R.; Robinson, G. H. *J. Am. Chem. Soc.* **2011**, *133*, 8874.

(10) Malcolm, A. C. M.Sc. Thesis 2012, University of Alberta

(11) (a) Stender, M.; Phillips, A. D.; Wright, R. J.; Power, P. P. *Angew. Chem., Int. Ed.* **2002**, *41*, 1785. (b) Stender, M.; Phillips, A. D.; Power, P. P. *Chem. Commun.* **2002**, 1312. (c) Power, P. P. *Organometallics* **2007**, *26*, 4362. (d) Brown, Z. D.; Vasko, P.; Fettinger, J. C.; Tuononen, H. M.; Power, P. P. *J. Am. Chem. Soc.* **2012**, *134*, 4045.

(12) (a) Davidson, P. J.; Lappert, M. F. *J. Chem. Soc. Chem. Commun.* **1973**, 317. (b) Goldberg, D. E.; Harris, D. H.; Lappert, M. F.; Thomas, K. M. *J. Chem. Soc. Chem. Commun.* **1976**, 261.

(13) West, R.; Fink, M. F.; Michl, J. *Science* **1981**, *214*, 1343.

(14) (a) Pluta, C.; Pörschke, K.–R.; Krüger, C.; Hildenbrand, K. *Angew. Chem., Int. Ed.* **1993**, *32*, 388. (b) Su, J.; Li, X, -W.; Crittendon, R. C.; Robinson, G. H. *J. Am. Chem. Soc.* **1997**, *119*, 4571. (c) Uhl, W. *Rev. Inorg. Chem.* **1998**, *18*, 29. (d) Sekiguchi, A.; Zigler, S. S.; West, R. J.; Michl, J. *J. Am. Chem. Soc.* **1986**, *108*, 4241. (e) Eichler, B. E.; Power, P. P. *J. Am. Chem. Soc.* **2000**, *122*, 8785. (f) Driess, M.; Yao, S.; Brym, M.; van Wüllen, C.; Lentz, D. *J. Am. Chem. Soc.* **2006,** *128,* 9629. (g) Sen, S. S.; Khan, S.; Kratzert, D.; Roesky, H. W.; Stalke, D. *Eur. J. Inorg. Chem.* **2011**, 1370. (h) Sen, S. S.; Khan, S.; Nagendran, S.; Roesky, H. W. *Acc. Chem. Res.* **2012**, *45*, 578.

(15) Nguyen, T.; Sutton, A. D.; Brynda, M.; Fettinger, J. C.; Long, G. J.; Power, P. P. *Science* **2005**, *310*, 844.

(16) (a) McMurry, J. *Organic Chemistry with Biological Applications, 2nd Ed.* **2011**, Cengage Learning. (b) Laffel, L.; *Diabetes Metab. Res. Rev.* **1999**, *15*, 412.

(17) (a) Pi, X. D.; Liptak, P. W.; Nowak, J. D.; Wells, N. P.; Carter, C. B.; Campbell, S. A.; Kortshagen, U. *Nanotechnology*, **2008**, *19*, 245603. (b) Wolkin, M. V.; Jorne, J.; Fauchet, P. M.; Allan, G.; Delerue, C. *Phys. Rev. Lett.* **1999**, *82*, 87. (c) Kovalev, D. I,; Yaroshetzkii, I. D.; Musschik, T.; Petrova-Koch, V.; Koch, F.; *Appl. Phys. Lett.* **1994**, *64*, 214. (d) Bertino, M.; Corazza, A.; Martini, M.; Mervic, A.; Spinolo, G. *J. Phys.: Condens.*

Matter **1994**, *6*, 6345.

(18) (a) Kapp, J.; Remko, M.; Schleyer, P. v. R. *J. Am. Chem. Soc.* **1996**, *118*, 5745. (b) Kapp, J.; Remko, M.; Schleyer, P. v. R. *Inorg. Chem.* **1997**, *36*, 4241.

(19) Kimura, M.; Nagase, S. *Chem. Lett.* **2001**, 1098.

(20) Kipping, F. S.; Lloyd, L. L. *J. Chem. Soc. Trans.* **1901**, 79, 449.

(21) (a) Xiong, Y.; Yao, S.; Driess, M. *J. Am. Chem. Soc.* **2009**, *131*, 7562. (b) Xiong, Y.; Yao, S.; Müller, R.; Kaupp, M.; Driess, M. *Nature. Chem.* **2010**, *2*, 577.

(22) Arya, R.; Boyer, J.; Carré, F.; Corriu, R.; Lanneau, G.; Lapasset, J.; Perrot, M.; Priou, C. *Angew. Chem., Int. Ed. Engl.* **2089**, *28*, 1016.

(23) Suzuki, H.; Tokitoh, N.; Okazaki, R.; Nagase, S.; Goto, M. *J. Am. Chem. Soc.* **1998**, *120*, 11096.

(24) Tokitoh, N.; Matsumoto, T.; Manmaru, K.; Okazaki, R. *J. Am. Chem. Soc.* **1993**, *115*, 8855.

(25) (a) Barrau, J.; Massol, M.; Mesnard, D.; Satgé, J. *J. Organomet. Chem.* **1971**, *30*, C67. (b) Barrau, J.; Escudié, J.; Satgé, J. *Chem. Rev.* **1990**, *90*, 283.

(26) Yao, S.; Xiong, Y.; Driess, M. *Chem. Commun.* **2009**, 6466.

(27) Li, L.; Fukawa, T.; Matsuo, T.; Hashizume, D.; Fueno, H.; Tanaka, K.; Tamao, K. *Nature Chem*. **2012**, *4*, 361.

(28) See for a brief history of carbenes: Kirmse, W. *Carbene Chemistry;* Academic Press: 1964, New York.

(29) Dumas, J. B. *Ann. Chim. Phys*. **1835**, *58,* 28.

(30) Regnault, H. V. *Ann. Chim. Phys*. **1839**, *71,* 427.

(31) Nef, J. U. *Ann*. **1897**, *298,* 202.

(32) (a) Staudinger, H.; Kupfer, O. *Ber. Dtsch. Chem. Ges*. **1911**, *44,* 2197. (b) Staudinger, H.; Endle, R. *Ber. Dtsch. Chem. Ges*. **1913**, *46,* 1437. (c) Staudinger, H.; Goldstein, J. *Ber. Dtsch. Chem. Ges*. **1916**, *49,* 1923. (d) Staudinger, H.; Anthes, E.; Pfenninger, F. *Ber. Dtsch. Chem. Ges*. **1916**, *49,* 1928.

(33) Breslow, R. *J. Am. Chem. Soc*. **1957**, *79*, 1762.

(34) (a) Wanzlick, H. W. *Angew. Chem*. **1960**, *72*, 494. (b) Wanzlick, H. W. *Angew. Chem., Int. Ed. Engl*. **1962**, *1*, 75. (c) Gleiter, R.; Hoffmann, R. *J. Am. Chem. Soc*. **1968**, *90*, 5457.

(35) Fischer, E. O.; Maasböl, A. *Angew. Chem., Int. Ed. Engl*. **1964**, *3*, 580.

(36) Igau, A.; Grutzmacher, H.; Baceiredo, A.; Bertrand, G. *J. Am. Chem. Soc*. **1988**, *110,* 6463.

(37) Arduengo, A. J., III; Harlow, R. L.; Kline, M. *J. Am. Chem. Soc.* **1991**, *113,* 361.

(38) Trinquier, G. *J. Am. Chem. Soc.* **1990**, *112,* 2130.

(39) Harrison, J. F. *J. Am. Chem. Soc.* **1971**, *93,* 4112. (b) Harrison, J. F.; Liedtke, C. R.; Liebman, J. F. *J. Am. Chem. Soc.* **1979**, *101,* 7162.

(40) (a) Wang, Y.; Xie, Y.; Wei, P.; King, R. B.; Schaefer, H. F., III; Schleyer, P. v. R.; Robinson, G. H. *Science* **2008**, *321*, 1069. (b) Ghadwal, R. S.; Roesky, H. W.; Merkel, S.; Henn, J.; Stalke, D. *Angew. Chem., Int. Ed.* **2009**, *48*, 5683. (c) Filippou, A. C.; Chernov, O.; Schnakenburg, G. *Angew. Chem., Int. Ed.* **2009**, *48*, 5687. (d) Back, O.; Kuchenbeiser, G.; Donnadieu, B.; Bertrand, G. *Angew. Chem., Int. Ed.* **2009**, *48*, 5530. (e) Wang, Y.; Xie, Y.; Abraham, M. Y.; Gilliard, R. J., Jr.; Wei, P.; Schaefer, H. F., III; Schleyer, P. v. R.; Robinson, G. H. *Organometallics* **2010**, *29*, 4778.

(41) For selected references, see: (a) Sidiropoulos, A.; Jones, C.; Stasch, A.; Klein, S.; Frenking, G. *Angew. Chem., Int. Ed.* **2009**, *48*, 9701. (b) Filippou, A. C.; Chernov, O.; Stumpf, K. W.; Schnakenburg, G. *Angew. Chem., Int. Ed.* **2010**, *49*, 3296. (c) Ghadwal, R. S.; Roesky, H. W.; Pröpper, K.; Dittrich, B.; Klein, S.; Frenking, G. *Angew. Chem., Int. Ed.* **2011**, *50*, 5374. (f) Katir, N.; Matioszek, D.; Ladeira, S.; Escudié, J.; Castel, A. *Angew. Chem., Int. Ed.* **2011**, *50*, 5352.

(42) (a) Herrmann, W. A.; Elison, M.; Fischer, J.; Köcher, C.; Artus, G. R. J. *Angew. Chem., Int. Ed. Engl.* **1995,** *34,* 2371. (b) Herrmann, W. A. *Angew. Chem., Int. Ed. Engl.* **2002**, *41,* 1290 and references therein.

(43) (a) Schwab, P.; Grubbs, R. H.; Ziller, J. W. *J. Am. Chem. Soc.* **1996,** *118,* 100. (b) Scholl, M.; Ding, S.; Lee, C. W.; Grubbs, R. H. *Org. Lett.* **1999**, *1*, 963.

(44) (a) Gaspar, P. P.; Xiao, M.; Pae, D. H; Berger, D. J.; Haile, T.; Chen, T.; Lei, D.; Winchester, W. R.; Jiang, J. P. *J. Organomet. Chem.* **2002**, *646*, 68. (b) Lee, V. Y.; Sekiguchi, A. *Heavy Analogs of Carbenes: Silylenes, Germylenes, Stannylenes and Plumbylenes*. In *Organometallic Compounds of Low-Coordinate Si, Ge, Sn and Pb*; Wiley: London, **2010**; Chapter 4, 139-197.

(45) (a) Gillette, G. R.; Noren, G. H.; West, R. *Organometallics* **1989**, *8*, 487. (b) Gillette, G. R.; Noren, G. H.; West, R. *Organometallics* **1987**, *6*, 2617. (c) Pearsall, M. –A.; West, R. *J. Am. Chem. Soc.* **1998**, *110*, 7228.

(46) Drahnak, T. J.; Michl, J. West, R. *J. Am. Chem. Soc.* **1979**, *101*, 5427.

(47) A few formally divalent silicon compounds were known prior to the Arduengo's discovery of stable NHCs, see: (a) Jutzi, P.; Kanne, D.; Keüger, C. *Angew. Chem., Int. Ed. Engl.* **1986**, *25*, 164. (b) Karsch, H. M.; Keller, U.; Gamper, S.; Müller, G. *Angew. Chem., Int. Ed. Engl.* **1990**, *29*, 295. (c) Lappert, M. F. *Main Group Metal Chem.* **1994**, *17*, 183.

(48) Denk, M.; Lennon, R.; Hayashi, R.; West, R.; Haaland, A.; Belyakov, H.; Verne, P.; Wanger, M.; Metzler, N. *J. Am. Chem. Soc.* **1994**, *116*, 2691.

(49) Gehrhus, B.; Lappert, M. F.; Heinicke, J.; Boese, R.; Balser, D. *J. Chem. Soc., Chem. Commun.* **1995**, 1931. (b) Heinicke, J.; Oprea, A.; Kindermann, M. K.; Karpati, T.; Nyulaszi, L.; Veszpremi, T. *Chem. Eur. J.* **1998**, *4*, 541.

(50) Kira, M.; Ishida, S.; Iwamato, T.; Kabuto, C. *J. Am. Chem. Soc.* **1999**, *121*, 9722.

(51) Yao, S.; Brym, M.; van Wüllen, C.; Driess, M. *Angew. Chem., Int. Ed.* **2007**, *46*, 4159.

(52) Yao, S.; Xiong, Y.; Driess, M. *Organometallics* **2011**, *30*, 1748.

(53) (a) Peng, Y.; Fan, H.; Zhu, H.; Roesky, H. W.; Magull, J.; Hughes, C. E. *Angew. Chem., Int. Ed.* **2004**, *43*, 3443. (b) Tavcar, G.; Sen, S. S.; Roesky, H. W.; Hey, J.; Kratzert, D.; Stalke, D. *Organometallics* **2010**, *29*, 3930. (c) Ghadwal, R. S.; Sen, S. S.; Roesky, H. W.; Granitzka, M.; Kratzert, D.; Merkel, S.; Stalke, D. *Angew. Chem., Int. Ed.* **2010**, *49*, 3952. (d) Sen, S. S.; Roesky, H. W.; Kathrin, Meindl; Stern, D.; Henn, J.; Stuückl, A. C.; Stalke, D. *Chem. Commun.* **2010**, *46*, 5873 (e) Jana, A.; Roesky, H. W.; Schulzke, C.; Samuel, P. P. *Organometallics* **2009**, *28*, 6574. (f) Jana, A.; Schulzke, C.; Roesky, H. W. *J. Am. Chem. Soc.* **2009**, *131*, 4600. (g) Sen, S. S.; Jana, A.; Roesky, H. W.; Schulzke, C. *Angew. Chem., Int. Ed.* **2009**,

48, 8536.

(54) (a) Rodriguez, R.; Gau, D.; Contie, Y.; Kato, T.; Saffon-Merceron, N.; Baceiredo, A. *Angew. Chem., Int. Ed.* **2011**, *50*, 11492. (b) Rodriguez, R.; Gau, D.; Contie, Y.; Kato, T.; Saffon-Merceron, N.; Cózar, D.; Cossío, F. P.; Baceiredo, A. *Angew. Chem., Int. Ed.* **2011**, *50*, 8354.

(55) Lee, G.; West. R.; Müller, T. *J. Am. Chem. Soc.* **2003**, *125*, 8114.

(56) Gaspar, P. P.; Xiao, M.; Pae, D. H.; Berger, D. J.; Haile, T.; Chen, T.; Lei, D.; Winchester, W. R.; Jiang, P. *J. Organomet. Chem.* **2002**, *646,* 68.

(57) (a) Slipchenko, L. V.; Krylov, A. I. *J. Chem. Phys.* **2002**, *117,* 4694. (b) Weidenbruch, M. *J. Organomet. Chem.* **2002**, *646,* 39. (c) Yoshida, M.; Tamaoki, N. *Organometallics* **2002**, *21,* 2587.

(58) Colvin, M. E.; Breulet, J.; Schaefer, H. F., III. *Tetrahedron* **1985**, *41,* 1429.

(59) (a) Bent, H. A. *Chem. Rev.* **1961**, *61*, 275. (b) Huheey, J. *Inorg. Chem.* **1981**, *20*, 4033.

(60) Rekken, B. D.; Brown, T. M.; Fettinger, J. C.; Tuononen, H. M.; Power, P. P. *J. Am. Chem. Soc.* **2012**, *134*, 6504.

(61) Protchenko, A. V.; Birjkumar, K. H.; Dange, D.; Schwarz, A. D.; Vidovic, D.; Jones, C.; Kaltsoyannis, N.; Mountford, P.; Aldridge, S. J. *Am. Chem. Soc.* **2012**, *134*, 6500.

(62) Wang, Y.; Quillan, B.; Wei, P.; Wannere, C. S.; Xie, Y.; King, R. B.; Schaefer, H. F., III; Schleyer, P. v. R.; Robinson, G. H. *J. Am. Chem. Soc.* **2007**, *129*, 12413.

(63) (a) Moezzi, A.; Olmstead, M. M.; Power, P. P. *J. Am. Chem. Soc.* **1992**, *114,* 2715. (b) Moezzi, A.; Bartlett, R. A.; Power, P. P. *Angew. Chem., Int. Ed.* **1992**, *31,* 1082.

(64) Nöth, H.; Knizek, J.; Ponikwar, W. *Eur. J. Inorg. Chem.* **1999**, 1931.

(65) Bonyhady, S. J.; Jones, C.; Nembenna, S.; Stasch, A.; Edwards, A. J.; Mclntyre, G. J. *Chem. Eur. J.* **2010**, *16*, 938.

(66) Jones, C.; Sidiropoulos, A.; Holzmann, N.; Frenking, G.; Stasch, A. *Chem. Commun.* **2012**, *48*, 9855.

(67) Wilson, D. J. D.; Couchman, S. A.; Dutton, J. L. *Inorg. Chem.* **2012**, *51*, 7657.

(68) Timms, P. L. *Acc. Chem. Res* **1973**, *6*, 118.

(69) Ghadwal, R. S.; Roesky, H. W.; Merkel, S.; Stalke, D. *Chem. Eur. J.* **2010**, 85.

(70) Li. J.; Merkel, S.; Henn. J.; Meindl, K.; Dörling, A.; Roesky, H. W.; Ghadwal, R. S.; Stalke, D. *Inorg. Chem.* **2010**, *49*, 775.

(71) Tavcar, S.; Sen. S. S.; Azhakar, R.; Thorn, A.; Roesky, H. W. *Inorg.*

Chem. **2010**, *49*, 10199.

(72) Ghadwal, R. S.; Roesky, H. W.; Schulzke, C.; Grantizka, M. *Organometallics* **2010**, *29*, 6329.

(73) (a) Shirobokov, O. G.; Gorelsky, S. I.; Simionescu, R.; Kuzmina, L. G.; Nikonov, G. I. *Chem. Commun*. **2010**, *46*, 7831. (b) Beard, C. D.; Craig, J. C. *J. Am. Chem. Soc*. **1974**, *96*, 7950. (c) Saegusa, T.; Ito, Y.; Kobayashi, S.; Hirota, K. *J. Am. Chem. Soc*. **1967**, *89*, 2240. (d) Bradley, G. F.; Stobart, S. R. *J. Chem. Soc., Dalton Trans*. **1974**, 264. (e) Terstige, I.; Maleczka Jr., R. E. *J. Org. Chem*. **1999**, *64*, 342.

(74) Ekerdt, J. G.; Sun, Y.-M.; Szabo, A.; Szulczewski, G. J.; White, J. M. *Chem. Rev*. **1996**, *96*, 1499 and references therein.

(75) (a) Bundhun, A.; Ramasami P.; Schaefer, H. F., III. *J. Phys. Chem. A*, **2009**, *113*, 8080 and references therein. (b) Isobe, C.; Cho, H.-C.; Sewell, J. E. *Surf. Sci*. **1993**, *295*, 117. (c) Weerts, W. L. M.; de Croon, M. H. J. M.; Marin, G. B. J. *Electrochem. Soc*. **1998**, *145*, 1318. (d) Jasinski, J. M.; Gates S. M. *Acc. Chem. Res*. **1991**, *24*, 9. For related synthesis of nanocrystals, see: (e) Kortshagen, U.; Anthony, R.; Gresback, R.; Holman, Z.; Ligman, R.; Liu, C. –Y.; Mangolini, L.; Campbell, S. A. *Pure Appl. Chem*. **2008**, *80*, 1901. (f) Li, X.; He, Y.; Talukdar, S. S.; Swihart, M. T. *Langmuir* **2003**, *19*, 8490.

(76) (a) Fischer, E. O. *Adv. Organomet. Chem*. **1976**, *14*, 1. (b) Schrock, R. R.

Acc. Chem. Res. **1979**, *12*, 98. (c) Bourissou, D.; Guerret, O.; Gabbaï, F. P.; Bertrand, G. *Chem. Rev.* **2000**, *100*, 39. (d) Grubbs, R. H, Ed. *Handbook of Metathesis*; Wiley-WCH: Weinheim, **2008**. (e) Hahn, F. E.; Jahnke, M. C. *Angew. Chem., Int. Ed.* **2008**, *47*, 3122. (f) Diez-González, S.; Marion, N.; Nolan, S. P. *Chem. Rev.* **2009**, *109*, 3612. (g) Petz, W. *Chem. Rev.* **1986**, *86*, 1019.

(77) (a) Smith, G. R.; Guillory, W. A. *J. Chem. Phys.* **1972**, *56*, 1423. (b) Wang, X.; Andrews, L.; Chertihin, G. V.; Souter, P. F. *J. Phys. Chem. A* **2002**, *106*, 6302. (c) Lemierre, V.; Chrostowska, A.; Dargelos, A.; Baylére, P.; Leigh, W. J.; Harrington, C. R. *Appl. Organometal. Chem.* **2004**, *18*, 676. (d) Smith, T. C.; Clouthier, D. J.; Sha, W.; Adam, A. G. *J. Chem. Phys.* **2000**, *113*, 9567.

(78) (a) Jacobsen, H.; Ziegler, T. *Inorg. Chem.* **1996**, *35*, 775. (b) Frison, G.; Sevin, A. *J. Chem. Soc., Perkin Trans. 2* **2002**, 1692. (c) Lein, M.; Szabó, A.; Kovács, A.; Frenking, G. *Faraday Discuss.* **2003**, *124*, 365.

(79) (a) Becerra, R.; Boganov, S. E.; Egorov, M. P.; Nefedov, O. M.; Walsh, R. *Chem. Phys. Lett.* **1996**, *260*, 433. (b) Becerra, R.; Boganov, S. E.; Egorov, M. P.; Faustov, V. I.; Nefedov, O. M.; Walsh, R. *J. Am. Chem. Soc.* **1998**, *120*, 12657 and references therein.

(80) Pineda, L. W.; Jancik, V.; Starke, K.; Oswald, R. B.; Roesky, H. W. *Angew. Chem., Int. Ed.* **2006**, *45*, 2602.

(81) Jana, A.; Ghoshal, D.; Roesky, H. W.; Objartel, I.; Schwab, G.; Stalke, D. A. *J. Am. Chem. Soc.* **2009**, 131, 1288.

(82) Jana, A.; Roesky, H. W.; Schulzke, C.; Döring, A. *Angew. Chem., Int. Ed.* **2009**, *48*, 1106.

(83) Jana, A.; Leusser, D.; Objartel, I.; Roesky, H. W.; Stalke, D. *Dalton Trans.* **2011**, *40*, 5458.

(84) Chizmeshya, A. V. G.; Ritter, C. J.; Hu, C.; Tice, J. B.; Tolle, J.; Nieman, R. A.; Tsong, I. S. T.; Kouvetakis, J. *J. Am. Chem. Soc.* **2006**, *128*, 6919.

(85) (a) Sekiguchi, A.; Kinjo, R.; Ichinohe, M. *Science* **2004**, *305*, 1755. (b) Pu, L.; Twamley, B.; Power, P. P. *J. Am. Chem. Soc.* **2000**, *122*, 3524. (c) Wiberg, N.; Niedermayer, W.; Fischer, G.; Nöth, H.; Suter, M. *Eur. J. Inorg. Chem.* **2002**, 1066. (d) Wiberg, N.; Vasisht, S. K.; Fischer, G.; Mayer, P. *Z. Anorg. Allg. Chem.* **2004**, *630*, 1823.

(86) (a) Power, P. P. *Acc. Chem. Res.* **2011**, *44*, 627. (b) Wright, R. J.; Phillips, A. D.; Power, P. P. *J. Am. Chem. Soc.* **2003**, *125*, 10784. (b) Wright, R. J.; Fettinger, J. C.; Power, P. P. *Angew. Chem., Int. Ed.* **2006**, *45*, 5953.

(87) (a) Fischer, R. C.; Power, P. P. *Chem. Rev.* **2010**, *110*, 3877. (b) Driess, M. Grützmacher, H. *Angew. Chem., Int. Ed. Engl.* **1996**, *35*, 828.

(88) Carter, E. A.; Goddard, W. A. *J. Phys. Chem.* **1986**, *90,* 998.

(89) (a) Trinquier, G.; Malrieu, J. -P. *J. Am. Chem. Soc.* **1987**, *109,* 5303. (b)

Trinquier, G.; Malrieu, J. -P. *J. Am. Chem. Soc.* **1989**, *111,* 5916. (c) Trinquier, G.; Malrieu, J. -P. In *The Chemistry of Functional Groups, Supplement A: The Chemistry of Double Bonded Functional Groups;* Patai, S., Ed.; Wiley: Chichester, **1989**; Vol. 2, Part 1, p 1. (d) Trinquier, G.; Malrieu, J. -P.; Rivière, P. *J. Am. Chem. Soc.* **1982**, *104,* 4529.

(90) Power, P. P. *Angew. Chem., Int. Ed. Engl.* **1990**, *29,* 449. (b) Paine, R. T.; Nöth, H. *Chem. Rev.* **1995**, *95,* 343.

(91) (a) Bader, R. F. W. *Can. J. Chem.* **1962,** *40,* 1164. (b) Pearson, R. G. *J. Am. Chem. Soc.* **1969**, *91,* 4947.

(92) Goldberg, D. E.; Hitchcock, P. B.; Lappert, M. F.; Thomas, K. M.; Fjelberg, T.; Haaland, A.; Schilling, B. E. R. *J. Chem. Soc., Dalton Trans.* **1986**, 2387.

(93) Grev, R. S. *Adv. Organomet. Chem.* **1991**, *33,* 125.

Chapter 2

Synthesis of Sterically Tunable Ligands Featuring Triarylsilyl "Umbrella" Motifs to Support Low Coordinate Tetrel-Chalcogen Complexes

Chapter 2

Synthesis of Sterically Tunable Ligands Featuring Triarylsilyl "Umbrella" Motifs to Support Low Coordinate Tetrel-Chalcogen Complexes

2.1 Abstract

The synthesis and coordination chemistry of a series of dianionic bis(amino)silyl $[NSiN]^{SiPh3}$ and $[NSiN]^{Dipp}$ chelates with N-bound "umbrella"-shaped triarylsilyl ($SiPh_3$) groups were explored. Two areas of steric modification involving this general ligand class were explored: (1) The incorporation of substituents on the phenyl rings of the $SiPh_3$ groups to increase the steric bulk of the ligand; (2) Changing the backbone type and chelate ring size in order to push the pendent groups on the nitrogen centers deeper into the coordination sphere of the chelated element. In order to provide a consistent comparison of the steric coverage afforded by each ligand construct, various two-coordinate N-heterocyclic germylene complexes featuring each ligand set were prepared, and oxidative oxygen- and sulfur-atom transfer chemistry were investigated. In the case of the unsubstituted ligand $[NSiN]^{SiPh3}$ the formation of oxo- and sulfido- bridged dimers $[LGe(\mu\text{-}O)]_2$ and $[LGe(\mu\text{-}S)]_2$ [L = bis(amidosilyl) ligands] were observed in lieu of the target monomeric germanones (LGe=O) and germathiones (LGe=S). Similar sulfido-bridged centrosymmetric germanium(IV) dimers were also obtained with modified $[NSiN]^{SiAr3}$ and $[NSiSiN]^{SiAr3}$ (Ar = 4-$^{i}PrC_6H_4$) ligands and the reaction of these species with oxygen sources were unsuccessful. These

results indicate that these $[NSiN]^{SiPh3}$, $[NSiN]^{SiAr3}$ and $[NSiSiN]^{SiAr3}$ chelates possess sufficient conformational flexibility to allow for the dimerization of LGeS units to occur. Notably, the new ligands with N-bound triarylsilyl groups (4-$RC_6H_4)_3Si$- [R = ^{t}Bu and ^{i}Pr] still offer considerably expanded degrees of steric coverage relative to the parent congener -$SiPh_3$ and thus the use of substituted triarylsilyl groups within ligand design strategies should be a generally useful concept in advancing low-coordination main group and transition-metal chemistry.

2.2 Introduction

The development of sterically encumbered ligands that contain modifiable steric and electronic properties has played a tremendous role in the synthesis of a variety of new main Group and transition metal complexes with interesting bonding and/or catalytic activity.[1-4] For example, the isolation of a Cr-Cr quintuple bond within the dimeric chromium complex Ar'CrCrAr' [Ar' = C_6H_3-2,6-(C_6H_3-2,6-$^iPr_2$)$_2$] was achieved by the Power group with the aid of sterically demanding supporting terphenyl ligands.[2j] Furthermore, the metal-assisted formation of chemical linkages in a chiral manner has been achieved *via* manipulation of a ligand structure.[3]

Sterically demanding ligands with anionic nitrogen donor sites also represent an active field of study in main group chemistry.[5] The widespread success of nitrogen containing amido (or amide) ligands can be rationalized by the dual σ- and π-donor ability of nitrogen and the facile nature of their synthesis that allows incorporation of a library of different pendent groups.[1-6] The very recent synthesis of a stable phosphinonitrene R_2PN (R = bulky amide ligand) a monomer of polyphosphazene is a nice illustration of this concept.[6b] The above mentioned successes provided inspiration to explore the synthesis of new bis(amido) ligands with –$SiPh_3$ groups positioned at the nitrogen sites so that the pendant phenyl rings can create a steric pocket due to their "umbrella- shaped" spatial orientation. In addition, these phenyl rings can be further modified with different substituents depending on the steric requirements (Chart 2.1). Another important aspect of

ligand design is the ability to incorporate different functional groups along the ligand backbone. Thus, by manipulating the ligand backbone, the bite angle and the ring size of chelate can be controlled, thus changing the steric bulk about a coordination site; therefore, a series of [NSiN] and [NSiSiN] chelates were prepared. Moreover, these ancillary groups can serve as useful spectroscopic handles for the monitoring of reactions. In order to compare the steric coverage offered by -$SiPh_3$ groups the synthesis of related ligands containing 2,6-diisopropylphenyl (Dipp) groups at the nitrogen centers was explored (Chart 2.1).

It was anticipated that the flanking groups on the nitrogen will create a steric shield around the chelated element leading to the discovery of new forms of bonding *via* the kinetic stabilization effect (see Chapter 1). For example, an area that would benefit from such ligand advances would be the synthesis of heavy ketone analogues such as silanones and germanones, [LE=O (L = bidentate ligand) or R_2E=O (R = monodentate ligand); E = Si and Ge]. The E=O double bonds in these targets are anticipated to be highly reactive due to their polarized nature, that arises from poor π-orbital overlap along with a large electronegativity difference between the two elements. The isolation of a silanone will therefore require sufficient steric shielding from the proximal ligands in order to suppress the thermodynamically favored formation of oligomers.[8] Although Tamao has very recently reported the elegant synthesis of a monomeric germone R_2Ge=O (R = 1,1,3,3,5,5,7,7-octaethyl-*s*-hydrindacen-4-yl),[9] these species and their heavier chalcogen derivatives are still quite rare.[10] A further inspiration for exploring the coordination chemistry of Ge and Sn is that these elements can be atomic models

for 1st and 2nd row transition metals, and thus could guide the future use of sterically hindered silylamido ligands in the realm of transition-metal mediated catalysis.

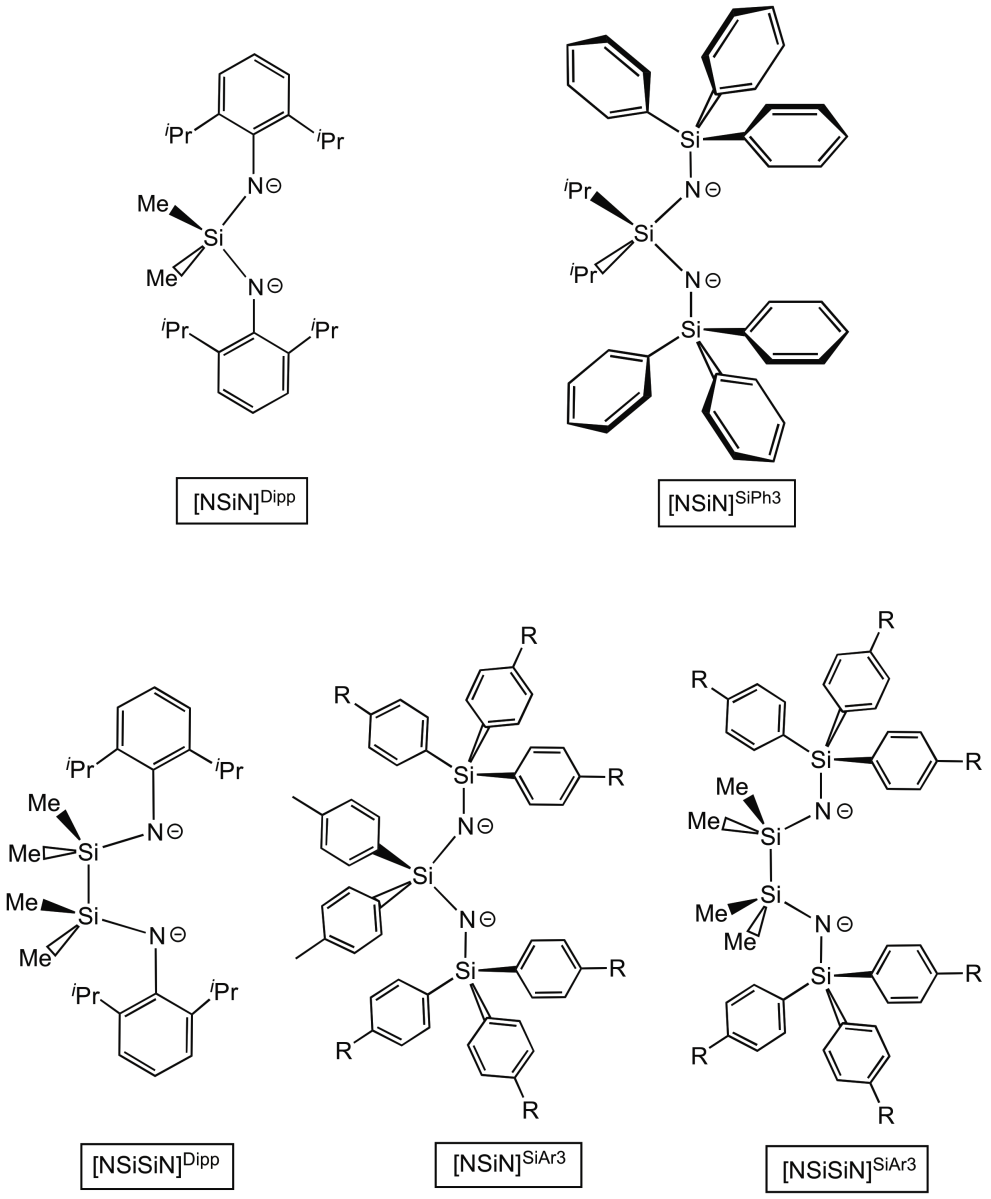

Chart 2.1. Dianionic bis(amido)silyl ligands featuring "umbrella-shaped" -SiR_3 or planar Dipp groups.

2.3 Results and discussion

2.3.1 Synthesis of the $[NSiN]^{Dipp}$ and $[NSiN]^{SiPh3}$ ligand precursors

The bis(amine) ligand precursors, $(RNH)_2Si^iPr_2$ (R = Dipp = 2,6-^{i}Pr$_2$C$_6$H$_3$, **1**; R = $SiPh_3$, **2**) were assembled using the general protocol outlined in Scheme 2.1. Starting from the readily available primary amines, $DippNH_2$ and Ph_3Si-NH_2,[11] the target chelates **1** and **2** were prepared in modest yields *via* two-step procedures and isolated as colorless moisture-sensitive solids (55 and 67% overall yields for **1** and **2**, respectively). The identities of **1** and **2** were established using a combination of NMR and IR spectroscopy, satisfactory elemental analyses (C, H, N), and single-crystal X-ray crystallography (Figure 2.1).

Despite the steric crowding present at the nitrogen centers in both **1** and **2**, all associated metrical parameters, including intrachain Si-N and adjacent Si-C(^{i}Pr) bond distances, were within expected values in accordance with the molecular structures depicted in Scheme 2.1.

2.3.2 Synthesis of the monomeric N-heterocyclic germylenes and stannylenes, (3 and 4) containing the $[NSiN]^{Dipp}$ ligand

In order to test the ability of the bis(amido)silyl ligands $[NSiN]^{Dipp}$ and $[NSiN]^{SiPh3}$ to stabilize low-coordinate Group 14 complexes R_2Ge: and R_2Sn:, termed as germylenes and stannylenes[12] was investigated. Following established literature procedures,[7d,13,14] the aryl-substituted bis(amine) (**1**) was reacted with two equivalents of ^{n}BuLi in Et_2O to generate the dilithiated precursor $Li_2[NSiN]^{Dipp}$ *in situ* and reacted with $GeCl_2$•dioxane and $SnCl_2$ to give the target Ge(II) and Sn(II) complexes [{^{i}Pr$_2$Si(NDipp)$_2$}E:] (E = Ge, **3**; E = Sn, **4**; Scheme

2.1) by salt metathesis chemistry. X-ray quality crystals of **3** and **4** were subsequently grown from diethyl ether and single-crystal X-ray crystallography confirmed the presence of monomeric heterocycles with dicoordinate Ge(II) and Sn(II) centers.

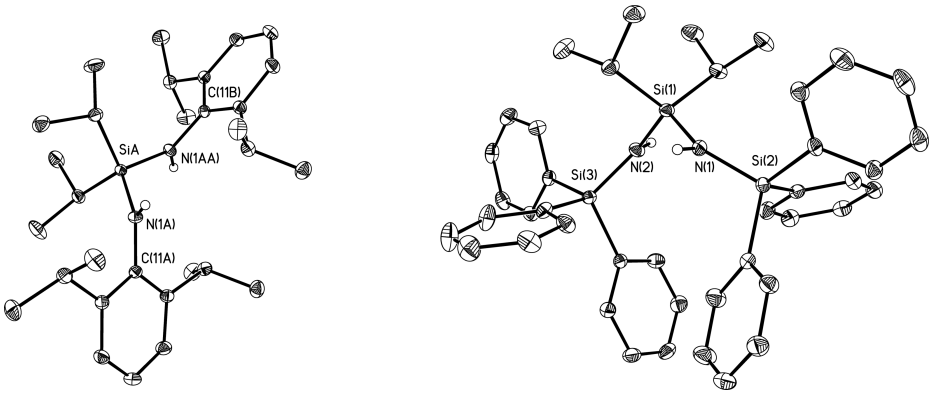

Figure 2.1. Molecular structures of $(DippNH)_2Si^iPr_2$ (**1**) and $(Ph_3SiNH)_2Si^iPr_2$ (**2**) with thermal ellipsoids presented at the 30% probability level. All carbon-bound hydrogen atoms and solvate molecules have been omitted for clarity. Primed atoms are related to unprimed via a two-fold rotation axis that bisects the N-Si-N angle in **1**. Selected bond lengths [Å] and angles [°] with values belonging to a second molecule within the asymmetric unit of **1** in square brackets: Compound **1**: Si(1)-N(1) 1.7397(11) [1.7413(11)], Si(1)-C(1) 1.8896(13) [1.8873(13)]; N(1)-Si(1)-N(1´ 115.04(8) [116.74(8)], C(1)-Si(1)-C(1)´ 116.86(9) [116.82(9)]. Compound **2**: Si(1)-N(1) 1.7391(16), Si(1)-N(2) 1.7402(19), Si(2)-N(1) 1.7228(16), Si(3)-N(2) 1.7182(16), Si(1)-C(1) 1.892(2), Si(1)-C(4) 1.892(2); N(1)-Si(1)-N(2) 114.43(8), Si(1)-N(1)-Si(2) 139.33(10), Si(1)-N(2)-Si(3) 140.09(11), C(1)-Si(1)-C(4) 116.31(9).

As shown in Figure 2.2, compounds **3** and **4** adopt similar overall geometries with planar four-membered NSiNE rings (E = Ge and Sn) and trigonal planar geometries about the chelating nitrogen atoms.

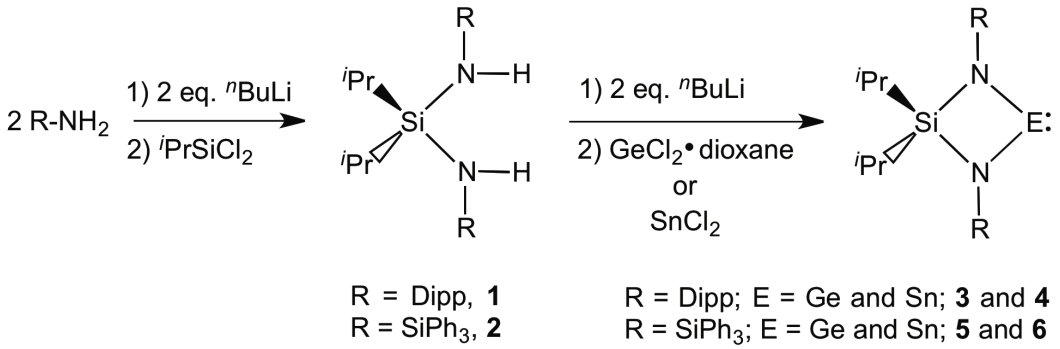

Scheme 2.1 Preparation of the monomeric germylenes and stannylenes, **3**-**6**, supported by $[NSiN]^{Dipp}$ and $[NSiN]^{SiPh3}$ ligands.

The Ge-N and Sn-N bond distances in **3** and **4** are 1.8627(10) and 2.067(2) Å (*avg*.), respectively, while nearly identical Si-N endocyclic bond lengths are present in both complexes [1.7471(10) in **3**; 1.745(2) Å (*avg*.) in **4**]. Compound **3** represents the first crystallographically characterized uncomplexed germylene heterocycle featuring an NSiNGe core. An analogous Ge(II) heterocycle [$Me_2Si(NtBu)_2Ge$:] was prepared by Veith et al. as a stable yellow oil and this species was identified as a monomeric species in benzene solvent by cryoscopic measurements.[15,16] Russell and coworkers recently reported the synthesis of a structurally related tin(II) heterocycle {$Ph_2Si(NDipp)_2$}Sn:].[14b] As with **4** a planar NSiNSn unit was present, however the Sn-N bond distances in the diphenylsilane analogue were elongated [2.101(6) and 2.259(5) Å] with respect to those found in **4** [2.067(2) Å (*avg*.)].[14] Moreover, additional molecular interactions were observed in [{$Ph_2Si(NDipp)_2$}Sn:] involving the flanking aryl rings of the Dipp groups and adjacent Sn centers, resulting in the formation of a weakly associated coordination polymer with close intermolecular Sn•••η^6 aryl(centroid) contacts of *ca*. 3.2 Å.[14b]

By contrast, compound **4** is monomeric with no close-range intermolecular interactions observed within 4.0 Å. This difference in solid-state packing is a likely consequence of added intraligand crowding in **4**. The presence of encumbered $^{i}Pr_2Si$ and Dipp groups within the same heterocycle results in the aryl rings in **4** being pushed even further toward the Sn center, leading to a greater degree of steric coverage.[17] This effect is observed both in the solid-state structure of **4**, wherein the Si-N-C(*ipso*, Dipp) angles are considerably wide [134.98(10) and 137.71(10)°], and *via* the presence of spectroscopically distinct ^{i}Pr environments within the Dipp ligands by ^{1}H and $^{13}C\{^{1}H\}$ NMR spectroscopy. In the less hindered analogue [{$Ph_2Si(NDipp)_2$}Sn:] the exocyclic Si-N-C(ipso, Dipp) angles are reduced to 130.2(2) and 132.7(2)°, while free rotation of the Dipp moieties and one ^{i}Pr environment was observed by NMR spectroscopy at ambient temperature.[14b] The Ge(II) heterocycle **3** possesses a similar overall geometry as its heavier congener **4** with correspondingly wide Si-N-C(ipso) angles of 139.41(8)° observed.

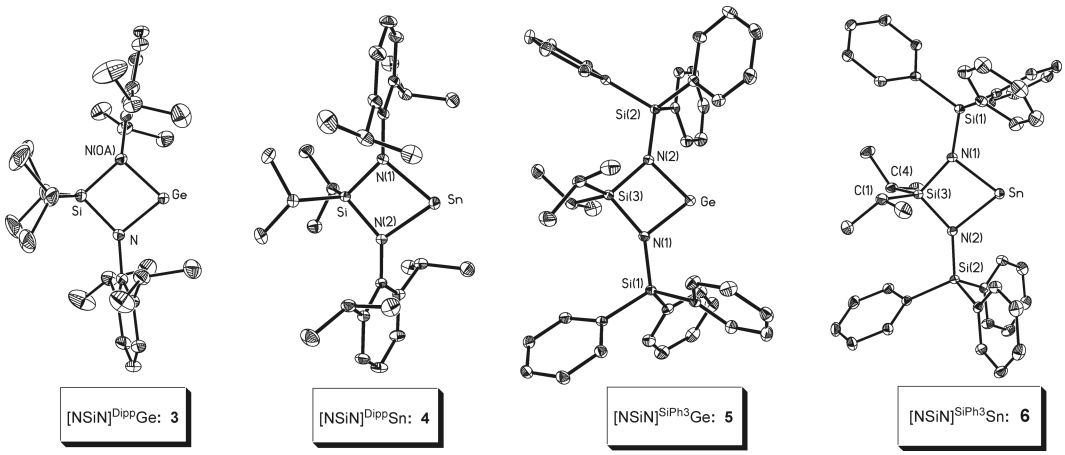

Figure 2.2. Molecular structures of heterocycles **3**-**6** with thermal ellipsoids at a 30% probability level. All hydrogen atoms have been omitted for clarity. Primed atoms for **3** are related to unprimed via a two-fold rotational axis upon which the Ge and Si atoms are located. Selected bond lengths [Å] and angles [°]: Compound **3**: Ge(1)-N(1) 1.8627(10), Si(1)-N(1) 1.7471(10); N(1)-Ge(1)-N(1)´ 81.26(6), N(1)-Si(1)-N(1)´ 87.94(7), C(1)-Si(1)-C(1)´ 112.72(12), Si(1)-N(1)-C(11) 139.41(8). Compound **4**: Sn(1)-N(1) 2.0709(12), Sn(1)-N(2) 2.0631(12), Si(1)-N(1) 1.7440(12), Si(1)-N(2) 1.7463(12); N(1)-Sn(1)-N(2) 74.60(5), C(1)-Si(1)-C(4) 111.87(7), Si(1)-N(1)-C(11) 137.71(10). Compound **5**: Ge(1)-N(1) 1.8834(14), Ge(1)-N(2) 1.8829(14), Si(1)-N(1) 1.7210(14), Si(2)-N(2) 1.7164(14), Si(3)-N(1) 1.7458(14), Si(3)-N(2) 1.7481(14); N(1)-Ge(1)-N(2) 83.31(6), C(1)-Si(3)-C(4) 110.52(10), Si(3)-N(1)-Si(1) 146.23(9). Compound **6**: Sn(1)-N(1) 2.0888(15), Sn(1)-N(2) 2.0882(15), Si(1)-N(1) 1.7102(16), Si(2)-N(2) 1.7083(16), Si(3)-N(1) 1.7402(16), Si(3)-N(2) 1.7446(16); N(1)-Sn(1)-N(2) 76.28(6), C(1)-Si(3)-C(4) 109.50(11), Si(3)-N(1)-Si(1) 146.51(10).

2.3.3 Synthesis of the monomeric N-heterocyclic germylenes and stannylenes (4 and 5) featuring the $[NSiN]^{SiPh3}$ ligand

As mentioned earlier, in order to further expand the steric bulk of the dianionic [NSiN] chelates, umbrella-shaped triarylsilyl groups were installed at the nitrogen-donor sites $[NSiN]^{SiPh3}$ (Chart 2.1). The -$SiPh_3$ groups not only provide a wide swath of steric bulk that radiates outward from the Si centers but should also allow for further ligand modification *via* chemical functionalization of the peripheral aryl groups.[18] The syntheses of the Ge(II) and Sn(II) complexes

[{[NSiN]^{SiPh3}}Ge:] (**5**) and [{[NSiN]^{SiPh3}}Sn:] (**6**) proceeded in a similar fashion as for the less hindered Dipp analogues **3** and **4** (Scheme 2.1), with the noted exception that the triphenylsilyl-substituted heterocycles exhibited significantly reduced solubility in organic solvents.[19] As a consequence of the hydrolytically prone Si-N and Ge-N/Sn-N linkages within **5** and **6**, these compounds were observed to react readily with trace quantities of moisture to yield Ph_3Si-O-$SiPh_3$ as a soluble byproduct (identified by X-ray crystallography and ^{1}H and $^{13}C\{^{1}H\}$ NMR spectroscopy).[20] However when compounds **5** and **6** are handled under strictly anhydrous conditions these compounds are thermally stable with no noticeable signs of decomposition in the solid state up to 300 °C (under N_2). High-quality crystals of **5** and **6** for X-ray diffraction studies were obtained from diethyl ether and their molecular structures are presented as part of Figure 2.2. These triarylsilyl-capped heterocycles display a higher degree of intramolecular repulsion involving the backbone positioned $^{i}Pr_2Si$ groups relative to the Dipp analogues, **3** and **4**. These $^{i}Pr_2Si$•••$SiPh_3$ interactions cause the -$SiPh_3$ moieties to be tilted forward toward the Ge and Sn centers to produce highly distorted Si(endo)-N-Si(exo) angles [Si(3)-N(1)-Si(1,2) angles = 146.23(9) and 140.10(9)° for **5**; 146.51(10) and 140.14(9)° for **6**]. Furthermore, space filling models indicate that the -$SiPh_3$ groups create a much deeper steric pocket about the capping Ge and Sn centers with respect to the coverage offered by the flanking Dipp groups in **3** and **4** hence the use of triarylsilyl groups as structural motifs is a promising strategy for the stabilization of low-coordinate bonding environments.

2.3.4 Initial chalcogen atom-transfer chemistry involving germylenes and stannylenes (3 and 4)

Divalent germylenes (R_2Ge:) and stannylenes (R_2Sn:) exhibit diverse reaction chemistry due to their dual donor/acceptor nature and proclivity for oxidative bond forming reactions.[12,21] As mentioned earlier, intramolecular steric repulsions within the [NSiN]E: (E = Ge and Sn) heterocycles **3**-**6** leads to the positioning of the flanking groups at nitrogen (Dipp or $SiPh_3$) in closer proximity to the Group 14 centers.

In order to benchmark the steric coverage offered by the $[NSiN]^{Dipp}$ and $[NSiN]^{SiPh3}$ chelates with respect to known ligands, preliminary chalcogen atom-transfer chemistry involving the germylenes and stannylenes (**3**-**6**) was explored with the goal of isolating hitherto rare examples of Ge=O and Ge=S multiple bonds.[12e] The interaction of the arylamido germylene $[\{(NSiN)^{Dipp}\}Ge:]$ with the chalcogen sources Me_3NO and S_8 (one atomic equivalent) afforded a new Ge product in each case; notably, the products obtained exhibited analogous NMR spectroscopic signatures, suggesting that these products were of similar structure in solution. X-ray crystallography substantiated the successful transfer of chalcogen atoms to germanium in both instances and revealed the formation of the corresponding oxo- and sulfido-bridged dimers $[\{^iPr_2Si(NDipp)_2\}Ge(\mu\text{-}O)]_2$ and $[\{^iPr_2Si(NDipp)_2\}Ge(\mu\text{-}S)]_2$ (**7** and **8**, Scheme 2.2 and Figure 2.3). The oxo-bridged dimer $[\{[NSiN]^{Dipp}\}Ge(\mu\text{-}O)]_2$ (**7**) contains planar NSiNGe and Ge_2O_2 arrays that are mutually rotated by 73.0 and 71.6°, with average endocyclic Ge-O and Ge-N bond lengths of 1.805(4) and 1.830(5) Å. A related amide-substituted 1,3-cyclodigermoxane $[Ge\{N(SiMe_3)_2\}_2(\mu\text{-}O)]_2$ was synthesized by Lappert and

coworkers through the direct reaction of the germanium(II) bisamide, $Ge\{N(SiMe_3)_2\}_2$ with molecular oxygen.[20] Dimeric $[Ge\{N(SiMe_3)_2\}_2(\mu\text{-}O)]_2$ features a similar planar Ge_2O_2 core as in **7** with Ge-O distances ranging from 1.804(11) to 1.836(10) Å and accompanying Ge-N distances that vary from 1.8317(10) to 1.830(10) Å.[22] For further comparison, the centrosymmetric diarylgermone dimer $[(2,6\text{-}Et_2C_6H_3)_2Ge(\mu\text{-}O)]_2$ exhibites an average Ge-O bond length of 1.817(3) Å and an endocyclic O-Ge-O angle of 87.6 (1)°;[23] this O-Ge-O bond angle compares well with those found in **7** [86.43(8) and 86.51(8)°]. Notably, the Ge-N distances in **7** are *ca*. 0.03 Å shorter than in **3**, while the intraring N-Ge-N angles are slightly wider in **7** [84.10(6) and 83.79(10)°] relative to the corresponding angle of 81.26(6)° in the Ge(II) precursor **3**. The decrease in the observed Ge-N bond lengths upon oxidation of **3** with Me_3NO is likely due to a reduction in the covalent radii on going from a formal Ge(II) site in **3** to a Ge(IV) center in **7**.[24] Similarly, when **4** was combined with sulfur and Me_3NO no reaction was observed by ^1H NMR spectroscopy. The reluctance of stannylene $[NSiN]^{Dipp}Sn$: to be oxidized can be rationalized from the reluctance of tin-based s-electrons to participate in the bonding relative to its lighter congeners C, Si and Ge (known as the "Inert Pair Effect").

The formation of a dimeric arrangement in $[\{(NSiN)^{Dipp}\}Ge(\mu\text{-}O)]_2$ (**7**) underscores the difficulty associated with isolating a monomeric germanone ($R_2Ge{=}O$) under ambient conditions; a major factor for the lack of wide spread success thus far lies in the highly polar nature of the Ge-O π-bond, which makes this unit prone to dimerization/oligomerization to yield thermodynamically more

stable σ-linkages (and the formation of extended Ge-O rings and/or chains).[8f,25] Notably, Veith's heterocyclic germylene [$Me_2Si(N^tBu)_2Ge$:] also participates in smooth oxo-transfer chemistry with Me_3NO, however due to the reduced steric bulk in this germelene, a system relative to **3**, a trimeric product [{$Me_2Si(N^tBu)_2$}Ge(μ-O)]$_3$ containing a Ge_3O_3 core was obtained.[21a]

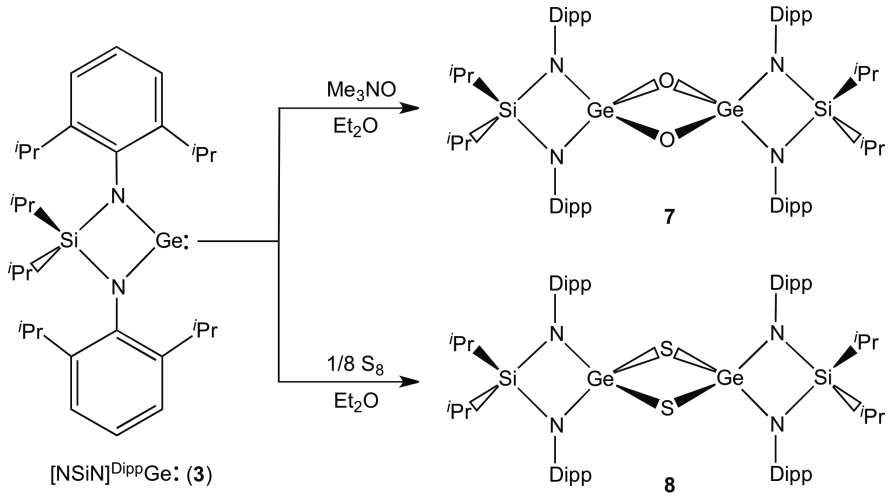

Scheme 2.2. Chalocogen atom-transfer chemistry involving [NSiN]^{Dipp}Ge: to produce oxo- and sulfido-bridged dimers (**7** and **8**).

The sulfido dimer [{[NSiN]^{Dipp}}Ge(μ-S)]$_2$ (**8**) (Figure 2.3) has an overall structure that mirrors the oxo-bridge dimer **7** with the primary difference being the presence of an expanded Ge_2S_2 core [Ge-S = 2.1992(3) and 2.2577(3) Å] due to the larger covalent radius of S relative to O.[27] It is salient to mention that an example of a stable monomeric germanethione has been isolated at ambient temperature [Tbt(Tip)Ge=S] (Tbt = 2,4,6-{$(Me_3Si)_2CH$}C_6H_2; Tip = 2,4,6-$^iPr_3C_6H_2$),[10] and that this species contains a significantly shorter Ge-S distance [2.049(3) Å] that is consistent with a Ge=S double bond.

The structures of **7** and **8** reveal that the flanking Dipp groups can readily twist away from the germanium-chalcogen rings, thus providing a pathway for the dimerization of any putative Ge=O and Ge=S double bonds initially formed. In addition, the relative positions between the Dipp groups in **7** and **8** and the Ge centers in these dimers are similar to that found in the precursor **3**, as evidenced by only minor deviations in the Si-N-C(*ipso*, Dipp) angles in all three complexes. This suggests that the degree of repulsion between the cofacial Dipp groups in the dimers **7** and **8** was minimal.

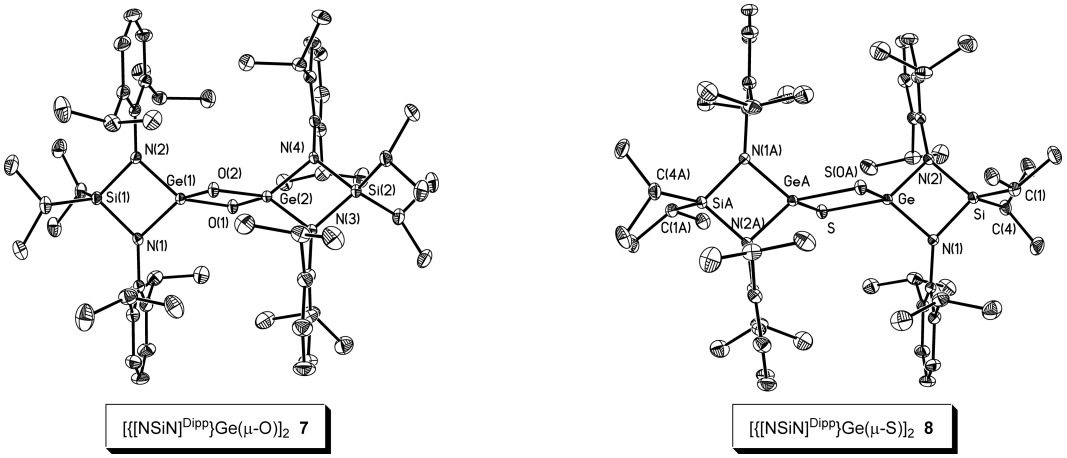

Figure 2.3. Molecular structure of $[\{[NSiN]^{Dipp}\}Ge(\mu\text{-}O)]_2$ (**7**) and $[\{[NSiN]^{Dipp}\}Ge(\mu\text{-}S)]_2$ (**8**) with thermal ellipsoids presented at a 30% probability level. All hydrogen atoms and ether solvate molecules have been omitted for clarity. Primed atoms in **8** are related to unprimed by an inversion center. Selected bond lengths [Å] and angles [°]: Compound **7**: Ge(1)-O(1) 1.8045(18), Ge(1)-O(2) 1.8063(19), Ge(2)-O(1) 1.8044(19), Ge(2)-O(2) 1.8032(18), Ge(1)-N(1) 1.828(2), Ge(1)-N(2) 1.833(2), Ge(2)-N(3) 1.830(2), Ge(2)-N(4) 1.828(2), Si(1)-N(1) 1.768(2), Si(1)-N(2) 1.763(2), Si(1)-C(1) 1.879(3), Si(1)-C(4) 1.877(3), Si(2)-N(3) 1.761(2), Si(2)-N(4) 1.762(2); O(1)-Ge(1)-O(2) 86.43(8), N(1)-Ge(1)-N(2) 84.10(10), O(1)-Ge(2)-O(2) 86.51(8), N(1)-Si(1)-N(2) 87.95(11), C(1)-Si(1)-C(4) 112.08(14), Si(1)-N(1)-C(21) 134.65(19), Si(1)-N(2)-C(41) 135.79-(19), Ge(1)-N(1)-C(21) 131.27(19). Compound **8**: Ge(1)-S(1) 2.1992(3), Ge(1)-S(1)´ 2.2577(3), Ge(1)-N(1) 1.8344(9), Ge(1)-N(2) 1.8471(9), Si(1)-N(1) 1.7606(9), Si(1)-N(2) 1.7675(10), Si(1)-C(1) 1.8925(13), Si(1)-C(4) 1.8755(13); S(1)-Ge(1)-S(1)´ 95.956(10), Ge(1)-S(1)-Ge(1)´ 84.043(10), N(1)-Ge(1)-N(2) 83.65(4), N(1)-Si(1)-N(2) 88.19(4), C(1)-Si(1)-C(4) 109.35(6), Si(1)-N(1)-C(11) 137.62(9), Si(1)-N(2)-C(31) 138.00(8), Ge(1)-N(1)-C(11) 128.19(7).

2.3.5 Chalcogen atom-transfer chemistry involving the germylenes and stannylenes, 5 and 6

In order to more thoroughly compare the steric effects created by the Dipp and -$SiPh_3$ groups within our chelates, analogous chalcogen-transfer chemistry involving the triarylsilylsubstituted germylene **5** was explored (Equation 2.1). Interaction of the Ph_3Si-flanked germylene [{[NSiN]^{SiPh3}}Ge:] (**5**) with Me_3NO did not yield any products that could be isolated in pure form. However, treatment of **5** with elemental sulfur yielded a clean product that was marginally soluble in diethyl ether. Single-crystal X-ray crystallography (Figure 2.4) later identified the compound as the sterically congested germanethione dimer [{[NSiN]^{SiPh3}}Ge(μ-S)]$_2$ (**9**) (Equation 2.1).

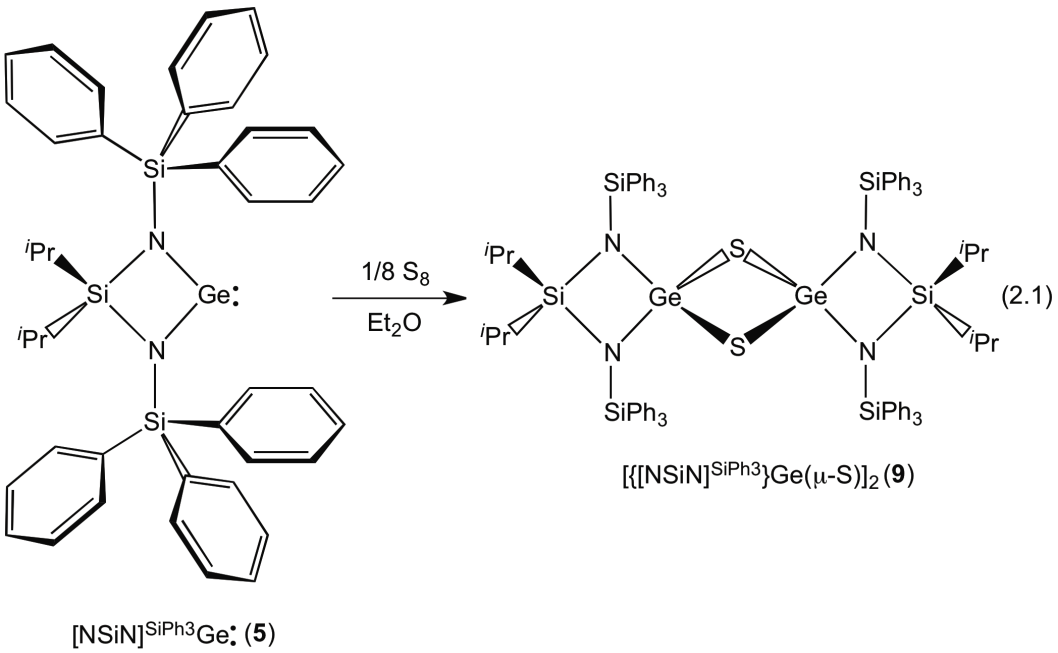

[NSiN]^{SiPh3}Ge: (**5**)

[{[NSiN]^{SiPh3}}Ge(μ-S)]$_2$ (**9**) (2.1)

As with the less hindered derivative [{[NSiN]^{Dipp}}Ge(μ-S)]$_2$ (**8**) the Ge_2S_2 core in **9** was found to be planar with similar Ge-S distances of 2.2197(5) and 2.2484(5) Å and a slightly narrower intraring S-Ge-S angle of 94.28(2)°; the Ge-S bond lengths in **9** are in the range expected for single bonds (2.17-2.25 Å).[10b] Particularly noteworthy is the significant degree of intramolecular repulsion in **9** involving proximal $SiPh_3$ groups that are mutually located on the same side of the plane created by the central Ge_2S_2 core.

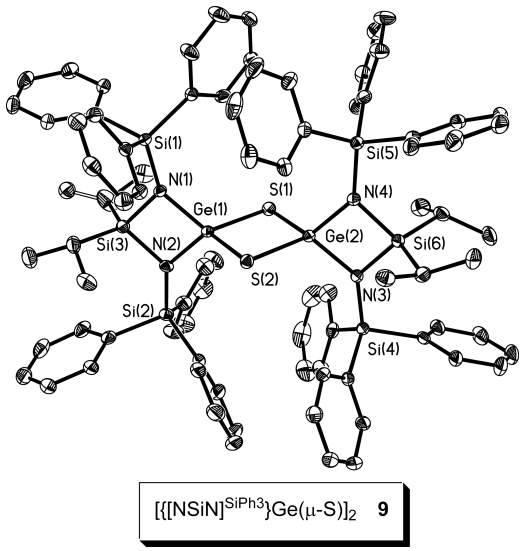

Figure 2.4. Molecular structure of [{[NSiN]^{SiPh3}}Ge(μ-S)]$_2$ (**9**) with thermal ellipsoids presented at the 30% probability level with primed atoms related to nonprimed by an inversion center. All hydrogen atoms and ether solvate molecules have been omitted for clarity. Selected bond lengths [Å] and angles [°]: Ge(1)-S(1) 2.2197(5), Ge(1)-S(1)´ 2.2484(5), Ge(1)-N(1) 1.8534(13), Ge(1)-N(2) 1.8519(13), Si(1)-N(1) 1.7337(14), Si(2)-N(2) 1.7326(14), Si(3)-N(1) 1.7704(14), Si(3)-N(2) 1.7675(14); S(1)-Ge(1)-S(1)´ 94.28(2), N(1)-Ge(1)-N(2) 85.38(6), N-(1)-Si(3)-N(2) 90.49(6), C(1)-Si(3)-C(4) 110.96(9), Si(3)-N(1)-Si-(1) 131.13(8), Si(3)-N(2)-Si(2) 134.47(8), Ge(1)-N(1)-Si(1) 136.91(8), Ge(1)-N(2)-Si(2) 133.22(8).

The intramolecular -$SiPh_3$•••Ph_3Si- interactions in **9** lead to very large molecular distortions as revealed by a widening of the Ge-N-$SiPh_3$ angles [133.22(8) and 136.91(8)°] relative to in the less-hindered precursor **5** [121.13(8) and 127.42(8)°]. This effect is in stark contrast to in the sulfido-dimer **8** where little perturbation of the Dipp groups is observed relative to the free germylene **3**.

Surprisingly, when the stannylene [(NSiN)^{SiPh3}]Sn: (**6**) was reacted with molar equivalent of Me_3NO in Et_2O, the formation of a new product was observed by ^{1}H NMR spectroscopy (Equation 2.2). A ^{119}Sn resonance for this new product was detected at 6.2 ppm which is distinctly shifted from the ^{119}Sn{^{1}H} signal found in compound **6** [527 ppm]. X-ray crystallographic analysis later revealed the formation of the adduct {[NSiN]^{SiPh3}}Sn-O-NMe_3 (**10**).

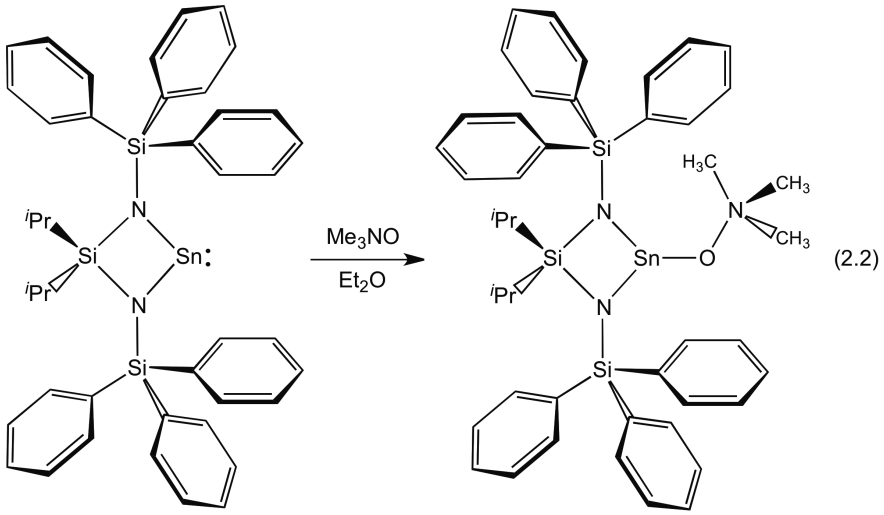

[NSiN]^{SiPh3}Sn: (**6**) {[NSiN]^{SiPh3}}Sn-O-NMe_3 (**10**)

As shown in Figure 2.5 compound **10** adopts a distorted trigonal pyramidal geometry around the tin center indicating the presence of a stereochemically active lone pair. The presence of a very weak Sn-O interaction in **10** is evident from the very elongated Sn-O bond distance of 2.2151(16) Å; for comparison, the Sn-O bond length in oxo-bridged dimer [{$R_2Sn(\mu$-O)}$_2$] (R = $CH(SiMe_3)_2$) was 1.960(2) Å (*avg.*).[28] In addition, there was no significant change in bond length in the donor Me_3NO component; the O-N(3) bond distance 1.406(2) Å in **10** is similar within the experimental error to the N-O bond distance in free Me_3NO [1.388(5) Å].[29]

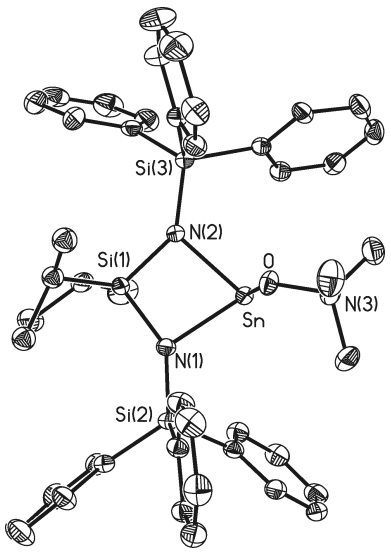

Figure 2.5. Molecular structure of {[NSiN]^{SiPh3}}Sn-O-NMe_3 (**10**) with thermal ellipsoids presented at a 30% probability level. All hydrogen atoms and solvate molecules have been omitted for clarity. Selected bond lengths [Å] and angles [°]: Sn(1)-N(1) 2.1586(18), Sn(1)-N(2) 2.1242(17), Si(1)-N(1) 1.7279(19), Si(2)-N(2) 1.7270(18), Si(2)-N(1) 1.6793(18), Si(3)-N(2) 1.6872(18), Sn(3)-Si(1) 2.8377(7), Sn-O 2.2151(16), O-N(3) 1.406(2); N(1)-Sn(1)-N(2) 74.46(7), N(1)-Si(1)-N(2) 97.19(9), Si(1)-N(1)-Si(2) 144.69(12), Si(1)-N(2)-Si(3) 140.75(11), O-Sn-N(1) 95.10(6), O-Sn-N(2) 88.42(6).

Given the formation of oxo- and sulfido-bridged germanium dimers in the presence of the $[NSiN]^{Dipp}$ and $[NSiN]^{SiPh3}$ ligands, it is tempting to postulate that the addition of bulk to the aryl groups in $[NSiN]^{SiPh3}$ ligand would result in further repulsion between the $SiAr_3$ units and cause a steric preference for monomeric species with discrete Ge=O and Ge=S double bonds. The next section of this Chapter will discuss the synthesis of new bis(amido)silyl ligands *via* modification of the -$SiAr_3$ groups at nitrogen and their application in the kinetic stabilization of highly reactive bonding environments.

2.3.6 Expanding the steric coverage offered by bis(amido)silyl chelates

Motivated by the high degree of steric bulk present in the dianionic bis(amido)silyl chelates, $[NSiN]^{Dipp}$ and $[NSiN]^{SiPh3}$ and keeping the products of the above mentioned chalcogen transfer chemistry in mind, a series of [NSiSiN] chelates bearing elongated tetramethyldisilyl, -$SiMe_2$-$SiMe_2$-, backbones in conjunction with new sterically expanded triarylsilyl $(4\text{-}R\text{-}C_6H_4)_3Si$-, umbrella-shaped moieties (R = ^{t}Bu and ^{i}Pr) were targeted.[30] The presence of -$SiMe_2$-$SiMe_2$- groups in these modified ligands will generate five membered heterocycles upon coordination with Ge(II) and Sn(II), and should direct the flanking $SiAr_3$ groups deeper into the coordination sphere around the chelated atoms. With these added features incorporated into the modified ligands, it was anticipated that highly monomeric species such as LE=O (L = bidentate ligand; E = Si and Ge) might be isolable.

2.3.7 Synthesis of the bis(amido)disilyl germylene and stannylene heterocycles [$(Me_2SiNDipp)_2E$:] (E = Ge and Sn; 12 and 13)

Starting from the known bis(amine) $[Me_2SiNHDipp]_2$ (**11**),[31] the monomeric germylene and stannylene complexes, $[(Me_2SiNDipp)_2E$:] (E = Ge and Sn; **12** and **13**) were prepared in high yields of 88 and 91%, respectively (Scheme 2.3). The germanium heterocycle **12** was obtained as an orange solid of modest stability in the solid state (decomposition noted at 80 °C under N_2), while its tin congener **13** was isolated as a thermally stable yellow solid. As shown in Figure 2.6, compounds **12** and **13** adopt monomeric structures in the solid state with the peripheral, nitrogen-bound Dipp groups oriented in an orthogonal manner to the ENSiSiN ring planes in **12** and **13** (E = Ge and Sn). In each heterocycle, slight canting of the $SiMe_2$ groups relative to one another is noted with N-Si-Si-N intraring torsion angles of 11.58(6)° and 22.17(6)° for **12** and **13**, respectively. As expected, the Dipp substituents are also bent considerably forward towards the Ge and Sn centers, as evidenced by the narrow C(ipso, Dipp)-N-E angles of 113.99(12)° (*avg*.) and 117.12(13)° (*avg*.) for compounds **12** and **13**. For comparison, the Dipp groups within the four-membered [NSiNE] chelates $[\{^iPr_2Si(NDipp)_2\}E$:] (**3** and **4**; E = Ge and Sn) were also positioned orthogonal to the inorganic ring planes, but were located further away from the Group 14 centers as indicated by significantly wider C(ipso, Dipp)-N-E angles of 124.96(8)° (E = Ge) and 126.30(13)° *avg*. (E = Sn).[32] The backbone Si-Si distances in heterocycles **12** [2.3339(5) Å] and **13** [2.3269(5) Å] are nearly

identical within experimental error and in the range expected for Si-Si single bonds.[33]

Compound **12** represents the first heterocyclic, two-coordinate-germylene that contains a disilane unit as part of the ring skeleton.[34] Notably, structurally related Sn(II) silylamino complexes $[(Me_2SiNR)_2Sn]_{1or2}$ (R = alkyl groups) were prepared by the group of Wrackmeyer.[35]

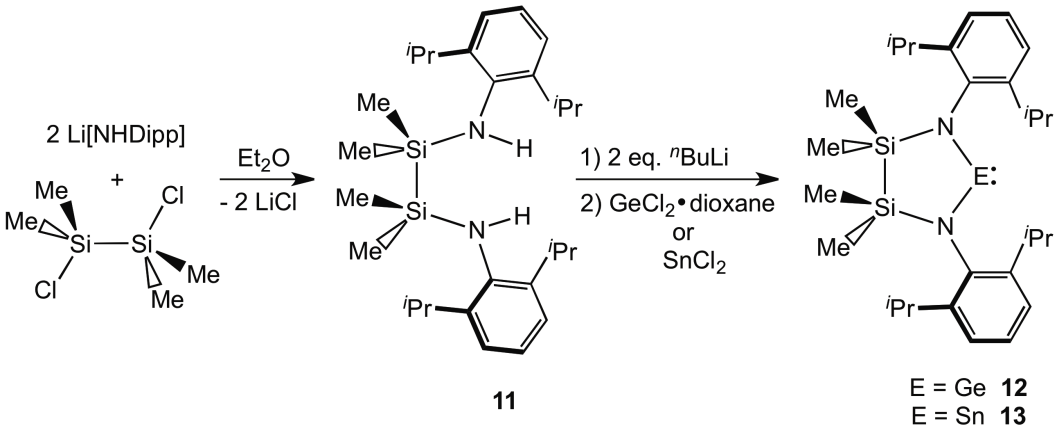

Scheme 2.3. Synthesis of the diaminodisilyl germylene and stannylene heterocycles $[(Me_2SiNDipp)_2E:]$ (E = Ge and Sn; **12** and **13**).

When bulky side groups were appended to nitrogen, monomeric stannylenes $[(Me_2SiN^tBu)_2Sn:]$ were observed in solution, however upon decreasing the steric bulk of the substituent at nitrogen, dimerization via intermolecular Sn•••N interactions transpired, and in some instances, monomer-dimer equilibria were identified using variable-temperature ^1H and ^{119}Sn NMR studies.[35] For comparison, the hindered stannylene **13** is stable indefinitely at room temperature and in the presence of light, while the less-sterically protected Sn complexes of Wrackmeyer slowly decompose in solution when exposed to

ambient light; this decomposition process generally leads to ligand redistribution to give the homoleptic complexes $[(Me_2SiNR)_2]_2Sn$.[35]

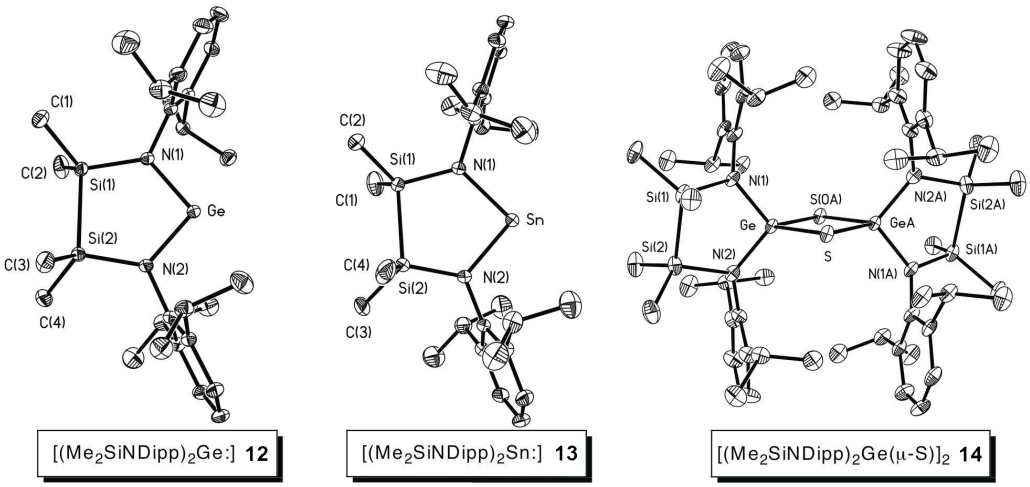

Figure 2.6. Molecular structures of $[(Me_2SiNDipp)_2\}E:]$ (E = Ge and Sn; **12** and **13**) and $[(Me_2SiNDipp)_2Ge(\mu\text{-}S)]_2$ (**14**) with thermal ellipsoids presented at a 30% probability level. The hydrogen atoms have been omitted for clarity. Selected bond lengths [Å] and angles [°]: Compound **12**: Ge-N(1) 1.8615(10), Ge-N(2) 1.8623(10), N(1)-Si(1) 1.7535(11), N(2)-Si(2) 1.7560(11), Si(1)-Si(2) 2.3339(5); N(1)-Ge-N(2) 98.75(5), Si(1)-N(1)-Ge 122.49(6), Si(2)-N(2)-Ge 121.70(6), Si(1)-N(1)-C(11) 123.50(8), C(11)-N(1)-Ge 113.93(8), Si(2)-N(2)-C(31) 124.26(8), C(31)-N(2)-Ge 114.05(8), 98.00(4). Compound **13**: Sn-N(1) 2.0597(11), Sn-N(2) 2.0646(11), N(1)-Si(1) 1.7477(11), N(2)-Si(2) 1.7533(12), Si(1)-Si(2) 2.3269(5); N(1)-Sn-N(2) 93.35(4), Si(1)-N(1)-Sn 121.05(6), Si(2)-N(2)-Sn 120.45(6), Si(1)-N(1)-C(11) 122.10(9), C(11)-N(1)-Sn 116.79(8), Si(2)-N(2)-C(31) 121.93(9), C(31)-N(2)-Sn 117.44(8). Compound **14**: Ge-S 2.2763(17), Ge-S´ 2.2245(17), Ge-N(1) 1.853(5), Ge-N(2) 1.840(6), N(1)-Si(1) 1.765(6), N(2)-Si(2) 1.792(6), Si(1)-Si(2) 2.303(3); S-Ge-S(A) 93.39(6), Ge-S-Ge 86.61(6), N(1)-Ge-N(2) 101.7(2), Ge-N(1)-C(11) 127.3(4), Ge-N(2)-C(31) 130.2(4), N(1)-Si(1)-Si(2) 96.9(2), N(2)-Si(1)-Si(2) 98.2(2).

The high degrees of thermal stability, coupled with the monomeric nature of the germylene and stannylene complexes **12** and **13**, suggest that the consitituent $[NSiSiN]^{Dipp}$ chelates are promising ligands for the stabilization of

other reactive inorganic bonding environments.[36] As a starting point, chalcogen atom transfer chemistry between the two-coordinate germylene [(Me-$_2$SiNDipp)$_2$Ge:] **12** and elemental sulfur was explored in order to potentially access a rare example of a stable species featuring a Ge=S double bond.[10]

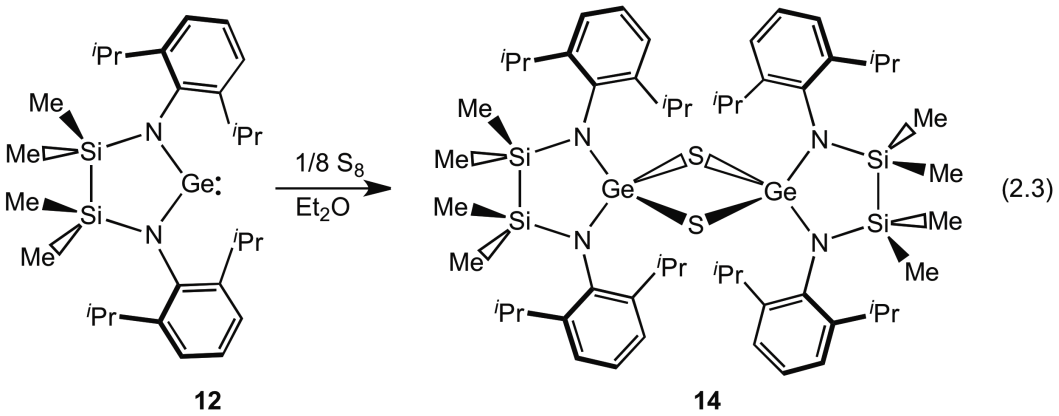

12 **14** (2.3)

Treatment of **12** with an atomic equivalent of sulfur resulted in the gradual bleaching of the initially orange colored solution and the eventual recovery of a white microcrystalline solid. X-ray crystallographic analysis later revealed the successful installation of a sulfur atom at Ge, however, in place of isolating the desired monomeric germanethione, a dimeric complex [(Me$_2$SiNDipp)$_2$Ge(μ-S)]$_2$ (**14**) was obtained (Equation 2.3; Figure 2.6).

As shown in Figure 2.6, compound **14** adopts a centrosymmetric structure comprised of two GeNSiSiN heterocycles joined by a central Ge_2S_2 array. The overall geometry of this germanium sulfide complex is reminiscent of that observed within the previously discussed dimers [{^{i}Pr$_2$Si(NDipp)$_2$}Ge(μ-S)]$_2$ (**7**) and [{^{i}Pr$_2$Si(NSiPh$_3$)$_2$}Ge(μ-S)]$_2$ (**8**). For example, the Ge-S distances in **14** are 2.2245(17) and 2.2763(17) Å, while in the abovementioned dimers featuring

[NSiN] chelates, distances in the range of 2.1992(3) to 2.2577(3) Å were observed.[32a] The Ge-S distances in **14** are consistent with the presence of Ge-S single bonds[10b] and these bond lengths are expectedly lengthened in comparison to the Ge=S double bond distance of 2.049(3) Å found in [Tbt(Tip)Ge=S] (Tbt = 2,4,6-{$(Me_3Si)_2CH\}_3C_6H_2$; Tip = 2,4,6-$^iPr_3C_6H_2$).[10a]

The backbone-positioned $SiMe_2$ groups in **14** are mutually twisted in comparison to the nearly eclipsed Me_2Si-$SiMe_2$ arrangement found in the Ge(II) precursor **12**, as evidenced by widened N-Si-Si-N torsion angles of 23.6(3)° in **14** versus 11.58(6)° in **12**; this effect is likely due to an increase in intraligand Dipp•••$SiMe_2$ repulsion in the oxidized dimer $[(Me_2SiNDipp)_2Ge(\mu\text{-}S)]_2$ (**14**). Another potential indicator of intraligand repulsion would be the presence of substantial widening of the Ge-N-C(ipso, Dipp) angles as the cofacial Dipp groups in **14** are pushed away from each other (and away from the Ge centers). In compound **14**, the average Ge-N-C(ipso, Dipp) angles are 128.8(5)° and indicate that the Dipp groups in this complex subtend at an angle that is only *ca*. 3° wider than in the precursor **12**. This data suggests that, despite some increase in intraligand repulsion involving the Dipp groups in **14**, the overall level of intraligand strain in this dimer is still relatively low, thus the dimerization of putative $[(Me_2SiNDipp)_2Ge{=}S]$ units can still proceed to form **14**.

2.3.8 Synthesis of ligand frameworks bearing sterically expanded triarylsilyl groups, $(4\text{-}RC_6H_4)_3Si$- (R = ^{i}Pr and ^{t}Bu)

Earlier in this Chapter it was shown that replacement of Dipp groups by "umbrella-shaped" triphenylsilyl, -$SiPh_3$, moities within [NSiN] chelates lead to

an increase in the overall steric bulk of the resulting ligand.[32a] Building upon this concept, the synthesis of sterically expanded analogues with the flanking triarylsilyl groups contained pendant ^{t}Bu and ^{i}Pr functionlity at the para-positions of the aryl rings (4-$RC_6H_4)_3Si$- (R = ^{i}Pr and ^{t}Bu) was explored.

Somewhat surprisingly, examples of species with the desired triarylsilyl motifs (4-$RC_6H_4)_3Si$- (R = ^{i}Pr and ^{t}Bu) were unknown in the literature prior to the investigations outlined in this Chapter. Consequently, new synthetic routes to the requisite silylamine ligand precursors (4-$RC_6H_4)_3SiNH_2$ (R = ^{i}Pr and ^{t}Bu) had to be developed. The first step in the general procedure outlined in Scheme 2.4 involved the preparation of the hindered triarylsilylchlorides (4-$RC_6H_4)_3SiCl$ (R = ^{i}Pr and ^{t}Bu; **15** and **16**) *via* the condensation of aryl Grignard reagents 4-RC_6H_4MgBr with $SiCl_4$. Fortunately the selective installation of three aryl groups at silicon was possible in high yield and conversion of the chlorosilanes **15** and **16** into the target silylamines (4-$RC_6H_4)_3SiNH_2$ (R = ^{i}Pr and ^{t}Bu; **17** and **18**) was readily accomplished by treating the chlorosilanes with a slight excess of $Li[NH_2]$ in THF. The silane reagents **15**-**18** were each obtained as lipophilic, moisture-sensitive colorless solids, while the ^{i}Pr-substituted (cumyl) derivatives **15** and **17** were characterized further by single-crystal X-ray crystallography (Figure 2.7); the metrical parameters for both **15** and **17** were within expected values and thus will not be discussed further in this Thesis.

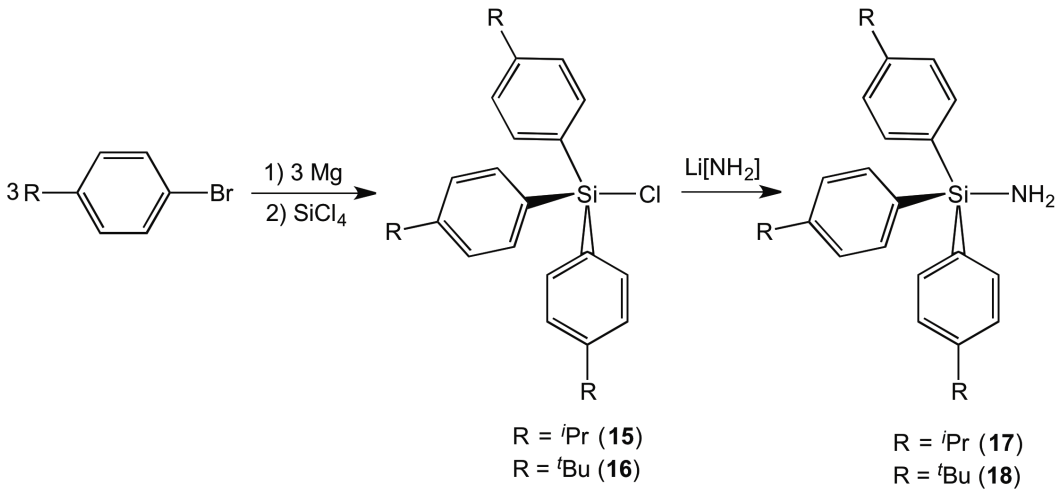

Scheme 2.4. Synthesis of the hindered triarylchlorosilane and triarylsilylamine precursors **15** -**18**.

With the silylamine (4-^{i}PrC$_6$H$_4$)$_3$SiNH$_2$ (**17**) in hand, both the monosilyl [(4-^{i}PrC$_6$H$_4$)$_3$SiNH]$_2$Si(tolyl)$_2$ **19** and disilyl-bridged [(4-^{i}PrC$_6$H$_4$)$_3$SiNHSiMe$_2$]$_2$ **20** ligand precursors were then prepared using the straightforward one-pot procedures outlined in Scheme 2.4. In the case of the monosilyl precursor [(4-^{i}PrC$_6$H$_4$)$_3$SiNH]$_2$Si(tolyl)$_2$ (**19)** the presence of the backbone-positioned tolyl groups were used to add structural rigidity to the ligand framework and to serve as spectroscopic handles. Both bis(amine) precursors **19** and **20** were obtained as analytically pure, moisture-sensitive materials in 58 and 77% yields, respectively, and exhibited NMR and IR spectral data consistent with the assigned structures.

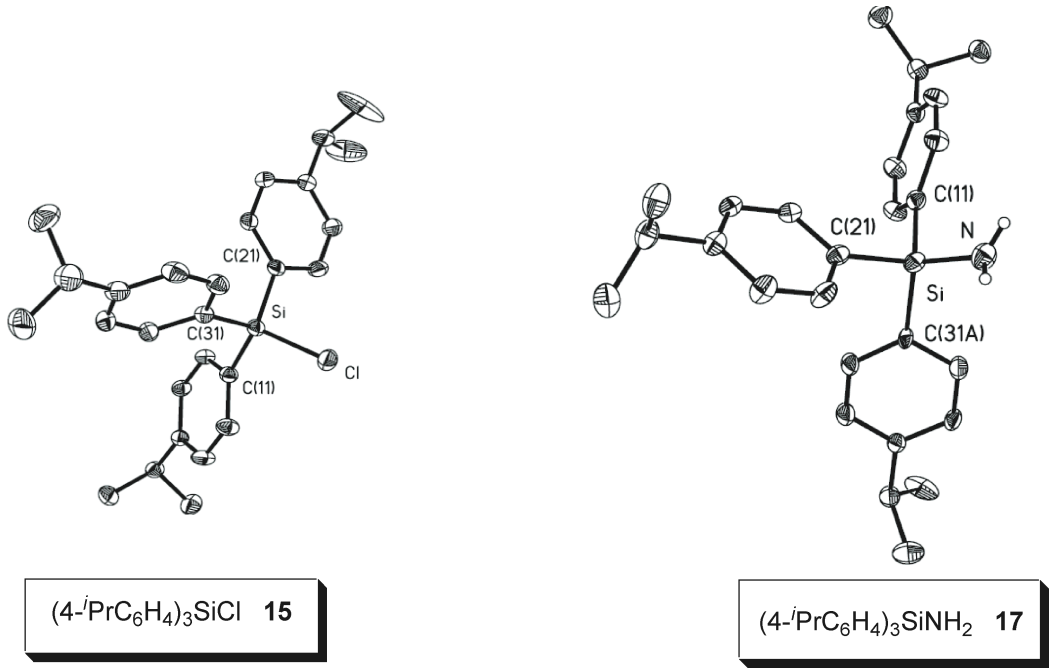

Figure 2.7. Molecular structures of $(4\text{-}^{i}PrC_6H_4)_3SiCl$ (**15**) and $(4\text{-}^{i}PrC_6H_4)_3SiNH_2$ (**17**) with thermal ellipsoids at a 30% probability level. All carbon-bound hydrogen atoms have been omitted for clarity; values due to a disorded $4\text{-}^{i}PrC_6H_4$ group in **17** are listed in square brackets. Selected bond lengths [Å] and angles [°]: **15**: Si-Cl 2.0841(6), Si-C(11) 1.8573(17), Si-C(21) 1.8605(18), Si-C(31) 1.8569(18); Cl-Si-C angles: 107.41(6) to 111.64(8), C-Si-C angles: 110.44(8) to 111.64(8). **17**: Si-N 1.7144(16), Si-C(11) 1.8679(15), Si-C(21) 1.8721(15), Si-C(31) 1.881(4) [1.884(5)]; N-Si-C angles: 105.3(6) to 113.6(4); C-Si-C angles: 103.4(3) to 109.8(5).

It was significantly difficult to construct the ligand analogues to **19** and **20** with *para*-^{t}Bu substituents in place of ^{i}Pr. For example, when $^{i}Pr_2SiCl_2$ was reacted with *in situ* generated $[(4\text{-}^{t}BuC_6H_4)_3SiNH]Li$, complex product mixtures were obtained from which the desired *tert*-butylated silylbis(amine) ligand precursors could not be isolated in pure form. One contributing reason for the lack of success lies in the extreme solubility of these *tert*-butylated derivatives that precluded further purification of the impure products by crystallization; moreover, attempts

to triturate the oily products with $Me_3SiOSiMe_3$ or lyophilization with benzene also failed to yield tractable products.

Motivated by the successful use of ^{i}Pr-bound aryl groups within ligand designs to aid in crystallization/purification,[37,17b] the remaining synthetic efforts were focused on [NSiN] and [NSiSiN] chelates bearing $(4\text{-}^{i}PrC_6H_4)_3Si$- substituents at the ligating nitrogen atoms.

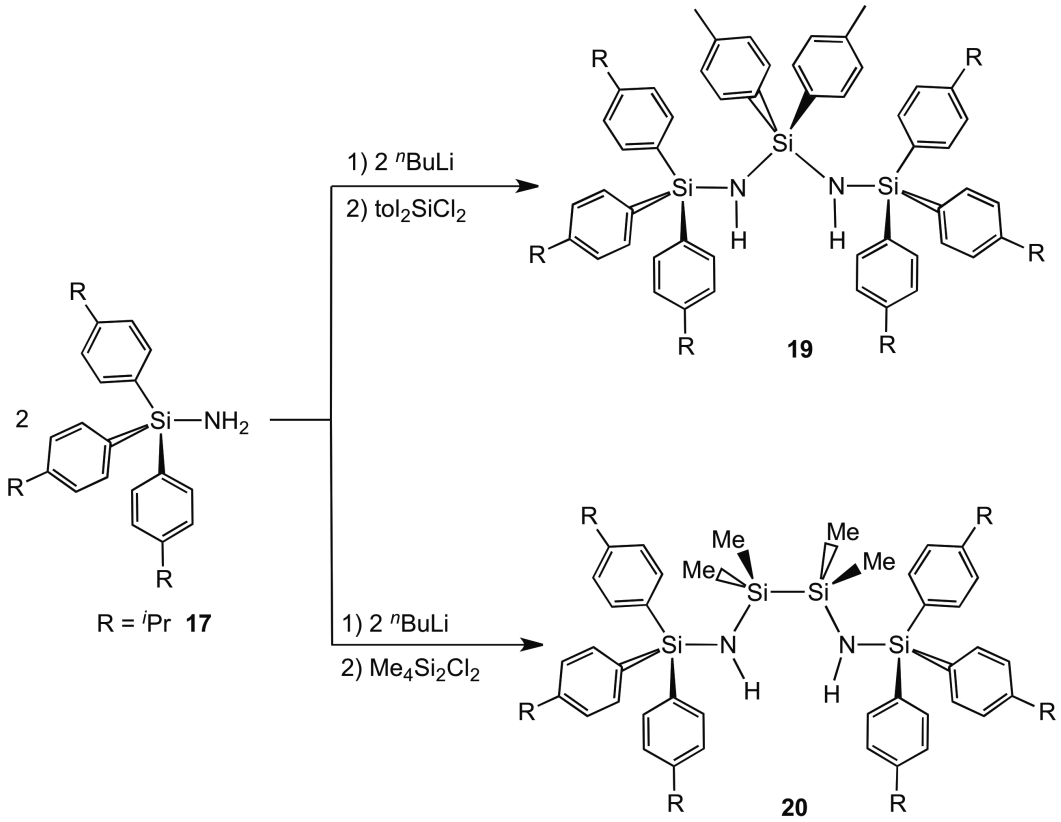

Scheme 2.5. Synthesis of the silyl and disilyl bis(amine) ligand precursors $[(4\text{-}^{i}PrC_6H_4)_3SiNH]_2Si(tol)_2$ **(19)** and $[(4\text{-}^{i}PrC_6H_4)_3SiNHSiMe_2]_2$ (**20**).

2.3.9 Synthesis of the monomeric N-heterocyclic germylenes and stannylenes, (21 and 22) containing modified [NSiSiN] ligands

In order to access new low-valent germylene complexes with $[NSiN]^{SiAr3}$ and $[NSiSiN]^{SiAr3}$ chelates, a procedure similar to that outlined in Scheme 2.3 was used (Scheme 2.6). The required dilithio-amide precursors $[tol_2Si\{(4\text{-}^{i}PrC_6H_4)_3SiN\}_2]Li_2$ and $[\{Me_2Si(4\text{-}^{i}PrC_6H_4)_3SiN\}_2]Li_2$ were each generated *in situ* via the reaction of the bis(amines) **19** and **20** with two equivalents of ^{n}BuLi in diethyl ether, and then reacted with $GeCl_2$•dioxane to afford the air- and moisture-sensitive germylenes $[\{tol_2Si[(4\text{-}^{i}PrC_6H_4)_3SiN]_2\}Ge:]$ **(21)** and $[\{Me_4Si_2[(4\text{-}^{i}PrC_6H_4)_3SiN]_2\}Ge:]$ (**22**) in moderate yields. Compounds **21** and **22** were obtained as colorless and pale yellow air- and moisture-sensitive solids, with the germylene **21** decomposing at 245 °C under a nitrogen atmosphere, while the disilylamido germylene heterocycle **22** exhibited a much lower decomposition temperature of 80 °C. The solid-state structure of the **21** could not be verified by X-ray crystallography, however, crystals of **22** of suitable quality for single-crystal X-ray crystallography were obtained from a cold (-35 °C) hexanes/$Me_3SiOSiMe_3$ solution (Figure 2.8). The five-membered germylene heterocycle $[\{Me_4Si_2[(4\text{-}^{i}PrC_6H_4)_3SiN]_2\}Ge:]$ (**22**) is monomeric in the solid state (Figure 2.8) with a planar GeNSiSiN ring and mutually eclipsed backbone $SiMe_2$ groups [N(1)-Si(1)-Si(2)-N(2) torsion angle = 1.74(6)°]. What is evident upon inspection of the structure of **22** is that the flanking nitrogen-bound $(4\text{-}^{i}PrC_6H_4)_3Si$ groups serve to create a much tighter steric pocket about the Ge center when compared to the Dipp analogue $[(Me_2SiNDipp)_2Ge:]$ **(12)**. The backbone Si-Si bond length in **22** [2.3400(15) Å] is the same within experimental error as the

related linkage in **12**, while the Ge-N bond lengths in **22** [1.875(3) and 1.886(3) Å] are typical for single bonding interactions and suggest a lack of appreciable Ge-N π-bonding within the heterocycle.

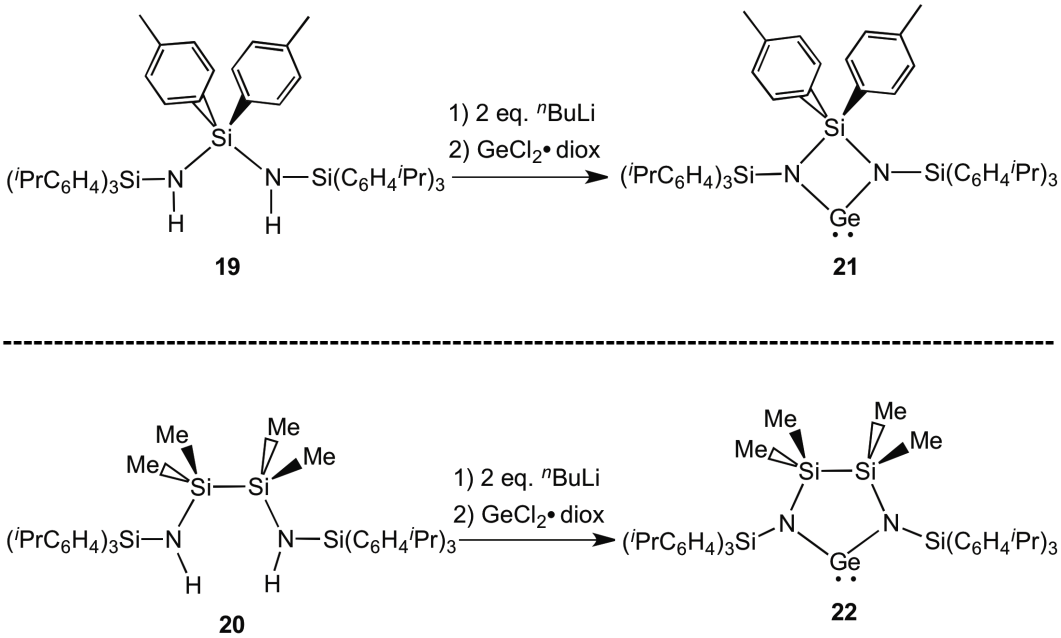

Scheme 2.6. Synthesis of the germylene complexes [{tol$_2$Si[(4-^{i}PrC$_6$H$_4$)$_3$SiN]$_2$}Ge:] (**21**) and [Me$_4$Si$_2$[(4-^{i}PrC$_6$H$_4$)$_3$SiN]$_2$}Ge:] (**22**).

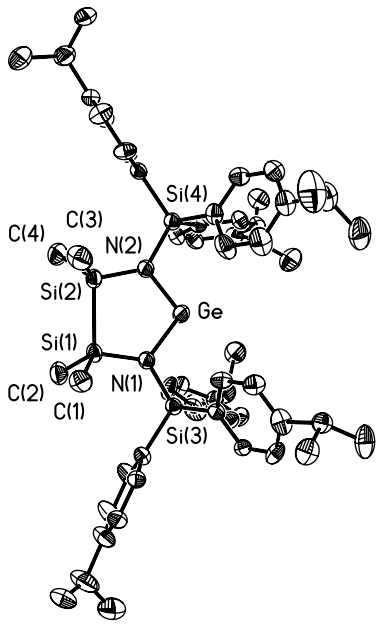

Figure 2.8. Molecular structure of [{Me_4Si_2[(4-^{i}PrC_6H_4)$_3$SiN]$_2$}Ge:] (**22**) with thermal ellipsoids at a 30% probability level. All hydrogen atoms and disordered 4-^{i}PrC_6H_4 groups have been omitted for clarity. Selected bond lengths [Å] and angles [°]: Ge-N(1) 1.875(3), Ge-N(2) 1.886(3), Si(1)-Si(2) 2.3400(15), Si(1)-N(1) 1.744(3), Si(2)-N(2) 1.745(3), N(1)-Si(3) 1.732(3), N(2)-Si(4) 1.737(3); N(1)-Ge-N(2) 101.46(13), N(1)-Si(1)-Si(2) 99.30(11), N(2)-Si(2)-Si(1) 99.53(11), Ge-N(1)-Si(1) 119.99(17), Ge-N(1)-Si(3) 110.55(15), Ge-N(2)-Si(2) 119.56(17), Ge-N(2)-Si(4) 110.07(15).

2.2.10 Chalcogen atom-transfer chemistry involving the germylenes [{tol$_2$Si[(4-^{i}PrC_6H_4)$_3$SiN]$_2$}Ge:] (21) and [Me_4Si_2[(4-^{i}PrC_6H_4)$_3$SiN]$_2$}Ge:] (22)

The Ge(II) centers within the monomeric germylenes **21** and **22** were expected to undergo facile oxidation chemistry to yield stable products with germanium centers in the +4 oxidation state. As anticipated, the bis(amido)germylene **21** reacted rapidly with elemental sulfur, however, as with **3** the product obtained was a sulfido-linked dimer, [{(4-^{i}PrC_6H_4)$_3$SiN]$_2$Si(tol)$_2$}Ge(μ-S)]$_2$ (**23**). Due to the high lipophilicity of **23**, the use

of hexamethyldisiloxane as a co-solvent was required to obtain crystals of suitable quality for X-ray crystallography.

The refined structure of $[\{(4\text{-}^{i}PrC_6H_4)_3SiN\}_2Si(tol)_2\}Ge(\mu\text{-}S)]_2$ (**23**) is presented in Figure 2.9 and reveals the formation of a dimeric germanethione containing a similar Ge_2S_2 diamond core arrangement as in **14**; however, in **23** the Ge_2S_2 unit is much more sterically shielded as a result of interdigitating cumyl groups ($4\text{-}^{i}PrC_6H_4$) that are positioned on each side of the Ge_2S_2 core. Furthermore, the close intraligand interactions between the cumyl side groups results in significant intraligand repulsion which is manifested in the form of wide Ge-N-$SiAr_3$ angles of 141.76(17) and 142.01(18)°. For comparison, the related angles in $[^{i}Pr_2Si(NSiPh_3)_2Ge(\mu\text{-}S)]_2$ (**9**) were, on average, considerably smaller [135.07(11)°].[32a] Despite the substantial buckling of the $(4\text{-}^{i}PrC_6H_4)_3Si$ groups in **23**, the Ge-S bond lengths [2.2253(10) and 2.2392(9) Å] are similar to the Ge-S bond lengths noted within related sulfido-bridged Ge(IV) complexes featuring silylamido chelates [2.1992(3) to 2.2577(3)].[32a]

Unfortunately our attempts to react the sterically shielded germylene $[Me_4Si_2[(4\text{-}^{i}PrC_6H_4)_3SiN]_2Ge:]$ (**22**) with elemental sulfur failed to yield clean products that could be structurally authenticated. When the reaction of **22** with one atom equiv. of sulfur was conducted, significant amount (ca. 20-30%) of unreacted **22** was noted along with another major product (ca. 50% spectroscopic yield). Increasing the amount of sulfur in the reaction to two equiv. improved the spectroscopic yield of the major species to *ca*. 60%, however, our efforts to separate this product from the remaining byproducts (at least four by ^{1}H NMR

spectroscopy) *via* fractional crystallization were unsuccessful. At this stage it is unknown if monomeric germanium polysulfides, such as $[Me_4Si_2\{(4\text{-}{}^iPrC_6H_4)_3SiN\}_2]Ge(S)_x$ (x = 2, 3…), are formed (as in the case of the reaction of Tbt(Trip)Ge: with S_8)[10] or if bridging sulfido Ge-S_x-Ge moieties are present. Moreover, attempts to selectively oxidize **22** with Me_3NO or MesCNO[13] to give the germanium(IV) oxo complex $[Me_4Si_2\{(4\text{-}{}^iPrC_6H_4)_3SiN\}_2]Ge(O)$ gave multiple products as confirmed by NMR spectroscopy. Interestingly, a number of downfield-positioned $SiMe_2$ ^1H NMR resonances (relative to in **22**) were observed and suggested that oxidation of the backbone Si-Si linkages in **22** to give siloxane moieties, -$SiMe_2OSiMe_2$- transpired. Support for this mode of reactivity exists in the literature, wherein the oxidation of Si-Si bonds by Me_3NO has been reported by various groups.[37]

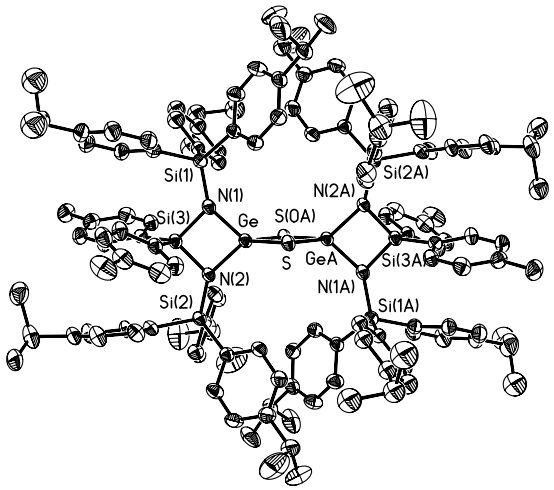

Figure 2.9. Molecular structure of $[\{[(4\text{-}{}^iPrC_6H_4)_3SiN]_2Si(tol)_2\}Ge(\mu\text{-}S)]_2$ (**23**) with thermal ellipsoids at a 30% probability level. All hydrogen atoms and solvate molecoles have been omitted for clarity. Selected bond lengths [Å] and angles [°]: Ge-S 2.2253(10), Ge-S´ 2.2392(9), Ge-N(1) 1.837(3), Ge-N(2) 1.850(3), N(1)-Si(1) 1.738(3), N(1)-Si(3) 1.764(3), N(2)-Si(2) 1.741(3), N(2)-Si(3) 1.762(3); S-Ge-S´ 95.14(3), Ge-S-Ge´ 84.86(3), N(1)-Ge-N(2) 85.68(12), Ge-N(1)-Si(1) 142.01(18), Ge-N(2)-Si(2) 141.76(17), Ge-N(1)-Si(3) 91.85(14), Ge-N(2)-Si(3) 91.43(12), N(1)-Si(3)-N(2) 85.68(12).

2.4 Conclusion

The synthesis of a ligand class featuring "umbrella" triarylsilyl motifs has been developed. This ligand class offers significant potential for the kinetic stabilization of low-coordinate bonding environments in the realm of main group and transition-metal chemistry. A number of low coordinate-germylenes and stannylenes featuring each ligand set were synthesized in order to inspect the level of steric coverage offered by these amidosilyl ligands. The N-heterocylic germylenes were further reacted with chalcogen sources, such as Me_3NO and S_8, with the goal of accessing kinetically stabilized three-coordinate germanones (LGe=O) and germathiones (LGe=S) (L = [NSiN] and [NSiSiN] chelates). Unfortunately, the exclusive formation of thermodynamically favorable germanes with σ-bonded Ge_2O_2 and Ge_2S_2 cores was observed. Modification of the amidosilyl ligands was explored by incorporating substituents on the phenyl rings, and these alterations allowed extension of steric protection deeper into the coordination sphere of the chelated Ge atoms. Despite these structural adjustments, the formation of dimeric species $[(LGeS)_2]$ was noted upon oxidative addition of sulfur. The inherent structural flexibility of these amidosilyl ligands limit their application for the kinetic stabilization of highly reactive bonds such as Si=O, Ge=O and Ge=S; nevertheless, the ease of synthesis and high level of substituent control with the reported ligands might lead to future advances in metal-mediated catalysis.

2.5 Experimental Section

2.5.1 Materials and Instrumentation

All reactions were performed using standard Schlenk techniques under an atmosphere of nitrogen or in a nitrogen-filled glove box (Innovative Technology, Inc.). Solvents were dried using a Grubbs-type solvent purification system[38] manufactured by Innovative Technology, Inc., and degassed (freeze-pump-thaw method) and stored under an atmosphere of nitrogen prior to use. 2,6-Diisopropylaniline, *n*-butyl lithium (2.5 M or 1.6 M solution in hexanes), $GeCl_2$•dioxane, $SnCl_2$, $Li[NH_2]$, magnesium, iodine, triphenyl chlorosilane and elemental sulfur were purchased from Aldrich and used as received. Dichloroditolylsilane, dichlorodiisopropylsilane and dichlorotetramethyldisilane were obtained from Gelest, degassed (freeze-pump-thaw) and stored under an N_2 atmosphere prior to use. Anhydrous Me_3NO (Aldrich) was recrystallized from dry and degassed DMF layered with hexanes (-35 °C). 4-$^{i}PrC_6H_4Br$, 4-$^{t}BuC_6H_4Br$, Li[NHDipp] (Dipp = 2,6-$^{i}Pr_2C_6H_3$) and MesCNO (Mes = 2,4,6-$Me_3C_6H_2$) were prepared according to literature procedures.[39-42] ^{1}H, $^{13}C\{^{1}H\}$, $^{29}Si\{^{1}H\}$ and $^{119}Sn\{^{1}H\}$ NMR spectra were recorded on a Varian iNova-400 spectrometer and referenced externally to $SiMe_4$ (^{1}H, $^{13}C\{^{1}H\}$, $^{29}Si\{^{1}H\}$) and $SnMe_4$ ($^{119}Sn\{^{1}H\}$) by setting the resonance for residual H, C, Si and Sn at 0.0 ppm. X-ray crystallographic analyses were performed by the X-ray Crystallography Laboratory at the University of Alberta. Elemental analyses and mass spectrometry were performed by the Analytical and Instrumentation Laboratory at the University of Alberta. Infrared spectra were recorded with a Nic-Plan FTIR

Microscope. Melting points were obtained in sealed glass capillaries under nitrogen using a MelTemp melting point apparatus and are uncorrected.

2.5.2 X-ray Crystallography

Crystals of appropriate quality for single-crystal X-ray diffraction studies were removed from either a Schlenk tube under a stream of nitrogen, or from a vial (glove box) and immediately covered with a thin layer of hydrocarbon oil (Paratone-N). A suitable crystal was then selected, attached to a glass fiber, and quickly placed in a low-temperature stream of nitrogen.[43] All data were collected using a Bruker APEX II CCD detector/D8 diffractometer using Mo or Cu Ka radiation, with the crystal cooled to -100 °C. The data were corrected for absorption through use of a multiscan model (SADABS[44] [**2**, **5**, **6**] or TWINABS[45] [**7**]) or through Gaussian integration from indexing of the crystal faces. Structures were solved using the direct methods programs SHELXS-97[46] (compounds **1**, **2**, **7**, **9**, **12**, **14**, **15**, **17**, **22** and **23**) and SIR97[47] (compound **5**, **6**, **8**, **10** and **13**), or using the Patterson search/structure expansion facilities within the DIRDIF-2008[48] and SHELXD[51] program suites (compound **4** and **12**). Refinements were completed using the program SHELXL-97.[46] Hydrogen atoms were assigned positions based on the sp^2 or sp^3 hybridization geometries of their attached carbon or nitrogen atoms, and were given thermal parameters 20% greater than those of their parent atoms. See Tables 2.1 – 2.6 for a listing of the crystallographic data.

2.5.2.1 Special Refinement Conditions

Compound **7**: The crystal used for data collection exhibited nonmerohedral twinning. Both components were indexed with the program CELL_NOW.[50] The second twin component can be related to the first component by a 180° rotation about the [1 0 0] axis in reciprocal space and the [1 -0.135 -0.144] axis in real space. Integration intensities for the reflections from the two components were written into a SHELXL-97 HKLF 5 reflection file with the data integration program SAINT (version 7.68 A)[51] using all reflection data (exactly and partially overlapped and nonoverlapped). The following restraints were applied to the disordered solvent Et_2O molecules: O-C, 1.43(1); C-C, 1.53(1); C---C, 2.34(2); O---C, 2.42(2) Å.

Compound **9**: The following restraints were applied to the disordered solvent Et2O molecules: O-C, 1.430(4); C-C, 1.534(4); C---C, 2.340(8); O---C, 2.420(8) Å.

Compound **14**: The following distance restraints were applied to the solvent tetrahydrofuran molecules: O-C, 1.43(1); C-C, 1.53(1) Å. The solvent toluene molecule phenyl ring was constrained to be an idealized hexagon with C-C distances of 1.39 Å, and C22S---C27S and C26S---C27S distances restrained to be 2.51(2) Å.

Compound **18**: The Si-C31A and Si-C31B distances (involving disordered positions for the ipso carbon of one of the 4-isopropylphenyl groups) were constrained to be equal (within 0.02 Å) during the refinement.

Compound **22**: The geometries of the isopropyl groups defined by atoms C27B to C29B and C47B to C49B (the minor orientations) were restrained to be the same as that of C37 to C39. Additionally, the phenyl rings defined by atoms C21A to C26A, C21B to C26B, C31B to C36B, C41A to C46A and C41B to C46B were constrained to be idealized hexagons with C-C distances of 1.39 Å.

Compound **23**: Attempts to refine peaks of residual electron density as disordered or partial-occupancy solvent hexane carbon atoms were unsuccessful. The data were corrected for disordered electron density through use of the SQUEEZE procedure as incorporated in *PLATON*.[52] A total solvent accessible void volume of 591 $Å^3$ with a total electron count of 89 (consistent with 2 molecules of solvent hexane, or 1 molecule per asymmetric unit) was found in the unit cell. The C44B-C47B, C47B-C48B and C47B-C49B distances were restrained to be 1.51(1) Å. The C17-C18A, C17-C19A, C17-C18B and C17-C19B distances were restrained to be the same by the *SHELX* **SAME** instruction. Additionally, the phenyl ring defined by carbon atoms C41B to C46B was constrained to be an idealized hexagon with C-C distances of 1.39 Å.

2.5.3 Synthetic Procedures

2.5.3.1 Preparation of $Ph_3Si\text{-}NH_2$.[11] THF (30 mL) was added to a pre-cooled mixture of Ph_3SiCl (6.02 g, 20.4 mmol) and $Li[NH_2]$ (0.519 g, 22.4 mmol) at -78 °C. The reaction mixture was then warmed to room temperature and stirred overnight to eventually yield a pale-pink solution. The solvent was then removed under vacuum to give an off-white oil. Addition of 50 mL of dry Et_2O to the oil

resulted in the precipitation of a white solid (presumably LiCl), and the mixture was filtered using a filter-tipped cannula. The solvent was then removed from the colorless filtrate to give a white solid that was recrystallized from hexanes (ca. -30 °C) to give pure $Ph_3Si\text{-}NH_2$ as a colorless solid (4.5 g, 80%). ^{1}H NMR (C_6D_6): δ 0.75 (br, 2H, -N*H*$_2$), 7.16-7.19 (m, 9H, Ar*H*), 7.62-7.64 (m, 6H, Ar*H*). ^{13}C{^{1}H} NMR(C_6D_6): δ 128.1 (Ar*C*), 129.8 (Ar*C*), 135.6 (Ar*C*) and 137.3 (Ar*C*). NMR spectroscopic data were also obtained in $CDCl_3$ and matched those reported previously.[4]

2.5.3.2 Preparation of (DippNH)$_2$Si^{i}Pr$_2$ (1). To a white slurry of Li[NHDipp] (1.67 g, 9.10 mmol) in 35 mL of Et_2O at -78 °C was added dropwise ^{i}Pr$_2$SiCl$_2$ (0.85 mL, 4.7 mmol). The reaction mixture was subsequently warmed to room temperature and stirred for 6 h. The resulting white slurry was filtered with a filter-tipped cannula to give a clear colorless solution. Concentration of the filtrate to *ca*. 20 mL followed by cooling to ca. -30 °C produced large colorless blocks of **1** after 2 days (1.16 g, 55%); these crystals were of suitable quality for X-ray crystallography. ^{1}H NMR (C_6D_6): δ 1.06 (d, $^3J_{HH}$ = 6.9 Hz, 12H, CH(C*H*$_3$)$_2$,-Si^{i}Pr$_2$-), 1.20 (d, $^3J_{HH}$ = 6.6 Hz, 24H, CH(C*H*$_3$)$_2$, Dipp), 1.23 (septet, $^3J_{HH}$ = 6.6 Hz, 2H, C*H*(CH$_3$)$_2$, -Si^{i}Pr$_2$-), 2.93 (s, 2H, N*H*), 3.67 (septet, $^3J_{HH}$ = 6.6 Hz, 4H, C*H*(CH$_3$)$_2$, Dipp), and 7.06 - 7.14 (m, 6H, Ar*H*). ^{13}C{^{1}H} NMR (C_6D_6): δ 14.3 (*C*H(CH$_3$)$_2$, -Si^{i}Pr$_2$-), 18.5 (CH(*C*H$_3$)$_2$, -Si^{i}Pr$_2$-), 24.0 (*C*H(CH$_3$)$_2$, Dipp), 28.6 (CH(*C*H$_3$)$_2$, Dipp), 123.7 (Ar*C*), 124.0 (Ar*C*), 140.1 (Ar*C*), and 143.6 (Ar*C*). ^{29}Si{^{1}H} NMR (C_6D_6): δ -11.8. IR (FT-IR microscope/cm^{-1}): 3394 (m, υN-H). Anal. Calcd for

$C_{30}H_{50}N_2Si$: C, 77.19; H, 10.80; N, 6.00. Found: C, 77.17; H, 10.98; N, 6.05. Mp (°C): 104-106.

2.5.3.3 Synthesis of $(Ph_3SiNH)_2Si^iPr_2$ (2). To a solution of Ph_3SiNH_2 (2.53 g, 9.14 mmol) in 30 mL dry diethyl ether was added dropwise one equiv. of ^{n}BuLi (3.66 mL, 9.15 mmol, 2.5 M solution in hexanes) at 0 °C. The reaction mixture was then warmed at room temperature and stirred for 3 h. The resulting white slurry was cooled at -78 °C, then 0.82 mL of $Cl_2Si^iPr_2$ (0.5 equiv., 4.57 mmol) was added dropwise and the mixture was warmed to room temperature and stirred overnight. The resulting mixture was filtered through Celite to give a pale orange colored solution, and subsequent removal of volatiles afforded an orange-colored oil that was recrystallized from diethyl ether (-35 °C) to give colorless crystals of **2** after 3 days (2.05 g, 67%). ^{1}H NMR (C_6D_6): δ 0.69 (septet, $^3J_{HH}$ = 7.6 Hz, 2H, C*H*(CH3)$_2$, -Si^{i}Pr$_2$-), 0.95 (d, $^3J_{HH}$ = 7.6 Hz, 12H, CH(C*H*$_3$)$_2$, -Si^{i}Pr$_2$-), 1.06 (br, 2H, N*H*), 7.13-7.18 (m, 18H, Ar*H*), and 7.71-7.74 (m, 12H, Ar*H*). ^{13}C{^{1}H} NMR (C_6D_6): δ 15.4 (*C*H(CH$_3$)$_2$, -Si^{i}Pr$_2$-), 18.5 (CH(CH$_3$)$_2$, -Si^{i}Pr$_2$-), 128.1 (Ar*C*), 129.9 (Ar*C*), 136.1 (Ar*C*), and 137.3 (Ar*C*). ^{29}Si{^{1}H} NMR ($CDCl_3$): -18.2 (s, -*Si*Ph$_3$), 1.2 (s, -*Si*^{i}Pr$_2$-). IR (FT-IR microscope/cm^{-1}): 3334 (m, υN-H). Anal. Calcd for $C_{42}H_{46}N_2Si_3$: C, 76.08; H, 6.99; N, 4.22. Found: C, 75.82; H, 6.82; N, 4.22. Mp (°C): 121-123.

2.5.3.4 Preparation of [{^{i}Pr$_2$Si(NDipp)$_2$}Ge:], [NSiN]^{Dipp}Ge (3). To a solution of **1** (0.23 g, 0.50 mmol) in 6 mL of Et_2O was added dropwise two equiv. of ^{n}BuLi

(2.5 M solution in hexanes, 0.40 mL, 1.00 mmol) at -35 °C. The resulting mixture was warmed to room temperature and stirred for 1.5 h to give a pale-yellow solution. This solution was then added dropwise to a cold (-35 °C) slurry of $GeCl_2$•dioxane (0.115 g, 0.50 mmol) in 5 mL of Et_2O. Upon the addition of the lithiated ligand, a purple color was generated which dissipated rapidly upon stirring. After the addition was complete, an orange solution was seen over a white precipitate. The resulting slurry was then warmed to ambient temperature and stirred overnight and then filtered through Celite to yield an orange filtrate from which **3** was isolated as a tan colored solid upon removal of the volatiles (0.251 g, 94%). X-ray quality crystals of **3** (colorless plates) were subsequently obtained by slowly cooling a solution of **3** in Et_2O to -35 °C (2 days). ^{1}H NMR (C_6D_6): δ 1.02 (d, $^3J_{HH}$ = 7.2 Hz, 12H, *C*H(CH_3)$_2$, Dipp), 1.31 (d, $^3J_{HH}$ = 6.8 Hz, 24H, CH(CH_3)$_2$, Dipp, and ^{i}Pr$_2$Si, coincident; confirmed by an ^{1}H-^{13}C HSQC correlation experiment), 1.71 (septet, $^3J_{HH}$ = 6.8 Hz, 2H, C*H*(CH3)$_2$, -Si^{i}Pr$_2$-), 3.80 (septet, $^3J_{HH}$ = 6.8 Hz, 4H, C*H*(CH_3)$_2$, Dipp), 7.10 (m, 2H, Ar*H*), and 7.20 (d, $^3J_{HH}$ = 8.2 Hz, 4H, Ar*H*). ^{13}C{^{1}H} NMR (C_6D_6): δ 18.2 (CH(*C*H_3)$_2$, Dipp), 23.5 (*C*H(CH_3)$_2$, Dipp), 24.2 (*C*H(CH_3)$_2$, -Si^{i}Pr$_2$-), 28.5 (CH(*C*H_3)$_2$, -Si^{i}Pr$_2$-), 123.5 (Ar*C*), 124.4 (Ar*C*), 142.6 (Ar*C*), and 144.1 (Ar*C*). Anal. Calcd for $C_{30}H_{48}GeN_2Si$: C, 67.05; H, 9.00; N, 5.21. Found: C, 66.84; H, 9.29; N, 5.09. Mp (°C): 171-173.

2.5.3.5 Preparation of [{^{i}Pr$_2$Si(NDipp)$_2$}Sn:], [NSiN]^{Dipp}Sn (4). To a solution of **1** (0.270 g, 0.58 mmol) in 6 mL of Et_2O was added dropwise a solution of ^{n}BuLi (2.5 M solution in hexanes, 0.463 mL, 1.16 mmol). The resulting colorless

solution was then stirred for 1.5 h and added dropwise to a cold (-35 °C) slurry of $SnCl_2$ (0.128 g, 0.68 mmol) in 4 mL of Et_2O. After the addition was completed within 15 min, a red-brown solution was observed over unreacted $SnCl_2$. The reaction mixture was then warmed to ambient temperature and stirred for 2 days. The resulting orange slurry was filtered through Celite, and the volatiles were removed from the orange filtrate to give a yellow solid (0.336 g, quantitative yield). Crystals of suitable for X-ray crystallography were subsequently grown by cooling a saturated solution of **4** in Et_2O to -35 °C to afford yellow rods. ^{1}H NMR (C_6D_6): δ 1.04 (d, $^3J_{HH}$ = 7.6 Hz, 12H, CH(CH_3)$_2$, Dipp), 1.28 (br, 24H, CH(CH_3)$_2$, Dipp and ^{i}Pr$_2$Si, coincident; confirmed by a ^{1}H-^{13}C{^{1}H} HSQC correlation experiment), 1.57 (septet, $^3J_{HH}$ =7.6 Hz, 2H, CH(CH$_3$)$_2$, -Si^{i}Pr$_2$-), 3.90 (septet, $^3J_{HH}$ = 6.8 Hz, 4H, CH(CH$_3$)$_2$, Dipp), 7.02 (t, $^3J_{HH}$ = 7.6 Hz, 2H, ArH), and 7.20 (d, $^3J_{HH}$ = 7.6 Hz, 4H, ArH). ^{13}C{^{1}H} NMR (C_6D_6): δ 18.4 (CH(CH$_3$)$_2$, Dipp), 23.3 (CH(CH$_3$)$_2$, Dipp), 24.1 (CH(CH$_3$)$_2$,-Si^{i}Pr$_2$-), 28.0 (CH(CH$_3$)$_2$,-Si^{i}Pr$_2$-), 123.2 (ArC), 123.4 (ArC), 143.6 (ArC), and 144.8 (ArC). ^{119}Sn{^{1}H} NMR (C_6D_6): δ 536. Anal. Calcd for $C_{30}H_{48}N_2SiSn$: C, 61.75; H, 8.29; N, 4.80. Found: C, 60.22; H, 8.65; N, 4.41. Mp (°C): 129-131.

2.5.3.6 Synthesis of [{^{i}Pr$_2$Si(NSiPh$_3$)$_2$}Ge:], [NSiN]^{SiPh3}Ge (5). To a solution of **2** (95 mg, 0.14 mmol) in 10 mL of Et_2O was added dropwise two equiv. of ^{n}BuLi (2.5 M solution in hexanes, 0.120 mL, 0.30 mmol) at -35 °C. The reaction mixture was warmed to room temperature and stirred overnight to give a yellow solution. The solution was then added dropwise to a cold (-35 °C) slurry of $GeCl_2$•dioxane

(0.035 g, 0.15 mmol) in 5 mL of Et_2O. The solution turned red-yellow immediately, and the formation of a white precipitate was observed. The reaction mixture was then warmed to ambient temperature, stirred overnight and filtered yield a clear yellow filtrate from which **5** was isolated as a yellow-colored solid upon removal of the volatiles (88 mg, 84%). X-ray quality crystals (colorless) of **5** were subsequently obtained by slowly cooling a solution in Et_2O (-35 °C, 5 days). ^{1}H NMR (C_6D_6): δ 0.81 (septet, $^3J_{HH}$ = 6.4 Hz, 2H, C*H*$(CH_3)_2$, -Si^{i}Pr$_2$-), 0.87 (d, $^3J_{HH}$ = 6.4 Hz, 12H, CH(C*H*$_3)_2$, -Si^{i}Pr$_2$-), 7.15-7.17 (m, 18H, Ar*H*), and 7.78- 7.80 (m, 12H, Ar*H*). ^{13}C{^{1}H} NMR (C_6D_6): δ 15.0 (*C*H$(CH_3)_2$, -Si^{i}Pr$_2$-), 17.0 (CH(*C*H$_3)_2$, -Si^{i}Pr$_2$-), 128.2 (Ar*C*), 129.9 (Ar*C*), 136.4 (Ar*C*), and 137.3 (Ar*C*). Anal. Calcd for $C_{42}H_{44}GeN_2Si_3$: C, 68.75; H, 6.04; N, 3.82. Found: C, 68.76; H, 5.61; N, 3.79. Mp (°C): 196-198.

2.5.3.7 Synthesis of [{^{i}Pr$_2$Si(NSiPh$_3)_2$}Sn:], [NSiN]^{SiPh3}Sn (6). To a solution of **2** (0.100 g, 0.150 mmol) in 10 mL of Et_2O was added dropwise two equiv. of ^{n}BuLi (2.5 M solution in hexanes, 0.12 mL, 0.30 mmol) at -35 °C. The resulting solution was warmed to room temperature and stirred overnight and then added dropwise to a cold (-35 °C) slurry of $SnCl_2$ (0.029 g, 0.15 mmol) in 5 mL of Et_2O. The reaction mixture was then warmed to ambient temperature and stirred overnight to give a bright-yellow slurry. Filtration of the resulting slurry through Celite yielded a bright-yellow filtrate from which **6** was isolated as a yellow-colored solid upon removal of the volatiles (93 mg, 79%). Crystals of **6** (yellow blocks) were grown by cooling a saturated ether solution to -35 °C for 5 days. ^{1}H NMR (C_6D_6): δ 0.80

(septet, $^{3}J_{HH}$ = 7.2 Hz, 2H, C*H*$(CH_3)_2$, -Si^{i}Pr$_2$-), 0.94 (d, $^{3}J_{HH}$ = 7.2 Hz, 12H, CH$(CH_3)_2$, -Si^{i}Pr$_2$-), 7.16-7.19 (m, 18H, Ar*H*), and 7.77-7.79 (m, 12H, Ar*H*). ^{13}C{^{1}H} NMR (C_6D_6): δ 15.8 (*C*H$(CH_3)_2$, -Si^{i}Pr$_2$-), 17.5 (CH(*C*$H_3)_2$, -Si^{i}Pr$_2$-), 128.1 (Ar*C*), 129.7 (Ar*C*), 136.3 (Ar*C*), and 138.9 (Ar*C*). ^{119}Sn{^{1}H} NMR (C_6D_6): δ 527. Anal. Calcd for $C_{42}H_{44}N_2Si_3Sn$: C, 64.69; H, 5.69; N, 3.59. Found: C, 65.02; H 5.81; N 3.57. Mp (°C): 113-115.

2.5.3.8 Preparation of [{^{i}Pr$_2$Si(NDipp)$_2$}Ge(μ-O)]$_2$, {[NSiN]^{Dipp}-Ge(μ-O)}$_2$ (7). Toluene (10 mL) was added to a mixture of **3** (60 mg, 0.11 mmol) and trimethylamine N-oxide (8.3 mg, 0.12 mmol) in a 20 mL scintillation vial in a glove box. The reaction mixture was stirred overnight at ambient temperature and resulted in the formation of a clear pale-yellow solution. The solution was filtered through Celite, and volatiles were removed in *vacuo* to obtain **7** as a colorless solid (48 mg, 78%), which was recrystallized from hexanes (-35 °C, 7 days). ^{1}H NMR (C_6D_6): δ 0.94 (d, $^{3}J_{HH}$ = 7.5Hz, 24H, CH(C*H*$_3)_2$, -Si^{i}Pr$_2$-), 1.04 (d, $^{3}J_{HH}$ = 6.9 Hz, 24H, CH(C*H*$_3)_2$, Dipp), 1.28 (d, $^{3}J_{HH}$ = 6.9 Hz, 24H, CH(C*H*$_3$), Dipp), 1.58 (septet, $^{3}J_{HH}$ = 6.9 Hz, 4H, C*H*$(CH_3)_2$, -Si^{i}Pr$_2$-), 3.77 (septet, $^{3}J_{HH}$ = 6.9 Hz, 8H, C*H*$(CH_3)_2$, Dipp), and 6.99 - 7.10 (m, 12H, Ar*H*). ^{13}C{^{1}H} NMR (C_6D_6): δ 19.0 (CH(*C*$H_3)_2$, -Si^{i}Pr$_2$-), 19.3 (*C*H$(CH_3)_2$, -Si^{i}Pr$_2$-), 26.2 (*C*H$(CH_3)_2$, Dipp), 28.4 (CH(*C*$H_3)_2$, Dipp), 123.9 (Ar*C*), 125.7 (Ar*C*), 138.2 (Ar*C*), and 146.9 (Ar*C*). Anal. Calcd. for $C_{60}H_{96}Ge_2N_4O_2Si_2$ C, 65.11; H 8.74; N, 5.06. Found: C, 64.02; H, 8.68; N, 5.03. Mp (°C): > 300.

2.5.3.9 Preparation of [{^{i}Pr$_2$Si(NDipp)$_2$}Ge(μ-S)]$_2$, {[NSiN]^{Dipp}Ge(μ-S)}$_2$ (8). of Dry Et_2O (10 mL) was added to a mixture of **4** (60 mg, 0.11 mmol) and one equiv. of sulfur (3.7 mg, 0.12 mmol) in a 20 mL scintillation vial in a glove box. The reaction mixture was stirred overnight at ambient temperature, which resulted in the formation of a clear yellow solution. The solution was filtered through Celite, and volatiles were removed in *vacuo* to give white solid (58 mg, 91%), which was recrystallized from a toluene/hexanes mixture (5:1 ratio, -35 °C, 10 days). ^{1}H NMR (C_6D_6): δ 0.91 (d, $^{3}J_{HH}$ = 7.5 Hz, 24H, CH(CH_3)$_2$,-Si^{i}Pr$_2$-), 1.20 (d, $^{3}J_{HH}$ =7.0 Hz, 24H, CH(CH_3)$_2$, Dipp), 1.29 (d, $^{3}J_{HH}$ =7.0Hz, 24H, CH(CH_3), Dipp), 1.44 (septet, $^{3}J_{HH}$ = 7.5 Hz, 4H, CH(CH$_3$)$_2$, -Si^{i}Pr$_2$-), 3.96 (septet, $^{3}J_{HH}$ = 7.0 Hz, 8H, CH(CH$_3$)$_2$,Dipp), and 6.99-7.17 (m, 12H, ArH). ^{13}C{^{1}H} NMR (C_6D_6): δ 15.6 (*C*H(CH$_3$)$_2$, -Si^{i}Pr$_2$-), 18.7 (CH(*C*H$_3$)$_2$, -Si^{i}Pr$_2$-), 27.6 (*C*H(CH$_3$)$_2$, Dipp), 28.2 (CH(*C*H$_3$)$_2$, Dipp), 124.2 (Ar*C*), 125.6 (Ar*C*), 138.3 (Ar*C*), and 147.6 (Ar*C*). Anal. Calcd for $C_{60}H_{96}Ge_2N_4S_2Si_2$: C, 63.27; H, 8.50; N, 4.92. Found: C, 63.55; H, 8.80; N, 4.59. Mp (°C): > 300.

2.5.3.10 Synthesis of [{^{i}Pr$_2$Si(NSiPh$_3$)$_2$}Ge(μ-S)]$_2$, {[NSiN]^{SiPh3}Ge(μ-S)}$_2$ (9). Diethyl ether (10 mL) was added to a mixture of **5** (51 mg, 0.070 mmol) and sulfur (2.2 mg, 0.069 mmol) in a 20 mL scintillation vial in a glove box. The reaction mixture was stirred for 24 h and resulted in the formation of white slurry. The slurry was filtered through Celite, and the volatiles were removed from the filtrate in *vacuo* to give a white solid (18 mg, 35%). X-ray quality crystals of **9** were obtained by redissolving the product in Et_2O (8 mL), followed by layering

with hexanes (-35 °C, 9 days). ^{1}H NMR (C_6D_6): δ -0.02 (septet, $^3J_{HH}$ = 7.5 Hz, 2H, C*H*(CH_3)$_2$, -Si^{i}Pr$_2$-), 0.51 (d, $^3J_{HH}$ = 7.5 Hz, 12H, CH(C*H*$_3$)$_2$, -Si^{i}Pr$_2$-), 1.15 (septet, $^3J_{HH}$ = 7.5 Hz, 2H, C*H*(CH_3)$_2$, -Si^{i}Pr$_2$-), 1.28 (d, $^3J_{HH}$ = 7.5 Hz, 12H, CH(C*H*$_3$)$_2$, -Si^{i}Pr$_2$-), 6.97 (t, $^3J_{HH}$ = 7.5Hz, 24H, Ar*H*), 7.12 (t, $^3J_{HH}$ = 7.5 Hz, 12H, Ar*H*), and 7.65 (d, $^3J_{HH}$ = 7.5 Hz, 24H, Ar*H*). The ^{13}C{^{1}H} NMR spectrum was uninformative due to the low solubility of the product. Anal. Calcd for $C_{92}H_{108}Ge_2N_4O_2S_2Si_6$ (**9**•2 Et_2O): C, 65.80; H 6.49; N, 3.34. Found: C, 65.35; H, 6.53; N, 3.23. Mp (°C): > 300.

2.5.3.11 Synthesis of {^{i}Pr$_2$Si(NSiPh$_3$)$_2$}Sn-O-NMe$_3$ (10). Diethyl ether (7 mL) was added to a mixture of **6** (92 mg, 0.12 mmol) and Me_3NO (8.9 mg, 0.12 mmol) in a 20 mL scintillation vial in a glove box. The reaction mixture was stirred overnight to give a pale yellow solution. The resulting solution was filtered through Celite, and the volatiles were removed from the filtrate in *vacuo* to yield a pale yellow solid (47 mg, 47%). X-ray quality crystals of **10** were obtained by cooling a saturated Et_2O solution of **10** layered with hexanes (-35 °C, 9 days). ^{1}H NMR (C_6D_6): δ 0.72 (septet, $^3J_{HH}$ = 6.5 Hz, 2H, C*H*(CH_3)$_2$, -Si^{i}Pr$_2$-), 0.99 (d, $^3J_{HH}$ = 6.5 Hz, 6H, CH(C*H*$_3$)$_2$, -Si^{i}Pr$_2$-), 1.30 (d, $^3J_{HH}$ = 6.5 Hz, 6H, CH(C*H*$_3$)$_2$, -Si^{i}Pr$_2$-), 1.81 (s, 9H, (C*H*$_3$)$_3$NO), 7.20-7.24 (m, 18H, Ar*H*), and 8.06-8.08 (m, 12H, Ar*H*). The ^{13}C{^{1}H} NMR spectrum was uninformative due to the low solubility of the product. Anal. Calcd for $C_{50.5}H_{66}N_3O_{1.25}Si_3Sn$ (**10**•0.25 Et_2O•0.75 C_6H_{14}): C, 64.66; H 7.09; N, 4.48. Found: C, 64.44; H, 7.03; N, 4.65. Mp (°C): > 300.

2.5.3.12 Preparation of $(DippNH)_2Si_2Me_4$ (11).[31] To a solution of Li[NHDipp] (1.043 g, 5.69 mmol) in 10 mL of cold (-35 °C) Et_2O was added dropwise a cold (-35 °C) solution of $ClSiMe_2SiMe_2Cl$ (0.532 g, 2.84 mmol) in 5 mL of Et_2O. The resulting mixture was slowly warmed to room temperature and stirred for 12 h to give a yellow solution over a white precipitate. The reaction mixture was then filtered through Celite and the volatiles were removed to yield **11** as a light yellow oil (1.300 g, 98%). ^1H NMR (C_6D_6): δ 0.25 (s, 12H, SiCH_3), 1.21 (d, 24H, $^3J_{HH}$ = 7.2 Hz, CH(CH_3)$_2$), 2.28 (s, 2H, N*H*), 3.47 (septet, 4H, $^3J_{HH}$ = 6.8 Hz, C*H*(CH_3)$_2$) and 7.07-7.18 (m, 6H, Ar*H*). $^{13}C\{^1H\}$ NMR (C_6D_6): δ 1.1 (Si*C*H_3), 26.4 (CH(*C*H_3)$_2$), 29.3 (*C*H(CH_3)$_2$), 124.0 (Ar*C*), 124.8 (Ar*C*), 140.6 (Ar*C*) and 144.7 (Ar*C*). IR (FT-IR microscope/cm^{-1}): 3384 (m, υN-H). Anal. Calcd. for $C_{29}H_{51}N_2Si_2$: C, 71.98; H, 10.62; N, 5.79. Found: C, 71.04; H, 10.30; N, 5.76.

2.5.3.13 Preparation of $[(Me_2SiNDipp)_2Ge:]$ (12). A solution of ^{n}BuLi (3.5 mL, 1.6 M solution in hexanes, 5.6 mmol) was slowly added to a solution of **11** (1.30 g, 2.80 mmol) in 6 mL of Et_2O at -35 °C. The resulting mixture was warmed to room temperature and stirred for 2 h, re-cooled to -35 °C and then slowly added to a slurry of $GeCl_2$•dioxane (0.648 g, 2.80 mmol) in 7 mL of Et_2O. The reaction mixture was then warmed to room temperature and allowed to stir at room temperature for 15 h to give an orange solution over a white precipitate (LiCl). Filtration of the mixture through Celite gave an amber solution, which afforded **12** as a pale orange waxy solid upon removal of the volatiles (1.314 g, 88%). Recrystallization of **12** from hexanes/Et_2O at -35 °C resulted in the formation of

large plate-shaped orange crystals of suitable quality for X-ray crystallography. ^{1}H NMR (C_6D_6): δ 0.22 (s, 12H, SiCH_3), 1.17 (d, 12H, $^{3}J_{HH}$ = 7.2 Hz, CH(CH_3)$_2$), 1.29 (d, 12H, $^{3}J_{HH}$ = 6.8 Hz, CH(CH_3)$_2$), 3.55 (septet, 4H, $^{3}J_{HH}$ = 6.8 Hz, CH(CH$_3$)$_2$), and 7.08-7.18 (m, 6H, ArH). ^{13}C{^{1}H} NMR (C_6D_6): δ 0.8 (SiCH$_3$), 23.0 (CH(CH$_3$)$_2$), 27.5 (CH(CH$_3$)$_2$), 28.1 (CH(CH$_3$)$_2$), 123.9 (ArC), 125.5 (ArC), 139.6 (ArC) and 146.4 (ArC). HR-MS, EI (m/z): Calcd. for [M$^+$]: 540.24115. Found: 540.24176 (Δ ppm = 1.1 ppm). Anal. Calcd. for $C_{28}H_{46}GeN_2Si_2$: C, 62.34; H, 8.59; N, 5.19. Found: C, 62.02; H, 8.83; N, 4.86. Mp (°C) = *ca*. 80 (turns red), 126-132 (melts).

2.5.3.14 Preparation of [(Me$_2$SiNDipp)$_2$Sn:] (13). A solution of ^{n}BuLi (0.623 mL, 1.6 M solution in hexanes, 1.00 mmol) was slowly added to a solution of **11** (0.231 g, 0.50 mmol) in 5 mL of Et_2O at -35 °C. The resulting mixture was warmed to room temperature and stirred for 2 h, then re-cooled to -35 °C and slowly added to a slurry of $SnCl_2$ (0.11 g, 0.55 mmol) in 5 mL of Et_2O. Afterwards, the reaction mixture was warmed to room temperature and stirred for 15 h to give a deep yellow solution over a white precipitate (LiCl). Filtration of the mixture through Celite yielded a pale yellow solution, which afforded a pale yellow solid once the solvent was removed (0.266 g, 91%). This product was recrystallized from cold (-35 °C) Et_2O to give **13** as yellow rhomboid-shaped crystals. ^{1}H NMR (C_6D_6): δ 0.27 (s, 12H, SiCH_3), 1.15 (d, 12H, $^{3}J_{HH}$ = 6.8 Hz, CH(CH_3)$_2$), 1.32 (d, 12H, $^{3}J_{HH}$ = 6.8 Hz, CH(CH_3)$_2$), 3.68 (septet, 4H, $^{3}J_{HH}$ = 6.8 Hz, CH(CH$_3$)$_2$), 7.07-7.10 (m, 2H, ArH) and 7.19 (d, 4H, $^{3}J_{HH}$ = 8.0 Hz, ArH).

$^{13}C\{^1H\}$ NMR (C_6D_6): δ 2.2 (Si*C*H_3), 23.2 (*C*H(CH_3)$_2$), 27.7 (CH(*C*H_3)$_2$), 28.1 (CH(*C*H_3)$_2$), 123.8 (Ar*C*), 124.5 (Ar*C*), 141.5 (Ar*C*) and 145.4 (Ar*C*). HR-MS, EI (m/z): Calcd. for [M^+]: 586.22217. Found: 586.22284 (Δ ppm = 1.1 ppm). Anal. Calcd for $C_{28}H_{46}N_2Si_2Sn$: C, 57.43; H, 7.92; N, 4.78. Found: C, 57.56; H, 8.06; N, 4.86. Mp (°C): 169-171.

2.5.3.15 Preparation of [(Me$_2$SiNDipp)$_2$Ge(μ-S)]$_2$ (14). Elemental sulfur (8.3 mg, 0.26 mmol) and 1**2** (0.149 g, 0.261 mmol) were combined in 5 mL of Et_2O and the resulting reaction mixture was then stirred for 24 h. Removal of the volatiles yielded a white microcrystalline powder from which X-ray quality crystals of **14** (needles) were subsequently grown from a solution of toluene and THF at -35 °C (34 mg, 22%). ^1H NMR (C_6D_6): δ 0.06 (s, 12H, SiCH_3), 1.04 (br, 12H, CH(CH_3)$_2$), 1.23 (d, 12H, $^3J_{HH}$ = 6.8 Hz, CH(CH_3)$_2$), 3.46 (septet, 4H, $^3J_{HH}$ = 6.8 Hz, C*H*(CH_3)$_2$) and 7.02-7.08 (m, 6H, Ar*H*). $^{13}C\{^1H\}$ NMR (C_6D_6): δ 1.2 (br, Si*C*H_3), 26.3 (^{i}Pr), 27.1 (^{i}Pr), 28.2 (^{i}Pr), 125.0 (Ar*C*), 126.1 (Ar*C*), 140.0 (Ar*C*) and 148.3 (Ar*C*). Anal. Calcd. for $C_{56}H_{92}Ge_2N_4S_2Si_4$: C, 58.84; H, 8.11; N, 4.90; S: 5.61. Found: C, 58.84; H, 8.08; N, 4.82; S, 5.71. Mp (°C): 215 (dec.).

2.5.3.16 Synthesis of (4-^{i}PrC$_6$H$_4$)$_3$SiCl (15). The Grignard reagent, (4-^{i}PrC$_6$H$_4$)MgBr was first prepared by slowly adding 4-^{i}PrC$_6$H$_4$Br (29.38 g, 0.148 mol) in 75 mL of THF (75 mL) to dried magnesium metal (4.20 g, 0.170 mol) in 75 mL of THF, followed by heating of the solvent to reflux overnight. The resulting brown solution of (4-^{i}PrC$_6$H$_4$)MgBr was then filtered into a separate

flask, and then slowly added via cannula to a solution of $SiCl_4$ (5.65 mL, 0.049 mol) in 50 mL of THF at -78 °C. The resulting greenish-yellow solution was allowed to warm to room temperature and was then heated under reflux for two days to yield a pale yellow solution. 15 mL of 1,4-dioxane was then added to precipitate the MgX_2 byproduct (in the form of MgX_2•dioxane; X = Cl and/or Br), and the resulting heterogeneous mixture was filtered. Removal of the volatiles from the filtrate afforded a colorless solid that was recrystallized from hexanes (*ca*. 75 mL; -35 °C) to give **15** as colorless X-ray quality crystals (7.635 g, 36%). ^{1}H NMR (C_6D_6): δ 1.07 (d, 18H, $^3J_{HH}$ = 7.0 Hz, CH(C*H*$_3$)$_2$), 2.63 (septet, 3H, $^3J_{HH}$ = 7.0 Hz, C*H*(CH$_3$)$_2$), 7.07 (d, 6H, $^3J_{HH}$ = 8.0 Hz, Ar*H*) and 7.77 (d, 6H, $^3J_{HH}$ = 8.0 Hz, Ar*H*). ^{13}C{^{1}H} NMR (C_6D_6): δ 23.8 (CH(*C*H$_3$)$_2$), 34.4 (*C*H(CH$_3$)$_2$), 126.6 (Ar*C*), 131.0 (Ar*C*), 136.0 (Ar*C*) and 151.6 (Ar*C*). HR-MS, EI (m/z): Calcd. for [M]$^+$: 422.20105. Found: 422.20269 (Δ ppm = 0.3). Anal. Calcd. for $C_{27}H_{33}ClSi$: C, 77.01; H, 7.90. Found: C, 76.79; H, 7.50. Mp (°C): 156-168.

2.5.3.17 Synthesis of (4-^{t}BuC$_6$H$_4$)$_3$SiCl (16). A 500 mL three-necked round bottom flask equipped with a magnetic stirring bar and a condenser was flushed with nitrogen and then charged with dried magnesium turnings (1.1 g, 0.046 mol), 10 mL of THF and a small crystal of iodine. The mixture was stirred at room temperature until the color of the iodine faded away and a solution of 1-bromo-4-tert-butylbenzene (6.0 g, 0.028 mol) in 20 mL of THF was then added dropwise. The resulting brown solution was refluxed overnight, then cooled to room temperature and filtered to remove unreacted magnesium. This solution of aryl

magnesium bromide was then added dropwise to a cold (-78 °C) solution of $SiCl_4$ (1.07 mL, 9.35 mmol) in 20 mL of THF. The reaction mixture was allowed to warm to room temperature and then refluxed overnight to yield a pale green solution. Removal of the volatiles from the solution afforded a white powder that was redissolved in 15 mL of THF and then 6 mL of 1,4-dioxane was added. The resulting slurry was stirred for 2 h and the precipitates were allowed to settle, then the mother liquor was filtered through Celite to yield a colorless filtrate. Removal of the volatiles from the filtrate gave **16** as a white powder that was then recrystallized from THF (5 mL) to yield spectroscopically pure **16** as colorless crystals (1.87 g, 43%). ^{1}H NMR ($CDCl_3$): δ 1.34 (s, 27H, C(C*H*$_3$)$_3$), 7.43 (d, 6H, $^3J_{HH}$ = 8.4 Hz, Ar*H*) and 7.60 (d, 6H, $^3J_{HH}$ = 8.4 Hz, Ar*H*). ^{13}C{^{1}H} NMR ($CDCl_3$): δ 31.4 (C(*C*H$_3$)$_3$), 35.0 (*C*(CH$_3$)$_3$), 125.2 (Ar*C*), 130.0 (Ar*C*), 135.3 (Ar*C*) and 153.8 (Ar*C*). HR-MS, EI (m/z): Calcd. for $[M]^+$: 462.25086. Found: 462.25095 (Δ ppm = 0.2). Mp (°C): 233-235.

2.5.3.18 Synthesis of (4-^{i}PrC$_6$H$_4$)$_3$SiNH$_2$ (17). (4-^{i}PrC$_6$H$_4$)$_3$SiCl (6.435 g, 0.0152 mol) and Li[NH_2] (0.456 g, 0.0199 mol) were combined in 25 mL of THF and the resulting white slurry was stirred overnight. A slightly turbid reaction mixture was obtained and the volatiles were removed under vacuum. The product was extracted with 50 mL of hexanes and the LiCl salt was removed by filtration. The resulting filtrate was cooled to -35 °C to give a crop of colorless crystals, while further concentration and cooling of the mother liquor yielded additional pure **17** as a white solid (combined yield of both crops = 4.896 g, 80%). ^{1}H NMR (C_6D_6):

δ 0.83 (br. s, 2H, NH_2), 1.13 (d, 18H, $^3J_{HH}$ = 7.0 Hz, CH(CH_3)$_2$), 2.70 (septet, 3H, $^3J_{HH}$ = 7.0 Hz, CH(CH$_3$)$_2$), 7.14 (d, 6H, $^3J_{HH}$ = 8.0 Hz, ArH) and 7.72 (d, 6H, $^3J_{HH}$ = 8.0 Hz, ArH). ^{13}C{^{1}H} NMR (C_6D_6): δ 24.1 (CH(CH$_3$)$_2$), 34.5 (CH(CH$_3$)$_2$), 126.3 (ArC), 134.9 (ArC), 136.0 (ArC) and 150.3 (ArC). HR-MS, EI (m/z): Calcd. for [M]$^+$: 401.25388. Found: 401.25374 (Δ ppm = 3.9). Anal. Calcd. for $C_{27}H_{35}NSi$: C, 80.74; H, 8.78; N, 3.49. Found: C, 80.42; H, 8.66; N, 3.48. Mp (°C): 65-70.

2.5.3.19 Synthesis of (4-^{t}BuC$_6$H$_4$)$_3$SiNH$_2$ (18). Compound **16** (1.50 g, 3.2 mmol) and Li[NH$_2$] (0.10 g, 4.4 mmol) were combined in 12 mL of THF and the reagent mixture was stirred for two days at room temperature to give a colorless solution. The solvent was then removed *in vacuo* to yield a white powder. The product was then extracted with 20 mL of Et_2O and the resulting slurry was filtered through Celite to give a colorless solution. Removal of the volatiles from the filtrate afforded spectroscopically pure **18** as a white powder (0.41 g, 28%). ^{1}H NMR ($CDCl_3$): δ 1.32 (s, 27H, C(CH_3)$_3$), 7.38 (d, 6H, $^3J_{HH}$ = 8.1 Hz, ArH) and 7.57 (d, 6H, $^3J_{HH}$ = 8.1 Hz, ArH); the N-H resonance could not be located. ^{13}C{^{1}H} NMR ($CDCl_3$): δ 31.4 (C(CH$_3$)$_3$), 34.9 (C(CH$_3$)$_3$), 124.9 (ArC), 133.6 (ArC), 135.2 (ArC) and 152.5 (ArC). HR-MS, EI (m/z): Calcd. for [M]$^+$: 443.30036. Found: 443.30084 (Δ ppm = 1.1). IR (FT-IR microscope/cm^{-1}): 3390 (br, υN-H). Anal. Calcd. for $C_{30}H_{41}NSi$: C, 81.20; H, 9.31; N, 3.16. Found: C, 81.03; H, 9.07; N, 3.08. Mp (°C): 167-169.

2.5.3.20 Preparation of $[(4\text{-}^{i}PrC_6H_4)_3SiNH]_2Si(tol)_2$ (19). $(4\text{-}^{i}PrC_6H_4)_3SiNH_2$ (0.774 g, 1.92 mmol) was dissolved in 8 mL of Et_2O and cooled to -35 °C. A solution of ^{n}BuLi (1.20 mL, 1.6 M solution in hexanes, 1.92 mmol) was then added dropwise, followed by stirring for 3 h. The resulting slurry was then cooled to -35° C, and neat di-p-tolyldichlorosilane (0.259 mL, 1.01 mmol) was then added followed by stirring at room temperature overnight. The resulting mixture was filtered to yield a colorless filtrate and the volatiles were then removed from the filtrate under vacuum. The crude product was then recrystalized from hexanes (-35 °C) to yield **19** as a white microcrystalline solid (0.568 g, 58%). ^{1}H NMR (C_6D_6): δ 1.14 (d, 36H, $^{3}J_{HH}$ = 6.8 Hz, CH(C*H*$_3$)$_2$), 1.78 (br. s, 2H, N*H)*, 2.08 (s, 3H, tolyl-C*H*$_3$), 2.71 (septet, 6H, $^{3}J_{HH}$ = 6.8 Hz, C*H*(CH$_3$)$_2$), 6.87 (d, 4H, *J* = 8.0 Hz, tolyl-Ar*H*), 7.05 (d, 12H, *J* = 8.0 Hz, Ar*H*), 7.55 (d, 4H, $^{3}J_{HH}$ = 8.0 Hz, tolyl-Ar*H*) and 7.67 (d, 12H, $^{3}J_{HH}$ = 8.0 Hz, Ar*H*). ^{13}C{^{1}H} NMR (C_6D_6): δ 21.5 (tolyl-*C*H$_3$), 24.0 (CH(*C*H$_3$)$_2$), 34.4 (*C*H(CH$_3$)$_2$), 126.1 (Ar*C*), 128.4 (Ar*C*), 134.7 (Ar*C*), 135.6 (Ar*C*), 135.9 (Ar*C*), 136.4 (Ar*C*), 138.7 (Ar*C*) and 149.8 (Ar*C*). IR (FT-IR microscope/cm^{-1}): 3330 (br, υN-H). Anal. Calcd. for $C_{68}H_{82}N_2Si_3$: C, 80.73; H, 8.17; N, 2.77. Found: C, 80.95; H, 8.06; N, 2.77. Mp (°C): 178-181.

2.5.3.21 Synthesis of $[(4\text{-}^{i}Pr\text{-}C_6H_4)_3SiNHSiMe_2]_2$ (20). $(4\text{-}^{i}Pr\text{-}C_6H_4)_3SiNH_2$ (1.04 g, 2.60 mmol) was dissolved in 20 mL of Et_2O and cooled to -35 °C, and a solution of ^{n}BuLi (1.62 mL, 1.6 M solution in hexanes, 2.60 mmol) was added dropwise. The reaction mixture was then stirred for 3 h, cooled to -35 °C, and dichlorotetramethyldisilane (0.245 mL, 1.32 mmol) was then added. The resulting

cloudy white suspension was then warmed to room temperature, stirred for 16 h and filtered through Celite. Removal of the volatiles from the filtrate (*in vacuo*) afforded a viscous yellow oil that was freed from residual LiCl (as evidenced by a flame test) by redissolving the crude material in 10 mL of hexanes, followed by filtration through Celite. Removal of the volatiles from the filtrate gave **20** as a spectroscopically pure pale yellow oil (0.92 g, 77%). ^{1}H NMR (C_6D_6): δ 0.18 (s, 12H, Si(C*H*$_3$)$_2$), 1.02 (br, 2H, N*H*), 1.14 (d, 36H, $^{3}J_{HH}$ = 7.0 Hz, CH(C*H*$_3$)$_2$), 2.71 (septet, 6H, $^{3}J_{HH}$ = 7.0 Hz, C*H*(CH$_3$)$_2$), 7.14 (d, 12H, $^{3}J_{HH}$ = 8.0 Hz, Ar*H*) and 7.83 (d, 12H, $^{3}J_{HH}$ = 8.0 Hz, Ar*H*). ^{13}C{^{1}H} NMR (C_6D_6): δ 2.0 (Si(*C*H$_3$)$_2$), 24.0 (CH(*C*H$_3$)$_2$), 34.5 (*C*H(CH$_3$)$_2$), 126.5 (Ar*C*), 135.2 (Ar*C*), 136.3 (Ar*C*) and 150.3 (Ar*C*). ^{29}Si{^{1}H} NMR (C_6D_6): δ -7.2 (s), -16.6 (s). IR (FT-IR microscope/cm^{-1}): 3349 cm^{-1} (m, υN-H). EI-MS (m/z): 459 {[(4-^{i}PrC$_6$H$_4$)$_3$SiNHSiMe$_2$]$^{+}$, 6%}, 401 {[(4-^{i}PrC$_6$H$_4$)$_3$SiNH$_2$]$^{+}$, 38%}, {[(4-^{i}PrC$_6$H$_4$)$_3$Si]$^{+}$, 22%}. Anal. Calcd. for $C_{58}H_{50}N_2Si_4$: C, 75.92; H, 8.79; N, 3.05. Found: C, 74.29; H, 8.84; N, 2.81; despite repeated attempts the analyses were consistently low in C (*ca*. 2%).

2.5.3.22 Preparation of [tol$_2$Si[(4-^{i}PrC$_6$H$_4$)$_3$SiN]$_2$Ge:] (21). Compound **19** (0.259 g, 0.256 mmol) was dissolved in 7 mL of Et$_2$O and cooled to -35 °C and ^{n}BuLi (320 μL, 1.6 M solution in hexanes, 0.512 mmol) was added dropwise; the reaction mixture was then allowed to warm to room temperature and stirred for 3 h. This solution was then added dropwise to GeCl$_2$•dioxane (59 mg, 0.26 mmol) in 4 mL of Et$_2$O, and stirred overnight to yield a cloudy white mixture. The resulting LiCl precipitate was separated by filtration, and the volatiles were removed from the yellow filtrate to give a white solid that was recrystallized from

Et_2O at -35 °C to give an analytically pure sample of **21** as a colorless microcrystalline solid (95 mg, 34%). ^{1}H NMR (C_6D_6): δ 1.08 (d, 36H, $^3J_{HH}$ = 6.5 Hz, CH(C*H*$_3$)$_2$), 2.08 (s, 6H, tolyl-C*H*$_3$), 2.63 (septet, 6H, $^3J_{HH}$ = 6.5 Hz, ArC*H*(CH$_3$)$_2$), 6.86 (d, 4H, $^3J_{HH}$ = 7.5 Hz, tolyl-Ar*H*), 7.00 (d, 12H, $^3J_{HH}$ = 8.0 Hz, ArH), 7.47 (d, 4H, $^3J_{HH}$ = 7.5 Hz, tolyl-ArH) and 7.65 (d, 12H, $^3J_{HH}$ = 8.0 Hz, Ar*H*). ^{13}C{^{1}H} NMR (C_6D_6): δ 1.5 (Ar-*C*H$_3$), 23.9 (CH(*C*H$_3$)$_2$), 34.3 (*C*H(CH$_3$)$_2$), 126.1 (Ar*C*), 128.7 (Ar*C*), 133.8 (Ar*C*), 134.7 (Ar*C*), 135.6 (Ar*C*), 136.5 (Ar*C*), 139.1 (Ar*C*) and 149.9 (Ar*C*). Anal. Calcd. for $C_{68}H_{80}GeN_2Si_3$: C, 75.46; H, 7.45; N, 2.59. Found: C, 75.23; H, 7.46; N, 2.56. Mp (°C): 245 – 248.

2.5.3.23 Synthesis of [{Me$_4$Si$_2$[(4-^{i}PrC$_6$H$_4$)$_3$SiN]$_2$}Ge:] (22). Silylamine **20** (0.377 g, 0.410 mmol) was dissolved in 14 mL of Et_2O and cooled to -35 °C, and ^{n}BuLi (0.513 mL, 1.6 M solution in hexanes, 0.82 mmol) was added; the reaction mixture was then allowed to warm to room temperature and stirred for 3 h. This resulting solution was then added dropwise to $GeCl_2$•dioxane (95 mg, 0.41 mmol) in 3 mL of Et_2O, and stirred overnight to yield a cloudy yellow mixture. The precipitate was separated by filtration, and the volatiles were removed form the filtrate to give a tacky yellow solid. This product was recrystallized from 5 mL of a 5:1 hexanes/hexamethyldisiloxane mixture at -35 °C to yield pale yellow crystals of **22** of suitable quality for single-crystal X-ray crystallography (154 mg, 38%). ^{1}H NMR (C_6D_6) δ 0.21 (s, 12H, Si(C*H*$_3$)$_2$), 1.12 (d, 36H, $^3J_{HH}$ = 7.0 Hz, CH(C*H*$_3$)$_2$), 2.67 (septet, 6H, $^3J_{HH}$ = 7.0 Hz, C*H*(CH$_3$)$_2$), 7.13 (d, 12H, $^3J_{HH}$ = 8.0 Hz, Ar*H*) and 7.87 (d, 12H, $^3J_{HH}$ = 8.0 Hz, Ar*H*). ^{13}C{^{1}H} NMR (C_6D_6): δ 2.8

(Si(CH$_3$)$_2$), 24.0 (CH(CH$_3$)$_2$), 34.4 (CH(CH$_3$)$_2$), 126.2 (ArC), 135.4 (ArC), 137.0 (ArC) and 150.3 (ArC). Anal. Calcd. for $C_{58}H_{78}GeN_2Si_4$: C, 70.49; H, 7.96; N, 2.83. Found: C, 70.83; H, 7.96; N, 2.79. Mp (°C): 80-83 (dec.).

2.5.3.24 Preparation of [{[(4-^{i}PrC$_6$H$_4$)$_3$SiN]$_2$Si(tol)$_2$}Ge(μ-S)]$_2$ (23). To a mixture of **21** (81 mg, 0.075 mmol) and elemental sulfur (2.4 mg, 0.075 mmol) was added 10 mL of Et_2O. The reaction mixture was stirred overnight at room temperature to give a white suspension that was then filtered through Celite to obtain a pale yellow solution. Removal of volatiles from the filtrate afforded **23** as a white powder (73 mg, 87%). X-ray quality crystals were obtained by cooling a solution of **23** in 2:1 hexanes/hexamethyldisiloxane mixture (6 mL) at -35 °C for 3 days. ^{1}H NMR (C_6D_6) δ 0.14 (d, 36H, $^3J_{HH}$ = 7.0 Hz, CH(CH_3)$_2$), 2.03 (s, 6H, tolyl-CH_3) 2.67 (septet, 6H, $^3J_{HH}$ = 7.0 Hz, CH(CH$_3$)$_2$), 6.71 (d, 4H, $^3J_{HH}$ = 7.5 Hz, ArH), 6.83 (br. d, 12H, $^3J_{HH}$ = 6.5 Hz, ArH), 7.20 (d, 4H, $^3J_{HH}$ = 7.5 Hz, ArH) and 7.41 (br. d, 12H, $^3J_{HH}$ = 6.5 Hz, ArH). ^{13}C{^{1}H} NMR (C_6D_6): δ 21.6 (tolyl-CH$_3$), 24.1 (CH(CH$_3$)$_2$), 34.4 (CH(CH$_3$)$_2$), 125.7 (ArC), 132.4 (ArC), 134.2 (ArC), 136.5 (ArC), 137.3 (ArC), 139.1 (ArC) and 149.1 (ArC); one ArC resonance could not be located. Anal. Calcd. for $C_{136}H_{160}Ge_2N_4S_2Si_6$: C, 73.29; H, 7.24; N, 2.51. Found: C, 73.45; H, 7.20; N, 2.60. Mp(°C): > 260.

Table 2.1: Crystallographic data for **1**-**3**.

Compound	**1**	**2**	**3**
Formula	$C_{30}H_{50}N_2Si$	$C_{42}H_{46}N_2Si_3$	$C_{30}H_{48}GeN_2Si$
formula weight	466.81	663.08	537.38
crystal system	trigonal	monoclinic	monoclinic
space group	$P3_12_1$	$P2_1/c$	$C2/c$
a(Å)	10.2694(3)	10.5347(9)	10.4149(4)
b (Å)		15.3080(13)	23.1176(8)
c (Å)	46.7860(14)	12.1157(10)	13.4528(5)
α (deg)	90	90	90
β (deg)	90	111.6950(10)	107.5710(4
γ (deg)	90	90	3087.9(2)
V (Å^3)	4273.0(2)	1815.4(3)	2823.1(11)
Z	6	2	4
ρ (g cm^{-3})	1.088	1.213	1.156
abs coeff (mm^{-1})	0.102	0.163	1.050
T (K)	173(1)	173(1)	173(1)
$2\theta_{max}$ (°)	55.10	52.92	55.00
total data	38035	14514	13517
unique data (R_{int})	6589 (0.0201)	7441 (0.0232)	3556 (0.0112)
Obs data [$I > 2\sigma(I)$]	6421	7063	3371
params	299	425	155
R_1 [$I > 2\sigma(I)$][a]	0.0331	0.0349	0.0240
wR_2 [all data][a]	0.0894	0.0940	0.0701
max/min $\Delta\rho$ (e$^-$ Å^{-3})	0.282/-0.268	0.533/-0.217	0.317/-0.235

[a] $R_1 = \Sigma \big| \, |F_o| - |F_c| \, \big| / \Sigma |F_o|$; $wR_2 = [\Sigma\, w(F_o^2 - F_c^2)^2 / \Sigma\, w(F_o^4)]^{1/2}$.

Table 2.2: Crystallographic data for **4**-**6**.

Compound	**4**	**5**	**6**
Formula	$C_{30}H_{48}N_2SiSn$	$C_{42}H_{44}GeN_2Si_3$	$C_{42}H_{44}N_2Si_3Sn$
formula weight	583.48	733.65	779.75
crystal system	monoclinic	monoclinic	monoclinic
space group	$P2_1/c$	$P2_1/n$	$P2_1/n$
a(Å)	16.6257(7)	8.6077(9)	8.6497(7)
b (Å)	11.2475(4)	25.628(3)	25.761(2)
c (Å)	17.6079(7)	17.1827(1)	17.1292(13)
α (deg)	90	90	90
β (deg)	110.7814(4)	91.3020(10)	91.3450(10)
γ (deg)	90	90	90
V (Å^3)	3078.4(2)	3789.5(7)	3815.8(5)
Z	4	4	4
ρ (g cm^{-3})	1.259	1.286	1.357
abs coeff (mm^{-1})	0.888	0.935	0.796
T (K)	173(1)	173(1)	173(1)
$2\theta_{max}$ (°)	55.02	55.26	55.06
total data	26638	33203	33162
unique data (R_{int})	7080 (0.0116)	8784 (0.0301)	8760 (0.0228)
Obs data [$I > 2\sigma(I)$]	6777	7290	7616
params	307	433	433
R_1 [$I > 2\sigma(I)$][a]	0.0208	0.0331	0.0284
wR_2 [all data][a]	0.0574	0.0983	0.0787
max/min $\Delta\rho$ (e$^-$ Å^{-3})	0.437/-0.392	0.577/-0.561	0.559/-0.695

[a] $R_1 = \Sigma \big| |F_o| - |F_c| \big| / \Sigma |F_o|$; $wR_2 = [\Sigma\, w(F_o^2 - F_c^2)^2 / \Sigma\, w(F_o^4)]^{1/2}$.

Table 2.3: Crystallographic data for **7**, **8**•Et_2O and **9**•**Et_2O**.

Compound	**7**	**8**•Et_2O	**9**•2Et_2O
Formula	$C_{68}H_{116}Ge_2N_4O_4Si_2$	$C_{64}H_{106}Ge_2N_4OS_2Si_2$	$C_{92}H_{108}Ge_2N_4O_2S_2Si_6$
formula weight	1255.01	1213.01	1679.66
crystal system	triclinic	monoclinic	triclinic
space group	$P\bar{1}$	$P2_1/n$	$P\bar{1}$
a(Å)	12.8221(6)	14.0842(6)	11.766(2)
b (Å)	15.7103(7)	14.8807(7)	13.955(3)
c (Å)	19.1054(9)	16.6170(8)	15.759(3)
α (deg)	82.9780(10)	90	65.862(2)
β (deg)	78.9340(10)	72.296(2)	105.8690(10)
γ (deg)	79.303(10)	90	71.013(2)
V (Å^3)	3696.4(3)	3349.9(3)	2188.5(7)
Z	4	2	1
ρ(g cm^{-3})	1.128	1.203	1.274
abs coeff (mm^{-1})	0.890	1.036	0.866
T (K)	173(1)	173(1)	173(1)
$2\theta_{max}$ (°)	50.50	55.10	55.30
total data	16911	29458	19736
unique data (R_{int})	16911(0.0323)	7700 (0.0156)	10089 (0.0096)
Obs data [$I > 2\sigma(I)$]	13235	7028	9505
params	696	375	530
R_1 [$I > 2\sigma(I)$][a]	0.0411	0.0211	0.0313
wR_2 [all data][a]	0.1229	0.0582	0.0903
max/min $\Delta\rho$ (e$^-$ Å^{-3})	1.164/-0.584	0.444/-0.197	0.995/-0.330

[a] $R_1 = \Sigma \big| \, |F_o| - |F_c| \, \big| / \Sigma |F_o|$; $wR_2 = [\Sigma\, w(F_o^2 - F_c^2)^2 / \Sigma\, w(F_o^4)]^{1/2}$.

Table 2.4: Crystallographic data for **10**-**13**.

Compound	**10**	**12**	**1 3**
Formula	$C_{50.55}H_{66}N_3O_{1.25}Si_3N$	$C_{28}H_{46}GeN_2Si_2$	$C_{28}H_{46}N_2Si_2Sn$
formula weight	938.02	539.44	585.54
crystal system	tetragonal	monoclinic	triclinic
space group	$I4_1/a$	$P2_1/n$	$P\bar{1}$
a(Å)	37.276 (3)	13.5706(4)	9.1347(5)
b (Å)		15.5783(5)	10.0168(5)
c (Å)	13.8978 (13)	14.5196(4)	19.1344(10)
α (deg)	90	90	76.6557(5)
β (deg)	90	97.2967(3)	86.6259(5)
γ (deg)	90	90	66.6516(5)
V (Å^3)	19311 (3)	3044.69(13)	1562.99(14)
Z	16	4	2
ρ(g cm^{-3})	1.291	1.177	1.244
abs coeff (mm^{-1})	0.643	1.102	0.911
T (K)	173(1)	173(1)	173(1)
$2\theta_{max}$ (°)	52.80	55.18	55.10
total data	76297	26915	14072
unique data (R_{int})	9902(0.0421)	7038(0.0159)	7151(0.0072)
Obs data [$I > 2\sigma(I)$]	8417	6181	6802
params	475	298	302
R_1 [$I > 2\sigma(I)$][a]	0.0349	0.0250	0.0186
wR_2 [all data][a]	0.0930	0.0763	0.0586
max/min $\Delta\rho$ (e$^-$ Å^{-3})	1.282/–0.336	0.467/-0.309	0.531/-0.332

[a] $R_1 = \Sigma \big| \, |F_o| - |F_c| \, \big| / \Sigma |F_o|$; $wR_2 = [\Sigma\, w(F_o^2 - F_c^2)^2 / \Sigma\, w(F_o^4)]^{1/2}$.

Table 2.5: Crystallographic data for **14**•Tol•THF, **15** and **17**.

Compound	**14**•Tol•THF	**15**	**1 7**
Formula	$C_{67}H_{108}Ge_2N_4SiOS_2Si_4$	$C_{27}H_{33}ClSi$	$C_{27}H_{35}NSi$
formula weight	1307.2	421.07	401.65
crystal system	triclinic	triclinic	monoclinic
space group	$P\bar{1}$	$P\bar{1}$	$P2_1/n$
a(Å)	9.960(2)	10.1381(3)	15.0786(16)
b (Å)	14.101(3)	11.5933(4)	6.8829(7)
c (Å)	15.228(3)	11.6907(4)	23.297(3)
α (deg)	102.871(3)	83.9233(3)	90
β (deg)	93.857(3)	65.1785(3)	93.6135(14)
γ (deg)	107.097(2)	89.4459(3)	90
V (Å^3)	1972.6(8)	1239.19(7)	2413.0(4)
Z	1	2	4
ρ(g cm^{-3})	1.100	1.128	1.106
abs coeff (mm^{-1})	0.913	0.213	0.110
T (K)	173(1)	173(1)	173(1)
$2\theta_{max}$ (°)	50.50	55.26	52.80
total data	14188	11052	18635
unique data (R_{int})	7124(0.0641)	5692(0.0095)	4941(0.0351)
Obs data [$I > 2\sigma(I)$]	5240	5111	3734
params	363	262	352
R_1 [$I > 2\sigma(I)$][a]	0.0870	0.0497	0.0371
wR_2 [all data][a]	0.2703	0.1428	0.1018
max/min $\Delta\rho$ (e$^-$ Å^{-3})	1.865/-1.461	0.963/-0.491	0.238/-0.233

[a] $R_1 = \Sigma \big| \, |F_o| - |F_c| \, \big| / \Sigma |F_o|$; $wR_2 = [\Sigma\, w(F_o^2 - F_c^2)^2 / \Sigma\, w(F_o^4)]^{1/2}$.

Table 2.6: Crystallographic data for **22** and **23**.

Compound	**22**	**23**
Formula	$C_{55}H_{78}GeN_2Si_4$	$C_{148}H_{188}Ge_2N_4S_2Si_6$
formula weight	988.17	2400.86
crystal system	monoclinic	triclinic
space group	$P2_1/n$	$P\bar{1}$
a(Å)	18.6549(5)	15.3279(11)
b (Å)	16.2623(4)	16.5942(12)
c (Å)	21.0055(5)	16.8715(13)
α (deg)	90	62.851(3)
β (deg)	116.4250(10)	66.564(4)
γ (deg)	90	83.170(4)
V (Å^3)	5706.7(2)	3493.2(4)
Z	4	1
ρ (g cm^{-3})	1.150	1.141
abs coeff (mm^{-1})	1.800	1.668
T (K)	173(1)	173(1)
$2\theta_{max}$ (°)	138.88	140.40
total data	28066	23551
unique data (R_{int})	10446(0.0317)	12426(0.0423)
Obs data [$I > 2\sigma(I)$]	8581	8900
params	694	696
R_1 [$I > 2\sigma(I)$][a]	0.0675	0.0722
wR_2 [all data][a]	0.1928	0.2328
max/min $\Delta\rho$ (e$^-$ Å^{-3})	0.846/-1.623	1.279/-0.829

[a] $R_1 = \Sigma \big| |F_o| - |F_c| \big| / \Sigma |F_o|$; $wR_2 = [\Sigma\, w(F_o^2 - F_c^2)^2 / \Sigma\, w(F_o^4)]^{1/2}$.

2.6 References

(1) (a) King, R. B.; Bisnette, M. B. *J. Organomet. Chem.* **1967**, *8*, 287. (b) Bradley, D. C.; Chisholm, M. H. *Acc. Chem. Res.* **1976**, *9, 273*. (c) Eaborn, C. *J. Organomet. Chem.* **1982**, *239*, 93. (d) Trofimenko, S. *Chem. Rev.* **1993**, *93*, 943. (e) Schrock, R. R. *Acc. Chem. Res.* **1997**, *30*, 9. (f) Cummins, C. C. *Chem. Commun.* **1998**, 1777. (g) Power, P. P. *J. Organomet. Chem.* **2004**, *689*, 3904. (h) MacLachlan, E. A.; Fryzuk, M. D. *Organometallics* **2006**, *25*, 1530. (i) Holland, P. L. *Acc. Chem. Res.* **2008**, *41*, 905. (j) Wolczanski, P. T. *Chem. Commun.* **2009**, 740.

(2) (a) Cummins, C. C.; Baxter, S. M.; Wolczanski, P. T. *J. Am. Chem. Soc.* **1988**, *110*, 8732. (b) Laplaza, C. E.; Cummins, C. C. *Science* **1995**, *268*, 861. (c) Albrecht, M.; van Koten, G. *Angew. Chem., Int. Ed.* **2001**, *40*, 3750. (d) Pool, J. A.; Lobkovsky, E.; Chirik, P. J. *Nature* **2004**, *427*, 527. (e) Betley, T. A.; Peters, J. C. *J. Am. Chem. Soc.* **2004**, *126*, 6252. (f) Gunanathan, C.; Ben-David, Y.; Milstein, D. *Science* **2007**, *317*, 790. (g) Ni, C.; Ellis, B. D.; Long, G. J.; Power, P. P. *Chem. Commun.* **2009**, 2332. (h) Takaoka, A.; Mankad, N. P.; Peters, J. C. *J. Am. Chem. Soc.* **2011**, *133*, 8440. (i) Rodriguez, M. M.; Bill, E.; Brennessel, W. W.; Holland, P. L. *Science* **2011**, *334*, 780. (j) Nguyen, T.; Sutton, A. D.; Brynda, M.; Fettinger, J. C.; Long, G. J.; Power, P. P. *Science* **2005**, *310*, 844.

(3) (a) Uematsu, N.; Fujii, A.; Hashiguchi, S.; Ikariya, T.; Noyori, R. *J. Am. Chem. Soc.* **1996**, *118*, 4916. (b) Mikhailine, A.; Maishan, M. I.; Lough,

A. J.; Morris, R. H. *J. Am. Chem. Soc.* **2012**, *134*, 12266. (c) Daley, C. J. A.; Bergens, S. H. *J. Am. Chem. Soc.* **2002**, *124*, 3680. (d) Zhang, W.; Chai, Y.; Zhang, X. *Acc. Chem. Res.* **2007**, *40*, 1278. (e) Niwa, T.; Nakada, M. *J. Am. Chem. Soc.* **2012**, *134*, 13538. (f) Diéguez, M.; Mazuela, J.; Pamies, O.; Verendel, J. J.; Andersson, P. G. *J. Am. Chem. Soc.* **2008**, *130*, 7208. (g) Monfette, S. Zoë, R. T.; Semproni, S. P.; Chirik, P. J. *J. Am. Chem. Soc.* **2012**, *134*, 4561. (h) Xu, Z. J.; Fang, R.; Zhao, C.; Huang, J. S.; Li, G. Y.; Zhu, N.; Che, C. M. *J. Am. Chem. Soc.* **2009**, *131*, 4405. (i) Hayashi, T. *Acc. Chem. Res.* **2000**, *33*, 354. (j) Knowles, W. S.; Noyori, R. *Acc. Chem. Res.* **2007**, *40*, 1238.

(4) (a) Okazaki, R.; Tokitoh, N. *Acc. Chem. Res.* **2000**, *33*, 625. (b) Resa, I.; Carmona, E.; Gutierrez-Puebla, E.; Monge, A. *Science* **2004**, *305*, 1136. (c) Rupar, P. A.; Staroverov, V. N.; Baines, K. M. *Science* **2008**, *322*, 1360. (d) Wang, Y.; Robinson, G. H. *Chem. Commun.* **2009**, 5201. (e) Fischer, R. C.; Power, P. P. *Chem. Rev.* **2010**, *110*, 3877. (f) Asay, M.; Jones, C.; Driess, M. *Chem. Rev.* **2011**, *111*, 354. (g) Li, J.; Schenk, C.; Goedecke, C.; Frenking, G.; Jones, C. *J. Am. Chem. Soc.* **2011**, *133*, 18622.

(5) (a) Cummins, C. C.; Schaller, C. P.; Van Duyne, G. D.; Wolczanski, P. T.; Chan, A. W. E.; Hoffmann, R. *J. Am. Chem. Soc.* **1991**, *113*, 2985. (b) Fryzuk, M. D. *Can. J. Chem.* **1992**, *70*, 2839. (c) Macbeth, C. E.; Golombek, A. P.; Young, V. G., Jr.; Yang, C.; Kuzera, K.; Hendrich, M. P.; Borovik, A. S. *Science*, **2000**, *289*, 938. (d) Gade, L. H. *Acc. Chem.*

Res. **2002**, *35*, 575. (e) Yandulov, D.; Schrock, R. R. *Science*, **2003**, *301*, 76. (f) Figueroa, J. S.; Cummins, C. C. *Dalton Trans*. **2006**, 2161. (k) Waterman, R. *Dalton Trans*. **2009**, 18.

(6) (a) Lappert, M.; Power, P. P.; Protchenko, A.; Seeber, A. *Metal Amide Chemistry*; John Wiley and Sons Ltd.: West Sussex, UK, **2008**. (b) Dielmann, F.; Back, O.; Ellinger, M. H.; Jerabek, P.; Frenking, G.; Bertrand, G. Science, **2012**, *337*, 1526.

(7) (a) Harris, D. H.; Lappert, M. F. *Chem*. *Commun*. **1974**, 895. (b) Niecke, E.; Flick, W. *Angew*. *Chem*., *Int*. *Ed*. *Engl*. **1974**, *13*, 134. (c) Veith, M. *Angew*. *Chem*., *Int*. *Ed*. *Engl*. **1975**, *14*, 263. (d) Gynane, M. J. S.; Harris, D. H.; Lappert, M. F.; Power, P. P.; Riviére , P.; Rivière-Baudet, M. *Dalton Trans*. **1977**, 2004. (e) Arduengo, A. J.; Harlow, R. L.; Kline, M. *J*. *Am*. *Chem*. *Soc*. **1991**, *113*, 361. (f) Herrmann, W. A.; Denk, M.; Behm, J.; Scherer, W.; Klingan, F. R.; Bock, H.; Solouki, B.; Wagner, M. *Angew*. *Chem*., *Int*. *Ed*. *Engl*. **1992**, *31*, 1485. (g) West, R.; Denk, M. *Pure Appl*. *Chem*. **1996**, *68*, 785. (h) Schmidt, E. S.; Jockisch, A.; Schmidbaur, H. *J*. *Am*. *Chem*. *Soc*. **1999**, *121*, 9758. (i) Stahl, L. *Coord*. *Chem*. *Rev*. **2000**, *210*, 203. (j) Baker, R. J.; Farley, R. D.; Jones, C.; Kloth, M.; Murphy, D. M. *J*. *Chem*. *Soc*., *Dalton Trans*. **2002**, 3844.

(8) (a) Steele, A. R.; Kippings, F. S. *J*. *Chem*. *Soc*. **1929**, 357. (b) Maruoka, K.; Ito, T.; Araki, T.; Shirasaka, T.; Yamamoto, H. *Bull*. *Chem*. *Soc*. *Jpn*. **1988**, *61*, 2975. (c) Mizuhata, Y.; Sasamori, T.; Tokitoh, N. *Chem*. *Rev*.

2009, *109*, 3479. (d) Tokitoh, N.; Kishikawa, K.; Okazaki, R.; Sasamori, T.; Nakata, N.; Takeda, N. *Polyhedron* **2002**, *21*, 563. (e) Witnall, R.; Andrews, L. *J. Phys. Chem.* **1985**, *89*, 3261. (f) Khabashesku, V. N.; Boganov, S. E.; Kudin, K. N.; Margrave, J. L.; Nefedov, O. M. *Organometallics* **1998**, *17*, 5041. (g) Xiong, Y.; Yao, S.; Driess, M. *J. Am. Chem. Soc.* **2009**, *131*, 7562. (h) Muraoka, T.; Abe, K.; Haga, Y.; Nakamura, T.; Ueno, K. *J. Am. Chem. Soc.* **2011**, *133*, 15365.

(9) Li, L.; Fukawa, T.; Matsuo, T.; Hashizume, D.; Fueno, H.; Tanaka, K.; Tamao, K. *Nature Chem.* **2012**, *4*, 361.

(10) For related studies involving chalcogen atom transfer to germylenes, see: (a) Tokitoh, N.; Matsumoto, T.; Manmaru, K.; Okazaki, R. *J. Am. Chem. Soc.* **1993**, *115*, 8855. (b) Matsumoto, T.; Tokitoh, N.; Okazaki, R. *J. Am. Chem. Soc.* **1999**, *121*, 8811. (c) Veith, M.; Becker, S.; Huch, V. *Angew. Chem., Int. Ed. Engl.* **1989**, *28*, 1237. (d) Nagendran, S.; Roesky, H. W. *Organometallics* **2008**, *27*, 457. (e) Yao, S.; Xiong, Y.; Driess, M. *Chem. Eur. J.* **2010**, 1281.

(11) Li, Y.; Banerjee, S.; Odom, A. L. *Organometallics* **2005**, *24*, 3272.

(12) (a) Neumann, W. P. *Chem. Rev.* **1991**, *91*, 311. (b) Lappert, M. F. *Main Group Metal Chem.* **1994**, *17*, 183. (c) Haaf, M.; Schmedake, T. A.; West, R. *Acc. Chem. Res.* **2000**, *33*, 704. (d) Weidenbruch, M. J. *Organomet. Chem.* **2002**, *646*, 39.

(13) (a) Fink, W. *Helv. Chim. Acta* **1964**, *47*, 498. (b) Bush, R. P.; Lloyd, N. C. *J. Chem. Soc. A* **1969**, 257.

(14) (a) Hill, M. S.; Hitchcock, P. B. *Organometallics* **2002**, *21*, 3258. (b) Mansell, S. M.; Russell, C. A.; Wass, D. F. *Inorg. Chem.* **2008**, *47*, 11367.

(15) (a) Veith, M. *Angew. Chem., Int. Ed.* **1987**, *26*, 1. (b) Veith, M.; Grosser, *M. Z. Naturforsch.* **1982**, *37*, 1375.

(16) For related work on N-heterocyclic germylenes (a) Kühl, O.; Lönnecke, P.; Heinicke, *J. Polyhedron* **2001**, *20*, 2215. (b) Kühl, O. *Coord. Chem. Rev.* **2004**, *248*, 411. (c) Zabula, A. V.; Hahn, F. E.; Pape, T.; Hepp, A. *Organometallics* **2007**, *26*, 1972.

(17) (a) Spencer, D. J. E.; Aboelella, N. W.; Reynolds, A. M.; Holland, P. L.; Tolman, W. B. *J. Am. Chem. Soc.* **2002**, *124*, 2108. (b) Stanciu, C.; Richards, A. F.; Fettinger, J. C.; Brynda, M.; Power, P. P. *J. Organomet. Chem.* **2006**, *691*, 2540. (c) Wolf, R.; Brynda, M.; Ni, C.; Long, G. J.; Power, P. P. *J. Am. Chem. Soc.* **2007**, *129*, 6076. (d) Zhu, Z.; Fischer, R. C.; Ellis, B. D.; Rivard, E.; Merrill, W. A.; Olmstead, M. M.; Power, P. P.; Guo, J. D.; Nagase, S.; Pu, L. *Chem. Eur. J.* **2009**, *15*, 5263.

(18) Watkin, J. G.; Click, D. R. *Polymerization Catalysts containing Electron Withdrawing Amide Ligands. WO Patent 9845039*, **1998**.

(19) For the use of $SiPh_3$ groups in ligands, see: (a) Bartlett, R. A.; Power, P. P. *J. Am. Chem. Soc.* **1987**, *109*, 6509. (b) Bott, S. G.; Sullivan, A. C. *J.*

Chem. Soc., Chem. Commun. **1988**, 1577. (c) Wehmschulte, R. J.; Power, P. P. *Inorg. Chem.* **1998**, *37*, 6906. (d) Bindl, M.; Stade, R.; Heilmann, E. K.; Picot, A.; Goddard, R.; Fürstner, A. *J. Am. Chem. Soc.* **2009**, *131*, 9468.

(20) For spectroscopic data, see: (a) Blankenship, C.; Cremer, S. E. *J. Organomet. Chem.* **1989**, *371*, 19. Crystals of non-solvated $Ph_3SiOSiPh_3$ and those containing toluene solvate were isolated in separate reactions, and identified by comparison of their unit cell parameters with those found in the literature: (b) Glidwell, C.; Liles, D. C. *Acta Crystallogr.* **1978**, *B34*, 124. (c) Honle, W.; Manriquez, V.; von Schnering, H. G. *Acta Crystallogr.* **1990**, *C46*, 1982.

(21) (a) Veith, M.; Nötzel, M.; Huch,V. *Z. Anorg. Allg. Chem.* **1994**, *620*, 1264. (b) Klein, B.; Neumann, W. P. *J. Organomet. Chem.* **1994**, *465*, 119. (c) Rakebrandt, H. -J.; Klingebiel, U. *Z. Anorg. Allg. Chem.* **1997**, *623*, 1264.

(22) Ellis, D.; Hitchcock, P. B.; Lappert, M. F. *J. Chem. Soc., Dalton Trans.* **1992**, 3397.

(23) Masamune, S.; Batcheller, S. A.; Park, J.; Davis, W. M.; Yamashita, O.; Ohta, Y.; Kabe, Y. *J. Am. Chem. Soc.* **1989**, *111*, 1888.

(24) Bokii, N. G.; Yu, T.; Struchkov, T.; Kolesnikov, S. P.; Rogozhin, I. S.; Nefedov, O. M. *Izv. Akad. Nauk SSSR, Ser. Khim* **1975**, *4*, 812.

(25) (a) Trinquier, G.; Barthelat, J. C.; Satge, J. *J. Am. Chem. Soc.* **1982**, *104*, 5931. (b) Kapp, J.; Remko, M.; Schleyer, P. v. R. *J. Am. Chem. Soc.* **1996**, *118*, 5745.

(26) (a) Barrau, J.; Rima, G.; Lavayssiere, H.; Dousse, G.;Satge, J. *J. Organomet. Chem.* **1983**, *246*, 227. (b) Tokitoh, N.; Matsumoto, T.; Okazaki, R. *Chem. Lett.* **1995**, 1087. (c) Weidenbruch, M.; Sturmann, M.; Kilian, H.; Pohl, S.; Saak, W. *Chem. Ber.* **1997**, *130*, 735. (d) Samuel, M. S.; Jennings, M. C.; Baines, K. M. *J. Organomet. Chem.* **2001**, *636*, 130. (e) Iwamoto, T.; Masuda, H.; Ishida, S.; Kabuto, C.; Kira, M. *J. Organomet. Chem.* **2004**, *689*, 1337.

(27) Cordero, B.; Gomez, V.; Platero-Plats, A. E.; Revés, M.; Echeverría, J.; Cremades, E.; Barragán, F.; Alvarez, S. *Dalton Trans.* **2008**, 2832.

(28) Edelman, M. A.; Hitchcock, P. B.; Lappert, M. A. *J. Chem. Soc., Chem. Commun.* **1990**, 1116.

(29) Caron, A.; Ralneik, G. J.; Goldish, E.; Donohue, J. *Acta. Cryst.* **1964**, *17*, 102.

(30) For the effective use of $SiAr_3$ groups (Ar = Ph or tolyl) in ligand design, see: (a) Danopoulos, A. A.; Redshaw, C.; Vaniche, A.; Wilkinson, G.; Hussain-Bates, B.; Hursthouse, M. B. *Polyhedron* **1993**, *12*, 1061. (b) Suzuki, E.; Komuro, T.; Kanno, Y.; Okazaki, M.; Tobita, H. *Organometallics* **2010**, *29*, 1839. (c) Malassa, A.; Herzer, N.; Görls, H.;

Westerhausen, M. *Dalton Trans*. **2010**, 5356. (d) Li, J.; Stasch, A.; Schenk, C.; Jones, C. *Dalton Trans*. **2011**, 10448.

(31) Jäger, F.; Roesky, H. W.; Dorn, H.; Shah, S.; Noltemeyer, M.; Schmidt, H. –G. *Chem. Ber./Receuil* **1997**, *130*, 399.

(32) a) Al-Rafia, S. M. I.; Lummis, P. A.; Ferguson, M. J.; McDonald, R.; Rivard, E. *Inorg. Chem*. **2010**, *49*, 9709 and references therein. For recent reports involving related chelates, see: (b) Yang, D.; Guo, J.; Wu, H.; Ding, Y.; Zheng, W. *Dalton. Trans* **2012**, 2187. (c) West, J. K.; Stahl, L. *Organometallics* **2012**, *31*, 2042.

(33) Choi, N.; Asano, K.; Ando, W. *Organometallics* **1995**, *14*, 3146.

(34) For examples of four-coordinate Ge(IV) complexes with NSiSiN chelates, see: Wannagat, v. U.; Seifert, R.; Schlingmann, M. *Z. Anorg. Allg. Chem*. **1978**, *439*, 83.

(35) (a) Horschler, K.; Stader, C.; Wrackmeyer, B. *Inorg. Chim. Acta* **1986**, *117*, L39. (b) Stader, C.; Wrackmeyer, B.; Schlosser, D. *Z. Naturforsch. B* **1988**, *43*, 288. (c) Wrackmeyer, B.; Stader, C.; Horchler, K.; Zhou, H.; Schlosser, D. *Inorg. Chim. Acta* **1990**, *176*, 205.

(36) (a) Power, P. P. *Chem. Rev*. **1999**, *99*, 3463. (b) West, R. *Polyhedron* **2002**, *21*, 467. (c) Weidenbruch, M. *Organometallics* **2003**, *22*, 4348. (d) Jones, C. *Coord. Chem. Rev*. **2010**, *254*, 1273. (e) Wang, Y.; Robinson, G.

H. *Dalton Trans*. **2012**, 337. (f) Sen, S. S.; Khan, S.; Samuel, P. P.; Roesky, H. W. *Chem. Sci*. **2012**, *3*, 659.

(37) Rivard, E.; Power, P. P. *Inorg. Chem*. **2007**, *46*, 10047, and references therein.

(38) Pangborn, A. B.; Giardello, M. A.; Grubbs, R. H.; Rosen, R. K.; Timmers, F. J. *Organometallics* **1996**, *15*, 1518.

(39) Marvel, C. S.; Johnston, H. W.; Meier, J. W.; Mastin, T. W.; Whitson, J.; Himel, C. M. *J. Am. Chem. Soc*. **1944**, *66*, 914.

(40) Hall, M. A.; Xi, J.; Lor, C.; Dai, S.; Pearce, R.; Dailey, W. P.; Eckenhoff, R. G. *J. Med. Chem*. **2010**, *53*, 5667.

(41) Patton, J. T.; Feng, S. G.; Abboud, K. A. *Organometallics* **2001**, *20*, 3399.

(42) (a) Bode, J. W.; Hachisu, Y.; Matsuura, T.; Suzuki, K. *Tetrahedron Lett*. **2003**, *44*, 3555. (b) Barybin, M. V.; Diaconescu, P. L.; Cummins, C. C. *Inorg. Chem*. **2001**, *40*, 2892.

(43) Hope, H. *Prog. Inorg. Chem*. **1993**, *41*, 1.

(44) Sheldrick, G. M. *SADABS*, version 2008/1; Universität Göttingen: Göttingen, Germany, 2008.

(45) Sheldrick, G. M. *TWINABS*, version 2008/2; Universität Göttingen: Göttingen, Germany, 2008.

(46) Sheldrick, G. M. *Acta Crystallogr*. **2008**, *A64*, 112.

(47) Altomare, A.; Burla, M. C.; Camalli, M.; Cascarano, G. L.; Giacovazzo, C.; Guagliardi, A.; Moliterni, A. G. G.; Polidori, G.; Spagna, R. *J. Appl. Crystallogr.* **1999**, *32*, 115.

(48) Beurskens, P. T.; Beurskens, G.; de Gelder, R.; Smits, J. M. M.; Garcia-Garcia, S.; Gould, R. O. *DIRDIF-2008*; Crystallography Laboratory, Radboud University: Nijmegen, The Netherlands, 2008.

(49) Schneider, T. R.; Sheldrick, G. M. *Acta Crystallogr.* **2002**, *D58*, 1772.

(50) Sheldrick, G. M. *CELL_NOW*, version2008/2; Universität Göttingen: Göttingen, Germany, 2008.

(51) Sheldrick, G. M. *SAINT*, version 7.68A; Bruker AXS Inc.: Madison, WI, 2008.

(52) (a) Sluis, P. v. der; Spek, A. L. *Acta Crystallogr.* **1990**, *A46*, 194. (b) Spek, A. L. *J. Appl. Cryst.* **2003**, *36*, 7. (c) *PLATON* – a multipurpose crystallographic tool. Utrecht University, Utrecht, The Netherlands.

Chapter 3

Donor-Acceptor Stabilization: A New Approach Towards the Isolation of Heavy Group 14 Methylene Analogues

Chapter 3

Donor-Acceptor Stabilization: A New Approach Towards the Isolation of Heavy Group 14 Methylene Analogues

3.1 Abstract

A new synthetic strategy for the isolation of heavy Group 14 element hydrides in the form of stable complexes, LB•EH_2•LA (LB = Lewis base; E = Si, Ge and Sn; LA = Lewis acid), is described in this Chapter. The Lewis base (LB) donates electron density into the empty p orbital of the :EH_2 unit while the Lewis acid (LA) interacts with the lone pair of the :EH_2 array to form stable donor-acceptor adducts, LB•EH_2•LA. The N-heterocyclic carbene IPr [IPr = {$(HCNDipp)_2$}C: and Dipp = 2,6-$^{i}Pr_2C_6H_3$] and the sterically encumbered N-heterocyclic olefin IPr=CH_2 were found to the effective donors, while Lewis acids such as BH_3, $W(CO)_5$ and $Cr(CO)_5$ were appropriate acceptors for the stabilization of the :EH_2 (E = Si, Ge and Sn) units. Thermal decomposition of these donor-acceptor adducts was studied as a potential route for the controlled (low temperature) synthesis of Group 14 (tetrel) elements nanoparticles and nanoclusters. On the basis of the observed decomposition temperatures, it was found that the borane adducts LB•EH_2•BH_3 (E = Si and Ge) are thermally less stable in comparison to the :EH_2 complexes with $W(CO)_5$ or $Cr(CO)_5$ acceptors, while the tin congener IPr•SnH_2•BH_3 could not be prepared. Furthermore, the element-borane interactions (E-BH_3) in the IPr•EH_2•BH_3 (E = Si and Ge) are sufficiently labile in THF to allow the IPr•EH_2 moieties to be transferred onto transition metal centers

such as $W(CO)_5$ or $Cr(CO)_5$. The N-heterocyclic olefin adducts, $IPrCH_2{\bullet}EH_2{\bullet}W(CO)_5$ (E = Ge and Sn) also exhibited clean ligand exchange chemistry with IPr to give $IPr{\bullet}EH_2{\bullet}W(CO)_5$ and free $IPr{=}CH_2$. These $BH_3/W(CO)_5$ and $IPrCH_2$/IPr exchange reaction are noteworthy since they illustrate that the associated donor-acceptor interactions are labile. As anticipated on the basis of electronegativity, the hydrogen atoms within the EH_2 units are hydridic and in the case of the tin(II) hydride adduct $IPr{\bullet}SnH_2{\bullet}W(CO)_5$ clean hydrostannylation chemistry with excess benzaldehyde transpired.

3.2 Introduction

The isolation of reactive inorganic species is an active field of modern synthetic chemistry and often provides considerable fundamental insight into the nature of chemical bonding and reactivity.[1] In general, chemical exploration of the heavy Group 14 elements (E = Si-Pb) is largely motivated by a desire to compare their reactivity to that displayed by the lightest congener, carbon.[2] Experimental verification of important bonding and reactivity patterns within this element group have been uncovered as a result of new advances in synthetic methodology. For example, the preparation of stable heavy element alkyne analogues, ArEEAr (E = Si-Pb), relied upon the development of extremely bulky aryl ligands,[3] while novel main group entities such as disilene :Si=Si:, digermene :Ge=Ge:, P_2, PN, HB=BH and B≡B have been isolated in the condensed phase using N-heterocyclic carbenes (NHCs) as stabilizing ligands.[4]

Historically, compounds featuring main group elements were thought to participate in completely different chemistry as complexes based upon transition metals. However, recent advances in the study of p-block chemistry have uncovered examples of reactivity once thought to be the exclusive domain of transition metal complexes.[5] This transition metal-like behavior originates from the fact that compounds containing heavy main group elements have frontier orbitals (HOMO and LUMO) that are often close in energy and also with a judicious choice of substituents, contain available coordination sites.[1] In 2005, the Power group uncovered the first example of H_2 activation at ambient temperature

using a low-coordinate germanium alkyne analogue, Ar'GeGeAr' (Ar' = C_6H_3-2,6-(C_6H_3-2,6-^{i}Pr$_2$)$_2$) to give the hydrogenated products Ar'(H)GeGe(H)Ar', Ar'$(H)_2$GeGe$(H)_2$Ar' and H_3GeAr'.[7a] The mechanism of the reaction is analogous to that of transition-metal complexes in terms of the overall symmetry of the orbital interactions, whereby a synergistic donation from the σ-orbital of hydrogen into the LUMO of Ar'GeGeAr', and donation from the π-HOMO of the germanium complex into the σ*-orbital of hydrogen is involved.[5,7a] Soon after main group element compounds were shown to activate other small molecules such as CO_2, NH_3, C_2H_4 and C_2H_2.[7]

The highly reactive low oxidation state (+2) Group 14 dihydrides :EH_2 (E = Si-Pb) and their substituted analogues have attracted considerable attention due to their potential role as intermediates in semiconductor syntheses and metal-mediated bond-forming reactions.[8] For example, silylene (:SiH_2) and germylene (:GeH_2) have been postulated as intermediates in the synthesis of semiconducting Si and Ge films and nanostructures *via* the thermal decomposition of silane (SiH_4) and germane (GeH_4), respectively.[8] The lightest member of this series, methylene, can be stabilized *via* M=CH_2 coordination with transition metals (M = transition metal), and participates in many useful C-C bond-forming processes ranging from olefin metathesis to carbonyl methylenations.[9,10] The heavier Group 14 element methylene analogues, :EH_2 (E = Si-Pb), have remained elusive due to a lack of suitable synthetic methods and the expected instability of these entities in the condensed phase.[11,12] In general, E(II) hydrides (E = Ge and Sn) are highly unstable in the absence of very bulky anionic ligands (e.g. (Ar'EH_2)$_2$; Ar' = C_6H_3-

2,6-(C_6H_3-2,6-^{i}Pr$_2$)$_2$),[13] however, free heavy methylene analogues, :EH_2, have been intercepted *via* matrix isolation (<10 K).[12b,14] It has been predicted that these heavy methylene analogues can exhibit dual Lewis acid and basic character due to the presence of a vacant p orbital and low energy lone pair at the Group 14 element center (E). These structural features prompted us to postulate that inorganic methylenes can be isolated in the form of donor-acceptor complexes LB•EH_2•LA. Recently, the use of N-heterocyclic carbenes (NHCs) as σ-donating ligands has proven to be an effective way to isolate/stabilize reactive main group bonding environments.[4] Motivated by these results it was reasoned that NHCs would be suitable Lewis bases to isolate heavy methylenes in the presence of additional Lewis acid acceptor such as BH_3 and $W(CO)_5$.[15]

3.3 Results and discussion

As an entry point into stabilizing heavy methylene analogues as donor-acceptor adducts IPr•EH_2•LA (E = Si-Pb; LA = Lewis acid) it was decided to first prepare a Ge(II) halide carbene adduct IPr•$GeCl_2$ from which halide/hydride metathesis would then afford the desired germanium dihydride complex, IPr•GeH_2•LA. Following prior work in the field,[16] the reaction of N-heterocyclic carbene,[17] IPr, [(HCNDipp)$_2$C:, Dipp = 2,6-^{i}Pr$_2$C$_6$H$_3$] with $GeCl_2$•dioxane[18] in toluene gave the expected adduct IPr•$GeCl_2$ (**1**) as a white moisture-sensitive solid in a 86% yield. The molecular structure of **1** was subsequently verified by X-ray crystallography, and the result is depicted in Figure 3.1.

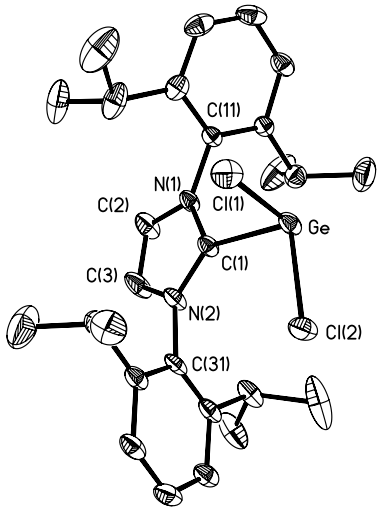

Figure 3.1. Thermal ellipsoid plot (30% probability level) of IPr•$GeCl_2$ (**1**). Hydrogen atoms have been omitted for clarity. Selected bond lengths [Å] and angles [°]: Ge-Cl(1) 2.2810(9), Ge-Cl(2) 2.2731(8), Ge-C(1) 2.112(2); Cl(1)-Ge-Cl(2) 95.95(3), Cl(1)-Ge-C(1) 94.31(8), Cl(2)-Ge-C(1) 97.68(7), N(1)-C(1)-N(2) 104.8(2).

As shown in the Figure 3.1, IPr•$GeCl_2$ (**1**) features a trigonal pyramidal arrangement around the germanium center [angle sum at Ge = 287.94(11)°]. The C_{IPr}-Ge bond length in **1** was determined to be 2.112(2) Å and is longer than the Ge-C single bond distance found in the metallogermylene complex, (η^5-C_5H_5)$(CO)_3$W-Ge-C_6H_3-2,6-$Trip_2$ (Trip = C_6H_2-2,4,6-$^i Pr_3$) [1.99(2) Å],[19] suggesting the presence of a weak dative interaction between the carbene and the $GeCl_2$ fragment in **1**.

With the desired Ge(II) dihalide adduct **1** in hand, its reactivity towards various hydride sources was investigated. Surprisingly, no discernable reaction was observed between **1** and NaH in either THF or Et_2O; similar results were obtained with the hydride sources $HSiEt_3$ and $HSnBu_3$. However, when **1** was

combined with an excess of $Li[BH_4]$ in Et_2O, a new product was formed, as evidenced by NMR spectroscopy (Equation 3.1). Notably, the appearance of additional non-carbene resonances were observed in the ^1H NMR spectrum at δ 3.92 (quartet, $^3J_{HH}$ = 4.8 Hz), along with a broad feature at 0.6-1.6 ppm. The latter resonance is characteristic of a B-H moiety, as close inspection of this signal indicated that a 1 : 1 : 1 : 1 quartet was present (due to coupling of hydrogen with the quadrupolar ^{11}B nucleus, I = 3/2). The presence of boron in the product was also established by ^{11}B NMR spectroscopy, which yielded a quartet resonance at δ -40.0 ($^1J_{BH}$ = 99 Hz), corresponding to a coordinated -BH_3 fragment.[20] The GeH_2 ^1H NMR resonance was located at 3.92 ppm and the quartet pattern of this resonance suggested coupling was occurring between the hydrogen bound to Ge and those of a proximal BH_3 unit. The formation of a germanium hydride was substantiated by the location of an IR stretching band at 1987 cm^{-1};[21] moreover, characteristic υB-H vibrations at 2310 and 2349 cm^{-1} were also observed. For comparison, the Ge-H stretching frequency in the germanium(IV) hydride, $Ar^*_2Ge(H)NH_2$ ($Ar^* = C_6H_3$-2,6-(C_6H_2-2,4,6-$Me_3)_2$) occurs at 2110 cm^{-1}.[21b] The formation of a Ge(II) hydride complex was subsequently confirmed by X-ray crystallography (Figure 3.2).

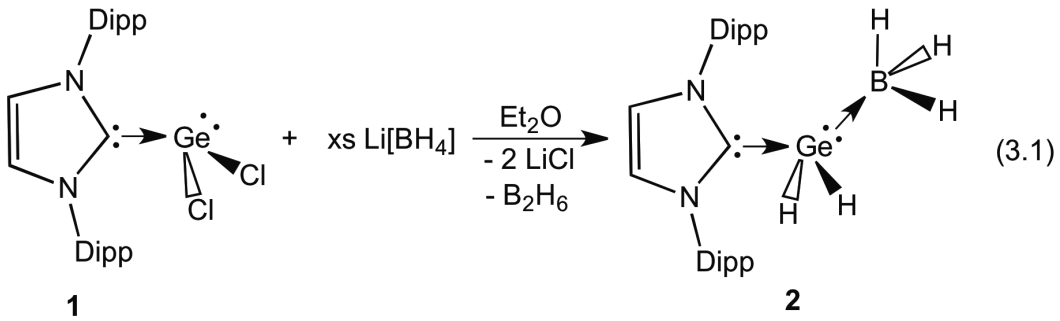

(3.1)

As shown in Figure 3.2, the structure of the isolated product was that of a donor/acceptor-stabilized Ge(II) dihydride IPr•GeH_2•BH_3 (**2**). The quality of the data was sufficient to allow for the location and refinement of the two hydrogen atoms bound to Ge. The observed Ge-H bond lengths are in the range of 1.460(18)-1.485(16) Å, while the Ge-B distances were determined to be 2.053(3) Å (averaged over two independent molecules). The Ge-B distances in **2** are elongated when compared to the corresponding Ge-B bond found within Roesky's Ge(II) hydride-BH_3 adduct, [{$HC(CMeAr)_2$}GeH•BH_3] [2.016(8) Å],[21a] and similar to the Ge-B distance in the Ge(II) heterocycle [{$N(SiMe_3)C(Ph)C(SiMe_3)(C_5H_4N$-2)GeH•$BH_3$] [2.064(6) Å].[21c] The Ge–C_{IPr} distances in **2** are 2.011(2) Å (*avg*.) and are short when compared to the Ge-C distance in the carbene germanium(II) chloride adduct IPr•$GeCl_2$ (**1**) [2.112(2) Å]. The bond angles encompassing the Ge-H units in **2** range from 97.3(9) to 98.2(9)°, while the C-Ge-B angle is considerably wider [118.82(7)°]. Notably, the H-Ge-H bond angle within the Ge(II) dihydride unit in **2** is 97.4(9)° (*avg*.), which is considerably wider than the angle of 91.2(8)° determined in free :GeH_2 consistent with an increase in s character within the Ge-H bonds in **2**.[11a,22]

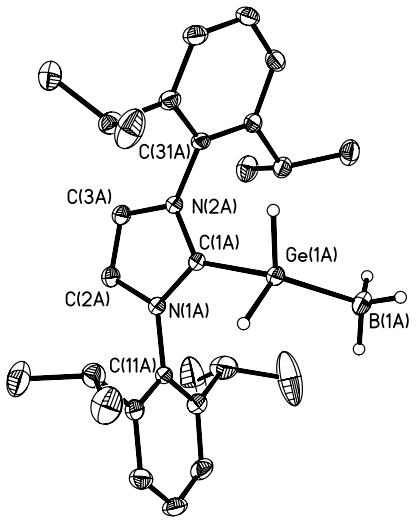

Figure 3.2. Thermal ellipsoid plot (30% probability level) of IPr•GeH_2•BH_3 (**2**). Carbon-bound are hydrogen atoms have been omitted for clarity. Only one molecule of the two in the asymmetric unit is shown. Selected bond lengths [Å] and angles [°] with metrical parameters for the second molecule listed in brackets: Ge(1)-C(1) 2.0148(13) [2.0065(13)], Ge(1)-B(1) 2.0567(18) [2.049(2)], Ge(1)-H(1) 1.485(16) [1.460(18)], Ge(1)-H(2) 1.464(16) [1.462(18)]; C(1)-Ge(1)-B(1) 118.82(7) [118.26(8)], C(1)-Ge(1)-H(1) 97.7(6) [98.7(7)], C(1)-Ge(1)-H(1) 97.4(6) [97.3(7)], C(1)-N(1)-C(2) 110.92(11) [110.63(11)].

The success in isolating a donor-acceptor complex of germanium(II) dihydride provided inspiration to explore the synthesis of other heavy Group 14 dihydride complexes, such as the stannylene IPr•SnH_2•BH_3. In order to construct a carbene-tin(II) chloride adduct, IPr was reacted with $SnCl_2$ in toluene to give IPr•$SnCl_2$ (**3**) in moderate yield (73%). The formation of **3** was supported by the ^{119}Sn NMR spectroscopy, which yielded a tin resonance at -68.7 ppm. Conclusive structural evidence for the formation of **3** was obtained from X-ray crystallography (Figure 3.3). The C_{IPr}-Sn bond distance in **3** [2.341(8) Å] was determined to be significantly longer than the Sn-C bond length in the Sn(II) heterocycle [$HC(CMeNAr)_2SnMe$] [2.253(2) Å][23] and the constituent Cl-Sn-Cl

angle [94.19(10)°] is same within the experimental error as the Cl-Ge-Cl bond angle in the lighter Ge congener **1** [94.31(8)°].

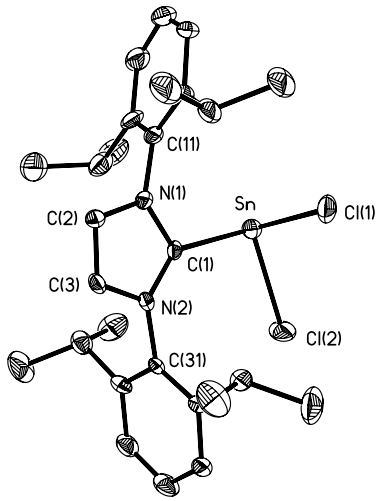

Figure 3.3. Thermal ellipsoid plot (30% probability level) of IPr•$SnCl_2$ (**3**). Hydrogen atoms have omitted for clarity. Selected bond lengths [Å] and angles [°]: Sn-Cl(1) 2.439(3), Sn-Cl(2) 2.426(2), Sn-C(1) 2.341(8); Cl(1)-Sn-Cl(2) 94.19(10), Cl(1)-Sn-C(1) 89.80(19), Cl(2)-Sn-C(1) 96.04(19), N(1)-C(1)-N(2) 105.7(6).

Tin(II) chloride adduct **3** reacted with NaH to give a complex product mixture, from which a pure product could not be isolated. When **3** was combined with Li[BH_4] in Et_2O, a vigorous reaction transpired that was accompanied by the evolution of a gas and the formation of metallic Sn on the walls of the reaction vessel. Similar results were obtained in toluene, however, gas evolution transpired after an initial induction period of *ca*. 15 min. In each case, a soluble product was isolated and identified as the known adduct IPr•BH_3 by ^{1}H, ^{11}B and $^{13}C\{^{1}H\}$ NMR spectroscopy.[4k] Attempts to isolate and identify the potential intermediate IPr•SnH_2•BH_3 in the above reaction mixtures were unsuccessful, even at low

temperatures (e.g. -35 °C).

Interestingly, the thermolysis of **2** in refluxing toluene (16 h, *ca*. 0.05 M concentration) led to the formal extrusion of GeH_2 and the generation of IPr•BH_3 in high yield, along with the formation of Ge metal (Scheme 3.1). These results imply that if the putative Sn(II) dihydride intermediate IPr•SnH_2•BH_3 is generated in the reaction of **3** with Li[BH_4], it is much less stable than its Ge(II) counterpart. The instability of the tin analogue could be due to the weaker nature of the Sn-H bond relative to the Ge-H bond[18] and/or the poorer electron-donor- and electron-accepting ability of Sn(II) species relative to Ge(II), leading to a weakening of the C_{IPr}-Sn and Sn-B bonds.

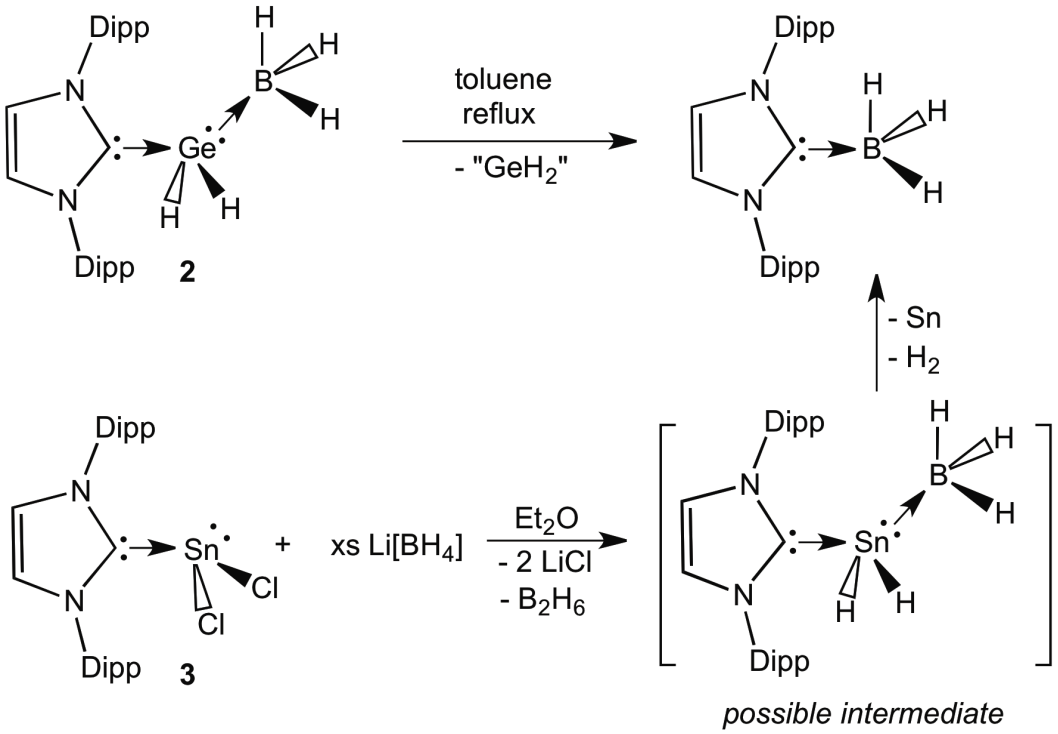

Scheme 3.1. Thermal decomposition of the IPr•$GeCl_2$•BH_3 (**2**) and reaction of IPr•$SnCl_2$with Li[BH_4] to give carbene-borane adduct IPr•BH_3 as a decomposition product.

On the basis of recent theoretical studies,[24] it was hoped that replacement of the Lewis acidic BH_3 group with the stronger electron acceptor $W(CO)_5$ would lead to the formation of more stable adducts, thus increasing the number of reactive species that could be intercepted and studied. To test the validity of this approach, the preparation of the tin(II) complex IPr•SnH_2•$W(CO)_5$ was set as an initial target.

Starting from the readily available precursor $(THF)_2SnCl_2$•$W(CO)_5$,[25] the required Sn(II) chloride precursor IPr•$SnCl_2$•$W(CO)_5$ (**4**) was synthesized by a ligand substitution reaction involving N-heterocyclic carbine as a σ-donor (Scheme 3.2). The tin(II) chloride precursor **4** was isolated as an air- and moisture-sensitive pale yellow solid in a 90% yield. The formation of the adduct **4** was supported by ^{119}Sn NMR specroscopy which yields a resonance at -71.3 ppm; for comparison, the ^{119}Sn NMR resonance for the parent tin(II) adduct, IPr•$SnCl_2$ was located at -68.7 ppm.

The desired tin(II) hydride adduct IPr•SnH_2•$W(CO)_5$ (**5**) was subsequently synthesized by chloride/hydride metathesis chemistry using a stoichiometric amount of $Li[BH_4]$ in Et_2O (Scheme 3.2). Evidence for the formation of a tin(II) dihydride adduct was obtained by NMR spectroscopy. Namely, the SnH_2 moiety was detected at 5.56 ppm in the ^{1}H NMR spectrum along with additional satellites ($^2J_{W\text{-}H}$ = 8.0 Hz) due to the coupling with NMR active tungsten nuclei (I = ½, natural abundance of ^{183}W = 14.31%). Furthermore, a triplet at -309 ppm was observed in the proton coupled ^{119}Sn NMR spectrum ($^1J_{Sn\text{-}H}$ = 1158 Hz) along with

additional satellites due to coupling with tungsten ($^1J_{Sn\text{-}W}$ = 828 Hz). A weak Sn-H band was detected at 1786 cm^{-1} in the IR spectrum of **5**, and assignment of this band in the presence of proximal carbonyl vibrations was supported by a deuterium labeling experiment (*vide infra*). For comparison, the Fe(II) stannane complex $[Fe\{PPh(OEt)_2\}_4(SnH_3)_2]$ exhibits a Sn-H vibration at 1755 cm^{-1},[26] while the terminal Sn-H bonds in the asymmetric tin hydride, Ar"$SnSn(H)_2$Ar" (Ar" = C_6H-2,6(C_6H_2-2,4,6-$^i Pr_3$)$_2$-3,5-$^i Pr_2$) yields IR bands at 1783 and 1810 cm^{-1}.[27] Crystals of IPr•SnH_2•$W(CO)_5$ (**5**) of suitable quality for X-ray crystallography were grown by cooling a saturated Et_2O/hexanes mixture to -35 °C.

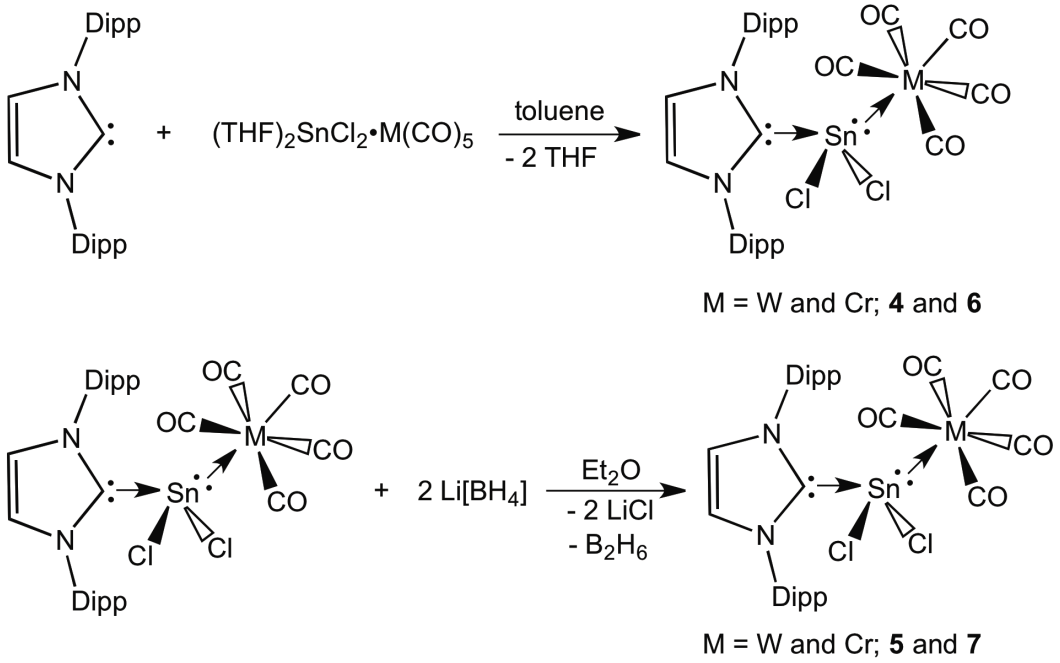

Scheme 3.2. Synthesis of the Sn(II) dichloride adducts, IPr•$SnCl_2$•$M(CO)_5$ (M = W and Cr; **4** and **6**) and their subsequent reaction with $Li[BH_4]$ to give the tin(II) hydride complexes IPr•SnH_2•$M(CO)_5$ (M = W and Cr; **5** and **7**).

As shown in Figure 3.4, IPr•SnH_2•$W(CO)_5$ (**5**) features a central SnH_2 moiety flanked by electron-donating IPr and electron-accepting $W(CO)_5$ groups. The respective Sn-C_{IPr} and Sn-W bond lengths are 2.230(6) and 2.7703(9) Å, and the latter distance is shorter than the Sn-C_{IPr} distance found in the tin(II) chloride adduct, IPr•$SnCl_2$ [2.341(8) Å], suggesting the presence of a stronger C_{IPr}-Sn donor/acceptor interaction in **5**. In addition, the Sn-W-CO_{trans} unit is nearly linear with an observed Sn-W-C(1) angle of 176.1(2)°. The Sn-W distance in **5** [2.7703(9) Å] is slightly elongated (~0.05 Å) in relation to the dative Sn-W bond lengths found within the dianionic cluster $[Sn_6\{W(CO)_5\}_6]^{2-}$ and the distannyl alkoxide complex [{(^{t}BuO)$_2$Sn}$_2$]•$W(CO)_5$.[28]

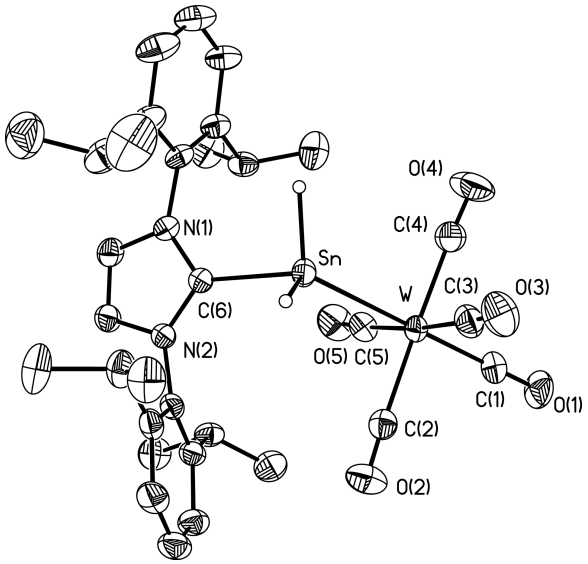

Figure 3.4. Thermal ellipsoid (30% probability level) plot of IPr•SnH_2•$W(CO)_5$ (**5**). Carbon-bound hydrogen atoms and hexane solvate have been omitted for clarity. Selected bond lengths [Å] and angles [°]: Sn-W 2.7703(9), Sn-C(6) 2.230(6), Sn-H 1.81(11) and 1.67(10), W-C(1) 1.961(7), W-C(2-5) 2.006(9) to 2.042(8); C(6)-Sn-W 120.06(14), Sn-W-C(1) 176.1(2), Sn-W-C(2-5) 84.6(2) to 91.7(2).

The deutero analogue IPr•SnD_2•$W(CO)_5$ (**5D**) was also prepared using a deuteride/chloride metathesis reaction between Li[BD_4] and **4**. The $^2H\{^1H\}$ NMR spectrum of **5D** yielded a resonance at 5.56 ppm corresponding to the SnD_2 moiety, while a diagnostic quintet resonance was observed in the ^{119}Sn NMR spectrum ($^1J_{Sn\text{-}D}$ = 179 Hz). Unfortunately, isotopically shifted Sn-D stretching band could not be identified due to the presence of proximal aromatic C=C vibrations.

The chromium adduct IPr•$SnCl_2$•$Cr(CO)_5$ (**6**) was also synthesized from the reaction of the coordinatively labile chromium THF adduct $(THF)_2SnCl_2$•$Cr(CO)_5$ with IPr. Compound **6** was isolated in 93% yield and was subsequently combined with two equivalents of Li[BH_4] to give the desired Sn(II) hydride complex, IPr•SnH_2•$Cr(CO)_5$ (**7**) (Scheme 3.2); compound **7** was isolated as a air- and moisture-sensitive brown solid and was characterized by a combination of NMR spectroscopy, elemental analysis (C, H, N) and X-ray crystallography. The resonance for the SnH_2 moiety in **7** was located at 5.51 ppm in ^1H NMR spectrum with flanking satellites due to the coupling with tin nuclei (satellites: $^1J_{H\text{-}119Sn}$ = 1180.9 Hz; $^3J_{H\text{-}117Sn}$ = 1128.8 Hz), while a triplet resonance was detected at -106 ppm in the proton coupled ^{119}Sn NMR spectrum. The IR spectrum of **7** yields an absorption band at 1772 cm^{-1} corresponding to the SnH_2 group, while the vibration for the carbonyl group trans to the SnH_2 unit appears as a strong band at 2037 cm^{-1}.

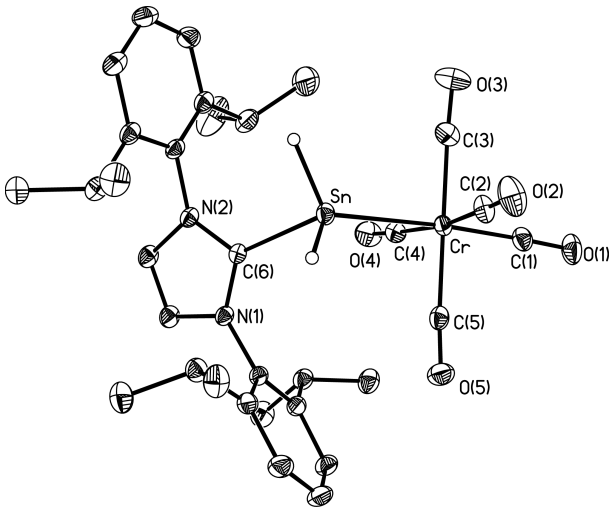

Figure 3.5. Thermal ellipsoid (30% probability level) plot of IPr•SnH_2•$Cr(CO)_5$ (**7**). Carbon-bound hydrogen atoms and hexane solvate have been omitted for clarity. Selected bond lengths [Å] and angles [°]: Sn-Cr 2.6247(3), Sn-C(6) 2.2358(15), Sn-H 1.59(3) and 1.67(2), Cr-C(1) 1.8347(19), Cr-C(2-5) 1.870(2) to 1.8939(19); C(6)-Sn-Cr 118.69(4), Sn-Cr-C(1) 175.36(6), Sn-Cr-C(2-5) 85.49(6) to 86.76(5).

As depicted in the Figure 3.5, compound **7** is isostructural with the tungsten adduct IPr•SnH_2•$W(CO)_5$ (**5**). The C_{IPr}-Sn distance in **7** [2.2358(15) Å] is identical within the experimental error to the corresponding distance in IPr•SnH_2•$W(CO)_5$ (**5**) [2.230(6) Å], thus suggesting presence of a similar dative interaction between the IPr and SnH_2 moieties in both compounds. The constituent Sn-Cr bond distance in **7** [2.6247(3) Å] is marginally shorter than the Sn-Cr interaction found in the Sn(II) alkyl pyridinopentacarbonylchromium adduct C_5H_5N•(^{t}Bu)$_2$Sn•$Cr(CO)_5$ [2.654(3) Å].[29]

Congruent with the stabilizing influence of the IPr and $W(CO)_5$ groups in **5**, this complex is stable up to 141 °C under a nitrogen atmosphere; however,

complete decomposition of **5** occurrs in hot toluene (100 °C, 1.5 days) to give an insoluble black precipitate, along with IPr, IPr•$W(CO)_5$ (**8**) and the aminal [$(HCNDipp)_2CH_2$] (**9**) as soluble products. The formation of these products was further confirmed by their independent syntheses. For instance, the carbene adduct, IPr•$W(CO)_5$ (**8**) was synthesized in a quantitative yield from the reaction of IPr with THF•$W(CO)_5$ in THF. The aminal [$(HCNDipp)_2CH_2$] (**9**) was prepared from the reaction of the known imidazolium salt, [$(HCNDipp)_2CH$]Cl with Li[$HBEt_3$] in Et_2O. Compounds **8** and **9** were characterized by NMR spectroscopy and elemental analysis (C, H, N). A similar decomposition pathway was also observed in the thermal decomposition of IPr•SnH_2•$Cr(CO)_5$ (**7**) and complete decomposition of **7** occurred in hot toluene (100 °C, 1.5 days) to give the IPr•$Cr(CO)_5$ (**10**) (*ca*. 35%) and [$(HCNDipp)_2CH_2$] (*ca*. 65%). Compound **10** was characterized by NMR spectroscopy and the formation of IPr•$Cr(CO)_5$ (**10**) was further confirmed by its independent synthesis using a similar protocol as described for the tungsten adduct **8**.

The analogous germanium dichloride adduct IPr•$GeCl_2$•$W(CO)_5$ (**11**) was prepared by reacting the N-heterocyclic carbene IPr with the germylene-tungsten complex (THF)$GeCl_2$•$W(CO)_5$.[25b] Compound **11** was isolated as a air- and moisture-sensitive pale yellow solid in a 90% yield and its structure was authenticated by a combination of NMR spectroscopy, elemental analysis and single-crystal X-ray crystallography.

As shown in Figure 3.6, IPr•$GeCl_2$•$W(CO)_5$ (**11**) contains a central $GeCl_2$

unit coordinated to electron-donating IPr, and electron-accepting $W(CO)_5$ groups. The C_{IPr}-Ge bond lengths in **11** [2.083(13) Å (*avg.*)] are slightly shorter compared to the related dative bond in the Ge(II) chloride adduct IPr•$GeCl_2$ (**1**) [2.112(2) Å]; this bond length contraction might be arising from the greater electron accepting ability of the $GeCl_2$•$W(CO)_5$ moiety relative to $GeCl_2$ which leads to a strengthening of the C_{IPr}-Ge interaction. In addition, the Ge-W linkage in **11** [2.5833(9) Å (*avg.*)] is comparable in length to the Ge-W bond in the germanium(II) adduct LGeCl•$W(CO)_5$ (L = PhNC(Me)CHC(Me)NPh) [2.567(5) Å].[30] Furthermore, a slightly wider Cl-Ge-Cl bond angle [97.1(2)° (*avg.*)] was observed in **11** compared to the Cl-Ge-Cl angle in the Ge(II) chloride adduct IPr•$GeCl_2$ (**1**) [95.95(3)°].

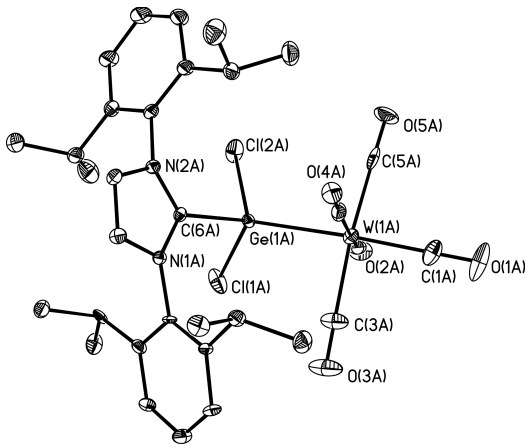

Figure 3.6. Thermal ellipsoid (30% probability level) plot of IPr•$GeCl_2$•$W(CO)_5$ (**11**). Carbon-bound hydrogen atoms have been omitted for clarity. One molecule of the three present in the asymmetric unit is shown. Selected bond lengths [Å] and angles [°]: *Molecule A:* Ge-W 2.5843(9), Ge-C(6) 2.083(7), Ge-Cl(1) 2.227(2), Ge-Cl(2) 2.210(2), W-C(1) 1.995(10); Cl(1)-Ge-Cl(2) 97.23(12), C(6)-Ge-W 126.6(2), Ge-W-C(1) 176.5(3). *Molecule B:* Ge-W 2.5833(9), Ge-C(6) 2.079(8), Ge-Cl(1) 2.201(2), Ge-Cl(2) 2.223(3), W-C(1) 2.002(11); Cl(1)-Ge-Cl(2) 96.83(14), C(6)-Ge-W 126.1(2), Ge-W-C(1) 176.8(4). *Molecule C:* Ge-W 2.5824(9), Ge-C(6) 2.085(7), Ge-Cl(1) 2.231(2), Ge-Cl(2) 2.222(2), W-C(1) 1.997(10); Cl(1)-Ge-Cl(2) 97.34(12), C(6)-Ge-W 126.7(2), Ge-W-C(1) 176.2(4).

The germanium dihydride complex IPr•GeH_2•$W(CO)_5$ (**12**) was prepared by two distinct routes. The first route involved the reaction of **11** with two equivalents of Li[BH_4] in Et_2O (Equation 3.2), and the latter route involved a BH_3/$W(CO)_5$ metathesis reaction starting from the Ge(II) hydride-borane adduct IPr•GeH_2•BH_3 (**2**) (Equation 3.3). The GeH_2 transfer chemistry outlined in Equation 3.3 is noteworthy as it could represent a general method to install reactive GeH_2 groups onto a variety of metal centers.

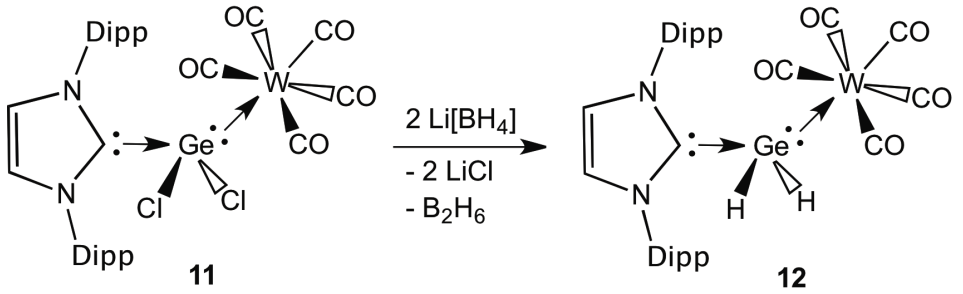

(3.2)

The ^{1}H NMR spectrum of **12** yields a singlet resonance at 4.23 ppm with accompanying satellites due to coupling with an NMR active tungsten nucleus in the adjacent $W(CO)_5$ moiety ($^3J_{HW}$ = 4.4 Hz). In the IR spectrum of **12** a Ge-H vibration appears at 1981 cm^{-1} which is in the range expected for state Ge(II) hydrides. For example, the IR absorption band for Ge-H was observed at 1905 cm^{-1} in Power's germanium (II) hydride complex Ar'$(H)_2$GeGeAr'(PMe_3) (Ar' = C_6H_3-2,6-(C_6H_3-2,6-^{i}Pr$_2$)$_2$).[7a] The assignment of the Ge-H absorption band amongst proximal carbonyl vibrations was aided by recording the IR spectrum of corresponding isotopologue IPr•GeD_2•$W(CO)_5$ (**12D**). The deuterium complex

12D was synthesized by either reacting IPr•$GeCl_2$•$W(CO)_5$ (**11**) with Li[BD_4] or by BD_3/$W(CO)_5$ metathesis chemistry starting from the Ge(II) deutride adduct, IPr•GeD_2•BD_3 (**2D**). Interestingly, the Ge(II) hydride adduct IPr•GeH_2•$W(CO)_5$ (**12**) displays an enhanced thermal stability relative to the tin analogue IPr•SnH_2•W(CO) (**5**) and is stable for extended periods of time in hot toluene (100 °C, 16 h). Complex **12** is a colorless solid that is highly moisture-sensitive and crystals suitable for the X-ray single crystal analysis were obtained by cooling (-35 °C) a THF solution of **12** layered with hexanes.

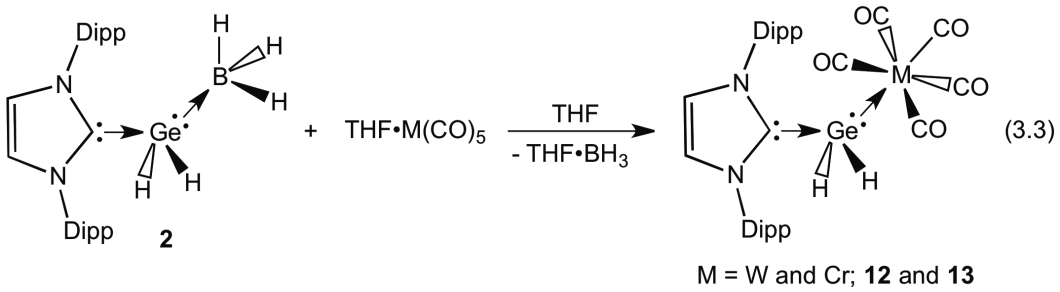

(3.3)

As shown in Figure 3.7, compound **12** has an overall structure that is analogous to the related tin(II) hydride complex IPr•SnH_2•$W(CO)_5$ (**5**). The Ge-C_{IPr} and Ge-H distances in **12** [2.0151(18) and 1.42(3) Å] are similar to the values found in the germanium hydride adduct IPr•GeH_2•BH_3 (**2**), while the corresponding Ge-W distance in **5** [2.6318(2) Å] is significantly longer than the Ge-W distance [2.4289(8) Å] the hydrogermylene $Cp^*(CO)_2(H)W{=}Ge(H)[C(SiMe_3)_3]$,[31a] and is in the range typically observed for W-Ge single bonds (2.50-2.75 Å).[31b]

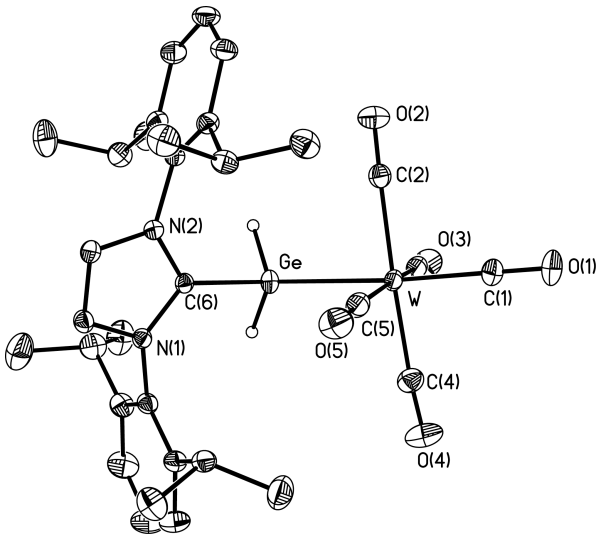

Figure 3.7. Thermal ellipsoid plot (30% probability level) of IPr•GeH_2•$W(CO)_5$ (**12**). Carbon-bound hydrogen atoms and THF solvate molecules have been omitted for clarity. Selected bond lengths [Å] and angles [°]: Ge-W 2.6318(2), Ge-C(6) 2.0151(18), Ge-H(1A) 1.42(2), Ge-H(1B) 1.43(3), W-C(1) 1.982(2), W-C(2) to W-C(5) 2.047(2) to 2.044(2); C(6)-Ge-W 121.44(5), Ge-W-C(1) 175.70(6), Ge-W-C(2) to Ge-W-C(5) 85.12(6) to 90.66(6), H(1A)-Ge-H(1B) 100.9(15).

The analogous chromium adduct IPr•GeH_2•$Cr(CO)_5$ (**13**) has an overall arrangement that is almost identical to that adopted by the tungsten complex IPr•GeH_2•$W(CO)_5$ (**12**) with a significantly canted transoid arrangement of C(6)-Ge-Cr-C(1) [torsion angle = -138(2)°] (Figure 3.8). The constituent C_{IPr}-Ge bond distance in **13** [2.018(3) Å] is similar in length to the corresponding bond in the tungsten adduct, IPr•GeH_2•$W(CO)_5$ (**12**), [2.0151(18) Å], suggesting the presence of a similar dative carbene-germanium interaction in each adduct. The Ge-Cr linkage in **13** [2.4805(7) Å] is longer than the Ge-Cr interaction in the Lappert's germylene complex $(CO)_5$Cr•Ge{$CH(SiMe_3)_2$} [2.378(4) Å].[32]

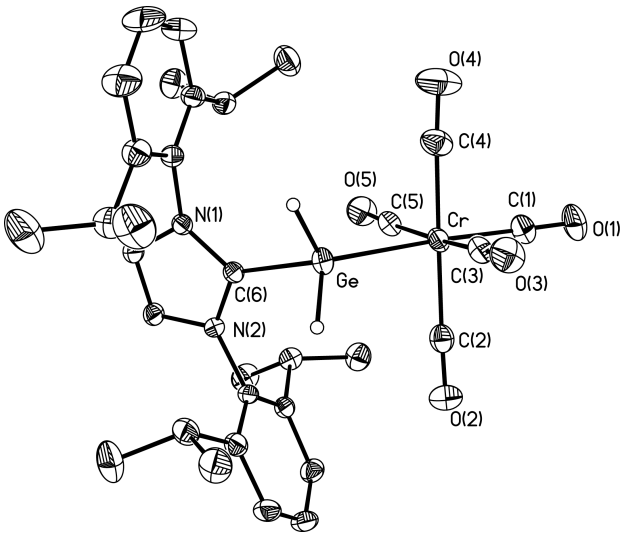

Figure 3.8. Thermal ellipsoid plot (30% probability level) of IPr•GeH_2•$Cr(CO)_5$ (**13**). Carbon-bound hydrogen atoms and THF solvate molecules have been omitted for clarity. Selected bond lengths ([Å] and angles [°]: Ge-Cr 2.4805(7), Ge-C(6) 2.018(3), Ge-H(1A) 1.42(4), Ge-H(1B) 1.49(5), Cr-C(1) 1.847(4), Cr-C(2) to Cr-C(5) 1.899(5) to 1.888(4); C(6)-Ge-Cr 122.45(9), Ge-Cr-C(1) 176.05(13), Ge-Cr-C(2) to Ge-Cr-C(5) 85.69(12) to 89.74(12), H(1A)-Ge-H(1B) 101(2).

As anticipated on the basis of electronegativities,[33] the hydrogen atoms within the EH_2 units in the abovementioned adducts were hydridic. This prediction was borne out in the observed reactivity of the Sn-H groups in **5** with the electrophile benzaldehyde. As shown in Equation 3.4, the racemic insertion product **14** was isolated as the sole tin-containing species in a 46% yield. The hydrostannylation product **14** was identified by NMR spectroscopy, elemental analysis (C, H, N) and single-crystal X-ray analysis (Figure 3.9). Although the exact mechanism for this process is not fully certain, the related hydrostannylation of ketones by Sn(II) hydrides has been reported.[34]

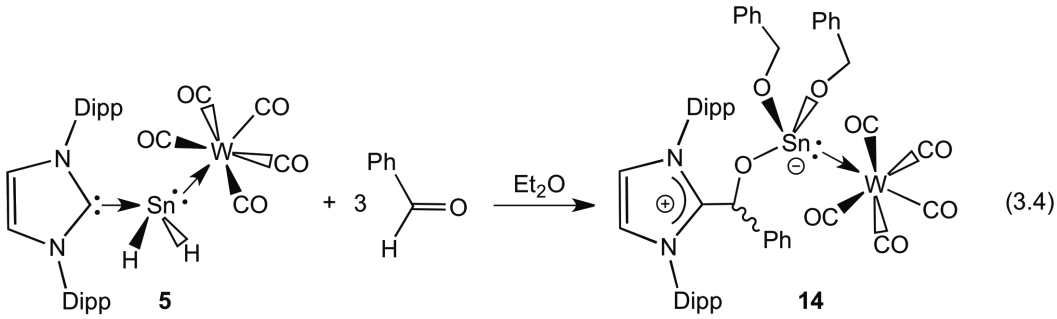

(3.4)

Compound **14** features a slightly distorted tetrahedral arrangement about the tin center. The dative Sn-W interaction in **14** [2.7430(4) Å] is shorter than the related Sn-W bond length in the tin(II) hydride adduct IPr•SnH_2•$W(CO)_5$ [2.7703(9) Å] and also significantly shorter than the Sn-W single bond distance of 2.9030(8) Å found in Power's Sn(II) complex [(η^5-C_5H_5)$W(CO)_3$-SnAr*] (Ar* = 2,6-^{i}Pr$_2C_6H_3$).[35] The Sn-O bond distances in **14** [2.0143 (3) Å (*avg.*)] are significantly shorter than the Sn-O length found in the organostannylene complex, [({2,6-$(MeOCH_2)_2C_6H_3$}SnCl)$Cr(CO)_5$] [2.3936(12) and 2.407(3) Å].[36] The internal C_{IPr}-C(50) bond in **14** is 1.514(4) Å and is slightly shorter than a standard C(sp^3)-C(sp^3) single bond, (*ca.* 1.54 Å),[37] in line with the presence of a covalent interaction between the imidazolium (C_{IPr}) carbon and the benzyloxy carbon center.

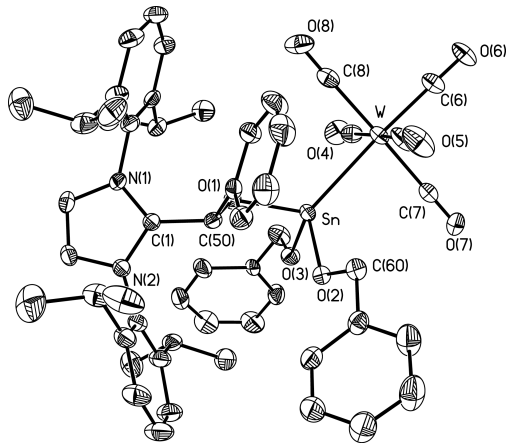

Figure 3.9. Thermal ellipsoid plot (30% probability level) for IPr-C(H)PhO-$Sn(OCH_2Ph)_2$•$W(CO)_5$ (**14**). Hydrogen atoms and Et_2O solvate molecules have been omitted for clarity. Selected bond lengths [Å] and angles [°]: Sn-W 2.7430(4), Sn-O(1) 2.029(2), Sn-O(2) 2.002(2), Sn-O(3) 2.012(2), C(1)-C(50) 1.514(4), C(50)-O(1) 1.402(4), W-C(6) 1.990(4), W-C(4) 2.039(4), W-C(5) 2.031(4), W-C(7) 2.026(4), W-C(8) 2.028(4); Sn-W-C(6) 176.15(13), Sn-W-C(4) 87.19(11), Sn-W-C(5) 88.50(11), Sn-W-C(7) 86.23(10), Sn-W-C(8) 92.27(10), O(1)-Sn-W 123.50(7), O(2)-Sn-O(3) 94.11(9), C(1)-C(50)-O(1) 105.5(3), N(1)-C(1)-C(50) 128.8(3), N(2)- C(1)-C(50) 124.0(3), N(1)-C(1)-N(2) 106.9(3).

As mentioned earlier, silylene :SiH_2 has been postulated to exist in the gas phase during the thermolytic synthesis of Si films from SiH_4, while metallosilylenes (M=SiR_2) have been implicated as intermediates in hydrosilane polymerization and in the synthesis of halomethylsilanes.[38] Recently, Robinson and coworkers reported the synthesis a compound bearing a formal :SiH_2 unit, IPr•SiH_2•BH_2-$SiH(B_3H_7)$•IPr, *via* a borane-induced Si–Si cleavage reaction involving the disilene bis-adduct IPr•Si=Si•IPr.[39]

Roesky and coworkers reported the synthesis of Si(II) dichloride-carbene adduct IPr•$SiCl_2$ in 2009[4c] which provided the chemical community with a standard source of $SiCl_2$ in order to access parent silylene adducts such as

IPr•SiH_2•BH_3 or IPr•SiH_2•$W(CO)_5$ by using a similar donor-acceptor stabilization protocol as used to form :GeH_2 and :SnH_2 complexes. Towards this goal, the Roesky group attempted to prepare the Si(II) hydride IPr•SiH_2•BH_3 by treating IPr•$SiCl_2$ with Li[BH_4] in THF. Interestingly, this reaction resulted in an unusual LiH elimination reaction, and the formation of the halosilylene adduct IPr•$SiCl_2$•BH_3 in high yield.[40] The reluctance of the Si-Cl bonds in IPr•$SiCl_2$•BH_3 to undergo hydride replacement chemistry with Li[BH_4] was consistent with observation reported in Chapter 4 of this Thesis wherein Si-H bond formation from Si-Cl precursors required the use of Li[AlH_4] to install hydride functionality (e.g. in the synthesis of IPr•H_2SiGeH_2•$W(CO)_5$ from IPr•$Cl_2SiGeCl_2$•$W(CO)_5$).[41]

Initial attempts to generate IPr•SiH_2•BH_3 (**15**) from the reaction of IPr•$SiCl_2$•BH_3 with Li[AlH_4] in ethereal solvents led to the formation of the known alane complex IPr•AlH_3 as a major product,[42] with only trace amounts (< 5%) of the desired silylene adduct **15** (as noted by ^{1}H NMR spectroscopy). In order to mitigate IPr•AlH_3 formation, the hydride transfer reaction was repeated in a solvent combination with lower polarity (toluene/Et_2O mixture) while concurrently decreasing the reaction time to 1.5 h. Fortunately these alterations in the reaction parameters led to the clean formation of the desired Si(II) dihydride adduct IPr•SiH_2•BH_3 (**15**) as a colorless solid in a moderate isolated yield of 55% (Equation 3.5).

The identification of Si(II) dihydride adduct IPr•SiH_2•BH_3 (**15**) was readily made using NMR spectroscopic analysis due to the presence of multiple

NMR active nuclei. For example, the ^{1}H NMR spectrum of **15** yielded a quartet resonance at δ 3.76 that was assigned to the SiH_2 moiety on the basis of its integration, while the quartet pattern of this resonance was consistent with the presence of a coordinated BH_3 unit at Si ($^{3}J_{HH}$ = 5.6 Hz). The ^{29}Si{^{1}H} NMR spectrum featured a well-resolved quartet pattern centered at -55.6 ppm ($^{1}J_{Si\text{-}B}$ = 46 Hz), while the -BH_3 acceptor unit in **15** appeared as a quartet in the ^{11}B NMR spectrum [δ = -46.2; $^{1}J_{BH}$ = 93 Hz]. A sharp band was located at 2096 cm^{-1} in the IR spectrum due to coincident symmetric and asymmetric Si-H stretching modes, and diagnostic υ($^{10/11}$B–H) stretching vibrations were observed from 2328 to 2345 cm^{-1}. The analogous deutride adduct IPr•SiD_2•BH_3 (**15D**) was also prepared following a similar procedure using Li[AlD_4] as a deutride source and **15D** yielded a υ(Si-D) IR absorption band at 1522 cm^{-1}, congruent with the expected change in Si–H/D harmonic oscillator strength on going from **15** to **15D**.

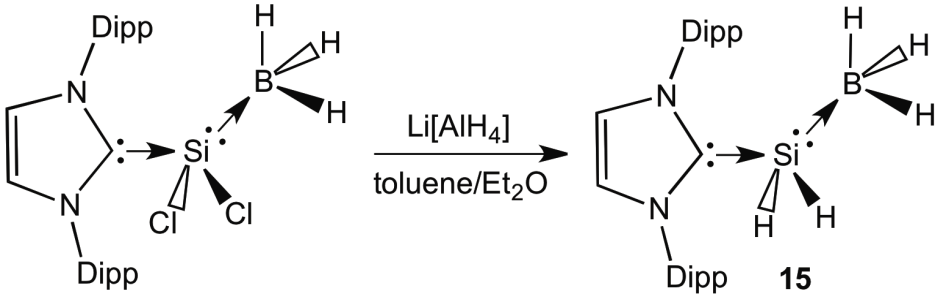

15 (3.5)

The structure of IPr•SiH_2•BH_3 (**15**) is presented in Figure 3.10 and bears geometric features that closely resemble those found within the germanium congener IPr•GeH_2•BH_3 (**2**). The dative C_{IPr}-Si bond length in **15** [1.9284(15) Å] is slightly shorter than the related C_{IPr}-Si interactions found within the SiH_2 adduct, IPr•SiH_2•BH_2–$SiH(B_2H_7)$•IPr [1.934(4) and 1.944(4) Å], and in

IPr•$SiCl_2$•BH_3 [1.937(2) Å].[39,40] The adjacent Si-B distance in **15** [1.992(2) Å] lies in the range reported for previously known BH_3 adducts involving formal Si(II) donor sites [1.965(2) to 1.996(4) Å].[39,40,43] Each of the hydrogen atoms bound to Si and B in **15** were located in the electron difference map and refined isotropically to expected Si-H and B-H distances.

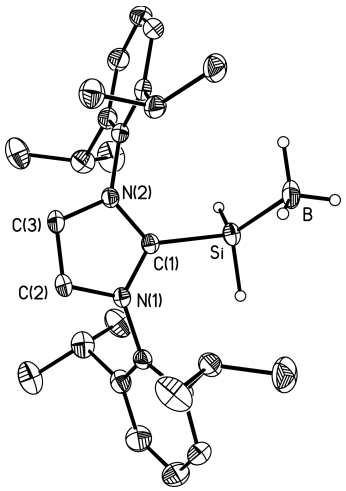

Figure 3.10. Thermal ellipsoid plot (30% probability level) for IPr•SiH_2•BH_3 (**15**). Carbon-bound hydrogen atoms have been omitted for clarity. Selected bond lengths [Å] and angles [°]: C(1)-Si 1.9284(15), Si-B 1.992(2), Si-H 1.409(18) and 1.439(18), B-H 1.02(2), 1.02(3) and 1.12(2); C(1)-Si-B 112.11(8), H-Si-H 102.0(10).

The SiH_2 complex **15** appears to be significantly more thermally stable than its Ge analogue IPr•GeH_2•BH_3 (**2**). For example, IPr•SiH_2•BH_3 (**15**) is stable up to *ca*. 230 °C in the solid state and remains unaltered in hot toluene (100 °C, 12 h). By comparison, complex **2** has a decomposition temperature (T_{dec}) of 130 °C in the solid state, while decomposition to Ge metal, H_2 and IPr•BH_3 is rapid at *ca*. 100 °C in toluene. Moreover, IPr•SiH_2•BH_3 is unreactive towards Cy_3P at

room temperature, whereas the GeH_2 adduct **2** reacts with Cy_3P to give the known phosphine-borane adduct $Cy_3P{\bullet}BH_3$, $IPr{\bullet}BH_3$ and the aminal $[(HCNDipp)_2CH_2]$ (**9**) as soluble products (*ca*. 25% conversion after 24 h). These observations are in line with the expected increase in both the electron donating and accepting abilities of the SiH_2 unit relative to GeH_2 leading to a higher degree of stability for $IPr{\bullet}SiH_2{\bullet}BH_3$.

An interesting silylene group transfer reaction was observed when $IPr{\bullet}SiH_2{\bullet}BH_3$ (**15**) was combined with $THF{\bullet}W(CO)_5$. In this process the $IPr{\bullet}SiH_2$ unit remained intact to give the tungsten complex $IPr{\bullet}SiH_2{\bullet}W(CO)_5$ (**16**) in a 66% yield with concomitant loss of $THF{\bullet}BH_3$ (Equation 3.6). It is important to mention that the related germanium hydride adduct $IPr{\bullet}GeH_2{\bullet}BH_3$ also exhibited similar $W(CO)_5/BH_3$ metathesis chemistry, thus this method could be used to install reactive $:EH_2$ (E = Si and Ge) groups onto a variety of electron deficient metal centers.

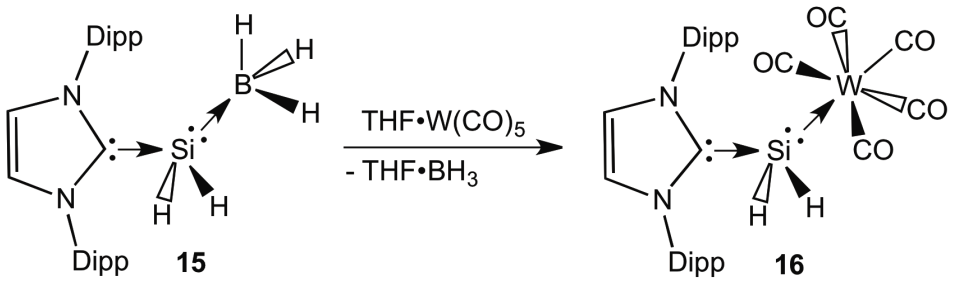

(3.6)

$IPr{\bullet}SiH_2{\bullet}W(CO)_5$ (**16**) has a singlet resonance in the ^1H NMR spectrum at δ 3.76 with neighboring satellites stemming from $^1J_{Si\text{-}H}$ coupling (164 Hz). A triplet resonance appears at -71.6 ppm as a triplet due to the coupling with two silicon-bound hydrogen atoms ($^1J_{Si\text{-}H}$ = 164 Hz) in the ^{29}Si NMR. The IR spectrum

of **16** affords sharp bands at 2086 and 2107 cm^{-1} that are assigned as symmetric and asymmetric Si-H stretching modes, respectively. The Si-H vibration frequencies in **16** are of similar value as in the Si(II) hydride adduct [^{t}BuNC(Ph)N^{t}Bu]SiH•BH_3 [2107 cm^{-1}].[43] The *trans*-disposed carbonyl ligand in IPr•SiH_2•$W(CO)_5$ (**16**) (relative to the SiH_2 donor) yields a characteristic A_1 vibration at 2044 cm^{-1}; this value is slightly lower than the related stretching frequencies in the heavier element analogues IPr•EH_2•$W(CO)_5$ (E = Ge and Sn; $\upsilon(CO)_{trans}$ = 2047 cm^{-1} in both cases). These data suggest that the IPr•SiH_2 group is a marginally stronger electron donor than both of the Ge and Sn derivatives. Of further note, West's N-heterocyclic silylene [$(HCN^tBu)_2Si$:] does not form an adduct with BH_3, thus implying that the IPr•SiH_2 unit is a stronger Lewis base than this classic Si(II) heterocyclic donor.[44]

As shown in the Figure 3.11, IPr•SiH_2•$W(CO)_5$ (**16**) consists of SiH_2 unit within the coordination sphere of a carbene donor and $W(CO)_5$ acceptor. The C_{IPr}-Si-W bond angle in **16** was determined to be 121.4(4)° and is within the experimental error as the related C_{IPr}-Ge-W bond angle in the germanium analogue IPr•GeH_2•$W(CO)_5$ (**12**) [121.44(5)°]; however, the C_{IPr}-Si-B bond angle is significantly narrower in the borane adduct IPr•SiH_2•BH_3 (**15**) [112.11(8)°]. The C_{IPr}-Si distance in **16** is 1.928(13) Å and is notably shorter than the carbene-silicon interaction in the Si(II) dihalide adducts IPr•SiX_2 [X = Cl, 1.985(4) Å and X = Br, 1.989(3) Å].[4c,d] Furthermore, the flanking Si-W bonding interaction in **16** [2.573(4) Å] is longer than the silicon-tungsten double bond length observed in the bicyclic silylene complex $Cp_2W(\eta^1\text{-}Si_4R_2)$ (Cp = η^5-C_5H_5; R = SiMe^tBu_2)

[2.4202(14) Å][45] and also slightly longer than the Si-W bond length of 2.543(2) Å found in the side-on bound silene complex, $Cp_2W(\eta^2\text{-}Me_2Si{=}CH_2)$.[46]

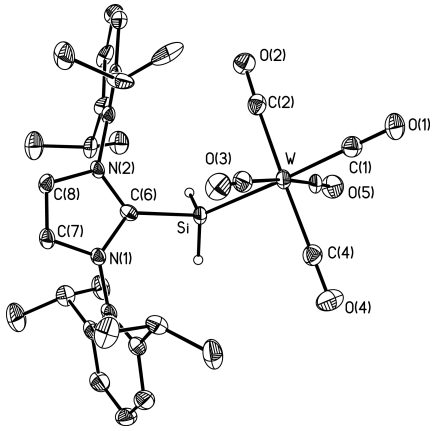

Figure 3.11. Thermal ellipsoid plot (30% probability) of IPr•SiH_2•$W(CO)_5$ (**16**). IPr-bound hydrogen atoms and hexane solvent have been omitted for clarity; Si–H distances were constrained to equal values during the refinement. Selected bond lengths [Å] and angles [°]: C(6)-Si 1.928(13), Si-W 2.573(4), W-C(1) 1.966(15), W-C(2-5) 1.997(16) to 2.059(17), Si-H 1.32(9); C(6)-Si-W 121.4(4), Si-W-C(1) 176.2(4), Si-W-C(2-5) 85.0(4) to 91.6(4).

In an attempt to better gauge the electron donating ability of the IPr•SiH_2 unit the reactivity of IPr•SiH_2•BH_3 (**15**) in the presence of different transition metal complexes was investigated with a hope to gain access to novel late transition metal silylene complexes, such as [IPr•SiH_2•$Rh(CO)_2Cl$]. As discussed earlier in this Chapter, IPr•EH_2•BH_3 (E = Si and Ge; **15** and **2**) can participate in the $W(CO)_5/BH_3$ metathesis chemistry, on the basis of these facile transformations it was proposed that IPr•SiH_2•BH_3 (**15**) can dissociate in solution to generate IPr•SiH_2 as a transient species, which then can be transferred onto Lewis acidic transition metal centers to give complexes of general form $[(IPr{\bullet}SiH_2)_nML_x]$ (M = transition metal, L = ligand). Complexes such as [L•$Rh(CO)_2Cl$] (L = $2e^-$ donor) are used to benchmark relative ligand donor strengths by monitoring changes in

the CO stretching frequencies.[47] As a starting point, the reaction between IPr•SiH_2•BH_3 and $[Rh(CO)_2Cl]_2$ was investigated and the rapid formation of Rh metal along with the generation of a large number of inseparable carbene-containing products were observed. Interestingly, a stable Rh-silylene complex was obtained when IPr•$SiCl_2$ was reacted with $[Rh(CO)_2Cl]_2$. In place of forming the target monometallic complex [IPr•$SiCl_2$•$Rh(CO)_2Cl$], its coordination isomer *trans*-[(IPr•$SiCl_2$)$_2$$Rh(CO)_2$]*cis*-[$Rh(CO)_2Cl_2$] (**17**) was obtained as an orange crystalline solid (Equation 3.7); compound **17** can be isolated in a 87% of yield with the use of excess $[Rh(CO)_2Cl]_2$.

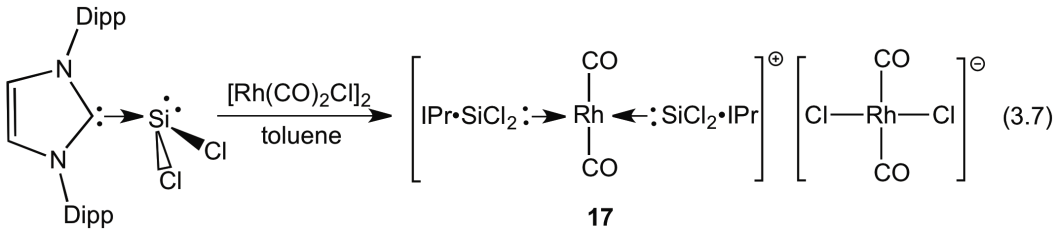

17

The formation of the coordination complex **17** was confirmed by NMR spectroscopy. The resonance for the carbene-carbon was detected as a doublet in the $^{13}C\{^1H\}$ spectrum due to the coupling with the NMR active ^{103}Rh nuclei ($^2J_{Rh\text{-}C}$ = 4.9 Hz), while two distinct carbonyl resonances were observed due to the presence of chemically distinct carbonyl groups in the anionic and cationic moities. The $^{29}Si\{^1H\}$ NMR spectrum of **17** yielded a doublet resonance at 27.9 ppm due to coupling with a neighboring coordinated Rh center ($^1J_{Si\text{-}Rh}$ = 69 Hz). The ligation of two IPr•$SiCl_2$ units to a sole Rh center in **17** is a likely consequence of the reduced proximal bulk at the donor site of this two electron donor ligand relative to NHCs which generally give the mono-substituted

complexes [(NHC)Rh(CO)$_2$Cl].[47] Unfortunately, attempts to generate a Rh-bound silylene complex featuring reactive Si–H groups *via* the reaction of **17** with various hydride sources exclusively led to the formation of metallic Rh and complicated product mixtures.

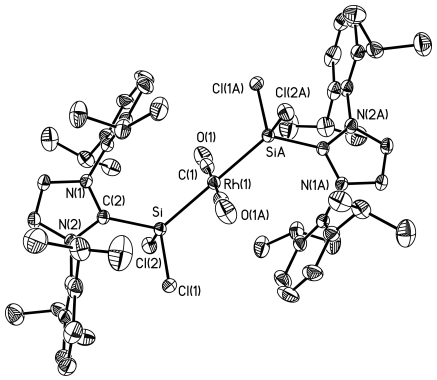

Figure 3.12. Thermal ellipsoid plot (30% probability) of the *trans*-[(IPr•SiCl$_2$)$_2$Rh(CO)$_2$]$^+$ cation in **17**. IPr-bound hydrogen atoms and CH_2Cl_2 solvent have been omitted for clarity. Selected bond lengths [Å] and angles [°]: Rh(1)-Si 2.3605(8), Rh(1)-C(1) 1.901(4), C(2)-Si 1.939(3); C(2)-Si-Rh(1) 123.41(10), Cl(1)-Si-Cl(2) 102.56(5), Si-Rh(1)-C(1) 90.94(11), Si-Rh(1)-Si(A) 180.0.

As shown in Figure 3.12, the [(IPr•SiCl$_2$)$_2$Rh(CO)$_2$]$^+$ cation in **17** has an overall centrosymmetric arrangement with two flanking IPr•SiCl$_2$ units mutually *trans* to each other [Si-Rh-Si = 180.0° by crystallographically imposed symmetry]. The Si-Rh bond lengths were determined to be 2.3605(8) Å and are longer than the silicon-rhodium bond distance found in RhI(H)(SiMe$_2$-O-SiMe$_3$)(PPh$_3$)$_2$ [2.291(2) Å].[48] The adjacent C$_{IPr}$-Si bond length in **17** [1.939(2) Å] is comparable to the related C$_{IPr}$-Si interactions observed within the SiH$_2$ adduct IPr•SiH$_2$•BH$_2$–SiH(B$_2$H$_7$)•IPr [1.934(4) and 1.944(4) Å] and in IPr•SiCl$_2$•BH$_3$ [1.937(2) Å].[39,40]

As mentioned earlier in this Chapter, the success of the donor-acceptor stabilization protocol relies upon the dual Lewis acidic and basic nature of the Group 14 dihydrides (:EH_2, E = Si–Pb), wherein their singlet ground states afford an accessible lone pair donor site, along with a low-lying vacant p-orbital on the tetrel elements. Thus far, strong electron donors such as the N-heterocyclic carbene, IPr (IPr = [$(HCNDipp)_2C$:], Dipp = 2,6-$^{i}Pr_2C_6H_3$), and electron acceptors such as BH_3 or $W(CO)_5$ are required to form stable adducts with EH_2 moieties. It has been found that common electron donating ligands such as phosphines and pyridines are ineffective at stabilizing main group hydrides. To further investigate the role of σ-donating ligands on the stability of EH_2 complexes, the application of sterically demanding N-heterocyclic olefins as potential donor ligands was explored.

The nucleophilic character of N-heterocyclic olefins was convincingly demonstrated by Kuhn and coworkers who reported the formation of stable adducts between the diamino olefin [$(MeCNMe)_2C=CH_2$] and Lewis-acidic borane (BH_3), phosphenium (PR_2^+) and metal carbonyl species.[49] With these observations in mind, the nucleophilic character of IPr=CH_2 and its analogues can be described by the canonical forms presented in Scheme 3.3. More recently, the hindered analogue IPr=CH_2 was generated *in situ* by the Beller group and used to prepare the cationic phosphine [$IPrCH_2–PCy_2]^+$ *via* a halide displacement reaction involving $ClPCy_2$.[50] However, the synthesis of IPr=CH_2 developed by the Beller group involves a complicated work-up procedure due the presence of LiI as a byproduct.

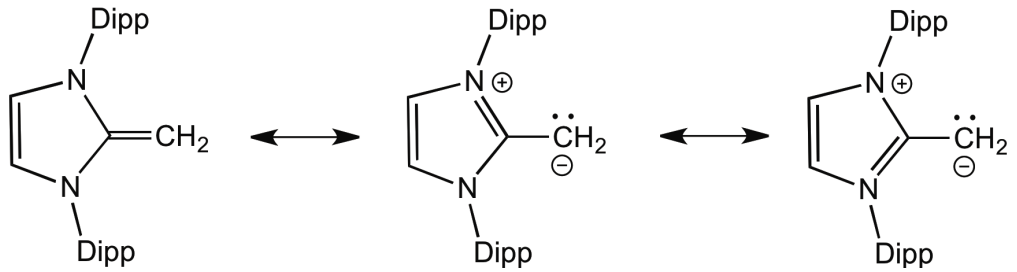

Scheme 3.3. Representative resonance structures of the N-heterocyclic olefin, IPr=CH_2 (**18**) (IPr = [(HCNDipp)$_2$C:], Dipp = 2,6-^{i}Pr$_2$C$_6$H$_3$).

In order to study the ability of N-heterocyclic olefins as donor ligands, the investigation started with the development of a convenient and efficient synthetic route for the preparation of the sterically hindered olefin IPr=CH_2 (**18**) (IPr = [(HCNDipp)$_2$C:], Dipp = 2,6-^{i}Pr$_2$C$_6$H$_3$). It was found that IPr=CH_2 (**18**) could be synthesized in a 90% yield directly from the reaction of two equivalents of IPr and MeI (Equation 3.8). The work-up procedure of this one-pot synthesis was greatly facilitated by the fact that **18** could be readily separated from the insoluble imidazolium salt byproduct [IPrH]I by filtration. IPr=CH_2 (**18**) was isolated as a highly moisture-sensitive colorless solid, and structural assignment of **18** was achieved by NMR spectroscopy and X-ray crystallography (Figure 3.13).

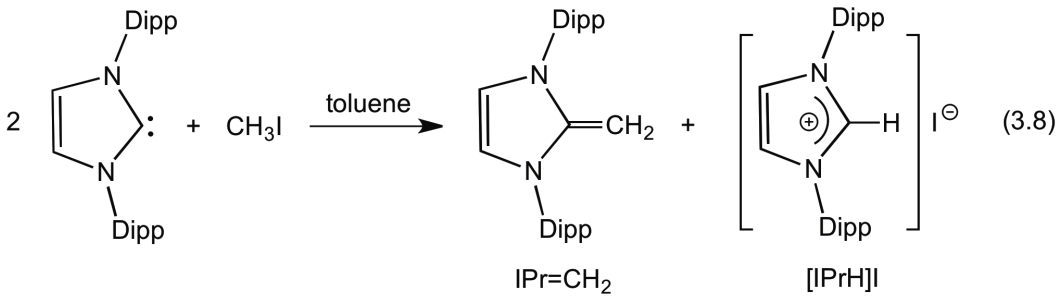

The terminal $-CH_2$ resonance in **18** was located at 2.42 ppm in the ^1H NMR spectrum, while this group appeared in the $^{13}C\{^1H\}$ NMR spectrum as a singlet at 40.2 ppm. For comparison, resonances for the methylene group in the related diamino olefin [$(MeCNMe)_2C=CH_2$] were found at 2.77 and 40.2 ppm by the ^1H and $^{13}C\{^1H\}$ NMR, respectively.[49b] As shown in the Figure 3.13, **18** adopts a planar arrangement within the five-membered C_3N_2 ring. The C(1)-C(2) bond distance in **18** was found to be 1.331(8) Å (*avg*.) and the presence of a short C-C bond further demonstrates the ylidic nature of the bond as represented by the resonance forms in Scheme 3.3. It is important to note that in the methyl-substituted nucleophilic olefin [$(MeCNMe)_2C=CH_2$] the C(1)-C(2) bond distance was determined to be 1.357(3) Å.[49b]

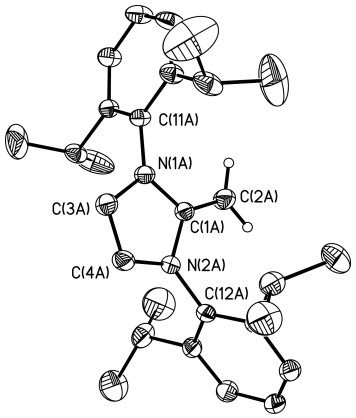

Figure 3.13. Thermal ellipsoid plot (30% probability level) of IPr=CH_2 (**18**). Carbon-bound hydrogen atoms have been omitted for clarity. One molecule of the four present in the asymmetric unit is shown. Selected bond lengths [Å] and angles [°]: *Molecule A:* C(1)-C(2) 1.332(4), C(1)-N(1) 1.391(3), C(1)-N(2) 1.391(3); N(1)-C(1)-N(2) 104.3(2), N(1)-C(1)-C(2) 127.8(3), N(2)-C(1)-C(2) 128.0(3). *Molecule B:* C(1)-C(2) 1.322(4), C(1)-N(1) 1.388(3), C(1)-N(2) 1.395(3); N(1)-C(1)-N(2) 103.8(2), N(1)-C(1)-C(2) 128.3(3), N(2)-C(1)-C(2) 127.9(3). *Molecule C:* C(1)-C(2) 1.337(4), C(1)-N(1) 1.391(3), C(1)-N(2) 1.396(3); N(1)-C(1)-N(2) 104.3(2), N(1)-C(1)-C(2) 127.6(3), N(2)-C(1)-C(2) 128.0(3). *Molecule D:* C(1)-C(2) 1.334(4), C(1)-N(1) 1.396(3), C(1)-N(2) 1.385(3); N(1)-C(1)-N(2) 104.7(2), N(1)-C(1)-C(2) 126.8(3).

In order to investigate the role of the N-heterocyclic olefin as a donor ligandon the stability of :EH_2 complexes (E = Si, Ge and Sn), a series of low-coordinate heavy Group 14 (tetrel) dichloride precursor complexes of general formula $IPrCH_2ECl_2$ (E = Si, Ge and Sn) had to be prepared from these complexes it was expected that hydride/chloride exchange chemistry would generate the dihydride adducts $IPrCH_2{\bullet}EH_2{\bullet}LA$ (E = Si, Ge and Sn; LA = Lewis acids). If IPr=CH_2 acts as a weaker σ-donor compared to IPr then the resulting olefin-hydride complexes $IPrCH_2{\bullet}EH_2{\bullet}LA$ might exhibit enhanced reactivity in comparison to their IPr counterparts ($IPr{\bullet}EH_2{\bullet}LA$).

Following the synthetic pathway outlined above, IPr=CH_2 was reacted with $GeCl_2$•dioxane in toluene resulting in the clean formation of a new product which was later identified as the expected N-heterocyclic olefin adduct $IPrCH_2{\bullet}GeCl_2$ (**19**). Compound **19** was isolated as an air- and moisture-sensitive white powder in a 86% yield. As an entry point into the synthesis of heavy methylene analogues :EH_2 using N-heterocyclic olefin donor IPr=CH_2, the germanium(II) chloride adduct $IPrCH_2{\bullet}GeCl_2$ (**19**) was reacted with Li[BH_4] in Et_2O. Unfortunately, instead of obtaining the desired hydide adduct $IPrCH_2{\bullet}GeH_2{\bullet}BH_3$, the formation of the N-heterocyclic olefin-borane adduct $IPrCH_2{\bullet}BH_3$ (**20**) was observed (Scheme 3.4). The ^{1}H NMR spectrum of **20** yields a quartet resonance at 2.05 ppm ($^3J_{HH}$ = 6.0 Hz) due to the coupling of the CH_2 group with a flanking BH_3 moiety, while the -BH_3 group was detected as a quartet resonance at -28.5 ppm ($^1J_{HH}$ = 85.9 Hz) by ^{11}B NMR spectroscopy. Compound **20** can also be synthesized in a quantitative yield from the direct reaction of IPr=CH_2

with H_3B•THF using hexanes as a solvent. X-ray quality crystals of **20** were obtained by cooling a saturated Et_2O layered with hexanes and the molecular structure **20** is shown in Figure 3.14.

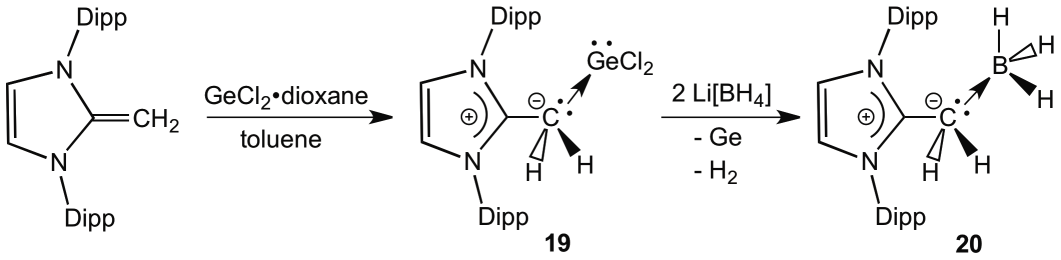

Scheme 3.4. Synthesis of the N-heterocyclic olefin adduct IPrCH_2•$GeCl_2$ (**19**) and its subsequent reaction with Li[BH_4] to IPrCH_2•BH_3 (**20**).

As illustrated in Figure 3.14, a slightly distorted tetrahedral arrangement around the olefinic carbon *C*H_2 center in IPrCH_2•BH_3 (**20**) is present. The C_{IPrCH2}-B bond length involving a terminal BH_3 group was determined to be 1.673(8) Å and is significantly longer than the C_{IPr}-B bond distance found in the carbene-borane adduct, IPr•BH_3 [1.585(4) Å],[4k] thus suggesting that IPr=CH_2 is a weaker donor than IPr.

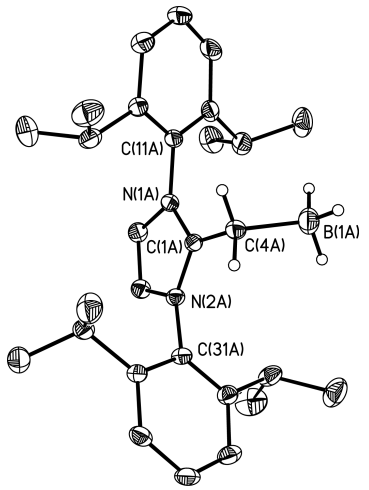

Figure 3.14. Thermal ellipsoid plot (30% probability level) of $IPrCH_2 \bullet BH_3$ (**20**). Carbon-bound hydrogen atoms have been omitted for clarity. Only one molecule of the two in the asymmetric unit is shown. Selected bond lengths [Å] and angles [°] with metrical parameters for the second molecule listed in square brackets: N(1)-C(1) 1.351(4) [1.343(4)], N(1)-C(2) 1.391(4) [1.398(4)], C(1)-C(4) 1.457(4) [1.459(4)], C(4)-B(1) 1.676(5) [1.670(6)]; N(1)-C(1)-N(2) 106.5(3) [106.2(2)], C(1)-C(4)-B(1) 112.2(3) [114.2(3)].

In order to further expand the known coordination chemistry between the N-heterocyclic olefin donor $IPr{=}CH_2$ and main group species, two equivalents of $IPr{=}CH_2$ were reacted with $HSiCl_3$ following a similar procedure developed by Roesky and coworkers to prepare $IPr \bullet SiCl_2$. Surprisingly, the formation of $IPr{=}CH\text{-}Si(H)Cl_2$ (**21**) was observed along with the known imidazolium salt, $[IPrCH_3]Cl$, instead of the target Si(II) chloride adduct, $IPrCH_2 \bullet SiCl_2$ (Equation 3.9). The formation of compound **21** can be rationalized from the fact that the olefinic proton becomes considerably acidic when bound to $HSiCl_3$, and thus can be deprotonated by an additional equivalent of $IPr{=}CH_2$ to yield **21**. The ^{1}H NMR spectrum of **21** contains a doublet resonance at δ 2.60 ppm corresponding to the IPrC*H* group, and the observed splitting pattern arises from coupling of an

olefinic proton with the adjacent Si-H unit ($^3J_{HSi}$ = 7.0 Hz). The ^{1}H NMR resonance for the Cl_2Si-H moiety appeares as a doublet at 4.39 ppm with flanking satellites due to the coupling with an NMR-active ^{29}Si nucleus ($^3J_{SiH}$ = 7.0 Hz, $^1J_{HSi}$ = 291.4 Hz). In addition, **21** yields a doublet of doublets in the ^{29}Si NMR spectrum ($^1J_{HSi}$ = 291.4 Hz, $^3J_{HSi}$ = 7.0 Hz) resulting from coupling between a silane unit (Si-H) and the proximal olefinic proton.

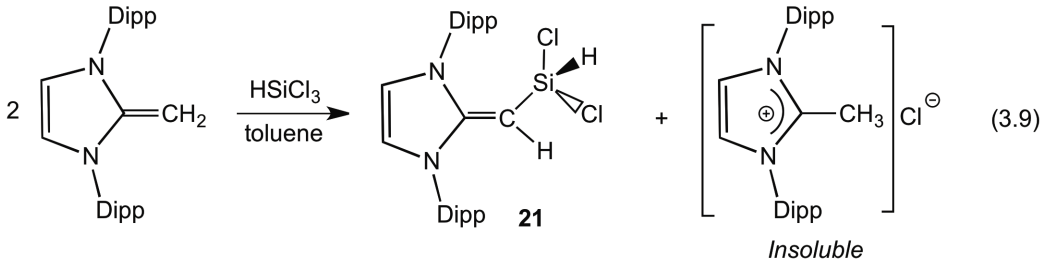

(3.9)

The molecular structure of **21** was determined by single crystal X-ray analysis and the refined structure is presented in Figure 3.15. The C_{IPrCH2}-Si bond length in **21** 1.7773(18) Å and is marginally longer than typical Si=C double bonds (1.70 – 1.76 Å),[51] but is still significantly shorter than structurally authenticated Si-C single bonds (1.86 – 1.91 Å),[52] thus the presence of partial multiple bond character in the C_{IPrCH2}-Si interaction can not be ruled out by the structural information obtained. The adjacent C(1)-C(2) bond length [1.379(2) Å] in **21** is elongated with respect to the C=C bond in IPr=CH_2 [1.331(8) Å (*avg*.)] indicating that electron density originally of π-character (*i.e*. C=C π-bond) has been transferred to the –$SiHCl_2$ moiety.

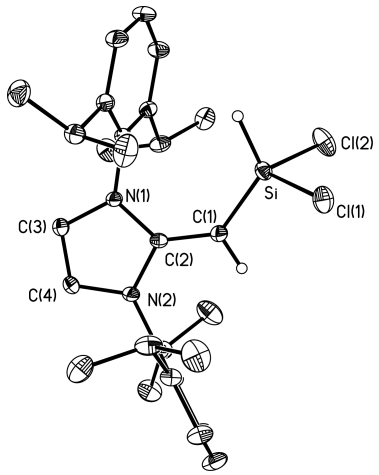

Figure 3.15. Thermal ellipsoid plot (30% probability level) of IPr=CH-Si(H)Cl_2 (**21**). All carbon-bound hydrogen atoms except the one on C(1) have been omitted for clarity. Selected bond lengths [Å] and angles [°]: C(1)-Si 1.7773(18), C(2)-C(1) 1.379(2), N(1)-C(2) 1.376(2), N(2)-C(2) 1.383(2), Si-Cl(1) 2.0801(7), Si-Cl(2) 2.0786(7), Si-H 1.37(2); Cl(1)-Si-Cl(2) 101.67(3), Cl(1)-Si-C(1) 107.94(6), Cl(2)-Si-C(1) 115.59(7), C(1)-Si-H 122.0(9).

Earlier in this Chapter, it was demonstrated that carbene group 14 element linkages can be efficiently constructed by reacting the carbene donor IPr with coordinatively labile tungsten complexes, $(THF)_xECl_2•W(CO)_5$ (E = Ge and Sn). In a similar fashion, an efficient two-step procedure was devised to access stable $IPrCH_2$ complexes of SnH_2 and GeH_2. The construction of donor–acceptor $IPrCH_2$-E coordinative bonds (E = Sn and Ge) was first accomplished by reacting $(THF)_xECl_2•W(CO)_5$ with $IPr=CH_2$ to cleanly afford the halogenated complexes $IPrCH_2•ECl_2•W(CO)_5$ (E = Sn and Ge; **22** and **23**) in 93 and 95% yields, respectively (Equation 3.10). Characterization of the Group 14 dihalide adducts **22** and **23** was achieved using a combination of X-ray crystallography, NMR and IR spectroscopy and elemental analyses.

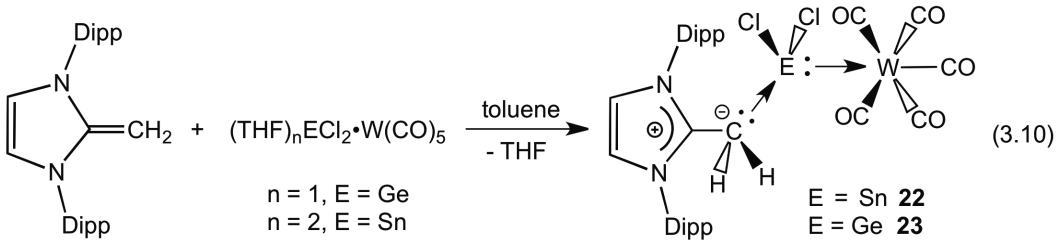

(3.10)

The tin(II) chloride adduct $IPrCH_2•SnCl_2•W(CO)_5$ (**22**) gives a resonance at -96 ppm by ^{119}Sn NMR spectroscopy and this signal is upfield shifted compared to the analogous carbene complex $IPr•SnCl_2•W(CO)_5$ (**4**) [δ = -71.3]. As shown in Figure 3.16, the molecular structure of $IPrCH_2•SnCl_2•W(CO)_5$ (**22**) features a $SnCl_2$ moiety that is encapsulated within a canted C(7)-C_{IPrCH2}-Sn-W array [torsion angle = 125.5(3)°]. The corresponding C_{IPrCH2}-Sn bond length in **22** is 2.178(4) Å and significantly elongated compared to the C_{IPr}-Sn interaction found in the carbene-tin(II) dichloride adduct $IPr•SnCl_2$ (**3**) [2.341(8) Å]. The adjacent C(7)-C_{IPrCH2} bond distance in **22** [1.452(4) Å] is longer than the C=C length in free $IPr=CH_2$ [1.331(8) Å (*avg.*)] consistent with the transfer of π-electron density to the Sn(II) center. The adjacent Sn-W bond length [2.755(2) Å] is slightly shorter than the similar dative interaction found in $IPr•SnCl_2•W(CO)_5$ (**4**) [2.7703(9) Å].

The structure of the Ge(II) chloride complex $IPrCH_2•GeCl_2•W(CO)_5$ (**23**) is shown in Figure 3.17 and this molecule adopts a similar structural motif as its heavier tin congener $IPrCH_2•SnCl_2•W(CO)_5$ (**22**). The C_{IPrCH2}-Ge bond length in **23** [2.056(3) Å] is slightly shorter than the C_{IPr}-Ge interaction in $IPr•GeCl_2•W(CO)_5$ (**11**) [2.083(13) Å (*avg.*)]. The Ge-W linkage in **23** [2.5803(3)

Å] is also the same within experimental error as the Ge-W bond distance in IPr•$GeCl_2$•$W(CO)_5$ (**11**) [2.5833(9) Å (*avg.*)]; but longer than the Ge-W bond length in the heterocyclic Ge(II) chloride adduct [PhN(Me)CHC(Me)NPh](Cl)Ge•$W(CO)_5$ [2.571(7) Å].[30]

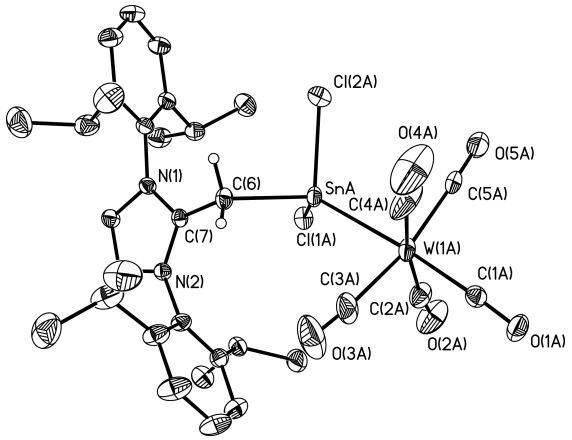

Figure 3.16. Thermal ellipsoid plot (30% probability level) of IPrCH_2•$SnCl_2$•$W(CO)_5$ (**22**). Carbon-bound hydrogen atoms and toluene solvate have been omitted for clarity. Selected bond lengths [Å] and angles (°) with values belonging to the disordered $SnCl_2$•$W(CO)_5$ residue in square brackets: Sn-W 2.755(2) [2.761(3)], Sn-C(6) 2.178(4) [2.309(5)], C(7)-C(6) 1.452(4), Sn-Cl(1) 2.354(17) [2.47(3)], Sn-Cl(2) 2.392(4) [2.397(6)], W-C(1) 1.970(9) [1.973(14)], W-C(2-5) 2.010(8) to 2.045(7); C(6)-Sn-W 124.90(14) [123.96(19)], C(7)-C(6)-Sn 124.0(2) [120.0(2)]; C(7)-C(6)-Sn-W torsion angle = -125.5(3) [-122.4(3)].

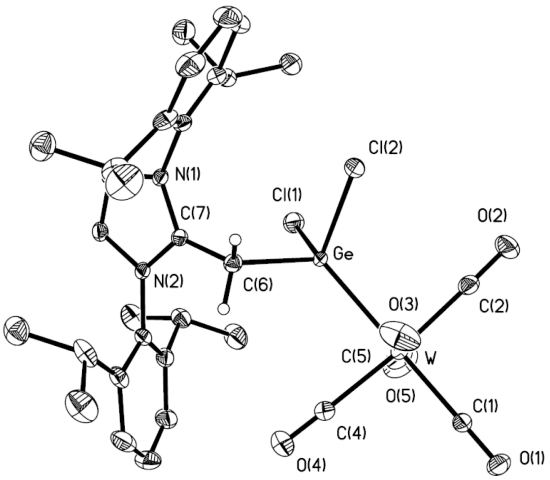

Figure 3.17. Thermal ellipsoid plot (30% probability level) of $IPrCH_2•GeCl_2•W(CO)_5$ (**23**). Carbon-bound hydrogen atoms except on C(6) have been omitted for clarity. Selected bond lengths [Å] and angles [°]: Ge-W 2.5803(3), Ge-C(6) 2.056(3), C(7)-C(6) 1.463(4), Ge-Cl(1) 2.2245(10), Ge-Cl(2) 2.2534(9), W-C(1) 2.000(3), W-C(2-5) 2.029(4) to 2.042(4); C(6)-Ge-W 120.37(9), C(7)-C(6)-Ge 118.7(2), Cl(1)-Ge-Cl(2) 99.73(4), Ge-W-C(1) 176.33(10), Ge-W-C(2-5) 86.74(11) to 92.70(13).

Having these dichloride complexes $IPrCH_2•ECl_2•W(CO)_5$ (E = Ge and Sn; **22** and **23**) in hand, the next goal was the investigation of their reactivity with different hydride sources as a potential way to prepare the desired dihydride adducts $IPrCH_2•EH_2•W(CO)_5$ (E = Ge and Sn). The target tin dihydride complexe $IPrCH_2•SnH_2•W(CO)_5$ (**24**) was prepared by reacting the Sn(II) dichloride adduct, $IPrCH_2•SnH_2•W(CO)_5$ (**22**) with $Li[BH_4]$ in Et_2O (equation 3.11). The formation of the expected Sn(II) hydride adduct $IPrCH_2•SnH_2•W(CO)_5$ (**24**) was evident by the NMR spectroscopy. The ^1H NMR spectrum of **24** gave a triplet corresponding to the SnH_2 moiety at 5.48 ppm with additional satellites due to the coupling with NMR active tungsten and tin nuclei ($^3J_{HH}$ = 2.0 Hz; $^2J_{HW}$ = 9.5 Hz; $^1J_{119Sn-H}$ = 1060

Hz and $^{1}J_{117Sn-H}$ = 1013), while a resonance for the adjacent CH_2 group was observed at 3.21 ppm along with satellites due to the coupling with tungsten ($^{3}J_{HW}$ = 21 Hz). In addition, the SnH_2 group resonated as a triplet at -229 ppm ($^{1}J_{119Sn-H}$ = 1060 Hz) in the proton-coupled ^{119}Sn NMR spectrum. For comparison, the magnitude of the ^{119}Sn-H coupling in IPr•SnH_2•$W(CO)_5$ (**5**) was determined to be 1158 Hz, while a $^{1}J_{119Sn-H}$ value of 1302 Hz was found in Jurkschat's 5-coordinate tin(II) hydride adduct [{2,6-$(Me_2NCH_2)_2C_6H_3$}SnH•$W(CO)_5$].[15e] A weak Sn-H stretching band was detected at 1758 cm^{-1} in the IR spectrum of **24**, while the related Sn-H vibration in IPr•SnH_2•$W(CO)_5$ (**5**) was located at 1786 cm^{-1}. These data is conjunction with X-ray crystallography (Figure 3.18) confirms the formation of IPrCH_2•SnH_2•$W(CO)_5$ (**24**).

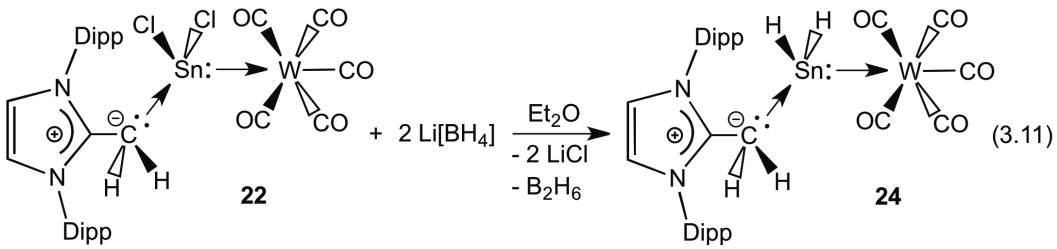

(3.11)

The deutero analogue IPrCH_2•SnD_2•$W(CO)_5$ (**24D**) was also synthesized by a clean chloride/deutride metathesis reaction. A diagnostic pentet resonance was observed in the ^{119}Sn{^{1}H} NMR spectrum ($^{1}J_{119Sn-D}$ = 164 Hz). The $^{1}J_{119Sn-D}$ value in the related tin(II) deutride complex IPr•SnD_2•$W(CO)_5$ (**5D**) was determined to be 179 Hz suggesting that a similar Sn-D bonding interactions were

present in both species.

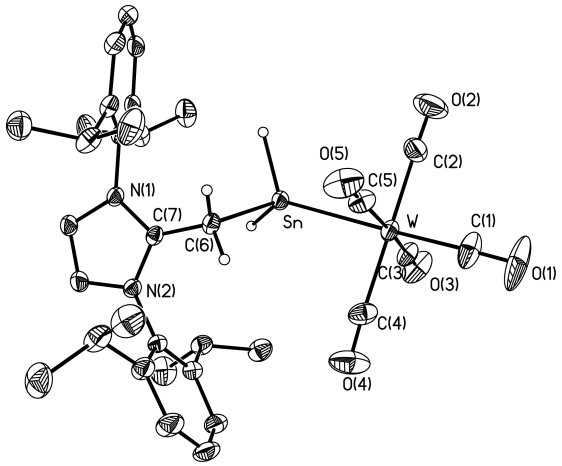

Figure 3.18. Thermal ellipsoid (30%) plot of $IPrCH_2•SnH_2•W(CO)_5$ (**24**). IPr-bound hydrogen atoms have been omitted for clarity. Selected bond lengths [Å] and angles [°]: Sn-C(6) 2.2547(17), Sn-W 2.7819(5), Sn-H 1.68(2) and 1.66(2), C(6)-C(7) 1.446(2), W-C(1) 1.965(2), W-C(2-5) 2.027(2) to 2.030(3); C(7)-C(6)-Sn 116.30(11), C(6)-Sn-W 109.76(4), Sn-W-C(1) 175.46(7), Sn-W-C(2-5) 83.52(7) to 90.75(6).

As shown in Figure 3.18, $IPrCH_2•SnH_2•W(CO)_5$ (**24**) contains a central SnH_2 array that is bound by electron donating $IPrCH_2$ and accepting $W(CO)_5$ units. The core C_{IPrCH2}-Sn bond length was determined to be 2.2547(17) Å and is the same value within error as the C-Sn bond length in Roesky's Sn(II) heterocycle [$HC(CMeNDipp)_2SnMe$] [2.253(2) Å].[23] Although, this C_{IPrCH2}-Sn interaction is much shorter than the C-Sn(II) interaction found in Veith's Ph_3PCH_2 adduct $Me_2Si(N^tBu)_2Sn•CH_2PPh_3$ [2.442(6) Å].[53] While the Sn-W distance in **24** [2.7819(5) Å] is in the range observed for Sn(II)–W bonds.[15e,54] The adjacent C_{IPrCH2}-C(7) bond length is considerably elongated [1.446(2) Å] with respect to the C=C distance in $IPr=CH_2$ (**18**) [1.331(8) Å (*avg.*)], indicating that a significant

degree of C-C π-bonding electron density is involved in coordinating the SnH_2 center. This process is accompanied by an increase in intraring N–C(7) π-bonding relative to that in **18**, and the retention of a planar geometry at C(7).

Surprisingly, the reaction of Ge(II) chloride complex $IPrCH_2•GeCl_2•W(CO)_5$ (**23**) with $Li[BH_4]$ did not lead to formation of the germanium hydride complex $IPrCH_2•GeH_2•W(CO)_5$ (**25**). However, the desired hydride functionality can be installed by reacting the germanium chloride complex $IPrCH_2•GeCl_2•W(CO)_5$ (**23**) with the stronger reducing agent, $Li[AlH_4]$ (Equation 3.12). The ^1H NMR spectrum of **25** was consistent with the assigned structure, and the GeH_2 array appeared as a well-resolved triplet at 4.07 ppm ($^3J_{HH}$ = 4.0 Hz) with expected satellites due to the coupling with an adjacent tungsten nuclei ($^3J_{HW}$ = 14.5 Hz), while a resonance for the -CH_2 group was located at 2.41 ppm as a triplet due to coupling with the -GeH_2 group ($^3J_{HH}$ = 4.0 Hz). Identification of the Ge–H stretching band in **25** by IR spectroscopy was unsuccessful due to the presence of overlapping υ(CO) bands from the $W(CO)_5$ group. Notably, the A_1 υ(CO) band in **25** was located at 2047 cm^{-1}, whereas in the $GeCl_2$ precursor $IPrCH_2•GeCl_2•W(CO)_5$ (**23**), this vibrational mode was found at 2063 cm^{-1}; these result suggests that the $IPrCH_2•GeH_2$ unit is more electron releasing than its chloro-counterpart $IPrCH_2•GeCl_2$ resulting in increased W-CO π-backbonding in **25**.[55]

The deutride analogue of **25**, $IPrCH_2•GeD_2•W(CO)_5$ (**25D**) was readily

prepared from **23** using $Li[AlD_4]$ as a deutride source. The corresponding Ge-D vibration was detected at 1407 cm^{-1} in the IR spectrum of $IPrCH_2•GeD_2•W(CO)_5$ (**25D**) from which the Ge-H stretching vibration in **25** could be estimated to be at *ca*. 1990 cm^{-1} based on the relative H/D mass ratio.

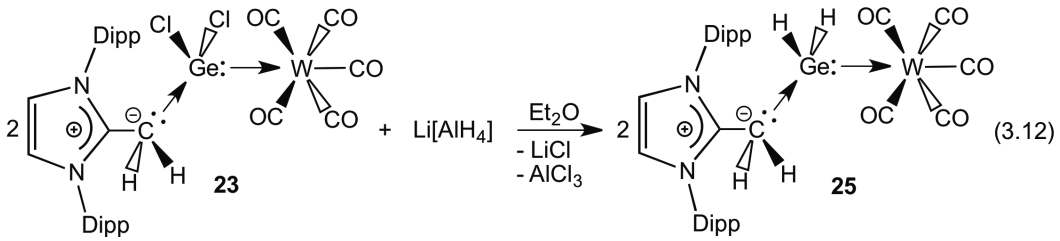

(3.12)

Overall, the GeH_2 adduct **25**, adopts an isostructural motif with its tin congener **24** (Figure 3.19). The C_{IPrCH2}-Ge distance in **25** [2.057(2) Å] is significantly longer than the Ge-C bond lengths in the germanium hydride complex $[\{Mo(CO)_4(\mu\text{-}\eta^2\text{-H-}GeEt_2)\}_2]$ [1.969(2) Å],[56] and $IPr•GeH_2•BH_3$ [2.011(2) Å]. The proximal C(6)-C_{IPrCH2} bond length was 1.463(3) Å and lies within the range expected for a C-C single bond; while the endocyclic C(7) center in the Ge adduct is planar [angle sum = 360.0(3)°] in line with the resonance form drawn in Equation 3.12.

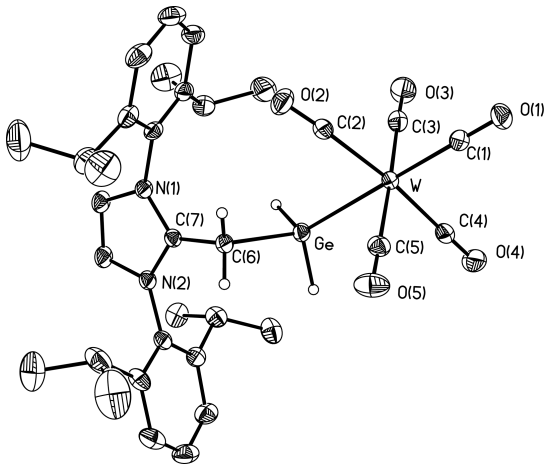

Figure 3.19. Thermal ellipsoid plot (30% probability level) of $IPrCH_2•GeH_2•W(CO)_5$ (**25**). IPr-bound hydrogen atoms and Et_2O solvate have been omitted for clarity. Selected bond lengths [Å] and angles [°]: Ge-W 2.6503(3), Ge-C(6) 2.057(2), Ge-H 1.46(3) and 1.50(3), C(6)-C(7) 1.463(3), W-C(1) 1.986(3), W-C(2-5) 2.026(3) to 2.037(3); C(6)-Ge-W 113.90(6), Ge-W-C(1) 175.89(7), Ge-W-C(2-5) 64.26(6) to 91.97(7).

$IPrCH_2•SnH_2•W(CO)_5$ (**24**) is highly sensitive to moisture and decomposes at *ca*. 95 °C in the solid state (under N_2). Complete decomposition of **24** occurs upon heating a solution of **24** in C_6D_6 to 85 °C for 30 h, whereupon a black precipitate was generated along with free $IPr=CH_2$ as the sole identifiable soluble product by ^1H and $^{13}C\{^1H\}$ NMR spectroscopy; these observations indicate that scission of the dative C_{IPrCH2}-Sn bond is a viable reaction pathway for **24**. The analogous germanium hydride $IPrCH_2•GeH_2•W(CO)_5$ (**25**) displays significantly enhanced thermal stability relative to **24** and is stable for extended periods of time (30 h) without sign of decomposition in hot C_6D_6 (85 °C).

In order to verify the dative (labile) nature of the $IPrCH_2$-E interactions in $IPrCH_2{\bullet}EH_2{\bullet}W(CO)_5$ (E = Sn and Ge; **24** and **25**), these hydride complexes were reacted with the carbene donor, IPr. As illustrated in Equation 3.13, quantitative $IPr{=}CH_2$/IPr exchange reactions transpired to give free $IPr{=}CH_2$ and the corresponding N-heterocyclic carbene adducts, $IPr{\bullet}EH_2{\bullet}W(CO)_5$, in high spectroscopic yields (> 90%) (E = Sn and Ge; **5** and **12**). This reactivity clearly indicates that these complexes are best regarded as $IPrCH_2$ adducts of GeH_2 and SnH_2 with weak $IPrCH_2$-EH_2 interactions, in place of adducts with coordinative $IPr{\bullet}CH_2$ interactions (e.g. $IPr{\bullet}H_2C{\bullet}EH_2{\bullet}W(CO)_5$).

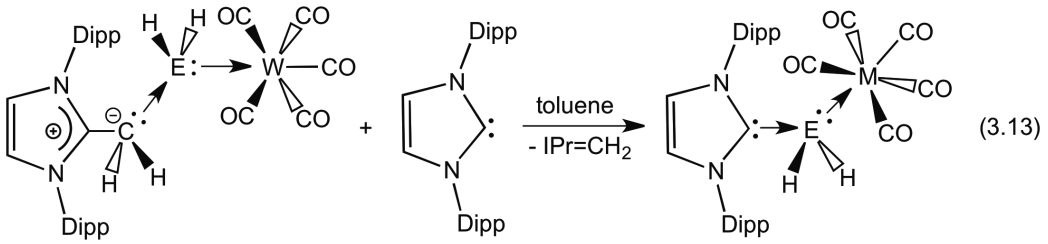

(3.13)

E = Ge and Sn; **24** and **25**

The above chemistry implied that there is an increased propensity for ligand dissociation in the olefin-bound hydrides **24** and **25** in relation to their carbene-stabilized counterparts; this property could be used to uncover new forms of reactivity. To test this hypothesis, the Sn(II) hydride adduct $IPrCH_2{\bullet}SnH_2{\bullet}W(CO)_5$ (**24**) was reacted with $ClSiMe_3$, which resulted in the formation of $IPrCH_2{\bullet}SnCl_2{\bullet}W(CO)_5$ (**22**) and $HSiMe_3$ (by ^1H NMR spectroscopy)

(Equation 3.14). Particularly noteworthy is the fact that IPr•SnH_2•$W(CO)_5$ is inert to $ClSiMe_3$ under similar conditions, thus illustrating an inherent increase in the ability of the SnH_2 unit to act as a reducing agent when a $IPrCH_2$ donor is present. No evidence of chlorosilane reduction was observed with the Ge analogue **25**, presumably due to a reduction in hydridic character of the Ge-H groups relative to the Sn-H bonds in **24**. The mechanism by which **24** reduces $ClSiMe_3$ is not understood at this time.

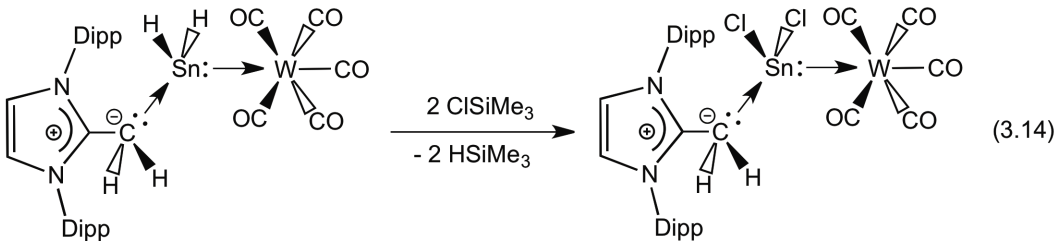

(3.14)

3.4 Conclusion

In summary, the first examples of donor-acceptor complexes of the parent heavy Group 14 methylenes EH_2 (E = Si, Ge and Sn) have been reported. This general donor-acceptor synthetic strategy involves the use of strong Lewis-basic donors such as N-heterocyclic carbenes and N-heterocyclic olefins in combination with Lewis-acids to isolate various Group 14 dihydrides. Of note, the use of sterically demanding phosphine and amine donors in this strategy were unsuccessful. In general, the N-heterocyclic carbene adducts IPr•EH_2•$W(CO)_5$ (E

= Si, Ge and Sn) are thermally more stable than their N-heterocyclic olefin counter parts; this higher degree of thermal stability originates from stronger σ-donation ability of IPr. As expected from the relative Lewis acidity and Lewis basicity of $:EH_2$ units, the Si(II) adduct $IPr{\bullet}SiH_2{\bullet}W(CO)_5$ is the most stable complex of the series followed by the germanium and tin analogues. Interestingly, the element-boron ($E\text{-}BH_3$) interactions in the borane adducts $IPr{\bullet}EH_2{\bullet}BH_3$ (E = Si and Ge) are labile enough in THF to allow $IPr{\bullet}EH_2$ units be transferred onto Lewis acidic metal centers such as $W(CO)_5$ and $Cr(CO)_5$ *via* $M(CO)_5/BH_3$ (M = Cr and W) metathesis chemistry. This unique $M(CO)_5/BH_3$ (M = Cr and W) metathesis chemistry can serve a general way to install $:EH_2$ moieties on wide variety of Lewis-acidic transition metal complexes. The E-H bonds in these hydride adducts $IPr{\bullet}EH_2{\bullet}W(CO)_5$ (E = Si, Ge and Sn) are hydridic and accordingly the tin hydride complex $IPr{\bullet}SiH_2{\bullet}W(CO)_5$ participated in a clean hydrostannylation reaction with excess benzaldehyde.

3.5 Experimental Section

3.5.1 Materials and Instrumentation

All reactions were performed using standard Schlenk line techniques under an atmosphere of nitrogen or in an inert atmosphere glove box (Innovative Technology, Inc.). Solvents were dried using Grubbs-type solvent purification system[38] manufactured by Innovative Technology, Inc., degassed (freeze-pump-thaw method) and stored under an atmosphere of nitrogen prior to use. $SnCl_2$, $Li[BH_4]$, $Li[BD_4]$, $Li[AlH_4]$, $Li[AlD_4]$, $Li[HBEt_3]$ (1.0 M solution in THF), CH_3I, ^{n}BuLi (1.6 M or 2.5 M solution in Hexanes), benzaldehyde and $GeCl_2$•dioxane were purchased from Aldrich and used as received. $W(CO)_6$ and $Cr(CO)_6$ were obtained from Aldrich and sublimed under vacuum and stored under nitrogen prior to use. Trichlorosilane (Cl_3SiH) and trimethylsilyl chloride (Me_3SiCl) were obtained from Aldrich and used as received. 1,3-Bis-(2,6-diisopropylphenyl)-imidazol-2-ylidene (IPr),[17] 1,3-bis-(2,6-diisopropylphenyl)-imidazolium chloride [IPrH]Cl,[17] IPr•$SiCl_2$,[4c] $(THF)_2SnCl_2$•$W(CO)_5$[25a] and (THF)$GeCl_2$•$W(CO)_5$[25b] were prepared following literature procedures. ^1H, $^2H\{^1H\}$, $^{13}C\{^1H\}$, ^{29}Si, ^{11}B and ^{119}Sn NMR spectra were recorded on a Varian iNova-400 spectrometer and referenced externally to $SiMe_4$ (^1H, $^{13}C\{^1H\}$ and ^{29}Si), $Si(CD_3)_4$ ($^2H\{^1H\}$), F_3B•OEt_2 (^{11}B) and $SnMe_4$ (^{119}Sn) respectively, by setting the resonance for residual H, D, C, Si, B and Sn at 0.0 ppm. X-ray crystallographic analyses were performed by the X-ray Crystallography Laboratory at the University of Alberta. Elemental analyses were performed by the Analytical and Instrumentation Laboratory at the University of

Alberta. Infrared spectra were recorded Nicolet IR100 FTIR spectrometer as a Nujol mulls between NaCl plates. Melting points were measured in sealed glass capillaries under nitrogen using a MelTemp melting point apparatus and are uncorrected.

3.5.2 X-ray Crystallography

Crystals of suitable quality for X-ray diffraction studies were removed from a vial in a glove box and immediately covered with a thin layer of hydrocarbon oil (Paratone-N). A suitable crystal was selected, mounted on a glass fiber and quickly placed in a low temperature stream of nitrogen on an X-ray diffractometer.[57] All data were collected using a Bruker APEX II CCD detector/D8 diffractometer using Mo Kα or Cu Kα radiation with the crystals cooled to -100 °C. The data were corrected for absorption through Gaussian integration from the indexing of the crystal faces.[58] Structures were solved using the direct methods program SHELXS-97[59] (compounds **1**, **3**, **5**, **11**-**14**, **17**, **18, 21** and **22**) and SIR97[60] (compounds **23** and **25**) or using the Patterson search/structure expansion facilities within the DIRDIF-2008[61] (compounds **2**, **9**, **16** and **24**) and SHELXD[62] program suites (compounds **15** and **20**); structure refinement was accomplished using SHELXL-97. Hydrogen atoms were assigned positions based on the sp^2 or sp^3 hybridization geometries of their attached carbon atoms, and were given thermal parameters 20% greater than those of their parent atoms. See Tables 3.1-3.6 for listings of the crystallographic data.

3.5.2.1 Special Refinement Conditions

Compound **3**: The crystal used for data collection was found to display non-merohedral twinning. Both components of the twin were indexed with the program *CELL_NOW* (Bruker AXS Inc., Madison, WI, 2004).[63] The second twin component was related to the first component by 180º rotation about the [0.003 0 1] axis in real space and about the [0.093 0.006 1] axis in reciprocal space. Integrated intensities for the reflections from the two components were written into a *SHELXL-93* HKLF 5 reflection file with the data integration program *SAINT* (version 7.60A),[64] using all reflection data (exactly overlapped, partially overlapped and non-overlapped).

Compound **11**: The minor (6%) orientation of the disordered $GeCl_2$–$W(CO)_5$ fragment of *moiety C* was restrained to have the same geometry as that of the major conformation by use of the *SHELXL* **SAME** instruction.

Compound **13**: The C–C distances within the disordered solvent tetrahydrofuran molecule were restrained to be approximately equal by use of the *SHELXL* instruction **SADI** during refinement; the C–O distances of the tetrahydrofuran molecule were treated in the same manner.

Compound **16**: The Si–H1 and Si–H2 distances were constrained to be equal (within 0.01 Å) during refinement. (b) The C–C distances within the disordered solvent n-hexane molecule were restrained during refinement: d(C1SA–C1SA') = d(C1SA–C2SA) = d(C2SA–C3SA) = d(C1SB–C1SB') = d(C1SB–C2SB) = d(C2SB–C3SB) = 1.52(1) Å (primed atoms are related to unprimed ones via the

crystallographic inversion center (½, 0, ½).

Compound **17**: Bond distances within the disordered solvent CH_2Cl_2 molecules were restrained during refinement: d(Cl1S–C1S) = d(Cl2S–C1S) = d(Cl3S–C2S) = d(Cl4S–C2S) = d(Cl5S–C3S) = d(Cl6S–C3S) = 1.75(1) Å.

Compound **20**: The crystal used for data collection was found to display non-merohedral twinning. Both components of the twin were indexed with the program *CELL_NOW* (Bruker AXS Inc., Madison, WI, 2004).[63] The second twin component can be related to the first component by 180º rotation about the [0.229 0 1] axis in real space and about the [0 0 1] axis in reciprocal space. Integrated intensities for the reflections from the two components were written into a *SHELXL-97* HKLF 5 reflection file with the data integration program *SAINT* (version 7.68A)[64] and absorption correction program *TWINABS* (version 2008/4)[65] using all reflection data from component one. The refined value of the twin fraction (*SHELXL-97* BASF parameter) was 0.3843(15).

The solvent diethylether molecules had the following restraints applied: O–C, 1.430(2) Å; C–C, 1.530(2) Å. The minor orientation of the disordered solvent diethylether molecule had the additional following restraints applied: C···C, 2.340(4) Å; O···C, 2.420(4) Å.

Compound **22**: Distances involving the methyl carbon of the inversion-disordered solvent toluene molecule were restrained during the refinement: d(C1S-C7S) = 1.50(1) Å; d(C2S...C7S) = d(C6S...C7S) = 2.50(1) Å. The phenyl ring of this molecule was modeled as an idealized regular hexagon with d(C-C) = 1.39 Å. All

carbon atoms of this molecule were refined with a common isotropic displacement parameter.

3.5.3 Synthetic Procedures.

3.5.3.1 Synthesis of IPr•$GeCl_2$ 1. IPr (0.372 g, 0.96 mmol) and $GeCl_2$•dioxane (0.220 g, 0.95 mmol) were combined in 12 mL of toluene at room temperature. The reaction mixture was allowed to proceed for 12 h, giving a white slurry. The white precipitate was isolated by filtration and identified as **1** (0.348 g). A further crop of **1** (colorless crystals of X-ray quality) was obtained by cooling the filtrate to -35 °C for 2 days (0.089 g; combined yield = 0.437 g, 86%). ^{1}H NMR (C_6D_6): δ 0.99 (d, 12H, $^3J_{HH}$ = 6.8 Hz, CH(CH_3)$_2$), 1.41 (d, 12H, $^3J_{HH}$ = 6.8 Hz, CH(CH_3)$_2$), 2.80 (septet, 4H, $^3J_{HH}$ = 7.2 Hz, C*H*(CH3)2), 6.42 (s, 2H, N–C*H*–), 7.07 (d, 4H, $^3J_{HH}$ = 8.0 Hz, Ar*H*), 7.21 (t, 2H, $^3J_{HH}$ = 8.0 Hz, ArH). ^{13}C{^{1}H} NMR (C_6D_6): δ 23.2 (CH(*C*H$_3$)$_2$), 25.7 (CH(*C*H$_3$)$_2$), 29.2 (*C*H(CH$_3$)$_2$), 124.4 (Ar*C*), 124.6 (Ar*C*), 131.3 (N–*C*H–), 133.2 (Ar*C*), 145.9 (Ar*C*), 174.9 (N–*C*–N). Anal. Calcd. for $C_{27}H_{36}Cl_2GeN_2$: C, 60.94; H, 6.82; N, 5.26. Found: C, 60.88; H, 6.80; N, 5.16. Mp (°C): 230–233.

3.5.3.2 Synthesis of IPr•GeH_2•BH_3 2. To a mixture of **1** (0.137 g, 0.260 mmol) and Li[BH_4] (0.027 g, 1.2 mmol) was added 9 mL of cold (-35 °C) Et_2O. The reaction mixture was then warmed to room temperature and stirred for 14 h to give a pale orange slurry. The volatiles were removed under vacuum and the product was extracted with 10 mL of benzene. Filtration of the mixture followed

by removal of the solvent from the filtrate afforded **2** as a pure white solid (0.100 g, 81%). Crystals suitable for X-ray crystallography were grown by cooling a toluene/hexanes solution to -35 °C for 2 days. ^{1}H NMR (C_6D_6): δ 0.6–1.6 (br, q, 3H, –B*H*$_3$), 0.97 (d, 12H, $^{3}J_{HH}$ = 6.9 Hz, CH(C*H*$_3$)$_2$), 1.39 (d, 12H, $^{3}J_{HH}$ = 6.6 Hz, CH(C*H*$_3$)$_2$), 2.62 (septet, 4H, $^{3}J_{HH}$ = 6.6 Hz, C*H*(CH$_3$)$_2$), 3.92 (q, 2H, $^{3}J_{HH}$ = 4.8 Hz, –Ge*H*$_2$–), 6.47 (s, 2H, N–C*H*–), 7.08 (d, 4H, $^{3}J_{HH}$ = 7.8 Hz, Ar*H*), 7.22 (t, 2H, $^{3}J_{HH}$ = 7.8 Hz, Ar*H*). ^{13}C{^{1}H} NMR (C_6D_6): δ 23.0 (CH(*C*H$_3$)$_2$), 25.5 (CH(*C*H$_3$)$_2$), 29.2 (*C*H(CH$_3$)$_2$), 124.6 (Ar*C*), 124.7 (Ar*C*), 131.3 (N–*C*H–), 133.9 (Ar*C*), 145.6 (Ar*C*), 171.4 (N–*C*–N). ^{11}B{^{1}H} NMR (C_6D_6): δ -40.0 (s). ^{11}B NMR (C_6D_6): δ -40.0 (quartet, $^{1}J_{BH}$ = 99 Hz). IR (Nujol/cm^{-1}): 1987 (m, υGe-H), and 2310 (sh, υB-H) and 2349 (sh, υB-H). Anal. Calcd. for $C_{27}H_{41}BGeN_2$: C, 67.97; H, 8.66; N, 5.87. Found: C, 67.45; H, 8.67; N, 6.09. Mp (°C): 130 (dec.).

3.5.3.3 Preparation of IPr•GeD$_2$•BD$_3$ (2D). To a mixture of IPr•GeCl$_2$ (0.11 g, 0.21 mmol) and Li[BD$_4$] (13 mg, 0.50 mmol) was added 12 mL of cold (-35 °C) Et$_2$O. The reaction mixture was then warmed to room temperature and stirred overnight to give a pale orange slurry. Filtration of this mixture through Celite afforded a colorless filtrate which upon removal of the volatiles gave pure IPr•GeD$_2$•BD$_3$ as a colorless solid (48 mg, 48%). ^{1}H NMR (C_6D_6): Similar to **2** except with the resonances for GeH$_2$ and BH$_3$ were absent. ^{2}H{^{1}H} NMR (C_6H_6): δ 1.03 (br, BD$_3$) and 3.88 (s, GeD$_2$). ^{11}B{^{1}H} NMR (C_6H_6): δ -40.6 (br).

3.5.3.4 Synthesis of IPr•SnCl$_2$ 3. IPr (0.574 g, 1.48 mmol) and SnCl$_2$ (0.281 g, 1.49 mmol) were combined in 12 mL of toluene at room temperature. The

reaction mixture was allowed to proceed for 24 h to give a white slurry. The white precipitate was isolated by filtration and identified as **3** (0.531 g). A further crop of **3** (colorless crystals of X-ray quality) was obtained by cooling the filtrate to -35 °C for 2 days (0.095 g; combined yield = 0.626 g, 73% yield). ^{1}H NMR (C_6D_6): δ 0.98 (d, 12H, $^{3}J_{HH}$ = 6.4 Hz, CH(CH_3)$_2$), 1.41 (d, 12H, $^{3}J_{HH}$ = 6.8 Hz, CH(CH_3)$_2$), 2.78 (septet, 4H, $^{3}J_{HH}$ = 6.8 Hz, CH(CH$_3$)$_2$), 6.45 (s, 2H, N–CH–), 7.08 (d, 4H, $^{3}J_{HH}$ = 8.0 Hz, ArH), 7.22 (t, 2H, $^{3}J_{HH}$ = 8.0 Hz, ArH). ^{13}C{^{1}H} NMR (C_6D_6): δ 23.2 (CH(CH$_3$)$_2$), 25.8 (CH(CH$_3$)$_2$), 29.2 (CH(CH$_3$)$_2$), 124.5 (ArC), 124.7 (ArC), 131.3 (N–CH–), 133.5 (ArC), 145.4 (ArC), 184.2 (N–C–N). ^{119}Sn NMR (C_6D_6): δ -68.7 (s). Anal. Calcd. for $C_{27}H_{36}Cl_2SnN_2$: C, 56.09; H, 6.28; N 4.84. Found: C, 55.37; H, 6.06; N, 4.69. Mp (°C): 190 (dec.).

3.5.3.5 Reaction of 3 with Li[BH$_4$]. IPr•SnCl$_2$ (**3**) (122 mg, 0.210 mmol) and an excess of Li[BH$_4$] (16 mg, 0.73 mmol) were combined in 6 mL of cold ether (-35 °C) and allowed to warm slowly to room temperature with stirring. A vigorous reaction resulted that was accompanied by gas evolution and a rapid darkening of the solution (with the deposition of a grey precipitate). After 5 h, the volatiles were removed, the residue was extracted with 10 mL of benzene and filtered. Removal of the solvent afforded a white solid that was identified as pure IPr•BH$_3$ by NMR spectroscopy (65 mg, 77%).[4k]

3.5.3.6 Thermolysis of IPr•GeH$_2$•BH$_3$ (2). Compound **2** (98 mg, 0.20 mmol) was dissolved in 3 mL of toluene and the solution heated to reflux. Within 45 min, a black suspension was obtained and the heating was then continued for a total of

16 h. Afterwards, the volatiles were removed, the resulting black solid stirred with 10 mL of benzene and the mixture was filtered. Removal of the solvent from the filtrate gave IPr•BH_3 in high yield (77 mg, 93%) as a white solid.

3.5.3.7 Synthesis of IPr•$SnCl_2$•$W(CO)_5$ 4. To a mixture of IPr (0.18 g, 0.46 mmol) and $(THF)_2SnCl_2$•$W(CO)_5$ (0.30 g, 0.46 mmol) was added 12 mL of toluene. The reaction mixture was stirred overnight to give a pale yellow slurry. The precipitate was isolated by filtration and identified as **4** (0.31 g). A further crop of **4** was isolated by cooling the filtrate to -35 °C (0.070 g; combined yield = 0.37 g, 90%). ^{1}H NMR (C_6D_6): δ 0.90 (d, $^3J_{HH}$ = 6.8 Hz, 12H, CH(CH_3)$_2$), 1.42 (d, $^3J_{HH}$ = 6.8 Hz, 12H, CH(CH3)2), 2.67 (septet, $^3J_{HH}$ = 6.8 Hz, 4H, C*H*(CH_3)$_2$), 6.32 (s, 2H, N-C*H*-), 7.07 (d, $^3J_{HH}$ = 7.6 Hz, 4H, Ar*H*) and 7.21 (t, $^3J_{HH}$ = 7.6 Hz, 2H, Ar*H*). ^{13}C{^{1}H} NMR (C_6D_6): δ 23.2 (CH(*C*H_3)$_2$), 25.7 (CH(*C*H_3)$_2$), 29.3 (*C*H(CH_3)$_2$), 125.3 (Ar*C*), 125.9 (Ar*C*), 131.9 (Ar*C*), 132.7 (Ar*C*), 145.4 (-N-*C*H-), 166.9 (N-*C*-N), 197.3 (equat. *C*O), 199.8 (ax. *C*O). ^{119}Sn{^{1}H} NMR (C_6D_6, referenced externally to $SnMe_4$): δ = -71.3. IR (Nujol, cm^{-1}): 1922 (br, υCO) and 2067 (m, υCO). Anal. Calcd. for $C_{32}H_{36}Cl_2N_2O_5SnW$: C, 42.61; H, 4.02; N, 3.11. Found: C, 42.08; H, 4.33; N, 3.26. Mp (°C): 181-183.

3.5.3.8 Preparation of IPr•SnH_2•$W(CO)_5$ 5. To a mixture of **4** (46 mg, 0.051 mmol) and Li[BH_4] (2.3 mg, 0.11 mmol) was added 10 mL of cold (-35 °C) Et_2O. The reaction mixture was warmed to room temperature and stirred overnight to yield a light brown slurry. The volatiles were removed under vacuum and the product was extracted with 8 mL of toluene and filtered. Removal of the solvent

from the filtrate afforded a pale yellow **5** as a spectroscopically pure solid (41 mg, 96%). Crystals of suitable quality for X-ray crystallography were grown from a saturated Et_2O/hexanes mixture at -35 °C. ^{1}H NMR (C_6D_6): δ 0.89 (d, $^3J_{HH}$ = 6.8 Hz, 12H, CH(C*H*$_3$)$_2$), 1.37 (d, $^3J_{HH}$ = 6.8 Hz, 12H, CH(C*H*$_3$)$_2$), 2.55 (septet, $^3J_{HH}$ = 6.8 Hz, 4H, C*H*(CH$_3$)$_2$), 5.55 (s, 2H, SnH_2, satellites: $^3J_{HW}$ = 8.0 Hz; $^1J_{H\text{-}119Sn}$ = 1159.4 Hz; $^3J_{H\text{-}117Sn}$ = 1108.2 Hz), 6.44 (s, 2H, N-C*H*-), 7.07 (d, $^3J_{HH}$ = 7.6 Hz, 4H, Ar*H*) and 7.20 (t, $^3J_{HH}$ = 7.6 Hz, 2H, Ar*H*). ^{13}C{^{1}H} NMR (C_6D_6): δ 22.8 (CH(*C*H$_3$)$_2$), 25.6 (CH(*C*H$_3$)$_2$), 29.1 (*C*H(CH$_3$)$_2$), 124.8 (Ar*C*), 125.4 (Ar*C*), 131.5 (Ar*C*), 134.4 (Ar*C*), 145.1 (-N-*C*H-), 167.5 (N-*C*-N), 200.8 (equat. *CO*, $^1J_{C\text{-}W}$ = 60.0 Hz), 203.1 (ax. *CO)*. ^{119}Sn{^{1}H} NMR (C_6D_6): δ -309 (s). ^{119}Sn NMR (C_6D_6): δ -309 (t, $^1J_{H\text{-}119Sn}$ = 1158 Hz, *Sn*H$_2$; $^1J_{Sn\text{-}W}$ = 828 Hz*)*. IR (Nujol/cm^{-1}): 1786 (w, υSn-H), 1878 (s, υCO), 1896 (s, υCO), 1909 (s, υCO) and 2047 (m, υCO). Anal. Calcd. for $C_{32}H_{38}N_2O_5SnW$: C, 46.13; H, 4.60; N, 3.36. Found: C, 47.50; H, 5.09; N, 3.17. Mp (°C): 149-151 (dec., turns black), 162-165 (melts).

3.5.3.9 Synthesis of IPr•SnD$_2$•W(CO)$_5$ 5D. To a mixture of **4** (50 mg, 0.055 mmol) and Li[BD_4] (3.4 mg, 0.13 mmol) was added 12 mL of cold (-35 °C) Et_2O. The reaction mixture was then warmed to room temperature and stirred overnight to afford a beige colored slurry. The resulting slurry was then filtered through Celite and the volatiles were removed to afford **5D** as a very pale yellow solid (45 mg, 97%). ^{1}H NMR (C_6D_6): essentially the same as **5** with the absence of the SnH_2 resonance. ^{2}H{^{1}H} NMR (C_6H_6): δ 5.58 (s, -Sn*D*$_2$-). ^{119}Sn{^{1}H} NMR (C_6D_6): δ -309.5 (pentet, $^1J_{119Sn\text{-}D}$ = 179 Hz); in addition, a resonance due to IPr•SnHD•W(CO)$_5$ was detected (ca. 20%): δ -309.2 (1:1:1 triplet, $^1J_{119Sn\text{-}D}$ = 179

Hz). IR (Nujol/cm^{-1}): Similar to **5** except for absence of υSn-H at 1786 cm^{-1}; the location of the Sn-D stretch could not be determined due to overlapping IPr vibrations.

3.5.3.10 Synthesis of $(THF)_2SnCl_2$•$Cr(CO)_5$ To a mixture of $Cr(CO)_6$ (500 mg, 2.27 mmol) and $SnCl_2$ (431 mg, 2.27 mmol) was added 85 mL of dry THF and the mixture was irradiated with a 450 W mercury lamp for 6 h to give a pale orange solution. Volatiles were removed from the reaction mixture and then extracted with 30 mL of hexanes. Spectroscopically pure $(THF)_2SnCl_2$•$Cr(CO)_5$ can be isolated as bright orange crystals by cooling the hexanes extract to -35 °C. Occasionally, a small amount of $Cr(CO)_6$ co-crystallized with the $(THF)_2SnCl_2$•$Cr(CO)_5$ (as evident from $^{13}C\{^1H\}$ NMR) and a further recrystallization from hexanes was required to remove $Cr(CO)_6$ and afford clean $(THF)_2SnCl_2$•$Cr(CO)_5$. (238 mg, 26%). ^1H NMR (C_6D_6): δ 1.12 (m, 4H, C_4H_8O (THF)), 3.59 (m, 4H, C_4H_8O (THF)). $^{13}C\{^1H\}$ NMR (C_6D_6): δ 25.2 (C_4H_8O (THF)), 69.6 (C_4H_8O (THF)), 215.8 (equat. *C*O), 222.6 (ax. *C*O). $^{119}Sn\{^1H\}$ NMR (C_6D_6): δ -250.1 (s). Anal. Calcd. for $C_{13}H_{316}Cl_2CrO_7Sn$: C, 29.69; H, 3.07. Found: C, 28.80; H, 2.35. Mp (°C): 166-168.

3.5.3.11 Synthesis of IPr•$SnCl_2$•$Cr(CO)_5$ 6. To a mixture of IPr (0.083 g, 0.213 mmol) and $(THF)_2SnCl_2$•$Cr(CO)_5$ (0.112 g, 0.213 mmol) was added 4 mL of toluene. The reaction mixture was stirred for 40 minutes to obtain a pale green slurry. The precipitate was isolated by filtration and identified as **6** (0.148 g, 93%). ^1H NMR (C_6D_6): δ 0.91 (d, $^3J_{HH}$ = 6.8 Hz, 12H, $CH(CH_3)_2$), 1.42 (d, $^3J_{HH}$ =

6.8 Hz, 12H, $CH(CH_3)_2$), 2.68 (septet, $^3J_{HH}$ = 6.8 Hz, 4H, C*H*$(CH_3)_2$), 6.32 (s, 2H, N-C*H*-), 7.07 (d, $^3J_{HH}$ = 7.6 Hz, 4H, Ar*H*) and 7.20 (t, $^3J_{HH}$ = 7.6 Hz, 2H, Ar*H*). $^{13}C\{^1H\}$ NMR (C_6D_6): δ 23.1 ($CH(CH_3)_2$), 25.7 ($CH(CH_3)_2$), 29.3 ($CH(CH_3)_2$), 125.2 (Ar*C*), 126.0 (Ar*C*), 131.9 (Ar*C*), 132.8 (Ar*C*), 145.4 (-N-*C*H-), 170.9 (N-*C*-N), 217.1 (equat. *C*O), 224.5 (ax. *C*O). $^{119}Sn\{^1H\}$ NMR (C_6D_6): δ 165.6. IR (Nujol/cm^{-1}): 1922 (br, υCO) and 2055 (m, υCO). Anal. Calcd. for $C_{32}H_{36}Cl_2CrN_2O_5Sn$: C, 49.90; H, 4.71; N, 3.64. Found: C, 50.15; H, 4.66; N, 3.57. Mp (°C): 152-154.

3.5.3.12 Synthesis of IPr•SnH_2•$Cr(CO)_5$ 7. To a mixture of **6** (200 mg, 0.260 mmol) and $Li[BH_4]$ (12 mg, 0.55 mmol) was added 6 mL of cold (-35 °C) Et_2O. The reaction mixture was warmed to room temperature and stirred for 45 minutes to yield a pale brown solution over a yellow precipitate. The precipitae was allowed to settle and the mother liquor was then filtered through Celite to give a beige filtrate. Removal of the volatiles from the filtrate afforded **7** as a brown solid (171 mg, 94%). Crystals of suitable quality for X-ray crystallography were grown by cooling a saturated Et_2O/hexanes mixture to -35 °C. ^1H NMR (C_6D_6): δ 0.89 (d, $^3J_{HH}$ = 6.8 Hz, 12H, $CH(CH_3)_2$), 1.37 (d, $^3J_{HH}$ = 6.8 Hz, 12H, $CH(CH_3)_2$), 2.58 (septet, $^3J_{HH}$ = 6.8 Hz, 4H, C*H*$(CH_3)_2$), 5.51 (s, 2H, SnH_2, satellites: $^1J_{H\text{-}119Sn}$ = 1180.9 Hz; $^3J_{H\text{-}117Sn}$ = 1128.8 Hz), 6.47 (s, 2H, N-C*H*-), 7.07 (d, $^3J_{HH}$ = 7.6 Hz, 4H, Ar*H*) and 7.19 (t, $^3J_{HH}$ = 7.6 Hz, 2H, Ar*H*). $^{13}C\{^1H\}$ NMR (C_6D_6): δ 22.4 ($CH(CH_3)_2$), 25.5 ($CH(CH_3)_2$), 28.8 ($CH(CH_3)_2$), 124.5 (Ar*C*), 125.3 (Ar*C*), 131.2 (Ar*C*), 133.9 (Ar*C*), 144.8 (-N-*C*H-), 169.5 (N-*C*-N), 222.4 (equat. *CO*), 203.1 (ax. *CO)*. $^{119}Sn\{^1H\}$ NMR (C_6D_6): δ -104.8 (s). ^{119}Sn NMR (C_6D_6): δ -106.6 (t, $^1J_{H\text{-}}$

$_{119Sn}$ = 1185 Hz, *Sn*H_2*)*. IR (Nujol/cm^{-1}): 1772 (m, υSn-H), 1882 (s, υCO), 1898 (br, υCO) and 2037 (m, υCO). Anal. Calcd. for $C_{32}H_{38}CrN_2O_5Sn$: C, 54.80; H, 5.46; N, 3.99. Found: C, 54.98; H, 5.62; N, 3.95. Mp (°C): 136-138 (dec., turns dark brown), 153-155 (melts).

3.5.3.13 Thermolysis of IPr•SnH_2•$W(CO)_5$. A solution of IPr•SnH_2•$W(CO)_5$ (55 mg, 0.066 mmol) in 10 mL of toluene was heated to 100 °C for 36 hrs to obtain a pale yellow solution over a black precipitate. The solution was decanted and the residue was extracted with 6 mL of toluene. The combined extracts were filtered through Celite and the volatiles were removed to obtain a pale yellow powder (33 mg). ^{1}H NMR (C_6D_6) analysis of the soluble fraction revealed the presence of IPr (39%), IPr•$W(CO)_5$ (52%) and [$(HCNDipp)_2CH_2$ (9%). Data for IPr: ^{1}H NMR (C_6D_6): δ 1.18 (d, $^3J_{HH}$ = 6.9 Hz, 12H, $CH(CH_3)_2$), 1.28 (d, $^3J_{HH}$ = 6.9 Hz, 12H, $CH(CH_3)_2$), 2.96 (septet, $^3J_{HH}$ = 6.8 Hz, 4H, $CH(CH_3)_2$), 6.61 (s, 2H, N-C*H*-), 7.17 (d, $^3J_{HH}$ = 7.2 Hz, 4H, Ar*H*) and 7.29 (t, $^3J_{HH}$ = 7.2 Hz, 2H, Ar*H*).

3.5.3.14 Independent synthesis of IPr•$W(CO)_5$ 8. 30 mL of dry THF was added to $W(CO)_6$ (121 mg, 0.344 mmol) and the mixture was irradiated with a 450 W mercury lamp for 1.5 h to give a bright yellow solution of $W(CO)_5$•THF. IPr (133 mg, 0.342 mmol) was dissolved in a 1:1 toluene/THF mixture (ca. 5 mL) and then added dropwise to the solution of $W(CO)_5$•THF. The immediate formation of a red solution was observed and the reaction mixture was stirred overnight; the volatiles were then removed under vacuum to give a pale yellow powder, which was further purified by recrystallization from a mixture of hexanes and toluene at

-35 °C (145 mg, 59%). ^{1}H NMR (C_6D_6): δ 0.98 (d, $^{3}J_{HH}$ = 6.8 Hz, 12H, CH(CH_3)$_2$), 1.36 (d, $^{3}J_{HH}$ = 6.8 Hz, 12H, CH(CH_3)$_2$), 2.75 (septet, $^{3}J_{HH}$ = 6.8 Hz, 4H, CH(CH$_3$)$_2$), 6.47 (s, 2H, N-CH-), 7.11 (d, $^{3}J_{HH}$ = 7.6 Hz, 4H, ArH) and 7.26 (t, $^{3}J_{HH}$ = 7.6 Hz, 2H, ArH). ^{13}C{^{1}H} NMR (C_6D_6): δ 22.9 (CH(*C*H$_3$)$_2$), 25.8 (CH(*C*H$_3$)$_2$), 29.1 (*C*H(CH$_3$)$_2$), 124.7 (Ar*C*), 131.2 (Ar*C*), 138.1 (Ar*C*), 146.2 (Ar*C*), 188.7 (-N-*C*H-), 191.2 (N-*C*-N), 197.3 (equat. *C*O) and 199.9 (ax. *C*O). IR (Nujol/cm^{-1}): 1880 (br, υCO), 1918 (br, υCO), 1981 (m, υCO), 2056 (s, υCO). Anal. Calcd. for $C_{32}H_{36}N_2O_5W$: C, 53.94; H, 5.09; N, 3.93. Found: C, 53.35; H, 4.92; N 3.77. Mp (°C): 258-260.

3.5.3.15 Independent synthesis of IPrH$_2$, ([(HCNDipp)$_2$CH$_2$]) 9. To a cold (-35 °C) slurry of [IPrH]Cl (49 mg, 0.12 mmol) in 10 mL of Et_2O was added dropwise a solution of Li[HBEt$_3$] (1.0 M solution in THF, 0.12 mL, 0.12 mmol). The reaction mixture was warmed to room temperature and stirred overnight to give a colorless solution over a white precipitate. The slurry was filtered through Celite and the volatiles were removed from the filtrate to give a white powder. Compound **9** (28 mg, 61%) was obtained as a white powder by washing the crude product with cold (-35 °C) hexanes (2 mL). ^{1}H NMR (C_6D_6): δ 1.26 (d, $^{3}J_{HH}$ = 6.9 Hz, 12H, CH(CH_3)$_2$), 3.88 (septet, $^{3}J_{HH}$ = 6.9 Hz, 2H, CH(CH$_3$)$_2$), 5.32 (s, 2H, N-CH_2-N), 5.62 (s, 2H, N-CH-), 7.11 (d, $^{3}J_{HH}$ = 7.5 Hz, 4H, ArH) and 7.19 (t, $^{3}J_{HH}$ = 7.5 Hz, 2H, ArH). ^{13}C{^{1}H} NMR (C_6D_6): δ 28.4 (CH(*C*H$_3$)$_2$), 28.9 (CH(*C*H$_3$)$_2$), 29.1 (*C*H(CH$_3$)$_2$), 78.6 (N-*C*H$_2$-N), 118.1 (-N-*C*H-), 124.7 (Ar*C*), 128.3 (Ar*C*), 139.8 (Ar*C*) and 149.9 (Ar*C*). HR-MS: [M–H]$^{+}$; Calcd. 389.29513. Found: 389.29459 (Δ ppm = 1.36). Mp (°C): 101-103. The product also contained minor

(ca. 5%) quantities of the known adduct, IPr•BEt_3.[7f]

3.5.3.16 Thermolysis of IPr•SnH_2•$Cr(CO)_5$. A solution of IPr•SnH_2•$Cr(CO)_5$ (40 mg, 0.057 mmol) in 8 mL of toluene was heated to 100 °C for 36 hours to obtain a greenish yellow solution over a black precipitate. The solution was decanted and the residue was extracted with 4 mL of toluene. The combined extracts were filtered through Celite and the volatiles were removed to obtain a greenish yellow powder (27 mg). ^{1}H NMR (C_6D_6) analysis of the soluble fraction revealed the presence of IPr•$Cr(CO)_5$ (*ca*. 35%) and [$(HCNDipp)_2CH_2$] (*ca*. 65%).

3.5.3.17 Independent synthesis of IPr•$Cr(CO)_5$ 10. 25 mL of dry THF was added to $Cr(CO)_6$ (116 mg, 0.527 mmol) and the mixture was irradiated with a 450 W mercury lamp for 1.5 h to give a bright orange solution of $(CO)_5$Cr•THF. IPr (204 mg, 0.527 mmol) was dissolved in 10 mL of toluene and then added dropwise to the solution of $(CO)_5$Cr•THF. The immediate formation of a pale yellow-orange solution was observed and the reaction mixture was stirred overnight; the volatiles were then removed under vacuum to give a pale green powder, which was further purified by recrystallization from a mixture of hexanes and toluene at -35 °C (197 mg, 64%). ^{1}H NMR (C_6D_6): δ 0.98 (d, $^3J_{HH}$ = 6.8 Hz, 12H, $CH(CH_3)_2$), 1.38 (d, $^3J_{HH}$ = 6.8 Hz, 12H, $CH(CH_3)_2$), 2.78 (septet, $^3J_{HH}$ = 6.8 Hz, 4H, $CH(CH_3)_2$), 6.51 (s, 2H, N-C*H*-), 7.11 (d, $^3J_{HH}$ = 7.6 Hz, 4H, Ar*H*), 7.25 (t, $^3J_{HH}$ = 7.6 Hz, 2H, Ar*H*). ^{13}C{^{1}H} NMR (C_6D_6): δ 22.4 ($CH(CH_3)_2$), 25.6 ($CH(CH_3)_2$), 28.5 ($CH(CH_3)_2$), 124.3 (Ar*C*), 125.2 (Ar*C*), 130.8 (Ar*C*), 137.5 (Ar*C*), 146.21 (Ar*C*), 200.1 (-N-*C*H-), 191.2 (N-*C*-N), 216.4 (equat. *C*O), 220.7

(ax. *C*O). IR (Nujol/cm^{-1}): 1880 (br, υCO), 1918 (br, υCO), 1981 (m, υCO), 2056 (s, υCO). Anal. Calcd. for $C_{32}H_{36}N_2O_5W$: C, 53.94; H, 5.09; N, 3.93. Found: C, 53.35; H, 4.92; N 3.77. Mp (°C): 258-260.

3.5.3.18 Synthesis of IPr•GeCl$_2$•W(CO)$_5$ 11. A solution of W(CO)$_6$ (147 mg, 0.42 mmol) in 30 mL of THF was irradiated with a 450 W mercury lamp for 2 h to yield a bright yellow solution of W(CO)$_5$•THF. A solution of IPr•GeCl$_2$ (222 mg, 0.42 mmol) in 20 mL of THF was then added dropwise and the resulting mixture was stirred overnight. The volatiles were then removed under vacuum to give a yellow powder that was redissolved in THF and filtered through Celite. Removal of the volatiles from the filtrate followed by washing of the crude solid obtained with Et$_2$O (3 × 5 mL) gave pure **11** as a colorless solid (48 mg, 13%). ^{1}H NMR (C_6D_6): δ 0.90 (d, $^3J_{HH}$ = 6.9 Hz, 12H, CH(C*H*$_3$)$_2$), 1.43 (d, $^3J_{HH}$ = 6.9 Hz, 12H, CH(C*H*$_3$)$_2$), 2.72 (septet, $^3J_{HH}$ = 6.9 Hz, 4H, C*H*(CH$_3$)$_2$), 6.26 (s, 2H, N-C*H*-), 7.06 (d, $^3J_{HH}$ = 7.6 Hz, 4H, Ar*H*), 7.18 (t, $^3J_{HH}$ = 7.6 Hz, 2H, Ar*H*). ^{13}C{^{1}H} NMR (C_6D_6): δ 23.0 (CH(*C*H$_3$)$_2$), 25.8 (CH(*C*H$_3$)$_2$), 29.6 (*C*H(CH$_3$)$_2$), 125.1 (Ar*C*), 126.0 (Ar*C*), 131.8 (Ar*C*), 133.5 (Ar*C*), 145.3 (-N-*C*H-), 160.0 (N-*C*-N), 198.2 (equat. *C*O), 200.7 (ax. *C*O). Anal. Calcd. for $C_{32}H_{36}Cl_2GeN_2O_5W$: C, 44.90; H, 4.24; N, 3.27. Found: C, 44.63; H, 4.31; N, 3.22. Mp (°C): 178 (dec.), 193-195 (melts).

3.5.3.19 Alternate Synthesis of IPr•GeCl$_2$•W(CO)$_5$ 11. To a mixture of IPr (0.13 g, 0.34 mmol) and (THF)GeCl$_2$•W(CO)$_5$ (0.18 g, 0.34 mmol) was added 10 mL of toluene. The reaction mixture was stirred for 2 hours to give a pale yellow

slurry. The precipitate was isolated by filtration and identified as **11** (0.228 g). A further crop of **11** was isolated by cooling the filtrate to -35 °C (0.049 g; combined yield = 0.277 g, 96%).

3.5.3.20 Synthesis of IPr•GeH$_2$•W(CO)$_5$ 12. To a mixture of **11** (30 mg, 0.035 mmol) and Li[BH$_4$] (1.8 mg, 0.084 mmol) was added 10 mL of Et$_2$O. The reaction was then stirred overnight to give a pale yellow slurry, which was subsequently filtered through Celite. Removal of the volatiles afforded **12** as a pale pink powder (15 mg, 54%). ^{1}H NMR (C$_6$D$_6$): δ 0.88 (d, $^3J_{HH}$ = 6.8 Hz, 12H, CH(C*H*$_3$)$_2$), 1.36 (d, $^3J_{HH}$ = 6.8 Hz, 12H, CH(C*H*$_3$)$_2$), 2.55 (septet, $^3J_{HH}$ = 6.8 Hz, 4H, C*H*(CH$_3$)$_2$), 4.23 (s, 2H, GeH$_2$, satellites: $^3J_{HW}$ = 4.4 Hz), 6.42 (s, 2H, N-C*H*-), 7.07 (d, $^3J_{HH}$ = 7.6 Hz, 4H, Ar*H*), 7.19 (t, $^3J_{HH}$ = 7.6 Hz, 2H, Ar*H*). ^{13}C{^{1}H} NMR (C$_6$D$_6$): δ 22.7 (CH(C*H*$_3$)$_2$), 25.9 (CH(C*H*$_3$)$_2$), 29.2 (C*H*(CH$_3$)$_2$), 125.0 (Ar*C*), 125.2 (Ar*C*), 131.5 (Ar*C*), 133.9 (Ar*C*), 145.1 (-N-*C*H-), 170.2 (N-*C*-N), 200.9 (equat. *CO*, $^1J_{CW}$ = 122 Hz), 203.3 (ax. *CO)*. IR (Nujol/cm^{-1}): 1873 (s, υCO), 1893 (s, υCO), 1910 (s, υCO) 1981 (m, υGe-H), 2047 (m, υCO). Anal. Calcd. for C$_{32}$H$_{38}$GeN$_2$O$_5$W: C, 48.83; H, 4.87; N, 3.56. Found: C, 49.43; H, 5.27; N, 3.25. Mp (°C): 173- 175 (dec. turns black); 199-202 (melts).

3.5.3.21 Alternate synthesis of IPr•GeH$_2$•W(CO)$_5$ 12. A solution of W(CO)$_6$ (0.090 g, 0.26 mmol) in 50 mL of THF was irradiated with a 450 W mercury lamp for 1.5 h to give a clear, bright yellow solution of THF•W(CO)$_5$. IPr•GeH$_2$•BH$_3$ (**2**) (0.12 g, 0.25 mmol) was then dissolved in 12 mL of a 1:1 THF/toluene mixture and then added dropwise to the solution of THF•W(CO)$_5$. The reaction

was then stirred overnight to give pale yellow solution, and the volatiles were removed *in vacuo*. The product was extracted with 10 mL of toluene and filtered through a bed of Celite. The solvent was then removed to give a pale red solid that was recrystallized from THF/hexanes (-35 °C) to give **12** as colorless crystals of suitable quality for X-ray crystallography (0.085 g, 43%).

3.5.3.22 Synthesis of IPr•GeD_2•$W(CO)_5$ 12D. $W(CO)_6$ (67 mg, 0.19 mmol) was dissolved in 40 mL of THF and irradiated with a 450 W mercury lamp for 1.5 h to give a bright yellow solution of THF•$W(CO)_5$. A solution of IPr•GeD_2•BD_3 (**2D**) (92 mg, 0.19 mmol) in 8 mL of a 1:1 THF/toluene mixture was then added dropwise to the *in situ* generated solution of $W(CO)_5$•THF. The reaction mixture was stirred overnight and the reaction was filtered through Celite. Removal of the volatiles from the filtrate gave **12D** as a colorless solid (63 mg, 42%). ^1H NMR (C_6D_6): essentially the same as **12** except for the absence of the GeH_2 resonance. $^2H\{^1H\}$ NMR (C_6H_6): δ 4.28 (br, -GeD_2-). IR (Nujol/cm^{-1}): Similar to **12** except for the absence of υGeH at 1981 cm^{-1}; the location of the Ge-D stretch could not be determined due to overlapping IPr vibrations.

3.5.3.23 Synthesis of IPr•GeH_2•$Cr(CO)_5$ 13. A solution of $Cr(CO)_6$ (0.036 g, 0.163 mmol) in 20 mL of THF was irradiated with a 450 W mercury lamp for 1.5 h to give a clear, bright yellow solution of THF•$Cr(CO)_5$. IPr•GeH_2•BH_3 (**2**) (0.076 g, 0.163 mmol) was then dissolved in 12 mL of a 1:1 THF/toluene mixture and then added dropwise to the solution of THF•$W(CO)_5$. The reaction mixture was then stirred overnight to give a pale yellow solution, and the volatiles were

removed *in vacuo*. The product was extracted with 10 mL of toluene and filtered through a bed of Celite. The solvent was then removed to give a pale red solid that was recrystallized from THF/hexanes (-35 °C) to give **13** as colorless crystals of suitable quality for X-ray crystallography (0.068 g, 65%). ^{1}H NMR (C_6D_6): δ 0.88 (d, $^{3}J_{HH}$ = 6.8 Hz, 12H, CH(CH_3)$_2$), 1.36 (d, $^{3}J_{HH}$ = 6.8 Hz, 12H, CH(CH_3)$_2$), 2.62 (septet, $^{3}J_{HH}$ = 6.8 Hz, 4H, CH(CH$_3$)$_2$), 4.11 (s, 2H, GeH$_2$), 6.46 (s, 2H, N-CH-), 7.07 (d, $^{3}J_{HH}$ = 7.6 Hz, 4H, ArH), 7.20 (t, $^{3}J_{HH}$ = 7.6 Hz, 2H, ArH). ^{13}C{^{1}H} NMR (C_6D_6): δ 22.5 (CH(CH_3)$_2$), 25.9 (CH(CH_3)$_2$), 29.1 (CH(CH$_3$)$_2$), 124.9 (ArC), 125.4 (ArC), 131.5 (ArC), 133.7 (ArC), 145.2 (-N-CH-), 172.3 (N-C-N), 222.3 (equat. *CO*), 227.2 (ax. *CO)*. Anal. Calcd. for $C_{36}H_{46}CrGeN_2O_6$: C, 59.44; H, 6.37; N, 3.85. Found: C, 61.72; H, 6.34; N, 3.80. Mp (°C): 176-178 (dec. turns black); 213-216 (melts).

3.5.3.24 Reaction of IPr•SnH$_2$•W(CO)$_5$ (5) with excess benzaldehyde: Synthesis of IPr-CPh(H)OSn(OCH$_2$Ph)$_2$•W(CO)$_5$ (14). IPr•SnH$_2$•W(CO)$_5$ (42 mg, 0.050 mmol) was dissolved in Et$_2$O (7 mL) and benzaldehyde (0.0155 mL, 0.141 mmol) was added. Upon the addition of benzaldehyde, the solution immediately turned orange and became slightly cloudy. The reaction mixture was then filtered through Celite and the volatiles were removed *in vacuo* to give an orange solid. The product was dissolved in a 1:1 hexanes/Et$_2$O mixture (~6 mL) and the solution was filtered through Celite. Cooling of the filtrate to *ca*. -35 °C afforded **14** as orange crystals of suitable quality for single-crystal X-ray diffraction (25 mg, 46%). Data for **14** (racemic mixture; integrations based upon *both* R and S forms, assignment made with APT and gHSQC experiments): ^{1}H

NMR (C_6D_6): δ 0.79 (d, $^3J_{HH}$ = 7.0 Hz, 12H, CH(CH_3)$_2$), 0.88 (d, $^3J_{HH}$ = 7.0 Hz, 12H, CH(CH_3)$_2$), 0.97 (d, $^3J_{HH}$ = 7.0 Hz, 12H, CH(CH_3)$_2$), 1.46 (d, $^3J_{HH}$ = 7.0 Hz, 12H, CH(CH_3)$_2$), 2.26 (septet, $^3J_{HH}$ = 7.0 Hz, 4H, C*H*(CH$_3$)$_2$), 2.79 (septet, $^3J_{HH}$ = 7.0 Hz, 4H, CH(CH$_3$)$_2$), 4.81 (d, $^2J_{HH}$ = 13.5 Hz, 2H, -O-C(*H*)HPh diastereotopic), 4.95 (d, $^2J_{HH}$ = 13.5 Hz, 2H, -O-C(*H*)HPh diastereotopic), 5.09 (d, $^2J_{HH}$ = 13.5 Hz, 2H, -O-C(*H*)HPh diastereotopic), 5.17 (d, $^2J_{HH}$ = 13.5 Hz, 2H, -O-C(*H*)HPh diastereotopic), 6.19 (s, 2H, N-C*H*- in IPr group), 6.61 (s, 4H, CIPr-C*H*(Ph)O-), 6.72-6.85 (m, 10H, Ar-*H*), 6.93 (dd, *J* = 8.0, 1.6 Hz, 4H, Ar-H), 6.98-7.07 (m, 4H, Ar-H), 7.08-7.14 (m, 6H, Ar*H*), 7.16-7.23 (m, 6H, Ar*H*), 7.24-7.30 (m, 8H, Ar*H*) and 7.48-7.52 (m, 4H, Ar*H*). $^{13}C\{^1H\}$ NMR (C_6D_6): δ 22.1 (CH(CH_3)$_2$), 22.5 (CH(*C*H$_3$)$_2$), 26.0 (CH(*C*H$_3$)$_2$), 26.1 (CH(*C*H$_3$)$_2$), 29.24 (*C*H(CH$_3$)$_2$), 29.29 (*C*H(CH$_3$)$_2$), 66.1 (O- *C*H$_2$-Ph*),* 66.2 (O-*C*H$_2$-Ph), 69.5 (C_{IPr}-*C*H(Ph)O-), 124.7 (Ar*C*), 124.9 (Ar*C*), 125.6 (Ar*C*), 125.8 (Ar*C*), 125.9 (Ar*C*), 126.7 (Ar*C*), 126.8 (Ar*C*), 128.49 (Ar*C*), 128.52 (Ar*C*), 129.3 (Ar*C*), 131.2 (Ar*C*), 132.2 (Ar*C*), 139.4 (Ar*C*), 145.7 (Ar*C*), 146.0 (Ar*C*), 146.2 (Ar*C*), 146.6 (Ar*C*), 152.7 (Ar*C*), 198.5 (*C*O), 201.1 (*C*O). $^{119}Sn\{^1H\}$ NMR (C_6D_6): δ -60.0. Anal. Calcd. for $C_{53}H_{57}N_2O_8SnW$: C, 55.23; H, 4.98; N, 2.43. Found: C, 54.56; H, 5.08; N, 2.30. Mp (°C): 152-153.

3.5.3.25 Synthesis of IPr•SiH$_2$•BH$_3$ 15. To mixture of IPr•SiCl$_2$•BH$_3$ (102 mg, 0.204 mmol) and Li[AlH$_4$] (5.42 mg, 0.143 mmol) was added 8 mL of toluene and the mixture was stirred at room temperature for 1 h to obtain a cloudy mixture. Afterwards, 3 mL of Et$_2$O was added to the mixture followed by stirring for another 30 minutes. The reaction mixture was then filtered through Celite to

obtain a pale yellow solution. Removal of the volatiles from the filtrate afforded **15** as a white powder (47 mg, 55%). Crystals suitable for X-ray crystallography (colorless blocks) were grown by cooling a saturated Et_2O solution layered with hexanes to -35 °C for 2 days. ^{1}H NMR (C_6D_6): δ 0.96 (d, $^3J_{HH}$ = 6.9 Hz, 12H, CH(C*H*$_3$)$_2$), 1.38 (d, $^3J_{HH}$ = 6.9 Hz, 12H, CH(C*H*$_3$)$_2$), 2.63 (septet, $^3J_{HH}$ = 6.9 Hz, 4H, C*H*(CH$_3$)$_2$), 3.76 (q, $^3J_{HH}$ = 5.6 Hz, 2H, -Si*H*$_2$-, assignment made by ^{29}Si-^{1}H gSHQC experiment), 6.40 (s, 2H, N-C*H*-), 7.05 (d, $^3J_{HH}$ = 7.8 Hz, 4H, Ar*H*), 7.19 (t, $^3J_{HH}$ = 7.8 Hz, 2H, Ar*H*). ^{13}C{^{1}H} NMR (C_6D_6): δ 22.9 (CH(*C*H$_3$)$_2$), 25.5 (CH(*C*H$_3$)$_2$), 29.2 (*C*H(CH$_3$)$_2$), 124.6 (-N-*C*H-), 124.7 (Ar*C*), 131.4 (Ar*C*), 133.5 (Ar*C*), 145.6 (Ar*C*), 168.8 (N-*C*-N). ^{11}B{^{1}H} NMR (128 MHz, C_6D_6): δ - 46.2. ^{11}B NMR (C_6D_6): δ - 46.2 (quartet, $^1J_{BH}$ = 93 Hz). ^{29}Si (C_6D_6): δ - 55.6 (quartet, $^1J_{SiB}$ = 46 Hz). IR (Nujol/cm^{-1}): 2096 (s, υSi-H), 2238 (sh, υB-H), 2304 (m, υB-H) and 2345 (sh, υB-H). Anal. Calcd. for: $C_{27}H_{41}BN_2Si$: C, 74.98; H, 9.55; N, 6.48. Found: C, 73.92; H, 9.50; N, 6.16. Mp (°C): 233-235.

3.5.3.26 Synthesis of IPr•SiD$_2$•BH$_3$ 15D. To mixture of IPr•$SiCl_2$•BH_3 (100 mg, 0.204 mmol) and Li[AlD_4] (5.9 mg, 0.141 mmol) was added 8 mL of toluene, and the mixture was stirred at room temperature for 1 h to obtain a cloudy mixture. Afterwards, 3 mL of Et_2O was added to the mixture and the reaction was stirred for another 30 minutes. The mixture was then filtered through Celite to obtain a pale yellow solution. Removal of the volatiles from the filtrate afforded **15D** as a white powder (45 mg, 52%). ^{1}H NMR (C_6D_6): All the peaks were identical as for compound **15**, except the -SiH_2- resonance was absent. ^{13}C{^{1}H} NMR (C_6D_6): essentially same as for the compound **15**. ^{2}H{^{1}H} NMR (C_6H_6): δ 3.75 (-Si*D*$_2$-).

IR (Nujol/cm^{-1}): 1522 (m, υSi-D), 2236 (sh, υB-H), 2302 (m, υB-H) and 2344 (w, υB-H).

3.5.3.27 Synthesis of IPr•SiH$_2$•W(CO)$_5$ 16. 12 mL of dry THF was added to W(CO)$_6$ (49 mg, 0.14 mmol) and irradiated with a 450 W mercury lamp for 2 h to give a bright yellow solution. A solution of IPr•SiH$_2$•BH$_3$ (60 mg, 0.14 mmol) in 5 mL of THF was added dropwise to the bright yellow solution of W(CO)$_5$•THF and heated overnight at 40 °C to yield a pale orange solution. The volatiles were removed from the reaction mixture and then washed with 3 mL of hexanes to yield **16** as a yellow solid (83 mg, 66%). X-ray quality crystals of **16** were grown by cooling a saturated Et$_2$O solution layered with hexanes at - 35 °C for 3 days. ^{1}H NMR (C$_6$D$_6$): δ 0.88 (d, $^3J_{HH}$ = 6.9 Hz, 12H, CH(C*H*$_3$)$_2$), 1.35 (d, $^3J_{HH}$ = 6.9 Hz, 12H, CH(C*H*$_3$)$_2$), 2.62 (septet, $^3J_{HH}$ = 6.9 Hz, 4H, C*H*(CH$_3$)$_2$), 4.16 (s, 2H, -Si*H*$_2$-, satellites: $^1J_{SiH}$ = 164 Hz), 6.40 (s, 2H, N-C*H*-), 7.08 (d, $^3J_{HH}$ = 7.2 Hz, 4H, Ar*H*), 7.20 (t, $^3J_{HH}$ = 7.2 Hz, 2H, Ar*H*). ^{13}C{^{1}H} NMR (C$_6$D$_6$): δ 22.4 (CH(*C*H$_3$)$_2$), 25.9 (CH(*C*H$_3$)$_2$), 29.1 (*C*H(CH$_3$)$_2$), 124.9 (-N-*C*H-), 125.2 (Ar*C*), 131.5 (Ar*C*), 133.5 (Ar*C*), 145.1 (Ar*C*), 168.7 (N-*C*-N), 201.4 (s, $^1J_{WC}$ = 122.2 Hz, equat. *C*O), 203.1 (ax. *C*O). ^{29}Si NMR (C$_6$D$_6$): δ -71.6 (t, $^1J_{Si-H}$ = 164 Hz). Anal. Calcd. for: C$_{32}$H$_{38}$N$_2$O$_5$SiW: C, 51.76; H, 5.16; N, 3.77. Found: C, 52.69; H, 5.99; N, 3.77. IR (Nujol/cm^{-1}): 1876 (s, υCO), 1919 (s, υCO), 1949 (sh, υCO), 2044 (s, υCO), 2086 (m, υSi-H) and 2108 (m, υSi-H). Mp (°C): 157-159 (dec., turns gray), 186-188 (melts).

3.5.3.28 Reaction of IPr•$SiCl_2$ with $[Rh(CO)_2Cl]_2$: Synthesis of [*trans*-(IPr•$SiCl_2$)$_2$Rh$(CO)_2$][*cis*-Rh$(CO)_2Cl_2$] 17. To a mixture of IPr•$SiCl_2$ (103 mg, 0.211 mol) and $[Rh(CO)_2Cl]_2$ (82 mg, 0.211 mmol) was added 10 mL of toluene. The reaction mixture was stirred at room temperature for 20 min. to obtain a bright yellow-orange slurry. The reaction mixture was allowed to settle and the precipitate was isolated by filtration. Removal of the volatiles from the precipitate afforded **17** as a orange powder (131 mg, 87%). Crystals suitable for the X-ray crystallography (orange needles) were grown by cooling a saturated CH_2Cl_2 solution of **17** layered with hexanes at -35 °C. ^{1}H NMR (CD_2Cl_2): δ 1.11 (d, $^3J_{HH}$ = 7.0 Hz, 12H, CH(CH_3)$_2$), 1.32 (d, $^3J_{HH}$ = 7.0 Hz, 12H, CH(CH_3)$_2$), 2.47 (septet, $^3J_{HH}$ = 7.0 Hz, 4H, C*H*(CH$_3$)$_2$), 7.30 (d, $^3J_{HH}$ = 8.0 Hz, 4H, Ar*H*), 7.44 (s, 2H, N-C*H*-), 7.52 (t, $^3J_{HH}$ = 8.0 Hz, 2H, Ar*H*). ^{13}C{^{1}H} NMR (CD_2Cl_2): δ 23.1 (CH(*C*H$_3$)$_2$), 26.2 (CH(*C*H$_3$)$_2$), 29.9 (*C*H(CH$_3$)$_2$), 125.2 (-N-*C*H-), 137.6 (Ar*C*), 132.4 (Ar*C*), 132.5 (Ar*C*), 145.8 (Ar*C*), 153.9 (N-*C*-N, $^2J_{RhC}$ = 4.9 Hz), 182.6 (cis-[Rh(*C*O)$_2$Cl$_2$]$^-$, $^1J_{RhC}$ = 71.9 Hz), 191.6 ([(IPr•$SiCl_2$)$_2$Rh(*C*O)$_2$]$^+$, $^1J_{RhC}$ = 63.4 Hz). ^{29}Si NMR (CD_2Cl_2): δ 27.9 (d, $^1J_{Si-Rh}$ = 69 Hz). Anal. Calcd. for: $C_{58}H_{72}Cl_6N_4O_4Rh_2Si_2$: C, 51.08; H, 5.32; N, 4.11. Found: C, 51.27; H, 5.60; N, 4.26. IR (Nujol/cm^{-1}): 1993 (s, υCO), 2009 (s, υCO), 2066 (s, υCO), 2090 (w, υCO). Mp (°C): 167-170.

3.5.3.29 Reaction of IPr•SiH_2•BH_3 with Cy_3P: To a mixture of **15** (26 mg, 0.049 mmol) and Cy_3P (14 mg, 0.049 mmol) was added 6 mL of toluene. The reaction mixture was stirred for 24 h. No sign of a reaction was observed by NMR spectroscopy. The solution was heated at 35 °C for 48 h and afterwards the

volatiles were removed *in vacuo*; ^{1}H and ^{31}P NMR spectroscopy revealed ~15% decomposition of IPr•SiH_2•BH_3 into IPr•BH_3 and [$(HCNDipp)_2CH_2$]; a conversion of Cy_3P (*ca*. 15%) into Cy_3P•BH_3 was also noted.

3.5.3.30 Reaction of IPr•GeH_2•BH_3 with Cy_3P: To a mixture of IPr•GeH_2•BH_3 (19 mg, 0.040 mmol) and Cy_3P was added to 4 mL of toluene. After stirring for 24 h, the volatiles were removed and ^{1}H, ^{11}B and ^{31}P NMR analysis revealed ~25% decomposition of IPr•GeH_2•BH_3 into IPr•BH_3 and [$(HCNDipp)_2CH_2$]; a conversion of Cy_3P (*ca*. 20%) into Cy_3P•BH_3 was also noted.

3.5.3.31 Synthesis of IPr=CH_2 18. To a white slurry [IPrH]Cl (1.95 g, 4.59 mmol) in 20 mL of THF at -78 °C, was added dropwise *n*-BuLi (3.15 mL, 5.05 mmol, 1.6 M solution in hexanes), and the reaction mixture was stirred for 10 min. to give a clear solution. The reaction mixture was warmed to room temperature and stirred for another 5 min. and then MeI (0.315 mL, 5.05 mmol) was added at -78 °C to yield a white precipitate of the 2-methyl-imidazolium salt, [IPr-CH_3]I. The resulting 2-methyl-imidazolium salt was then deprotonated with *n*-BuLi (3.15 mL, 5.05 mmol, 1.6 M solution in hexanes) at -78 °C to obtain a pale yellow solution. The resulting solution was stirred at ambient temperature for 30 min. and afterwards the volatiles were removed to give a yellow solid. The yellow solid was extracted with hexanes (20 mL) and filtered through Celite to give yellow filtrate from which crude **18** was isolated as a pale yellow solid upon removal of the volatiles. Recrystallization of crude product from hexanes (-35 °C)

afforded pure **18** (527 mg, 29%). Crystals suitable for X-ray crystallography were grown by cooling a saturated hexanes solution to -35 °C. ^{1}H NMR (C_6D_6): δ 1.22 (d, $^{3}J_{HH}$ = 6.9 Hz, 12H, CH(CH_3)$_2$), 1.36 (d, $^{3}J_{HH}$ = 6.9 Hz, 12H, CH(CH_3)$_2$), 2.42 (s, 2H, -CH_2), 3.35 (septet, $^{3}J_{HH}$ = 6.9 Hz, 4H, CH(CH$_3$)$_2$), 5.85 (s, 2H, N-CH-), 7.17 (d, $^{3}J_{HH}$ = 7.0 Hz, 4H, ArH), 7.22 (t, $^{3}J_{HH}$ = 7.0 Hz, 2H, ArH). ^{13}C{^{1}H} NMR (C_6D_6): δ 23.8 (CH(*C*H$_3$)$_2$), 24.3 (CH(*C*H$_3$)$_2$), 28.8 (*C*H(CH$_3$)$_2$), 44.3 (-*C*H$_2$), 114.6 (-N-*C*H-), 124.5 (Ar*C*), 129.3 (Ar*C*), 134.9 (Ar*C*), 148.9 (Ar*C*), 152.5 (N-*C*-N). HR-MS: [M]$^{+}$; Calcd. 402.30255. Found. 402.30350 (Δ ppm = 2.4). (Nujol/cm^{-1}): 3067 (s, υCH$_2$) and 3130 (br, υCH$_2$). Mp (°C): 119-121.

3.5.3.32 Alternate Preparation of IPr=CH$_2$ 18. To a solution of IPr (0.200 g, 0.515 mmol) in 6 mL of toluene, was added MeI (17.7 μL, 0.283 mmol) at ambient temperature. A white precipitate of [IPrH]I was formed immediately and the reaction mixture stirred for a further 1 hour. Filtration of the reaction mixture through Celite gave a pale yellow filtrate and removal of volatiles from the filtrate afforded spectroscopically pure **18** (0.93 g, 90%).

3.5.3.33 Synthesis of IPrCH$_2$•GeCl$_2$ 19. To a mixture of IPr=CH$_2$ (147 mg, 0.364 mmol) and GeCl$_2$•dioxane (85 mg, 0.364 mmol) was added 10 mL of toluene. The reaction mixture was stirred at room temperature for 1 h to obtain a white slurry. The resulting mixture was allowed to settle and the precipitate was separated by filtration. Removal of the volatiles from the filtrate afforded **19** as a white powder (173 mg, 86%). ^{1}H NMR (CD_2Cl_2): δ 1.21 (d, $^{3}J_{HH}$ = 7.0 Hz, 12H, CH(CH_3)$_2$),

1.39 (d, $^{3}J_{HH}$ = 7.0 Hz, 12H, CH(CH_3)$_2$), 2.62 (septet, $^{3}J_{HH}$ = 7.0 Hz, 4H, CH(CH$_3$)$_2$), 2.66 (s, 2H, -CH_2-), 7.15 (s, 2H, N-CH-), 7.42 (d, $^{3}J_{HH}$ = 8.0 Hz, 4H, ArH), 7.62 (t, $^{3}J_{HH}$ = 8.0 Hz, 2H, ArH). ^{13}C{^{1}H} NMR (CD_2Cl_2): δ 22.4 (CH(*C*H$_3$)$_2$), 24.5 (CH(*C*H$_3$)$_2$), 29.1 (*C*H(CH$_3$)$_2$), 37.9 (-*C*H$_2$-), 121.9 (-N-*C*H-), 125.1 (Ar*C*), 130.4 (Ar*C*), 131.6 (Ar*C*), 145.6 (Ar*C*), 155.5 (N-*C*-N). Anal. Calcd. for $C_{28}H_{38}Cl_2GeN_2$: C, 61.58; H, 7.01; N, 5.13. Found: C, 60.64; H, 6.95; N, 5.10. Mp (°C): 211-213.

3.5.3.34 Reaction of IPrCH$_2$•GeCl$_2$ with Li[BH$_4$]: Synthesis of IPrCH$_2$•BH$_3$ 20. To a mixture of **19** (60 mg, 0.11 mmol) and Li[BH_4] (5.7 mg, 0.26 mmol) was added 8 mL of cold (-35 °C) Et_2O. The reaction mixture was warmed at ambient temperature and stirred overnight to give a colorless solution over a yellow precipitate. The precipitate was allowed to settle and the mother liquor was filtered through Celite to give a colorless filtrate. Removal of the volatiles from the filtrate afforded **20** as a white powder (38 mg, 82%). Crystals suitable for X-ray crystallography were grown by cooling an Et_2O solution of **20** layered with hexanes to -35 °C for 3 days. ^{1}H NMR (C_6D_6): δ 0.97 (d, $^{3}J_{HH}$ = 7.0 Hz, 12H, CH(CH_3)$_2$), 1.31 (d, $^{3}J_{HH}$ = 7.0 Hz, 12H, CH(CH_3)$_2$), 1.47 (t, $^{3}J_{HH}$ = 6.0 Hz, 3H, BH_3; determined by ^{1}H{^{11}B} NMR spectroscopy), 2.05 (q, $^{3}J_{HH}$ = 6.0 Hz, 2H, -CH_2-), 2.89 (septet, $^{3}J_{HH}$ = 7.0 Hz, 4H, CH(CH$_3$)$_2$), 6.24 (s, 2H, N-CH-), 7.05 (d, $^{3}J_{HH}$ = 8.0 Hz, 4H, ArH), 7.18 (t, $^{3}J_{HH}$ = 8.0 Hz, 2H, ArH). ^{13}C{^{1}H} NMR (CD_2Cl_2): δ 22.9 (CH(*C*H$_3$)$_2$), 25.7 (CH(*C*H$_3$)$_2$), 29.1 (*C*H(CH$_3$)$_2$), resonance for the -*C*H$_2$- could not be located, 120.4 (-N-*C*H-), 124.7 (Ar*C*), 131.1 (Ar*C*), 132.9 (Ar*C*), 146.3 (Ar*C*), resonance for the N-*C*-N could not be located. ^{11}B{^{1}H} NMR

(C_6D_6): δ -28.5. ^{11}B NMR (C_6D_6): δ -28.5 (q, $^1J_{BH}$ = 85.9 Hz). Anal. Calcd. for $C_{28}H_{41}BN_2$: C, 80.75; H, 9.92; N, 6.73. Found: C, 79.78; H, 10.04; N, 6.55. Mp (°C): 187-189.

3.5.3.35 Alternate synthesis of IPrCH$_2$•BH$_3$ 20. To a solution of IPr=CH$_2$ (100 mg, 0.248 mmol) in 6 mL of Et_2O and H_3B•THF (0.273 mL, 1.0 M solution in THF) was added at -35 °C. The reaction mixture was stirred at room temperature for 1 h to obtain a white slurry. The resulting mixture was allowed to settle and the precipitate was separated by filtration. Removal of the volatiles from the precipitate afforded **20** as a white powder (93 mg, 90%).

3.5.3.36 Synthesis of IPr=CH-SiHCl$_2$ 21. To a cold (-35 °C) solution of IPr=CH$_2$ (140 mg, 0.35 mmol) was in 8 mL of toluene was added trichlorosilane (19.6 μL, 0.38 mmol) at ambient temperature. A white precipitate was formed immediately and the reaction mixture was stirred overnight at ambient temperature to obtain a pale yellow solution over white precipitate. The precipitate was allowed to settle and the mother liquor was filtered through Celite to obtain pale yellow filtrate. Removal of the volatiles from the filtrate afforded **21** (83 mg, 45%). Crystals suitable for X-ray crystallography were grown from a saturated toluene/hexanes solution to -35 °C. ^{1}H NMR (C_6D_6): δ 1.08 (d, $^3J_{HH}$ = 7.0 Hz, 6H, CH(CH_3)$_2$), 1.12 (d, $^3J_{HH}$ = 7.0 Hz, 6H, CH(CH_3)$_2$), 1.31 (d, $^3J_{HH}$ = 7.0 Hz, 6H, CH(CH_3)$_2$), 1.41 (d, $^3J_{HH}$ = 7.0 Hz, 6H, CH(CH_3)$_2$), 2.60 (dt, 1H, -C*H*-, $^3J_{HSi}$ = 7.0 Hz, $^5J_{HH}$ = 0.5 Hz), 2.94 (septet, $^3J_{HH}$ = 7.0 Hz, 2H, C*H*(CH$_3$)$_2$), 3.03 (septet, $^3J_{HH}$ = 7.0 Hz, 2H, C*H*(CH$_3$)$_2$), 4.39 (d, 1H, -Si*H*Cl$_2$-, $^3J_{SiH}$ = 7.0 Hz, satellites: $^1J_{HSi}$ = 291.4 Hz), 5.88

(m, 2H, N-C*H*-), 7.05 (d, $^{3}J_{HH}$ = 7.5 Hz, 2H, Ar*H*), 7.09 (d, $^{3}J_{HH}$ = 7.5 Hz, 2H, Ar*H*), 7.18 (t, $^{3}J_{HH}$ = 7.5 Hz, 2H, Ar*H*). $^{13}C\{^{1}H\}$ NMR (C_6D_6): δ 22.8 ($CH(CH_3)_2$), 23.7 ($CH(CH_3)_2$), 24.1 ($CH(CH_3)_2$), 24.9 ($CH(CH_3)_2$), 28.8 ($CH(CH_3)_2$), 28.9 ($CH(CH_3)_2$), 48.2 (-*C*H-), 103.1 (Ar*C*), 115.8 (-N-*C*H-), 116.6 (-N-*C*H-), 124.7 (Ar*C*), 125.4 (Ar*C*), 130.4 (Ar*C*), 130.9 (Ar*C*), 132.8 (Ar*C*), 134.1 (Ar*C*), 147.8 (Ar*C*), 147.9 (Ar*C*), 155.2 (N-*C*-N). $^{29}Si\{^{1}H\}$ NMR (C_6D_6): δ -10.0 (s). ^{29}Si NMR (C_6D_6): δ -10.0 (dd, $^{1}J_{HSi}$ = 291.4 Hz, $^{3}J_{HSi}$ = 7.0 Hz). Anal. Calcd. for $C_{28}H_{38}GeCl_2N_2Si$: C, 67.04; H, 7.64; N, 5.58. Found: C, 67.42; H, 7.72; N, 5.58. Mp (°C): 176-178.

3.5.3.37 Synthesis of $IPrCH_2{\bullet}SnCl_2{\bullet}W(CO)_5$ 22. To a mixture of IPr=CH_2 (46 mg, 0.11 mmol) and $(THF)_2SnCl_2{\bullet}W(CO)_5$ (74 mg, 0.11 mmol) was added 8 mL of toluene. The reaction mixture was stirred at room temperature for 1 h to give a pale yellow slurry. The precipitate was isolated by filtration (73 mg) and identified as **22** by ^{1}H NMR spectroscopy. A further crop of **22** was isolated as colorless crystals of suitable quality for X-ray crystallography by cooling the filtrate to -35 °C (13 mg, combined yield = 96 mg, 92%). ^{1}H NMR (C_6D_6): δ 0.84 (d, $^{3}J_{HH}$ = 7.0 Hz, 12H, $CH(CH_3)_2$), 1.30 (d, $^{3}J_{HH}$ = 7.0 Hz, 12H, $CH(CH_3)_2$), 2.69 (s, 2H, -CH_2-), 2.75 (septet, $^{3}J_{HH}$ = 7.0 Hz, 4H, $CH(CH_3)_2$), 6.28 (s, 2H, N-C*H*-), 7.06 (d, $^{3}J_{HH}$ = 8.0 Hz, 4H, Ar*H*), 7.20 (t, $^{3}J_{HH}$ = 8.0 Hz, 2H, Ar*H*). $^{13}C\{^{1}H\}$ NMR (C_6D_6): δ 22.8 ($CH(CH_3)_2$), 26.2 ($CH(CH_3)_2$), 29.1 ($CH(CH_3)_2$), 32.8 (-CH_2-), 121.9 (-N-*C*H-), 125.7 (Ar*C*), 130.4 (Ar*C*), 132.1 (Ar*C*), 145.5 (Ar*C*), 155.7 (N-*C*-N), 197.7 (equat. *C*O), 200.9 (ax. *C*O). $^{119}Sn\{^{1}H\}$ NMR (C_6D_6): δ -96 (s). IR

(Nujol/cm^{-1}): 1898 (br, υCO), 1914 (br, υCO), 1970 (br, υCO), 2063 (s, υCO), 3132 (s, υCH_2) and 3163 (s, υCH_2). Anal. Calcd. for $C_{73}H_{84}Cl_4N_4O_{10}Sn_2W_2$: C, 45.56; H, 4.40; N, 2.91. Found: C, 45.59; H, 4.35; N, 2.92. Mp (°C): 182-186.

3.5.3.38 Synthesis of IPrCH$_2$•GeCl$_2$•W(CO)$_5$ 23. To a mixture of IPr=CH_2 (100 mg, 0.248 mmol) and (THF)$GeCl_2$•$W(CO)_5$ (134 mg, 0.248 mmol) was added 12 mL of toluene. The reaction mixture was stirred at room temperature for 1 h to give a pale yellow slurry. The precipitate was isolated by filtration and identified as **23** (189 mg) by ^{1}H NMR. A further crop of **23** was isolated as colorless crystals suitable for X-ray crystallography by cooling the filtrate at -35 °C (17 mg, combined yield = 206 mg, 95%). ^{1}H NMR (C_6D_6): δ 0.84 (d, $^3J_{HH}$ = 6.6 Hz, 12H, CH(C*H*$_3$)$_2$), 1.31 (d, $^3J_{HH}$ = 6.6 Hz, 12H, CH(C*H*$_3$)$_2$), 2.73 (broad, 4H, C*H*(CH$_3$)$_2$), 3.18 (s, 2H, -C*H*$_2$), 6.33 (s, 2H, N-C*H*-), 7.04 (d, $^3J_{HH}$ = 7.6 Hz, 4H, Ar*H*), 7.20 (t, $^3J_{HH}$ = 7.6 Hz, 2H, Ar*H*). ^{13}C{^{1}H} NMR (C_6D_6): δ 22.6 (CH(*C*H$_3$)$_2$), 26.2 (CH(*C*H$_3$)$_2$), 29.1 (*C*H(CH$_3$)$_2$), 31.9 (-*C*H$_2$-), 122.5 (-N-*C*H-), 125.6 (Ar*C*), 130.6 (Ar*C*), 132.1 (Ar*C*), 145.3 (Ar*C*), 154.6 (N-*C*-N), 198.5 (equat. *C*O, $^1J_{CW}$ = 61.9 Hz), 202.3 (ax. *C*O). IR (Nujol/cm^{-1}): 1916 (br, υCO), 1978 (br, υCO), 2063 (s, υCO), 3148 (br, υCH_2) and 3171 (s, υCH_2). Anal. Calcd. for $C_{33}H_{38}Cl_2GeN_2O_5W$: C, 45.56; H, 4.40; N, 3.22. Found: C, 45.53; H, 4.50; N, 3.15. Mp (°C): ~155 (dec.) 184-186 (melts).

3.5.3.39 Synthesis of IPrCH$_2$•SnH$_2$•W(CO)$_5$ 24. To a mixture of **22** (54 mg, 0.06 mmol) and Li[BH_4] (2.7 mg, 0.12 mmol) was added 8 mL of cold (-35 °C) Et_2O. The reaction mixture was warmed at ambient temperature and stirred for 20 min

to obtain a pale yellow solution over a white precipitate. Filtration of the mixture through Celite followed by the removal of the volatiles afforded **24** as a pale brown powder (45 mg, 91%). Crystals suitable for X-ray crystallography were grown by cooling an Et_2O solution to -35 °C for 3 days. ^{1}H NMR (C_6D_6): δ 0.88 (d, $^3J_{HH}$ = 6.9 Hz, 12H, CH(C*H*$_3$)$_2$), 1.27 (d, $^3J_{HH}$ = 6.9 Hz, 12H, CH(C*H*$_3$)$_2$), 2.31 (t, 2H, -C*H*$_2$-, $^3J_{HH}$ = 2.0 Hz, satellites: $^3J_{HW}$ = 21 Hz), 2.58 (septet, $^3J_{HH}$ = 6.9 Hz, 4H, C*H*(CH$_3$)$_2$), 5.48 (t, 2H, Sn*H*$_2$, $^3J_{HH}$ = 2.0 Hz, satellites: $^2J_{HW}$ = 9.5 Hz, $^1J_{119Sn-H}$ = 1060 Hz, $^1J_{117Sn-H}$ = 1013), 6.15 (s, 2H, N-C*H*-), 7.02 (d, $^3J_{HH}$ = 8.0 Hz, 4H, Ar*H*), 7.19 (t, $^3J_{HH}$ = 8.0 Hz, 2H, Ar*H*). ^{13}C{^{1}H} NMR (C_6D_6): δ 22.7 (CH(*C*H$_3$)$_2$), 25.8 (CH(*C*H$_3$)$_2$), 29.2 (*C*H(CH$_3$)$_2$), 31.9 (*C*H$_2$), 120.9 (-N-*C*H-), 125.5 (Ar*C*), 130.4 (Ar*C*), 132.7 (Ar*C*), 145.5 (Ar*C*), 160.6 (N-*C*-N), 202.1 (equat. *C*O, $^1J_{CW}$ = 61.3 Hz), 204.8 (ax. *C*O). ^{119}Sn{^{1}H} NMR (C_6D_6): δ -228 (s). ^{119}Sn NMR (C_6D_6): δ -229 (t, $^1J_{SnH}$ = 1066 Hz, $^1J_{SnW}$ = 791.4 Hz). IR (Nujol/cm^{-1}): 1758 (sh, υSnH), 1889 (br, υCO), 1913 (br, υCO), 1980 (s, υCO), 2043 (s, υCO), 3150 (br, υCH$_2$) and 3177 (br, υCH$_2$). Anal. Calcd. for $C_{33}H_{40}N_2O_5SnW$: C, 46.78; H, 4.76; N, 3.31. Found: C, 48.50; H, 5.03; N, 3.25. Mp (°C): 95-97 (dec., turns black), 117-119 (melts).

3.5.3.40 Synthesis of IPrCH$_2$•SnD$_2$•W(CO)$_5$ 24D. To a mixture of **22** (53.1 mg, 0.058 mmol) and Li[BD$_4$] (3.1 mg, 0.121 mmol) was added 10 mL of cold (-35 °C) Et_2O. The reaction mixture was warmed at ambient temperature stirred for 20 min to give a beige colored slurry. The reaction was filtered through Celite and volatiles were removed to afford **24D** as a pale brown solid (43.6 mg, 88%). ^{1}H NMR (C_6D_6): essentially same as **24** with the absence of the SnH_2 resonance.

$^{2}H\{^{1}H\}$ NMR (C_6H_6): δ 5.51 (s, -SnD_2-). $^{119}Sn\{^{1}H\}$ NMR (C_6D_6): δ -309 (pentet, $^{1}J_{Sn\text{-}D}$ = 164.2 Hz). IR (Nujol/cm^{-1}): Similar to **24** except for the absence of υ SnH at 1758 cm^{-1}; the Sn-D stretch could not assigned due to the presence of IPr vibrations in the same region.

3.5.3.41 Synthesis of IPrCH_2•GeH_2•$W(CO)_5$ 25. To a mixture of **23** (97.1 mg, 0.112 mmol) and Li[AlH_4] (2.1 mg, 0.056 mmol) was added 10 mL of toluene. After stirring the reaction mixture for 20 min, 2 mL of Et_2O was added followed by stirring for another 10 min to give a pale yellow solution over a brown precipitate. Filtration of the solution through Celite followed by the removal of solvent from the filtrate afforded **25** as a beige powder (81 mg, 90%). Crystals suitable for X-ray crystallography were grown from a saturated Et_2O/hexanes solution to -35 °C. ^{1}H NMR (C_6D_6): δ 0.86 (d, $^{3}J_{HH}$ = 6.9 Hz, 12H, CH(CH_3)$_2$), 1.26 (d, $^{3}J_{HH}$ = 6.9 Hz, 12H, CH(CH_3)$_2$), 2.41 (t, 2H, -CH_2-, $^{3}J_{HH}$ = 4.0 Hz), 2.53 (septet, 4H, CH(CH$_3$)$_2$), 4.07 (t, 2H, -GeH_2-, $^{3}J_{HH}$ = 4.0 Hz, satellites: $^{3}J_{HW}$ = 14.5 Hz), 6.14 (s, 2H, N-CH-), 7.04 (d, $^{3}J_{HH}$ = 7.8 Hz, 4H, ArH), 7.13 (t, $^{3}J_{HH}$ = 7.8 Hz, 2H, ArH). $^{13}C\{^{1}H\}$ NMR (C_6D_6): δ 12.9 (-CH$_2$-), 22.6 (CH(CH$_3$)$_2$), 25.8 (CH(CH$_3$)$_2$), 29.3 (CH(CH$_3$)$_2$), 121.2 (-N-CH-), 125.4 (ArC), 130.3 (ArC), 132.2 (ArC), 145.4 (ArC), 160.1 (N-C-N), 202.5 (equat. CO), 205.5 (ax. CO). IR (Nujol/cm^{-1}): 1860 (br, υCO), 1901 (br, υCO), 1951 (br, υCO), 2047 (s, υCO), 3149 (br, υCH_2) and 3174 (br, υCH_2); Ge-H stretch could not conclusively identified due to overlapping $W(CO)_5$ vibrations. Anal. Calcd. for $C_{33}H_{40}GeN_2O_5W$: C, 49.47; H, 5.03; N, 3.50. Found: C, 49.76; H, 4.14; N, 3.52. Mp (°C): ~120 (dec.) 161-163 (melts).

3.5.3.42 Synthesis of $IPrCH_2•GeD_2•W(CO)_5$ 25D. To a mixture of **23** (50 mg, 0.057 mmol) and $Li[AlD_4]$ (1.2 mg, 0.029 mmol) was added a mixture of 10 mL toluene and Et_2O (4:1). The reaction mixture was stirred for 10 min at ambient temperature to obtain a beige slurry. Filtration of the reaction mixture through Celite afforded a pale yellow solution and volatiles were removed to yield **25D** as a pale yellow powder (43 mg, 91%). ^1H NMR (C_6D_6): essentially same as **25** with the absence of the GeH_2 resonance. $^2H\{^1H\}$ NMR (C_6H_6): δ 4.06 (s, -GeD_2-). IR (Nujol/cm^{-1}): Similar to **25** except a υGe-D stretching vibration was detected at 1407 cm^{-1}.

3.5.3.43 Thermolysis of $IPrCH_2•SnH_2•W(CO)_5$. A solution of IPr-$CH_2•SnH_2•W(CO)_5$ (17 mg, 0.02 mmol) in C_6D_6 was heated to 85 °C in a J-Young tube for 30 hours to give a pale yellow solution over a black precipitate. ^1H NMR analysis of the soluble fraction revealed the formation of free IPr=CH_2 (~96% by ^1H NMR spectroscopy) as a soluble product from the thermal decomposition.

3.5.3.44 Thermolysis of $IPrCH_2•GeH_2•W(CO)_5$. A solution of IPr-$CH_2•GeH_2•W(CO)_5$ (32 mg, 0.04 mmol) in toluene was heated at 110 °C for 48 hours to give a pale yellow solution over black precipitate. The solution was decanted and the volatiles were removed to afford a pale yellow powder (7.4 mg). ^1H NMR (C_6D_6) analysis of the soluble fraction revealed the presence of starting material, IPr-$CH_2•GeH_2•W(CO)_5$ (77%) and IPr=CH_2 (23%) as a decomposition product.

3.5.3.45 Reaction of IPrCH$_2$•SnH$_2$•W(CO)$_5$ with IPr. To mixture of IPr-CH$_2$•SnH$_2$•W(CO)$_5$ (0.037 g, 0.043 mmol) and IPr (0.018 g, 0.048 mmol) was added to 6 mL of toluene. The reaction mixture was stirred at ambient temperature overnight to give a pale yellow solution. Removal of the volatiles afforded a pale yellow powder (55 mg). ^{1}H NMR (C_6D_6) analysis of the product indicated the quantitative formation of IPr•SnH$_2$•W(CO)$_5$ (**5**) and free IPr=CH$_2$ in a 1:1 ratio.

3.5.3.46 Reaction of IPrCH$_2$•SnH$_2$•W(CO)$_5$ with excess ClSiMe$_3$. To a solution of IPrCH$_2$•SnH$_2$•W(CO)$_5$ (28 mg, 0.03 mmol) in 8 mL of Et$_2$O, was added ClSiMe$_3$ (34 mg, 0.31 mmol). The reaction mixture was stirred for 18 h at room temperature to give a beige solution. Removal of the solvent afforded pale yellow powder (22 mg) and ^{1}H NMR (C_6D_6) analysis of the product revealed the presence of IPr-CH$_2$•SnCl$_2$•W(CO)$_5$ (85% by ^{1}H NMR) along with a minor amount of unidentified product. The other product of the reaction was HSiMe$_3$ (g), the formation of which was confirmed by ^{1}H NMR spectroscopy by repeating the reaction in a J-Young NMR tube.

3.5.3.47 Reaction of IPr=CH$_2$•GeH$_2$•W(CO)$_5$ with IPr. To mixture of IPr-CH$_2$•GeH$_2$•W(CO)$_5$ (0.027 g, 0.033 mmol) and IPr (0.013 g, 0.033 mmol) was added to 5 mL of toluene. The reaction mixture was stirred at ambient temperature overnight to give a pale yellow solution. Removal of the volatiles afforded a pale yellow oil (40 mg). ^{1}H NMR (C_6D_6) analysis of the products revealed the quantitative conversion to IPr•GeH$_2$•W(CO)$_5$ and free IPr=CH$_2$ had occurred.

Table 3.1: Crystallographic data for **1**, **2**•toluene and **3**.

Compound	**1**	**2**•toluene	**3**
Formula	$C_{27}H_{36}Cl_2GeN_2$	$C_{28}H_{38}BGeN_2$	$C_{27}H_{36}Cl_2N_2Sn$
formula weight	532.07	569.15	578.17
crystal system	monoclinic	triclinic	orthorhombic
space group	$P2_1/n$	$P\bar{1}$	$P2_12_12_1$
a(Å)	10.0830(11)	10.7242(8)	9.325(2)
b (Å)	19.115(2)	16.9846(13)	15.529(4)
c (Å)	14.7562(16)	19.3106(15)	19.495(4)
α (deg)	90	84.4220(10)	90
β (deg)	99.571(2)	80.5350(10)	90
γ (deg)	90	73.4210(10)	90
V (Å^3)	2804.5(5)	3320.5(4)	2823.1(11)
Z	4	4	4
ρ (g cm^{-3})	1.260	1.138	1.360
abs coeff (mm^{-1})	1.299	0.945	1.111
T (K)	173(1)	173(1)	173(1)
$2\theta_{max}$ (°)	52.92	52.80	51.00
total data	10788	26986	20478
unique data (R_{int})	10788(0.0569)	26986(0.0271)	5247(0.1245)
Obs data [$I > 2\sigma(I)$]	7693	22024	3521
params	290	722	289
R_1 [$I > 2\sigma(I)$][a]	0.0476	0.0351	0.0596
wR_2 [all data][a]	0.1158	0.0926	0.1513
max/min $\Delta\rho$ (e$^-$ Å^{-3})	0.890 /-0. 661	0.595 /-0.363	1.209 /-0.564

[a] $R_1 = \Sigma \left| \left| F_o \right| - \left| F_c \right| \right| / \Sigma \left| F_o \right|$; $wR_2 = [\Sigma\, w(F_o^2 - F_c^2)^2 / \Sigma\, w(F_o^4)]^{1/2}$.

Table 3.2: Crystallographic data for **5**•0.25 Hexane, **7**•0.5 Hexane and **11**.

Compound	**5**•0.25 Hexane	**7**•0.5 Hexane	**11**
Formula	$C_{33.5}H_{41.5}N_2O_5SnW$	$C_{35}H_{45}CrN_2O_5Sn$	$C_{32}H_{36}Cl_2GeN_2O_5W$
formula weight	854.73	744.42	855.97
crystal system	orthorhombic	monoclinic	monoclinic
space group	*Pbca*	$P2_1/n$	$P2_1/n$
a(Å)	14.330(6)	10.8773(5)	10.6058(9)
b (Å)	19.457(8)	20.1714(9)	18.9964(16)
c (Å)	26.718(10)	16.8178(7)	50.974(4)
α (deg)	90	90	90
β (deg)	90	103.0007(5)	92.1060(10)
γ (deg)	90	90	90
V (Å^3)	7450(5)	3595.4(3)	10263.0(15)
Z	8	4	12
ρ (g cm^{-3})	1.524	1.375	1.662
abs coeff (mm^{-1})	3.793	1.037	4.435
T (K)	173(1)	173(1)	173(1)
$2\theta_{max}$ (°)	55.38	55.10	55.12
total data	58643	31765	89628
unique data (R_{int})	8542(0.0305)	8260(0.0184)	23567(0.0430)
Obs data [$I > 2\sigma(I)$]	7640	7417	21124
params	402	405	1205
R_1 [$I > 2\sigma(I)$][a]	0.0446	0.0221	0.0675
wR_2 [all data][a]	0.1600	0.0634	0.1509
max/min $\Delta\rho$ (e$^-$ Å^{-3})	3.143 /-1.421	0.329 /-0.459	3.720 /-3.387

[a] $R_1 = \Sigma \big| \, |F_o| - |F_c| \, \big| / \Sigma |F_o|$; $wR_2 = [\Sigma\, w(F_o^2 - F_c^2)^2 / \Sigma\, w(F_o^4)]^{1/2}$.

Table 3.3: Crystallographic data for **12**•THF, **13**•THF and **14**•THF.

Compound	**12**•THF	**13**•THF	**14**•THF
Formula	$C_{36}H_{46}GeN_2O_6W$	$C_{36}H_{46}CrGeN_2O_6$	$C_{57}H_{66}N_2O_9SnW$
formula weight	859.19	744.42	1225.66
crystal system	orthorhombic	orthorhombic	orthorhombic
space group	*Pbca* (No. 61)	*Pbca* (No. 61)	$Pna2_1$ (No. 33)
a(Å)	14.6626(5)	14.7679(7)	17.910(4)
b (Å)	19.5017(6)	19.1109(9)	13.236(3)
c (Å)	26.3383(8)	26.3971(12)	23.515(5)
α (deg)	90	90	90
β (deg)	90	90	90
γ (deg)	90	90	90
V (Å^3)	7531.3(4)	7450.0(6)	5575(2)
Z	8	8	4
ρ(g cm^{-3})	1.516	1.297	1.460
abs coeff (mm^{-1})	3.894	1.141	2.564
T (K)	173(1)	173(1)	173(1)
$2\theta_{max}$ (°)	55.20	50.50	55.16
total data	64342	50659	47549
unique data (R_{int})	8727(0.0193)	6735(0.0770)	12822(0.0249)
Obs data [$I > 2\sigma(I)$]	7697	4731	12002
params	423	410	676
R_1 [$I > 2\sigma(I)$][a]	0.0175	0.0463	0.0227
wR_2 [all data][a]	0.0474	0.1264	0.0515
max/min $\Delta\rho$ (e$^-$ Å^{-3})	0.747 /-0.493	0.772 /-0.785	1.067 /-0.489

[a] $R_1 = \Sigma \big| |F_o| - |F_c| \big| / \Sigma |F_o|$; $wR_2 = [\Sigma\, w(F_o^2 - F_c^2)^2 / \Sigma\, w(F_o^4)]^{1/2}$.

Table 3.4: Crystallographic data for **15**, **23**•0.5 Hexane and **17**•3 CH_2Cl_2.

Compound	**15**	**16**•0.5 Hexane	**17•3CH$_2$Cl$_2$**
Formula	$C_{27}H_{41}BN_2Si$	$C_{36}H_{45}N_2O_5SiW$	$C_{61}H_{78}Cl_{12}N_2O_4Rh_2Si_2$
formula weight	432.52	785.67	1618.67
crystal system	monoclinic	orthorhombic	monoclinic
space group	$P2_1/n$	*Pbca*	$P2_1/c$
a(Å)	11.2366(7)	14.2434(15)	13.2122(2)
b (Å)	13.7989(8)	18.594(2)	21.2410(3)
c (Å)	17.9086(11)	27.175(3)	13.2241(2)
α (deg)	90	90	90
β (deg)	97.2660(10)	90	97.4269(6)
γ (deg)	90	90	90
V (Å^3)	2754.5(3)	7196.9(13)	3680.08(9)
Z	4	8	2
ρ (g cm^{-3})	1.043	1.450	1.461
abs coeff (mm^{-1})	0.100	3.284	8.308
T (K)	173(1)	173(1)	173(1)
$2\theta_{max}$ (°)	52.80	51.00	140.08
total data	21777	50262	24802
unique data (R_{int})	5649(0.0404)	6703(0.1106)	6813(0.0170)
Obs data [$I > 2\sigma(I)$]	4146	4839	6390
params	300	413	446
R_1 [$I > 2\sigma(I)$][a]	0.0418	0.0850	0.0452
wR_2 [all data][a]	0.1161	0.2254	0.1316
max/min $\Delta\rho$ (e$^-$ Å^{-3})	0.296 /-0.258	4.579 /-4.960	1.203 /-0.869

[a] $R_1 = \Sigma \big| \, |F_o| - |F_c| \, \big| / \Sigma |F_o|$; $wR_2 = [\Sigma\, w(F_o^2 - F_c^2)^2 / \Sigma\, w(F_o^4)]^{1/2}$.

Table 3.5: Crystallographic data for **22**•0.5 tol, **23**•0.5 Et_2O and **24**.

Compound	**22**•0.5 tol	**23**•0.5 Et_2O	**24**
Formula	$C_{36.5}H_{42}Cl_2N_2O_6SnW$	$C_{33}H_{38}Cl_2GeN_2O_5W$	$C_{33}H_{40}N_2O_5SnW$
formula weight	960.19	869.99	847.21
crystal system	monoclinic	orthorhombic	monoclinic
space group	$P2_1/c$ (No. 14)	$Pna2_1$ (No. 33)	$P2_1/n$
a(Å)	18.2204(7)	24.2684(11)	10.400(2)
b (Å)	13.8439(5)	11.1671(5)	22.212(5)
c (Å)	17.6027(7)	13.2380(6)	15.597(3)
α (deg)	90	90	90
β (deg)	118.0937(4)	90	91.626(3)
γ (deg)	90	90	90
V (Å^3)	3917.0(3)	3587.6(3)	3601.5(13)
Z	4	4	4
ρ (g cm^{-3})	1.632	1.611	1.562
abs coeff (mm^{-1})	3.749	4.230	3.922
T (K)	173(1)	173(1)	173(1)
$2\theta_{max}$ (°)	54.98	55.40	55.18
total data	34306	31057	31790
unique data (R_{int})	8962(0.0196)	8358(0.0163)	8303(0.0150)
Obs data [$I > 2\sigma(I)$]	7764	8171	7809
params	484	398	387
R_1 [$I > 2\sigma(I)$][a]	0.0302	0.0203	0.0156
wR_2 [all data][a]	0.0921	0.0501	0.0394
max/min $\Delta\rho$ (e$^-$ Å^{-3})	1.629/-0.863	1.136 /-0.670	0.738 /-0.597

[a] $R_1 = \Sigma \big| \, |F_o| - |F_c| \, \big| / \Sigma |F_o|$; $wR_2 = [\Sigma\, w(F_o^2 - F_c^2)^2 / \Sigma\, w(F_o^4)]^{1/2}$.

Table 3.6: Crystallographic data for **25**•0.5 Et_2O.

Compound	**25•0.5Et_2O**
Formula	$C_{33}H_{45}GeN_2O_{5.5}W$
formula weight	838.17
crystal system	monoclinic
space group	$P\bar{1}$
a(Å)	34.3772(15)
b (Å)	10.0524(5)
c (Å)	21.8558(10)
α (deg)	90
β (deg)	100.6360(10)
γ (deg)	90
V (Å^3)	7423.0(6)
Z	8
ρ (g cm^{-3})	1.500
abs coeff (mm^{-1})	3.948
T (K)	173(1)
$2\theta_{max}$ (°)	55.38
total data	32963
unique data (R_{int})	8636(0.0191)
Obs data [$I > 2\sigma(I)$]	7859
params	410
R_1 [$I > 2\sigma(I)$][a]	0.0196
wR_2 [all data][a]	0.0491
max/min $\Delta\rho$ (e$^-$ Å^{-3})	1.253 /-0.473

[a] $R_1 = \Sigma \left| \left| F_o \right| - \left| F_c \right| \right| / \Sigma \left| F_o \right|$; $wR_2 = [\Sigma\, w(F_o^2 - F_c^2)^2 / \Sigma\, w(F_o^4)]^{1/2}$.

3.6 References

(1) Power, P. P. *Chem. Rev.* **1999**, *99*, 3463.

(2) (a) *The Chemistry of Organic Germanium, Tin and Lead*; Rappoport, Z., Ed.; Wiley VCH: New York, **2003**; Vol. 2. (b) Elschenbroich, C.; Salzer, A. *Organometallics: A Concise Introduction (2nd Ed.)*, Wiley-VCH, Weinheim, Germany, **2006**. (c) Lappert, M. F.; Power, P. P.; Protchenko, A.; Seeber, A. *Metal Amide Chemistry*, Wiley, Chichester, UK, **2009**.

(3) (a) Pu, L.; Twamley, B.; Power, P. P. *J. Am. Chem. Soc.* **2000**, *122*, 3524. (b) Phillips, A. D.; Wright, R. J.; Olmstead, M. M.; Power, P. P. *J. Am. Chem. Soc.* **2002**, *124*, 5930. (c) Stender, M.; Phillips, A. D.; Wright, R. J.; Power, P. P. *Angew. Chem., Int. Ed.* **2002**, *41*, 1785. (d) Wiberg, N.; Vasisht, S. K.; Fischer, G.; Mayer, P. *Z. Anorg. Allg. Chem.* **2004**, *630*, 1823. (e) Sekiguchi, A.; Kinjo, R.; Ichinohe, M. *Science* **2004**, *305*, 1755. (f) Sugiyama, Y.; Sasamori, T.; Hosoi, Y.; Furukawa, Y.; Takagi, N.; Nagase, S.; Tokitoh, N. *J. Am. Chem. Soc.* **2006**, *128*, 1023. (g) Li, J.; Schenk, C.; Goedecke, C.; Frenking, G.; Jones, C. *J. Am. Chem. Soc.* **2011**, *133*, 18622. (h) Rekken, B. D.; Brown, T. M.; Fettinger, J. C.; Tuononen, H. M.; Power, P. P. *J. Am. Chem. Soc.* **2012**, *134*, 6504. (i) Protchenko, A. V.; Birjkumar, K. H.; Dange, D.; Schwarz, A. D.; Vidovic, D.; Jones, C.; Kaltsoyannis, N.; Mountford, P.; Aldridge, S. *J. Am. Chem. Soc.* **2012**, *134*, 6500. (j) Inoue, S.; Leszczyńska, K. *Angew. Chem., Int.*

Ed. **2012**, *51*, 8589.

(4) (a) Kinjo, R.; Donnadieu, B.; Celik, M. A.; Frenking, G.; Bertrand, G. *Science* **2011**, *333*, 610. (b) Wang, Y.; Xie, Y.; Wei, P.; King, R. B.; Schaefer, H. F., III; Schleyer, P. v. R.; Robinson, G. H. *Science* **2008**, *321*, 1069. (c) Ghadwal, R. S.; Roesky, H. W.; Merkel, S.; Henn, J.; Stalke, D. *Angew. Chem., Int. Ed.* **2009**, *48*, 5683. (d) Filippou, A. C.; Chernov, O.; Schnakenburg, G. *Angew. Chem., Int. Ed.* **2009**, *48*, 5687. (e) Wang, Y.; Xie, Y.; Wei, P.; King, R. B.; Schaefer, H. F., III; Schleyer, P. v. R.; Robinson, G. H. *J. Am. Chem. Soc.* **2008**, *130*, 14970. (f) Back, O.; Kuchenbeiser, G.; Donnadieu, B.; Bertrand, G. *Angew. Chem., Int. Ed.* **2009**, *48*, 5530. (g) Wang, Y.; Xie, Y.; Abraham, M. Y.; Gilliard, R. J., Jr.; Wei, P.; Schaefer, H. F., III; Schleyer, P. v. R.; Robinson, G. H. *Organometallics* **2010**, *29*, 4778. (h) Braunschweig, H.; Dewhurst, R. D.; Hammond, K.; Mies, J.; Radacki, K.; Vargas, A. *Science* **2012**, *336*, 11420. (j) Baker, R. J.; Farley, R. D.; Jones. C.; Kloth, M.; Murphy, D. M. *Chem. Commun.* **2002**, 1196. (k) Wang, Y.; Quillian, B.; Wei, P.; Wannere, C. S.; Xie, Y.; King, R. B.; Schaefer III, H. F.; Schleyer, P. v. R.; Robinson, G. H. *J. Am. Chem. Soc.* **2007**, *129*, 12412.

(5) Power, P. P. *Nature*, **2010**, *463*, 171.

(6) (a) Mizuhata, Y.; Sasamori, T.; Tokitoh, N. *Chem. Rev.* **2009**, *109*, 3479. (b) Linti, G.; Schnöckel, H. *Coord. Chem. Rev.* **2000**, *206*, 285. (c) Stephan, D. W. *Dalton Trans.* **2009**, 3129. (d) Pearson, R. G. *J. Am. Chem.*

Soc. **1988**, *110*, 2092. (e) Kutzelnigg, W. *Angew*. *Chem., Int*. *Ed*. *Engl*. **1984**, *23*, 272.

(7) (a) Spikes, G. H.; Fettinger, J. C.; Power, P. P. *J*. *Am*. *Chem*. *Soc*. **2005**, *127*, 12232. (b) Frey, G. D.; Lavallo, B.; Donnadieu, B.; Schoeller, W. W.; Bertrand, G. *Science* **2007**, *316*, 439. (c) Welch, G. C.; San Juan, R. R.; Masuda, J. D.; Stephan, D. W. *Science* **2006**, *314*, 1124. (d) Chase, P. A.; Stephan, D. W. *Angew*. *Chem., Int*. *Ed*. **2008**, *47*, 7433. (e) Peng, Y.; Ellis, B. D.; Wang, X.; Power, P. P. *J*. *Am*. *Chem*. *Soc*. **2008**, *130*, 12268. (f) Yamaguchi, Y.; Kashiwabara, T.; Ogata, K.; Miura, Y.; Nakamura, Y.; Kobayashi, K.; Ito, T. *Chem*. *Commun*. **2004**, 2160. (g) Peng, Y.; Ellis, B. D.; Wang, X.; Fettinger, J. C.; Power, P. P. *Science* **2009**, *325*, 1668. (h) Otten, E.; Neu, R. C.; Erker, G.; Stephan, D. W. *J*. *Am*. *Chem*. *Soc*. **2009**, *131*, 9918. (i) Mömming, C. M.; Otten, E.; Kehr, G.; Fröhlich, R.; Grimme, S.; Stephan, D. W.; Erker, G. *Angew*. *Chem., Int*. *Ed*. **2009**, *48*, 6643.

(8) (a) Bundhun, A.; Ramasami P.; Schaefer, H. F., III. *J*. *Phys*. *Chem*. *A*, **2009**, *113*, 8080 and references therein. (b) Isobe, C.; Cho, H. -C.; Sewell, J. E. *Surf*. *Sci*. **1993**, *295*, 117. (c) Weerts, W. L. M.; de Croon, M. H. J. M.; Marin, G. B. J. *Electrochem*. *Soc*. **1998**, *145*, 1318. (d) Jasinski, J. M.; Gates S. M. *Acc*. *Chem*. *Res*. **1991**, *24*, 9. For related synthesis of nanocrystals see: (e) Kortshagen, U.; Anthony, R.; Gresback, R.; Holman, Z.; Ligman, R.; Liu, C. –Y.; Mangolini, L.; Campbell, S. A. *Pure Appl*.

Chem. **2008**, *80*, 1901. (f) Li, X.; He, Y.; Talukdar, S. S.; Swihart, M. T. *Langmuir*, **2003**, *19*, 8490.

(9) (a) Fischer, E. O. *Adv*. *Organomet*. *Chem*. **1976**, *14*, 1. (b) Schrock, R. R. *Acc*. *Chem*. *Res*. **1979**, *12*, 98. (c) Bourissou, D.; Guerret, O.; Gabbaï, F. P.; Bertrand, G. *Chem*. *Rev*. **2000**, *100*, 39. (d) Grubbs, R. H, Ed. *Handbook of Metathesis*; Wiley-WCH: Weinheim, **2008**. (e) Hahn, F. E.; Jahnke, M. C. *Angew*. *Chem*., *Int*. *Ed*. **2008**, *47*, 3122. (f) Diez-González, S.; Marion, N.; Nolan, S. P. *Chem*. *Rev*. **2009**, *109*, 3612. For the reviews on the chemistry of heavy divalent tetrelenes (:ER_2, E = Si-Pb) see: (g) Petz, W. *Chem*. *Rev*. **1986**, *86*, 1019.

(10) (a) Tebbe, F. N.; Parshall, G. W.; Ovenall, D. W. *J*. *Am*. *Chem*. *Soc*. **1979**, *101*, 5074. (b) Schwab, P.; France, M. B.; Ziller, J. W.; Grubbs, R. H. *Angew*. *Chem*., *Int*. *Ed*. *Engl*. **1995**, *34*, 2039. (c) Scott, J.; Mindiola, D. *J*. *Dalton Trans*. **2009**, 8463.

(11) (a) Smith, G. R.; Guillory, W. A. *J*. *Chem*. *Phys*. **1972**, *56*, 1423. (b) Wang, X.; Andrews, L.; Chertihin, G. V.; Souter, P. F. *J*. *Phys*. *Chem*. *A* **2002**, *106*, 6302. (c) Lemierre, V.; Chrostowska, A.; Dargelos, A.; Baylére, P.; Leigh, W. J.; Harrington, C. R. *Appl*. *Organometal*. *Chem*. **2004**, *18*, 676. (d) Smith, T. C.; Clouthier, D. J.; Sha, W.; Adam, A. G. *J*. *Chem*. *Phys*. **2000**, *113*, 9567.

(12) Theoretical studies predict singlet ground states for the heavy Group 14 hydrides, :EH_2, and a reduced propensity for M=EH_2 π-bonding, see: (a)

Jacobsen, H.; Ziegler, T. *Inorg. Chem.* **1996**, *35*, 775. (b) Frison, G.; Sevin, A. *J. Chem. Soc., Perkin Trans. 2* **2002**, 1692. (c) Lein, M.; Szabó, A.; Kovács, A.; Frenking, G. *Faraday Discuss.* **2003**, *124*, 365.

(13) (a) Eichler, B. E.; Power, P. P. *J. Am. Chem. Soc.* **2000**, *122*, 8785. (b) Pineda, L. W.; Jancik, V.; Starke, K.; Oswald, R. B.; Roesky, H. W. *Angew. Chem., Int. Ed.* **2006**, *45*, 2602.

(14) (a) Becerra, R.; Boganov, S. E.; Egorov, M. P.; Nefedov, O. M.; Walsh, R. *Chem. Phys. Lett.* **1996**, *260*, 433. (b) Becerra, R.; Boganov, S. E.; Egorov, M. P.; Faustov, V. I.; Nefedov, O. M.; Walsh, R. *J. Am. Chem. Soc.* **1998**, *120*, 12657 and references therein.

(15) For selected examples of donor-acceptor stabilization, see: (a) Vogel, U.; Timoshkin, A. Y.; Scheer, M. *Angew. Chem., Int. Ed.* **2001**, *40*, 4409. (b) Rupar, P. A.; Jennings, M. C.; Ragogna, P. J.; Baines, K. M. *Organometallics* **2007**, *26*, 4109. (c) Adolf, A.; Vogel, U.; Zabel, M.; Timoshkin, A. Y.; Scheer, M. *Eur. J. Inorg. Chem.* **2008**, 3482. (d) Yamaguchi, T.; Sekiguchi, A.; Driess, M. *J. Am. Chem. Soc.* **2010**, *132*, 14061. (e) Xiong, Y.; Yao, S.; Driess, M. *Angew. Chem., Int. Ed.* **2010**, *49*, 6642. (e) Jambor, R.; Herres-Pawlis, S.; Schürmann, M. Jurkschat, K. *Eur. J. Inorg. Chem.* **2011**, 344.

(16) Arduengo III, A. J.; Rasika Dias, H. V.; Calabrese, J. C.; Davidson, F. *Inorg. Chem.* **1993**, *32*, 1541.

(17) Jafarpour, L.; Stevens, E. D.; Nolan, S. P. *J. Organomet. Chem.* **2000**, *606*, 49.

(18) Kolensnikov, S. P.; Shiryaev, V. I.; Nefedov, O. M. *Izv. Akad. Nauk SSSR, Ser. Khim.* **1966**, 584.

(19) Pu, L.; Twamley, B.; Haubrich, S. T.; Olmstead, M. M.; Mork, B. V.; Simons, R. S.; Power, P. P. *J. Am. Chem. Soc.* **2000**, *122*, 650.

(20) Nöth, H.; Wrackmeyer, B. *Nuclear Magnetic Resonance Spectroscopy of Boron Compounds*, in NMR Basic Principles and Progress, Vol. 14 (Eds.: Diehl, P.; Fluck, E.; Kosfeld), Springer, Berlin, **1978**.

(21) Some examples of substituted Ge(II) monohydrides have been reported. See: (a) Ding, Y.; Hao, H.; Roesky, H. W.; Noltemeyer, M.; Schmidt, H. -G. *Organometallics* **2001**, *20*, 4806. (b) Richards, A. F.; Phillips, A. D.; Olmstead, M. M.; Power, P. P. *J. Am. Chem. Soc.* **2003**, *125*, 3204. (c) Leung, W.-P.; So, C.-W.; Chong, K.-H.; Kan, K.-W.; Chan, H. -S.; Mak, T. C. W. *Organometallics* **2006**, *25*, 2851. (d) Khan, S.; Samuel, P. P.; Michel, R.; Dieterich, J. M.; Mata, R. A.; Demers, J. P.; Lange, A.; Roesky, H. W.; Stalke, D. *Chem. Commun.* **2012**, *48*, 4890.

(22) Karolczak, J.; Harper, W. W.; Grev, R. S.; Clouthier, D. J. *J. Chem. Phys.* **1995**, *103*, 2839.

(23) Jana, A.; Roesky, H. W.; Schulzke, C.; Döring, A.; Beck, T.; Pal, A.; Irmer, R. H. *Inorg. Chem.* **2009**, *48*, 193.

(24) Krapp, A.; Frenking, G. *J. Am. Chem. Soc.* **2008**, *49*, 16646.

(25) (a) Balch, A. L.; Oram, D. E. *Organometallics* **1988**, *7*, 155. (b) Jutzi, P.; Steiner, W. *Chem. Ber.* **1976**, *109*, 3473.

(26) Albertin, G.; Antoniutti, S.; Castro, J. *Organometallics* **2010**, *29*, 3808.

(27) Peng, Y.; Brynda, M.; Ellis, B. D.; Fettinger, J. C.; Rivard, E.; Power, P. P. *Chem. Commun.* **2008**, 6042.

(28) (a) Renner, G.; Kircher, P.; Huttner, G.; Rutsch, P.; Heinze, K. *Eur. J. Inorg. Chem.* **2001**, 973. (b) Veith, M.; Ehses, M.; Huch, V. *New. J. Chem.* **2005**, *29*, 154.

(29) Brice, M. D.; Cotton, F, A. *J. Am. Chem. Soc.* **1973**, *95*, 4529.

(30) Saur, I.; Rima, G.; Miqueu, K.; Gornitzk, H.; Barrau, J. *J. Organomet. Chem.* **2003**, *672*, 77.

(31) (a) Hashimoto, H.; Tsubota, T.; Fukuda, T.; Tobita, H. *Chem. Lett.* **2009**, *38*, 1196. (b) Hashimoto, H.; Fukuda, T.; Tobita, H. *New. J. Chem.* **2010**, *34*, 1723.

(32) Lappert, M. F.; Miles, S. J.; Power, P. P.; Carty, A. J.; Taylor, N. J. *J. Chem. Soc., Chem. Commun.* **1977**, 458.

(33) Pauling, L. *The Nature of the Chemical Bond*, 3rd ed., Cornell University Press: Ithaca, NY, **1960**.

(34) Jana, A.; Roesky, H. W.; Schulzke, C. *Inorg. Chem.* **2009**, *48*, 9543.

(35) Eichler, B. E.; Phillips, A. D.; Haubrich, S. T.; Mork, B. V.; Power, P. P. *Organometallics* **2002**, *21*, 5622.

(36) Dostálová, R.; Dostál, L.; Růžička, A.; Jambor, R. *Organometallics* **2011**, *30*, 2405.

(37) Baldridge, K. K.; Battersby, T. R.; Clark, R. V.; Siegel, J. S. *J. Am. Chem. Soc.* **1997**, *119*, 7048.

(38) (a) Waterman, R.; Hayes, P. G.; Tilley, T. D. *Acc. Chem. Res.* **2007**, *40*, 712. (b) Zybill, C.; Müller, G. *Angew. Chem., Int. Ed. Engl.* **1987**, *26*, 669. (c) Gusev, D. G.; Fontaine, F. -G.; Lough, A. J.; Zargarian, D. *Angew. Chem., Int. Ed.* **2003**, *42*, 216. (d) Ochiai, M.; Hashimoto, H.; Tobita, H. *Angew. Chem., Int. Ed.* **2007**, *46*, 8192.

(39) Abrahim, M. Y.; Wang, Y.; Xie, Y.; Wei, P.; Schaefer III, H. F.; Schleyer, P. v. R.; Robinson, G. H. *J. Am. Chem. Soc.* **2011**, *133*, 8874.

(40) Azhakar, R.; Tavcar, G.; Roesky, H. W.; Hey, J.; Stalke, D. *Eur. J. Inorg. Chem.* **2011**, *475*.

(41) Al-Rafia, S. M. I.; Malcolm, A. C.; McDonald, R.; Ferguson, M. J.; Rivard, E. *Angew. Chem., Int. Ed.* **2011**, *50*, 8354.

(42) (a) Baker, R. J.; Davies, A. J.; Jones, C.; Kloth, M. *J. Organomet. Chem.*, **2002**, *656*, 203. The direct reaction between IPr•$SiCl_2$ and Li[AlH_4] also

gave IPr•AlH_3 as the major product.

(43) Jana, A.; Leusser, D.; Objartel, I.; Roesky, H. W.; Stalke, D. *Dalton Trans*. **2011**, *40*, 5458.

(44) (a) Haaf, M.; Schmiedl, A.; Schmedake, T. A.; Powell, D. R.; Millevolte, A. J.; Denk, M.; West, R. *J. Am. Chem. Soc*. **1998**, *120*, 12714 and references therein. (b) Metzler, N.; Denk, M. *Chem. Commun*. **1996**, 2657.

(45) Takanashi, K.; Lee, V. Y.; Yokoyama, T.; Sekiguchi, A. *J. Am. Chem. Soc*. **2009**, *131*, 916.

(46) Koloski, T. S.; Carroll, P. J.; Berry, D. H. *J. Am. Chem. Soc*. **1990**, *112*, 6405.

(47) Khramov, D. M.; Lynch, V. M.; Bielawski, C. W. *Organometallics* **2007**, *26*, 6042.

(48) Nishihara, Y.; Takemura, M.; Kohtaro, K. *Organometallics* **2002**, *21*, 825.

(49) (a) Kuhn, N.; Bohnen, H.; Kreutzberg, J.; Bläser, D.; Boese, R. *J. Chem. Soc., Chem. Commun*. **1993**, 1136 (b) Kuhn, N.; Bohnen, H.; Kreutzberg, J.; Bläser, D.; Boese, R. *Chem. Ber*. **1994**, *127*, 1405.

(50) Dumrath, A.; Wu, X. F.; Neumann, H.; Spannenberg, A.; Jackstell, R.; Beller, M. *Angew. Chem., Int. Ed*. **2010**, *49*, 8988.

(51) (a) Brook, A. G.; Brook, M. A. *Adv. Organomet. Chem*. **1996,** *39,* 71. (b)

Sakaba, H.; Watanabe, S.; Kabuto, C.; Kabuto, K. *J. Am. Chem. Soc.* **2003**, *125*, 2842.

(52) Sheldrick, W. S. *The Chemistry of Organic Silicon Compounds;* Wiley: New York, 1989; Chapter 3.

(53) Veith, M.; Huch, V. *J. Organomet. Chem.* **1986**, *308*, 263.

(54) Tokitoh, N.; Manmaru, K.; Okazaki, R. *Organometallics* **1994**, *13*, 167.

(55) Bancroft, G. M.; Dignard-Bailey, L.; Puddephatt, R. J. *Inorg. Chem.* **1986**, *25*, 3675.

(56) Zyder, M.; Kochel, A.; Handzlik, J.; Buzar, T. S. *Organometallics* **2009**, *28*, 5857.

(57) Hope, H.; *Prog. Inorg. Chem.* **1994**, *43,* 1.

(58) Blessing, R. H.; *Acta Cryst.* **1995**, *A51,* 33.

(59) Sheldrick, G. M.; *Acta Cryst.* **2008**, *A64,* 112.

(60) Altomare, A.; Burla, M. C.; Camalli, M.; Cascarano, G. L.; Giacovazzo, C.; Guagliardi, A.; Moliterni, A. G. G.; Polidori, G.; Spagna, R. *J. Appl. Cryst.* **1999**, *32*, 115.

(61) Beurskens, P. T.; Beurskens, G.; de Gelder, R.; Smits, J. M. M.; Garcia-Garcia, S.; Gould, R. O. *DIRDIF-2008*, Crystallography Laboratory, Radboud University: Nijmegen, The Netherlands, **2008**.

(62) Schneider, T. R.; Sheldrick, G. M. *Acta Cryst*. **2002**, *D58*, 1772.

(63) Sheldrick, G. M. CELL_NOW, version 2008/2; Universität Göttingen: Göttingen, Germany, 2008.

(64) Sheldrick, G. M. SAINT, version 7.68A; Bruker AXS Inc.: Madison, WI, 2008.

(65) Sheldrick, G. M. TWINABS, version 2008/4; University of Göttingen: Göttingen, Germany, 2008.

Chapter 4

Trapping Parent Inorganic Ethylenes in the Form of Donor-Acceptor Adducts

Chapter 4

Trapping Parent Group 14 Element Inorganic Ethylenes in the Form of Donor-Acceptor Adducts

4.1 Abstract

The synthesis of a series of Group 14 element heavy ethylene analogues in the form of Lewis acid-base adducts LB•H_2EE'H_2•LA (LB = Lewis base; E = Si and Ge; E' = Ge and Sn; LA = Lewis acid) is described. The N-heterocyclic carbene IPr [IPr = {(HCNDipp)$_2$}C: and Dipp = 2,6-^{i}Pr$_2$C$_6$H$_3$] and the N-heterocyclic olefin, IPr=CH_2, were used as Lewis-basic donors, while $W(CO)_5$ was used as the Lewis-acid acceptor to stabilize these inorganic ethylenes in the condensed phase. The E-E' linkages were constructed by reacting the nucleophilic E(II) halide adducts, IPr•ECl_2 or IPrCH_2•ECl_2 (E = Si and/or Ge) with the coordinatively labile tungsten complexes [$(THF)_n$•E'Cl_2•$W(CO)_5$] (E' = Ge and Sn) to give perhalogenated complexes [IPr•Cl_2E-E'Cl_2•$W(CO)_5$] (E = Si and Ge; E' = Ge and Sn). The desired hydride functionalities were installed by reacting the perhalogenated complexes with Li[BH_4] or Li[AlH_4] to yield IPr•H_2E-E'H_2•$W(CO)_5$ (E = Si; E' = Ge and Sn) and LB•H_2Ge-GeH_2•$W(CO)_5$ (LB = IPr and IPrCH_2). In the presence of pentane-2,4-dione, the silagermene complex IPr•H_2Si-GeH_2•$W(CO)_5$ underwent a clean hydrosilylation to yield the novel anionic adduct [{MeC(O)H-CH=C(Me)O}SiH-GeH_2•$W(CO)_5$]$^-$ as a salt with the known imidiazolium countercation [IPrH]$^+$. This transformation indicates that the

C_{IPr}-Si interaction in the silagermene complex is labile in nature. The presence of a stable Si-Ge linkage in the silagermene adduct IPr•H_2Si-GeH_2•$W(CO)_5$ should facilitate the future synthesis of new SiGe hybrid nanomaterials *via* decomplexation/dehydrogenation of the silagermene unit.

4.2 Introduction

Ethylene is a key industrial precursor to numerous value added chemicals, and over the last decade its global production exceeded that of any other organic compound.[1] It is also a key regulatory component in plants and responsible for stimulating or regulating the ripping of fruits, the abscission (or shedding) of leaves and the opening flowers.[2] Moreover, ethylene can act as both π-donor and π-acceptor ligand and as a result its coordination chemistry led the development of bonding concepts in transition-metal chemistry.[3] In contrast, the heavier Group 14 element ethylene analogues $H_2E=EH_2$ (E = Si-Pb) have remained elusive owing to a lack of suitable synthetic routes for their preparation and the expected instability of these entities in the condensed phase.[4,5] The reactive nature of the heavy ethylene analogues originates from their weaker π-bonding interaction between the heavier Group 14 elements (E-E) and the increasingly reactive nature of E-H (E = Si-Pb) bonds which arise from their poor orbital overlap and considerable ionic character.[7] Despite such synthetic obstacles, these species are of considerable interest as they serve as structural models for Si and Ge surfaces (where E=E multiple bonds are likely present),[7] and as potential precursors to new inorganic hybrid materials.[8]

Pioneering work by Lappert and others revealed that the heavy Group 14 element dimetallenes $R_2E=ER_2$ can be stabilized using sterically demanding ligands (Scheme 4.1).[9] For example, Lappert et al. prepared the digemene $R_2Ge=GeR_2$ and distannene $R_2Sn=SnR_2$ (R = $-CH(SiMe_3)_2$) in the early 1970s.[9a,b]

These dimetallenes behave like singlet germelene (R_2Ge:) and stannylene (R_2Sn:) species in solution but in the solid state the R_2E: fragments dimerize to form the dimetallenes with elongated E-E bonds (E = Ge and Sn). Subsequently, in 1981 West *et al*. reported the synthesis of disilene $Mes_2Si=SiMes_2$ (Mes = 2,4,6-$(CH_3)_3C_6H_2$) using a similar strategy used by the Lappert group. The bonding features within these compounds are often vastly different from that of olefins, for example, the heavy ethylene congeners $R_2E=ER_2$ (E = Ge, Sn, or Pb) have a high propensity to dissociate into monomeric singlet R_2E: fragments in solution.[9] In addition, elongated E=E distances and *trans*-bent geometries are two key features of heavy Group 14 element dimetallenes $R_2E=ER_2$ (E = Si-Pb) in the solid state.[9] These experimental observations are in line with the bonding and structural arrangements predicted by theory.[10,11]

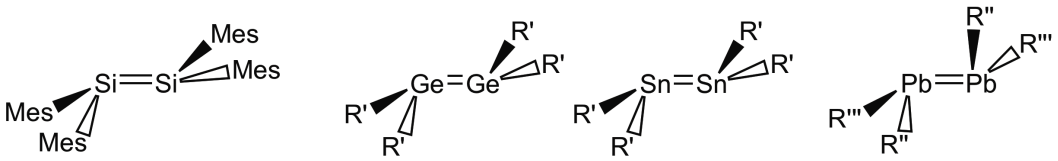

Scheme 4.1 Heavy Group 14 dimetallenes; $Mes_2Si=SiMes_2$, Mes = 2,4,6-$(CH_3)_3C_6H_2$; $R'_2Ge=GeR'_2$ and $R'_2Sn=SnR'_2$, R' = $CH(SiMe_3)_2$; R''R'''Pb=PbR''R''', R'' = 2,4,6-$(CF_3)_3C_6H_2$, R''' = $Si(SiMe_3)_3$.

As mentioned above, it has been predicted that the heavy ethylene analogues $H_2E=EH_2$ (E = Si-Pb) adopt *trans*-bent geometries, wherein both E centers can act either as electron donors or acceptors.[9–12] This unusual bonding feature is illustrated by the resonance forms **I–III** in Scheme 4.2. Based on the

canonical structure represented in Scheme 4.2, it was reasoned that the isolation of inorganic ethylenes $H_2E=E'H_2$ (E and E' = Si-Pb) could be possible in the form of donor-acceptor adducts by using suitable Lewis acidic and basic groups.[13,14]

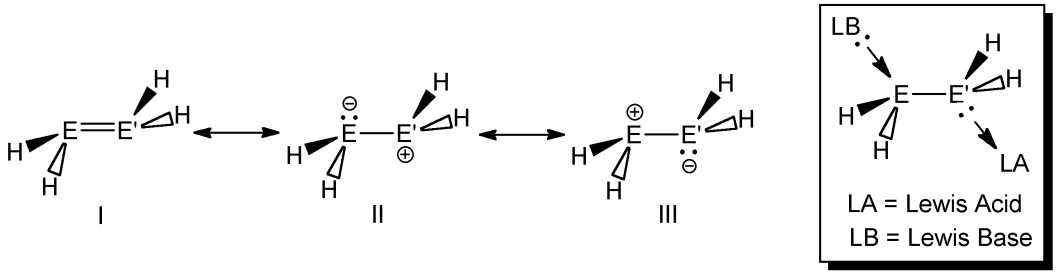

Scheme 4.2 Resonance description of the bonding within the heavy ethylene analogues $H_2E=E'H_2$ (E and E' = Si-Pb) and a possible way to isolate these inorganic ethylenes a using donor-acceptor strategy.

Recently, the Rivard group has developed a stabilization protocol to isolate heavy methylene analogues $:EH_2$ (E = Si, Ge and Sn).[13] This stabilization technique engages a N-heterocyclic carbenes (NHCs) as electron pair donors (Lewis base) and Lewis-acid acceptors such as BH_3 or $W(CO)_5$ (Chart 4.1).[13,14]

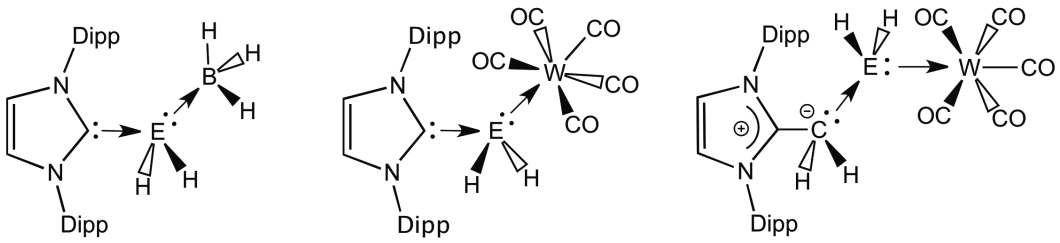

The abovementioned successes in isolating donor-acceptor adducts of Group 14 element methylenes provided the motivation to implement a similar approach to isolate heavy ethylene analogues in the form of stable adducts

IPr•H_2E-E'H_2•LA (LA = Lewis acid; E and E' = Si, Ge and/or Sn).

4.3 Results and discussion

The use of N-heterocyclic carbenes (NHCs) as supporting ligands has proven to be an efficient way to stabilize/isolate reactive inorganic bonding environments that previously remained unknown and/or elusive.[15] Recently, a number of novel main group species such as B≡B, :SiX_2 (X = Cl or Br), :Ge=Ge:, :Si=Si:, P_2, and PN have been isolated in the condensed phase using NHC ligands.[16] These discoveries have substantially improved our fundamental understanding of chemistry and also provided access to new families of chemical reagents for the future advancement of inorganic chemistry.

As mentioned earlier, the overall goal of the project described in this Chapter was to synthesize inorganic ethylene analogues in the form of stable adducts IPr•H_2E-E'H_2•LA (LA = Lewis acid; E and E' = Si, Ge and/or Sn). To attain the abovementioned target, the initial challenge was to make the hybrid group 14 elementchloride complexes [IPr•Cl_2E-E'Cl_2•$W(CO)_5$] (E and E' = Si, Ge and/or Sn), which can then be subsequently reacted with different hydride sources to incorporate desired hydride functionalities. The requisite Si-Ge and Si-Sn linkages were constructed by reacting Roesky's nucleophilic Si(II) halide adduct IPr•$SiCl_2$,[16c] with the coordinatively labile tungsten complexes [$(THF)_n$•E'Cl_2•$W(CO)_5$] (E' = Ge and Sn)[18] to give the perhalogenated complexes [IPr•Cl_2Si-E'Cl_2•$W(CO)_5$] (E' = Ge and Sn; **2** and **3**) (Scheme 4.3). Compounds **2** and **3** were isolated as air- and moisture-sensitive yellow solids in 87 and 97%

yields, respectively. The ^{29}Si NMR resonance for **2** was located at -6.1 ppm, which was up-field shifted relative to the ^{29}Si NMR signal in the Si(II) precursor IPr•$SiCl_2$ (δ = 19.1).[16c] The tin analogue, **3** affords a ^{119}Sn resonance at -350.3 ppm that is in an up-field spectral region compared to the related three-coordinate Sn(II) adduct IPr•$SnCl_2$ (δ = -68.7).[13a] Conclusive structural evidence for the formation of **2** was obtained by single-crystal X-ray crystallographic analysis and the refined structure is shown in Figure 4.1. Repetitive attempts of crystallization to obtain X-ray quality crystals of **3** failed but decisive evidence for its formation was obtained by elemental analysis (C, H, N), NMR and IR spectroscopy.

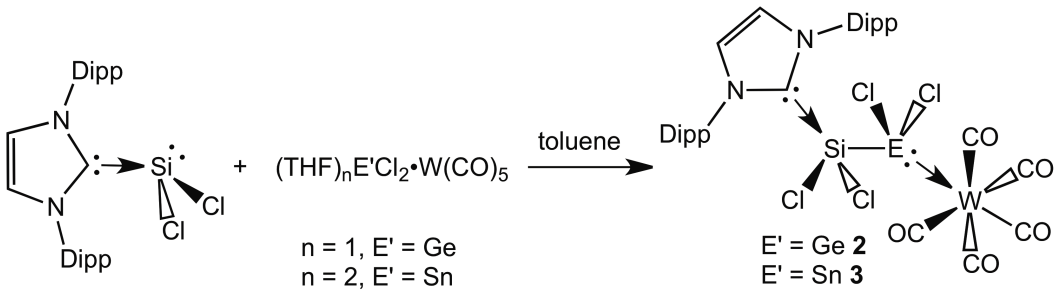

Scheme 4.3 Synthesis of the perhalogenated complexes IPr•Cl_2Si-E'Cl_2•$W(CO)_5$ (E' = Ge and Sn; **2** and **3**).

As shown in the Figure 4.1, IPr•Cl_2Si-$GeCl_2$•$W(CO)_5$ (**2**) contains a coordinated tetrachlorosilagermene Cl_2Si-$GeCl_2$ unit with a transoid C_{IPr}-Si-Ge-W arrangement [torsion angle = 71.84(12)°]. The C_{IPr}-Si bond length in **2** [1.921(3) Å] is shorter than the C_{IPr}-Si dative interactions in IPr•$SiCl_2$ [1.985(4) Å][16c] and in Robinson's chlorosilylene complex IPr•(Cl)Si=Si(Cl)•IPr [1.934(6) Å].[16b] While the observed Si-Ge bond length 2.4348(9) Å is slightly shorter than the Si-Ge

single-bond distance found in $R_2Si(H)$-Ge(OMe)Ar*$_2$ (R = $^tBu_2MeSi$, Ar* = 2,4,6-$(CH_3)_3C_6H_2$) [2.4614(8) Å].[19] The constituent Ge-W bond length in **2** was determined to be 2.5890(4) Å and is comparable to the Ge-W interaction in IPr•$GeCl_2$•$W(CO)_5$ [2.5833(9) Å],[20] thus suggesting the presence of a very similar dative interactions in both species.

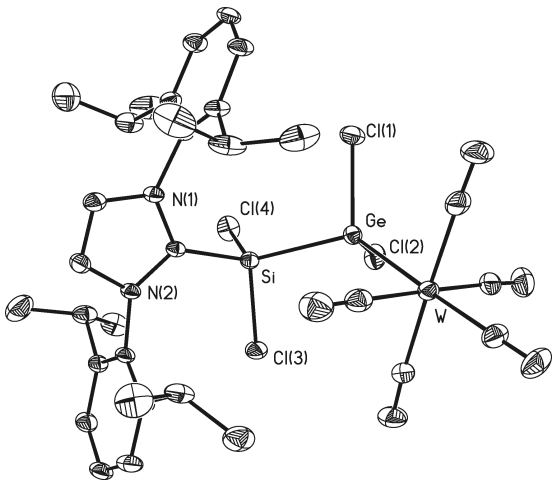

Figure 4.1. Thermal ellipsoid plot (30% probability level) of IPr•Cl_2Si-$GeCl_2$•$W(CO)_5$ (**2**). Carbon-bound hydrogen atoms and THF solvate have been omitted for clarity. Selected bond lengths [Å] and angles [°]: C(6)-Si 1.921(3), Si-Ge 2.4348(9), Si-Cl(3) 2.0409(12), Si-Cl(4) 2.0414(11), Ge-Cl(1) 2.2116(9), Ge-Cl(2) 2.2407(9), Ge-W 2.5890(4), W-C(1) 1.996(4), W-(C(2) to C(5)) 2.036(4) to 2.033(4); C(6)-Si-Ge 127.17(9), Si-Ge-W 127.94(2), Ge-W-C(1) 177.85(12); W-Ge-Si-C(6) torsion angle = 71.84(12).

It has been shown that Li[AlH_4] and Li[BH_4] can be used successfully for the preparation of new main group hydrides, particularly those containing group 14 elements.[13] It was anticipated that the reaction of the perhalogenated complexes IPr•Cl_2Si-E'Cl_2•$W(CO)_5$ (E' = Ge and Sn; **2** and **3**) with Li[AlH_4] or Li[BH_4] would lead to a hydride/chloride metathesis reaction to give the hydride complexes IPr•H_2Si-E'H_2•$W(CO)_5$. When compound **2** was reacted with Li[AlH_4]

the formation of new a product containing hydride functionalities at the Si and Ge centers was observed by ^{1}H NMR spectroscopy (Scheme 4.4). Initial evidence for the formation of the silagermene adduct IPr•H_2Si-GeH_2•$W(CO)_5$ (**4**) was obtained by ^{1}H NMR spectroscopy wherein second-order AA'XX' splitting patterns were observed at 1.90 and 3.73 ppm corresponding to the -GeH_2- and -SiH_2- fragments, respectively (Figure 4.2). These spectroscopic features arise from the magnetic inequivalence of each of the four-hydride substituents in GeH_2 and SiH_2 units. The presence of -SiH_2 functionality was further confirmed by proton coupled ^{29}Si NMR spectrum, which yielded a triplet resonance at δ -71.9 with silicon-hydrogen coupling, $^{1}J_{Si\text{-}H}$ of 192.2 Hz. The IR spectrum of **4** contained absorptions at 2140 and 2150 cm^{-1} representing Si-H stretching vibrations, while a Ge-H stretching band was located at 1959 cm^{-1}. The perdeutero complex IPr•D_2Si-GeD_2•$W(CO)_5$ (**4D**) was prepared using Li[AlD_4] as a deutride source and isotopically shifted Si-D (1549 and 1567 cm^{-1}) and Ge-D (1404 cm^{-1}) IR bands were observed; this study confirmed the initial assignment of the Ge-H vibration in **4** amongst proximal υ(CO) vibrations. Compound **4** was isolated as an air- and moisture-sensitive pale yellow solid in 82% yield and conclusive structural evidence for the formation of the parent hydride adduct **4** was obtained by single-crystal X-ray crystallographic analysis.

As shown in Figure 4.3, IPr•H_2Si-GeH_2•$W(CO)_5$ (**4**) features a coordinated H_2Si-GeH_2 silagermene unit within a canted transoid C_{IPr}-Si-Ge-W array. The corresponding Si-Ge distance in **4** was found to be 2.3717(14) Å and is similar in length as the Si-Ge single bond found in the cyclotrigermane [$Ge(SiMe_3)_2$]$_3$

[2.388(4) Å].[21] The flanking C_{IPr}-Si interaction was determined to be 1.915(5) Å and is the same within the experimental error as the C_{IPr}-Si bond in the perhalogenated starting material IPr•Cl_2Si-$GeCl_2$•$W(CO)_5$ [1.921(3) Å]; however, the C_{IPr}-Si distance in **4** is notably shorter than the carbene-silicon interactions in the silicon(II) dihalide adducts IPr•SiX_2 [X = Cl, 1.985(4) Å and X = Br, 1.989(3) Å].[16c,d] In addition, the observed Ge-W bond distance 2.5890(4) Å in **4** is slightly shorter than the Ge-W distance within the Ge(II) hydride adduct IPr•GeH_2•$W(CO)_5$ [2.6318(2) Å][13b] but significantly longer than the Ge-W bond length of [2.4289(8) Å] in the hydrogermylene complex $Cp^*(CO)_2(H)W=Ge(H)[C(SiMe_3)_3]$,[22a] however, it is in the range typical for Ge-W single bonds [2.50-2.75 Å].[22b]

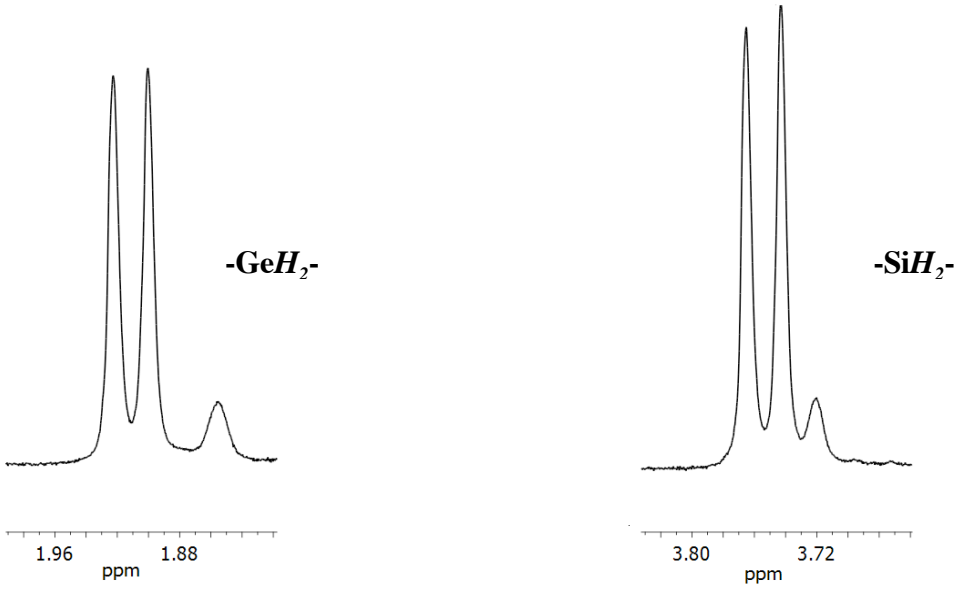

Figure 4.2. Second order AA'XX' splitting pattern for the –GeH_2- and -SiH_2- units in the ^{1}H NMR spectrum of the silagermene adduct IPr•H_2Si-GeH_2•$W(CO)_5$ (**4**).

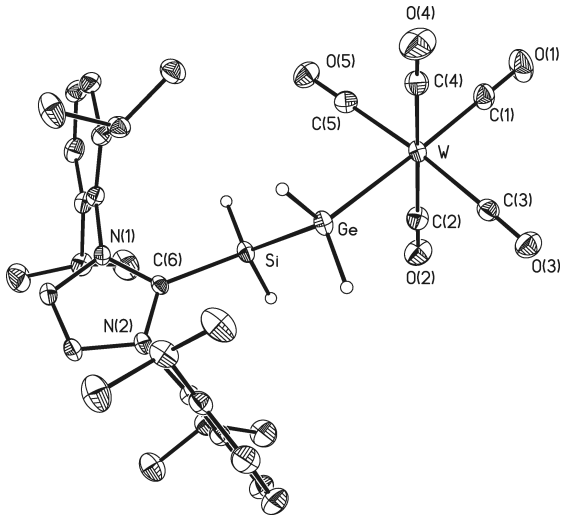

Figure 4.3. Thermal ellipsoid plot of IPr•H_2Si-GeH_2•$W(CO)_5$ (**4**). Ellipsoids set at a 30% probability level; all carbon-bound hydrogen atoms have been omitted for clarity. Selected bond lengths [Å] and angles [°]: C(6)-Si 1.915(5), Si-Ge 2.3717(14), Si-H 1.38(5) and 1.37(5), Ge-H distances fixed to 1.460(4) Å, Ge-W 2.6479(6), W-C(1) 1.996(5), W-(C(2)-C(5)) 2.014(5) to 2.049(6); C(6)-Si-Ge 119.96(13), Si-Ge-W 107.84(4), Ge-W-C(1) 177.26(12); W-Ge-Si-C(6) torsion angle = -164.77(15).

Interestingly, when **2** was reacted with two equivalents of $Li[BH_4]$, formation of the mixed halo/hydride adduct IPr•Cl_2Si-GeH_2•$W(CO)_5$ (**5**) resulted instead of the expected silagermene adduct IPr•H_2Si-GeH_2•$W(CO)_5$ (**4**) (Scheme 4.4). This observation is in line with previous studies wherein the Ge-Cl bonds in IPr•$GeCl_2$ were rapidly reduced by $Li[BH_4]$ to give IPr•GeH_2•BH_3,[13a] while Roesky and coworkers revealed that the Si-Cl groups in IPr•$SiCl_2$ remain largely unchanged in the presence of $Li[BH_4]$.[23] Compound **5** was isolated in a 74% yield as an air- and moisture-sensitive pale yellow solid. The GeH_2 resonance in **5** was located as a singlet at 2.99 ppm in the ^{1}H NMR spectrum and is slightly down-field shifted relative to the resonance belonging to the -GeH_2- group in IPr•H_2Si-GeH_2•$W(CO)_5$ (**4**). A stretching band for the GeH_2 unit in **5** was found at 1969 cm$^-$

[1] in the IR spectrum. Finally, compound **5** was structurally characterized by single-crystal X-ray analysis.

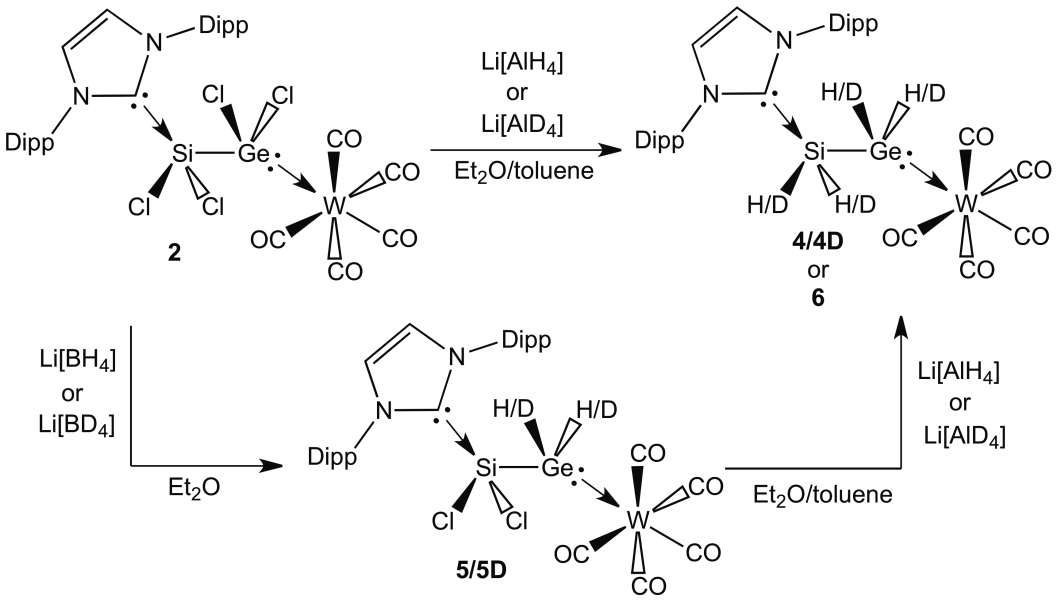

Scheme 4.4. Synthesis of sligermene, IPr•H_2Si-GeH_2•$W(CO)_5$ (**4**), chlorosilagermene IPr•Cl_2Si-GeH_2•$W(CO)_5$ (**5**) and their isotopologues.

As represented in the Figure 4.4, IPr•Cl_2Si-GeH_2•$W(CO)_5$ (**5**) has an overall structure that is analogous to that of the silagermene adduct, **4**. The constituent C_{IPr}-Si bond distance in **5** [1.920(5) Å] is identical within experimental error to the corresponding distance in the silagermene adduct IPr•H_2Si-GeH_2•$W(CO)_5$ (**4**) [1.915(5) Å]. The dative Ge-W interaction in **5** is [2.6208(6) Å] marginally shorter than the Ge-W bond distance of [2.6479(6) Å] in IPr•H_2Si-GeH_2•$W(CO)_5$, thus suggesting the presence of a somewhat stronger Ge-W dative interaction in **5**.

The deuterium analogue of **5** [IPr•Cl_2Si-GeD_2•$W(CO)_5$] (**5D**) was readily prepared from **2** using Li[BD_4], however, further treatment of **5** with the deuteride source Li[AlD_4] generated the novel silagermene isotopomer IPr•D_2Si-GeH_2•$W(CO)_5$ (**6**) in high yield. The formation of **6** was accompanied by discernable H/D exchange at Ge (as judged by ^{1}H and ^{2}H NMR spectroscopy), and the mechanism by which this exchange process occurs is not clearly understood at this time.

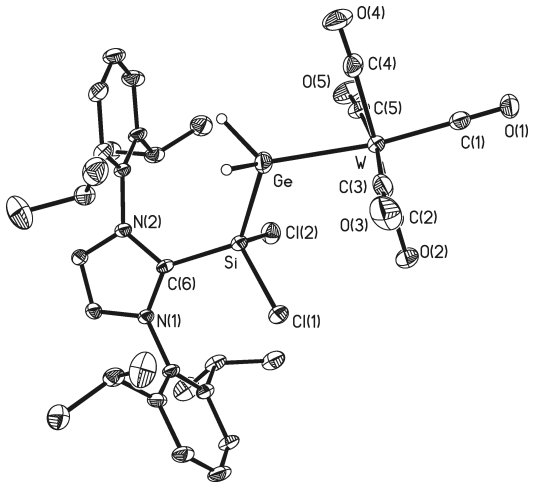

Figure 4.4. Thermal ellipsoid plot (30% probability level) of IPr•Cl_2Si-GeH_2•$W(CO)_5$ (**5**). Carbon-bound hydrogen atoms and Et_2O solvate have been omitted for clarity. Selected bond lengths [Å] and angles [°]: C(6)-Si 1.920(5), Ge-H 1.47(6) and 1.52(6), Si-Cl(1) 2.0537(17), Si-Cl(2) 2.0632(18), Ge-Si 2.3520(14), Ge-W 2.6208(6), W-C(1) 1.974(5), W-C(2-5) 2.017(6) to 2.036(6); C(6)-Si-Ge 125.23(13), Si-Ge-W 110.91(4), Cl(1)-Si-Cl(2)106.24(8), H-Si-H 88(3), Ge-W-C(1) 170.97(14), Ge-W-C(2-5) 80.80(15) to 97.33(13).

Surprisingly, a clean chloride/hydride metathesis reaction occurred when IPr•Cl_2Si-$SnCl_2$•$W(CO)_5$ (**3**) was treated with four equivalents of Li[BH_4]. Instead of the expected mixed halohydride complex [IPr•Cl_2Si-SnH_2•$W(CO)_5$], the

formation of silastannene complex [IPr•H_2Si-SnH_2•$W(CO)_5$] (**7**) (Equation 4.1) was clearly evident by NMR spectroscopy due to the presence of many different NMR active nuclei; this observation suggests that the Si-Cl bonds in **3** are more reactive compared to the silagermane analogue **2**. A second-order (AA'XX') spin system was observed for the SiH_2 and SnH_2 groups in the ^{1}H NMR spectrum of **7** (Figure 4.5), with added flanking satellites resulting from coupling with NMR-active ^{119}Sn and ^{117}Sn nuclei. Moreover, a distinct triplet of triplets pattern was noted in the proton-coupled ^{119}Sn NMR spectrum (δ = -537) of **7** owing to coupling between the ^{119}Sn nuclei and the hydrogen atoms of the SnH_2 ($^1J_{Sn\text{-}H}$ = 1109 Hz) and SiH_2 ($^2J_{Si\text{-}H}$ = 62 Hz) residues. For comparison, the magnitude of $^1J_{Sn\text{-}H}$ coupling in **7** is similar to that observed in the tin(II) hydride adduct [IPr•SnH_2•$W(CO)_5$] ($^1J_{Sn\text{-}H}$ = 1158 Hz ; δ = -309).[13b] The IR spectrum of **7** contained the expected number of υ(CO) vibrations for an L•$W(CO)_5$ coordination environment (L = monodentate ligand),[12c] while a Si-H stretching mode was detected at 2136 cm^{-1}. A Si-H stretching band was detected at 2096 cm^{-1} in the Si(II) hydride adduct IPr•SiH_2•BH_3 and the recently reported silicon(II) hydride complex [PhC(N^{t}Bu)$_2$]Si(H)•BH_3 gave a Si–H vibration at 2107 cm^{-1}.[13d,24] Despite NMR and crystallographic evidence for the presence of a SnH_2 group in **7**, the anticipated Sn–H IR vibrations could not be conclusively identified, which is presumably due to their low oscillator strengths. The isolation of **7** was complicated by the routine formation of the known adduct IPr•$SiCl_2$•BH_3 as a by-product (*ca*. 40%).[23] As a result, the isolation of **7** in pure form necessitated additional recrystallization steps resulting in a substantially reduced yet

reproducible, yield of about 9%.

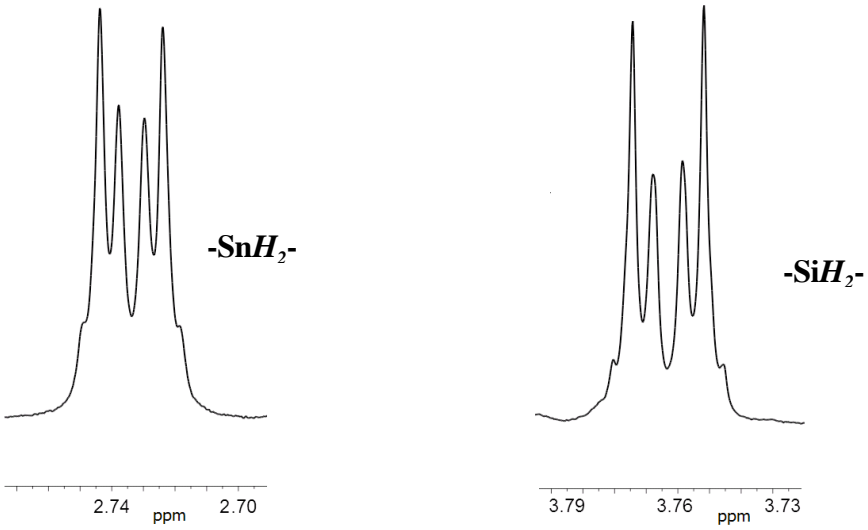

Figure 4.5. Second order AA'XX' splitting pattern for the –SiH_2- and -SnH_2- in the ^{1}H NMR spectrum of the silastannene adduct IPr•H_2Si-GeH_2•W(CO)$_5$ (**7**).

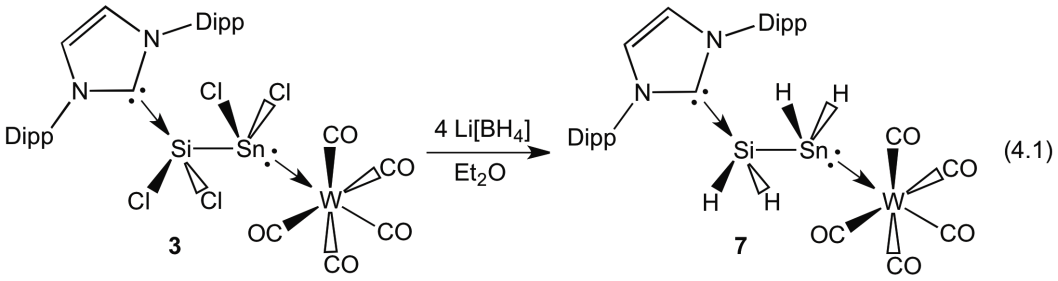

(4.1)

As shown in Figure 4.6 silastannene adduct **7** adopts a nearly isostructural motif as its Si-Ge congener **4**, with a Si-Sn distance of 2.5808(5) Å. This value is consistent with the presence of a Si-Sn single bond in **7**,[25] while the corresponding Si=Sn bond length in (^{t}Bu$_2$MeSi)$_2$Si=SnTrip$_2$ (Trip = 2,4,6-^{i}Pr$_3$C$_6$H$_2$) is as expected considerably shorter [2.4188(14) Å].[26] The adjacent C_{IPr}-Si bond length in **7** [1.9128(17) Å] is comparable to the related bond in **4** [1.915(5) Å] suggesting that a similar formally dative carbene-element interaction is present in each

adduct. The Sn-W linkage in **7** [2.79631(17) Å] is slightly longer than the Sn-W bond in IPr•SnH_2•$W(CO)_5$ [2.7703(9) Å], congruent with the stronger donating ability of IPr relative to the silylene adduct IPr•SiH_2.[13b] Furthermore, the Sn-W distance in **7** is much shorter than the Sn-W distance of 2.9030(8) Å found in Power's Sn(II) complex [(η^5-C_5H_5)$W(CO)_3$-SnAr*] (Ar* = 2,6-^{i}$Pr_2C_6H_3$) and is consistent with an increase in tin-derived s-orbital character within the Sn-W bond in **7**.[27] Of note, in each of the reported $W(CO)_5$ adducts (**4**, **5**, and **7**) quasi octahedral geometries are found about the tungsten centers with nearly colinear E-W-C(1) arrangements (E = Ge and Sn).

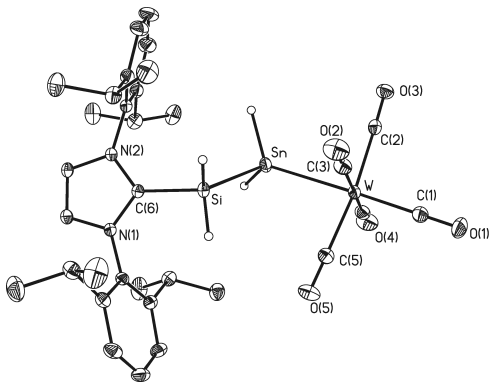

Figure 4.6. Thermal ellipsoid plot of IPr•H_2Si-SnH_2•$W(CO)_5$ (**7**). Ellipsoids set at a 30% probability; all carbon-bound hydrogen atoms have been omitted for clarity. Selected bond lengths [Å] and angles [°]: C(6)-Si 1.9128(17), Si-Sn 2.5808(5), Si-H 1.35(2) and 1.36(2), Sn-H 1.67(2) and 1.65(2), Sn-W 2.79631(17), W-C(1) 1.986(2), W-(C(2)-C(5) 2.0217(19) to 2.0467(18); C(6)-Si-Sn 120.14(5), Si-Sn-W 101.101(11), Sn-W-C(1) 177.82(6); W-Sn-Si-C(6) torsion angle = -164.67(5).

The above mentioned successes in isolating donor-acceptor adducts of hybrid group 14 element ethylenes provided inspiration to study the synthesis of related analogues such as H_2Ge-GeH_2, H_2Ge-SnH_2 and H_2Sn-SnH_2. Following an

established procedure IPr•$GeCl_2$ was reacted with (THF)•$GeCl_2$•$W(CO)_5$ with the goal of forming the perhalogenated complex IPr•Cl_2Ge-$GeCl_2$•$W(CO)_5$. However, instead of obtaining the desired product, only starting materials could be identified by NMR spectroscopy. The inability to construct Ge-Ge linkages is likely due to the diminished nucleophilicity of IPr•$GeCl_2$ compared with IPr•$SiCl_2$. In a similar fashion, the reaction of IPr•ECl_2 (E = Ge and Sn) with $(THF)_2$•$SnCl_2$•$W(CO)_5$ resulted in a clean metathesis reaction to give the known adducts IPr•ECl_2•$W(CO)_5$ (E = Ge and Sn), accompanied by the extrusion of $SnCl_2$ (Equation 4.2). An analogous metathesis reaction was also observed when the tin(II) chloride adduct IPr•$SnCl_2$ was reacted with (THF)•$GeCl_2$•$W(CO)_5$. As the products of the metathesis reactions were IPr•$GeCl_2$•$W(CO)_5$ and $SnCl_2$ (Equation 4.3).

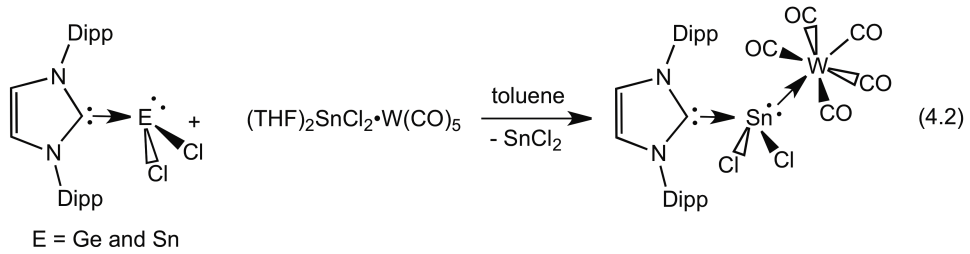

(4.2)

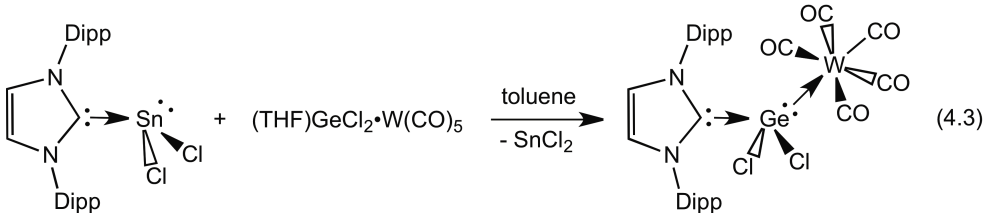

(4.3)

Interestingly, when a mixture of IPr•$GeCl_2$ and (THF)•$GeCl_2$•$W(CO)_5$ were reacted with four equivalents of Li[BH_4], the formation of a mixture containing the new compound IPr•H_2Ge-GeH_2•$W(CO)_5$ (**8**) (*ca*. 20%, *vide infra*) was observed along with the known compounds IPr•GeH_2•BH_3[13a] (*ca*. 40%) and IPr•GeH_2•$W(CO)_5$[13b] (*ca*. 40%) as shown in Equation 4.4. The digermene adduct, IPr•H_2Ge-GeH_2•$W(CO)_5$ (**8**) was isolated in pure form as pale yellow crystals (20% yield) by cooling a saturated Et_2O/hexanes solution of the crude product mixture to -35 °C. Initial evidence for the formation of IPr•H_2Ge-GeH_2•$W(CO)_5$ (**8**) was obtained by ^{1}H NMR spectroscopy where second-order AA'XX' splitting patterns were observed at 3.05 and 4.08 ppm corresponding to two chemically distinct GeH_2 environments (Figure 4.7). As discussed earlier, these splitting patterns arise from the presence of magnetically inequivalent hydrides in GeH_2 moieties. Two Ge-H stretching bands were located at 1961 cm^{-1} and 1954 cm^{-1} in the IR spectrum of **8**; for comparison a Ge-H vibration was found at 1981 cm^{-1} in the Ge(II) hydride adduct IPr•GeH_2•$W(CO)_5$.[13b] The formation of the digermene adduct IPr•H_2Ge-GeH_2•$W(CO)_5$ (**8**) was also confirmed by elemental analysis (C, H, N). Crystals suitable for X-ray single crystal analysis were obtained by cooling a saturated solution Et_2O solution of **8**, unfortunately each time the obtained crystal contained a minor chloride impurity.

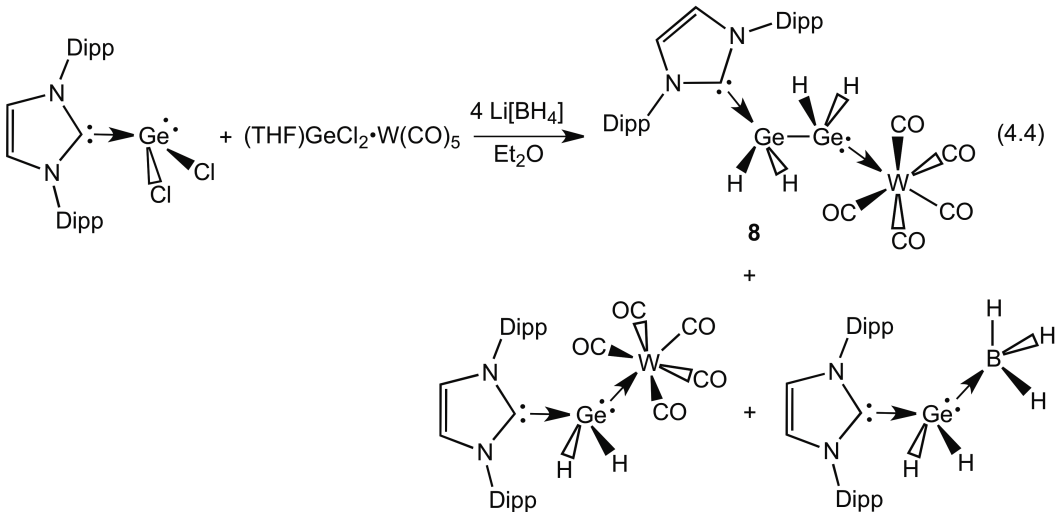

(4.4)

The perdeutero complex IPr•D_2Ge-GeD_2•W(CO)$_5$ (**8D**) was also synthesized using a deutride/chloride metathesis reaction where Li[BD_4] was used as a deutride source. Isotopically shifted Ge-D IR bands were located at 1405 cm^{-1} and 1407 cm^{-1} and thus supporting the initial assignment of the Ge-H stretching bands at 1961 cm^{-1} and 1954 cm^{-1} in **8**.

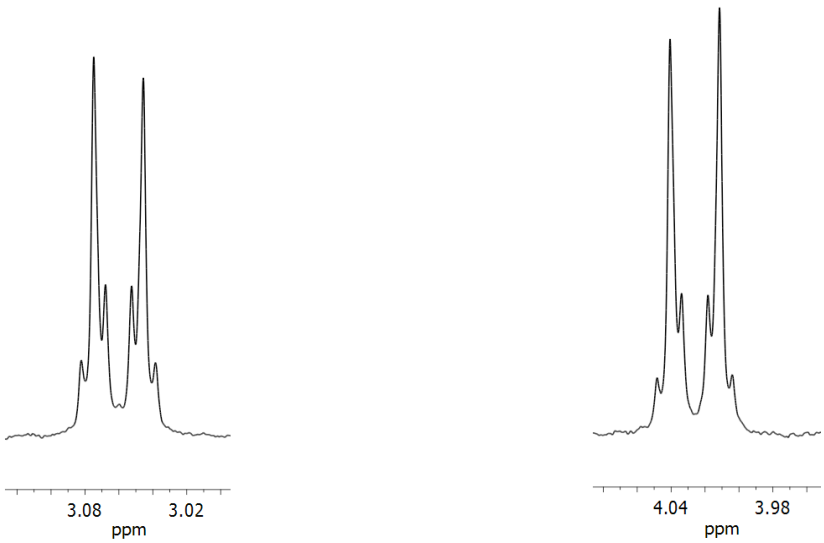

Figure 4.7. Second order AA'XX' splitting pattern for the -GeH_2- units in the ^{1}H NMR spectrum of the digermene adduct IPr•H_2Ge-GeH_2•W(CO)$_5$ (**8**).

Recently, the Rivard group has shown that the N-heterocyclic olefin IPr=CH_2 can be used as a donor in low coordinate Group 14 hydride complexes IPrCH_2•EH_2•$W(CO)_5$ (E = Ge and Sn).[13c] It has been found that N-heterocyclic olefin IPr=CH_2 is a weaker σ-donor compared to N-heterocyclic carbene IPr (see Chapter 3). Thus it was hypothesized that in the presence of IPr=CH_2 as a σ-donating ligand IPrCH_2•H_2E-E'H_2•$W(CO)_5$ (E = Ge and E' = Ge and Sn) complexes will be more reactive compared to their carbene analogues. To investigate the role of IPr=CH_2 as a σ-donating ligand for the stabilization of H_2E-EH_2 moieties, the synthesis of N-heterocyclic olefin complexes IPrCH_2•H_2E-E'H_2•$W(CO)_5$ (E = Ge and E' = Ge and Sn) was explored. Using a similar strategy as discussed earlier in this Chapter, the halogenated complex IPrCH_2•Cl_2Ge-$GeCl_2$•$W(CO)_5$ (**9**) was prepared by reacting the nucleophilic Ge(II) chloride IPrCH_2•$GeCl_2$ (see Chapter 3 for experimental details) with (THF)•$GeCl_2$•$W(CO)_5$ (Equation 4.5). Compound **9** was isolated as an air- and moisture-sensitive yellow solid and its composition was confirmed by elemental analysis (C, H, N), NMR and IR spectroscopy, and single-crystal X-ray crystallography (Figure 4.8).

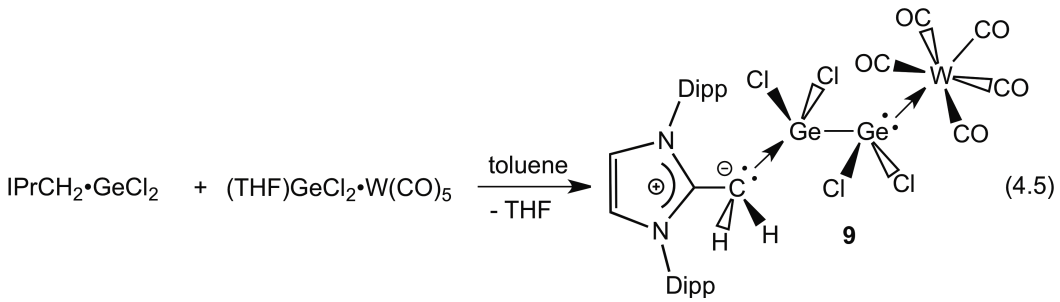

As shown in the Figure 4.8, compound **9** has an overall arrangement that is very similar to that adopted by the perhalogenated complex IPr•Cl_2Si-

$GeCl_2$•$W(CO)_5$ (**2**). The constituent C_{IPrCH2}-Ge and Ge-W bond lengths were determined to be 1.9815(8) Å (*avg*.) and 2.5451(10) Å (*avg*.) respectively, and are slightly shorter than the C_{IPrCH2}-Ge [2.056(3) Å] and Ge-W [2.5803(3) Å] bonds in $IPrCH_2$•$GeCl_2$•$W(CO)_5$. The proximal C_{IPrCH2}-C(7) bond length [1.4635(8) Å (*avg*.)] in **9** lies within the expected range for a C-C single bond and is identical within experimental error to the corresponding distance in the Ge(II) adduct $IPrCH_2$•$GeCl_2$•$W(CO)_5$ [1.463(4) Å]. In addition, the Ge(1)-Ge(2) separation [2.4478(14) Å (*avg*.)] in **9** is within the bond-length range of Ge-Ge single-bonds [2.40-2.50 Å];[30] for example, the Ge-Ge single bond length in elemental germanium has been reported to be 2.44 Å.[31] The Ge-Ge bond distance in **9** is significantly shorter than the Ge-Ge bond distance [2.7093(7) Å] found in digermylene [Ar*(Me_3Si)N]GeGe[N($SiMe_3$)Ar*] (Ar* = 2,6-$(Ph_2CH)_2$-4-Me-C_6H_2) synthesized by Jones and coworkers where considerable p character is present in the Ge-Ge σ-bond.[32]

The target tetrahydrodigermene adduct $IPrCH_2$•H_2Ge-GeH_2•$W(CO)_5$ (**10**) was prepared by reacting the halogenated complex **9** with four equivalents of $Li[BH_4]$ in Et_2O (Equation 4.6). Interestingly, there was no sign of the expected second-order splitting patterns due to the H_2Ge-GeH_2 unit by ^1H NMR spectroscopy; instead, well-resolved triplet resonances were detected for both the CH_2 and terminal GeH_2 fragments at 2.29 and 3.23 ppm, respectively ($^3J_{H\text{-}H}$ = 4.0 Hz). A pentet resonance was also located at 3.97 ppm corresponding to the central -GeH_2- unit ($^3J_{HH}$ = 4.0 Hz). Only one Ge-H stretching band was present in the IR spectrum of **10** (2028 cm^{-1}) and the other stretching band could not be detected

due to presence of strong carbonyl vibrations in the proximity.

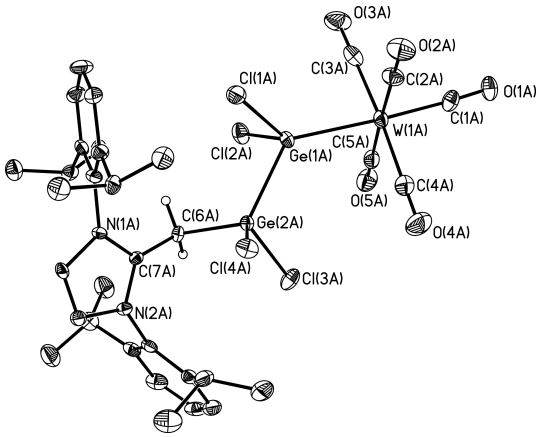

Figure 4.8. Thermal ellipsoid plot (30% probability level) of $IPrCH_2•Cl_2Ge$-$GeCl_2•W(CO)_5$ (**9**). Carbon-bound hydrogen atoms have been omitted for clarity. Only one molecule in the asymmetric unit is presented with metrical parameters for the second molecule listed in square brackets. Selected bond lengths [Å] and angles [°]: C(6)-C(7) 1.465(8) [1.462(8)], C(6)-Ge(2) 1.991(6) [1.972(6)], Ge(1)-Ge(2) 2.4486(10) [2.4469(10)], Ge(2)-Cl(3) 2.1562(17) [2.1601(18)], Ge(2)-Cl(4) 2.1653(19) [2.1715(19)], Ge(1)-Cl(1) 2.2274(19) [2.2274(19)], Ge(1)-Cl(2) 2.2412(19) [2.2339(18)], Ge(1)-W 2.5551(7) [2.5393(7)], W-C(1) 1.988(8) [1.996(9)], W-(C(2) to C(5)) 2.024(8) to 2.051(9) [2.035(8) to 2.048(9)]; C(6)-Ge(2)-Ge(1) 118.02(18) [113.93(18)], Ge(2)-Ge(1)-W 128.45(3) [126.88(3)], Ge(1)-W-C(1) 174.6(2) [178.1(2)]; W-Ge(1)-Ge(2)-C(6) torsion angle = -150.25(19) [-162.8(2)].

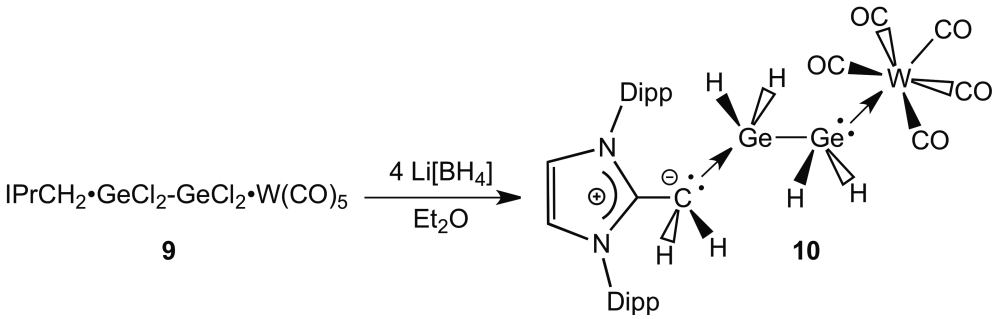

(4.6)

A complete structural picture of **10** was obtained by single-crystal X-ray crystallography and the refined structure is shown in Figure 4.9. $IPrCH_2•H_2Ge$-$GeH_2•W(CO)_5$ (**10**) features a central H_2Ge-GeH_2 fragment that is bound by electron donating $IPrCH_2$ and electron accepting $W(CO)_5$ units. The C_{IPrCH2}-Ge

bond distance in **10** [2.013(3) Å] is marginally shorter than the related C_{IPrCH2}-Ge bond length in the germanium dihydride adduct $IPrCH_2•GeH_2•W(CO)_5$ [2.057(2) Å][13c] but longer than the Ge-C distance in [{Mo(μ-η^2-H-$GeEt_2$)$(CO)_4$}$_2$] [1.969(2) Å].[33] The Ge(1)-Ge(2) bond length 2.4098(5) Å is, as expected, shorter than the Ge=Ge double distance in IPr•Ge=Ge•IPr [2.3490(8) Å][17a] and comparable with the Ge-Ge single bond length of 2.395(2) Å found in Li_2[Ar'(H)Ge-Ge(H)Ar'] (Ar' = C_6H_2-2,6-(C_6H_3-2,6-^{i}Pr$_2$)$_2$).[34] The dative Ge(1)-W bond length in **10** was determined to be 2.6295(4) Å and is slightly shorter than the Ge-W interaction in $IPrCH_2•GeH_2•W(CO)_5$ [2.6503(3) Å][13c] but longer than the Ge-W bond distance found in the heterocyclic Ge(II) adduct [PhN(Me)CHC(Me)NPh](Cl)Ge•$W(CO)_5$ [2.571(7) Å].[35]

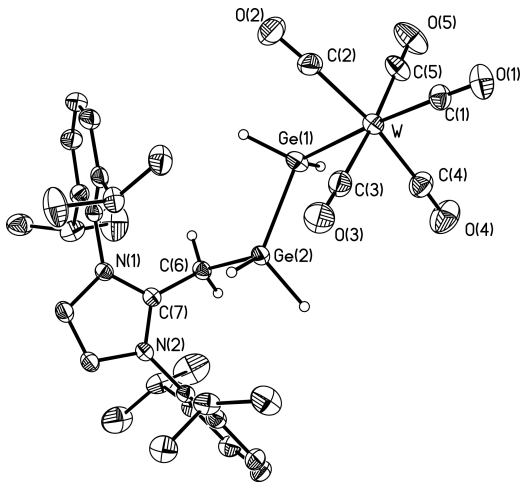

Figure 4.9. Thermal ellipsoid plot (30% probability level) of $IPrCH_2•H_2Ge$-$GeH_2•W(CO)_5$ (**10**). Carbon-bound hydrogen atoms have been omitted for clarity. Selected bond lengths [Å] and angles [°]: C(6)-C(7) 1.462(4), C(6)-Ge(2) 2.013(3), Ge(1)-H(1) 1.63(3), Ge(1)-H(2) 1.48(4), Ge(2)-H(3) 1.60(4), Ge(2)-H(4) 1.50(4), Ge(1)-Ge(2) 2.4098(5), Ge(1)-W 2.6295(4), W-C(1) 1.992(4), W-(C(2)-C(5)) 2.035(4) to 2.014(4); C(6)-Ge(2)-Ge(1) 111.10(9), Ge(2)-Ge(1)-W 114.706(17), H(1)-Ge(1)-H(2) 98.2(18), H(3)-Ge(2)-H(4) 97(2), Ge(1)-W-C(1) 176.36(10), Ge-W-(C(2)-C(5)) 86.64(11) to 87.12(11); W-Ge(1)-Ge(2)-C(6) torsion angle = 172.81(9).

The deutero isotopologue of **10** $IPrCH_2 \bullet D_2Ge\text{-}GeD_2 \bullet W(CO)_5$ (**10D**) was also prepared by reacting **9** with excess $Li[BD_4]$ in Et_2O. Unfortunately, the Ge-D stretching band could not be identified due to the presence of aromatic C=C vibrations which occur in the expected region of the IR spectrum.

The silagermene $IPr \bullet H_2Si\text{-}GeH_2 \bullet W(CO)_5$ (**4**) exhibits considerable thermal stability in the solid state ($T_{dec} \approx 135$ °C), and is stable for extended periods of time in refluxing toluene. The silastannene complex $IPr \bullet H_2Si\text{-}SnH_2 \bullet W(CO)_5$ (**7**) however, is significantly less stable, with decomposition in Et_2O solvent occurring even at -30 °C to give the known adduct $[IPr \bullet SnH_2 \bullet W(CO)_5]$[12b] and unidentified insoluble byproduct(s). Although the digermene adduct $IPr \bullet H_2Ge\text{-}GeH_2 \bullet W(CO)_5$ is quite stable at -30 °C over extended periods of time in the solid state but decomposition is observed within 24 hours in C_6D_6 at room temperature to generate the Ge(II) hydride adduct $IPr \bullet GeH_2 \bullet W(CO)_5$ with some unidentified insoluble yellow byproduct(s). The fate of the eliminated GeH_2 is not clear yet, however, it is possible that this unstable species presumably participates in further decomposition chemistry to give germanium metal/clusters with the liberation of H_2 gas.[36] Surprisingly, $IPrCH_2 \bullet H_2Ge\text{-}GeH_2 \bullet W(CO)_5$ (**10**) shows improved thermal stability compared to the corresponding IPr adduct (**8**) as heating to 60 °C in toluene is required to decompose **10** to give $IPr \bullet GeH_2 \bullet W(CO)_5$ as a soluble product. The origin of the enhanced thermal stability of **10** relative to **8** is not known at this time.

When $IPrCH_2•H_2Ge\text{-}GeH_2•W(CO)_5$ (**10**) was reacted with one equivalent of IPr, the clean formation of $IPr•GeH_2•W(CO)_5$ and free $IPrCH_2$ was observed, suggesting the formal loss of a GeH_2 unit according to Equation 4.7. Attempts to trap the liberated GeH_2 unit using either 2,3-dimethyl-1,3-butadiene or cyclohexene failed, and each time $IPr•GeH_2•W(CO)_5$, $IPr{=}CH_2$, unreacted 2,3-dimethy-1,3-butadiene or cyclohexene was present.

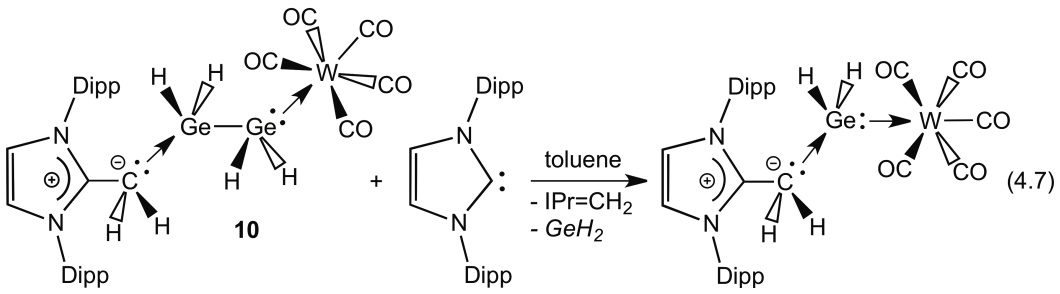

(4.7)

Attempts to induce H_2 elimination from the silagermene complex $IPr•H_2Si\text{-}GeH_2•W(CO)_5$ (**4**) and to generate the novel dimetallyne adduct $IPr•HSi{=}GeH•W(CO)_5$ by photolysis led only to the recovery of unreacted **4**. Furthermore, no reactivity was observed between **4** and either HC≡CPh or C≡NXyl (Xyl = 2,6-$Me_2C_6H_4$). Yet in the presence of acetylacetone, compound **4** underwent a clean hydrosilylation reaction to yield the novel anionic adduct $[\{MeC(O)H\text{-}CH{=}C(Me)O\}SiH\text{-}GeH_2•W(CO)_5]^-$ (**11**) as a salt with the known imidiazolium countercation $[IPrH]^+$ (Equation 4.8). The formation of hydrosilylation product **11** was evident from ^1H NMR spectrum where a second order resonance pattern was observed at 2.40 ppm corresponding to the -GeH_2- unit, while a triplet resonance was observed for the silicon bound proton at 5.67 ppm. The imidiazolium proton in the $[IPrH]^+$ counter cation gave a triplet

resonance at δ 9.60 due to the coupling with the olefinic protons of the N-heterocyclic backbone ($^4J_{HH}$ = 1.6 Hz). Although the proton coupled ^{29}Si experiment was unsuccessful, a resonance was observed at 3.9 ppm in the ^{29}Si{^{1}H} spectrum, representing a new Si environment compared to the starting material **4**. For comparison, the ^{29}Si NMR spectrum of **4** yielded a triplet resonance at δ -71.9.

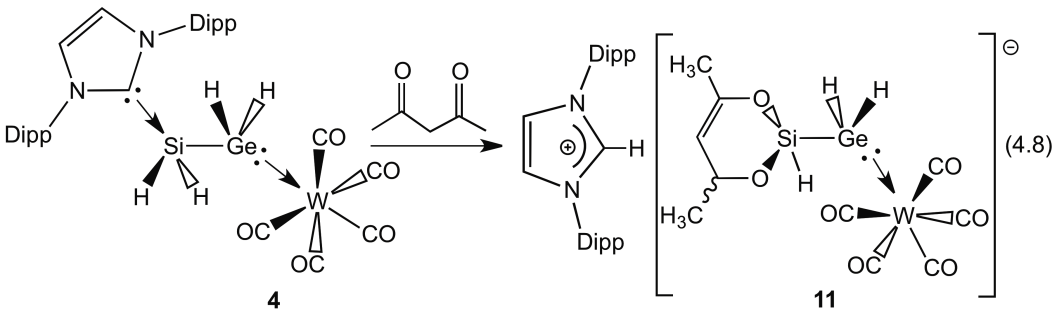

The NMR spectra of **11** corroborated the X-ray crystallographic data shown in Figure 4.10. The constituent Si-O bond lengths (*avg*. 2.643(3) Å) in **11** are marginally shorter than the Si-O distances observed in Roesky's $L_2Si_2O_2$ heterocycle (L = PhC(N^{t}Bu)$_2$) [1.60865(15) Å (*avg*.)].[37] The Si-Ge and Ge-W bond distances in **11** are 2.3620(12) and 2.6464(6) Å, respectively, and comparable with the similar interactions observed in silagermene adduct IPr•H_2Si-GeH_2•$W(CO)_5$ (**4**) [2.3717(14) and 2.6479(6) Å, respectively]; however, a wider Si-Ge-W bond angle [118.43(3)°] is observed in **11** compared to in the silagermene complex **4** [107.84(4)°].

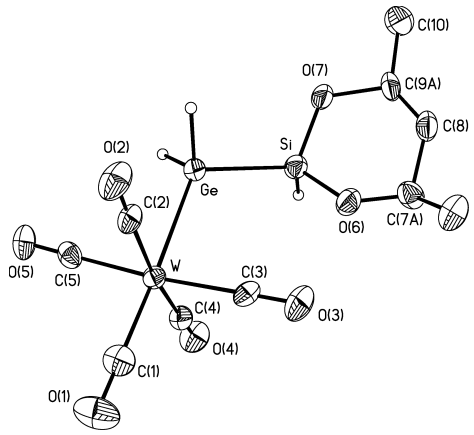

Figure 4.10. Thermal ellipsoid plot of $[IPrH]^+[\{MeC(O)H\text{-}CH{=}C(Me)O\}SiH\text{-}GeH_2{\bullet}W(CO)_5]^-$ (**11**). Ellipsoids set at 30% probability level; carbon-bound hydrogen atoms, Et_2O solvate and $[IPrH]^+$ have omitted for clarity; one view of the disordered silicon heterocycle is shown. Selected bond lengths [Å] and angles [°]: Si-Ge 2.3620(12), Si-H 1.33(4), Ge-H 1.44(4) and 1.47(4), Ge-W 2.6464(6), Si–O(6) 1.641(3), Si–O(7) 1.645(3), O(6)-C(7) 1.346(13) [1.484(13)], O(7)-C(9) 1.522(12) [1.344(13)], W-C(1) 1.948(6), W-(C(2)–C(5)) 2.012(5) to 2.045(5); O(6)-Si-O(7) 104.54(17), Si-Ge-W 118.43(3), Ge-W-C(1) 177.27(15).

As indicated by the formation of $[IPrH]^+$ the hydrosilylation reaction (Equation 4.8) involves the deprotonation of the acetylacetone group by the basic carbene IPr.[38] The fate of the activated Si-H and backbone C-H groups was confirmed by repeating the same reaction with the isotopomer $IPr{\bullet}D_2Si\text{-}GeD_2{\bullet}W(CO)_5$ (**4D**) whereby deuteride migration from the $-SiD_2-$ unit to the ketonic carbon of acetylacetonate was observed. This transformation suggests that the C_{IPr}-Si interaction in **4** is sufficiently labile to allow productive hydrosilylation chemistry to transpire while illustrating the stable nature of the Si-Ge linkage. The presence of strong Si-Ge bonding in **4** should facilitate the future synthesis of new SiGe hybrid nanomaterials by the decomplexation/dehydrogenation of the $H_2Si\text{-}GeH_2$ unit in **4**.[8]

4.4 Conclusion

In summary, the first stable complexes of the parent inorganic ethylenes $H_2EE'H_2$ (E = Si and Ge; E' = Ge and Sn) have been synthesized using a donor-acceptor stabilization protocol that engages N-heterocyclic carbene (IPr) or N-heterocyclic olefin (IPr=CH_2) donors in tandem with $W(CO)_5$ as an acceptor. The ability to generate these novel Group 14 element hydrides using readily available techniques should encourage the widespread study of these once elusive species, and thus opening an entirely new avenues of chemical exploration with potential applications in both the realms of molecular and materials chemistry.

4.5 Experimental Section

4.5.1 Materials and Instrumentation

All reactions were performed using standard Schlenk line techniques under an atmosphere of nitrogen or in an inert atmosphere glove box (Innovative Technology, Inc.). Solvents were dried using Grubbs-type solvent purification system[39] manufactured by Innovative Technology, Inc., degassed (freeze-pump-thaw method) and stored under an atmosphere of nitrogen prior to use. $SnCl_2$, $Li[BH_4]$, $Li[BD_4]$, $Li[AlH_4]$, $Li[AlD_4]$ and $GeCl_2$•dioxane were purchased from Aldrich and used as received. $W(CO)_6$ was obtained from Aldrich and sublimed under vacuum and stored under nitrogen prior to use. 2,4-Pentanedione was obtained from Aldrich and dried over molecular sieves (4 Å) prior to use. 1,3-Bis-(2,6-diisopropylphenyl)-imidazol-2-ylidene (IPr),[40] 1,3-bis-(2,6-diisopropylphenyl)-2methyleneimidazoline (IPr=CH_2),[13c] IPr•$GeCl_2$,[13a] IPr•$SiCl_2$,[16c] $(THF)_2SnCl_2$•$W(CO)_5$[18b] and $(THF)GeCl_2$•$W(CO)_5$[18a] were prepared following literature procedures. ^1H, $^2H\{^1H\}$, $^{13}C\{^1H\}$, ^{29}Si and ^{119}Sn NMR spectra were recorded on a Varian iNova-400 spectrometer and referenced externally to $SiMe_4$ (^1H, $^{13}C\{^1H\}$ and ^{29}Si), $Si(CD_3)_4$ ($^2H\{^1H\}$) and $SnMe_4$ (^{119}Sn), respectively, by setting the resonance for residual H, D, C, Si, B and Sn at 0.0 ppm. X-ray crystallographic analyses were performed by the X-ray Crystallography Laboratory at the University of Alberta. Elemental analyses were performed by the Analytical and Instrumentation Laboratory at the University of Alberta. Infrared spectra were recorded Nicolet IR100 FTIR spectrometer as a Nujol mulls

between NaCl plates. Melting points were measured in sealed glass capillaries under nitrogen using a MelTemp melting point apparatus and are uncorrected.

4.5.2 X-ray Crystallography

Crystals of suitable quality for X-ray diffraction studies were removed from a vial in a glove box and immediately covered with a thin layer of hydrocarbon oil (Paratone-N). A suitable crystal was then selected, mounted on a glass fiber and quickly placed in a low temperature stream of nitrogen on an X-ray diffractometer.[41] All data were collected using a Bruker APEX II CCD detector/D8 diffractometer using Mo Kα radiation with the crystals cooled to -100 °C. The data were corrected for absorption through Gaussian integration from the indexing of the crystal faces.[42] Structures were solved using the direct methods program SHELXS-97[43] (compounds **4**, **7** and **9**) or using the Patterson search/structure expansion facilities within the DIRDIF-2008[44] program suite (compounds **2**, **5**, **10** and **11**); structure refinement was accomplished using SHELXL-97.[43] Hydrogen atoms were assigned positions based on the sp^2 or sp^3 hybridization geometries of their attached carbon atoms, and were given thermal parameters 20% greater than those of their parent atoms. See Tables 1-3 for a listing of the crystallographic data.

4.5.3 Synthetic Procedures.

4.5.3.1 Synthesis of (THF)$GeCl_2$•$W(CO)_5$ 1. To a mixture of $GeCl_2$•dioxane (161 mg, 0.693 mmol) and $(THF)_2SnCl_2$•$W(CO)_5$ (450 mg, 0.693 mmol) was added 6 mL of toluene. The reaction mixture was stirred for 3 h at room

temperature to obtain a pale yellow solution over white precipitate ($SnCl_2$). The precipitate was then removed by filtration through Celite and removal of the volatiles from the filtrate afforded **1** as a pale yellow crystalline solid (361 mg, 97%). ^{1}H NMR (C_6D_6): δ 1.12 (m, 4H, C_4H_8O, THF), 3.59 (m, 4H, C_4H_8O, THF). $^{13}C\{^1H\}$ NMR (C_6D_6): δ 24.7 (C_4H_8O, THF), 72.4 (C_4H_8O, THF), 195.5 (equat. *CO*, $^1J_{W\text{-}C}$ = 124.9 Hz), 198.3 (ax. *CO)*. Anal. Calcd. for $C_{10}H_{11}Cl_2GeO_6W$: C, 21.66; H, 2.00. Found: C, 20.20; H, 1.51.

4.5.3.2 Synthesis of IPr•$SiCl_2$•$GeCl_2$•$W(CO)_5$ 2. To a mixture of IPr•$SiCl_2$ (125 mg, 0.256 mmol) and (THF)$GeCl_2$•$W(CO)_5$ (138 mg, 0.256 mmol) was added 6 mL of toluene. The reaction mixture was then stirred for 3 min at room temperature to give a orange solution over yellow precipitate. The precipitate was isolated by filtration and dried under vacuum to give **2** as pale yellow powder (213 mg, 87%). Crystals suitable for X-ray crystallography (pale yellow needles) were grown by cooling a saturated THF solution of **2** solution to -35 °C. ^{1}H NMR ([D_8]-THF): δ 1.17 (d, $^3J_{HH}$ = 6.6 Hz, 12H, CH(CH_3)$_2$), 1.44 (d, $^3J_{HH}$ = 6.6 Hz, 12H, CH(CH_3)$_2$), 2.69 (septet, $^3J_{HH}$ = 6.6 Hz, 4H, CH(CH$_3$)$_2$), 7.45 (d, $^3J_{HH}$ = 7.8 Hz, 4H, Ar*H*), 7.59 (t, $^3J_{HH}$ = 7.8 Hz, 2H, Ar*H*), 8.24 (s, 2H, N-C*H*-). $^{13}C\{^1H\}$ NMR ([D_8]-THF): δ 23.0 (CH(*C*H$_3$)$_2$), 25.9 (CH(*C*H$_3$)$_2$), 30.1 (*C*H(CH$_3$)$_2$), 125.8 (-N-*C*H-), 131.3 (Ar*C*), 133.1 (Ar*C*), 133.9 (Ar*C*), 146.4 (Ar*C*), 147.9 (N-*C*-N), 198.6 (equat. *CO*, $^1J_{W\text{-}C}$ = 125 Hz), 202.6 (ax. *CO)*. $^{29}Si\{^1H\}$ NMR ([D_8]-THF): δ -6.1. IR (Nujol/cm^{-1}): 1909 (br, υCO), 1931 (br, υCO), 1975 (sh, υCO), 2063 (s, υCO). Anal. Calcd. for $C_{32}H_{36}Cl_4GeN_2O_5SiW$: C, 40.24; H, 3.80; N, 2.93. Found: C, 40.30; H, 3.95; N, 2.96. Mp (°C): *ca*. 160 (dec., turns black), 176-178 (melts).

4.5.3.3 Synthesis of IPr•$SiCl_2$•$SnCl_2$•$W(CO)_5$ 3. To a mixture of IPr•$SiCl_2$ (137 mg, 0.281 mmol) and $(THF)_2SnCl_2$•$W(CO)_5$ (183 mg, 0.281 mmol) was added 7 mL of toluene, and the mixture was stirred for 5 min at room temperature to give an orange solution over yellow precipitate. The precipitate was isolated by filtration and dried under vacuum to give **3** as a pale yellow powder (273 mg, 97%). ^{1}H NMR (C_6D_6): δ 0.81 (d, $^3J_{HH}$ = 7.0 Hz, 12H, CH(CH_3)$_2$), 1.35 (d, $^3J_{HH}$ = 7.0 Hz, 12H, CH(CH_3)$_2$), 2.51 (septet, $^3J_{HH}$ = 7.0 Hz, 4H, CH(CH$_3$)$_2$), 6.27 (s, 2H, N-CH-), 6.99 (d, $^3J_{HH}$ = 8.0 Hz, 4H, ArH), 7.14 (t, $^3J_{HH}$ = 8.0 Hz, 2H, ArH). ^{13}C{^{1}H} NMR (C_6D_6): δ 23.0 (CH(*C*H$_3$)$_2$), 25.8 (CH(*C*H$_3$)$_2$), 29.5 (*C*H(CH$_3$)$_2$), 125.2 (-N-*C*H-), 129.2 (Ar*C*), 132.2 (Ar*C*), 132.7 (Ar*C*), 145.1 (Ar*C*), 150.7 (N-*C*-N), 197.9 (equat. *CO),* 200.7 (ax. *CO)*. ^{119}Sn{^{1}H} NMR (C_6D_6): δ -350.3. IR (Nujol/cm^{-1}): 1902 (br, υCO), 1980 (s, υCO), 2063 (s, υCO). Anal. Calcd. for $C_{32}H_{36}Cl_4N_2O_5SiSnW$: C, 38.39; H, 3.62; N, 2.80. Found: C, 38.22; H, 3.50; N, 2.85. Mp (°C): *ca*. 130 (dec., turns black), 146-148 (melts).

4.5.3.4 Synthesis of IPr•SiH_2•GeH_2•$W(CO)_5$ 4. To a mixture of **2** (85 mg, 0.090 mmol) and Li[AlH_4] (4.9 mg, 0.13 mmol) was added 8 mL of toluene. The reaction mixture was stirred for 10 min at room temperature to give a pale yellow slurry to which was added 2 mL of Et_2O. The reaction mixture was then stirred for 5 min resulting in a clear yellow solution. Filtration of the solution through Celite followed by the removal of the volatiles afforded **4** as a pale yellow powder (58 mg, 82%). Crystals suitable for X-ray crystallography (colorless blocks) were grown by cooling a saturated Et_2O solution of **4** layered with hexanes to -35 °C for 7 days. ^{1}H NMR ([D_8]-THF): δ 1.20 (d, $^3J_{HH}$ = 6.8 Hz, 12H, CH(CH_3)$_2$), 1.37

(d, $^3J_{HH}$ = 6.8 Hz, 12H, CH(CH_3)$_2$), 1.90 (m, second order AA'XX' pattern, 2H, -GeH_2-), 2.49 (septet, $^3J_{HH}$ = 6.8 Hz, 4H, CH(CH$_3$)$_2$), 3.73 (m, second order AA'XX' pattern, 2H, -SiH_2-), 7.46 (d, $^3J_{HH}$ = 8.0 Hz, 4H, ArH), 7.62 (t, $^3J_{HH}$ = 8.0 Hz, 2H, ArH), 8.18 (s, 2H, N-CH-). ^{1}H NMR (C_6D_6): δ 0.85 (d, $^3J_{HH}$ = 6.8 Hz, 12H, CH(CH_3)$_2$), 1.22 (d, $^3J_{HH}$ = 6.8 Hz, 12H, CH(CH_3)$_2$), 2.30 (septet, $^3J_{HH}$ = 6.8 Hz, 4H, CH(CH_3)$_2$), 2.45 (m, second order AA'XX' pattern, 2H, -GeH_2-), 3.95 (m, second order AA'XX' pattern, 2H, -SiH_2-), 6.32 (s, 2H, N-CH-), 6.95 (d, $^3J_{HH}$ = 7.8 Hz, 4H, ArH), 7.13 (t, $^3J_{HH}$ = 7.8 Hz, 2H, ArH). ^{13}C{^{1}H} NMR ([D_8]-THF): δ 22.9 (CH(*C*H$_3$)$_2$), 25.6 (CH(*C*H$_3$)$_2$), 29.9 (*C*H(CH$_3$)$_2$), 125.5 (-N-*C*H-), 128.4 (Ar*C*), 132.5 (Ar*C*), 145.7 (Ar*C*), 157.9 (N-*C*-N), 202.2 (equat. *CO),* 205.1 (ax. *CO).* ^{29}Si{^{1}H} NMR (gHSQC, [D8]-THF): δ -71 (s). ^{29}Si NMR ([D_8]-THF): δ -71.9 (t, $^1J_{Si-H}$ = 192.2 Hz). IR (Nujol/cm^{-1}): 1882 (br, υCO), 1943 (sh, υCO), 1959 (w, υGe-H), 2044 (s, υCO), 2140 (sh, υSi-H) and 2150 (m, υSi- H). Anal. Calcd. for $C_{32}H_{40}GeN_2O_5SiW$: C, 47.03; H, 4.93; N, 3.43. Found: C, 46.88; H, 3.94; N, 3.42. Mp (°C): *ca*. 135 (dec., turns black), 150-152 (melts).

4.5.3.5 Synthesis of IPr•SiD$_2$•GeD$_2$•W(CO)$_5$ 4D. To a mixture of **2** (52 mg, 0.050 mmol) and Li[AlD_4] (3.2 mg, 0.081 mmol) was added 5 mL of toluene, and the reaction mixture was stirred for 10 min at room temperature to obtain a pale yellow slurry. Afterwards, 2 mL of Et_2O was added to the reaction and the mixture was stirred for another 3 min to yield a clear yellow solution. The resulting solution was filtered through Celite and volatiles were removed *in vacuo* to obtain **4D** as a pale yellow powder (32 mg, 76%). ^{1}H NMR (C_6D_6): essentially same as the **4** with the absence of the -GeH_2- and -SiH_2- resonances. ^{2}H{^{1}H} NMR

(THF): δ 1.89 (s, -GeD_2-), 3.72 (s, -SiD_2-). IR (Nujol/cm^{-1}): Similar to **4** except for the absence of the SiH_2 (υ = 2150 cm^{-1} and 2140 cm^{-1}) and GeH_2 (υ = 1959 cm^{-1}) vibrations. The SiD_2 stretches were detected at 1549 $cm^{-1}$and 1567 cm^{-1}; a Ge-D stretching vibration was observed at 1404 cm^{-1}.

4.5.3.6 Synthesis of IPr•$SiCl_2$•GeH_2•$W(CO)_5$ 5. To a mixture of **2** (140 mg, 0.146 mmol) and Li[BH_4] (6.7 mg, 0.31 mmol) was added 10 mL of Et_2O. The reaction mixture was stirred for 4 h at room temperature to give a pale yellow slurry over a brown precipitate. The reaction mixture was filtered through Celite to afford a pale yellow solution. Removal of volatiles from the filtrate yielded **5** as a pale yellow crystalline solid (96 mg, 74%). Crystals suitable for X-ray crystallography (colorless needles) were grown by cooling a saturated Et_2O solution of **5** to -35 °C. ^{1}H NMR ([D_8]-THF): δ 0.98 (d, $^3J_{HH}$ = 6.5 Hz, 12H, CH(CH_3)$_2$), 1.19 (d, $^3J_{HH}$ = 6.5 Hz, 12H, CH(CH_3)$_2$), 2.32 (s, 2H, -GeH_2-), 2.34 (septet, $^3J_{HH}$ = 6.5 Hz, 4H, CH(CH_3)$_2$), 7.23 (d, $^3J_{HH}$ = 8.0 Hz, 4H, ArH), 7.40 (t, $^3J_{HH}$ = 8.0 Hz, 2H, ArH), 7.93 (s, 2H, N-CH-). ^{1}H NMR (C_6D_6): δ 0.79 (d, $^3J_{HH}$ = 6.9 Hz, 12H, CH(CH_3)$_2$), 1.22 (d, $^3J_{HH}$ = 6.9 Hz, 12H, CH(CH_3)$_2$), 2.36 (septet, $^3J_{HH}$ = 6.9 Hz, 4H, CH(CH_3)$_2$), 2.99 (s, 2H, -GeH_2-, $^2J_{HW}$ = 5.4 Hz), 6.23 (s, 2H, N-CH-), 6.93 (d, $^3J_{HH}$ = 7.8 Hz, 4H, ArH), 7.13 (t, $^3J_{HH}$ = 7.8 Hz, 2H, ArH). ^{13}C{^{1}H} NMR ([D_8]-THF): δ 22.7 (CH(*C*H_3)$_2$), 25.8 (CH(*C*H_3)$_2$), 30.1 (*C*H(CH_3)$_2$), 125.5 (-N-*C*H-), 129.4 (Ar*C*), 132.9 (Ar*C*), 133.2 (Ar*C*), 146.3 (Ar*C*), 149.9 (N-*C*-N), 201.2 (equat. *CO),* 204.1 (ax. *CO)*. ^{29}Si{^{1}H} NMR ([D_8]-THF): δ 7.8 (s). ^{29}Si NMR ([D_8]-THF): δ 7.8 (t, $^2J_{SiH}$ = 6.9 Hz). IR (Nujol/cm^{-1}): 1884 (br, υCO), 1901 (br, υCO), 1914 (br, υCO), 1948 (sh, υCO), 1969 (w, υGe-H), 2049 (s, υCO).

Anal. Calcd. for $C_{32}H_{38}Cl_2GeN_2O_5SiW$: C, 43.37; H, 4.32; N, 3.16. Found: C, 43.45; H, 4.89; N, 3.24. Mp (°C): 161-163.

4.5.3.7 Synthesis of IPr•$SiCl_2$•GeD_2•$W(CO)_5$ 5D. To a mixture of **2** (65 mg, 0.068 mmol) and Li[BD_4] (3.7 mg, 0.14 mmol) was added 7 mL of Et_2O. The reaction mixture was stirred for 4 h at room temperature to give a pale yellow slurry over a brown precipitate. Filtration of the mixture through Celite gave a pale yellow solution and the volatiles were removed *in vacuo* to yield **6D** as a pale yellow crystalline solid (53 mg, 88%). ^{1}H NMR (C_6D_6): essentially same as the **6** with the absence of the -GeH_2- resonances. ^{2}H{^{1}H} NMR (THF): δ 2.55 (s, -GeD_2-). IR (Nujol/cm^{-1}): Similar to **6** except for the absence of the -GeH_2- vibration at 1969 cm^{-1} and a -GeD_2- stretching frequency was observed at 1416 cm^{-1}.

4.5.3.8 Synthesis of IPr•SiD_2•GeH_2•$W(CO)_5$ 6. To a mixture of **5** (63 mg, 0.071 mmol) and Li[AlD_4] (1.54 mg, 0.037 mmol) was added 4 mL toluene, followed by stirring for 5 min at room temperature. After which, 3 mL of Et_2O was added and the mixture was stirred for another 5 min to yield a clear yellow solution. The reaction mixture was filtered through Celite and volatiles were removed *in vacuo* affording **6** as a pale yellow crystalline solid (46 mg, 79%). ^{1}H NMR (C_6D_6): essentially same as the **4** with the absence of the -SiH_2- resonance but the -GeH_2- resonance was slightly broadened. ^{2}H{^{1}H} NMR (C_6H_6): δ 3.73 (s, -SiD_2-) and 1.91 (s, -GeD_2-). IR (Nujol/cm^{-1}): Similar to **4** but both -SiH_2- (minor amount, 2140 cm^{-1} and 2152 cm^{-1}) and -SiD_2- (1549 cm^{-1} and 1567 cm^{-1}) vibrations were

observed. Similarly, a -GeH_2- (1961 cm^{-1}) stretching frequency was observed along with a minor -GeD_2- vibration at 1406 cm^{-1}.

4.5.3.9 Synthesis of IPr•SiH_2•SnH_2•$W(CO)_5$ 7. To a mixture of **3** (101 mg, 0.10 mmol) and Li[BH_4] (8.7 mg, 0.04 mmol) was added a mixture of toluene and Et_2O (10 mL, 1:1). The reaction mixture was stirred for 20 min at room temperature to give a red solution over a brown precipitate. Filtration of the reaction mixture through Celite followed by removal of volatiles afforded **7** as a red oil (67 mg, 62% overall; containing 40% IPr•$SiCl_2$•BH_3 in that product mixture). X-ray quality crystals of compound **7** were grown by cooling a saturated Et_2O solution to -35 °C (isolated yield 9%, 8 mg). Despite the low yield, this preparation was reproducible. ^{1}H NMR (C_6D_6): δ 0.83 (d, $^3J_{HH}$ = 6.9 Hz, 12H, CH(CH_3)$_2$), 1.23 (d, $^3J_{HH}$ = 6.9 Hz, 12H, CH(CH_3)$_2$), 2.30 (septet, $^3J_{HH}$ = 6.9 Hz, 4H, CH(CH_3)$_2$), 3.12 (m, second order AA'XX' pattern, 2H, -SnH_2-, satellites: $^1J_{119SnH}$ = 1111.4 Hz, $^1J_{117SnH}$ = 1062.8 Hz), 3.86 (m, second order AA'XX' pattern, 2H, -SiH_2-, $^1J_{SiH}$ = 187.7 Hz, $^2J_{SnH}$ = 61.2 Hz), 6.30 (s, 2H, N-CH-), 6.97 (d, $^3J_{HH}$ = 7.8 Hz, 4H, ArH), 7.16 (t, $^3J_{HH}$ = 7.8 Hz, 2H, ArH). ^{13}C{^{1}H} NMR (C_6D_6): δ 22.9 (CH(*C*H_3)$_2$), 25.5 (CH(*C*H_3)$_2$), 29.2 (*C*H(CH_3)$_2$), 125.2 (-N-*C*H-), 125.8 (Ar*C*), 132.2 (Ar*C*), 132.4 (Ar*C*), 144.9 (Ar*C*), 160.6 (N-*C*-N), 199.6 (ax. *CO),* 202.2 (equat. *CO)*. ^{29}Si{^{1}H} NMR (C_6D_6): δ -91.1 (s). ^{29}Si NMR (C_6D_6): δ -91.1 (t, $^1J_{Si-H}$ = 188.0 Hz). ^{119}Sn{^{1}H} NMR (C_6D_6): δ -537.1 (s). ^{119}Sn NMR (C_6D_6): δ -537.1 (tt, $^1J_{Sn-H}$ = 1108.9 Hz, $^2J_{Sn-H}$ = 62.3 Hz). IR (Nujol/cm^{-1}): 1886 (br, υCO), 1895 (br, υCO), 1945 (sh, υCO), 2040 (s, υCO), 2136 (m, υSi-H), 2141 (sh, υSi-H); the Sn-H vibrations could not be located. Anal. Calcd. For $C_{32}H_{40}N_2O_5SiSnW$: C, 44.52; H,

4.67; N, 3.24. Found: C, 44.65; H, 4.48; N, 3.54. Mp (°C): 113-115 (dec, turns black), 153-155 (melts).

NMR data for IPr•$SiCl_2$•BH_3:[23] ^{1}H NMR (C_6D_6): δ 0.91 (d, $^3J_{HH}$ = 6.8 Hz, 12H, CH(CH_3)$_2$), 1.41 (d, $^1J_{HH}$ = 6.8 Hz, 12H, CH(CH_3)$_2$), 2.64 (septet, $^3J_{HH}$ = 6.8 Hz, 4H, CH(CH$_3$)$_2$), 6.35 (s, 2H, N-CH-), 7.05 (d, $^3J_{HH}$ = 7.8 Hz, 4H, ArH), 7.18 (t, $^3J_{HH}$ = 7.8 Hz, 2H, ArH). ^{11}B{^{1}H} NMR (C_6D_6): δ -38 (s).

4.5.3.10 Synthesis of IPr•GeH_2•GeH_2•$W(CO)_5$ 8. To a mixture of IPr•$GeCl_2$ (56 mg, 0.10 mmol), (THF)$GeCl_2$•$W(CO)_5$ (57 mg, 0.10 mmol) and Li[BH_4] (9.4 mg, 0.43 mmol) was added 6 mL of Et_2O. The reaction mixture was stirred for 20 min to give a yellow solution over a pale yellow precipitate (presumably LiCl). The reaction mixture was allowed to settle and the mother liquor filtered through Celite to yield a yellow filtrate. Removal of the volatiles from the filtrate gave a yellow solid, which was identified as a mixture of **8** (*ca*. 20%), IPr•GeH_2•$W(CO)_5$ (*ca*. 40%), IPr•GeH_2•BH_3 (*ca*. 40%) by ^{1}H NMR spectroscopy. Spectroscopically pure **8** was isolated by fractional crystallization: by cooling a saturated Et_2O solution of the crude material layered with hexanes to -35 °C (18 mg, 20%). Despite the low yield, this preparation was reproducible. ^{1}H NMR (C_6D_6): δ 0.82 (d, $^3J_{HH}$ = 7.0 Hz, 12H, CH(CH_3)$_2$), 1.19 (d, $^3J_{HH}$ = 7.0 Hz, 12H, CH(CH_3)$_2$), 2.27 (septet, $^3J_{HH}$ = 7.0 Hz, 4H, CH(CH$_3$)$_2$), 3.05 (m, second order AA'XX' pattern, 2H, -GeH_2-), 4.08 (m, second order AA'XX' pattern, 2H, -GeH_2-), 6.30 (s, 2H, N-CH-), 6.96 (d, $^3J_{HH}$ = 7.5 Hz, 4H, ArH), 7.14 (t, $^3J_{HH}$ = 7.5 Hz, 2H, ArH). ^{13}C{^{1}H} NMR (C_6D_6): δ 22.8 (CH(*C*H$_3$)$_2$), 25.4 (CH(*C*H$_3$)$_2$), 29.2 (*C*H(CH$_3$)$_2$), 125.1 (-N-

*C*H-), 125.4 (Ar*C*), 132.2 (Ar*C*), 132.5 (Ar*C*), 144.9 (Ar*C*), 163.7 (N-*C*-N), 201.7 (equat. *CO*, $^{1}J_{W\text{-}C}$ = 125 Hz), 202.2 (ax. *CO*). IR (Nujol/cm^{-1}): 1887 (br, υCO), 1945 (br, υCO), 1954 (sh, υGe-H), 1961 (s, υGe-H), 2047 (s, υCO). Anal. Calcd. For $C_{32}H_{40}Ge_2N_2O_5W$: C, 44.60; H, 4.68; N, 3.25. Found: C, 44.17; H, 4.70; N, 3.13. Mp (°C): 65-67 (dec, turns red), 149-151 (melts).

4.5.3.11 Synthesis of IPr•GeD$_2$•GeD$_2$•W(CO)$_5$ 8D. To a mixture of IPr•$GeCl_2$ (63 mg, 0.12 mmol), (THF)$GeCl_2$•$W(CO)_5$ (0.64 mg, 0.12 mmol) and Li[BD_4] (13 mg, 0.51 mmol) was added 6 mL of Et_2O. The reaction mixture was stirred for 20 min at room temperature to give a yellow solution over a pale yellow precipitate (LiCl). The reaction mixture was allowed to settle and the mother liquor was filtered through Celite to yield a yellow filtrate. Removal of the volatiles from the filtrate gave a yellow solid, which was identified as a mixture of **8D** (*ca*. 20%), IPr•GeD_2•$W(CO)_5$ (*ca*. 40%) and IPr•GeD_2•DH_3 (*ca*. 40%) by ^{1}H NMR spectroscopy. Spectroscopically pure **8D** was isolated by fractional crystallization: by cooling a saturated Et_2O solution of the crude material layered with hexanes to -35 °C (19 mg, 19%). ^{1}H NMR (C_6H_6): essentially same as the **8** with the absence of the -GeH_2- resonances at 3.05 and 4.08 ppm. ^{2}H{^{1}H} NMR (C_6D_6): δ 3.05 (s, -Ge*D*$_2$-), 4.08 (s, -Ge*D*$_2$-). IR (Nujol/cm^{-1}): Similar to **8** except for the absence of the -GeH_2- vibrations at 1961 and 1964 cm^{-1} while -GeD_2- stretching bands were observed at 1405 and 1407 cm^{-1}.

4.5.3.12 Reaction of IPr•$SnCl_2$ with (THF)$_2$$SnCl_2$•$W(CO)_5$: Formation of IPr•$SnCl_2$•$W(CO)_5$. To a mixture of IPr•$SnCl_2$ (86 mg, 0.15 mmol) and

$(THF)_2SnCl_2•W(CO)_5$ (97 mg, 0.16 mmol) was added 6 mL of toluene. The reaction mixture was then stirred for 6 hrs at room temperature to give a pale solution over a white precipitate. The precipitate was isolated by filtration and dried under vacuum to yield a white powder, which was identified as $SnCl_2$ (by melting point).[45] The ^1H NMR spectrum of the filtrate supports clean formation of $IPr•SnCl_2•W(CO)_5$ in quantitative yield (quantitative yield).[13b] For full characterization details of $IPr•SnCl_2•W(CO)_5$ please refer to Chapter 3.

4.5.3.13 Reaction of $IPr•GeCl_2$ with $(THF)_2SnCl_2•W(CO)_5$: Formation of $IPr•GeCl_2•W(CO)_5$. To a mixture of $IPr•GeCl_2$ (110 mg, 0.21 mmol) and $(THF)_2SnCl_2•W(CO)_5$ (134 mg, 0.21 mmol) was added 8 mL of toluene. The reaction mixture was then stirred overnight at room temperature to give a pale yellow slurry. The reaction mixture was filtered through Celite and removal of the volatiles from the filtrate afforded a pale yellow powder which was identified as $IPr•GeCl_2•W(CO)_5$ by ^1H NMR spectroscopy (quantitative yield).[13b] For full characterization details of $IPr•GeCl_2•W(CO)_5$ please refer to Chapter 3.

4.5.3.14 Reaction of $IPr•SnCl_2$ with $(THF)GeCl_2•W(CO)_5$: Formation of $IPr•GeCl_2•W(CO)_5$. To a mixture of $IPr•SnCl_2$ (120 mg, 0.21 mmol) and $(THF)GeCl_2•W(CO)_5$ (112 mg, 0.21 mmol) was added 8 mL of toluene. The reaction mixture was then stirred overnight at room temperature to give a pale yellow solution over a pale yellow precipitate. The precipitate was isolated by filtration and the volatiles were removed from the filtrate to yield a pale yellow powder which was identified as $IPr•GeCl_2•W(CO)_5$ by ^1H NMR spectroscopy

(quantitative yield).[13b] For full characterization details of IPr•$GeCl_2$•$W(CO)_5$ please refer to Chapter 3.

4.5.3.15 Synthesis of IPrCH_2•$GeCl_2$•$GeCl_2$•$W(CO)_5$ 9. To a mixture of IPrCH_2•$GeCl_2$ (250 mg, 0.46 mmol) and (THF)$GeCl_2$•$W(CO)_5$ (246 mg, 0.46 mmol) was added 8 mL of toluene. The reaction mixture was then stirred for 20 min at room temperature to give a pale solution over a yellow precipitate. The precipitate was isolated by filtration and dried under vacuum to give **9** as a pale yellow powder (430 mg, 93%). Crystals suitable for X-ray crystallography were grown by cooling (-35 °C) a saturated solution of **9** in CH_2Cl_2 layered with hexanes. ^{1}H NMR (CD_2Cl_2): δ 1.19 (d, $^3J_{HH}$ = 7.0 Hz, 12H, CH(CH_3)$_2$), 1.40 (d, $^3J_{HH}$ = 7.0 Hz, 12H, CH(CH_3)$_2$), 2.60 (septet, $^3J_{HH}$ = 7.0 Hz, 4H, CH(CH_3)$_2$), 3.15 (s, 2H, -CH_2-), 7.40 (s, 2H, N-CH-), 7.45 (d, $^3J_{HH}$ = 7.5 Hz, 4H, ArH), 7.63 (t, $^3J_{HH}$ = 7.5 Hz, 2H, ArH). ^{13}C{^{1}H} NMR (CD_2Cl_2): δ 21.9 (-CH$_2$-), 22.8 (CH(CH$_3$)$_2$), 26.6 (CH(CH$_3$)$_2$), 29.6 (CH(CH$_3$)$_2$), 124.6 (-N-CH-), 126.2 (ArC), 129.9 (ArC), 132.9 (ArC), 145.6 (ArC), 150.3 (N-C-N), 197.1 (equat. *CO*), 201.62 (ax. *CO)*. IR (Nujol/cm^{-1}): 1919 (br, υCO), 1941 (br, υCO), 1983 (sh, υCO), 2065 (s, υCO). Anal. Calcd. for $C_{33}H_{38}Cl_4Ge_2N_2O_5W$: C, 39.10; H, 3.78; N, 2.76. Found: C, 39.80; H, 3.88; N, 2.80. Mp (°C): 189-191 (dec, turns dark brown), 201-203 (melts).

4.5.3.16 Synthesis of IPrCH_2•GeH_2•GeH_2•$W(CO)_5$ 10. To a mixture of IPrCH_2•$GeCl_2$•$GeCl_2$•$W(CO)_5$ (102 mg, 0.100 mmol) and Li[BH_4] (9.1 mg, 0.41

mmol) was added 10 mL of Et_2O. The reaction mixture was stirred for 30 min at room temperature to give a pale yellow slurry over a pale yellow precipitate. The resulting mixture was then allowed to settle and the mother liquor was filtered through Celite to yield a pale yellow filtrate. Removal of the volatiles from the filtrate afforded **10** as a pale yellow powder (82 mg, 93%). Crystals suitable for X-ray crystallography were grown by cooling a saturated Et_2O solution of **10** layered with hexanes to -35 °C for 5 days. ^{1}H NMR (C_6D_6): δ 0.82 (d, $^3J_{HH}$ = 7.0 Hz, 12H, CH(CH_3)$_2$), 1.91 (d, $^3J_{HH}$ = 7.0 Hz, 12H, CH(CH_3)$_2$), 2.29 (t, $^3J_{HH}$ = 4.0 Hz, 2H, -CH_2-), 2.32 (septet, $^3J_{HH}$ = 7.0 Hz, 4H, CH(CH$_3$)$_2$), 3.23 (t, $^3J_{HH}$ = 4.0 Hz, 2H, -GeH_2-), 3.97 (pentet, $^3J_{HH}$ = 4.0 Hz, 2H, -GeH_2-), 6.13 (s, 2H, N-CH-), 6.97 (d, $^3J_{HH}$ = 7.2 Hz, 4H, ArH), 7.14 (t, $^3J_{HH}$ = 7.2 Hz, 2H, ArH). ^{13}C{^{1}H} NMR (C_6D_6): δ 9.9 (-CH$_2$-), 22.4 (CH(CH$_3$)$_2$), 25.7 (CH(CH$_3$)$_2$), 29.3 (CH(CH$_3$)$_2$), 121.9 (-N-CH-), 125.5 (ArC), 129.6 (ArC), 132.6 (ArC), 145.1 (ArC), 156.5 (N-C-N), 202.8 (equat. *CO*), 205.5 (ax. *CO)*. IR (Nujol/cm^{-1}): 1865 (br, υCO), 1896 (br, υCO), 1950 (sh, υCO), 2028 (sh, υGe-H), 2044 (sh, υCO). Anal. Calcd. for $C_{33}H_{42}Ge_2N_2O_5W$: C, 45.83; H, 4.83; N, 3.20. Found: C, 45.54; H, 4.99; N, 3.20. Mp (°C): 61-63 (dec, turns red), 87-89 (melts).

4.5.3.17 Synthesis of IPrCH$_2$•GeD$_2$•GeD$_2$•W(CO)$_5$ 10D. To a mixture of IPrCH$_2$•GeCl$_2$•GeCl$_2$•W(CO)$_5$ (75 mg, 0.07 mmol) and Li[BH_4] (7.8 mg, 0.30 mmol) was added 6 mL of Et_2O. The reaction mixture was stirred for 30 min at room temperature to give a pale yellow slurry over pale yellow precipitate. The resulting mixture was then allowed to settle and filtered through Celite to yield a pale yellow filtrate. Removal of the volatiles from the filtrate afforded **10D** as a

pale yellow powder (62 mg, 95%). ^{1}H NMR (C_6H_6): essentially same as the **10D** with the absence of the -GeH_2- resonances at 3.23 and 3.97 ppm. ^{2}H{^{1}H} NMR (C_6D_6): δ 3.23 (s, -Ge*D*$_2$-), 3.97 (s, -Ge*D*$_2$-). IR (Nujol/cm^{-1}): Similar to **8** except for the absence of the -GeH_2- vibration at 2028 cm^{-1} and the -GeD_2- stretching frequency could not be located due to overlap with aromatic C=C vibrations.

4.5.3.18 Thermolysis of IPr•SiH_2•GeH_2•$W(CO)_5$. A solution of IPr•SiH_2•GeH_2•$W(CO)_5$ (15 mg, 0.016 mmol) in 8 mL of toluene was heated to 110 °C for 24 h to obtain a clear pale yellow solution. The volatiles were then removed from the solution to yield a pale yellow powder. ^{1}H NMR analysis (C_6D_6) of the powder shows the presence of starting material without any sign of decomposition.

4.5.3.19 Thermolysis of IPr•GeH_2•GeH_2•$W(CO)_5$. A solution of IPr•GeH_2•GeH_2•$W(CO)_5$ (8 mg) in C_6D_6 was kept in a J. Young NMR tube at room temperature for 48 h. ^{1}H NMR analysis (C_6D_6) after that period showed the complete conversion of **9** into IPr•GeH_2•$W(CO)_5$. For full characterization details of IPr•GeH_2•$W(CO)_5$ please refer to Chapter 3.

4.5.3.20 Thermolysis of IPrCH_2•GeH_2•GeH_2•$W(CO)_5$. A solution of IPrCH_2•GeH_2•GeH_2•$W(CO)_5$ (20 mg, 0.022 mmol) in 8 mL of toluene was heated to 60 °C for 24 h to obtain a clear pale yellow solution with dark brown precipitate on the wall of the reaction flask. The reaction mixture was filtered through Celite and volatiles were then removed from the filtrate to yield a pale yellow powder. ^{1}H NMR analysis (C_6D_6) of the powder shows the formation of

$IPrCH_2•GeH_2•W(CO)_5$ as the main soluble decomposition product. For full characterization details of $IPrCH_2•GeH_2•W(CO)_5$ please refer to Chapter 3.

4.5.3.21 Reaction of $IPr•SiH_2•GeH_2•W(CO)_5$ (4) with 2,4-pentanedione to form [{IPrH][{Me(O)H-CH=C(Me)O]SiH-$GeH_2•W(CO)_5$] 11.

$IPr•SiH_2•GeH_2•W(CO)_5$ (40 mg, 0.050 mmol) was dissolved in 7 mL of Et_2O and 2,4-pentanedione (7.0 mg, 0.071 mmol) was added to the solution. The reaction mixture was stirred overnight at room temperature to give a cloudy mixture. The mixture was then filtered through Celite and the volatiles were removed *in vacuo* to yield a pale yellow oil. The resulting oil was washed with 1 mL of hexanes and then dissolved in a 5 mL of 5:1 Et_2O/hexanes mixture. The resulting solution was filtered through Celite and cooled to -35 °C to give **11** as pale yellow needles of suitable quality for X-ray crystallography (34 mg, 75%). ^{1}H NMR ([D_8]-THF); peak assignments were made based on GCOSY and gHSQC experiments: δ 1.23 (d, $^3J_{HH}$ = 7.0 Hz, 12H, $CH(CH_3)_2$), 1.27 (m, 3H, $O(CH_3)CCH$), 1.32 (d, $^3J_{HH}$ = 7.0 Hz, 12H, $CH(CH_3)_2$), 1.66 (m, 3H, $CH_3C(O)HCH$), 2.04 (m, second order AA'XX' pattern, 2H, -GeH_2-), 2.48 (septet, $^3J_{HH}$ = 7.0 Hz, 4H, $CH(CH_3)_2$), 4.32 (m, 1H, $CH_3C(O)HCH$), 4.42 (m, 1H, $CH_3C(O)HCH$), 5.67 (t, $^3J_{HH}$ = 2.5 Hz, -SiH-), 7.52 (d, $^3J_{HH}$ = 7.6 Hz, 4H, ArH), 7.68 (t, $^3J_{HH}$ = 7.6 Hz, 2H, ArH), 8.25 (d, $^4J_{HH}$ = 1.6 Hz, 2H, N-CH-), 9.60 (t, $^4J_{HH}$ = 1.6 Hz, 1H, N-CH-N-). ^{13}C{^{1}H} NMR ([D_8]-THF): δ 23.5 ($CH_3C(O)HCH$), 23.7 ($CH(CH_3)_2$), 23.8 ($CH(CH_3)_2$), 29.9 ($OC(CH_3)CH$), 29.9 ($CH(CH_3)_2$), 66.3 ($OC(CH_3)HCH$), 68.1 ($OC(CH_3)CH$), 105.7 ($CH_3C(O)HCH$), 125.8 (-N-CH-), 127.5 (ArC), 131.2 (ArC), 133.3 (ArC), 140.1 (ArC), 146.2 (N-CH-N), 204.4 (ax. *CO),* 208.2 (equat. *CO)*. ^{29}Si{^{1}H} NMR

([D_8]-THF): δ = 3.9. Anal. Calcd. for $C_{37}H_{48}GeN_2O_7SiW$: C, 48.44; H, 5.27; N, 3.05. Found: C, 48.02; H, 5.60; N, 3.17. Mp (°C): 133-135.

4.5.3.22 Reaction of IPr•SiD_2•GeD_2•$W(CO)_5$ (4D) with 2,4-Pentanedione to form [$H_3CC(O)D$-CH=$C(CH_3)O$]SiD-GeD_2•$W(CO)_5$] 11D.

IPr•SiD_2•GeD_2•$W(CO)_5$ (40 mg, 0.041 mmol) was dissolved in 6 mL of Et_2O and 2,4-pentanedione (6.0 mg, 0.061 mmol) was added to the solution and the reaction was stirred overnight at room temperature to obtain a cloudy, pale yellow, mixture. This mixture was then filtered through Celite and volatiles were removed *in vacuo* to yield a pale yellow oil. The oil was washed with 1 mL of hexanes and then dried under vacuum to obtain **11D** as a pale yellow oil (32 mg, 76%). ^1H NMR ([D_8]-THF): essentially same as **11** with the absence of -GeH_2- (δ = 2.04), $CH_3C(O)HCH$ (δ = 4.44) and -SiH- (δ = 5.67). $^2H\{^1H\}$ NMR (THF): δ 2.05 (s, -GeD_2-), 4.37 (br, $CH_3C(O)DCH$), 5.67 (s, -Si*D*-).

Table 4.1: Crystallographic data for **2**•THF, **4 and 5**•Et_2O.

Compound	**2**•THF	**4**	**5**•Et_2O
Formula	$C_{36}H_{44}Cl_4GeN_2O_6SiW$	$C_{32}H_{40}GeN_2O_5SiW$	$C_{36}H_{48}Cl_2GeN_2O_6SiW$
formula weight	1027.06	817.19	960.19
crystal system	triclinic	orthorhombic	monoclinic
space group	$P\bar{1}$	*Pbca* (No. 61)	*C*2/*c* (No. 15)
a(Å)	10.0601(4)	20.608(3)	37.006(5)
b (Å)	11.0700(4)	15.168 (2)	10.7703(13)
c (Å)	20.4081(7)	22.932(4)	21.044(3)
α (deg)	75.8474(4)	90	90
β (deg)	86.0770(5)	90	92.8633(16)
γ (deg)	76.1582(5)	90	90
V (Å^3)	2139.66(14)	7168(2)	8376.9(18)
Z	2	8	8
ρ (g cm^{-3})	1.594	1.514	1.523
abs coeff (mm^{-1})	3.709	4.116	3.660
T (K)	173(1)	173(1)	173(1)
$2\theta_{max}$ (°)	55.10	55.56	52.78
total data	19023	60585	32883
unique data (R_{int})	9783(0.0229)	8390(0.0465)	8578(0.0680)
Obs data [$I > 2\sigma(I)$]	8259	6246	6509
params	460	391	451
R_1 [$I > 2\sigma(I)$][a]	0.0282	0.0432	0.0370
wR_2 [all data][a]	0.0670	0.1275	0.0902
max/min $\Delta\rho$ (e$^-$ Å^{-3})	1.327/-0.700	4.317/-1.533	0.941/-1.459

[a] $R_1 = \Sigma \big| \, |F_o| - |F_c| \, \big| / \Sigma |F_o|$; $wR_2 = [\Sigma\, w(F_o^2 - F_c^2)^2 / \Sigma\, w(F_o^4)]^{1/2}$.

Table 4.2: Crystallographic data for **7**, **9** and **10**.

Compound	**7**	**9**	**10**
Formula	$C_{32}H_{40}N_2O_5SiSnW$	$C_{33}H_{38}Cl_4Ge_2N_2O_5W$	$C_{33}H_{42}Ge_2N_2O_6W$
formula weight	863.29	1013.48	875.72
crystal system	orthorhombic	monoclinic	monoclinic
space group	*Pbca* (No. 61)	$P2_1/c$ (No. 14)	$P2_1/n$
a(Å)	20.9929(11)	16.2246(15)	13.1383(5)
b (Å)	15.0611(8)	20.6128(19)	15.3167(5)
c (Å)	22.9501(12)	24.111(2)	18.6925(6)
α (deg)	90	90	90
β (deg)	90	98.9410(10)	101.9760(4)
γ (deg)	90	90	90
V (Å^3)	7256.3(7)	7965.6(13)	3679.7(2)
Z	8	8	4
ρ (g cm^{-3})	1.580	1.690	1.581
abs coeff (mm^{-1})	3.926	4.688	4.779
T (K)	173(1)	173(1)	173(1)
$2\theta_{max}$ (°)	55.06	50.50	52.78
total data	62228	56224	129119
unique data (R_{int})	8348(0.0188)	14432(0.0726)	7536(0.0243)
Obs data [$I > 2\sigma(I)$]	7493	10366	6473
params	396	847	404
R_1 [$I > 2\sigma(I)$][a]	0.0147	0.0403	0.0260
wR_2 [all data][a]	0.0403	0.0998	0.0675
max/min $\Delta\rho$ (e$^-$ Å^{-3})	0.500 /-0.382	1.285/-0.969	1.351/-0.476

[a] $R_1 = \Sigma \big| \, |F_o| - |F_c| \, \big| / \Sigma |F_o|$; $wR_2 = [\Sigma\, w(F_o^2 - F_c^2)^2 / \Sigma\, w(F_o^4)]^{1/2}$.

Table 4.3: Crystallographic data for **11**•Et_2O.

Compound	**11•Et_2O**
Formula	$C_{41}H_{58}GeN_2O_8SiW$
formula weight	991.42
crystal system	monoclinic
space group	*Pn* (No. 7)
a(Å)	11.1107(4)
b (Å)	9.9270(3)
c (Å)	21.7330(7)
α (deg)	90
β (deg)	104.4957(4)
γ (deg)	90
V (Å^3)	7168(2)
Z	2
ρ (g cm^{-3})	1.419
abs coeff (mm^{-1})	3.197
T (K)	173(1)
$2\theta_{max}$ (°)	55.14
total data	20199
unique data (R_{int})	10628(0.0277)
Obs data [$I > 2\sigma(I)$]	8689
params	501
R_1 [$I > 2\sigma(I)$][a]	0.0263
wR_2 [all data][a]	0.0517
max/min $\Delta\rho$ (e$^-$ Å^{-3})	0.726/-0.378

[a] $R_1 = \Sigma \big| \, |F_o| - |F_c| \, \big| / \Sigma |F_o|$; $wR_2 = [\Sigma\, w(F_o^2 - F_c^2)^2 / \Sigma\, w(F_o^4)]^{1/2}$.

4.6 References

(1) (a) Alt, H. G.; Köppl, A. *Chem. Rev.* **2000**, *100*, 1205. (b) Elschenbroich, C.; Salzer, A. *Organometallics: A Concise Introduction (2nd Ed.)*, Wiley-VCH, Weinheim, Germany, **2006**.

(2) (a) Yang; S. F.; Hoffman, N. E. *Annu. Rev. Plant Physiol.* **1984**, *35*, 155. (b) Chang, C.; Stadler, R. *BioEssays*, **2001**, *23*, 619. (c) Wilmowicz, E.; Kęys, J.; Kopcewicz, J. *J. Plant. Physol*, **2008**, *165*, 1917.

(3) Zeise, W. C. *Ann. Phys.* **1831**, *97*, 33.

(4) (a) Weidenbruch, M. *Organometallics* **2003**, *22*, 4348. (b) Fischer, R. C.; Power, P. P. *Chem. Rev.* **2010**, *110*, 3877. (c) Asay, M.; Jones, C.; Driess, M. *Chem. Rev.* **2011**, *111*, 354.

(5) (a) Andrews, L.; Wang, X. *J. Phys. Chem. A* **2002**, *106*, 7696. (b) Wang, X.; Andrews, L.; Kushto, G. P. *J. Phys. Chem. A* **2002**, *106*, 5809. (c) Carrier, W.; Zheng, W.; Osamura, Y.; Kaiser, R. I. *Chem. Phys.* **2006**, *330*, 275. (d) Wang, X.; Andrews, L. *J. Am. Chem. Soc.* **2003**, *125*, 6581.

(6) Lee, V. Ya.; Sekiguchi, A. *Organometallics* **2004**, *23*, 2822.

(7) Buriak, J. M. *Chem. Rev.* **2002**, *102*, 1271.

(8) Chizmeshya, A. V. G.; Ritter, C. J.; Hu, C.; Tice, J. B.; Tolle, J.; Nieman, R. A.; Tsong, I. S. T.; Kouvetakis, J. *J. Am. Chem. Soc.* **2006**, *128*, 6919.

(9) (a) Davidson, P. J.; Lappert, M. F. *J. Chem. Soc. Chem. Commun.* **1973**, 317. (b) Goldberg, D. E.; Harris, D. H.; Lappert, M. F.; Thomas, K. M. *J.*

Chem. Soc. Chem. Commun. **1976**, 261. (c) Klinkhammer, K. W.; Fässler, T. F.; Grützmacher, H. *Angew. Chem., Int. Ed.* **1998**, *37*, 124. (d) Chaubon, M.–A.; Escudié, J.; Ranaivonjatovo, H.; Stagé, J. *J. Chem. Soc. Chem. Commun.* **1996**, 2621. (e) West, R.; Fink, M. F.; Michl, J. *Science*, **1981**, *214*, 1343. (f) Stürmann, M.; Weidenbruch, M.; Klinkhammer, K. W.; Lissener, F.; Marsmann, H. *Organometallics* **1998**, *17*, 4425.

(10) (a) Zabula, A. V.; Hahn, F. E.; *Eur. J. Inorg. Chem.* **2008**, 5165. (b) Mizuhata, Y.; Sasamori, T.; Tokitoh, N. *Chem. Rev.* **2009**, *109*, 3479.

(11) (a) Trinquier, G. *J. Am. Chem. Soc.* **1990**, *112*, 2130. (b) Grev, R. S.; Schaefer, H. F., III; Baines, K. M. *J. Am. Chem. Soc.* **1990**, *112*, 9458. (c) Windus, T. L.; Gordon, M. S.; *J. Am. Chem. Soc.* **1992**, *114*, 9559. (d) Jacobsen, H.; Ziegler, T. *J. Am. Chem. Soc.* **1994**, *116*, 3667.

(12) Yamaguchi, T.; Sekiguchi, A.; Driess, M. *J. Am. Chem. Soc.* **2010**, *132*, 14061.

(13) (a) Thimer, K. C.; Al-Rafia, S. M. I.; Ferguson, M. J.; McDonald, R.; Rivard, E. *Chem. Commun.*, **2009**, 7119. (b) Al-Rafia, S. M. I.; Malcolm, A. C.; Liew, S. K.; Ferguson, M. J.; Rivard, E. *J. Am. Chem. Soc.* **2011**, *133*, 777. (c) Al-Rafia, S. M. I.; Malcolm, A. C.; Liew, S. K.; Ferguson, M. J.; McDonald, R.; Rivard, E. *Chem. Commun.* **2011**, *47*, 6987. (d) Al-Rafia, S. M. I.; Malcolm, A. C.; McDonald, R.; Ferguson, M. J.; Rivard, E. *Chem. Commun.* **2012**, *48*, 1308. (e) Inoue, S.; Driess, M. *Angew. Chem., Int. Ed.* **2011**, *50*, 5614.

(14) (a) Vogel, U.; Timoshkin, A. Y.; Scheer, M. *Angew. Chem., Int. Ed.* **2001**, *40*, 4409. (b) Rupar, P. A.; Jennings, M. C.; Ragogna, P. J.; Baines, K. M. *Organometallics* **2007**, *26*, 4109. (c) Adolf, A.; Vogel, U.; Zabel, M.; Timoshkin, A. Y.; Scheer, M. *Eur. J. Inorg. Chem.* **2008**, 3482. (d) Yamaguchi, T.; Sekiguchi, A.; Driess, M. *J. Am. Chem. Soc.* **2010**, *132*, 14061. (e) Xiong, Y.; Yao, S.; Driess, M. *Angew. Chem., Int. Ed.* **2010**, *49*, 6642. (e) Jambor, R.; Herres-Pawlis, S.; Schürmann, M.; Jurkschat, K. *Eur. J. Inorg. Chem.* **2011**, 344.

(15) (a) Arduengo, A. J., III; Rasika Dias, H. V.; Harlow, R. L.; Kline, M. *J. Am. Chem. Soc.* **1992**, *114*, 5530. (b) Kuhn, N.; Al-Sheikh, A. *Coord. Chem. Rev.* **2005**, *249*, 829. (c) Wang, Y.; Robinson, G. H. *Inorg. Chem.* **2011**, *50*, 12326.

(16) (a) Kinjo, R.; Donnadieu, B.; Celik, M. A.; Frenking, G.; Bertrand, G. *Science* **2011**, *333*, 610. (b) Wang, Y.; Xie, Y.; Wei, P.; King, R. B.; Schaefer, H. F., III; Schleyer, P. v. R.; Robinson, G. H. *Science* **2008**, *321*, 1069. (c) Ghadwal, R. S.; Roesky, H. W.; Merkel, S.; Henn, J.; Stalke, D. *Angew. Chem., Int. Ed.* **2009**, *48*, 5683. (d) Filippou, A. C.; Chernov, O.; Schnakenburg, G. *Angew. Chem., Int. Ed.* **2009**, *48*, 5687. (e) Wang, Y.; Xie, Y.; Wei, P.; King, R. B.; Schaefer, H. F., III; Schleyer, P. v. R.; Robinson, G. H. *J. Am. Chem. Soc.* **2008**, *130*, 14970. (f) Back, O.; Kuchenbeiser, G.; Donnadieu, B.; Bertrand, G. *Angew. Chem., Int. Ed.* **2009**, *48*, 5530. (g) Wang, Y.; Xie, Y.; Abraham, M. Y.; Gilliard, R. J., Jr.;

Wei, P.; Schaefer, H. F., III; Schleyer, P. v. R.; Robinson, G. H. *Organometallics* **2010**, *29*, 4778. (h) Braunschweig, H.; Dewhurst, R. D.; Hammond, K.; Mies, J.; Radacki, K.; Vargas, A. *Science* **2012**, *336*, 11420.

(17) (a) Sidiropoulos, A.; Jones, C.; Stasch, A.; Klein, S.; Frenking, G. *Angew. Chem., Int. Ed.* **2009**, *48*, 9701. (b) Filippou, A. C.; Chernov, O.; Stumpf, K. W.; Schnakenburg, G. *Angew. Chem., Int. Ed.* **2010**, *49*, 3296. (c) Bonyhady, S. J.; Collis, D.; Frenking, G.; Holzmann, N.; Jones, C.; Stasch, A. *Nat. Chem.* **2010**, *2*, 865. (d) Yao, S.; Xiong, Y.; Driess, M. *Chem.—Eur. J.* **2010**, 1281. (e) Ghadwal, R. S.; Roesky, H. W.; Pröpper, K.; Dittrich, B.; Klein, S.; Frenking, G. *Angew. Chem., Int. Ed.* **2011**, *50*, 5374. (f) Katir, N.; Matioszek, D.; Ladeira, S.; Escudié, J.; Castel, A. *Angew. Chem., Int. Ed.* **2011**, *50*, 5352. (g) Abraham, M. Y.; Wang, Y.; Xie, Y.; Wei, P.; Schaefer, H. F., III; Schleyer, P. v. R.; Robinson, G. H. *J. Am. Chem. Soc.* **2011**, *133*, 8874.

(18) (a) Jutzi, P.; Steiner, W. *Chem. Ber.* **1976**, *109*, 3473. (b) Balch, A. L.; Oram, D. E. *Organometallics* **1988**, *7*, 155.

(19) Ichinohe, M.; Arai, Y.; Sekiguchi, A.; Takagi, N. Nagase, S. *Organometallics* **2001**, *20*, 4141.

(20) See: Chapter 3 for the structural details of IPr•$GeCl_2$•$W(CO)_5$.

(21) Mallela, S. P.; Hill, S.; Geanangel, R. A. *Inorg. Chem.* **1997**, *36*, 6247.

(22) (a) Hashimoto, H.; Tsubota, T.; Fukuda, T.; Tobita, H. *Chem. Lett.* **2009**, *38*, 1196. (b) Hashimoto, H.; Tsubota, T.; Fukuda, T.; Tobita, *New. J. Chem.* **2010**, *34*, 1723.

(23) Azhakar, R.; Tavcar, G.; Roesky, H. W.; Hey, J.; Stalke, D.; *Eur. J. Inorg. Chem.* **2011**, 475.

(24) Jana, A.; Leusser, D.; Objartel, I.; Roesky, H. W.; Stalke, D. *Dalton Trans.* **2011**, *40*, 5458.

(25) A typical Si-Sn single bond length is about 2.60 Å; see: Mackay, K. M. *The Chemistry of Organic Germanium, Tin and Lead Compounds* (Ed.: S. Patai), Wiley, New York, **1995**, chap. 2.

(26) Sekiguchi, A.; Izumi, R.; Lee, V. Ya.; Ichinohe, M. *J. Am. Chem. Soc.* **2002**, *124*, 14822.

(27) Eichler, B. E.; Phillips, A. D.; Haubrich, S. T.; Mork, B. V.; Power, P. P. *Organometallics* **2002**, *21*, 5622.

(28) (a) Kudo, T.; Nagase, S. *J. Chem. Phys. Lett.* **1981**, *84*, 375. (b) Trinquier, G.; Barthelat, J.; Satgé, J. *J. Am. Chem. Soc.* **1982**, *104*, 5931. (c) Nagase, S.; Kudo, T. *Organometallics* **1984**, *3*, 324. (d) Dewar, M. J. S.; Grady, G. L.; Healy, E. F. *Organometallics* **1987**, *6*, 186. (e) Trinquier, G.; Malrieu,; J. -P.; Rivière, P. *J. Am. Chem. Soc.* **1982**, *104*, 4529. (f) Nagase, S.; Kudo, T. *J. Mol. Struct.* **1983**, *103*, 35. (g) Liang, C.; Allen, L. C. *J. Am. Chem. Soc.* **1990**, *112*, 1039.

(29) Márquez, A.; Gonzales, G. G.; Fernandez, S. *J. Chem. Phys.* **1989**, *138,* 99.

(30) (a) Schäfer, H.; Saak, W.; Weidenbruch, M. *Organometallics* **1999**, *18*, 3159. (b) Beattie, I. R.; Jones, P. J.; Reid, G.; Webster, M. *Inorg. Chem.* **1998**, *37*, 6032. (c) Pu, L.; Senge, M. O.; Olmstead, M. M.; Power, P. P. *J. Am. Chem. Soc.* **1998**, *120*, 12682. (d) Ishida, Y.; Sekiguchi, A.; Kobayashi, K.; Nagase, S. *Organometallics* **2004**, *23*, 4891. (e) Pu, L.; Philips, A. D.; Richards, A. F.; Stender, M.; Simons, R. S.; Olmstead, M. M.; Power, P. P. *J. Am. Chem. Soc.* **2003**, *125*, 11626. (f) Ramaker, G.; Saak, W.; Weidenbruch, M. *Organometallics* **2003**, *22*, 5212. (g) Sekiguchi, A.; Fukaya, N.; Ichinohe, M.; Takagi, N.; Nagase, S. *J. Am. Chem. Soc.* **1999**, *127*, 11587. (h) Sen, S. S.; Kratzet, D.; Stern, D.; Roesky, H. W.; Stalke D. *Inorg. Chem.* **2010**, *49*, 5786. (i) Simons, R. S.; Pu, L.; Olmstead, M. M.; Power, P. P. *Organometallics* **1997**, *16*, 1920.

(31) (a) Baines, K. M.; Stibbs, W. G. *Adv. Organomet. Chem.* **1996**, *39*, 275. (b) Cui, C.; Brynda, M.; Olmstead, M. M.; Power, P. P. *J. Am. Chem. Soc.* **2004**, *126*, 6510.

(32) Li, J.; Schenk, C.; Goedecke, C.; Frenking, G.; Jones, C. *J. Am. Chem. Soc.* **2011**, *133*, 18622.

(33) Zyder, M.; Kochel, A.; Handzilk, J.; Buzar, T. S. *Organometallics* **2009**, *28*, 5857.

(34) Richards, A. F.; Brynda, M.; Power, P. P. *J. Am. Chem. Soc.* **2004**, *126*, 10530.

(35) Saur, I.; Rima, G.; Miqueu, K.; Gornitzk, H.; Barrau, J. *J. Organomet. Chem.* **2003**, *672*, 77.

(36) Billone, P.S.; Beleznay, K.; Harrington, C. R.; Huch, L. A.; Leigh, W. J. *J. Am. Chem. Soc.* **2011**, *133*, 10523.

(37) Sen, S. S.; Tavčar, G.; Roesky, H. W.; Kratzert, D.; Hey, J.; Stalke, D. *Organometallics* **2010**, *29*, 2343.

(38) Jutzi, P.; Bunte, E. A.; Holtmann, U.; Neumann, B.; Stammler, H. G. *J. Organomet. Chem.* **1993**, *446*, 139.

(39) Pangborn, A. B.; Giardello, M. A.; Grubbs, R. H.; Rosen, R. K.; Timmers, F. *J. Organometallics* **1996**, *15,* 1518.

(40) Jafarpour, L.; Stevens, E. D.; Nolan, S. P. *J. Organomet. Chem.* **2000**, *606,* 49.

(41) Hope, H.; *Prog. Inorg. Chem.* **1995**, *43,* 1.

(42) Blessing, R. H. *Acta Cryst.* **1995**, *A51,* 33.

(43) Sheldrick, G. M. *Acta Cryst.* **2008**, *A64,* 112.

(44) Beurskens, P. T.; Beurskens, G.; de Gelder, R.; Smits, J. M. M.; Garcia-Garcia, S.; Gould, R. O. *DIRDIF-2008*, Crystallography Laboratory, Radboud University: Nijmegen, The Netherlands, **2008**.

(45) For melting point of $SnCl_2$ please refer to: Abbott, A. P.; Capper, G.; Davies, D. L.; Rashed, R. K.; Tambyrajah, V. *Chem. Commun.* **2003**, 70.

Chapter 5

Preparation of Stable Low Oxidation State Group 14 Element Amidohydrides and Hydride-mediated Ring-Expansion Chemistry of N-Heterocyclic Carbenes

Chapter 5

Preparation of Stable Low Oxidation State Group 14 Element Amidohydrides and Hydride-mediated Ring-Expansion Chemistry of N-Heterocyclic Carbenes

5.1 Abstract

Various low oxidation state (+2) Group 14 element amidohydrides adducts IPr•EH(BH_3)NHDipp (E = Si and Ge; IPr = [(HCNDipp)$_2$C:], Dipp = 2,6-^{i}Pr$_2$C$_6$H$_3$) were synthesised. The thermolysis of these amidohydrides was investigated as a potential route to access Si- and Ge-based clusters; however, unexpected transmetallation chemistry occurred to yield the carbene-borane adduct IPr•BH_2NHDipp. When a solution of IPr•BH_2NHDipp was heated to 100 °C, a rare C-N bond activation/ring-expansion reaction involving the bound N-heterocyclic carbene donor, IPr, transpired.

5.2 Introduction

The use of the electron donating ability of N-heterocyclic carbenes (NHCs) to stabilize reactive main group species is a rapidly expanding area of inorganic chemistry.[1] In many instances the resulting coordinative NHC-element interactions are of sufficient strength to enable the isolation of complexes featuring molecular entities that only exist as fleeting intermediates or were previously unknown altogether. For example, the recent isolation of stable molecular adducts of parent borylene (:BH)[2] and disilylene (:Si=Si:)[3] represent synthetic breakthroughs made possible *via* carbene coordination chemistry. In addition, NHC-BH_3 adducts have been recently shown to be versatile precatalysts in main group element-based catalysis, such as in the photoinduced radical polymerization of methacrylates.[4] It is therefore of significant interest to improve our general knowledge regarding potential decomposition/activation pathways involving N-heterocyclic carbenes ligands due to their increasing use in catalysis.[4]

Recently, the Rivard group has prepared a series of parent low-valent Group 14 element hydride donor-acceptor adducts of the general form: IPr•EH_2•LA and IPr•H_2E-EH_2•LA (E = Si, Ge and/or Sn; IPr = $[HCNDipp)_2C:]$, Dipp = 2,6-$^{i}Pr_2C_6H_3$; LA = Lewis acids such as BH_3 and $W(CO)_5$).[5,6] These hydrides are considered as promising precursors for the controlled synthesis of clusters and nanoparticles as evidence by the clean formation of Ge metal from the solution phase thermolysis of the germanium(II) hydride adduct IPr•GeH_2•BH_3.[5a,7] The synthesis of Group 14 element clusters is highly desirable since they possess structural and bonding features which approach those of the

bulk element while providing valuable insight into the nature of the chemical transformations that occur at or near the surface of the bulk material;[8] in addition, Group 14 (tetrel) element particles of nanometer dimensionality have been shown to exhibit useful electronic properties such as tunable luminescence.[9]

Over the years a number of tetrel element clusters have been reported in the literature, and their syntheses generally involve the reduction of RE-Cl (R = aryl or amide group) precursors with alkali metal-based reagents (*e.g.* KC_8).[10] Power, Lappert and coworkers have devised an alternate route to clusters *via* the thermolysis of either *in situ* generated or isolable Sn(II) hydrides, such as the metastable amide "[(Me_3Si)NDipp]SnH" or the room temperature stable species, $[Ar´Sn(\mu\text{-}H)]_2$; Ar´ = $(2,6\text{-}Dipp)_2C_6H_2$, to form novel Sn_{17} and Sn_7 clusters.[11a, 11b] In addition, Klinkhammer *et al*. have generated Pb clusters *via* the decomposition of putative Pb(II) hydride intermediates.[11c] Drawing inspiration from this chemistry, it was anticipated that the preparation of N-heterocyclic carbene-stabilized amidohydride complexes of the general form IPr•EH-NHDipp (E = Si, Ge and Sn) might provide access to new clusters *via* mild, controllable thermolytic pathways. In pursuit of this goal, a novel decomposition pathway involving the carbene-borane adduct IPr•BH_2NHDipp leading to C-N bond activation/ring-expansion of the generally inert donor, IPr, was uncovered; this discovery has widespread implications as IPr and related NHCs are often used as supporting ligands in catalysis.

5.3 Results and discussion

5.3.1 Synthesis of E(II) aminohalide adducts IPr•E(Cl)-NHDipp (E = Si, Ge and Sn)

As mentioned in the Introduction, low valent Group 14 element hydrides REH (R = aryl or amine group) are often unstable and can readily decompose to give clusters.[11] With this knowledge in mind, the initial target was the preparation of stable aminohydride adducts of N-heterocyclic carbenes IPr•E(H)-NHDipp (E = Si, Ge and Sn) in order to access new cluster archetypes (*e.g.* $IPr_x•E_y$; x < y) upon controlled thermolysis chemistry. As an entry point, the requisite E(II) amidohalide adducts IPr•E(Cl)-NHDipp (E = Si, Ge and Sn; **1**-**3**) were prepared *via* treating the known adducts IPr•ECl_2 with one equivalent of Li[NHDipp] in Et_2O solvent (Equation 5.1).

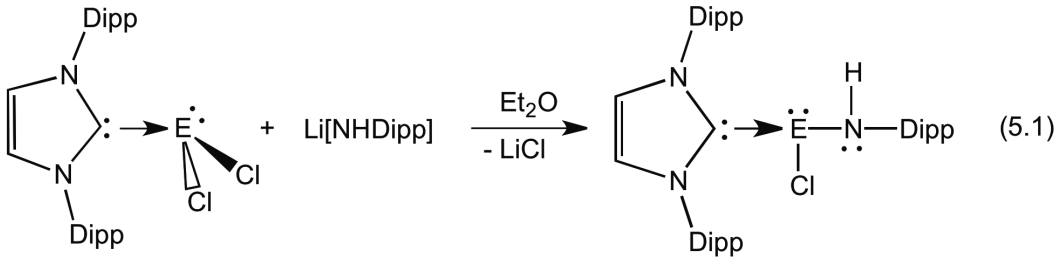

(5.1)

While examples of Ge(II) and Sn(II) amides are common in the literature,[12] compound **1** represents a rare example of a silicon(II) amide that is stable at ambient temperature.[13] In the absence of sterically encumbered groups at nitrogen, the free heavy Group 14 amidochlorides E(Cl)-N(H)R (E = Ge and Sn) show a tendency to spontaneously oligomerize and/or participate in further

condensation chemistry.[14] However, the presence of σ-donating carbenes in **1**-**3** leads to occupation of the initially vacant p-orbital at the Group 14 centers enabling the stabilization of the low valent heavy element amidochlorides in the form of monomeric adducts.

Compounds **1-3** IPr•E(Cl)-NHDipp (E = Si, Ge and Sn) were isolated as air- and moisture-sensitive yellow solids in 45, 98 and 85% yields, respectively. The formation of adducts **1-3** was confirmed by elemental analysis (C, H, N), NMR and IR spectroscopy. The ^{1}H NMR data for these complexes exhibit similar spectral features with well-resolved singlet resonances belonging to the N-H groups at 4.14, 4.11 and 3.82 ppm for **1**-**3** respectively. Moreover, each of the six -^{i}Pr groups exists in magnetically distinct environments (to give six doublet resonances). The ^{29}Si NMR resonance for **1** is present at -6.0 ppm, and is upfield-shifted relative to the ^{29}Si NMR signal in the Si(II) precursor IPr•$SiCl_2$ (δ = 19.1).[15] The tin(II) amide **3** yields a ^{119}Sn resonance at -96.2 ppm which is in a similar spectral region as the related three-coordinate Sn(II) adduct IPr•$SnCl_2$ (δ = -68.7).[5a] The IR spectra for **1**-**3** corroborated the abovementioned NMR assignments with stretching frequencies belonging to the N-H residues observed in the narrow range of 3357 to 3371 cm^{-1}. Conclusive evidence for the formation of IPr•E(Cl)-NHDipp (E = Si, Ge and Sn; **1**-**3**) was obtained by single-crystal X-ray crystallography and the refined structures are collectively shown in Figure 5.1.

Compounds **1**-**3** are isostructural with distorted trigonal pyramidal geometries at each of the three-coordinate E centers (E = Si, Ge and Sn), consistent with the presence of a stereochemically active lone pair at the tetrel

element centers. Furthermore, the E-Cl bonds in **1**-**3** are each oriented towards the steric cradle created by the flanking Dipp groups of the IPr donor. The C_{IPr}-Si bond length in **1** [1.980(3) Å] is identical within experimental error to the corresponding distance in the Si(II) adduct IPr•$SiCl_2$ [1.985(4) Å],[15] but is significantly longer than the C_{IPr}-Si interactions in Robinson's chlorosilylene complex IPr•(Cl)Si=Si(Cl)•IPr [1.934(6) Å] and five coordinate Si(IV) adduct IPr•$SiCl_4$ [1.928(2) Å].[3] In the heavier element congeners, **2** and **3**, the respective C_{IPr}-Ge [2.098(4) Å *avg*.] and C_{IPr}-Sn [2.3220(19) Å] bond distances are very similar to those of their parent Ge(II) and Sn(II) compounds, IPr•$GeCl_2$ and IPr•$SnCl_2$ [C_{IPr}-Ge = 2.112(2) Å; C_{IPr}-Sn = 2.341(8) Å].[5a] The Si-N bond distance in **1** [1.765(2) Å] is marginally longer than the Si-N bond distances found in Roesky's dimeric silaisonitrile [{(2,4,6-$^{i}Pr_3C_6H_2)_2C_6H_3$}NSi:]$_2$ [1.756(1) Å *avg*.].[16] Similarly, the E-N (E = Ge and Sn) bond distances in **2** and **3** are 1.900(3) Å (*avg*.) and 2.1142(16) Å, respectively, and in the range expected for single bonds; for comparison, the Ge-N bonds found in the acyclic Ge(II) bisamide $(Ar''NH)_2Ge$: [Ar´´ = 2,6-(2,4,6-$Me_3C_6H_2)_2C_6H_3$] were 1.896(2) Å, while an average Sn-N separation of 2.101(3) Å was noted in the tin congener $(Ar''NH)_2Sn$:.[17] As expected, the C_{IPr}-E-N angles in **1**-**3** become narrower as the Group 14 element becomes heavier from a value of 98.49(1)° in **1** to 94.83(6)° in **3**.

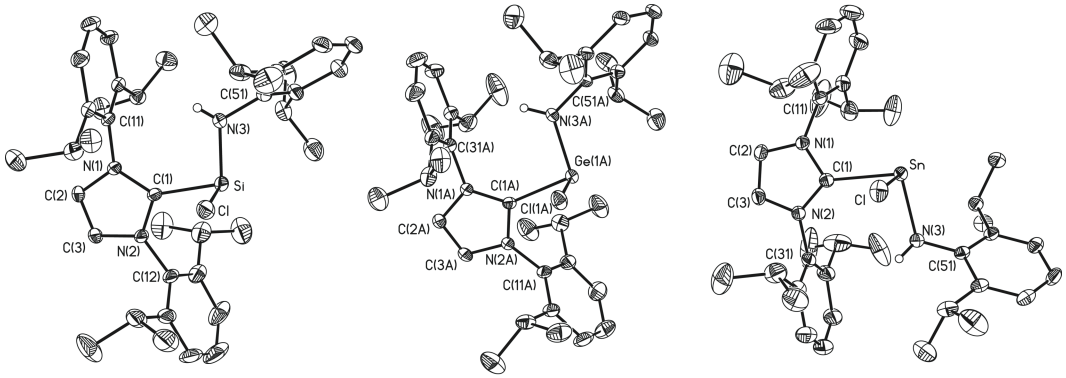

IPr•Si(Cl)NHDipp **1** IPr•Ge(Cl)NHDipp **2** IPr•Sn(Cl)NHDipp **3**

Figure 5.1. Molecular structures of IPr•E(Cl)NHDipp (E = Si, Ge and Sn; **1**, **2** and **3**) with thermal ellipsoids presented at a 30% probability level. All carbon-bound hydrogen atoms and solvate molecules have been omitted for clarity. For compound **2** only one molecule of the two in the asymmetric unit is shown with metrical parameters for the second molecule listed in square brackets. Selected bond lengths [Å] and angles [°]: Compound **1**: Si-C(1) 1.980(3), Si-N(3) 1.765(2), Si-Cl 2.2463(11), N(3)-C(51) 1.433(3); N(1)-C(1)-N(2) 103.7(2), Cl-Si-N(3) 101.87(9), Cl-Si-C(1) 89.88(8), N(3)-Si-C(1) 98.49(11), Si-N(3)-C(51) 118.64(18). Compound **2**: Ge(1A)-C(1A) 2.103(3) [2.093(3)], Ge(1A)-N(3A) 1.903(3) [1.897(2)], Ge(1A)-Cl(1A) 2.3548(9) [2.3632(9)], N(3A)-C(51A) 1.419(4) [1.420(4)]; Cl(1A)-Ge(1A)-N(3A) 99.05(8) [98.23(8)], Cl(1A)-Ge(1A)-C(1A) 88.96(8) [90.14(8)], N(3A)-Ge(1A)-C(1A) 96.14(11) [96.81(11)], Ge(1A)-N(3A)-C(51A) 117.9(2). Compound **3**: Sn-C(1) 2.3220(19), Sn-N(3) 2.1142(16), Sn-Cl(1) 2.4898(6), N(3)-C(51) 1.403(2); Cl-Sn-N(3) 95.21(5), Cl-Sn-C(1) 89.59(5), N(3)-Sn-C(1) 94.83(6), Sn-N(3)-C(51) 116.53(12).

5.3.2 Synthesis of the E(II) aminohydride complexes IPr•EH(BH_3)NHDipp (E = Si, Ge and Sn)

The reaction of IPr•Si(Cl)NHDipp **1** with one equivalent of Li[BH_4] in Et_2O resulted in the formation of a mixture of the new compounds IPr•SiH(BH_3)NHDipp (**4**) and IPr•BH_2NHDipp (**6**) (*vide infra*) along with the known compounds IPr•BH_3[18] and IPrH_2[5b] as shown in Scheme 5.1. The silicon(II) hydride complex **4** was isolated in pure form (34% yield) by cooling a saturated

Et_2O/hexanes solution of the crude product mixture to -35 °C. Initial evidence for the formation of IPr•SiH(BH_3)NHDipp (**4**) was obtained by NMR spectroscopy where a broad Si-*H* resonance was located at 5.13 ppm in the ^{1}H NMR spectrum which was flanked by resolvable ^{29}Si satellites ($^1J_{SiH}$ = 160.3 Hz). The proximal NHDipp group appeared as a doublet resonance at δ = 1.94 ($^3J_{HH}$ = 5.5 Hz) due to coupling of an N-*H* hydrogen atom with the adjacent silicon-bound hydride. The presence of coordinated BH_3 in **4** was confirmed by ^{11}B NMR spectroscopy which gave a quartet resonance at δ -44.1 with an expected coupling constant $^1J_{BH}$, of 89.5 Hz.[5e,19] For comparison, the previously reported Si(II) dihydride adduct IPr•SiH_2•BH_3 gave a -SiH_2 resonance at 3.76 ppm in ^{1}H NMR spectrum and the corresponding silylene-bound BH_3 group was located at -46.2 ppm ($^1J_{BH}$ = 93.0 Hz) by ^{11}B NMR spectroscopy.[5e] The IR spectrum of **4** contained an absorption at 3559 cm^{-1} due to an N-H stretching vibration along with broadened $^{10/11}$B-H stretching modes from 2326 to 2237 cm^{-1} and a sharp Si–H stretching band at 2096 cm^{-1}; the latter vibration is identical in frequency (within experimental error) to the ν(Si-H) band observed in IPr•SiH_2•BH_3.[5e]

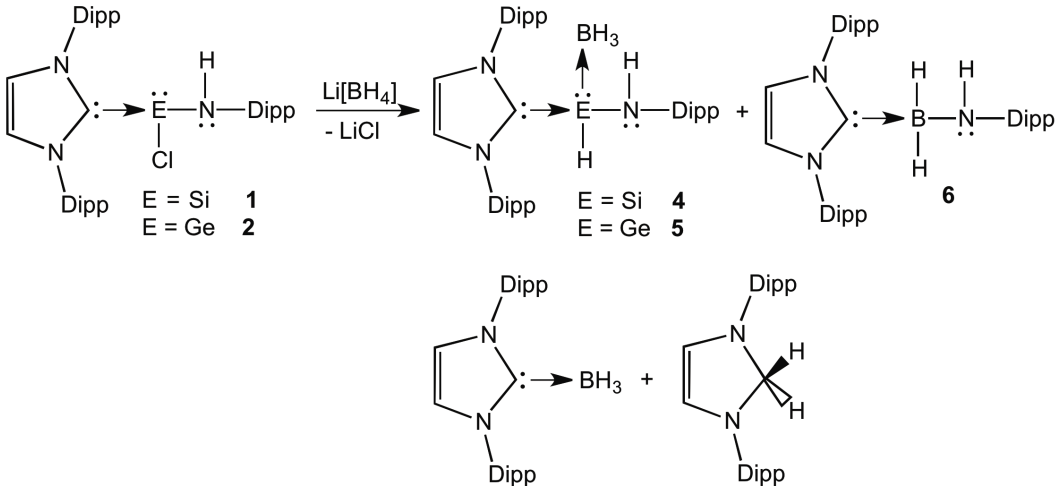

Scheme 5.1. Synthesis of the Si(II) and Ge(II) amidohydride complexes IPr•EH(BH_3)NHDipp (E = Si and Ge; **4** and **5**).

Similarly, when the Ge(II) aminochloride IPr•Ge(Cl)NHDipp (**2**) was reacted with Li[BH_4], the formation of a new product IPr•GeH(BH_3)NHDipp (**5**) was observed as a component of the product mixture that also contained IPr•BH_2NHDipp (**6**), IPr•BH_3 and IPrH_2 (as evidenced by ^{1}H, ^{13}C{^{1}H} and ^{11}B NMR spectroscopy). The borane-capped Ge(II) hydride adduct IPr•GeH(BH_3)NHDipp (**5**) was isolated as an analytically pure solid following a similar procedure as used to obtain the silicon congener **4**. The Ge-*H* unit gave a broad singlet at 5.66 ppm in the ^{1}H NMR spectrum, while a doublet resonance was located at 1.97 ppm and assigned to the amine proton of the -N*H*Dipp group with discernable coupling to a proximal Ge-*H* residue ($^{3}J_{HH}$ = 6.5 Hz). As in IPr•SiH(BH_3)NHDipp (**4**), the BH_3 unit in **5** was identified by ^{11}B NMR spectroscopy, which yielded a quartet resonance at -39.1 ppm. Similarly, the IR spectrum of **5** displayed a characteristic N-H stretching vibration at 3346 cm^{-1} with expected $^{10/11}$B-H and Ge-H stretching vibrations at 2371 to 2253 cm^{-1} and

1997 cm^{-1}, respectively. The ν(Ge-H) band in **5** is in the range expected for Ge(II) compounds with terminal Ge-H residues.[5,20] Additional evidence for the formation of the silylene and germylene borane adducts (**4** and **5**) was obtained by X-ray crystallography and the molecular structures of these adducts are shown in Figure 5.2.

IPr•SiH(BH_3)NHDipp (**4**) and IPr•GeH(BH_3)NHDipp (**5**) each represent formal donor-acceptor complexes of encapsulated heavy Group 14 aminohydride units E(H)-NHDipp with the four-coordinated Si and Ge centers in **4** and **5** located within slightly canted transoid C_{IPr}-E-N-C_{Dipp} bonding arrangements [torsion angles = 177.58(13) and 177.98(19)°, respectively]. The dative C_{IPr}-Si bond length in **4** is 1.9431(15) Å and is considerably longer than the C_{IPr}-Si distance in the donor-acceptor adduct IPr•SiH_2•BH_3 [1.9284(15) Å],[5e] but is similar in length as the carbene-silicon linkages in the formal SiH_2 adduct IPr•SiH_2•BH_2-SiH(B_3H_7)•IPr [1.934(4) Å and 1.944(4) Å].[19b] The adjacent Si-B bond length in **4** is 1.9760(19) Å and lies in the bond length range previously reported for silylene-borane Si(II)-BH_3 adducts involving pseudotetrahedral geometries at silicon [1.965(2) to 1.996(4) Å].[19,21] IPr•GeH(BH_3)NHDipp (**5**) adopts an analogous solid state geometry as its Si(II) congener **4**. The constituent C_{IPr}-Ge and Ge-B bond distances in **5** are 2.020(2) Å and 2.032(3) Å, respectively and of similar values as the C_{IPr}-Ge [2.0148(13) Å] and Ge-B [2.0567(18) Å] interactions present in IPr•GeH_2•BH_3,[5a] suggesting the existence of similar dative bonding interactions in **5**.

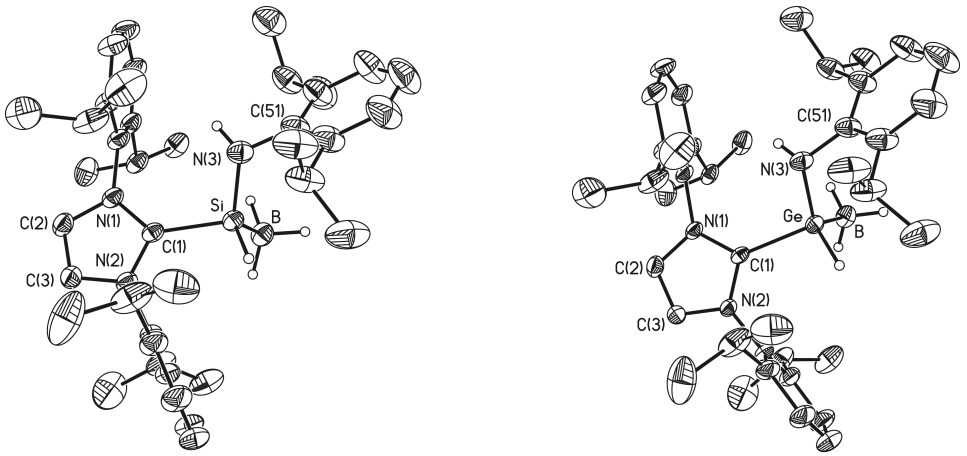

IPr•SiH(BH_3)NHDipp **4** IPr•GeH(BH_3)NHDipp **5**

Figure 5.2 Thermal ellipsoid plots (30% probability level) for IPr•SiH(BH_3)NHDipp (**4**) and IPr•GeH(BH_3)NHDipp (**5**). All carbon-bound hydrogen atoms and solvate molecules have been omitted for clarity. Selected bond lengths [Å] and angles [°]: Compound **4**: Si-C(1) 1.9431(15), Si-B 1.9760(19), Si-H 1.400(16), Si-N(3) 1.7680(14), N(3)-C(51) 1.422(2); N(3)-Si-C(1) 103.00(7), N(3)-Si-B 119.27(8), C(1)-Si-B 110.04(8), Si-N(3)-C(51) 120.63(13). Compound **5**: Ge-C(1) 2.020(2), Ge-B 2.032(3), Ge-H 1.53(2), Ge-N(3) 1.883(2), N(3)-C(51) 1.416(3); N(3)-Ge-C(1) 100.90(10), N(3)-Ge-B 119.36(12), C(1)-Ge-B 110.57(11), Ge-N(3)-C(51) 117.27(18).

Motivated by the above chemistry the tin(II) amide IPr•Sn(Cl)NHDipp **3**, was treated with one equivalent of Li[BH_4] in Et_2O. The rapid evolution of gas was noted accompanied by the precipitation of metallic Sn. Analysis of the soluble fraction of the product mixture by ^{1}H NMR spectroscopy revealed the formation of IPr•BH_2NHDipp (**6**, 50% yield; *vide infra*) IPr•BH_3[17] (37%) and IPrH_2[5b] (13%) with no sign of the target hydridostannylene adduct IPr•SnH(BH_3)NHDipp (Scheme 5.2). Despite the absence of a stable tin hydride product, the remaining species generated from the reaction were also present during the synthesis of IPr•EH(BH_3)NHDipp (E = Si and Ge; **4** and **5**). The formation of similar products in the reaction of **3** with Li[BH_4] can be rationalized

by the decomposition of a putative IPr•SnH(BH_3)NHDipp intermediate; thus far, our attempts to identify this intermediate at low temperatures (*e.g.* -78 to 0 °C) by NMR spectroscopy have been unsuccessful.

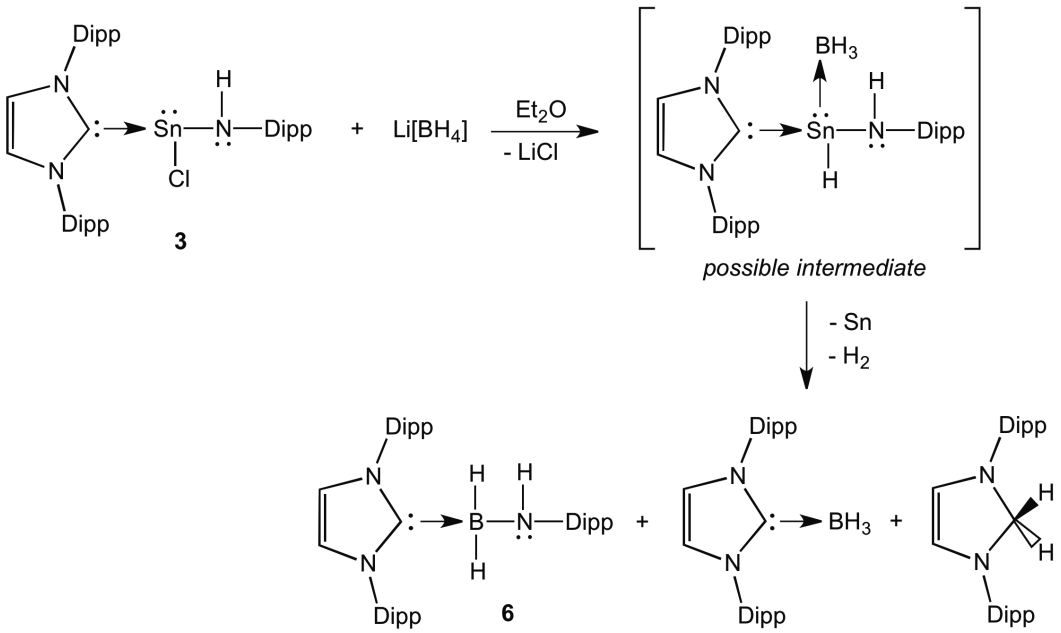

Scheme 5.2 Formation of IPr•BH_2NHDipp (**6**) from the reaction of IPr•Sn(Cl)NHDipp (**3**) with Li[BH_4].

The soluble products formed from the reaction of IPr•Sn(Cl)NHDipp (**3**) with Li[BH_4] were identified by NMR spectroscopy, while the new amino-borane adduct IPr•BH_2NHDipp (**6**) was isolated in pure form as a colorless solid by fractional crystallization (58% yield) from Et_2O. The ^{1}H NMR spectrum of **6** affords a broad singlet at 2.55 ppm belonging to the boron-bound hydrogen atoms within the -BH_2NHDipp unit, while the –N-*H* group yields a signal δ 1.64. The *B*H_2NHDipp residue in **6** resonates to give a broad signal at -16 ppm in the proton-coupled ^{11}B NMR spectrum with no resolvable coupling to hydrogen. The

remaining IPr donor in **6** gave expected ^{1}H and $^{13}C\{^{1}H\}$ NMR resonances for a coordinated NHC unit, for example, the carbenic carbon (C_{IPr}) can be located located as a broad resonance at 150.3 ppm by $^{13}C\{^{1}H\}$ NMR spectroscopy in C_6D_6. An N-H stretching band is present at 3402 cm^{-1} in the IR spectrum of **6** while lower frequency ν(B-H) stretching modes appear between 2310 and 2393 cm^{-1}. Crystals of **6** of suitable quality for single-crystal X-ray analysis were grown by cooling an Et_2O/hexanes solution to - 35 °C, and the refined structure is presented in Figure 5.3. Notably, attempts to directly prepare compound **6** in higher yields by reacting the haloborane adducts, IPr•BH_2X (X = Cl or I)[22] with Li[NHDipp] were unsuccessful and led only to the recovery of the starting materials.

IPr•BH_2NHDipp (**6**) adopts a transoid C_{IPr}-B-N-C_{Dipp} core with an average C_{IPr}-B bond distance of 1.627(5) Å between two crystallographically independent molecules. These interactions are longer than those found in the diborane bisadduct IPr•H_2B-BH_2•IPr [1.577(2) Å],[18] suggesting that a weaker C_{IPr}-B donor-acceptor interaction is present in **6**; however a similar C_{IPr}-B bond length exists in the structurally related four-coordinate azido-borane adduct IPr•BH_2N_3 [1.614(2) Å].[22] The central B-N bond distance in **6** is 1.538(8) Å (*av*g.) and is comparable to the B-N distance found in the four-coordinate azido boron adduct IPr•BH_2N_3 [1.573(2) Å].[22]

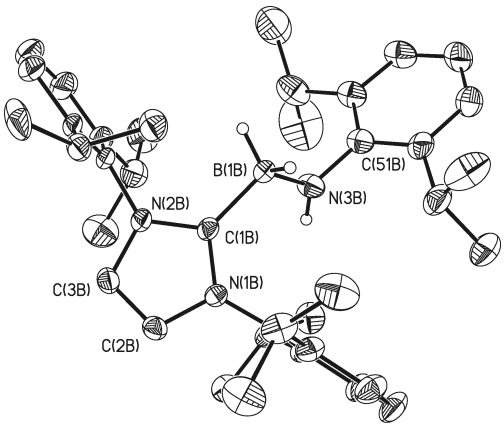

Figure 5.3. Thermal ellipsoid plot (30% probability level) for IPr•BH_2NHDipp (**6**). All carbon-bound hydrogen atoms and solvate Et_2O molecules have been omitted for clarity. Only one molecule in the asymmetric unit is presented, with metrical parameters for a disordered BH_2-NHDipp unit in the *Molecule A* listed in brackets. Selected bond lengths [Å], angles [°]: *Molecule A*: C(1)-B(1) 1.627(4) [1.627(4)], N(3)-B(1) 1.542(8) [1.541(8)], N(3)-C(51) 1.427(4) [1.427(4)]; N(3)-B(1)-C(1) 109.2(3) [108.7(5)], B(1)-N(3)-C(51) 118.1(6) [132.6(7)]. *Molecule B*: C(1)-B(1) 1.626(3), N(3)-B(1) 1.534(3), N(3)-C(51) 1.426(3); N(3)-B(1)-C(1) 112.07(17), B(1)-N(3)-C(51) 116.70(17).

Occasionally during the synthesis of IPr•BH_2NHDipp (**6**) from the reaction of the stannyl chloride adduct IPr•Sn(Cl)NHDipp (**3**) with Li[BH_4] the formation of trace quantities (< 2% by ^{1}H NMR) of a new carbene-containing product was observed. Given the existence of a lone pair on the nitrogen center in **6** and the likely presence of free borane in reaction mixture, it was postulated that the amine-borane adduct IPr•BH_2NHDipp(BH_3) might be the unknown species formed. Therefore, IPr•BH_2NHDipp (**6**) was subsequently treated with a stoichiometric quantity of H_3B•THF to give the new complex IPr•BH_2NHDipp(BH_3) (**7**) in 81% isolated yield as a moisture-sensitive colorless solid. Importantly, the ^{1}H NMR spectrum of **7** matched that of the minor product produced in the reaction of **3** with Li[BH_4], thus confirming our original postulate.

In addition to resonances belonging to the IPr and NHDipp groups in **7**, two broad resonances for BH_2 and BH_3 groups were observed at 3.14 and 2.34 ppm in the ^{1}H NMR spectrum, while the corresponding ^{11}B NMR resonances for these units were located as broad resonances at -14.4 and -16.5 ppm, respectively. The molecular structure of **7** was determined by single-crystal X-ray crystallography (Figure 5.4) and the observed C_{IPr}-B bond distance in this complex [1.607(3) Å] was found to be slightly shorter than the C_{IPr}-B interaction in **6** [1.627(3) Å].

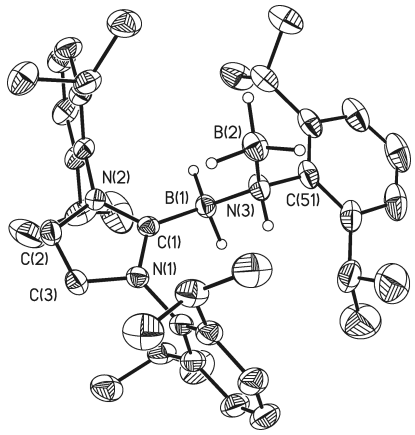

Figure 5.4. Thermal ellipsoid plot (30% probability level) for IPr•BH_2NHDipp(BH_3) (**7**). All carbon-bound hydrogen atoms and hexane solvate molecules have been omitted for clarity. Selected bond lengths [Å] and angles [°]: C(1)-B(1) 1.607(3), N(3)-B(1) 1.585(3), N(3)-B(2) 1.604(3), N(3)-C(51) 1.477(2); N(3)-B(1)-C(1) 113.73(15), N(3)-B(2)-B(1) 124.76(16), C(51)-N(3)-B(1) 109.05(14), C(51)-N(3)-B(2) 115.64(16).

As mentioned above, it was expected that hydridoamide complexes containing the E(H)-NHDipp structural unit (as found within the isolated complexes IPr•EH(BH_3)NHDipp; E = Si and Ge; **4** and **5**) might undergo thermally-induced elimination of H_2NDipp to form new Group 14 element clusters with potentially novel structural and electronic properties. In order to investigate this possibility complexes **4** and **5** were each heated at 70 °C in

toluene. However, in place of isolating products with cluster motifs the formation of a colorless solution over a bright orange precipitate was observed in both instances.[23] The soluble products from the thermal decomposition of **4** and **5** were identified as a mixture of IPr•BH_2NHDipp (**6**), IPr•BH_3 and IPrH_2 (^{1}H and ^{11}B NMR spectroscopy) with no sign of soluble carbene-encapsulated clusters. A similar product mixture was observed in the reaction of IPr•Sn(Cl)NHDipp with Li[BH_4] thus lending support that IPr•SnH(BH_3)NHDipp is a plausible intermediate in this reaction; in line with these results, carbene-bound Sn(II) hydride complexes are generally much less thermally stable than their Si and Ge counterparts.[5] While both **4** and **5** are stable at ambient temperature in the solid state, they both decompose slowly in THF solution (*ca*. 20% decomposition in 10 days at room temperature). The exact mechanism by which IPr•EH(BH_3)NHDipp (E = Si and Ge; **4** and **5**) decompose to give IPr•BH_2NHDipp (**6**) is unclear at this time, however the related isotopologue IPr•BD_2NHDipp (**6D**) can be isolated as a spectroscopically pure product from the reaction of **3** with Li[BD_4], revealing that the BH_2 and BD_2 units are generated directly from Li[BH_4] and Li[BD_4], respectively. One possible pathway to form **6** (and **6D**) involves transmetallation chemistry between a BH_3 unit and the Si- and Ge-bound amide group -NHDipp to yield the transient amino-borane H_2B-NHDipp that is later intercepted by free IPr to form **6** (or **6D**). Although there is no direct evidence at this time, the decomposition of IPr•SnH_2•$W(CO)_5$ yields both free-carbene IPr and IPrH_2 as soluble products,[5b] implying that any IPr•SnH_2 formed by transmetallation chemistry could undergo a similar decomposition process. Related

transmetallation chemistry was used by Power and coworkers to generate the aryltin(II) hydride dimer $[Ar´Sn(\mu\text{-}H)]_2$ from the reaction of $[Ar´Sn\text{-}NMe_2]_2$ with $H_3B•THF$ yielding volatile $[Me_2NBH_2]_x$ as a co-product.[11b]

5.3.3 Thermal Decomposition Study of IPr•BH_2NHDipp

Due to the presence of both acidic ($N\text{-}H^{\delta+}$) and hydridic ($B\text{-}H^{\delta-}$) functionalities in IPr•BH_2NHDipp (**6**) it was proposed that liberation of H_2 from **6** could transpire to yield a carbene-stabilized iminoborane IPr•HB=NDipp.[24] To explore this possibility **6** was combined with the known dehydrogenation catalyst, $[Rh(COD)Cl]_2$ (COD = 1,5 cyclooctadiene),[24a] however, no sign of hydrogen loss was observed at ambient temperature with a 5 mol% catalyst loading. When the reaction mixture was heated to elevated temperature (100 °C) in toluene in the presence of $[Rh(COD)Cl]_2$ the quantitative formation of a new product was detected; a similar product with a new ^{11}B resonance at 28.6 ppm was also detected when **6** was heated to 100 °C in the absence of any Rh complex. This new product was isolated as a colorless, crystalline solid and identified by X-ray crystallography (Figure 5.5) as the novel ring-expanded product $[(HCNDipp)_2CH_2BNHDipp]$ (**8**) (Equation 5.2).

The ^1H NMR spectrum of **8** corroborated the X-ray crystallographic data as a singlet resonance at δ 3.17 corresponding to a -CH_2 moiety was present while the backbone C-H groups of the newly formed boracycle appeared as two distinct doublet resonances at 4.95 and 5.31 ppm ($^3J_{HH}$ = 6.0 Hz). The intraring methylene group appeared at 40.2 ppm in the $^{13}C\{^1H\}$ NMR spectrum while the initially

present resonance due to the carbenic carbon in **6** was absent in **8**. As mentioned, the compound **8** yields an ^{11}B NMR spectrum that contains a signal at 28.6 ppm typical for three-coordinate boron compounds.[25]

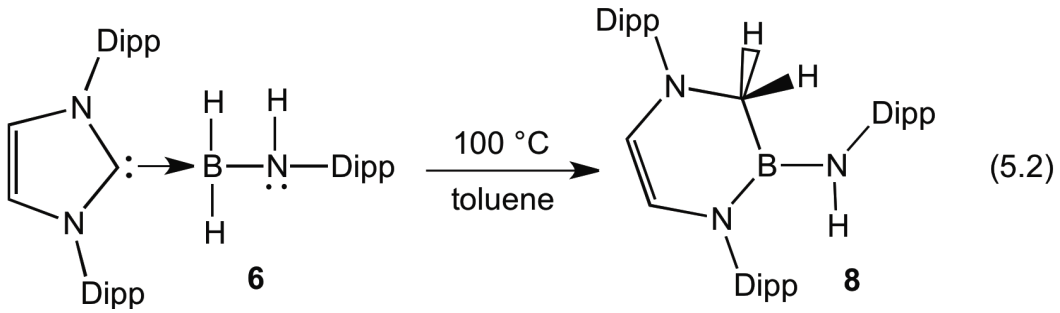

(5.2)

As shown in Figure 5.5, compound **8** consists of a six-membered boron-containing heterocycle with pseudo-envelop conformation. The C(1)-B interatomic distance in **8** was determined to be 1.586(3) Å (average of two crystallographically independent molecules) and is typical for B-C bonds in three-coordinate boranes [*e.g.* 1.589(5) in Ph_3B; 1.574(4) in $[2,6\text{-}(MeO)_2C_6H_3]_3B$].[26] The average endocyclic B-N(1) [1.420(3) Å *avg.*] and exocyclic B-N(3) [1.413(3) Å *avg.*], bond distances in **8** are identical within experimental error to each other and slightly shorter than the B-N bond distances in N-triphenylborazine $[PhNBH]_3$ [1.429(2) to 1.431(2) Å],[27] suggesting the presence of some partial B=N bond character between the boron atom and nitrogen centers in **8**.

In order to gain mechanistic insight into the thermal conversion of IPr•BH_2NHDipp (**6**) into the carbene-activated product **8**, the ring-expansion reaction was repeated with the deuterium isotopologue IPr•BD_2NHDipp (**6D**). Heating a sample of **6D** to 100 °C for 12 h yielded a product with NMR and IR

spectroscopic data consistent with the formation of the isotopically labeled species [(HCNDipp)$_2$CD$_2$BNHDipp] (**8D**). For example, ^{2}H{^{1}H} NMR spectroscopy revealed the exclusive presence of deuterium at the intraring methylene carbon -C*D*$_2$ at 3.17 ppm, while the corresponding resonance was absent in the ^{1}H NMR spectrum. This result revealed that the direct transfer of two boron-bound deuterium atoms from the -BD$_2$ unit in **6D** to the carbene carbon center of the IPr group transpired to form [(HCNDipp)$_2$CD$_2$BNHDipp] **8D** as the sole isotopologue; since no H/D exchange was observed with the pendant –NHDipp group it can be concluded that the N-H bond does not participate in the deuterium migration process (Equation 5.2).

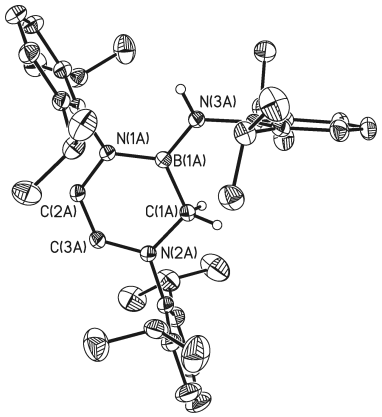

Figure 5.5. Thermal ellipsoid plot (30% probability level) for [(HCNDipp)$_2$CH$_2$BNHDipp] (**8**). All carbon-bound hydrogen atoms except those bonded to C(1) have been omitted for clarity. Only one molecule of the two crystallographically independent molecules is shown; metrical parameters for the second molecule listed in square brackets. Selected bond lengths [Å] and angles [°]: N(1A)-B(1A) 1.4213(18) [1.4183(19)], B(1A)-C(1A) 1.5889(19) [1.583(2)], N(2A)-C(1A) 1.4601(18) [1.4591(18)], N(3A)-B(1A) 1.4148(19) [1.4103(19)]; N(2A)-C(1A)-B(1A) 111.60(11) [111.07(11)], N(1A)-B(1A)-N(3A) 121.62(12) [121.77(13)], N(1A)-B(1A)-C(1A) 117.30(12) [117.51(12)], N(3A)-B(1A)-C(1A) 121.08(12) [120.72(12)].

The observation of C-N bond insertion chemistry involving the N-heterocyclic carbene-borane adduct IPr•BH_2NHDipp (**6**) is significant given the recent role NHC-borane adducts have had in advancing catalytic transformations.[4] In general C-H bond activation of a ring backbone-positioned hydrogen atom is a more commonly observed reactivity pathway in N-heterocyclic carbenes such as IPr.[28] However, recently Hill and coworkers reported a related Be-H mediated C-N bond activation/ring-expansion reaction as the formation of **8**. Moreover the authors provided parallel evidence for the migration of hydrides directly from the main group element beryllium to the carbenic carbon of IPr.[29] Therefore our combined research efforts indicate that main group element hydrides have the potential to undergo C-N bond activation/ring-expansion chemistry even with typically inert NHCs, thus leading to possible catalyst deactivation pathways when NHC-based catalysts (or precatalysts) are exposed to elevated temperatures.

5.4 Conclusion

A series of low-oxidation state heavy Group 14 element aminochlorides stabilized by N-heterocyclic carbenes IPr•E(Cl)NHDipp, **1**-**3** (E = Si, Ge and Sn) have been reported. Compounds **1** and **2** reacted with Li[BH_4] to give the novel low-valent hydrido-amide adducts IPr•EH(BH_3)NHDipp **4** and **5** (E = Si and Ge). The tin congener IPr•Sn(Cl)NHDipp (**3**) reacted with Li[BH_4] to give the amino-borane adduct IPr•BH_2NHDipp (**6**) as the major product, with no evidence for the formation of IPr•SnH(BH_3)NHDipp as a stable species. Thermolysis of **4** and **5** was also investigated as a potential route to Si- and Ge-based clusters, however in each case, the formation of IPr•BH_2NHDipp (**6**) transpired. Upon further heating, IPr•BH_2NHDipp (**6**) participated in a rare ring-expansion reaction involving C-N bond activation of the coordinated N-heterocyclic carbene IPr which was mediated by B-H hydride group transfer chemistry. This ring-expansion reaction shows that N-heterocyclic carbenes are prone to ring-opening processes in the presence of reactive main group hydrides at elevated temperatures, and thus highlights a potential deactivation pathway in NHC-based catalysis.

5.5 Experimental Section

5.5.1 Materials and Instrumentation

All of the reactions were performed using standard Schlenk line techniques under an atmosphere of nitrogen or in an inert atmosphere glove box (Innovative Technology, Inc.). Solvents were dried using Grubbs-type solvent purification system[30] manufactured by Innovative Technology, Inc., degassed (freeze-pump-thaw method) and stored under an atmosphere of nitrogen prior to use. $Li[BH_4]$ and $Li[BD_4]$ were purchased from Aldrich and used as received. 1,3-Bis-(2,6-diisopropylphenyl)-imidazol-2-ylidene (IPr),[31] IPr•$SiCl_2$,[15] IPr•$GeCl_2$,[5a] IPr•$SnCl_2$,[5a] and Li[NHDipp][32] (Dipp = 2,6-$^i Pr_2C_6H_3$) were synthesized following literature procedures. ^1H, $^{13}C\{^1H\}$, ^{29}Si, ^{11}B, and ^{119}Sn NMR spectra were recorded either on Varian iNova-400 or Varian iNova-500 spectrometers and referenced externally to $SiMe_4$ (^1H, $^{13}C\{^1H\}$ and ^{29}Si), $Et_2O•BF_3$ (^{11}B) and $SnMe_4$ (^{119}Sn), respectively by setting the resonance for residual H, D, C, Si, B and Sn at 0.0 ppm. X-ray crystallographic analyses were performed by the X-ray Crystallography Laboratory at the University of Alberta. Elemental analyses were performed by the Analytical and Instrumentation Laboratory at the University of Alberta. Infrared spectra were recorded on a Nicolet IR100 FTIR spectrometer as Nujol mulls between NaCl plates. Melting points were measured in sealed glass capillaries under nitrogen using a MelTemp melting point apparatus and are uncorrected.

5.5.2 X-ray Crystallography

Crystals of suitable quality for X-ray diffraction studies were removed from a vial in a glove box and immediately covered with a thin layer of hydrocarbon oil (Paratone-N). A suitable crystal was then selected, mounted on a glass fiber and quickly placed in a low temperature stream of nitrogen on an X-ray diffractometer.[33] All data were collected using a Bruker APEX II CCD detector/D8 diffractometer using Mo Kα or Cu Kα radiation, with the crystals cooled to -100 °C. The data were corrected for absorption through Gaussian integration from the indexing of the crystal faces.[34] Structures were solved using the direct methods programs SHELXS-97[35] (compound **5**) and SIR97[36] (compounds **2** and **6**) or using the Patterson search/structure expansion facilities within the DIRDIF-2008[37] (compounds **1** and **3**) and SHELXD[38] program suites (compounds **4** and **7**); structure refinement was accomplished using SHELXS-97.[35] Hydrogen atoms were assigned positions based on the sp^2 or sp^3 hybridization geometries of their attached carbon atoms, and were given thermal parameters 20% greater than those of their parent atoms. See Tables 5.1 and 5.2 for a listing of the crystallographic data.

5.5.2.1 Special Refinement Conditions

Compound **2**: The following distance restraints were applied to the disordered solvent diethylether molecules: C-C, 1.530(2) Å; C-O, 1.430(2) Å; C---C, 2.340(4) Å; C---O, 2.420(4) Å.

Compound **3**: Attempts to refine peaks of residual electron density located about the inversion center (½, ½, 0) as disordered half-occupancy solvent tetrahydrofuran oxygen or carbon atoms were unsuccessful. The data were corrected for disordered electron density through use of the SQUEEZE procedure[38] as implemented in *PLATON*.[39] A total solvent-accessible void volume of 790.6 $Å^3$ with a total electron count of 177 (consistent with 4 molecules of solvent tetrahydrofuran, or 0.5 molecules per formula unit of the tin complex) was found in the unit cell in addition to the inversion-disordered solvent tetrahydrofuran molecule located near the inversion center (¼,¼, 0) that had been successfully modeled.

Compound **4**: Attempts to refine peaks of residual electron density as disordered or partial-occupancy solvent *n*-hexane-solvent carbon atoms were unsuccessful. The data were corrected for disordered electron density through use of the SQUEEZE procedure[39] as implemented in *PLATON*.[40] A total solvent-accessible void volume of 2346.5 $Å^3$ with a total electron count of 439 (consistent with 8 molecules of solvent *n*-hexane, or one molecule per formula unit of the {1,3-bis(2,6-diisopropylphenyl)-1,3-dihydro-2*H*-imidazol-2-ylidene}SiH(BH_3)NH(2,6-diisopropylphenyl) molecule) was found in the unit cell.

Compound **5**: Attempts to refine peaks of residual electron density as disordered or partial-occupancy solvent hexane carbon atoms were unsuccessful. The data were corrected for disordered electron density through use of the SQUEEZE procedure[39] as implemented in *PLATON*.[40] A total solvent-accessible void volume of 2392.7 $Å^3$ with a total electron count of 511 (consistent with 8 molecules of solvent hexane or 1 molecule per formula unit of **5**) was found in the unit cell.

Compound **6**: Pairs of distances for atoms C1–B1, B1–N3, and N3–C51 within the disordered BH_2–$NH(C_6H_3{}^iPr_2)$ fragment of *molecule A* were restrained to have the same bond lengths by use of the *SHELXL* **SAME** instruction. Additionally, the phenyl rings within this disordered fragment were constrained to be idealized hexagons. The minor (20%) orientation of the disordered diisopropylphenyl group in molecule B was restrained to have the same geometry as that of the major orientation by use of the *SHELXL* **SAME** instruction. The disordered solvent diethylether molecule had the following restraints applied: C-C, 1.53(1) Å; C-O, 1.43(1) Å; C---O, 2.42(1) Å; C---C, 2.34(1) Å. Finally, the following pairs of atoms were restrained to have equivalent anisotropic displacement parameters: C51A/C, C52A/C, C53A/C, C54A/C, C55A/C, C56A/C, C62A/C, B1A/C and O1S/O2S.

Compound **7**: Attempts to refine peaks of residual electron density as disordered or partial-occupancy solvent *n*-hexane carbon atoms were unsuccessful. The data were corrected for disordered electron density through use of the SQUEEZE procedure[39] as implemented in *PLATON*.[40] A total solvent-accessible void volume

of 1670.0 $Å^3$ with a total electron count of 370 (consistent with 8 molecules of solvent *n*-hexane, or one molecule per formula unit of the {1,3-bis(2,6-diisopropylphenyl)-1,3-dihydro-2*H*-imidazol-2-ylidene}$BH_2NH(BH_3)$(2,6-diisopropylphenyl) molecule) was found in the unit.

5.5.3 Synthetic procedures

5.5.3.1 Synthesis of IPr•Si(Cl)NHDipp (1). A solution of Li[NHDipp] (0.031 g, 0.17 mmol) in 10 mL of cold Et_2O (-35 °C) was added dropwise to a cold (-35 °C) slurry of IPr•$SiCl_2$ (0.081 g, 0.17 mmol) in 3 mL of Et_2O. The resulting mixture was warmed slowly to room temperature and stirred for 20 min to give an orange solution over a white precipitate (LiCl). The reaction mixture was filtered through Celite and then removal of volatiles from the filtrate yielded **1** as a yellow powder. Crystals suitable for X-ray crystallography were grown by cooling a THF/hexanes solution of **1** to -35 °C for 7 days (0.047 g, 45%). ^{1}H NMR (C_6D_6): δ 0.96 (d, $^3J_{HH}$ = 7.0 Hz, 6H, CH(CH_3)$_2$), 1.02 (d, $^3J_{HH}$ = 7.0 Hz, 6H, CH(CH_3)$_2$), 1.14 (d, $^3J_{HH}$ = 7.0 Hz, 6H, CH(CH_3)$_2$), 1.27 (d, $^3J_{HH}$ = 7.0 Hz, 6H, CH(CH_3)$_2$), 1.34 (d, $^3J_{HH}$ = 7.0 Hz, 6H, CH(CH_3)$_2$), 1.48 (d, $^3J_{HH}$ = 7.0 Hz, 6H, CH(CH_3)$_2$), 2.96 (septet, $^3J_{HH}$ = 7.0 Hz, 4H, CH(CH$_3$)$_2$), 3.20 (septet, $^3J_{HH}$ = 7.0 Hz, 2H, CH(CH$_3$)$_2$), 4.14 (s, 1H, -NH), 6.36 (s, 2H, N-CH-), 6.94 (t, $^3J_{HH}$ = 7.5 Hz, 1H, ArH), 6.99-7.19 (m, 8H, ArH). ^{13}C{^{1}H} NMR (C_6D_6): δ 22.9 (CH(*C*H$_3$)$_2$), 23.1 (CH(*C*H$_3$)$_2$), 24.8 (CH(*C*H$_3$)$_2$), 25.2 (CH(*C*H$_3$)$_2$), 25.8 (CH(*C*H$_3$)$_2$), 25.9 (CH(*C*H$_3$)$_2$), 27.8 (CH(*C*H$_3$)$_2$), 28.8 (*C*H(CH$_3$)$_2$), 29.5 (*C*H(CH$_3$)$_2$), 121.3 (Ar*C*), 123.7 (Ar*C*), 123.9 (Ar*C*), 124.3 (Ar*C*), 124.5 (-N-*C*H-), 131.4 (Ar*C*), 133.7 (Ar*C*), 140.5 (Ar*C*), 141.9 (Ar*C*), 145.8 (Ar*C*), 146.3 (Ar*C*), 171.7 (N-*C*-N). ^{29}Si NMR (C_6D_6): δ -6.0.

IR (Nujol/cm^{-1}): 3360 (s, υN-H). Anal. Calcd. for $C_{39}H_{54}ClN_3Si$: C, 74.54; H, 8.66; N, 6.69. Found: C, 74.54; H, 8.49; N, 6.58. Mp (°C): 179-181.

5.5.3.2 Synthesis of IPr•Ge(Cl)NHDipp (2). A solution of Li[NHDipp] (0.18 g, 0.98 mmol) in 12 mL of cold Et_2O (-35 °C) was added dropwise to a cold (-35 °C) slurry of IPr•$GeCl_2$ (0.51 g, 0.96 mmol) in 5 mL of Et_2O. The resulting mixture was warmed slowly to room temperature and stirred overnight to form a pale yellow solution over a white precipitate (LiCl). The reaction mixture was then filtered through Celite and the volatiles were removed *in vacuo* to yield **2** as a pale yellow powder (0.63 g, 98%). Crystals suitable for X-ray crystallography were grown by cooling a saturated Et_2O solution of **2** layered with hexanes to -35 °C. ^{1}H NMR (C_6D_6): δ 0.96 (d, $^3J_{HH}$ = 7.0 Hz, 6H, CH(CH_3)$_2$), 1.02 (d, $^3J_{HH}$ = 7.0 Hz, 6H, CH(CH_3)$_2$), 1.08 (d, $^3J_{HH}$ = 7.0 Hz, 6H, CH(CH_3)$_2$), 1.28 (d, $^3J_{HH}$ = 7.0 Hz, 6H, CH(CH_3)$_2$), 1.36 (d, $^3J_{HH}$ = 7.0 Hz, 6H, CH(CH_3)$_2$), 1.47 (d, $^3J_{HH}$ = 7.0 Hz, 6H, CH(CH_3)$_2$), 2.96 (septet, $^3J_{HH}$ = 7.0 Hz, 4H, CH(CH$_3$)$_2$), 3.20 (septet, $^3J_{HH}$ = 7.0 Hz, 2H, CH(CH$_3$)$_2$), 4.11 (s, 1H, -NH), 6.43 (s, 2H, N-CH-), 6.88 (t, $^3J_{HH}$ = 7.5 Hz, 1H, ArH), 7.01-7.20 (m, 8H, ArH). ^{13}C{^{1}H} NMR (C_6D_6): δ 23.1 (CH(*C*H$_3$)$_2$), 23.2 (CH(*C*H$_3$)$_2$), 25.2 (CH(*C*H$_3$)$_2$), 25.8 (CH(*C*H$_3$)$_2$), 25.86 (CH(*C*H$_3$)$_2$), 25.91 (CH(*C*H$_3$)$_2$), 27.6 (*C*H(CH$_3$)$_2$), 29.3 (*C*H(CH$_3$)$_2$), 29.4 (*C*H(CH$_3$)$_2$), 119.8 (Ar*C*), 123.8 (Ar*C*), 124.43 (Ar*C*), 124.46 (Ar*C*), 124.51 (-N-*C*H-), 131.4 (Ar*C*), 133.6 (Ar*C*), 139.1 (Ar*C*), 144.3 (Ar*C*), 145.9 (Ar*C*), 146.7 (Ar*C*), 177.1 (N-*C*-N). IR (Nujol/cm^{-1}): 3371 (br, υN-H). Anal. Calcd. for $C_{39}H_{54}ClN_3Ge$: C, 69.50; H, 8.23; N, 6.23. Found: C, 69.20; H, 8.22; N, 5.73. Mp (°C): 152-154.

5.5.3.3 Synthesis of IPr•Sn(Cl)NHDipp (3). A cold (-35 °C) solution of Li[NHDipp] (0.23 g, 1.2 mmol) in 12 mL of Et_2O was added dropwise to a cold (-35 °C) slurry of IPr•$SnCl_2$ (0.71 g, 1.2 mmol) in 5 mL of Et_2O. The resulting mixture was warmed slowly to room temperature and stirred for 2 h to give a beige solution over white a precipitate (LiCl). The reaction mixture was then filtered through Celite and the volatiles were removed *in vacuo* to afford **3** as a pale brown powder (0.83 g, 85%). X-ray quality crystals of **3** (pale yellow) were grown by cooling a THF solution layered with hexanes to -35 °C. ^{1}H NMR (C_6D_6): δ 0.96 (d, $^3J_{HH}$ = 7.0 Hz, 6H, CH(CH_3)$_2$), 1.03 (d, $^3J_{HH}$ = 7.0 Hz, 6H, CH(CH_3)$_2$), 1.12 (d, $^3J_{HH}$ = 7.0 Hz, 6H, CH(CH_3)$_2$), 1.30 (d, $^3J_{HH}$ = 7.0 Hz, 6H, CH(CH_3)$_2$), 1.36 (d, $^3J_{HH}$ = 7.0 Hz, 6H, CH(CH_3)$_2$), 1.48 (d, $^3J_{HH}$ = 7.0 Hz, 6H, CH(CH_3)$_2$), 2.92 (septet, $^3J_{HH}$ = 7.0 Hz, 4H, CH(CH$_3$)$_2$), 3.10 (septet, $^3J_{HH}$ = 7.0 Hz, 2H, CH(CH$_3$)$_2$), 3.82 (s, 1H, -NH), 6.46 (s, 2H, N-CH-), 6.83 (t, $^3J_{HH}$ = 7.5 Hz, 1H, ArH), 7.03-7.22 (m, 8H, ArH). ^{13}C{^{1}H} NMR (125 MHz, C_6D_6): δ 23.1 (CH(*C*H$_3$)$_2$), 23.4 (CH(*C*H$_3$)$_2$), 25.1 (CH(*C*H$_3$)$_2$), 25.73 (CH(*C*H$_3$)$_2$), 25.76 (CH(*C*H$_3$)$_2$), 25.81 (CH(*C*H$_3$)$_2$), 27.5 (*C*H(CH$_3$)$_2$), 29.2 (*C*H(CH$_3$)$_2$), 29.4 (*C*H(CH$_3$)$_2$), 117.7 (Ar*C*), 123.4 (Ar*C*), 124.4 (Ar*C*), 124.6 (Ar*C*), 131.3 (-N-*C*H-), 133.9 (Ar*C*), 137.1 (Ar*C*), 146.1 (Ar*C*), 146.2 (Ar*C*), 146.6 (Ar*C*), 147.2 (Ar*C*), 184.8 (N-*C*-N). ^{119}Sn{^{1}H} NMR (C_6D_6): δ -93.2. IR (Nujol/cm^{-1}): 3358 (m, υN-H). Anal. Calcd. for $C_{39}H_{54}ClN_3Sn$: C, 65.15; H, 7.57; N, 5.84. Found: C, 64.67; H, 7.93; N, 5.82. Mp (°C): 180-182.

5.5.3.4 Reaction of 1 with Li[BH_4]: Synthesis of IPr•SiH(BH_3)NHDipp (4). To a mixture of **1** (77 mg, 0.12 mmol) and Li[BH_4] (2.9 mg, 0.13 mmol) was added

10 mL of cold (-35 °C) Et_2O. The reaction mixture was then warmed to room temperature and stirred overnight to give a yellow solution over a white precipitate (LiCl). The precipitate was allowed to settle and the resulting supernatant was filtered through Celite to obtain a bright yellow solution. Removal of the volatiles from the filtrate yielded a pale yellow solid which was identified as a mixture of **4** (*ca*. 47%), **6** (*ca*. 3%), IPr•BH_3 (*ca*. 31%), and $IPrH_2$ (*ca*. 10%) by ^{1}H NMR spectroscopy. Spectroscopically pure **4** was isolated by fractional crystallization (cooling a saturated Et_2O solution of the crude material layered with hexanes to -35 °C). Crystals of **4** suitable for X-ray crystallography were grown by cooling an Et_2O solution layered with hexanes to -35 °C for 3 days (25 mg, 34%). ^{1}H NMR (C_6D_6): δ 0.01-0.62 (br. quartet, $^1J_{BH}$ = 89.5 Hz, 3H, BH_3), 0.93 (d, $^3J_{HH}$ = 6.9 Hz, 6H, CH(CH_3)$_2$), 0.97 (d, $^3J_{HH}$ = 6.9 Hz, 6H, CH(CH_3)$_2$), 0.99 (d, $^3J_{HH}$ = 6.9 Hz, 6H, CH(CH_3)$_2$), 1.27 (d, $^3J_{HH}$ = 6.9 Hz, 6H, CH(CH_3)$_2$), 1.38 (d, $^3J_{HH}$ = 6.9 Hz, 6H, CH(CH_3)$_2$), 1.47 (d, $^3J_{HH}$ = 6.9 Hz, 6H, CH(CH_3)$_2$), 1.94 (d, $^3J_{HH}$ = 5.5 Hz, 1H, -N*H*), 2.88 (septet, $^3J_{HH}$ = 6.9 Hz, 4H, C*H*(CH$_3$)$_2$), 3.19 (septet, $^3J_{HH}$ = 6.9 Hz, 2H, C*H*(CH$_3$)$_2$), 5.12 (s, 1H, -Si*H*-, satellites: $^1J_{H\text{-}Si}$ = 163.0 Hz), 6.39 (s, 2H, N-C*H*-), 7.01-7.19 (m, 9H, Ar*H*). ^{13}C{^{1}H} NMR (125 MHz, C_6D_6): δ 22.7 (CH(*C*H$_3$)$_2$), 22.9 (CH(*C*H$_3$)$_2$), 24.7 (CH(*C*H$_3$)$_2$), 25.5 (CH(*C*H$_3$)$_2$), 25.9 (CH(*C*H$_3$)$_2$), 26.1 (CH(*C*H$_3$)$_2$), 27.5 (*C*H(CH$_3$)$_2$), 29.3 (*C*H(CH$_3$)$_2$), 29.4 (*C*H(CH$_3$)$_2$), 123.1 (Ar*C*), 123.6 (Ar*C*), 124.6 (Ar*C*), 125.2 (Ar*C*), 131.7 (-N-*C*H-), 133.6 (Ar*C*), 139.9 (Ar*C*), 143.4 (Ar*C*), 145.7 (Ar*C*), 146.2 (Ar*C*), 166.4 (N-*C*-N). ^{11}B{^{1}H} NMR (C_6D_6): δ - 44.1 (s). ^{11}B NMR (C_6D_6): δ -44.1 (q, $^1J_{BH}$ = 89.5 Hz). IR (Nujol/cm^{-1}): 3359 (m, υN-H), 2326 (br, υB-H), 2237 (m, υB-H), 2096 (m,

υSi-H). Anal. Calcd. for $C_{39}H_{58}BN_3Si$: C, 77.07; H, 9.62; N, 6.91. Found: C, 77.07; H, 9.02; N, 6.30. Mp (°C): 182-184.

5.5.3.5 Reaction of 2 with Li[BH_4]: Synthesis of IPr•GeH(BH_3)NHDipp (5). Compound **2** (88 mg, 0.13 mmol) and Li[BH_4] (2.8 mg, 0.13 mmol) were combined in 10 mL of cold (-35 °C) Et_2O. The reaction mixture was stirred overnight at ambient temperature to give an orange solution with yellow precipitate. The resulting mixture was then filtered through Celite to give an orange filtrate. Removal of the volatiles from the filtrate yielded a yellow solid which was identified as a mixture of **5** (*ca*. 55%), **6** (*ca*. 30%), IPr•BH_3 (*ca*. 5%) and $IPrH_2$ (*ca*. 7%) by ^{1}H NMR spectroscopy. Spectroscopically pure **5** was isolated by fractional crystallization (cooling a saturated Et_2O solution of the crude material layered with hexanes to -35 °C). Crystals suitable for X-ray crystallography were grown by cooling an Et_2O solution layered with hexanes to -35 °C for 3 days (43 mg, 50%). ^{1}H NMR (C_6D_6): δ 0.93 (d, $^3J_{HH}$ = 6.5 Hz, 6H, CH(CH_3)$_2$), 0.97 (d, $^3J_{HH}$ = 7.0 Hz, 6H, CH(CH_3)$_2$), 1.01 (d, $^3J_{HH}$ = 7.0 Hz, 6H, CH(CH_3)$_2$), 1.29 (d, $^3J_{HH}$ = 6.5 Hz, 6H, CH(CH_3)$_2$), 1.41 (d, $^3J_{HH}$ = 7.0 Hz, 6H, CH(CH_3)$_2$), 1.48 (d, $^3J_{HH}$ = 6.5 Hz, 6H, CH(CH_3)$_2$), 1.97 (d, $^3J_{HH}$ = 6.5 Hz, 1H, -N*H*), 2.84 (septet, $^3J_{HH}$ = 7.0 Hz, 2H, C*H*(CH$_3$)$_2$), 2.85 (septet, $^3J_{HH}$ = 6.5 Hz, 2H, C*H*(CH$_3$)$_2$), 3.20 (septet, $^3J_{HH}$ = 7.0 Hz, 2H, C*H*(CH$_3$)$_2$), 5.67 (br, 1H, -Ge*H*), 6.41 (s, 2H, N-C*H*-), 6.95-7.21 (m, 9H, Ar*H*); the –BH_3 unit was not located. ^{13}C{^{1}H} NMR (125 MHz, C_6D_6): δ 22.7 (CH(*C*H$_3$)$_2$), 22.9 (CH(*C*H$_3$)$_2$), 24.7 (CH(*C*H$_3$)$_2$), 25.4 (CH(*C*H$_3$)$_2$), 25.8 (CH(*C*H$_3$)$_2$), 25.9 (CH(*C*H$_3$)$_2$), 27.3 (*C*H(CH$_3$)$_2$), 29.3 (*C*H(CH$_3$)$_2$), 29.4 (*C*H(CH$_3$)$_2$), 121.9 (Ar*C*), 123.5 (Ar*C*), 124.6 (Ar*C*), 125.2

(Ar*C*), 131.7 (-N-*C*H-), 133.5 (Ar*C*), 141.2 (Ar*C*), 143.2 (Ar*C*), 145.7 (Ar*C*), 146.3 (Ar*C*), 169.7 (N-*C*-N). $^{11}B\{^{1}H\}$ NMR (C_6D_6): δ - 39.0. IR (Nujol/cm^{-1}): 3346 (m, υN-H), 2371 (br, υB-H), 2253 (sh, υB-H), 1997 (m, υGe-H). Anal. Calcd. for $C_{39}H_{58}BN_3Ge$: C, 71.80; H, 8.96; N, 6.44. Found: C, 71.57; H, 9.11; N, 5.87. Mp (°C): 151-153 (decomp., turns red), 159-161 (melts).

5.5.3.6 Reaction of 3 with Li[BH_4]: Synthesis of IPr•BH_2NHDipp (6). To a mixture of **3** (366 mg, 0.51 mmol) and Li[BH_4] (11.1 mg, 0.51 mmol) was added 12 mL of cold Et_2O (-35 °C). The reaction mixture was stirred for 2 h at ambient temperature to give a clear solution along with an insoluble black precipitate. The precipitate was then allowed to settle and the mother liquor was filtered through Celite. Removal of the volatiles from the filtrate yielded **6** as a white solid which contained a mixture of **6** (*ca*. 58% yield), IPr•BH_3 (*ca*. 30% yield) and IPrH_2 (*ca*. 12% yield) as evidenced by ^{1}H NMR spectroscopy. Spectroscopically pure **6** was isolated by fractional crystallization (cooling a saturated Et_2O solution of the crude material to -35 °C). Crystals suitable for X-ray crystallography were grown by cooling an Et_2O solution to -35 °C for 2 days (163 mg, 55%). ^{1}H NMR (C_6D_6): δ 1.03 (d, $^{3}J_{HH}$ = 7.0 Hz, 12H, CH(CH_3)$_2$), 1.09 (d, $^{3}J_{HH}$ = 7.0 Hz, 12H, CH(CH_3)$_2$), 1.36 (d, $^{3}J_{HH}$ = 7.0 Hz, 12H, CH(CH_3)$_2$), 1.64 (t, $^{3}J_{HH}$ = 6.5 Hz, 1H, -N*H*), 2.55 (s, 2H, -BH_2; located in the $^{1}H\{^{11}B\}$ NMR spectrum), 2.74 (septet, $^{3}J_{HH}$ = 7.0 Hz, 4H, C*H*(CH$_3$)$_2$), 3.01 (septet, $^{3}J_{HH}$ = 7.0 Hz, 2H, C*H*(CH$_3$)$_2$), 6.35 (s, 2H, N-C*H*-), 6.98 (t, $^{3}J_{HH}$ = 7.5 Hz, 2H, Ar*H*), 7.08 (d, $^{3}J_{HH}$ = 7.5 Hz, 1H, Ar*H*), 7.10 (d, $^{3}J_{HH}$ = 7.5 Hz, 2H, Ar*H*), 7.23 (t, $^{3}J_{HH}$ = 7.5 Hz, 4H, Ar*H*). $^{13}C\{^{1}H\}$ NMR (C_6D_6): δ 22.9 (CH(*C*H$_3$)$_2$), 25.3 (CH(*C*H$_3$)$_2$), 25.4 (CH(*C*H$_3$)$_2$), 27.1 (*C*H(CH$_3$)$_2$), 29.2

(*C*H(CH_3)$_2$), 119.5 (Ar*C*), 122.3 (Ar*C*), 123.3 (Ar*C*), 124.2 (Ar*C*), 130.6 (-N-*C*H-), 134.5 (Ar*C*), 140.9 (Ar*C*), 145.9 (Ar*C*), 150.3 (N-*C*-N). $^{11}B\{^1H\}$ NMR (C_6D_6): δ –16.5. ^{11}B NMR (C_6D_6): δ –16.5 (t, broad) . IR (Nujol/cm^{-1}): 3373 (br, υN-H), 2393 (sh, υB-H), 2310 (br, υB-H). Anal. Calcd. for $C_{39}H_{56}BN_3$: C, 81.08; H, 9.77; N, 7.27. Found: C, 81.05; H, 9.92; N, 7.36. Mp (°C): 145-147.

5.5.3.7 Synthesis of IPr•BD_2NHDipp (6D). To a mixture of **3** (430 mg, 0.51 mmol) and Li[BD_4] (15.5 mg, 0.60 mmol) was added 12 mL Et_2O. The reaction mixture was stirred for 2 h at ambient temperature to give a clear solution over a black precipitate. The precipitate was then allowed to settle and the mother liquor was filtered through Celite to give a colorless filtrate. Removal of the volatiles from the filtrate yielded a white solid from which spectroscopically pure **6D** was isolated (188 mg, 54%) by fractional crystallization following the same procedure as **6**. ^1H NMR (C_6D_6): essentially same as **6** except the N-H resonance (δ = 1.64) was observed as a singlet. $^{11}B\{^1H\}$ NMR (C_6D_6): same as compound **6**. $^2H\{^1H\}$ NMR (C_6D_6): δ 2.53 (br, -BD_2-). IR (Nujol/cm^{-1}): similar to **6** except for the absence of B-H stretches; the B-D stretching frequencies were observed at 1724 (sh, υB-D) and 1630 (br, υB-D).

5.5.3.8 Reaction of 6 with H_3B•THF: Synthesis of IPr•BH_2NHDipp(BH_3) (7). To a solution of **6** (86 mg, 0.15 mmol) in 10 mL of Et_2O was added H_3B•THF (0.16 mL, 1.0 M solution in THF) dropwise. The reaction mixture was stirred overnight at room temperature to give a colorless solution and the volatiles were then removed *in vacuo* to yield a white powder. The powder was washed with 4

mL of hexanes and dried to afford spectroscopically pure **7**. Crystals of **7** suitable for X-ray crystallography were grown by cooling saturated Et_2O solution of **7** layered with hexanes to -35 °C for 4 days (71 mg, 81%). ^{1}H NMR (C_6D_6): δ 0.93 (d, $^3J_{HH}$ = 6.5 Hz, 3H, CH(CH_3)$_2$), 0.96 (d, $^3J_{HH}$ = 6.5 Hz, 9H, CH(CH_3)$_2$), 1.01 (d, $^3J_{HH}$ = 6.5 Hz, 3H, CH(CH_3)$_2$), 1.06 (d, $^3J_{HH}$ = 6.5 Hz, 9H, CH(CH_3)$_2$), 1.38-1.42 (overlapping broad doublets, $^3J_{HH}$ = 6.5 Hz, 9H, CH(CH_3)$_2$), 1.45 (d, $^3J_{HH}$ = 6.5 Hz, 3H, CH(CH_3)$_2$), 1.68 (septet, $^3J_{HH}$ = 6.5 Hz, 1H, CH(CH$_3$)$_2$), 2.34 (br, 3H, -BH_3), 2.90 (septet, $^3J_{HH}$ = 6.5 Hz, 2H, CH(CH$_3$)$_2$), 3.14 (br, 2H, -BH_2-), 4.15 (septet, $^3J_{HH}$ = 6.5 Hz, 1H, CH(CH$_3$)$_2$), 4.36 (br, 2H, CH(CH$_3$)$_2$), 4.70 (s, 1H, -NH-), 6.55 (s, 2H, N-CH-), 6.87-7.25 (m, 9H, ArH). ^{13}C{^{1}H} NMR (C_6D_6): δ 22.5 (CH(*C*H$_3$)$_2$), 22.9 (CH(*C*H$_3$)$_2$), 23.9 (CH(*C*H$_3$)$_2$), 24.6 (CH(*C*H$_3$)$_2$), 24.8 (CH(*C*H$_3$)$_2$), 25.6 (CH(*C*H$_3$)$_2$), 25.7 (CH(*C*H$_3$)$_2$), 26.2 (CH(*C*H$_3$)$_2$), 26.3 (CH(*C*H$_3$)$_2$), 27.7 (CH(*C*H$_3$)$_2$), 28.2 (*C*H(CH$_3$)$_2$), 28.9 (*C*H(CH$_3$)$_2$), 29.0 (*C*H(CH$_3$)$_2$), 122.4 (Ar*C*), 122.8 (-N-*C*H-), 124.4 (Ar*C*), 124.5 (Ar*C*), 124.7 (Ar*C*), 126.8 (Ar*C*), 130.7 (Ar*C*), 134.1 (Ar*C*), 138.6 (Ar*C*), 144.3 (-N-*C*H-), 145.5 (Ar*C*), 146.5 (N-*C*-N). ^{11}B{^{1}H} NMR (C_6D_6): δ -14.4 (-*B*H$_2$-), -16.5 (-*B*H$_3$). IR (Nujol/cm^{-1}): 3321 (m, υN-H), 2484 (m, υB-H), 2388 (sh, υB-H), 2308 (s, υB-H), 2266 (s, υB-H). Anal. Calcd. for $C_{39}H_{59}B_2N_3$: C, 79.19; H, 10.05; N, 7.10. Found: C, 78.99; H, 10.13; N, 6.98. Mp (°C): 156-158.

5.5.3.9 Thermolysis of IPr•BH$_2$NHDipp: Synthesis of [(HCNDipp)$_2$CH$_2$BNHDipp] (8). A solution of **6** (142 mg, 0.25 mmol) in 10 mL of toluene was heated at 100 °C for 12 h to form a pale yellow solution. The reaction mixture was then filtered through Celite and the volatiles were removed

in vacuo to yield crude **8** as a bright yellow oil. Crystals of **8** suitable for X-ray crystallography were grown by cooling a saturated hexanes solution of **8** layered with $(Me_3Si)_2O$ to -35 °C for 4 days (113 mg, 80%). ^{1}H NMR (C_6D_6): δ 1.14 (d, $^3J_{HH}$ = 7.0 Hz, 9H, CH(C*H*$_3$)$_2$), 1.20 (d, $^3J_{HH}$ = 7.0 Hz, 9H, CH(C*H*$_3$)$_2$), 1.31 (d, $^3J_{HH}$ = 7.0 Hz, 9H, CH(C*H*$_3$)$_2$), 1.34 (d, $^3J_{HH}$ = 7.0 Hz, 9H, CH(C*H*$_3$)$_2$), 3.17 (s, 2H, -C*H*$_2$-), 3.45 (septet, $^3J_{HH}$ = 7.0 Hz, 2H, C*H*(CH$_3$)$_2$) 3.58 (septet, $^3J_{HH}$ = 7.0 Hz, 2H, C*H*(CH$_3$)$_2$), 3.67 (s, 1H, -N*H*), 3.85 (septet, $^3J_{HH}$ = 7.0 Hz, 2H, C*H*(CH$_3$)$_2$), 4.95 (d, $^3J_{HH}$ = 6.0 Hz, 1H, N-C*H*-), 5.31 (d, $^3J_{HH}$ = 6.0 Hz, 1H, N-C*H*-), 6.95-7.22 (m, 9H, Ar*H*). ^{13}C{^{1}H} NMR (C_6D_6): δ 23.4 (CH(*C*H$_3$)$_2$), 23.8 (CH(*C*H$_3$)$_2$), 24.9 (CH(*C*H$_3$)$_2$), 25.7 (CH(*C*H$_3$)$_2$), 27.8 (*C*H(CH$_3$)$_2$), 28.1 (*C*H(CH$_3$)$_2$), 29.4 (*C*H(CH$_3$)$_2$), 40.2 (-*C*H$_2$-), 109.5 (-N-*C*H-), 118.7 (-N-*C*H-), 122.9 (Ar*C*), 124.1 (Ar*C*), 124.2 (Ar*C*), 126.2 (Ar*C*), 135.9 (Ar*C*), 140.1 (Ar*C*), 145.3 (Ar*C*), 145.7 (Ar*C*), 147.2 (Ar*C*), 147.9 (N-*C*-N). ^{11}B{^{1}H} NMR (C_6D_6): δ 28.6. IR (Nujol/cm^{-1}): 3391 (br, υN-H). Anal. Calcd. for $C_{39}H_{56}BN_3$: C, 81.08; H, 9.77; N, 7.27. Found: C, 81.17; H, 9.74; N, 7.23. Mp (°C): 124-126.

5.5.3.10 Thermolysis of IPr•BD$_2$NHDipp: Synthesis of [(HCNDipp)$_2$CD$_2$BNHDipp] (8D). A solution of **6D** (85 mg, 0.15 mmol) in 10 mL of toluene was heated at 100 °C for 12 h to give a pale yellow solution. The reaction was then filtered through Celite and the volatiles were removed *in vacuo* to yield **8D** as a bright yellow oil (57 mg, 79%). ^{1}H NMR (C_6D_6): essentially same as compound **8** except the absence of a resonance for the -C*H*$_2$- group (δ 3.17). ^{2}H{^{1}H} NMR (C_6H_6): δ 3.16 (–C*D*$_2$-).

Table 5.1: Crystallographic Data for **1**, **2**•Et_2O and **3**•THF.

Compound	**1**	**2**•Et_2O	**3**•THF
Formula	$C_{39}H_{54}ClN_3Si$	$C_{43}H_{64}ClGeN_3O$	$C_{43}H_{62}ClN_3OSn$
formula weight	628.39	747.01	791.10
crystal system	monoclinic	monoclinic	monoclinic
space group	$P2_1/n$	$P2_1/n$	$C2/c$
a(Å)	19.8052 (17)	19.4351 (11)	43.642 (3)
b (Å)	12.3167 (11)	23.3885 (14)	12.0988 (8)
c (Å)	15.8436 (14)	20.1177 (12)	16.7555 (11)
α (deg)	90	90	90
β (deg)	98.8045 (12)	104.8410 (10)	104.3880 (8)
γ (deg)	90	90	90
V (Å^3)	3819.3 (6)	8839.6 (9)	8569.8 (10)
Z	4	8	8
ρ (g cm^{-3})	1.093	1.123	1.226
abs coeff (mm^{-1})	0.160	0.786	0.692
T (K)	173(1)	173(1)	173(1)
$2\theta_{max}$ (°)	51.40	50.50	54.98
total data	27859	17242	37306
unique data (R_{int})	7257 (0.0946)	17242 (0.0428)	9835 (0.0143)
Obs data [$I > 2\sigma(I)$]	4223	14046	9255
params	401	857	444
R_1 [$I > 2\sigma(I)$][a]	0.0527	0.0483	0.0309
wR_2 [all data][a]	0.1378	0.1527	0.0786
max/min $\Delta\rho$ (e$^-$ Å^{-3})	0.256 /-0.304	0.843/-0.598	0.677/-0.627

[a] $R_1 = \Sigma \big| \, |F_o| - |F_c| \, \big| / \Sigma |F_o|$; $wR_2 = [\Sigma\, w(F_o^2 - F_c^2)^2 / \Sigma\, w(F_o^4)]^{1/2}$.

Table 5.2: Crystallographic Data for **4, 5** and **6**•0.4Et_2O.

Compound	**4**	**5**	**6**•0.4Et_2O
Formula	$C_{45}H_{72}BN_3Si$	$C_{45}H_{72}BGeN_3$	$C_{40.6}H_{60}BN_3O_{0.4}$
formula weight	693.96	738.46	607.33
crystal system	monoclinic	monoclinic	monoclinic
space group	*I*2/*a*	*I*2/*a*	*C*2/*c*
a(Å)	23.8535 (4)	23.8622 (12)	47.114 (3)
b (Å)	14.3021 (2)	14.3819 (7)	12.1840 (7)
c (Å)	27.0924 (4)	27.3526 (14)	29.0791 (17)
α (deg)	90	90	90
β (deg)	95.4166 (9)	95.6700 (10)	110.5450 (7)
γ (deg)	90	90	90
V (Å^3)	9201.4 (2)	9341.0 (8)	15630.6 (16)
Z	8	8	16
ρ (g cm^{-3})	1.002	1.050	1.032
abs coeff (mm^{-1})	0.663	0.686	0.060
T (K)	173(1)	173(1)	173(1)
$2\theta_{max}$ (°)	51.40	50.50	50.50
total data	27859	32964	52431
unique data (R_{int})	7257 (0.0946)	8477 (0.0699)	14167 (0.0460)
Obs data [$I > 2\sigma(I)$]	4223	5797	9171
params	417	408	856
R_1 [$I > 2\sigma(I)$][a]	0.0530	0.0439	0.0666
wR_2 [all data][a]	0.1669	0.397/-0.313	0.246/-0.243
max/min $\Delta\rho$ (e$^-$ Å^{-3})	0.280/-0.263	0.397/-0.313	0.246/-0.243

[a] $R_1 = \Sigma \big| \, |F_o| - |F_c| \, \big| / \Sigma |F_o|$; $wR_2 = [\Sigma\, w(F_o^2 - F_c^2)^2 / \Sigma\, w(F_o^4)]^{1/2}$.

Table 5.3: Crystallographic Data for **7**•Hexane and **8**.

Compound	**7**•Hexane	**8**
Formula	$C_{45}H_{73}B_2N_3$	$C_{39}H_{56}BN_3$
formula weight	677.68	577.68
crystal system	monoclinic	monoclinic
space group	*C*2/*c* (No. 15)	$P2_1/n$ (No. 14)
a(Å)	22.5387 (11)	10.5312 (1)
b (Å)	14.7074 (7)	18.7236 (3)
c (Å)	25.9542 (13)	36.5391 (5)
α (deg)	90	90
β (deg)	90.5331 (8)	90.1432 (6)
γ (deg)	90	90
V (Å^3)	8603.1 (7)	7204.83 (17)
Z	8	8
ρ (g cm^{-3})	1.065	1.065
abs coeff (mm^{-1})	0.059	0.456
T (K)	173(1)	173(1)
$2\theta_{max}$ (°)	50.80	141.48
total data	30770	48851
unique data (R_{int})	7934 (0.0422)	13784 (0.0197)
Obs data [$I > 2\sigma(I)$]	4747	12394
params	421	775
R_1 [$I > 2\sigma(I)$][a]	0.0574	0.0532
wR_2 [all data][a]	0.1751	0.1463
max/min $\Delta\rho$ (e$^-$ Å^{-3})	0.246/-0.243	0.775 /–0.450

[a] $R_1 = \Sigma \big| \, |F_o| - |F_c| \, \big| / \Sigma |F_o|$; $wR_2 = [\Sigma\, w(F_o^2 - F_c^2)^2 / \Sigma\, w(F_o^4)]^{1/2}$.

5.6 References

(1) See the following reviews: (a) Kuhn, N.; Al-Sheikh, A. *Coord. Chem. Rev.* **2005**, *249*, 829. (b) Wolf, R.; Uhl, W. *Angew. Chem., Int. Ed.* **2009**, *48*, 6774. (c) Wang, Y.; Robinson, G. H. *Inorg. Chem.* **2011**, *50*, 12326. (d) Feldmann, K. –O.; Weigand, J. J. *Angew. Chem., Int. Ed.* **2012**, *51,* 6566. (e) Braunschweig, H.; Dewhurst, R. D.; Hammond, K.; Mies, J.; Radacki, K.; Vargas, A. *Science*, **2012**, *336*, 1420. (f) Tanaka, H.; Ichinohe, M.; Sekiguchi, A. *J. Am. Chem. Soc.* **2012**, *134*, 5540 (g) Katir, N.; Matioszek, D.; Ladeira, S.; Escudié, J.; Castel, A. *Angew. Chem., Int. Ed.* **2011**, *50*, 5352. (h) Al-Rafia, S. M. I.; Ferguson, M. J.; Rivard, E. *Inorg. Chem.* **2011**, *50*, 10543.

(2) Kinjo, R.; Donnadieu, B.; Celik, M. A.; Frenking, G.; Bertrand, G. *Science*, **2011**, *333*, 610.

(3) Wang, Y.; Xie, Y.; Wei, P.; King, R. B.; Schaefer III, H. F.; Schleyer, P. v. R.; Robinson, G. H. *Science*, **2008**, *321*, 1069.

(4) (a) Tehfe, M. –A.; Makhlouf Brahmi, M.; Fouassier, J. –P.; Curran, D. P.; Malacria, M.; Fensterbank, L.; Lacôte, E.; Lalevée, J. *Macromolecules*, **2010**, *43*, 2261. (b) Curran, D. P.; Solovyev, A.; Makhlouf Brahmi, M.; Fensterbank, L.; Malacria, M.; Lacôte, E. *Angew. Chem., Int. Ed.* **2011**, *50*, 10294. (c) Tehfe, M. –A.; Monot, J.; Malacria, M.; Fensterbank, L.; Fouassier, J. –P.; Curran, D. P.; Lacôte, E.; Lavalée, J. *ACS Macro Lett.* **2012**, *1*, 92.

(5) (a) Thimer, K. C.; Al-Rafia, S. M. I.; Ferguson, M. J.; McDonald, R.; Rivard, E. *Chem. Commun.*, **2009**, 7119. (b) Al-Rafia, S. M. I.; Malcolm, A. C.; Liew, S. K.; Ferguson, M. J.; Rivard, E. *J. Am. Chem. Soc.* **2011**, *133*, 777. (c) Al-Rafia, S. M. I.; Malcolm, A. C.; Liew, S. K.; Ferguson, M. J.; McDonald, R.; Rivard, E. *Chem. Commun.* **2011**, *47*, 6987. (d) Al-Rafia, S. M. I.; Malcolm, A. C.; McDonald, R.; Ferguson, M. J.; Rivard, E. *Angew. Chem., Int. Ed.* **2011**, *50*, 8354. (e) Al-Rafia, S. M. I.; Malcolm, A. C.; McDonald, R.; Ferguson, M. J.; Rivard, E. *Chem. Commun.* **2012**, *48*, 1308. (f) Inoue, S.; Driess, M. *Angew. Chem., Int. Ed.* **2011**, *50*, 5614.

(6) For selected examples of donor-acceptor stabilization, see: (a) Vogel, U.; Timoshkin, A. Y.; Scheer, M. *Angew. Chem. Int., Ed.* **2001**, *40*, 4409. (b) Rupar, P. A.; Jennings, M. C.; Ragogna, P. J.; Baines, K. M. *Organometallics* **2007**, *26*, 4109. (c) Adolf, A.; Vogel, U.; Zabel, M.; Timoshkin, A. Y.; Scheer, M. *Eur. J. Inorg. Chem.* **2008**, 3482. (d) Yamaguchi, T.; Sekiguchi, A.; Driess, M. *J. Am. Chem. Soc.* **2010**, *132*, 14061. (e) Xiong, Y.; Yao, S.; Driess, M. *Angew. Chem., Int. Ed.* **2010**, *49*, 6642. (e) Jambor, R.; Herres-Pawlis, S.; Schürmann, M. Jurkschat, K. *Eur. J. Inorg. Chem.* **2011**, 344.

(7) SiH_2 and GeH_2 are often implicated as intermediates in the synthesis of semi-conducting Si and Ge films *via* the thermal decomposition of silane and germane, respectively: (a) Jasinski, J. M.; Gates, S. M. *Acc. Chem. Res.* **1991**, *24*, 9. (b) Smith, T. C.; Clouthier, D. J.; Sha, W.; Adam, A. G. *J. Chem. Phys.* **2000**, *113*, 9567 and reference therein; For related

synthesis of nanocrystals, see: (c) Kortshagen, U.; Anthony, R.; Gresback, R.; Holman, Z.; Ligman, R.; Liu, C. –Y.; Mangolini, L.; Campbell, S. A. *Pure Appl. Chem.* **2008**, *80*, 1901. (d) Li, X.; He, Y.; Talukdar, S. S.; Swihart, M. T. *Langmuir*, **2003**, *19*, 8490.

(8) (a) Schnepf, A. *Chem. Soc. Rev.* **2007**, *36*, 745. (b) Pacher, A.; Schrenk, C.; Schnepf, A. *J. Organometal. Chem.* **2010**, *695*, 941. (c) Wiberg, N.; Power, P. P. *Molecular Clusters of the Main Group Elements* (Eds.: M. Driess, H. Nöth), Wiley-VCH, Weineim, **2004**, chap. 25, pp. 188-208.

(9) Kelly, J. A.; Henderson, E. J.; Veinot, J. G. C. *Chem. Commun.* **2010**, *46*, 8704.

(10) (a) Matsumoto, H.; Higuchi, K.; Hoshino, Y.; Koike, H.; Naoi, Y.; Nagai, Y. *J. Chem. Soc., Chem. Commun.* **1988**, 1083. (b) Richards, A. F.; Brynda, M.; Olmstead, M. M.; Power, P. P. *Organometallics* **2004**, *23*, 2841. (c) Richards, A. F.; Hope, H.; Power, P. P. *Angew. Chem., Int. Ed.* **2003**, *42*, 4071. (d) Eichler, B. E.; Power, P. P. *Angew. Chem. Int., Ed.* **2001**, *40*, 796. (e) Richards, A. F.; Eichler, B. E.; Brynda, M.; Olmstead, M. M.; Power, P. P. *Angew. Chem., Int. Ed.* **2005**, *44*, 2546.

(11) (a) Brynda, M.; Herber, R.; Hitchcock, P. B.; Lappert, M. F.; Nowik, I.; Power, P. P.; Protchenko, A. V.; Růžička, A.; Steiner, J. *Angew. Chem., Int. Ed.* **2006**, *45*, 4333. (b) Rivard, E.; Steiner, J.; Fettinger, J. C.; Giuliani, J. R.; Augustine, M. P.; Power, P. P. *Chem. Commun.* **2007**, 4919. (c) Klinkhammer, K. W.; Xiong, Y.; Yao, S. *Angew. Chem., Int. Ed.* **2004**, *43*, 6202.

(12) Lappert, M. F.; Power, P. P.; Protchenko, A.; Seeber, A. *Metal Amide Chemistry*, Wiley, Chichester, UK, **2009**, Chapter 9.

(13) (a) Denk, M.; Lennon, R.; Hayashi, R.; West, R.; Belyakov, A. V.; Verne, H. P.; Haaland, A.; Wagner, M.; Metzler, N. *J. Am. Chem. Soc.* **1994**, *116*, 2691. (b) So, C. -W.; Roesky, H. W.; Magull, J.; Oswald, R. B. *Angew. Chem., Int. Ed.* **2006**, *45*, 3948. (c) Driess, M.; Yao, S.; Brym, M.; van Wüllen, C.; Lentz, D. *J. Am. Chem. Soc.* **2006**, *128*, 9628. (d) Kong, L.; Zhang, J.; Song, H.; Cui, C. *Dalton Trans.* **2009**, 5444. (e) Rodriguez, R.; Gau, D.; Contie, Y.; Kato, T.; Saffon-Merceron, N.; Baceiredo, A. *Angew. Chem., Int. Ed.* **2011**, *50*, 11492. (f) Cui, H.; Cui, C. *Dalton Trans.* **2011**, 11937. (g) Protchenko, A. V.; Hassomal Birjkumar, K.; Dange, D.; Schwartz, A. D.; Vidovic, D.; Jones, C.; Kaltsoyannis, N.; Mountford, P.; Aldridge, S. *J. Am. Chem. Soc.* **2012**, *134*, 6500.

(14) (a) Merrill, W. A.; Steiner, J.; Betzer, A.; Nowik, I.; Herber, R.; Power, P. P. *Dalton Trans.* **2008**, 5905. (b) Meller, A.; Ossig, G.; Maringelle, W.; Stalke, D.; Herbst-Irmer, R.; Freitag, S.; Sheldrick, G. M. *J. Chem. Soc., Chem. Commun.* **1991**, 1123. (c) Padělková, Z.; Havlík, A.; Švec, P.; Nechaev, M. S.; Růžička, A. *J. Organometal. Chem.* **2010**, *695*, 2651.

(15) Ghadwal, R. S.; Roesky, H. W.; Merkel, S.; Henn, J.; Stalke, D. *Angew. Chem., Int. Ed.* **2009**, *48*, 5683.

(16) Ghadwal, R. S.; Roesky, H. W.; Pröpper, K.; Dittrich, B.; Klein, S.; Frenking, G. *Angew. Chem., Int. Ed.* **2011**, *50*, 5374.

(17) Merrill, W. A.; Wright, R. J.; Stanciu, C. S.; Olmstead, M. M.; Fettinger, J. C.; Power, P. P. *Inorg. Chem.* **2010**, *49*, 7097.

(18) Wang, Y.; Quillian, B.; Wei, P.; Wannere, C. S.; Xie, Y.; King, R. B.; Schaefer III, H. F.; Schleyer, P. v. R.; Robinson, G. H. *J. Am. Chem. Soc.* **2007**, *129*, 12412.

(19) (a) Azhakar, R.; Tavčar, G.; Roesky, H. W.; Hey, J.; Stalke, D. *Eur. J. Inorg. Chem.* **2011**, 475. (b) Abraham, M. Y.; Wang, Y.; Xie, Y.; Wei, P.; Schaefer III, H. F.; Schleyer, P. v. R.; Robinson, G. H. *J. Am. Chem. Soc.* **2011**, *133*, 8874.

(20) (a) Ding, Y.; Hao, H.; Roesky, H. W.; Noltemeyer, M.; Schmidt, H. –G. *Organometallics* **2001**, *20*, 4806. (b) Spikes, G. H.; Fettinger, J. C.; Power, P. P. *J. Am. Chem. Soc.* **2005**, *127*, 12232. (c) Leung, W.–P.; So, C.–W.; Chong, K.–H.; Kan, K. –W.; Chan, H.–S.; Mak, T. C. W. *Organometallics* **2006**, *25*, 2851.

(21) Jana, A.; Leusser, D.; Objartel, I.; Roesky, H. W.; Stalke, D. *Dalton Trans.* **2011**, *40*, 5458.

(22) Solovyev, A.; Chu, Q.; Geib, S. J.; Fensterbank, L.; Malacria, M.; Lacôte, E.; Curran, D. P. *J. Am. Chem. Soc.* **2010**, *132*, 15072.

(23) In general, main group element clusters are highly colored, thus we cannot rule out the presence of Si and Ge clusters as part of the orange precipitate formed.

(24) For related dehydrogenation chemistry with amine-boranes, $RNH_2 \bullet BH_3$, see: (a) Jaska, C. A.; Temple, K.; Lough, A. J.; Manners, I. *J. Am. Chem.*

Soc. **2003**, *125*, 9424. (b) Staubitz, A.; Robertson, A. P. M.; Sloan, M. E.; Manners, I. *Chem*. *Rev*. **2010**, *110*, 4023. (c) Staubitz, A.; Robertson, A. P. M.; Manners, I. *Chem*. *Rev*. **2010**, *110*, 4079.

(25) Nöth, H.; Wrackmeyer, B. *Nuclear Magnetic Resonance Spectroscopy of Boron Compounds*, Springer, Berlin, **1978**.

(26) (a) Wehmschulte, R. J.; Diaz, A. A.; Khan, M. A. *Organometallics* **2003**, *22*, 83. (b) Zettler, F.; Hausen, H. D.; Hess, H. *J*. *Organometal*. *Chem*. **1974**, *72*, 157. (c) Kahr, B.; Jackson, J. E.; Ward, D. L.; Jang, S. H.; Blount, J. F. *Acta*. *Cryst*. **1992**, *B48*, 324.

(27) Caruso Jr., A.; Siegler, M. A.; Tovar, J. D. *Angew*. *Chem., Int*. *Ed*. **2010**, *49*, 4213.

(28) (a) Arduengo III, A. J.; Davidson, F.; Dias, H. V. R.; Goerlich, J. R.; Khasnis, D.; Marshall, W. J.; Prakasha, T. K. *J*. *Am*. *Chem*. *Soc*. **1997**, *119*, 12742. (b) Bates, J. I.; Kennepohl, P.; Gates, D. P. *Angew*. *Chem*., *Int*. *Ed*. **2009**, *48*, 9844 and references therein. (c) Mendoza-Espinosa, D.; Donnadieu, B.; Bertrand, G. *J*. *Am*. *Chem*. *Soc*. **2010**, *132*, 7264.

(29) (a) Arrowsmith, M.; Hill, M. S.; Kociok-Köhn, G.; MacDougall, D. J.; Mahon, M. F. *Angew*. *Chem., Int*. *Ed*. **2012**, *51*, 2098. (b) Schmidt, D.; Berthel, J. H. J.; Pietsch, S.; Radius, U. *Angew*. *Chem., Int*. *Ed*. **2012**, *51*, 8881.

(30) Pangborn, A. B.; Giardello, M. A.; Grubbs, R. H.; Rosen, R. K.; Timmers, F. J. *Organometallics* **1996**, *15*, 1518.

(31) (a) Jafarpour, L.; Stevens, E. D.; Nolan, S. P. *J. Organometal. Chem.* **2000**, *606*, 49. (b) Hintermann, L. *Beilstein J. Org. Chem.*, **2007**, *3*, No 22, doi: 10.1186/1860-5397-3-22.

(32) Patton, J. T.; Feng, S. G.; Abboud, K. A. *Organometallics* **2001**, *20*, 3399.

(33) Hope, H. *Prog. Inorg. Chem.* **1994**, *41*, 1.

(34) Blessing, R. H. *Acta Cryst.* **1995**, *A51*, 33.

(35) Sheldrick, G. M. *Acta Cryst.* **2008**, *A64*, 112.

(36) Altomare, A.; Burla, M. C.; Camalli, M.; Cascarano, G. L.; Giacovazzo, C.; Guagliardi, A.; Moliterni, A. G. G.; Polidori, G.; Spagna, R. *J. Appl. Cryst.* **1999**, *32*, 115.

(37) Beurskens, P. T.; Beurskens, G.; de Gelder, R.; Smits, J. M. M.; Garcia-Garcia, S.; Gould, R. O. *DIRDIF-2008*, Crystallography Laboratory, Radboud University: Nijmegen, The Netherlands, **2008**.

(38) Schneider, T. R.; Sheldrick, G. M. *Acta Cryst.* **2002**, *D58*, 1772.

(39) van der Spek, P.; Sluis, A. L. *Acta Cryst.* **1990**, *A46*, 194.

(40) (a) Spek, A. L. *J. Appl. Cryst.* **2003**, *36*, 7. (b) *PLATON* – a multipurpose crystallographic tool. Utrecht University, Utrecht, The Netherlands.

Chapter 6

Interaction of N-Heterocyclic Carbene and Olefinic Donors with $[Cl_2P{=}N]_3$: Towards Stable Adducts of $(PN)_3$

Chapter 6

Interaction of N-Heterocyclic Carbene and Olefinic Donors with $[Cl_2P=N]_3$: Towards Stable Adducts of $(PN)_3$

6.1 Abstract

The synthesis of the iminophosphine-phosphazene [P(III)-P(V)] heterocyclic adduct [IPr•$PN(PCl_2N)_2$] was achieved *via* the dehalogenation of the cyclic phosphazene $[Cl_2P=N]_3$ in the presence of the carbene donor IPr [IPr = {$(HCNDipp)_2C$:} and Dipp = 2,6-$^{i}Pr_2C_6H_3$]. The coordination chemistry of [IPr•$PN(PCl_2N)_2$] was studied including the reaction of this heterocycle with BH_3 to give the borane adduct [IPr•$P(BH_3)N(PCl_2N)_2$]. An oxidative chalcogen transfer reaction occurred when [IPr•$PN(PCl_2N)_2$] was treated with an atomic equivalent of sulfur. In order to investigate the steric and electronic influences of the donor on the stability of the phosphazene adduct, the cyclic phosphazene $[Cl_2P=N]_3$ was reacted with the N-heterocyclic olefin, IPr=CH_2. In the presence of IPr=CH_2, nucleophilic halide displacement followed by deprotonation of the IPr=CH_2 fragment gave the olefin-grafted phosphazene ring [(IPr=CH)ClPN$(Cl_2PN)_2$]. Attempts to abstract a halide from this olefin-bound ring to generate the coordinatively unsaturated cyclophosphazene cation $[(IPr=CH)PN(PCl_2N)_2]^+$ were unsuccessful.

6.2 Introduction

The use of N-heterocyclic carbenes (NHCs) as supporting ligands to isolate/stabilize inorganic species that were either unknown or inaccessible using conventional methods is a rapidly developing avenue of research.[1] In this regard, the synthesis of NHC adducts featuring reactive entities such as HB=BH, B≡B, :SiX_2 (X = Cl and Br), :Si=Si:, P_2, and PH, represent particularly noteworthy achievements.[2] These breakthroughs have substantially expanded our general knowledge of bonding in inorganic chemistry and have facilitated the discovery of a number of useful chemical transformations involving once elusive inorganic species as reagents.[3]

The Rivard group has recently developed a stabilization protocol that involves use of a N-heterocyclic carbene (NHC) donor and a Lewis-acid acceptor to intercept highly reactive Group 14 hydrides, for example, the heavy methylene and ethylene analogues :EH_2 and $H_2EE'H_2$ (E and E' = Si, Ge, and/or Sn).[4,5] The above mentioned successes have provided an impetus to explore the application of donor-acceptor stabilization in the preparation of NHC-supported complexes of phosphorus mononitride (PN) and/or its oligomers $(PN)_x$. Phosphorus mononitride (PN) was identified as an important component of interstellar space and recently it has been discovered in the atmospheres of Jupiter and Saturn.[6] In addition, PN represents a heavier analogue of N_2 and is thus an attractive species from a fundamental standpoint.

In the laboratory, gaseous PN and $(PN)_3$ were generated by pyrolysis of various precursors and characterized by spectroscopy in a krypton matrix at 20 K.[7]

Although the phosphorus mononitride dimer $(PN)_2$ has not yet been detected experimentally a number of other binary PN species such as P_3N_5, P_3N_{21}, P_4N_4, PN_9 and PN_{15} have been observed and spectroscopically characterized.[8-10] Furthermore, in comparison to the numerous instances where N_2, P_2 and As_2 moieties are involved in coordination with transition metals, there is only one report by Timms and Atkins that describes the interaction of PN with Group 11 elements. These PN coordinated complexes were only characterized by IR spectroscopy at 10 K and proposed to display μ-P and η^1-P coordination.[11] It was anticipated that isolation of PN and/or its oligomers $(PN)_2$, $(PN)_3$ etc. in the condensed phase using a donor-acceptor stabilization technique would provide a better way to study their properties and reactivity. This chapter reports a full details of our efforts to develop a potential route towards the isolation of $(PN)_3$ in the form of a stable adduct at ambient temperature.

6.3 Results and discussion

The overall strategy of this chapter relies upon the reduction of the readily available cyclic precursor $[Cl_2PN]_3$ in the presence of N-heterocyclic carbene donors to yield stable complexes of $(PN)_3$ (equation 6.1).[12,13] It was postulated that the lone pairs on each phosphorus center of the donor-stabilized $(PN)_3$ unit can engage in additional dative interactions with suitable Lewis acids such as BH_3 or $W(CO)_5$. The ultimate goal of this study was to synthesize donor or donor/acceptor stabilized adducts of $(PN)_3$ that can be used as precursors for the

controlled synthesis of binary bulk P-N materials (e.g. PN) *via* low temperature thermolysis.

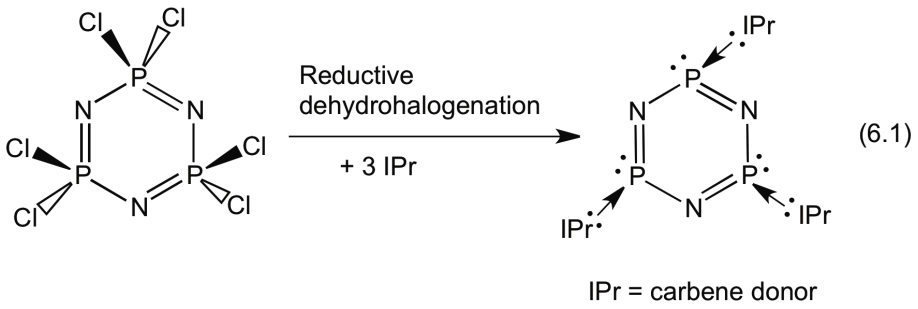

(6.1)

Recently, Bertrand and coworkers reported the synthesis of a formal adduct of a phosphorus mononitride PN and its radical cation ($PN^{+\cdot}$) using two carbenes (Scheme 6.1).[14] As shown in Scheme 6.1 the PN complex can be represented by two canonical structures: the phosphinidene-nitrene fragment (**a**) or the phosphabutadiene skeleton (**b**), with the latter form consistent with the X-ray crystallographic data. Interestingly, the P-N bond distance in this phosphorus mononitride complex 1.7085(16) Å is within the range of P-N single bonds; for comparison, the P≡N length in molecular PN was determined to be 1.462 Å by microwave spectroscopy and theoretically calculated to be 1.49 Å.[7a,7c,14]

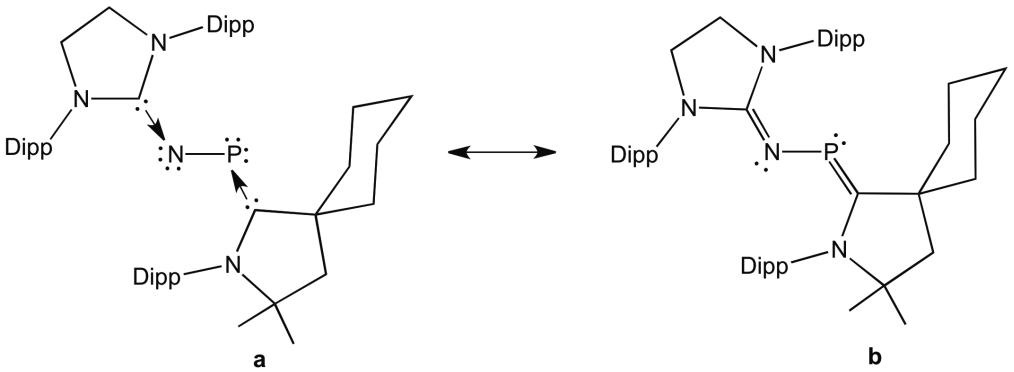

Scheme 6.1. Canonical structures of a bis(carbene)-PN adduct. Dipp = 2,6-diisopropylphenyl.

6.3.1 Synthesis of the iminophosphine-phosphazene adduct, [IPr•PN(PCl$_2$N)$_2$]

The interaction of the hindered carbene IPr [IPr = (HCNDipp)$_2$C:], where Dipp = 2,6-Pr$_2$C$_6$H$_3$] with [Cl$_2$PN]$_3$ in the presence of sodium metal as a reductant yielded a new crystalline product which exhibited an AX$_2$ splitting pattern in the ^{31}P NMR spectrum [δ_A 101.4 (t, J = 86.9 Hz); δ_X 6.1 (d, J = 86.9 Hz)]. The disparate nature of the observed chemical shifts suggested the presence of a single product with two phosphorus environments in different oxidation states. Single-crystal X-ray crystallography later identified this species as the novel iminophosphine-phosphazene [P(III)-P(V)] heterocyclic adduct [IPr•PN(PCl$_2$N)$_2$] **1** (Equation 6.2 and Figure 6.1). Compound **1** was isolated as an air- and moisture-sensitive solid in 55% yield. Attempts to further reduce the remaining P(V) centers in **1** with additional equivalents of IPr and sodium to obtain a formal carbene adduct of (PN)$_3$ (*i.e.* [IPr•PN]$_3$) yielded no discernible reaction. The observed inability to further reduce the remaining P(V) centers suggested that the steric bulk imposed by the hindered IPr ligand suppressed the approach of any further carbene to the unreduced phosphorus centers. In order to investigate the steric effect of the donor ligand, the cyclic phosphazene [Cl$_2$PN]$_3$ was reacted with six equivalents of the less hindered methyl-substituted carbene ImMe$_4$ (ImMe$_4$ = [(MeCNMe)$_2$C:]) in the presence of sodium. This reaction gave a product with a ^{31}P NMR spectrum consistent with the formation mono-carbene adduct [ImMe$_4$•PN(PCl$_2$N)$_2$]; thus steric effects are not responsible for the incomplete reduction of [Cl$_2$PN]$_3$. In addition, the reaction of **1** with carbene in the presence of strong reducing agents such as KC$_8$ resulted in the cleavage of IPr-

P(III) bond and led to the isolation of free IPr as a soluble product. This reaction implies that the P_3N_3 heterocycle core in **1** is electron rich and inhibits any further reduction of the remaining P(V) centers.

Compound **1** could also be obtained in low isolated yield (13%) when $[Cl_2PN]_3$ was directly combined with 2 equiv. of IPr in the absence of sodium; the low yield of **1** stems from the formation of a number of unidentified side products during the reaction that have to be separated from **1** by fractional crystallization. Importantly, this transformation reveals the role of IPr as a dehalogenation/reducing agent.[12] Interestingly, the reaction of IPr•$GeCl_2$ with $[Cl_2PN]_3$ in the presence of four equivalents of sodium also led to the formation of **1** in 85% yield. The exact mechanism of this reaction is not clear at this time, however, one of the probable pathways for this reaction would be initial formation of digermane/digermene intermediates such as IPr•(Cl)Ge-Ge(Cl)•IPr or IPr•Ge=Ge•IPr,[3a] and followed by the reduction of $[Cl_2PN]_3$ by these low oxidation state Ge species to yield **1**. Unfortunately, these possible intermediates could not be identified in the reaction mixture by NMR spectroscopy.

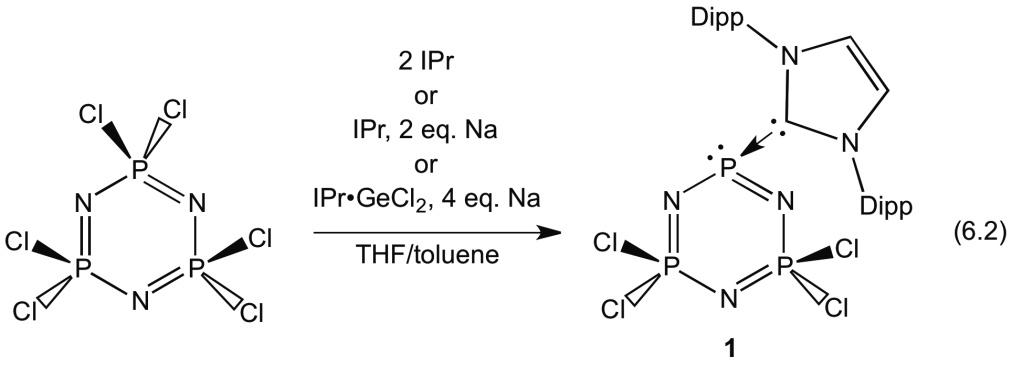

(6.2)

As shown in Figure 6.1, [IPr•$PN(PCl_2N)_2$] **1** contains a phosphorus-bound IPr ligand with a C_{IPr}-P distance [C(1)-P(1)] of 1.8791(13) Å. This elongated bond

length compared to the C-P distances in the cationic phosphorus bis(carbene) adduct [($ImMe_2{}^iPr_2$)•P•($ImMe_2{}^iPr_2$)]Cl (where $ImMe_2{}^iPr_2$ = [($MeCN{}^iPr)_2$]C:) [1.824(3) Å *avg*.][12b] and is much longer than the C_{IPr}-P linkages within Robinson's diphosphorus adduct IPr•P_2•IPr [1.7504(17) Å], wherein significant P-C_{IPr} π-bonding is present.[2e] The P_3N_3 heterocycle in **1** adopts an envelope conformation with a pyramidal geometry about the apical P(1) atom in the ring [angle sum = 307.3(1)°]. Compound **1** also features considerable intraring P-N bond-length variation, with long P-N bonds of 1.6770(12) and 1.6845(13) Å involving the three-coordinate P(1) center, while the remaining P-N distances vary from 1.5423(12) to 1.5923(13) Å. For comparison, the latter P-N bond lengths are in the range of normally observed for phosphazene [P(V)-N] rings and chains.[15]

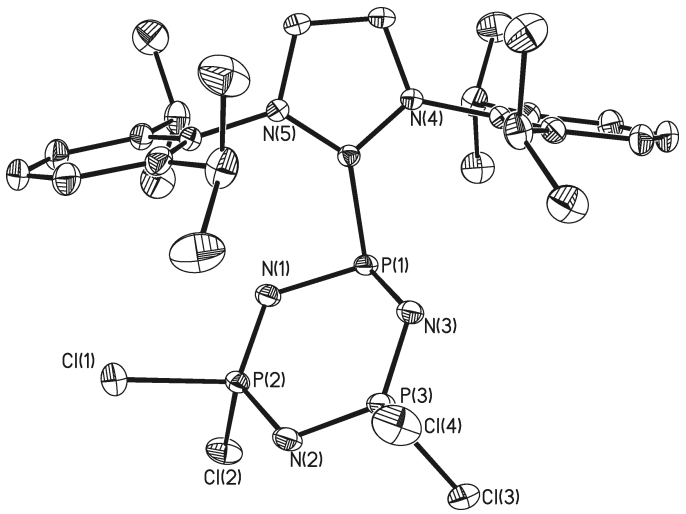

Figure 6.1 Thermal ellipsoid plot (30% probability level) for [IPr•$PN(PCl_2N)_2$] (**1**) with hydrogen atoms and toluene solvate omitted for clarity. Selected bond lengths [Å] and angles [°]: C(1)-P(1) 1.8791(13), P(1)-N(1) 1.6770(12), P(1)-N(3) 1.6845(13), P(2)-N(1) 1.5423(12), P(2)-N(2) 1.5900(13), P(3)-N(2) 1.5923(13), P(3)-N(3) 1.5543(13); C(1)-P(1)-N(1) 99.05(6), C(1)-P(1)-N(3) 100.14(6), N(1)-P(1)-N(3) 108.12(6).

6.3.2 Reaction of [IPr•PN(PCl$_2$N)$_2$] (**1**) with S$_8$ and H$_3$B•THF

The above mentioned data supported the presence of a sterochemically active lone pair on the P(III) center in **1**. Accordingly, when **1** was reacted with atomic equivalent of sulfur, the novel phosphine sulfide complex [IPr•(S)PN(PCl$_2$N)$_2$] (**2**) was formed as an air- and moisture-sensitive colorless solid in a 88% isolated yield (Scheme 6.2 and Figure 6.2). The NMR spectra for **2** are consistent with the presence of phosphazene environments, as AX$_2$ splitting patterns are present in the ^{31}P NMR spectrum [δ_A = 23.9 (t, $^2J_{PP}$ = 26.7 Hz); δ_X = 13.4 (d, $^2J_{PP}$ = 26.7 Hz)]. Correspondingly short P-N bond distances of 1.5595(17)-1.6256(16) Å are observed by X-ray crystallography. Despite the presence of a terminal sulfido group in **2**, the dative C_{IPr}-P(1) interaction [1.8582(18) Å] is similar in length to the carbene-phosphorus interaction within the reduced precursor **1** [1.8791(13) Å]. For comparison, the P=S bond distance in **2** [1.9361(7) Å] lies within the range of typical phosphorus sulfur double bonds observed in phosphine sulfides R$_3$P=S [e.g., 1.950(3) Å within Ph$_3$P=S].[16] The oxidation of the carbene-bound phosphorus center in **1** with a chalcogen is reminiscent of prior work by Kuhn and coworkers, who prepared the phosphonium selenide complex [Ph$_2$P(Se)•ImMe$_2$^{i}Pr$_2$]AlCl$_4$ *via* the direct oxidation of an NHC phosphenium (Ph$_2$P$^+$) adduct with selenium.[13c]

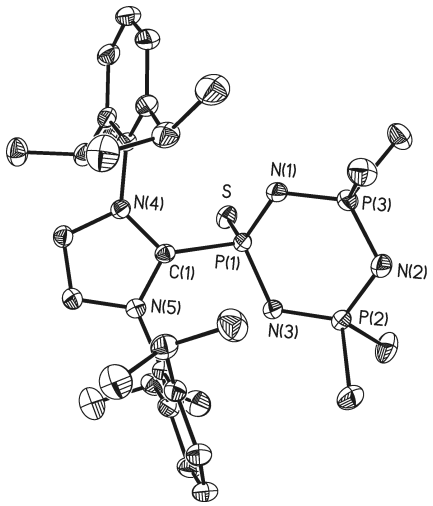

Figure 6.2 Thermal ellipsoid plot (30% probability level) for [IPr•(S)PN(Cl_2PN)$_2$] (**2**) with hydrogen atoms and toluene solvate omitted for clarity. Selected bond lengths [Å] and angles [°]: C(1)-P(1) 1.8582(18), P(1)-S 1.9361(7), P(1)-N(1) 1.6256(16), P(1)-N(3) 1.6252(16), P(2)-N(3) 1.5542(16), P(2)-N(2) 1.5791(18), P(3)-N(1) 1.5595(17); C(1)-P(1)-N(1) 104.14(8), C(1)-P(1)-N(3) 102.58(8), N(1)-P(1)-N(3) 111.72(8), C(1)-P(1)-S 105.02(6).

The coordination of the Lewis acid BH_3 to the phosphorus donor site in **1** was also investigated. Reaction of **1** with H_3B•THF resulted in the formation of the stable phosphine-borane adduct [IPr•P(BH_3)N(PCl_2N)$_2$] (**3**) (Scheme 6.2). Compound **3** was characterized by NMR (^{1}H, ^{31}P and ^{11}B NMR), mass spectroscopy and elemental analysis. However, attempts to obtain crystals of suitable quality for X-ray single-crystal crystallographic analysis were unsuccessful. The ^{31}P NMR spectrum of **3** yields an unresolvable broad resonance for the boron-bound phosphorus atom, while a well-resolved doublet resonance is present in the ^{11}B NMR spectrum at -30.0 ppm with a $^1J_{B\text{-}P}$ coupling value of 71.6 Hz, corresponding to a BH_3 unit bound to a P(III) center.

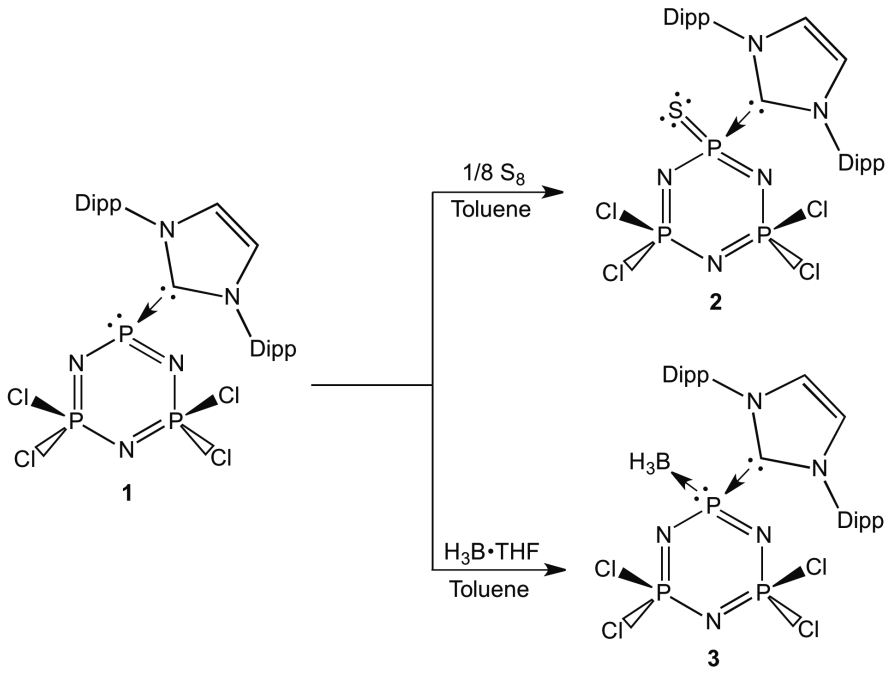

Scheme 6.2. Synthesis of [IPr•(S)PN(Cl_2PN)$_2$] (**2**) and phosphine-borane adduct, [IPr•P(BH_3)N(PCl_2N)$_2$] (**3**).

6.3.3 Attempted use of an N-heterocyclic olefin as a stabilizing ligand to access $(PN)_3$

Recently, it was shown by the Rivard group that the N-heterocyclic olefin IPr=CH_2 can be used as a donor ligand to stabilize low-oxidation-state Group 14 hydrides (Chapter 3).[4c,17] Since this N-heterocyclic olefin has a different steric environment around the donor site relative to the N-heterocyclic carbene IPr (due to the presence of spacer CH_2 group), it was assumed that use of IPr=CH_2 as a coordinating ligand in the above chemistry would allow the approach of multiple donors to the phosphorous centers in the P_3N_3 ring. Furthermore, the weaker donor nature of IPr=CH_2 compared to IPr might be able to compensate for the electronic barrier to reduction that was discussed earlier. Inspired by these potential advantages, the reaction of IPr=CH_2 with [Cl_2PN]$_3$ was investigated. As

illustrated in Scheme 6.3, the sole phosphorus-containing product in the reaction was the alkene-substituted heterocycle [(IPr=CH)P(Cl)N(PCl_2N)$_2$] (**4**). Intriguingly, the same product was also obtained when the reaction was performed in the presence of stoichiometric sodium metal as a potential reducing agent. The formation of **4** likely involves the initial nucleophilic displacement of a phosphorus-bound chloride in $[Cl_2PN]_3$ by IPr=CH_2, followed by deprotonation (HCl elimination) in the presence of excess basic IPr=CH_2 to generate an alkenyl IPr=CH group at phosphorus. The latter process yields the insoluble imidazolium salt [IPrCH_3]Cl, which was isolated in pure form by filtration. Efforts to isolate the olefin-bound cationic intermediate (as shown in the Scheme 6.3) *via* 1:1 reaction of IPr=CH_2 and $[Cl_2PN]_3$ failed and yielded only **4** and unreacted chlorophosphazene trimer, $[Cl_2P{=}N]_3$.

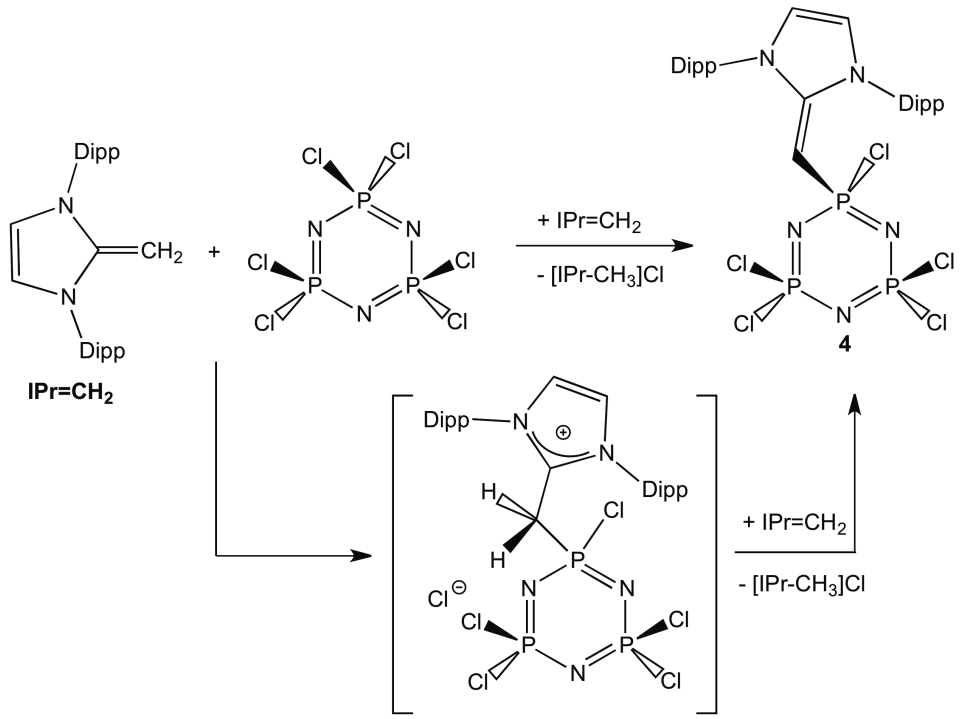

Scheme 6.3. Synthesis of alkene-substituted phosphazene [(IPr=CH)P(Cl)N(PCl_2N)$_2$] (**4**).

Attempts to functionalize the remaining P-Cl bonds in **4** with excess IPr=CH_2 failed even in the presence of sodium. As expected, the alkene-substituted heterocycle **4** yields an AX_2 pattern in the ^{31}P NMR spectrum [P_A = 25.6 ppm (t, $^2J_{P\text{-}P}$ = 17. 5 Hz); P_X 18.8 ppm (d, $^2J_{P\text{-}P}$ = 17. 5 Hz)]. In addition, a well-resolved doublet resonance found at 3.31 ppm in the ^1H NMR spectrum [$^2J_{H\text{-}P}$ = 6. 5 Hz] which is assigned to the alkene proton in the pendent IPr=C*H* group bound to P(V) center.

Compound **4** was structurally characterized by single-crystal X-ray crystallography (Figure 6.3). The phosphazene heterocycle [(IPr=CH)P(Cl)N(PCl_2N)$_2$] (**4**) contains P-N bond lengths in the narrow range of 1.5617(6) to 1.610(2) Å, while the exocyclic P-C interaction is significantly shorter [P(1A)-C(4) = 1.692(4) Å *avg*.] than the dative P-C_{IPr} linkages within the heterocyclic adducts **1** and **2**. Furthermore, the short P-C distance in **4** is accompanied by the substantial lengthening of the proximal P(1)-Cl(1) bond length [2.088(2) Å *avg*.] relative to the P-Cl distance observed in the phenyl-substituted phosphazene [PhP(Cl)N(PCl_2N)$_2$] [2.021(2) Å].[18] These metrical parameters suggest that the IPr=CH substituent is strongly electron-releasing, thereby leading to a weakening of the adjacent P-Cl interaction.

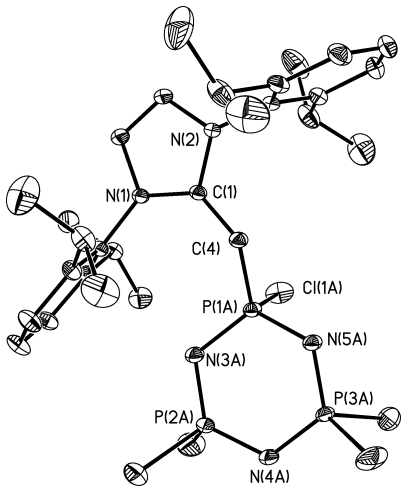

Figure 6.3. Thermal ellipsoid plot (30% probability level) for [(IPr=CH)P(Cl)N(PCl_2N)$_2$] (**4**) with hydrogen atoms and solvate omitted. The $N_3P_3Cl_5$ group was disordered over two positions (70:30), and only the major orientation is shown for clarity. Selected bond lengths [Å] and angles [°] metrical parameters for the minor orientation of the $N_3P_3Cl_5$ group in brackets: C(1)-C(4) 1.398(2), C(4)-P(1A) 1.687(2) [1.708(3)], P(1A)-N(3A) 1.6089(17), P(1A)-N(5A) 1.610(2), P(2A)-N(3A) 1.5617(16), P(2A)-N(4A) 1.583(2), P(3A)-N(4A) 1.583(2), P(3A)-N(5A) 1.567(2); C(1)-C(4)-P(1A) 129.07(14) [132.52(17)].

Attempts to functionalize the remaining P-Cl bonds in **4** with excess IPr=CH_2 failed presumably due to both electronic and steric factors. However, the pendent IPr=CH moiety in **4** can be removed from the phosphazene ring by treatment with anhydrous HCl (1.0 M solution in Et_2O) to give $[Cl_2P{=}N]_3$ along with the imidazolium salt [IPr-CH_3]Cl (Equation 6.3).

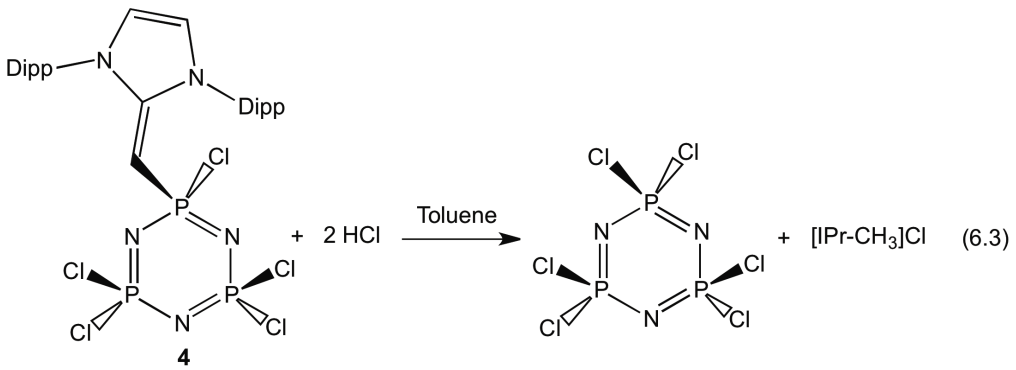

The presence of an elongated P-Cl bond in **4** provided inspiration to investigate the possibility of intercepting the cyclophosphazene cation $[(IPr{=}CH)PN(PCl_2N)_2]^+$. The halogenated cyclophosphazene cation $[N_3P_3Cl_5]^+$ is proposed to be an intermediate during the ring-opening polymerization (ROP) of $[Cl_2P{=}N]_3$.[19] It was expected that the steric shield created by the pedant IPr=CH group would kinetically stabilize a cationic phosphorus center and thus provide access to the cyclophosphazene cation $[(IPr{=}CH)PN(PCl_2N)_2]^+$. Isolation of this intermediate might provide valuable mechanistic insight into the ROP of cyclic chlorophosphazene trimer $[Cl_2PN]_3$ at elevated temperature. Unfortunately, attempts to remove a chloride ion from **4** using the known halide abstracting reagents $Ag[SbF_6]$ and $Ag[O_3SCF_3]$ led to the formation of inseparable product mixtures in place of the desired cyclophosphazene cation $[(IPr{=}CH)PN(PCl_2N)_2]^+$ $[\mathbf{4}]^+$.

6.4 Conclusion

In summary, partial reductive dehalogenation of $[Cl_2PN]_3$ in the presence of the carbene donor, IPr, afforded the novel mixed P(III)-P(V) heterocyclic adduct **1**. Reaction of **1** with sulfur yielded an oxidative sulfur addition product $[IPr•(S)PN(Cl_2PN)_2]$ **2** and the clean formation of a borane adduct, $[IPr•P(BH_3)N(PCl_2N)_2]$ **3** was observed when **1** was reacted with $H_3B•THF$. A divergent reaction pathway was discovered in the reaction of $IPr=CH_2$ and $[Cl_2PN]_3$ which led to the formation of the olefin-bound cyclophosphazene $[(IPr=CH)P(Cl)N(PCl_2N)_2]$ **4**. Repeated attempts to abstract a chloride from **4** in order to generate cyclophosphazene cation $[(IPr=CH)PN(PCl_2N)_2]^+$ $[\mathbf{4}]^+$ were unsuccessful.

6.5 Experimental Section

6.5.1 Materials and Instrumentation

All reactions were performed using standard Schlenk line techniques under an atmosphere of nitrogen or in an inert atmosphere glove box (Innovative Technology, Inc.). Solvents were dried using Grubbs-type solvent purification system[20] manufactured by Innovative Technology, Inc., degassed (freeze-pump-thaw method) and stored over molecular sieves under an nitrogen atmosphere prior to use. Phosphonitrilic chloride trimer $[Cl_2P=N]_3$, HCl (2.0 M solution in Et_2O), H_3B•THF (1.0 M solution in THF) and elemental sulfur were purchased from Aldrich and used as received. 1,3-Bis-(2,6-diisopropylphenyl)-imidazol-2-ylidene (IPr),[21] 1,3-bis-(2,6-diisopropylphenyl)-2-methyleneimidazoline (IPr=CH_2)[4c] were prepared following literature procedures. ^{1}H, $^{13}C\{^{1}H\}$ and ^{31}P NMR spectra were recorded on a Varian iNova-400 spectrometer and referenced externally to $SiMe_4$ (^{1}H and $^{13}C\{^{1}H\}$), F_3B•Et_2O (^{11}B) and 85% H_3PO_4 ($^{31}P\{^{1}H\}$), respectively by setting the resonance for residual H, C, B and P at 0.0 ppm. X-ray crystallographic analyses were performed by the X-ray Crystallography Laboratory at the University of Alberta. Elemental analyses were performed by the Analytical and Instrumentation Laboratory at the University of Alberta. Mass spectra were obtained on a Agilent 6220 spectrometer. Melting points were measured in sealed glass capillaries under nitrogen using a MelTemp melting point apparatus and are uncorrected.

6.5.2 X-ray Crystallography

Crystals of suitable quality for X-ray crystallography were removed from a vial (in glove box) and coated immediately with a thin layer of hydrocarbon oil (Paratone-N). A suitable crystal was picked and mounted on a glass fiber and then quickly placed in a low temperature stream of nitrogen on the X-ray diffractometer.[22] All data were collected using a Bruker APEX II CCD detector/D8 diffractometer using either Mo Kα radiation or Cu Kα (compound **4**), with the crystals cooled to -100 °C. The data were corrected for absorption[23] through Gaussian integration from the indexing of the crystal faces. Structures were solved using the direct methods program SHELXS-97, and refined using SHELXS-97.[24] Hydrogen atoms were assigned positions based on sp^2 or sp^3 hybridization geometries of their attached carbon atoms, and were given thermal parameters 20% greater than those of their parent atoms.

6.5.2.1 Special Refinement Conditions

Compound **2**: The geometry of the minor orientation of the disordered toluene solvent molecule was restrained to be the same as that of the major orientation during the refinement by use of the *SHELXL* **SAME** instruction.

Compound **4**: The minor orientation of the disordered $N_3P_3Cl_5$ ring was restrained to have the same geometry as that of the major orientation by use of the *SHELXL* **SAME** instruction.

6.5.3 Synthetic Procedures.

6.5.3.1 Synthesis of [IPr•PN(Cl_2PN)$_2$] 1. To a mixture of IPr (280 mg, 0.72 mmol), phosphonitrilic chloride trimer $[Cl_2PN]_3$ (100 mg, 0.29 mmol) and sodium (15 mg, 0.65 mmol) was added 15 mL of a 1:1 mixture of toluene and THF. The resulting mixture was stirred overnight at room temperature to give a pale green slurry. The reaction mixture was allowed to settle and the mother liquor was then filtered through Celite to yield a green solution. The volatiles were removed from the filtrate *in vacuo* and the resulting solid was then washed with 5 mL of hexanes and dried to give a pale green powder. Crystals (colorless blocks) suitable for X-ray crystallography were grown by cooling a saturated toluene solution layered with hexanes to -35 °C for 7 days (103 mg, 55%). ^{1}H NMR (C_6D_6): δ 0.94 (d, $^3J_{HH}$ = 6.8 Hz, 12H, CH(C*H*$_3$)$_2$), 1.45 (d, $^3J_{HH}$ = 6.8 Hz, 12H, CH(C*H*$_3$)$_2$), 2.63 (septet, $^3J_{HH}$ = 6.8 Hz, 4H, C*H*(CH$_3$)$_2$), 6.17 (s, 2H, N-C*H*-), 7.05 (d, $^3J_{HH}$ = 7.6 Hz, 4H, Ar*H*), 7.15 (t, $^3J_{HH}$ = 7.6 Hz, 2H, Ar*H*). ^{13}C{^{1}H} NMR (C_6D_6): δ 23.6 (CH(*C*H$_3$)$_2$), 24.8 (CH(*C*H$_3$)$_2$), 28.8 (*C*H(CH$_3$)$_2$), 121.6 (-N-*C*H-), 123.7 (Ar*C*), 124.6 (Ar*C*), 129.1 (Ar*C*), 139.1 (Ar*C*), 146.3 (N-*C*-N). ^{31}P{^{1}H} NMR (C_6D_6): δ 6.1 (d, -Cl$_2$*P*N, $^2J_{PP}$ = 86.9 Hz), 101.4 (t, IPr-*P*N, $^2J_{PP}$ = 86.9 Hz). Repeated attempts to obtain satisfactory elemental analysis consistently led to low analysis value for N (> 3% lower). Mp (°C): 153-155 (dec.), 225-227 (melts).

6.5.3.2 Alternate sodium-free synthesis of [IPr•PN(Cl_2PN)$_2$] 1. To a mixture of IPr (0.41 g, 1.1 mmol), phosphonitrilic chloride trimer, $[Cl_2PN]_3$ (0.18 g, 0.53 mmol) was added 15 mL of toluene. The reaction mixture was stirred overnight at room temperature to give a thick brown slurry. The resulting mixture was allowed

to settle and the mother liquor was then filtered through Celite to yield a pale brown solution. Removal of the volatiles from the filtrate afforded a brown oil. The oil was dissolved in 12 mL of toluene, layered with hexanes and cooled to -35 °C for 10 days to afford **1** as a white solid (45 mg, 13%).

6.5.3.3 Synthesis of [IPr•PN(Cl_2PN)$_2$] 1 using stoichiometric IPr•$GeCl_2$ as a carbene source. To a mixture of IPr•$GeCl_2$ (0.502 g, 0.945 mmol), phosphonitrilic chloride trimer, [Cl_2PN]$_3$ (0.327 g, 0.942 mmol) and sodium (0.130 g, 5.65 mmol) was added a 1:1 mixture of toluene and THF (12 mL). The reaction mixture was stirred for 72 h at room temperature to obtain a dark brown slurry. The resulting mixture was allowed to settle and the mother liquor was then filtered through Celite to yield a pale yellow solution. Removal of the volatiles from the filtrate afforded a white solid. X-ray quality crystals of **1** were obtained by cooling (-35 °C) a saturated solution of **1** layered with hexanes. (0.439 g, 83%).

6.5.3.4 Reaction of [IPr•PN(Cl_2PN)$_2$] with S_8: Synthesis of [IPr•(S)PN(Cl_2PN)$_2$] 2. To a mixture of **1** (72 mg, 0.11 mmol) and sulfur (3.5 mg, 0.11 mmol) was added 10 mL of toluene. The reaction mixture was stirred overnight at room temperature to give a slightly cloudy mixture. Filtration of the resulting mixture through Celite gave a colorless filtrate. Removal of the volatiles from the filtrate yielded colorless crystalline solid (67 mg, 88%). X-ray quality crystals of **2** were grown by cooling a saturated toluene solution to -35 °C for 2 days. ^{1}H NMR (C_6D_6): δ 0.93 (d, $^3J_{HH}$ = 6.5 Hz, 12H, CH(CH_3)$_2$), 1.50 (d, $^3J_{HH}$ =

6.5 Hz, 12H, CH(CH_3)$_2$), 2.79 (septet, $^3J_{HH}$ = 6.5 Hz, 4H, CH(CH$_3$)$_2$), 6.15 (d, $^4J_{HP}$ = 1.5 Hz, 2H, N-CH-), 7.04 (d, $^3J_{HH}$ = 7.5 Hz, 4H, ArH), 7.13 (t, $^3J_{HH}$ = 7.5 Hz, 2H, ArH). ^{13}C{^{1}H} NMR (C_6D_6): δ 23.3 (CH(CH$_3$)$_2$), 25.5 (CH(CH$_3$)$_2$), 26.6 (CH(CH$_3$)$_2$), 124.5 (-N-CH-), 124.6 (ArC), 127.6 (ArC), 131.4(ArC), 134.0 (ArC), 145.2 (N-C-N). ^{31}P{^{1}H} NMR (C_6D_6): δ 13.4 (d, -Cl$_2$$P$N, $^2J_{PP}$ = 26.7 Hz), 23.9 (t, IPr-PN, $^2J_{PP}$ = 26.7 Hz). Anal. Calcd. for $C_{27}H_{36}Cl_4N_5P_3S$: C, 46.50; H, 5.20; N, 10.40; S, 4.60. Found: C, 47.07; H, 5.60; N, 9.75; S, 4.21. Mp (°C): > 260 °C.

6.5.3.5 Synthesis of [IPr•(BH$_3$)P•N(Cl$_2$PN)$_2$] 3. To a solution of **1** (74 mg, 0.11 mmol) in 6 mL of toluene was added dropwise H$_3$B•THF (0.11 mL, 0.11 mmol, 1.0 M solution in THF). The reaction mixture turned slightly cloudy after two hours of stirring at room temperature. The solution was then filtered through Celite and the volatiles were removed from the filtrate to yield a crystalline white solid which was identified as **3** by NMR spectroscopy (65 mg, 87%). ^{1}H NMR (C_6D_6): δ 0.91 (d, $^3J_{HH}$ = 6.9 Hz, 12H, CH(CH_3)$_2$), 1.51 (d, $^3J_{HH}$ = 6.9 Hz, 12H, CH(CH_3)$_2$), 2.70 (septet, $^3J_{HH}$ = 6.9 Hz, 4H, CH(CH$_3$)$_2$), 6.17 (s, 2H, N-CH-), 7.03 (d, $^3J_{HH}$ = 7.6 Hz, 4H, ArH), 7.14 (t, $^3J_{HH}$ = 7.6 Hz, 2H, ArH). ^{13}C{^{1}H} NMR (C_6D_6): δ 23.1 (CH(CH$_3$)$_2$), 25.7 (CH(CH$_3$)$_2$), 29.6 (CH(CH$_3$)$_2$), 124.6 (-N-CH-), 125.7 (ArC), 131.6 (ArC), 133.6 (ArC), 136.2 (ArC), 145.2 (N-C-N). ^{31}P{^{1}H} NMR (C_6D_6): δ 12.6 (d, -Cl$_2$$P$N, $^2J_{PP}$ = 6.0 Hz), 72.5 (br, IPr-PN). ^{11}B{^{1}H} NMR (C_6D_6): δ -30.5 (d, IPr•P•BH$_3$, $^1J_{BP}$ = 71.6 Hz). MS (ESI, positive mode, high res.): [M+H]$^+$; 678.1352 (Δ = 1.39 ppm). Anal. Calcd. for $C_{27}H_{39}BCl_4N_5P_3$: C, 47.75; H, 5.79; N, 10.31. Found: C, 47.94; H, 5.82; N, 9.44. Mp (°C): 194-197 (dec.).

6.5.3.6 Synthesis of [(IPr=CH)PClN(Cl_2PN)$_2$] 4. To a mixture of IPr=CH_2 (140 mg, 0.35 mmol) and phosphonitrilic chloride trimer $[Cl_2PN]_3$ (60 mg, 0.17 mmol) was added 15 mL of toluene. The reaction mixture was heated to 60 °C in an oil bath for 30 hrs resulting in the formation of a pink solution over white precipitate. The reaction mixture was then filtered through Celite and the volatiles were removed from the filtrate *in vacuo* to yield a pink powder (110 mg, 88%). Crystals (colorless needles) suitable for X-ray crystallography were grown by cooling a saturated toluene solution layered with hexanes to -35 °C for 5 days. ^{1}H NMR (C_6D_6): δ 1.06 (d, $^3J_{HH}$ = 7.0 Hz, 12H, CH(CH_3)$_2$), 1.38 (d, $^3J_{HH}$ = 7.0 Hz, 12H, CH(CH_3)$_2$), 2.91 (septet, $^3J_{HH}$ = 7.0 Hz, 4H, CH(CH$_3$)$_2$), 3.31 (t, 1H, -CH-, $^4J_{HP}$ = 6.0 Hz, confirmed by selective ^{1}H{^{31}P} and ^{1}H-^{31}P gHSQC experiments), 5.96 (s, 2H, N-CH-), 7.06 (d, $^3J_{HH}$ = 8.0 Hz, 4H, ArH), 7.20 (t, $^3J_{HH}$ = 8.0 Hz, 2H, ArH). ^{13}C{^{1}H} NMR (C_6D_6): δ 23.3 (CH(*C*H$_3$)$_2$), 24.9 (CH(*C*H$_3$)$_2$), 29.1 (*C*H(CH$_3$)$_2$), 53.4 (doublet of triplets, -*C*H-P, $^1J_{CP}$ = 231.4 Hz, $^3J_{CP}$ = 16.1 Hz), 118.5 (-N-*C*H-), 124.9 (Ar*C*), 130.0 (Ar*C*), 132.9 (Ar*C*), 147.1 (Ar*C*), 152.0 (d, N-*C*-N, $^2J_{CP}$ = 15.2 Hz). ^{31}P{^{1}H} NMR (C_6D_6): δ 18.8 (d, -Cl$_2$*P*N-, $^2J_{PP}$ = 17.5 Hz), 25.6 (t, -HC-Cl*P*N-, $^2J_{PP}$ = 17.5 Hz). Anal. Calcd. for $C_{28}H_{37}Cl_5N_5P_3$: C, 47.11; H, 5.22; N, 9.81. Found: C, 47.70; H, 5.32; N, 9.66. Mp (°C): > 260 °C.

6.5.3.7 Reaction of [(IPr=CH)P(Cl)N(PCl_2N)$_2$] (4) with HCl: To a solution of **4** (85 mg, 0.12 mmol) in 10 mL of toluene was added a solution of HCl (0.120 mL, 0.24 mmol, 2.0 M solution in Et_2O). The reaction mixture clouded immediately and was stirred for 2 hours to give a white slurry. The slurry was allowed to settle

and the white precipitate was isolated by filtration. $^{31}P\{^{1}H\}$ NMR analysis of the filtrate reveled the quantitative formation of free phosphonitrilic chloride trimer, $[Cl_2PN]_3$.[25] The precipitate was dried *in vacuo* to give a white powder (51 mg, 97%) which was identified as [IPr-CH_3]Cl by ^{1}H NMR spectroscopy. ^{1}H NMR ($CDCl_3$): δ 1.17 (d, $^{3}J_{HH}$ = 6.8 Hz, 12H, $CH(CH_3)_2$), 1.27 (d, $^{3}J_{HH}$ = 6.8 Hz, 12H, $CH(CH_3)_2$), 2.07 (s, 3H, -CH_3), 2.32 (septet, $^{3}J_{HH}$ = 7.0 Hz, 4H, $CH(CH_3)_2$), 7.36 (d, $^{3}J_{HH}$ = 8.0 Hz, 4H, Ar*H*), 7.60 (t, $^{3}J_{HH}$ = 8.0 Hz, 2H, Ar*H*), 8.53 (s, 2H, N-C*H*-). $^{13}C\{^{1}H\}$ NMR ($CDCl_3$): δ 10.8 (s, -CH_3), 23.5 ($CH(CH_3)_2$), 24.9 ($CH(CH_3)_2$), 29.1 ($CH(CH_3)_2$), 125.4 (-N-*C*H-), 127.1 (Ar*C*), 129.2 (Ar*C*), 132.5 (Ar*C*), 144.5 (Ar*C*), 145.1 (N-*C*-N). MS (ESI, positive mode, low res.): $[M\text{-}Cl]^+$; 403.3. Anal. Calcd. for $C_{28}H_{39}ClN_2$: C, 76.59; H, 8.95; N, 6.38;. Found: C, 76.56; H, 8.87; N, 6.56.

Table 6.1 Crystallographic data for **1**, **2** and **4**.

Compound	**1**	**2**	**4**
Formula	$C_{34}H_{44}Cl_4N_5P_3$	$C_{34}H_{44}Cl_4N_5P_3S$	$C_{34}H_{44}Cl_5N_5P_3$
formula weight	757.45	789.91	805.92
crystal system	triclinic	monoclinic	triclinic
space group	$P\bar{1}$	$P2_1/c$	$P\bar{1}$
a(Å)	9.9329(3)	11.5334(2)	10.5636(4)
b (Å)	12.3748(4)	13.9852(2)	11.5438(5)
c (Å)	16.5363(5)	24.9658(10)	19.1398(5)
α (deg)	86.1689(3)	90	99.4845(5)
β (deg)	76.2264(3)	99.5850(10)	99.7811(5)
γ (deg)	80.9368(3)	90	114.9935(4)
V (Å^3)	1948.60(10)	3970.66(11)	2030.64(14)
Z	2	4	2
ρ(g cm^{-3})	1.291	1.321	1.318
abs coeff (mm^{-1})	0.458	4.586	0.507
T (K)	173(1)	173(1)	173(1)
$2\theta_{max}$ (°)	55.12	139.34	54.96
total data	17249	26061	18102
unique data (R_{int})	8886(0.0117)	7333(0.0220)	9252(0.0116)
Obs data [$I > 2\sigma(I)$]	7786	6717	7954
params	415	448	529
R_1 [$I > 2\sigma(I)$][a]	0.0325	0.0392	0.0429
wR_2 [all data][a]	0.0932	0.1126	0.1271
max/min $\Delta\rho$ (e$^-$ Å^{-3})	0.437/-0.397	0.631/-0.367	1.021/-0.534

[a] $R_1 = \Sigma \big| |F_o| - |F_c| \big| / \Sigma |F_o|$; $wR_2 = [\Sigma\, w(F_o^2 - F_c^2)^2 / \Sigma\, w(F_o^4)]^{1/2}$.

6.6 References

(1) (a) Arduengo, A. J., III; Rasika Dias, H. V.; Harlow, R. L.; Kline, M. *J. Am. Chem. Soc.* **1992**, *114*, 5530. (b) Kuhn, N.; Al-Sheikh, A. *Coord. Chem. Rev.* **2005**, *249*, 829. (c) Wang, Y.; Robinson, G. H. *Inorg. Chem.* **2011**, *50*, 12326.

(2) (a) Kinjo, R.; Donnadieu, B.; Celik, M. A.; Frenking, G.; Bertrand, G. *Science* **2011**, *333*, 610. (b) Wang, Y.; Xie, Y.; Wei, P.; King, R. B.; Schaefer, H. F., III; Schleyer, P. v. R.; Robinson, G. H. *Science* **2008**, *321*, 1069. (c) Ghadwal, R. S.; Roesky, H. W.; Merkel, S.; Henn, J.; Stalke, D. *Angew. Chem., Int. Ed.* **2009**, *48*, 5683. (d) Filippou, A. C.; Chernov, O.; Schnakenburg, G. *Angew. Chem., Int. Ed.* **2009**, *48*, 5687. (e) Wang, Y.; Xie, Y.; Wei, P.; King, R. B.; Schaefer, H. F., III; Schleyer, P. v. R.; Robinson, G. H. *J. Am. Chem. Soc.* **2008**, *130*, 14970. (f) Back, O.; Kuchenbeiser, G.; Donnadieu, B.; Bertrand, G. *Angew. Chem., Int. Ed.* **2009**, *48*, 5530. (g) Wang, Y.; Xie, Y.; Abraham, M. Y.; Gilliard, R. J., Jr.; Wei, P.; Schaefer, H. F., III; Schleyer, P. v. R.; Robinson, G. H. *Organometallics* **2010**, *29*, 4778. (h) Braunschweig, H.; Dewhurst, R. D.; Hammond, K.; Mies, J.; Radacki, K.; Vargas, A. *Science* **2012**, *336*, 11420.

(3) For selected references, see: (a) Sidiropoulos, A.; Jones, C.; Stasch, A.; Klein, S.; Frenking, G. *Angew. Chem., Int. Ed.* **2009**, *48*, 9701. (b) Filippou, A. C.; Chernov, O.; Stumpf, K. W.; Schnakenburg, G. *Angew.*

Chem., Int. Ed. **2010**, *49*, 3296. (c) Bonyhady, S. J.; Collis, D.; Frenking, G.; Holzmann, N.; Jones, C.; Stasch, A. *Nat. Chem.* **2010**, *2*, 865. (d) Yao, S.; Xiong, Y.; Driess, M. *Chem. Eur. J.* **2010**, 1281. (e) Ghadwal, R. S.; Roesky, H. W.; Pröpper, K.; Dittrich, B.; Klein, S.; Frenking, G. *Angew. Chem., Int. Ed.* **2011**, *50*, 5374. (f) Katir, N.; Matioszek, D.; Ladeira, S.; Escudié, J.; Castel, A. *Angew. Chem., Int. Ed.* **2011**, *50*, 5352. (g) Abraham, M. Y.; Wang, Y.; Xie, Y.; Wei, P.; Schaefer, H. F., III; Schleyer, P. v. R.; Robinson, G. H. *J. Am. Chem. Soc.* **2011**, *133*, 8874.

(4) (a) Thimer, K. C.; Al-Rafia, S. M. I.; Ferguson, M. J.; McDonald, R.; Rivard, E. *Chem. Commun.* **2009**, 7119. (b) Al-Rafia, S. M. I.; Malcolm, A. C.; Liew, S. K.; Ferguson, M. J.; Rivard, E. *J. Am. Chem. Soc.* **2011**, *133*, 777. (c) Al-Rafia, S. M. I.; Malcolm, A. C.; Liew, S. K.; Ferguson, M. J.; McDonald, R.; Rivard, E. *Chem. Commun.* **2011**, 6987. (d) Inoue, S.; Driess, M. *Angew. Chem., Int. Ed.* **2011**, *50*, 5614.

(5) Al-Rafia, S. M. I.; Malcolm, A. C.; McDonald, R.; Ferguson, M. J.; Rivard, E. *Angew. Chem., Int. Ed.* **2011**, *50*, 8354.

(6) (a) Dulley, D. D.; Williams, D. A. A.; *Interstellar Chemistry*, Academic Press, New York, **1984**. (b) Yung, Y. L.; DeMore, W. B. *Photochemistry of Planetary Atmospheres*, Oxford University Press, Oxford, **1998**. (c) Ziurys, L. M. *Astrophys. J.* **1987**, *321*, L81.

(7) (a) Ahlrichs, R.; Schunck, S.; Schnöckel, H. *Angew. Chem., Int. Ed. Engl.* **1988**, *27*, 421. (b) Ahlrichs, R.; Bär, M.; Plitt, H. S.; Schnöckel, H. *Chem.*

Phys. Lett. **1989**, *161*, 179. (c) Weber, L. *Angew. Chem., Int. Ed.* **2010**, *49*, 5829.

(8) Göbel, M.; Karaghiosoff, K.; Klapötke, T. M. *Angew. Chem., Int. Ed.* **2006**, *45*, 6037.

(9) (a) Horstmann, S.; Irran, E.; Schnick, W. *Angew. Chem., Int. Ed.* **1997**, *36*, 1873. (b) Landskorn, K.; Huppertz, H.; Senker, J.; Schnick, W. *Angew. Chem., Int. Ed.* **2001**, *40*, 2643.

(10) (a) Kober, E. H.; Lederel, H. F.; Ottmann, G. F. USA Patent US 32918645, 1966. (b) Zeng, X.; Wang, W.; Liu, F.; Ge, M.; Sun, Z.; Wang, D. *Eur. J. Inorg. Chem.* **2006**, 416. (c) Volgnandt, A.; Schmidt, A. *Z. Anorg. Allg. Chem.* **1976**, *425*, 189.

(11) Atkins, R. M.; Timms, P. L. *Spectrochim. Acta* **1977**, *33A*, 853.

(12) (a) Arduengo, A. J., III; Calabrese, J. C.; Cowley, A. H.; Rasika Dias, H. V.; Goerlich, J. R.; Marshall, W. J.; Riegel, B. *Inorg. Chem.* **1997**, *36*, 2515. (b) Ellis, B. D.; Dyker, C. A.; Decken, A.; Macdonald, C. L. B. *Chem. Commun.* **2005**, 1965.

(13) For related carbene chemistry involving phosphorus, see: (a) Schmidpeter, A.; Lochschmidt, S.; Willhalm, A. *Angew. Chem., Int. Ed. Engl.* **1983**, *22*, 545. (b) Arduengo, A. J., III; Carmalt, C. J.; Clyburne, J. A. C.; Cowley, A. H.; Pyati, R. *Chem. Commun.* **1997**, 981. (c) Kuhn, N.; Fahl, J.; Bläser, D.; Boese, R. *Z. Anorg. Allg. Chem.* **1999**, *625*, 729. (d) Burford, N.;

Dyker, C. A.; Phillips, A. D.; Spinney, H. A.; Decken, A.; McDonald, R.; Ragogna, P. J.; Rheingold, A. L. *Inorg. Chem.* **2004**, *43*, 7502. (e) Masuda, J. D.; Schoeller, W. W.; Donnadieu, B.; Bertrand, G. Angew. *Chem., Int. Ed.* **2007**, *46*, 7052. (f) Back, O.; Donnadieu, B.; Parameswaran, P.; Frenking, G.; Bertrand, G. *Nat. Chem.* **2010**, *2*, 369. (g) Weigand, J. J.; Feldmann, K, -O.; Henne, F. D. *J. Am. Chem. Soc.* **2010**, *132*, 16321.

(14) Kinjo, R.; Donnadieu, B.; Bertrand, G. *Angew. Chem., Int. Ed.* **2010**, *49*, 5930.

(15) Bartlett, S. W.; Coles, S. J.; Davies, D. B.; Hursthouse, M. B.; Ibisoglu, H.; Kilic, A.; Shaw, R. A.; Un, I. *Acta Crystallogr.* **2006**, *B62*, 321.

(16) Codding, P. W.; Kerr, K. A. *Acta Crystallogr.* **1978**, *B34*, 3785.

(17) Kuhn, N.; Bohnen, H.; Kreutzberg, J.; Bläser, D.; Boese, R. *J. Chem. Soc., Chem. Commun.* **1993**, 1136. (b) Dumrath, A.; Wu, X. F.; Neumann, H.; Spannenberg, A.; Jackstell, R.; Beller, M. *Angew. Chem., Int. Ed.* **2010**, *49*, 8988.

(18) Allcock, H. R.; Connolly, M. S.; Whittle, R. R. *Organometallics* **1983**, *2*, 1514.

(19) (a) Allcock, H. R. *Chem. Rev.* **1972**, *72*, 315. (b) Zhang, Y.; Huynh, K.; Manners, I.; Reed, C. A. *Chem. Commun.* **2008**, 494.

(20) Pangborn, A. B.; Giardello, M. A.; Grubbs, R. H.; Rosen, R. K.; Timmers, F. *J. Organometallics* **1996**, *15,* 1518.

(21) Jafarpour, L.; Stevens, E. D.; Nolan, S. P. *J. Organomet. Chem.* **2000,** *606,* 49.

(22) Hope, H.; *Prog. Inorg. Chem.* **1995**, *43,* 1.

(23) Blessing, R. H. *Acta Cryst.* **1995**, *A51,* 33.

(24) Sheldrick, G. M. *Acta Cryst.* **2008**, *A64,* 112.

(25) Huynh, K.; Rivard, E.; Lough, A. J.; Manners, I. *Chem. Eur. J.* **2007**, *13,* 3431.

Chapter 7

Growth of Dichlorogermanium Oligomers from N-Heterocyclic Carbene and N-Heterocyclic Olefin Hosts

Chapter 7

Growth of Dichlorogermanium Oligomers from N-Heterocyclic Carbene and N-Heterocyclic Olefin Hosts

7.1 Abstract

The synthesis of a new class of donor-supported oligogermanium complexes is reported. It has been found that the σ-donor ability of the supporting ligand dictates the nature of the oligomer formed (*i.e* linear *vs* branched). For example, the reaction of IPr•$GeCl_2$ (IPr = ([(HCNDipp)$_2$C:], Dipp = 2,6-^{i}Pr$_2$C$_6$H$_3$) with an additional equivalent of $GeCl_2$•dioxane leads to the formation of the linear tetrachlorodigermane complex IPr•$GeCl_2$-$GeCl_2$ (**1**), while IPrCH_2•$GeCl_2$ reacts with $GeCl_2$•dioxane to give a dicationic species containing a branched tetragermane array [(IPrCH_2•$GeCl_2$)$_3$Ge][$GeCl_3$]$_2$ (**4**). A chloride/hydride metathesis reaction involving **1** and Li[BH_4], with the goal of forming digermane the borane complex IPr•GeH_2-GeH_2•BH_3 was unsuccessful and resulted in the formation of the known Ge(II) hydride borane adduct IPr•GeH_2•BH_3. Interestingly, IPr•$GeCl_2$-$GeCl_2$ (**1**) interacted with two equivalents of $GeCl_2$•dioxane to afford the *catena*-tetragermane complex IPr•$GeCl_2$-Ge($GeCl_3$)$_2$ (**3**); the exact mechanism for the formation of **3** is not clear at this time, but oxidative addition (direct or stepwise) of two Ge(2)-Cl bonds in IPr•$GeCl_2$-$GeCl_2$ (**1**) to two separate $GeCl_2$ groups can be one of the possible pathways. Attempts to prepare the donor-

acceptor adduct IPr•$GeCl_2$•$GeCl_2$•$B(C_6F_5)_3$ from the treatment of **1** with the Lewis acid acceptor $B(C_6F_5)_3$, resulted in the formation of an unexpected linear trigermane complex [IPr•$GeCl_2$-GeCl-$GeCl_2$•IPr][Cl_3Ge-$B(C_6F_5)_3$] (**2**).

7.2 Introduction

The concept of catenation, the linking of similar atoms into extended molecular arrays, is often used to obtain materials with novel properties. A salient illustration of this point is the synthesis of industrially and commercially relevant organic polymers such as polyolefins.[1] Amongst the inorganic Group 14 elements it has been shown that catenation leads to species of the general form $[R_2E]_n$ (E = Si, Ge, Sn and Pb) display interesting optoelectronic properties as a result of increasing σ-σ* conjugation both as the length of the chains get longer and as the core element becomes heavier.[2] Thus oligomers and polymers featuring Group 14 elements often interact with visible light and in fact, polysilanes are now widely employed as efficient photoresist materials.[3]

In general the synthesis of polytetrels $[R_2E]_n$ involve harsh reducing conditions, such as Wurtz coupling, which limits the degree of molecular weight control;[4] however the use of transition-metals as catalysts to construct Group 14 element polymers *via* dehydrocoupling polymerization is emerging as a powerful strategy.[5] Despite the stable nature of the tin and lead dihalides $SnCl_2$ and $PbCl_2$, which have extended three dimensional network structures in solid state, much

less is known about the lighter congeners $(SiCl_2)_x$ and $(GeCl_2)_x$ which are both considered to have extended catenated structures in the solid state.[6] Both $SiCl_2$ and $GeCl_2$ have been stabilized as molecular adducts L•ECl_2 (E = Si and Ge; L = Lewis base),[7,8] however intercepting oligomers of these species with a high degree of control over chain length has posed a considerable challenge thus far. In recent years, the synthesis of *catena*-germanium compounds has drawn significant attention due to their potential application in the synthesis of germanium nanowires and wide variety of semiconductor heterostructures such as $Ge_{1-x}C_x$, $Si_{1-x}Ge$, $Si_{1-x-y}Ge_xC_y$.[9] Thus the development of a facile strategy for the controlled synthesis of *catena*-germanes (oligomers/polymers) could provide new precursors for the fabrication of germanium-based semiconducting materials of potential interest to the electronics industry.

This Chapter reports the synthesis, characterization and preliminary reactivity studies of a series of donor-supported oligodichlorogermanium complexes.

7.3 Results and discussion

The Rivard group has been exploring the use of N-heterocyclic carbenes (NHCs) to facilitate the isolation of complexes featuring the parent methylene and ethylenes units EH_2 and $H_2EE'H_2$ (E and E′ = Si, Ge and/or Sn).[8,10] Knowing that the Ge(II) adduct IPr•$GeCl_2$ (IPr = [(HCNDipp)$_2$C:]; Dipp = 2,6-^{i}Pr$_2$C$_6$H$_3$) contains a stereochemically active lone pair at Ge,[8a,c] it was postulated that this

complex might interact with further equivalents of $GeCl_2$ to give new carbene-stabilized oligomers of the general form IPr•$(GeCl_2)_x$ (x > 1). Each new Ge-Ge linkage would be formed *via* the formal donation of a Ge lone pair into an empty p-orbital of a neighboring $GeCl_2$ unit. To explore this hypothesis, a solution of IPr•$GeCl_2$ was reacted with one equivalent of $GeCl_2$•dioxane in toluene. This reaction afforded a new sparingly soluble product that was isolated as an air- and moisture-sensitive white powder in 75% yield and identified by X-ray crystallography as the tetrachlorodigermane-carbene adduct IPr•$GeCl_2$-$GeCl_2$ (**1**) (Equation 7.1). Note that, IPr•$GeCl_2$ can be illustrated by two forms (**I** and **II**) on the basis of how the C_{IPr}-Ge interaction is represented (*i.e.* covalent *vs* dative bonding). For simplicity, in this Chapter all the Ge-Ge interactions will be drawn as covalent bonds, however, further bonding analysis *via* theoretical methods will be required to clarify this point; prior work has shown that the C_{IPr}-Ge bond in **1** can be considered as dative in nature.

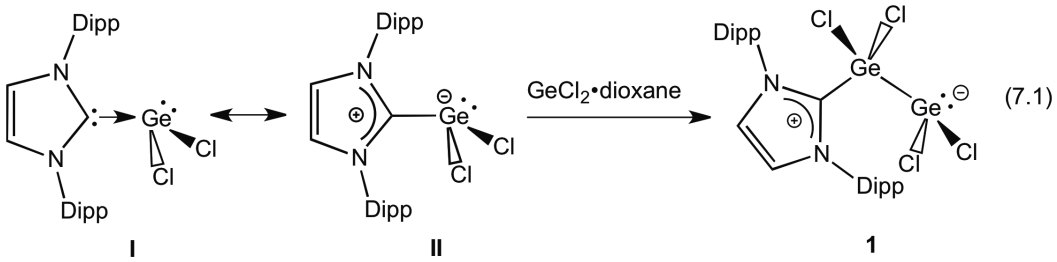

(7.1)

The ^{1}H NMR spectrum of **1** corroborated the X-ray crystallographic data as a resonance belonging to the olefinic protons of the carbene backbone was located at 7.39 ppm, while in the IPr•$GeCl_2$ starting material these protons appear at 7.24 ppm. Correspondingly shifted resonance signals for **1** were observed in the

$^{13}C\{^{1}H\}$ NMR spectrum relative to that of the starting Ge(II) chloride complex IPr•$GeCl_2$. For example, the carbenic carbon appeared at 146.2 ppm in **1** while the related resonance in IPr•$GeCl_2$ was located at 173.1 ppm.

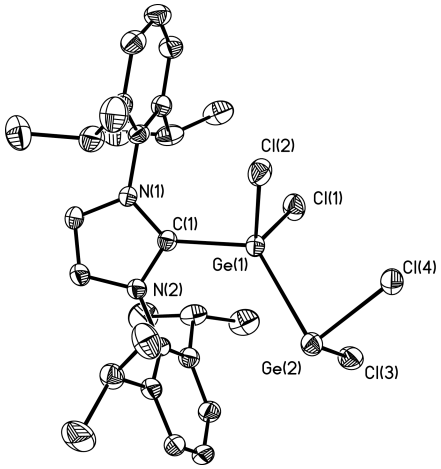

Figure 7.1. Thermal ellipsoid plot (30% probability level) of IPr•$GeCl_2$-$GeCl_2$ (**1**). Carbon-bound hydrogen atoms have been omitted for clarity. Selected bond lengths [Å] and angles [°]: C(1)-Ge(1) 2.032(5), Ge(1)-Cl(1) 2.1811(16), Ge(1)-Cl(2) 2.1780(15), Ge(1)-Ge(2) 2.6304(9), Ge(2)-Cl(3) 2.2568(16), Ge(2)-Cl(4) 2.2844(15); C(1)-Ge(1)-Ge(2) 125.04(14), C(1)-Ge(1)-Cl(1) 100.16(15), C(1)-Ge(1)-Cl(2) 99.80(14), Ge(1)-Ge(2)-Cl(3) 93.41(5), Ge(1)-Ge(2)-Cl(4) 86.73(4), Cl(3)-Ge(2)-Cl(4) 96.22(6); torsion angle = C(1)-Ge(1)-Ge(2)-Cl(3) 101.85(17), C(1)-Ge(1)-Ge(2)-Cl(4) -162.11(17), Cl(1)-Ge(1)-Ge(2)-Cl(3) -43.70(7), Cl(2)-Ge(1)-Ge(2)-Cl(4) 101.85(7).

As illustrated in Figure 7.1, IPr•$GeCl_2$-$GeCl_2$ (**1**) contains a coordinated tetrachlodigermane unit Cl_2Ge-$GeCl_2$ with a mutually twisted arrangement of constituent $GeCl_2$ groups. The C_{IPr}-Ge bond length in **1** [2.032(5) Å] is shorter than the C_{IPr}-Ge dative interaction in the IPr•$GeCl_2$ adduct [2.112(2) Å],[8c] and the contraction of carbene-germanium dative interaction might be arising from the greater electron accepting ability of the Cl_2Ge-$GeCl_2$ moiety relative to $GeCl_2$. The

Ge(1)-Ge(2) bond distance [2.6304(9) Å] in **1** is longer than the bond length range typically observed for Ge-Ge single bonds [2.40-2.50 Å],[11] suggesting the presence of a weak germanium-germanium interaction in **1**. Nevertheless, the Ge-Ge bond distance in **1** is shorter than the elongated Ge-Ge bond of 2.7093(7) Å found in Jones' digermylene [Ar*(Me_3Si)NGe-Ge($SiMe_3$)Ar*] (Ar* = 2,6-(Ph_2CH)$_2$-4-Me-C_6H_2) wherein considerable p-character is present in the Ge-Ge bond.[12] The terminal $GeCl_2$ moiety in **1** features a trigonal pyramidal arrangement around the germanium center with a sterochemically active lone pair [angle sum at Ge(2) = 276.36(9)°].

The UV-visible absorption spectrum of **1** exhibits a broad absorption at 289 nm and the value of molar absorption coefficient (ε) was 2.58×10^3 $M^{-1}cm^{-1}$ (Figure 7.3). For comparison, in $Ph_3GeGePh_3$ the absorption maxima (λ_{max}) was found to be at 241 nm and the value of the molar absorption coefficient (ε) was determined to be 3.9×10^4 $M^{-1}cm^{-1}$.[13]

The crystallographic data supports the presence of a stereochemically active lone pair on the terminal $GeCl_2$ unit in **1** and it has already been shown that the germanium based lone pair in IPr•$GeCl_2$ can participate in dative interactions with Lewis acids acceptors such as BH_3 and $W(CO)_5$.[8] In prior studies it was shown that IPr•$GeCl_2$ reacts with Li[BH_4] to generate a stable Ge(II) dihydride borane adduct IPr•GeH_2•BH_3 (Chapter 3).[8a,c] Therefore, it was anticipated that the tetrachlorodigermane adduct IPr•$GeCl_2$-$GeCl_2$ (**1**) might react with Li[BH_4] to give the hitherto unknown digermane borane complex IPr•GeH_2-GeH_2•BH_3.

Unfortunately, the reaction of IPr•$GeCl_2$•$GeCl_2$ (**1**) with four equivalents of Li[BH_4] resulted in the formation of the known hydride adduct IPr•GeH_2•BH_3, in 70% yield (Equation 7.2). This result hints that the Ge-Ge interaction in the expected product IPr•GeH_2-GeH_2•BH_3 is very labile and perhaps dissociation occurs in solution to give transient IPr•GeH_2 species which then reacts with excess BH_3 from the solution to form the stable germylene borane adduct IPr•GeH_2•BH_3 (Equation 7.2). The exact mechanism by which decomposition occurs is not clear at this time but similar chemistry was observed when IPr•GeH_2-GeH_2•$W(CO)_5$ decomposes at room temperature to give IPr•GeH_2•$W(CO)_5$ as a stable product (Chapter 4).

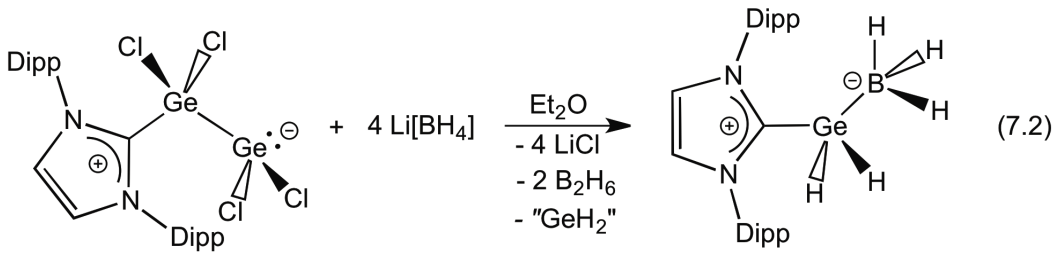

(7.2)

The labile nature of the Ge-Ge bond in **1** was further examined by the reaction of IPr•$GeCl_2$-$GeCl_2$ (1) with 2,3-dimethyl-1,3-butadiene. As shown in the Equation 7.3, **1** reacts cleanly with 2,3-dimethyl-butadiene to give IPr•$GeCl_2$ and known the germanium heterocycle, 3,4-dimethyl-1,1-dichlorogermacyclopent-3-ene.[14]

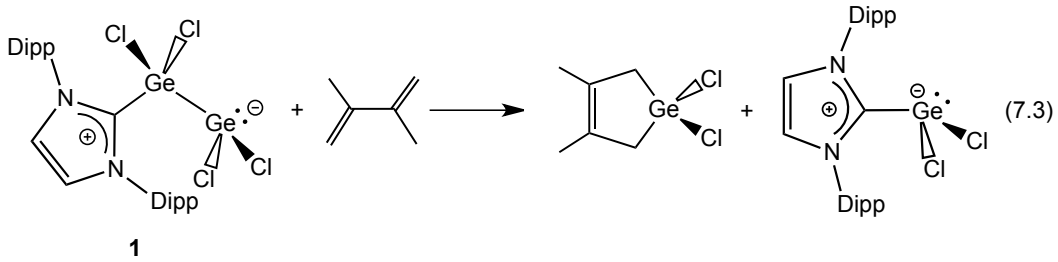

In addition, the labile nature of the Ge-Ge linkage in **1** was noted in the presence of THF in which IPr•$GeCl_2$-$GeCl_2$ (**1**) undergoes clean dissociation to form IPr•$GeCl_2$ and the metastable adduct THF•$GeCl_2$ as soluble products (Equation 7.4).

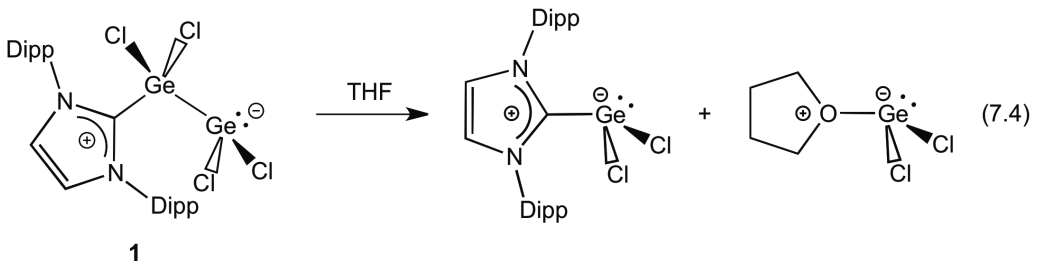

On the basis of our prior studies, where it was shown that Ge-Ge linkages can be stabilized by binding with a external Lewis basic donor and a Lewis acidic acceptor (Chapter 4), it was postulated that the use of stronger electron acceptor such as $B(C_6F_5)_3$ might lead to the strengthening of the Ge-Ge linkage in **1**. Thus this chemistry should potentially enable the syntheses of the borane adduct IPr•$GeCl_2$-$GeCl_2$•$B(C_6F_5)_3$ and IPr•GeH_2-GeH_2•$B(C_6F_5)_3$.[8,15,16] To test the validity of this approach IPr•$GeCl_2$-$GeCl_2$ (**1**) was treated with one equivalent of $B(C_6F_5)_3$ with the goal of forming the donor-acceptor adduct IPr•$GeCl_2$-$GeCl_2$•$B(C_6F_5)_3$. Surprisingly, this reaction afforded the novel cationic *catena*-chlorogermane

adduct, $[IPr•GeCl_2\text{-}GeCl\text{-}GeCl_2•IPr]^+$ (**2**) with a $[Cl_3Ge\text{-}B(C_6F_5)_3]^-$ counter anion (Equation 7.5).

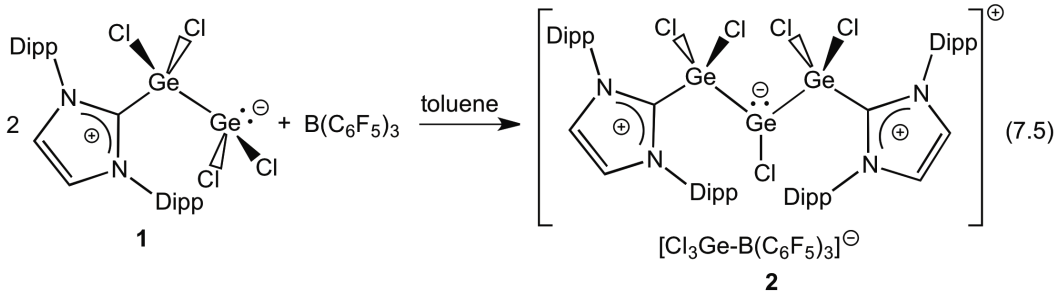

The formation of the $[Cl_3Ge\text{-}B(C_6F_5)_3]^-$ anion **2** was supported by $^{11}B\{^{19}F\}$ NMR spectrum where a broad resonance was observed at -5.7 ppm consistent with the presence of a four-coordinate boron center. The $^{19}F\{^1H\}$ NMR spectrum contained three well-resolved resonances at -129.3 (d), -157.6 (t) and 164.7 (m) ppm corresponding to the fluorine groups at *ortho*, *meta* and *para* positions, respectively in the $B(C_6F_5)_3$ unit. The ^1H NMR spectrum of **2** yields two broad doublets ($CH(CH_3)_2$) and a broad septet ($CH(CH_3)_2$), which were assigned to the isopropyl groups in the capping IPr donors, while resonances belonging to the olefinic protons at the carbene backbone and aromatic protons were quite sharp at room temperature. At lower temperatures (*i.e.* -60 °C) the broad isopropyl resonances in **2** became considerably sharper and interestingly exhibited rotational isomerism. Even at lower temperatures (-90 °C) the presences of two sets of ^1H NMR signals were noted in a *ca.* 19:1 ratio (on the basis of integration values), representing two rotational isomers, which was confirmed by saturation transfer and variable temperature ^1H NMR experiments. For example, when the resonance

for the septet corresponding to the major rotomer is selectively saturated at -60 °C, the corresponding resonance for the minor rotomer collapses. Furthermore, increasing the temperature to 25 °C results in the coalescence of these peaks into a broad resonance; unfortunately, experiments were limited by the low boiling point of CD_2Cl_2, *ca*. 40 °C. The UV-visible absorption spectrum of **2** displayed an absorption maximum (λ_{max}) at 291 nm with a molar absorption coefficient (ε) of 1.10×10^3 $M^{-1}cm^{-1}$ (Figure 7.3).

As shown in Figure 7.2, the trigermane cation [IPr•$GeCl_2$-GeCl-$GeCl_2$•IPr]$^+$ in **2** represents an all *trans* conformation along the C_{IPr}-Ge-Ge-Ge-C_{IPr} backbone with a Ge(1)-Ge(2)-Ge(3)-C(4) torsion angle of 163.98(10)°. The capping carbene-Ge bonding interactions in **2** [2.030(3) and 2.022(3) Å] are the same within the experimental error as the C_{IPr}-Ge bond length in the tetrachlorodigermane complex **1** [2.032(5) Å]. The Ge-Ge bond distances in **2** [2.5455(8) and 2.5700(5) Å] are significantly shorter than the corresponding distance in IPr•$GeCl_2$-$GeCl_2$ (1) [2.6304(9) Å], yet longer than the Ge-Ge bond distance in cyclotrigermane $[Ge(SiMe_3)_2]_3$ [2.460(1) Å][17] and the computed value of 2.45 Å in $(GeH_2)_3$.[18] While the Ge-B bond distance in the $[Cl_3Ge•B(C_6F_5)_3]^-$ counteranion is 2.174(4) Å and comparable to the Ge-B bond in the Ge(II) complex [Me_2ATI](Ph)Ge•BPh_3 (Me_2ATI = *N*-methyl-2-(methylamino)troponiminate) [2.156(4) Å].[19,20] The Ge(1)-Ge(2)-Ge(3) bond angle in **2** was determined to be 87.226(16)° and is significantly narrower than the Ge-Ge-Ge bond angle found within the trigermane chain $Ph_3GeGePh_2GePh_3$

[121.3(1)°];[21] this bond angle contraction in **2** might be due to the presence of a higher degree of p-character in the Ge(1)-Ge(2)-Ge(3) bond.

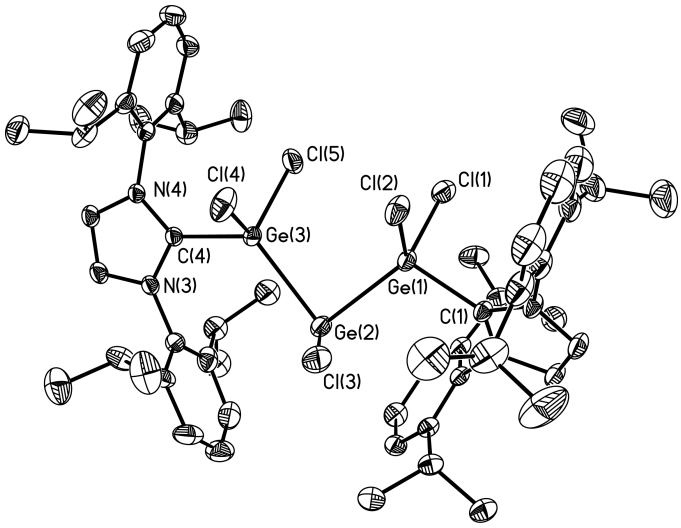

Figure 7.2. Thermal ellipsoid plot (30% probability level) of the [IPr•$GeCl_2$-GeCl-$GeCl_2$•IPr]$^+$ cation in (**2**). Carbon-bound hydrogen atoms, CH_2Cl_2 solvate and the $[Cl_3Ge\text{-}B(C_6F_5)_3]^-$ anion have been omitted for clarity. Selected bond lengths [Å] and angles [°]: C(1)-Ge(1) 2.030(3), Ge(1)-Cl(1) 2.1856(11), Ge(1)-Cl(2) 2.1489(19), Ge(1)-Ge(2) 2.5455(8), Ge(2)-Cl(3) 2.2610(13), Ge(2)-Ge(3) 2.5700(5), Ge(3)-C(4) 2.022(3), Ge(3)-Cl(4) 2.1581(11), Ge(1)-Cl(5) 2.022(3); C(1)-Ge(1)-Ge(2) 109.71(9), Cl(1)-Ge(1)-Cl(2) 100.40(5), Ge(1)-Ge(2)-Ge(3) 87.226(16), Ge(1)-Ge(2)-Cl(3) 83.94(4), Ge(3)-Ge(2)-Cl(3) 95.34(3); C(1)-Ge(1)-Ge(2)-Ge(3) 171.34(10), C(1)-Ge(1)-Ge(2)-Cl(3) 75.66(10), Ge(1)-Ge(2)-Ge(3)-C(4) 163.98(10). In the $[Cl_3Ge\text{-}B(C_6F_5)_3]^-$ anion: Ge(4)-B 2.174(4); Cl(6)-Ge(4)-Cl(7) 100.37(4), Cl(6)-Ge(4)-Cl(8) 102.63(4), Cl(6)-Ge(4)-Cl(8) 100.91(4).

The success in isolating a carbene adduct of tertachlorodigermane IPr•$GeCl_2$-$GeCl_2$ (**1**) provided an impetus to extend this synthetic protocol towards the synthesis of other polygermylene adducts [*e.g.* IPr•$(GeCl_2)_x$; x >2]. In order to construct the desired $GeCl_2$-$GeCl_2$-$GeCl_2$ chain, IPr•$GeCl_2$-$GeCl_2$ (**1**) was reacted with one equivalent of $GeCl_2$•dioxane in a 4:1 mixture of toluene/CH_2Cl_2.

Analysis of the reaction mixture by ^{1}H NMR spectroscopy in CD_2Cl_2 showed the formation of a new carbene-containing product (*ca*. 35%; *vide infra*) along with IPr•$GeCl_2$-$GeCl_2$ (**1**) and $GeCl_2$•dioxane starting materials (Scheme 7.1). The new carbene-bound product was isolated in pure form (33% overall yield) by fractional crystallization from a saturated CH_2Cl_2/hexanes solution of the crude product mixture at -35 °C and structurally characterized as the branched tetragermane IPr•$GeCl_2$-$Ge(GeCl_3)_2$ (**3**) by X-ray crystallography. It is important to mention that the reaction of **1** with two equivalents of $GeCl_2$•dioxane also gave a similar product mixture with no sign of the formation of extended polygermanes with greater than four Ge atoms. Compound **3** was isolated as an air- and moisture-sensitive pale yellow solid and its formation was confirmed by ^{1}H, and $^{13}C\{^{1}H\}$ NMR spectroscopy, elemental analysis (C, H, N) and UV-visible absorption spectroscopy.

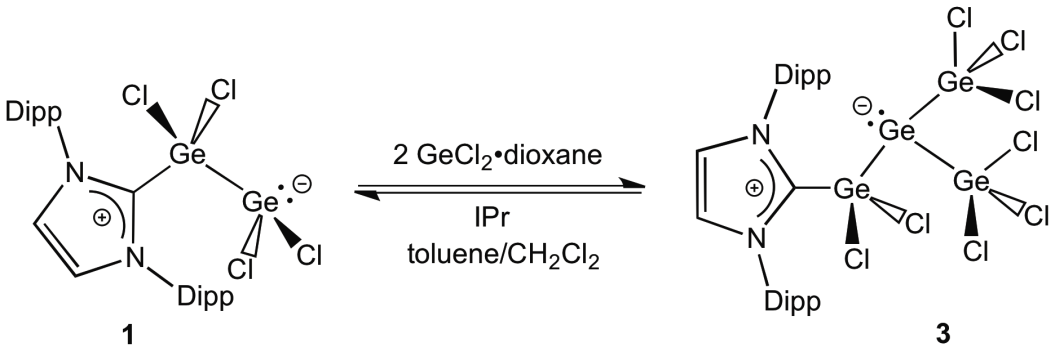

Scheme 7.1. Synthesis of *catena*-tetragermanium complex IPr•$GeCl_2$-$Ge(GeCl_3)_2$ (**3**) and its reversible reaction in the presence of IPr to give IPr•$GeCl_2$-$GeCl_2$ (**1**).

Compound **3** displayed a broad absorption band at 286 nm ($\varepsilon = 6.09 \times 10^3$ $M^{-1}cm^{-1}$) in the UV-visible absorption spectrum, which is slightly blue shifted in comparison to the absorption maxima for **1** and **2** [289 and 291 nm, respectively] (Figure 7.3). In general, branched oligogermanes exhibit bathochromic shifts compared to their linear congeners due to the two dimensional σ-delocalization,[21] therefore the similarities in absorption maxima for IPr•$GeCl_2$ and **1**-**3** indicate that the electronic transition is likely a π-π* transition involving the backbone of the olefinic group of the IPr donor. The nature of these electronic transitions is currently under investigation in our group using TD-DFT methods.

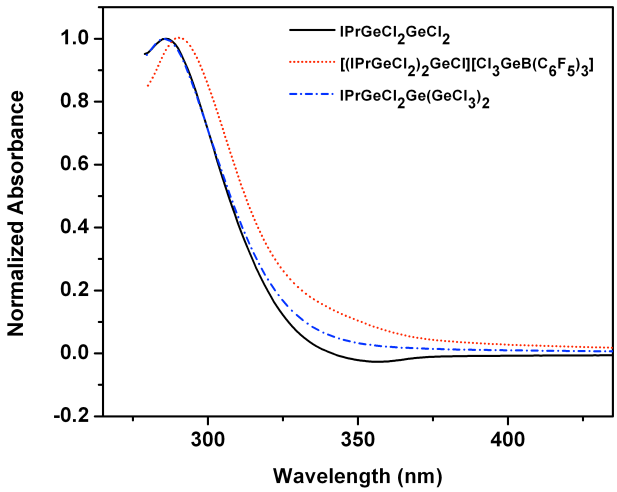

Figure 7.3. UV-visible spectra of IPr•$GeCl_2$-$GeCl_2$ (**1**), [IPr•$GeCl_2$-GeCl-$GeCl_2$•IPr][Cl_3Ge-B(C_6F_5)$_3$] (**2**) and IPr•$GeCl_2$-Ge($GeCl_3$)$_2$ (**3**) in CH_2Cl_2.

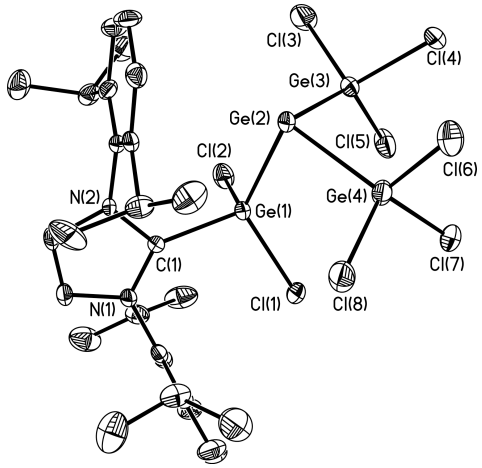

Figure 7.4. Thermal ellipsoid plot (30% probability level) of IPr•Cl_2Ge-Ge($GeCl_3$)$_2$ (**3**). Carbon-bound hydrogen atoms and CH_2Cl_2 solvate molecules have been omitted for clarity. Selected bond lengths [Å] and angles [°]: C(1)-Ge(1) 2.0024(5), Ge(1)-Cl(1) 2.1506(15), Ge(1)-Cl(2) 2.1734(16), Ge(1)-Ge(2) 2.4983(8), Ge(2)-Ge(3) 2.4870(8), Ge(3)-Ge(4) 2.4987(8), Ge(3)-Cl(3-5) 2.1549(18) to 2.1792(15), Ge(4)-Cl(6-8) 2.1525(19) to 2.1675(17); C(1)-Ge(1)-Ge(2) 117.46(14), Cl(1)-Ge(1)-Cl(2) 103.99(7), Ge(1)-Ge(2)-Ge(3) 90.90(3), Ge(1)-Ge(2)-Ge(4) 91.27(3), Ge(3)-Ge(2)-Ge(4) 89.20(3); torsion angle = C(1)-Ge(1)-Ge(2)-Ge(3) -152.89(16), C(1)-Ge(1)-Ge(2)-Ge(4) 117.89(16).

As depicted in Figure 7.4, IPr•Cl_2Ge-Ge($GeCl_3$)$_2$ (**3**) contains a branched array of mixed valent germanium centers anchored to a carbene donor. The C_{IPr}-Ge distance in **3** is 2.0024(5) Å and is comparable to the C_{IPr}-Ge dative bonds in IPr•$GeCl_2$-$GeCl_2$ (**1**) [2.032(5) Å] and [IPr•$GeCl_2$-GeCl-$GeCl_2$•IPr]$^+$ (**2**) [2.030(3) and 2.022(3) Å], thus indicating the presence of similar C-Ge interactions in all three compounds. The Ge-Ge bonds in **3** are in the narrow range of 2.4870(8)-2.4987(8) Å and slightly elongated compared to the Ge-Ge bonds in the branched oligogermane (Ph_3Ge)$_3$GePh [2.4692(4) Å].[23] Interestingly, the central germanium atom in **3** adopts a distorted trigonal pyramidal geometry [sum of angles around Ge(2) = 271.71 (3)°] in line with the presence of a stereochemically active lone

pair. The core Ge-Ge-Ge bond angles involving Ge(2) in **3** are significantly narrower than the intra-chain Ge-Ge-Ge bond angles in tetragermane $Ph_3GeGePh_2GePh_2GePh_3$ [average value of 115.6(2)°].[22] This bond-angle contraction in **3** can be attributed to the higher degree of p-character in the Ge-Ge-Ge linkage stemming from the presence of a stereochemically active lone pair on the Ge(2) center. Furthermore, the presence of narrow internal Ge-Ge-Ge bond angles in **3** [90.46(3)° (*avg*.)] compared to the Cl(3)-Ge-Cl(4) bond angle in **2** [96.22(6)°] suggests that the $GeCl_3$ groups are more strongly electron withdrawing than chlorides and therefore, higher participation of p-orbitals should be present in the Ge-Ge bonds in **3** in accordance with the Bent's rule.[24] Although, in terms of steric effect the presence of bulky $GeCl_3$ groups in **3** should make the Ge-Ge-Ge angles wider; hence, the electronic effect appears to dictate the narrow bond angles observed in **3**.

The mechanism by which IPr•Cl_2Ge-Ge$(GeCl_3)_2$ (**3**) forms is not clear at this time but one probable mechanism would be the chloride migration involving an internal Ge-Cl bond to an incoming $GeCl_2$ unit (Scheme 7.2).[25,26] Another possible mechanism by which compound **3** can form involves the direct oxidative addition of two terminal Ge(2)-Cl bonds in IPr•$GeCl_2$-$GeCl_2$ (**1**) to two separate $GeCl_2$ groups,[27] the net effect of this proposed processes is the formation of two Ge-$GeCl_3$ units to give IPr•Cl_2Ge-Ge$(GeCl_3)_2$ (**3**).

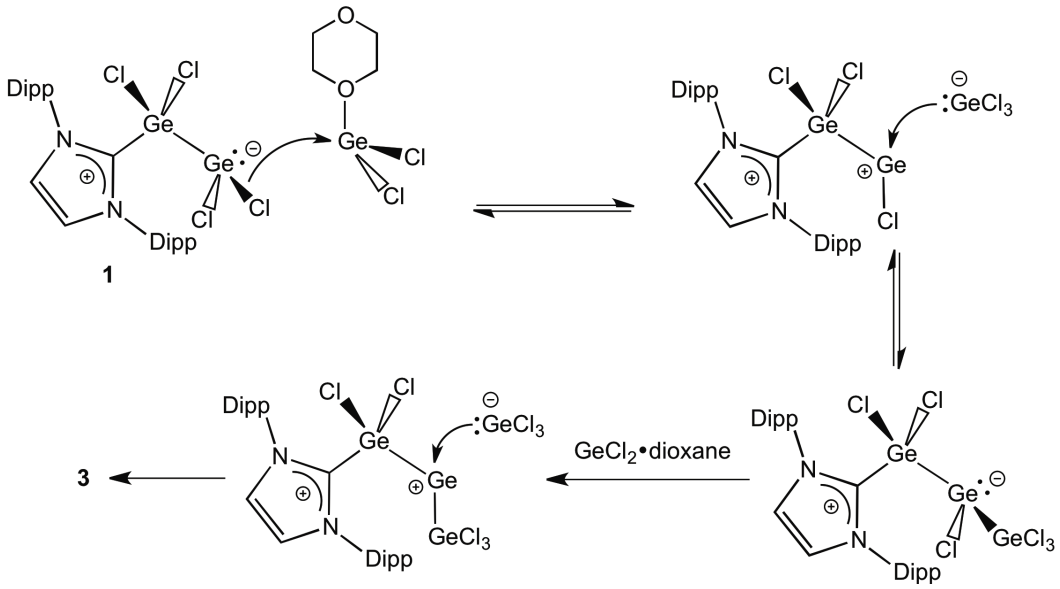

Scheme 7.2. Proposed mechanism for the formation of IPr•Cl_2Ge-Ge($GeCl_3$)$_2$ (**3**).

It is quite important to mention that IPr•Cl_2Ge-Ge($GeCl_3$)$_2$ (**3**) exhibits reversible chloride migration in the presence of IPr, leading the quantitative formation of IPr•$GeCl_2$-$GeCl_2$ (**1**) (Scheme 7.1).

In order to explore the strategy of donor-assisted germanium chain growth further, the application of the N-heterocyclic olefin IPr=CH_2 as a donor ligand was investigated. Recently, the Rivard group has shown that IPr=CH_2 can be used efficiently to stabilize low-coordinate main group hydride complexes, such as IPrCH_2•EH_2•$W(CO)_5$ (E = Ge and Sn).[10c] In early the 1990's, the Karsh group successfully used anionic bidentate PCP ligand to isolate different linear and branched germanium complexes, for example, [{(μ-[$(Me_3Si)C(PMe_2)_2$]}$_2$$Ge_2$]$_2$$GeCl_2$.[28] In general, it has been noted that IPr=CH_2 is a

weaker σ-donor compared to N-heterocyclic carbene IPr (Chapter 3), and it was hypothesized that the differing donor strength of IPr=CH_2 might provide access to a new family of *catena*-germanium complexes.

To explore the use of IPr=CH_2 as a donor for the stabilization of germanium dichloride oligomers IPrCH_2•$(GeCl_2)_x$ the known nucleophilic Ge(II) halide adduct IPrCH_2•$GeCl_2$[29] was reacted with $GeCl_2$•dioxane in a 4:1 mixture of toluene/CH_2Cl_2. After stirring overnight at room temperature, the clean formation of a new IPrCH_2 product was observed. This new product was isolated in pure form as pale yellow crystals by cooling (-35 °C) a saturated CH_2Cl_2 solution containing the product that was layered with hexanes. On the basis of X-ray crystallography the crystals were characterized as the trichlorogermate salt [(IPrCH_2•$GeCl_2)_3$Ge][$(GeCl_3)_2$] (**4**) (Equation 7.6, Figure 7.6).

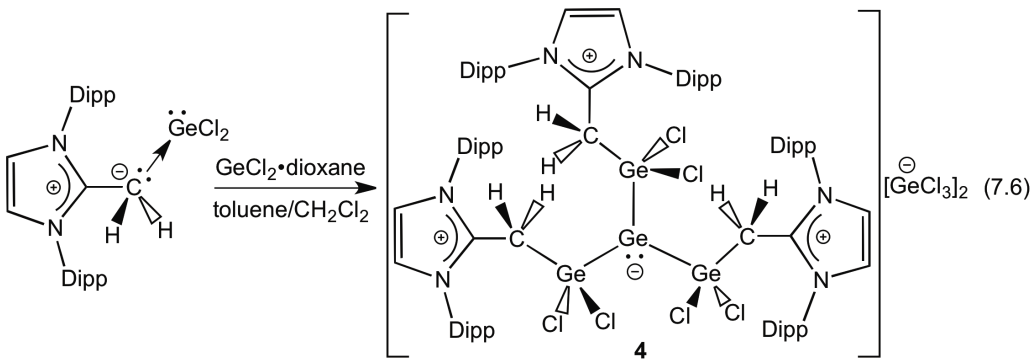

(7.6)

The ^{1}H NMR spectrum of **4** yielded broad resonances at room temperature with well-resolved signals present at -90 °C in CD_2Cl_2. The -*C*H_2 groups resonated at 2.68 ppm, while a sharp singlet resonance was obtained at 7.48 ppm

corresponding to the C-H groups of the IPr backbone. The $^{13}C\{^{1}H\}$ spectrum of **4** exhibited some broad resonance features even at -90 °C but the number of observed resonances matches the expected number of expected carbon resonances based on the symmetry of the complexes (*vide infra*). In addition, saturation transfer and variable temperature NMR experiments were performed to confirm the fluxional behavior of **4** in solution. For example, ^{1}H NMR spectrum of **4** yielded a broad resonance for the C*H*$(CH_3)_2$ protons, which resolved into two distinct resonances at -90 °C (in CD_2Cl_2); at this temperature, selective saturation of one of these resonance causes the collapse of the other signal, confirming the presence of exchange behavior between the two rotational conformations. The UV-visible absorption spectrum of **4** contains λ_{max} at 309 nm ($\varepsilon = 43.63 \times 10^3$ $M^{-1}cm^{-1}$) and is only slightly shifted from the λ_{max} in $IPrCH_2{\bullet}GeCl_2$ [309 nm; $\varepsilon = 4.01 \times 10^3$ $M^{-1}cm^{-1}$] (Figure 7.5).

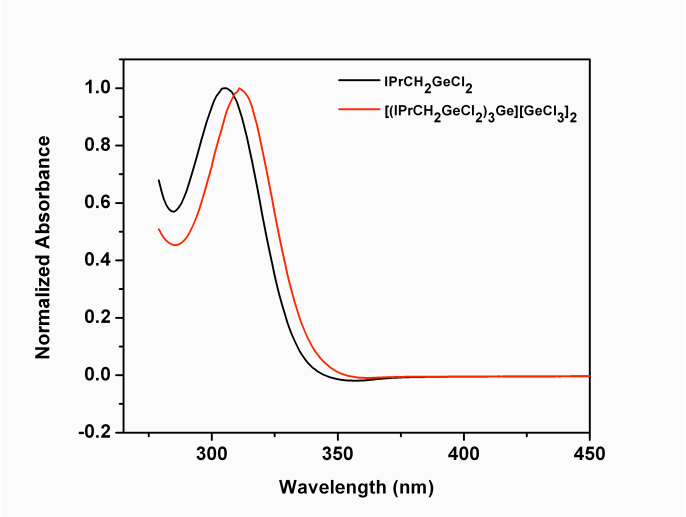

Figure 7.5. UV-visible spectram of $IPrCH_2{\bullet}GeCl_2$ and $[(IPrCH_2{\bullet}GeCl_2)_3Ge][(GeCl_3)_2]$ (**4**) in CH_2Cl_2.

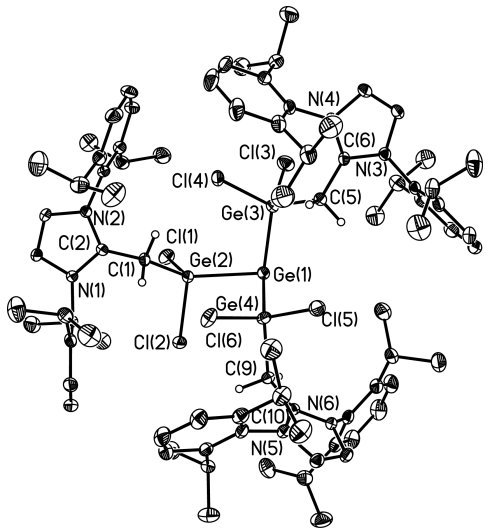

Figure 7.6. Thermal ellipsoid plot (30% probability level) of the $[(IPrCH_2{\bullet}GeCl_2)_3Ge]^{2+}$ dication in **4**. Carbon-bound hydrogen atoms, $[GeCl_3]^-$ anions and CH_2Cl_2 solvate have been omitted for clarity. Selected bond lengths [Å] and angles [°]: C(2)-C(1) 1.469(5), C(6)-C(5) 1.467(5), C(10)-C(9) 1.458(5), C(1)-Ge(2) 2.004(4), C(5)-Ge(3) 1.996(4), C(9)-Ge(4) 2.004(4), Ge(1)-Ge(2) 2.4899(6), Ge(1)-Ge(3) 2.4743(6), Ge(1)-Ge(4) 2.5005(6); C(1)-Ge(2)-Ge(1) 130.95(11), C(5)-Ge(3)-Ge(1) 118.32(12), C(9)-Ge(4)-Ge(1) 109.15(12), Ge(2)-Ge(1)-Ge(3) 98.75(2), Ge(2)-Ge(1)-Ge(4) 88.38(2), Ge(3)-Ge(1)-Ge(4) 95.61(2); torsion angle = C(2)-C(1)-Ge(2)-Ge(1) 156.5(2), C(6)-C(5)-Ge(3)-Ge(1) 142.5(3), C(10)-C(9)-Ge(4)-Ge(1) 142.2(3).

As illustrated in Figure 7.6, the $[(IPrCH_2{\bullet}GeCl_2)_3Ge]^{2+}$ dication in **4** has a trigonal pyramidal arrangement [sum of the bond angles = 282.74(2)°] with three flanking $IPrCH_2{\bullet}GeCl_2$ groups attached to the centeral Ge(II) atom. Each of the flanking $IPrCH_2{\bullet}GeCl_2$ groups in **4** features a $GeCl_2$ moiety that is bound to a central Ge atom to give a canted array of $C\text{-}C_{IPrCH2}\text{-}Ge\text{-}Ge$ [torsion angle = 147.07(5) (*avg*.)]. The constituent C_{IPrCH2}-Ge bond distances in **4** are 2.001(4) (*avg*.) and slightly elongated compared to the C_{IPrCH2}-Ge distance in $IPrCH_2{\bullet}Cl_2Ge\text{-}GeCl_2{\bullet}W(CO)_5$ [1.9815(8) Å (*avg*.)],[30] but shorter than the similar interaction in $IPrCH_2{\bullet}GeCl_2{\bullet}W(CO)_5$ [2.056(3) Å].[10c] The corresponding Ge-Ge bond lengths [2.488(6) Å (*avg*.)] are similar to the Ge-Ge bond distances present in the IPr-stabilized branched oligomer $IPr{\bullet}Cl_2Ge\text{-}Ge(GeCl_3)_2$ (**3**) [2.4947(8) Å, (*avg*.)], suggesting that the Ge-Ge bond distances are not greatly affected by the formal cationic character of the central germanium atom Ge(1) in **4**. Moreover, the Ge-Ge bond distances in $(Me_3Ge)_3GeK{\bullet}$18-crown-6 were determined to be 2.442(12) Å (*avg*.) and in $[(Me_3Ge)_3Ge]_2$ the germanium-germanium bond lengths were found to be 2.4495(9) Å (*avg*.).[31] Interestingly, the Ge(2)-Ge(1)-Ge(3), Ge(2)-Ge(1)-Ge(4) and Ge(3)-Ge(1)-Ge(4) bond angles in **4** [94.25(2)°, *avg*.] are *ca*. 3.8° wider than the similar bond angles in **3** and thus suggest the presence of similar Ge-Ge bond hybridization as in **3**.

7.4 Conclusion

A new synthetic strategy was developed for the synthesis of oligodichlorogermylenes L•$[GeCl_2]_x$ (x = 1-4, L = IPr and $IPrCH_2$). For example, a linear digermane complex IPr•$GeCl_2$-$GeCl_2$ (**1**) was obtained from the reaction of IPr•$GeCl_2$ with $GeCl_2$•dioxane. The Ge-Ge linkage in **1** is labile and accordingly disintrigates into IPr•$GeCl_2$ and metastable THF•$GeCl_2$ adducts in the presence of THF solvent. Furthermore, in the presence of $B(C_6F_5)_3$, IPr•$GeCl_2$-$GeCl_2$ (**1**) participated in a chloride transfer reaction that led to the formation of a new cationic trigermane complex [IPr•$GeCl_2$-GeCl-$GeCl_2$•IPr][Cl_3Ge-$B(C_6F_5)_3$] (**2**). While a neutral tetragermane complex IPr•Cl_2Ge-Ge$(GeCl_3)_2$ (**3**) was formed from the reaction of **1** with two equivalents of $GeCl_2$•dioxane. Interestingly, when compound **3** was reacted with IPr, the quantitative formation of IPr•$GeCl_2$-$GeCl_2$ (**1**) was noted. Different reactivity was observed when N-heterocyclic olefin ($IPr=CH_2$) was used as donor ligand. For example, reaction of $IPrCH_2$•$GeCl_2$ with an additional equivalent of $GeCl_2$•dioxane resulted in the formation of a di-cationic branched tetragermane complex $[(IPrCH_2•GeCl_2)_3Ge][GeCl_3]_2$ (**4**). Although further extension of the reported chain length unsuccessful, the chemistry described in this Chapter offers significant potential for the future controlled synthesis of other heavy Group 14 oligomers IPr•$(E'Cl_2)_n$ (E = Si and Ge; E' = Si-Sn) and possibly their hydride analogues.

7.5 Experimental Section

7.5.1 Materials and Instrumentation

All of the reactions were performed using standard Schlenk line techniques under an atmosphere of nitrogen or in an inert atmosphere glove box (Innovative Technology, Inc.). Solvents were dried using Grubbs-type solvent purification system[32] manufactured by Innovative Technology, Inc., degassed (freeze-pump-thaw method) and stored under an atmosphere of nitrogen prior to use. $Li[BH_4]$ and $GeCl_2$•dioxane were purchased from Aldrich and used as received. 1,3-Bis-(2,6-diisopropylphenyl)-imidazol-2-ylidene (IPr),[33] IPr•$GeCl_2$[8c] and IPr=CH_2[10c] were synthesized following literature procedures. ^{1}H, $^{13}C\{^{1}H\}$, $^{19}F\{^{1}H\}$ and $^{11}B\{^{19}F\}$ NMR spectra were recorded either on Varian iNova-400 or Varian iNova-500 spectrometers and referenced externally. X-ray crystallographic analyses were performed by the X-ray Crystallography Laboratory at the University of Alberta. Elemental analyses were performed by the Analytical and Instrumentation Laboratory at the University of Alberta. Infrared spectra were recorded on a Nicolet IR100 FTIR spectrometer as Nujol mulls between NaCl plates. UV-visible spectra were measured using a Varian Cary 300 spectrophotometer. Melting points were measured in sealed glass capillaries under nitrogen using a MelTemp melting point apparatus and are uncorrected.

7.5.2 X-ray Crystallography

Crystals of suitable quality for X-ray diffraction studies were removed from a vial in a glove box and immediately covered with a thin layer of hydrocarbon oil (Paratone-N). A suitable crystal was then selected, mounted on a glass fiber and quickly placed in a low temperature stream of nitrogen on an X-ray diffractometer.[34] All data were collected using a Bruker APEX II CCD detector/D8 diffractometer using Mo Kα (compounds **3** and **4**) or Cu Kα (compounds **1** and **2**) radiation, with the crystals cooled to -100 °C. The data were corrected for absorption through Gaussian integration from the indexing of the crystal faces.[35] Structures were solved using the direct methods programs SHELXS-97[36] (compounds **2** and **4**) or using the Patterson search/structure expansion facilities within the DIRDIF-2008[37] (compound **1**) and SHELXD[38] program suites (compounds **3**); structure refinement was accomplished using SHELXS-97.[36] Hydrogen atoms were assigned positions based on the sp^2 or sp^3 hybridization geometries of their attached carbon atoms, and were given thermal parameters 20% greater than those of their parent atoms. See Tables 7.1 and 7.2 for a listing of the crystallographic data.

7.5.2.1 Special Refinement Conditions

Compound **2**: The C56–C60A and C56–C60B distances were restrained to be the same by use of the *SHELXL* **SADI** instruction. The disordered solvent dichloromethane molecule was restrained to have the same geometry as that of the

ordered solvent dichloromethane molecule by use of the *SHELXL* **SAME** instruction.

Compound **3**: The C-Cl distances within the disordered solvent dichloromethane molecule were restrained to be the same by use of the *SHELXL* **SAME** instruction.

7.5.3 Synthetic Procedures.

7.5.3.1 Synthesis of IPr•$GeCl_2$-$GeCl_2$ 1. A solution of IPr•$GeCl_2$ (0.103 g, 0.193 mmol) in 10 mL of toluene was added to $GeCl_2$•dioxane (0.045 g, 0.193 mmol) and the resulting mixture was stirred overnight to give a white slurry. The precipitate was then allowed to settle and the mother liquor was separated by filtration through Celite. Removal of the volatiles from the precipitate afforded **1** as a white powder (0.086 g) and a second crop of **1** (0.012 g) was isolated by cooling the filtrate to -35 °C (75% overall yield). Crystals suitable for X-ray single crystallographic analysis were obtained by cooling (-35 °C) a saturated solution of **1** in CH_2Cl_2 layered with hexanes. ^{1}H NMR (500 MHz, CD_2Cl_2): δ 1.19 (d, $^3J_{HH}$ = 7.0 Hz, 12H, CH(C*H*$_3$)$_2$), 1.40 (d, $^3J_{HH}$ = 7.0 Hz, 12H, CH(C*H*$_3$)$_2$), 2.62 (septet, $^3J_{HH}$ = 7.0 Hz, 4H, C*H*(CH$_3$)$_2$), 7.39 (s, 2H, N-C*H*-), 7.41 (d, $^3J_{HH}$ = 8.0 Hz, 4H, Ar*H*), 7.61 (t, $^3J_{HH}$ = 8.0 Hz, 2H, Ar*H*). ^{1}H NMR (500 MHz, C_6D_6): δ 0.92 (d, $^3J_{HH}$ = 6.5 Hz, 12H, CH(C*H*$_3$)$_2$), 1.36 (d, $^3J_{HH}$ = 7.0 Hz, 12H, CH(C*H*$_3$)$_2$), 2.70 (septet, $^3J_{HH}$ = 7.0 Hz, 4H, C*H*(CH$_3$)$_2$), 6.34 (s, 2H, N-C*H*-), 7.01 (d, $^3J_{HH}$ = 7.5 Hz, 4H, Ar*H*), 7.16 (t, $^3J_{HH}$ = 7.5 Hz, 2H, Ar*H*). ^{13}C{^{1}H} NMR (125 MHz, CD_2Cl_2): δ 23.1 (CH(*C*H$_3$)$_2$), 26.1 (CH(*C*H$_3$)$_2$), 29.6 (*C*H(CH$_3$)$_2$), 125.2 (-N-*C*H-),

126.6 (Ar*C*), 128.6 (Ar*C*), 129.4 (Ar*C*), 132.3 (Ar*C*), 146.2 (N-*C*-N). Anal. Calcd. for $C_{27}H_{36}Cl_4Ge_2N_2$: C, 47.99; H, 5.37; N, 4.15. Found: C, 48.09; H, 5.39; N, 4.16. UV/visible (CH_2Cl_2): λ_{max} 289 nm ($\varepsilon = 2.58 \times 10^3$ $M^{-1}cm^{-1}$). Mp (°C): 179-181.

7.5.3.2 Synthesis of [(IPr•$GeCl_2$)$_2$-GeCl][Cl_3Ge-B(C_6F_5)$_3$] 2. To a mixture of IPr•$GeCl_2$-$GeCl_2$ (0.130 g, 0.192 mmol) and $B(C_6F_5)_3$ (0.049 g, 0.096 mmol) was added 10 mL of CH_2Cl_2 and the mixture was stirred overnight to give a pale yellow solution. Removal of the volatiles from the reaction mixture afforded **2** as a pale yellow powder. Crystals of **2** suitable for X-ray crystallography were grown by cooling a CH_2Cl_2 solution of **2** layered with hexanes to -35 °C for 5 days (0.171 g, 95%). ^{1}H NMR (400 MHz, CD_2Cl_2, 300 K): δ 1.15 (d, $^3J_{HH}$ = 6.8 Hz, 24H, CH(C*H*$_3$)$_2$), 1.33 (br, 24H, CH(C*H*$_3$)$_2$), 2.47 (br, 8H, C*H*(CH$_3$)$_2$), 7.39 (d, $^3J_{HH}$ = 7.6 Hz, 8H, Ar*H*), 7.43 (s, 4H, N-C*H*-), 7.64 (d, $^3J_{HH}$ = 7.6 Hz, 4H, Ar*H*), 7.60. ^{1}H NMR (400 MHz, CD_2Cl_2, 213 K, major and minor rotamers were present in a *ca*. 95:5 ratio and their chemical shifts are listed separately; the presence of two rotomers was confirmed by variable temperature (+ 40 to -90 °C) and saturation transfer NMR experiments). ^{1}H NMR data for major rotomer: δ 1.05 (d, $^3J_{HH}$ = 6.8 Hz, 24H, CH(C*H*$_3$)$_2$), 1.13 (d, $^3J_{HH}$ = 6.8 Hz, 12H, CH(C*H*$_3$)$_2$), 1.23 (d, $^3J_{HH}$ = 6.8 Hz, 12H, CH(C*H*$_3$)$_2$), 2.30 (two overlapping septets, $^3J_{HH}$ = 6.8 Hz, 8H, C*H*(CH$_3$)$_2$), 7.29 (d, $^3J_{HH}$ = 7.6 Hz, 4H, Ar*H*), 7.34 (d, $^3J_{HH}$ = 7.6 Hz, 4H, Ar*H*), 7.45 (s, 4H, N-C*H*-), 7.60 (t, $^3J_{HH}$ = 7.6 Hz, 4H, Ar*H*). ^{1}H NMR data for minor rotomer: δ 1.10 (d, $^3J_{HH}$ = 6.8 Hz, 24H, CH(C*H*$_3$)$_2$), 1.27 (d, $^3J_{HH}$ = 6.8 Hz, 24H, CH(C*H*$_3$)$_2$), 2.48 (septet, $^3J_{HH}$ = 6.8 Hz, *ca*. 8H, C*H*(CH$_3$)$_2$), 7.29 (d, $^3J_{HH}$ = 7.6 Hz, 4H, Ar*H*), 7.34 (d, $^3J_{HH}$ = 7.6 Hz, 4H, Ar*H*), 7.45 (s, 4H, N-C*H*-), 7.60 (t, $^3J_{HH}$ = 7.6 Hz, 4H,

Ar*H*).^{13}C{^{1}H, ^{19}F} NMR (125 MHz, CD_2Cl_2, -60 °C): δ 22.66 (CH(*C*H_3)$_2$), 22.71 (CH(*C*H_3)$_2$), 25.8 (CH(*C*H_3)$_2$), 25.9 (CH(*C*H_3)$_2$), 29.1 (*C*H(CH$_3$)$_2$), 29.3 (*C*H(CH$_3$)$_2$), 125.2 (-N-*C*H-), 127.4 (Ar*C*), 130.8 (Ar*C*), 132.5 (Ar*C*), 136.7 (Ar*C*), 139.6 (Ar*C*), 145.4 (Ar*C*), 145.6 (Ar*C*), 148.2 (Ar*C*), 154.5 (N-*C*-N). ^{19}F {^{1}H} NMR (377 MHz, CD_2Cl_2, -60 °C): δ 129.4 (d, $^{3}J_{FF}$ = 20.6 Hz, 6F, *o*-C_6F_5), -157.6 (t, $^{3}J_{FF}$ = 21.1 Hz, 3F, *p*-C_6F_5), -164.7 (m, 6F, *p*-C_6F_5). ^{11}B{^{19}F} NMR (128 MHz, CD_2Cl_2, -60 °C): δ -5.7. Anal. Calcd. for $C_{72}H_{72}BCl_8Ge_4N_4$: C, 46.41; H, 3.89; N, 3.01. Found: C, 46.36; H, 3.97; N, 3.01. UV/visible (CH_2Cl_2): λ_{max} 291 nm (ε = 1.10 × 10^3 M^{-1}cm^{-1}). Mp (°C): *ca*. 156-158 (decomp., turns brown), 193-195 (melts).

7.5.3.3 Synthesis of IPr•$GeCl_2$-Ge($GeCl_3$) 3. A solution of IPr•$GeCl_2$•$GeCl_2$ (0.079 g, 0.117 mmol) in a 4:1 mixture of toluene and CH_2Cl_2 (16 mL) was added to $GeCl_2$•dioxane (0.055 g, 0.234 mmol). The resulting reaction mixture was stirred overnight at room temperature to obtain a pale yellow solution. The reaction mixture was then filtered through Celite to yield a pale yellow filtrate. Removal of the volatiles from the filtrate afforded a pale yellow solid, which was identified as a mixture of **3** (*ca*. 35%) and **1** (*ca*. 65%) by ^{1}H NMR spectroscopy. Spectroscopically pure **1** was first isolated by fractional crystallization by cooling a saturated CH_2Cl_2 solution of the crude material layered with hexanes to -35 °C. Crystals suitable for X-ray crystallography were grown by cooling the remaining saturated solution (containing **3**) in CH_2Cl_2 layered with hexanes to -35 °C for 3 days. (37 mg, 33%). ^{1}H NMR (500 MHz, CD_2Cl_2): δ 1.16 (d, $^{3}J_{HH}$ = 6.5 Hz, 12H, CH(C*H*$_3$)$_2$), 1.43 (d, $^{3}J_{HH}$ = 6.5 Hz, 12H, CH(C*H*$_3$)$_2$), 2.56 (septet, $^{3}J_{HH}$ = 6.5 Hz,

4H, C*H*(CH_3)$_2$), 7.46 (d, $^3J_{HH}$ = 8.0 Hz, 4H, Ar*H*), 7.54 (s, 2H, N-C*H*-), 7.67 (t, $^3J_{HH}$ = 8.0 Hz, 2H, Ar*H*). $^{13}C\{^1H\}$ NMR (125 MHz, CD_2Cl_2): δ 22.8 (CH(*C*H_3)$_2$), 26.1 (CH(*C*H_3)$_2$), 29.4 (*C*H(CH_3)$_2$), 125.4 (-N-*C*H-), 127.6 (Ar*C*), 131.1 (Ar*C*), 133.1 (Ar*C*), 145.8 (Ar*C*), 152.6 (N-*C*-N). Mp (°C): *ca*. 137-139 (decomp., turns brown), 208-210 (melts). Anal. Calcd. for $C_{27}H_{36}Cl_8Ge_4N_2$: C, 33.68; H, 3.77; N, 2.91. Found: C, 34.26; H, 3.62; N, 3.10. UV/visible (CH_2Cl_2): λ_{max} 286 nm (ε = 6.09×10^3 $M^{-1}cm^{-1}$).

7.5.3.4 Synthesis of [(IPrCH$_2$•GeCl$_2$)$_3$-Ge](GeCl$_3$)$_2$ 4. A solution of IPrCH$_2$•$GeCl_2$ (0.086 g, 0.16 mmol) in a 4:1 mixture of toluene and CH_2Cl_2 (16 mL) was added to $GeCl_2$•dioxane (0.036 g, 0.16 mmol). The resulting reaction mixture was stirred overnight at room temperature to give a yellow solution and the volatiles were then removed *in vacuo* to obtain spectroscopically pure **4** as a yellow solid (106 mg, 97%). Crystals suitable for X-ray crystallography were grown by cooling a saturated solution of **4** in CH_2Cl_2 layered with hexanes to -35 °C for 3 days. ^1H NMR (500 MHz, CD_2Cl_2, 27 °C): δ 1.16 (d, $^3J_{HH}$ = 6.8 Hz, 36H, CH(C*H*$_3$)$_2$), 1.34 (br, 36H, CH(C*H*$_3$)$_2$), 2.43 (br, 6H, C*H*(CH_3)$_2$), 2.60 (br, 6H, C*H*$_2$), 2.83 (br, 6H, C*H*(CH_3)$_2$), 7.39 (br, 12H, Ar*H*), 7.59 (t, $^3J_{HH}$ = 7.5 Hz, 6H, Ar*H*). ^1H NMR (400 MHz, CD_2Cl_2, -90 °C): δ 0.97 (br, 18H, CH(C*H*$_3$)$_2$), 1.09 (br, 36H, CH(C*H*$_3$)$_2$), 1.17 (br, 18H, CH(C*H*$_3$)$_2$), 1.83 (br, 6H, C*H*(CH_3)$_2$), 2.68 (s, 6H, C*H*$_2$), 2.76 (br, 6H, C*H*(CH_3)$_2$), 7.27 (d, $^3J_{HH}$ = 7.6 Hz, 6H, Ar*H*), 7.35 (br, 6H, Ar*H*), 7.48 (s, 6H, N-C*H*-), 7.53 (t, $^3J_{HH}$ = 7.6 Hz, 6H, Ar*H*). $^{13}C\{^1H\}$ NMR (125 MHz, CD_2Cl_2, -90 °C): δ 22.1 (CH(*C*H_3)$_2$), 22.5 (CH(*C*H_3)$_2$), 23.3 (CH(*C*H_3)$_2$), 25.4 (CH(*C*H_3)$_2$), 26.1 (CH(*C*H_3)$_2$), 26.7 (*C*H(CH_3)$_2$), 27.8 (*C*H(CH_3)$_2$), 28.5

(*C*H(CH_3)$_2$), 29.1 (*C*H_2), 124.6 (br, Ar*C*), 125.3 (br, Ar*C*), 125.8 (Ar*C*), 128.6 (Ar*C*), 132.4 (br, Ar*C*), 143.3 (br, Ar*C*), 145.5 (br, Ar*C*), 147.2 (Ar*C*). Anal. Calcd. for $C_{84}H_{114}Cl_{12}Ge_6N_6$: C, 48.76; H, 5.55; N, 4.06. Found: C, 48.34; H, 5.47; N, 3.96. UV/visible (CH_2Cl_2): λ_{max} 309 nm ($\varepsilon = 43.63 \times 10^3$ $M^{-1}cm^{-1}$). Mp (°C): *ca.* 173-175.

7.5.3.5 Reaction of IPr•$GeCl_2$-Ge($GeCl_3$) (3) with IPr. To a mixture of **3** (50 mg, 0.052 mmol) and IPr (20 mg, 0.052 mmol) was added 6 mL of toluene and the resulting mixture was stirred overnight to give a pale yellow slurry. The precipitate was then allowed to settle and the mother liquor was separated by filtration. Removal of the volatiles from the precipitate yielded a pale yellow powder, which was identified as IPr•$GeCl_2$-$GeCl_2$ (**1**) by NMR spectroscopy (53 mg). Afterwards, the mother liquor was evaporated to dryness which afforded a pale yellow powder that was identified as **1** by NMR spectroscopy (11 mg, overall yield of both fractions, 91%).

7.5.3.6 Reaction of IPr•$GeCl_2$-$GeCl_2$ (1) with Li[BH_4]. To a mixture of **1** (0.056 g, 0.083 mmol) and Li[BH_4] (0.0072 g, 0.33 mmol) was added 8 mL of cold (-35 °C) Et_2O. The reaction mixture was then warmed to room temperature and stirred for 2 h to give a yellow slurry. The reaction mixture was then filtered through Celite to give a pale yellow filtrate and removal of the volatiles from the filtrate afforded pale yellow powder (0.028 g, 70%), which was identified as IPr•GeH_2•BH_3 by ^{1}H and ^{11}B NMR spectroscopy.

7.5.3.7 Reaction of IPr•$GeCl_2$-$GeCl_2$ (1) with 2,3-dimethyl-1,3-butadiene. 2,3-dimethyl-1,3-butadiene (0.026 mL, 0.23 mmol) was added to a solution of **1** (0.155 g, 0.23 mmol) 6 mL of in benzene. The reaction mixture was stirred for 3 hours and then the volatiles were removed under vacuum to obtain a white solid (0.146 g); ^{1}H and $^{13}C\{^{1}H\}$ NMR analysis revealed the formation of a mixture of IPr•$GeCl_2$ and 3,4-dimethyl-1,1-dichlorogermacyclopent-3-ene (*ca*. 1:1 ratio). NMR data for 3,4-dimethyl-1,1-dichlorogermacyclopent-3-ene: ^{1}H NMR (300 MHz, $CDCl_3$): δ 1.80 (t, CH_3, 6H), 2.22 (pentet, -CH_2, 4H). $^{13}C\{^{1}H\}$ NMR (300 MHz, $CDCl_3$): δ 18.7 (*C*H_3), 32.9 (-*C*H_2), 129.2 (*C*(CH_3)).[39]

Table 7.1: Crystallographic data for **1** and **2**•CH_2Cl_2.

Compound	**1**	**2**•CH_2Cl_2
Formula	$C_{27}H_{36}Cl_4Ge_2N_2$	$C_{74}H_{76}BCl_{12}F_{15}Ge_4N_4$
formula weight	675.56	2032.96
crystal system	orthorhombic	monoclinic
space group	*Pbca* (No. 61)	$P2_1/c$
a(Å)	18.2822(3)	11.3804 (2)
b (Å)	16.8572(3)	29.6549 (5)
c (Å)	20.7811(3)	25.9771 (4)
α (deg)	90	90
β (deg)	90	93.6960 (10)
γ (deg)	90	90
V (Å^3)	6404.46(18)	8748.6 (3)
Z	8	4
ρ (g cm^{-3})	1.401	1.543
abs coeff (mm^{-1})	5.513	5.603
T (K)	173(1)	173(1)
$2\theta_{max}$ (°)	139.26	140.38
total data	40949	58305
unique data (R_{int})	5814(0.0379)	15873 (0.0210)
Obs data [$I > 2\sigma(I)$]	4833	14533
params	334	996
R_1 [$I > 2\sigma(I)$][a]	0.0576	0.0471
wR_2 [all data] [a]	0.1669	0.1352
max/min $\Delta\rho$ (e$^-$ Å^{-3})	1.220 /-0.428	1.828/-1.089

[a] $R_1 = \Sigma \big| \, |F_o| - |F_c| \, \big| / \Sigma |F_o|$; $wR_2 = [\Sigma\, w(F_o^2 - F_c^2)^2 / \Sigma\, w(F_o^4)]^{1/2}$

Table 7.2: Crystallographic data for **4**•CH_2Cl_2 and **3**•$2CH_2Cl_2$.

Compound	**4**•CH_2Cl_2	**3**•$2CH_2Cl_2$
Formula	$C_{28}H_{38}Cl_{10}Ge_4N_2$	$C_{86}H_{118}Cl_{16}Ge_6N_6$
formula weight	1047.46	2238.60
crystal system	triclinic	triclinic
space group	$P\bar{1}$	$P\bar{1}$
a(Å)	10.8249 7)	10.7596(4)
b (Å)	11.1215(8)	17.7500(6)
c (Å)	19.3359(15)	28.2990(10)
α (deg)	81.6000(10)	90.1414(5)
β (deg)	73.8550(10)	99.8137(5)
γ (deg)	68.3800(10)	103.2628(5)
V (Å^3)	2076.2(3)	5178.6(3)
Z	2	2
ρ (g cm^{-3})	1.675	1.436
abs coeff (mm^{-1})	3.534	2.175
T (K)	173(1)	173(1)
$2\theta_{max}$ (°)	53.02	52.92
total data	16920	42118
unique data (R_{int})	8573(0.0371)	21309(0.0410)
Obs data [$I > 2\sigma(I)$]	6270	14462
params	418	1027
R_1 [$I > 2\sigma(I)$][a]	0.0518	0.0477
wR_2 [all data] [a]	0.1423	0.1413
max/min $\Delta\rho$ (e$^-$ Å^{-3})	1.333/-0.822	1.043 /-0. 962

[a] $R_1 = \Sigma \big| \, |F_o| - |F_c| \, \big| / \Sigma |F_o|$; $wR_2 = [\Sigma\, w(F_o^2 - F_c^2)^2 / \Sigma\, w(F_o^4)]^{1/2}$

7.6 References

1. (a) West, R. In *The Chemistry of Organic Silicon Compounds*; S. Patai, Z. Rappoport, Eds: John Wiley and Sons: New York, **1989**; pp 1207-1240. (b) Miller, R. D.; Michl, J. *Chem. Rev.* **1989**, *89*, 1359. (c) Trummer, M.; Choffat, F.; Smith, P.; Caseri, W. *Macromol. Rapid Comm.* **2012**, *33*, 448. (d) Stabenow, F.; Saak, W.; Marsmann, H.; Weidenbruch, M. *J. Am. Chem. Soc.* **2003**, *125*, 10172. (e) Manners, I. *Angew. Chem., Int. Ed.* **1996**, *35*, 1602. (f) Steinmetz, M. G. *Chem. Rev.* **1995**, *95*, 1527. (g) Sita, L. R. *Acc. Chem. Res.* **1994**, *27*, 191. (h) Weinert, C. S. *Dalton Trans.* **2009**, 1691. (i) Dyker, C. A.; Burford, N.; Lumsden, M. D.; Decken, A. *J. Am. Chem. Soc.* **2006**, *128*, 9632. (j) Dyker, C. A.; Burford, N. *Chem. Asian. J.* **2008**, *3*, 28. (k) Breuning, H. J.; Ghesner, I.; Lork, E. *Organometallics* **2001**, *20*, 1360. (l) Schacher, F. H.; Rupar, P. A.; Manners, I. *Angew. Chem., Int. Ed.* **2012**, *51*, 7898.

2. (a) Carraher Jr.; C. E. In *Macromolecules Containing Metal and Metal-Like Elements*; Eds. Abd-El-Aziz, A. S.; Carraher Jr., C. E.; Pittman Jr., C. U.; Sheat, J. E.; Zeldin, M. John Wiley and Sons: New Jersey, **2003**; pp 263-310. (b) Amadruge, M. L.; Weinert, C. S. *Chem. Rev.* **2008**, *108*, 4253. (c) Lu, V. Y.; Tilley, T. D. *Macromolecules* **2000**, *33*, 2403. (d) Wilks, E. S. *J. Chem. Inf. Comput. Sci.* **1997**, *37*, 224. (e) Lambert, J. B.;

Wu, H. *Organometallics* **1998**, *17*, 4904. (f) Lambert, J. B.; Pflug, J. L.; Denari, J. M. *Organometallics* **1996**, *15*, 615.

3. (a) Kani, R.; Nakano, Y.; Yohida, H.; Mikoshiba, S.; Hayase, S. *J. Polym. Sci. A* **1997**, *35*, 2355. (b) Miller, R. D. *Angew. Chem., Int. Ed. Engl.* **1989**, *28*, 1733. (c) Guo, C. S.; Luo, L. B.; Yuan, G. D.; Yang, X. B.; Zhang, R. Q.; Zhang, J.; Lee, S. T. *Angew. Chem., Int. Ed.* **2009**, *48*, 9896.

4. (a) Trujillo, R. E. *J. Organomet. Chem.* **1980**, *198*, C27. (b) Jones, R. G.; Benfield, R. E.; Cragg, R. H.; Swain, A. C.; Webb, S. J. *Maromolecules* **1993**, *26*, 4878. (c) Kim, H. K.; Matyjaszewski, K.; *J. Am. Chem. Soc.* **1988**, *110*, 3321. (d) Azemi, T.; Yokoyama, Y.; Mochida, K. *J. Organometal. Chem.* **2005**, *690*, 1588.

5. (a) Clark, T. J.; Lee, K.; Manners, I. *Chem. Eur. J.* **2006**, 8634. (b) Aitken, C.; Harrod, J. F.; Samuel, E. *J. Organomet. Chem.* **1985**, *279*, C11. (c) Reichl, J. A.; Popoff, C. M.; Gallagher, L. A.; Remsen, E. E.; Berry, D. H. *J. Am. Chem. Soc.* **1996**, *118*, 9430. (d) Woo, H. G.; Walzer, J. F.; Tilley, T. D. *J. Am. Chem. Soc.* **1992**, *114*, 7047. (e) Imori, T.; Tilley, T. D. *J. Chem. Soc., Commun.* **1993**, 1607. (f) Schittelkopf, K.; Fischer, R. C.; Meyer, S.; Wilfling, P.; Uhlig, F. *Appl. Organometal. Chem.* **2010**, *24*, 897.

6. (a) Koe, J. R.; Powell, D. R.; Buffy, J. J.; Hayase, S.; West, R. *Angew. Chem., Int. Ed.* **1998**, *37*, 1441. (b) Egorov, M. P.; Gaspar, P. P. In *Encyclopedia of Inorganic Chemistry*; John Wiley and Sons, **1989**, p13.

(c) Tsuchiya, M. J.; Hiroaki, H.; Tanaka, K.; Tanaka, T. *J. of Mol. Struct.* **1995**, *352*, 407.

7. (a) Ghadwal, R. S.; Roesky, H. W.; Merkel, S.; Henn, J.; Stalke, D. *Angew. Chem., Int. Ed.* **2009**, *48*, 5683. (b) Filippou, A. C.; Chernov, O.; Schnakenburg, G. *Angew., Chem. Int. Ed.* **2009**, *48*, 5687. (c) Kolesnikov, S. P.; Shiryaev, V. I.; Nefedov, O. M. *Izv. Akad. Nauk Ser. Khim.* **1966**, 584.

8. (a) Al-Rafia, S. M. I.; Malcolm, A. C.; Liew, S. K.; Ferguson, M. J.; Rivard, E. *J. Am. Chem. Soc.* **2011**, *133*, 777. (b) Al-Rafia, S. M. I.; Malcolm, A. C.; McDonald, R.; Ferguson, M. J.; Rivard, E. *Chem. Commun.* **2012**, 1308. (c) Thimer, K. C.; Al-Rafia, S. M. I.; Ferguson, M. J.; McDonald, R.; Rivard, E. *Chem. Commun.* **2009**, 7119. For related studies, see: (d) Arduengo III, A. J.; Rasika Dias, H. V.; Calabrese, J. C.; Davidson, F. *Inorg. Chem.* **1993**, *32*, 1541. (e) Rupar, P. A.; Staroverov, V. N.; Ragogna, P. J.; Baines, K. M. *J. Am. Chem. Soc.* **2007**, *129*, 15138.

9. (a) Sze, S. M. *Semiconductor Devices: Physics and Technology*, 1st Ed.; Wiley: New York, **1985**. (b) Hobbs, R. G.; Barth, S.; Petkov, N.; Zirngast, M.; Marchner, C.; Morris, M. A.; Holmes, J. D. *J. Am. Chem. Soc.* **2010**, *132*, 13742. (c) Kouvetakis, J.; Haaland, A.; Shorokhov, D. J.; Volden, H. V.; Girichev, G. V.; Sokolov, V. I.; Matsunaga, P. *J. Am. Chem. Soc.* **1998**, *120*, 6738. (d) Pan, W. Z.; Dai, S.; Rouleau, C. M.; Lowndes, D. H. *Angew. Chem., Int. Ed.* **2005**, *44*, 274. (e) Emmelius, M.; Pawlowski, G.; Wollmann, H. W. *Angew. Chem., Int. Ed. Engl.* **1989**, *28*, 1445. (f) Todd,

M.; Kouvetakis, J.; Smith, D. J. *Appl. Phys. Lett.* **1996**, 2407. (g) Soref, R. F. *J. Appl. Phys.* **1991**, *70*, 2470.

10. (a) Al-Rafia, S. M. I.; Malcolm, A. C.; McDonald, R.; Ferguson, M. J.; Rivard, E. *Angew. Chem., Int. Ed.* **2011**, *50*, 8354. (b) Al-Rafia, S. M. I.; McDonald, R.; Ferguson, M. J.; Rivard, E. *Chem. -Eur. J.* **2012**, 18, 13810. (c) Al-Rafia, S. M. I.; Malcolm, A. C.; Liew, S. K.; Ferguson, M. J.; McDonald, R.; Rivard, E. *Chem. Commun.* **2011**, *47*, 6987.

11. (a) Schäfer, H.; Saak, W.; Weidenbruch, M. *Organometallics* **1999**, *18*, 3159. (b) Beattie, I. R.; Jones, P. J.; Reid, G.; Webster, M. *Inorg. Chem.* **1998**, *37*, 6032. (c) Pu, L.; Senge, M. O.; Olmstead, M. M.; Power, P. P. *J. Am. Chem. Soc.* **1998**, *120*, 12682. (d) Ishida, Y.; Sekiguchi, A.; Kobayashi, K.; Nagase, S. *Organometallics* **2004**, *23*, 4891. (e) Pu, L.; Philips, A. D.; Richards, A. F.; Stender, M.; Simons, R. S.; Olmstead, M. M.; Power, P. P. *J. Am. Chem. Soc.* **2003**, *125*, 11626. (f) Ramaker, G.; Saak, W.; Weidenbruch, M. *Organometallics* **2003**, *22*, 5212. (g) Sekiguchi, A.; Fukaya, N.; Ichinohe, M.; Takagi, N.; Nagase, S. *J. Am. Chem. Soc.* **1999**, *127*, 11587. (h) Sen, S. S.; Kratzet, D.; Stern, D.; Roesky, H. W.; Stalke D. *Inorg. Chem.* **2010**, *49*, 5786. (i) Simons, R. S.; Pu, L.; Olmstead, M. M.; Power, P. P. *Organometallics* **1997**, *16*, 1920.

12. Li, J.; Schenk, C.; Goedecke, C.; Frenking, G.; Jones, C. *J. Am. Chem. Soc.* **2011**, *133*, 18622.

13. (a) Okano, M.; Mochida, K. *Chem. Lett.* **1990**, 701. (b) Amadoruge, M. L.; Gardinier, J. R.; Weinert, C. S. Organometallics **2008**, *27*, 3753. (c)

Castle, A.; Revière, Saint-Roch, B.; Stagé, J. *J. Organomet. Chem.* **1983**, *247*, 145.

14. Sugiyma, Y.; Sasamori, T.; Hosoi, Y.; Furukawa, Y.; Takagi, N.; Nagase, S.; Tokitoh, N. *J. Am. Chem. Soc.* **2006**, *128*, 1023.

15. Krapp, A.; Frenking, G. *J. Am. Chem. Soc.* **2008**, *49*, 16646.

16. Ghadwal, R. S.; Roesky, H. W.; Merkel, S.; Stalke, D. *Chem. Eur. J.* **2010**, *16*, 85.

17. Mallela, S. P.; Hill, S.; Geanangel, R. A. *Inorg. Chem.* **1997**, *36*, 6247.

18. Nagase, S.; Nakano, M. *J. Chem. Soc., Chem. Commun.* **1998**, 1077.

19. Dias, H. V.; Wang, Z. *J. Am. Chem. Soc.* **1997**, *119*, 4650.

20. Slriwardane, U.; Islam, M. S.; Maguire, J. A.; Hosmane, N. S. *Organometallics* **1988**, *7*, 1894.

21. Kraus, C. A.; Brown, C. L. *J. Am. Chem. Soc.* **1930**, *52,* 4031.

22. Roller, S.; Dräger, M. *J. Organomet. Chem.* **1986**, *316,* 57.

23. Amadoruge, M. L.; Golen, J. A.; Reingold, A. L.; Weinert, C. S. *Organometallics* **2008**, *27*, 1979.

24. (a) Bent, H. A. *Chem. Rev.* **1961**, *61*, 275. (b) Huheey, J. *Inorg. Chem.* **1981**, *20*, 4033.

25. Reichl, J. A.; Popoff, C. M.; Gallagher, L. A.; Remsen, E. E.; Berry, D. H. *J. Am. Chem. Soc.* **1996,** *118,* 9430.

26. Katz, S. M.; Reichl, J. A.; Berry, D. H. *J. Am. Chem. Soc.* **1998**, *120,* 9844.

27. Li, L.; Fukawa, T.; Matsuo, T.; Hashizume, D.; Fueno, H.; Tanaka, K.; Tamao, K. *Nature Chem*. **2012**, *4*, 361.

28. Karsch, H. H.; Deubely, B.; Riede, J.; Müller, G. *Angew. Chem., Int. Ed. Engl*. **1987**, *26*, 674.

29. For experimental and characterization details please refer to Chapter 2.

30. For details please refer to Chapter 3.

31. Hlina, J.; Baumgartner, J.; Marschner, C. *Organometallics* **2010**, *29*, 5289.

32. Pangborn, A. B.; Giardello, M. A.; Grubbs, R. H.; Rosen, R. K.; Timmers, F. J. *Organometallics* **1996**, *15*, 1518.

33. (a) Jafarpour, L.; Stevens, E. D.; Nolan, S. P. *J. Organometal. Chem*. **2000**, *606*, 49. (b) Hintermann, L. *Beilstein J. Org. Chem*. **2007**, *3*, No 22, doi: 10.1186/1860-5397-3-22.

34. Hope, H. *Prog. Inorg. Chem*. **1994**, *41*, 1.

35. Blessing, R. H. *Acta Cryst*. **1995**, *A51*, 33.

36. Sheldrick, G. M. *Acta Cryst*. **2008**, *A64*, 112.

37. Beurskens, P. T.; Beurskens, G.; de Gelder, R.; Smits, J. M. M.; Garcia-Garcia, S.; Gould, R. O. *DIRDIF-2008*, Crystallography Laboratory, Radboud University: Nijmegen, The Netherlands, **2008**.

38. Schneider, T. R.; Sheldrick, G. M. *Acta Cryst*. **2002**, *D58*, 1772.

39. Lemierre, V.; Chrostowska, A.; Dagelos, A.; Baylère, P.; Leigh, W. J.; Harrington, C. R. *Appl. Organomet. Chem*. **2004**, *18*, 676.

Chapter 8

Summary and Future Work

Chapter 8

Summary and Future Work

Chapter 2 described the synthesis of a new ligand class containing sterically modifiable umbrella-shaped triarylsilyl groups and use of these ligands for the isolation of low coordinate group 14 complexes. Unfortunately, due to the presence of a high degree of structural flexibility in these amidosilyl ligands the kinetic stabilization of reactive bonds such as Ge=O and Ge=S double bonds was not successful; instead, the formation of thermodynamically favorable germanes with σ-bonded Ge_2O_2 and Ge_2S_2 motifs was observed. Despite the inherent flexibility of the reported amidosilyl ligands, they can be quite useful in transition metal chemistry where flexible steric bulk is often considered to be one of the requirements for accommodating incoming substrates. During the course of these studies, the major focus was the isolation of reactive bonds between main Group elements. In future, it would be important to study the steric nature of these amidosilyl ligands when they are in the coordination sphere of a transition metal. In this regard, the initial goal could be amidosilyl ligand incorporation onto transition metals to support low-coordinate metal environments, which then can be tested for activation of small molecules such as N_2 and CO_2.

Chapter 3 reported the synthesis of heavy Group 14 element methylene adducts LB•EH_2•LA (E = Si, Ge and Sn), with the use of Lewis basic donors and Lewis acidic acceptors. It was demonstrated that N-heterocyclic carbenes (NHCs) and N-heterocyclic olefins in combination with Lewis acids such as BH_3, $W(CO)_5$ and $Cr(CO)_5$ can efficiently stabilize various Group 14 dihydrides, while the use

of sterically demanding phosphine and amine donors were unsuccessful. It was also noted that the relative Lewis acidity and Lewis basicity of :EH_2 units played a key role in the stability and reactivity of the resulting heavy methylene complexes. For example, the Si(II) adduct IPr•SiH_2•$W(CO)_5$ is the most stable complex of the series followed by the germanium and tin analogues. This trend mirrors the expected decrease in the HOMO-LUMO gap in SiH_2 relative to its heavier analogues; thus SiH_2 is expected to be a better donor and acceptor. Interestingly, the element-boron (E-BH_3) interactions in the borane adducts IPr•EH_2•BH_3 (E = Si and Ge) are labile enough in THF to allow the IPr•EH_2 units to be transferred onto Lewis acidic metal centers such as $W(CO)_5$ and $Cr(CO)_5$ *via* $M(CO)_5/BH_3$ (M = Cr and W) metathesis chemistry. This unique $M(CO)_5/BH_3$ (M = Cr and W) metathesis chemistry can be a general way to transfer :EH_2 moieties onto transition metal centers in the future. Future work in this area could involve studying the thermal decomposition of these heavy methylene analogues LB•EH_2•LA as low temperature routes to nanoparticles. The main challenge associated with the use of LB•EH_2•LA adducts is the low element contents (in terms of weight percent) within these complexes, which will need to be improved in order to achieve higher yields of nanomaterials *via* thermal decomposition. The use of smaller carbenes such as $ImMe_4$ or low molecular weight N-heterocyclic olefins or Wittig reagents (such as $Me_3P{=}CH_2$), could be a possible approach to solve this issue.

In Chapter 4, the preparation of the first stable complexes of the parent inorganic ethylenes $H_2EE'H_2$ (E = Si and Ge; E' = Ge and Sn) using the donor-

acceptor stabilization concept introduced in Chapter 2 was presented. The E-E' linkages were constructed by reacting the nucleophilic E(II) halide adducts, IPr•ECl_2 or IPrCH_2•ECl_2 (E = Si and/or Ge) with the coordinatively labile tungsten complexes, [$(THF)_n$•E'Cl_2•$W(CO)_5$] (E' = Ge and Sn) and then the desired hydride functionalities were installed by using chloride/hydride metathesis reactions. An interesting hydrosilylation reaction was observed when 2,4-pentanedione was reacted with the silagermene complex IPr•H_2Si-GeH_2•$W(CO)_5$, which yielded the novel anionic adduct [{MeC(O)H-CH=C(Me)O}SiH-GeH_2•$W(CO)_5]^-$ as a salt with the known imidiazolium countercation $[IPrH]^+$. This transformation indicates that the Ge-Si linkage in the silagermene complex is quite stable, which might facilitate the future synthesis of new SiGe hybrid nanomaterials *via* decomplexation/dehydrogenation of the silagermene unit. Furthermore, in the digermene complex IPr•H_2Ge-GeH_2•$W(CO)_5$ (**8**) (Chapter 4), the Ge-Ge interaction is labile and this phenomena might be used to prepare higher catenates of the series such as IPr•H_2Ge-$(EH_2)_n$-GeH_2•$W(CO)_5$ (E = Si-Sn) by inserting additional ECl_2 units into the Group 14 chain followed by chloride/hydride metathesis chemistry. Another possible future research direction in this area could involve the synthesis of the parent heavy alkyne analogues IPr•HE=E'H•$W(CO)_5$ (E and E' = Si, Ge and Sn). This target might be approached using two different routes: (1) reduction of the known chloro complexes [IPr•Cl_2E-E'Cl_2•$W(CO)_5$] using a mild reducing agent such as Jones' Mg(I) complex [{Mg[N(Mes)CMe]$_2$CH}$_2$] (Mes = 2,4,6-$Me_3C_6H_2$) to give IPr•ClE=E'Cl•$W(CO)_5$, which later can be reacted with a hydride source; (2) H_2

elimination from IPr•H_2E-E'H_2•W$(CO)_5$ with the use of a Frustrated Lewis Pair e.g. ^{t}BuP/B$(C_6F_5)_3$ or using an electrophilic carbene such as a cyclic alkylamino carbene (CAAC) (Scheme 8.1) as a dehydrogenating agent.

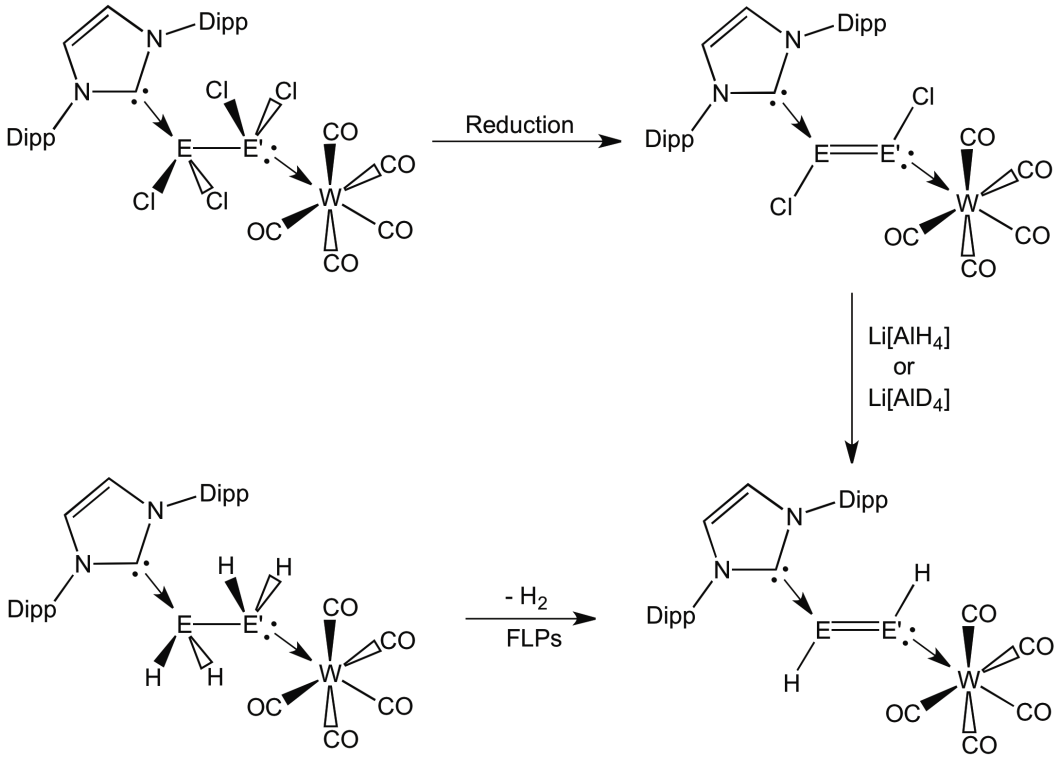

Scheme 8.1. Proposed synthetic routes for obtaining donor-acceptor stabilized heavy ethylene analogues IPr•HE=E'H•W$(CO)_5$ (E and E' = Si, Ge and Sn).

Chapter 5 focused on the preparation of a series heavy Group 14 element aminochloro and aminohydride adducts, IPr•E(Cl)NHDipp and IPr•EH(BH_3)NHDipp (E = Si, Ge and Sn). The thermal decomposition of these hydrido amine adducts IPr•EH(BH_3)NHDipp was investigated as a potential route to access Si- and Ge-based clusters. Although the synthesis/isolation of the desired nanomaterials was not possible, a rare C-N bond activation/ring-

expansion reaction involving the bound N-heterocyclic carbene donor IPr was discovered; this reaction could represent an important deactivation pathway in NHC-based catalysis. Future studies in this area could involve further investigation of thermal decomposition of analogous hydrido amide adducts with bulky groups at nitrogen in order to access new types of Group 14 element clusters.

Chapter 6 describes the synthesis of a novel mixed P(III)-P(V) heterocyclic adduct [IPr•PN(PCl_2N)$_2$]. Unfortunately, attempts to reduce the remaining P(V) centers in [IPr•PN(PCl_2N)$_2$] to prepare [IPr•PN]$_3$, a trapped oligomer of PN, were unsuccessful. A divergent reaction pathway was discovered in the reaction of IPr=CH_2 and [Cl_2PN]$_3$, which led to the formation of the olefin-bound cyclophosphazene [(IPr=CH)P(Cl)N(PCl_2N)$_2$]. Repeated attempts to abstract chloride from this olefin-bound cyclophosphazene in order to generate cyclophosphazene cation [(IPr=CH)PN(PCl_2N)$_2$]$^+$ were unsuccessful. Nevertheless, these studies provide the foundation of future research, which could include the discovery of a synthetic strategy to access the desired [IPr•PN]$_3$ complexes and the synthesis of new binary PN materials *via* thermolysis/carbene-decomplexation chemistry. One of the ways to attain this target heterocycle would be to engage electrophilic carbenes, such as CAACs. Since CAACs are strong σ-donors and good π-acceptors they might be able to stabilize a PN ring with fully reduced P(III) centers *via* C-P π-acceptor interactions. Another important area of research could be the generation of [(IPr=CH)PN(PCl_2N)$_2$]$^+$, as this species might

be an active ring-opening polymerization (ROP) catalyst to prepare polydichlorophosphazene from $[Cl_2PN]_3$.

The last research Chapter of this Thesis described a synthetic strategy for the preparation of oligomeric dichlorogermylenes, $[GeCl_2]_x$ (x = 1-4). These oligomeric species were stabilized with the application of N-heterocyclic carbene (IPr) and N-heterocyclic olefin (IPr=CH_2) donors. Interestingly, it was found that the σ-donor ability of the donor controls the geometry of the oligomers formed. For example, linear digermane complex IPr•$GeCl_2$-$GeCl_2$ was obtained from the reaction of IPr•$GeCl_2$ with $GeCl_2$•dioxane, while a similar reaction with the use of IPrCH_2•$GeCl_2$ resulted in the formation of dicationic branched tetragermane complex $[(IPrCH_2•GeCl_2)_3Ge][GeCl_3]_2$. Furthermore, in the presence of $B(C_6F_5)_3$, IPr•$GeCl_2$-$GeCl_2$ participated in a chloride transfer reaction to produce the new trigermane complex [IPr•$GeCl_2$-GeCl-$GeCl_2$•IPr][Cl_3Ge-$B(C_6F_5)_3$]. The neutral *catena*-tetragermane adduct IPr•Cl_2Ge-Ge$(GeCl_3)_2$ was formed from the reaction of IPr•$GeCl_2$-$GeCl_2$ with two equivalents of $GeCl_2$•dioxane indicating a propensity for forming branched germanes as the Ge content is increased. Although the synthesis of complexes with longer Ge chain lengths were unsuccessful, this synthetic strategy might offer a route for the controlled synthesis of other heavy Group 14 oligomers IPr•$(E'Cl_2)_n$ (E = Si and Ge; E' = Si-Sn). Future directions in this area of research might involve optimizing the reaction conditions to prepare dichlorogermylenes with increased chain length along with higher degree of control over their geometry (*i.e* linear *vs* branched).

One of the possible ways to attain this goal might be to use strong σ-donor carbenes with less steric bulk around the carbene center. The presence of a strong donor might help to make the terminal germanium centers more nucleophlic leading to stronger donor-acceptor interactions, while the reduced steric bulk around the carbene center might help to better understand the role of steric effects on the degree of branching. In addition to these experiments, theoretical studies will be needed to comprehend the bonding features in these molecules. Since these oligogermanes have higher element content, it would be quite interesting to explore the application of these complexes for the synthesis of germanium nanomaterials *via* low temperature thermal decomposition.